Exploiting natural variation in *Plantago* seed composition for food and human health applications

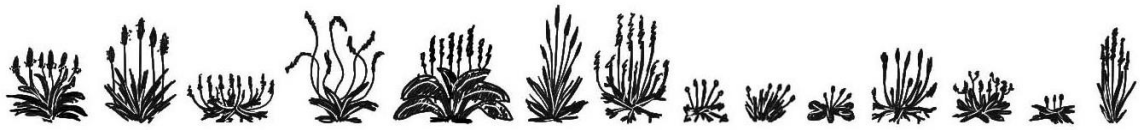

James M. Cowley

BAgS, BSc (Hons)

A thesis submitted to The University of Adelaide in fulfilment of the requirements for the degree of Doctor of Philosophy

THE UNIVERSITY of ADELAIDE

The University of Adelaide
Faculty of Sciences
School of Agriculture, Food and Wine
October 2020

Declaration

I certify that this work contains no material which has been accepted for the award of any other degree or diploma in my name, in any university or other tertiary institution and, to the best of my knowledge and belief, contains no material previously published or written by another person, except where due reference has been made in the text. In addition, I certify that no part of this work will, in the future, be used in a submission in my name, for any other degree or diploma in any university or other tertiary institution without the prior approval of the University of Adelaide and where applicable, any partner institution responsible for the joint-award of this degree.

I acknowledge that copyright of published works contained within this thesis resides with the copyright holder(s) of those works.

I also give permission for the digital version of my thesis to be made available on the web, via the University's digital research repository, the Library Search and also through web search engines, unless permission has been granted by the University to restrict access for a period of time.

I acknowledge the support I have received for my research through the provision of an Australian Government Research Training Program Scholarship.

James M. Cowley

20/10/2020

Acknowledgements

This thesis is dedicated to all the brilliant, inspiring women in science that I have been fortunate enough to be surrounded and supported by in my career. You have all been instrumental in helping me become the scientist I am today, and you will all forever have my deepest respect.

I struggle to put into words the appreciation and admiration I have for my supervisors, Prof. Rachel Burton and Dr Tina Bianco-Miotto. Your support and confidence in me, both inside and outside of the lab, has been instrumental in getting me to where I am today. Thank you for sticking by me through all my meltdowns. This thesis is dedicated to you and is a testament to your extraordinary ability as supervisors and scientists.

I acknowledge the financial support of the University of Adelaide, the Australian Research Council Centres of Excellence in Plant Cell Walls and Plant Energy Biology, the Barr Smith Trust and the Farrer Memorial Trust.

To my “fronds” Dr Jana Phan and Dr Bianca Warnock, your friendship and support through my highest highs and lowest lows did not and does not go unappreciated. I’m so appreciative and proud to call you my “Wednesday Friends”.

I’d like to thank the past and present members of Plant Cell Walls and RABLAB for creating such a friendly, inclusive and inspiring environment to undertake my PhD. In particular I’d like to thank my friends Dr Natalie Betts, Dr Helen Collins, Dr Andrea Matros, Dr Neil Shirley, Associate Professor Matt Tucker, Stav Manafis, Emma Drew, Kylie Neumann, Sandy Khor, Dr Laura Wilkinson, Dr Matt Aubert, Aaron Phillips, Jakob Schulz, Mel Ford, Ali Gill, Emma Aspin, Dayton Bird, Maple Ang, Mia Lou, Lina Herliana, Ghazwan Karem, Tate Hancox, Tharu Jayampathi, Jacqui Barsby, Amy

Doan, Dr Ben Keiller and Dr Trang Pham for making it so enjoyable to come to the lab every day.

I have to thank my friends from my stays at the University of Nottingham, Sutton Bonington Campus which was life-changing and essential to my studies. I'd like to express my sincerest thanks to Professor Tim Foster who was my host and mentor at Sutton Bonington Campus. To my friends Dr Yi Ren, Dr Gleb Yakubov, Dr Vincenzo Di Bari, Dr Olivia Cousins, Rosemary Young, Nat Ivanova, Sam Riley, Ethan Iles, Khatija Nawaz, Alex McIntyre, Jordan Robson, Dr Cindy Callens, Motolani Sobanwa and Dr Yangyi Chen, thank you for making my stays in Nottingham so productive and enjoyable.

To my family, my mum Julie, my dad Wayne, my sisters Carina and Elise, their husbands Paul and Zeke, and my gorgeous "niblings", Connor, Lila, Ezra, Arlo, and Logan, and my best and oldest friends, Heather, Daniel, and Hilary, thank you for always making me laugh thanks for always supporting me, making me smile, and letting me forge my own path.

Finally, to Chris, you were an unexpected gift from my PhD experience. Thank you for always listening to me talk science at you even when you didn't at all understand. Thank you for all of the trips to the theatre, all the dinners out, showing me the best of the UK's theme parks, suffering through hikes with me, and even sharing the times where we sat around and did and said nothing. Thanks for being "mine".

Table of Contents

List of Figure and Tables (in order of appearance in each chapter)

Chapter 1 – General Introduction

Chapter 2 – Literature Review

Chapter 3 – Method for rapid analysis of seed mucilage characteristics

Chapter 4 – *P. ovata* seed mucilage accumulation, storage and release

Chapter 5 – Seed characteristics and composition of Australian *Plantago* species

Chapter 6 – Pasting of *Plantago* flour and rice flour/starch blends

Chapter 7 – Augmenting gluten-free breads with *Plantago* flour

Chapter 8 – Effect of *Plantago* flour extracts on intestinal epithelial cell viability *in vitro*

List of publications, published and proposed

The following publications are listed in order of future submission

1. **Cowley JM**, Herliana L, Neumann KA, Ciani S, Cerne V, and Burton RA (2020) A small-scale fractionation pipeline for rapid analysis of seed mucilage characteristics. Plant Methods 16:20 https://doi.org/10.1186/s13007-020-00569-6
2. Phan JL, **Cowley JM,** Neumann KA, Herliana L, O'Donovan LA, and Burton RA (2020) The novel features of *Plantago ovata* seed mucilage accumulation, storage and release. Scientific Reports **10 11766** https://doi.org/10.1038/s41598-020-68685-w
3. **Cowley JM** and Burton RA (unpublished) Seed composition of Australian *Plantago* species: insights into drivers of natural variation and the benefit of whole seed consumption. Target journal: Annals of Botany
4. **Cowley JM,** Foster TJ, and Burton RA (unpublished) Polysaccharides in whole seed *Plantago* flour interact with amylose altering rice flour/starch pasting and retrogradation: a new synergistic interaction model. Target journal: Food Hydrocolloids
5. **Cowley JM,** Ren Y, Foster TJ, and Burton RA (unpublished) Augmenting rice flour-based gluten-free breads with naturalised and Australian native *Plantago* seeds. Target journal: Food Hydrocolloids
6. **Cowley JM,** Barsby JP, Leemaqz SY, Bastian SEP, Bianco-Miotto T and Burton RA (unpublished) Crude aqueous extracts from novel Australian *Plantago* flours increase viability of rat IEC-6 and human Caco-2 intestinal epithelial cells. Target journal: Food & Function

CHAPTER 1

Thesis Introduction

This chapter was written to the sounds of...	
Album	I'll Still Have Me (Aquilo Remix)
Artist	Cyn
Favourite Song	I'll Still Have Me (Aquilo Remix)

Thesis Introduction

Food manufacturing is a massive global industry that is constantly undergoing research and development to create products that meet customer expectations of sensory traits. The success of processed products can rely on careful manipulation of product texture, often through the addition of long-chain, hydrophilic polymers called hydrocolloids. Hydrocolloids can be synthetic, semisynthetic or natural, with natural food hydrocolloids increasing in importance due to a need to meet consumer perceptions and ease of production. An important class of natural food hydrocolloids are mucilage polysaccharides, produced from seeds of many plant species. However, mucilage-producing seeds like psyllium (*Plantago ovata*) are orphan crops and are plagued by agronomic constraints that severely limit consistent supply of high-quality product. The production constraints of psyllium are also compounded by high amounts of waste during processing, where the non-mucilaginous tissues (endosperm and embryo) are not put to good use. Due to poor knowledge about psyllium seed composition, this practice is routine but it is likely that the endosperm and embryo contain many beneficial nutrients that are unnecessarily wasted.

These factors raise several questions about new and/or improved sources of mucilage-containing materials. What valuable nutrients do whole *Plantago* seeds contain that are typically wasted during manufacturing processes? Could a whole seed flour be used in place of purified mucilage? Are there any added health advantages of using a whole seed flour in this way? Can mucilage and/or flour from non-commercial, evolutionarily-adapted species be used in the same or different ways to commercial psyllium? A summary of these research questions that has shaped this thesis can be found in Figure 1.1.

Thesis Structure / Abstract

This thesis is comprised of nine chapters: a general thesis introduction (Chapter 1), a review of the literature (Chapter 2), two published research articles (Chapters 3 and 4), four unpublished research manuscripts (Chapters 5, 6, 7 and 8) and a final general discussion (Chapter 9). A schematic overview of the thesis structure is presented in Figure 1.2.

Chapter 3 is a published research and methodology article describing a method for small-scale rapid fractionation of seed mucilage (Cowley *et al.* 2020, *Plant Methods*, 16:20). Most published seed mucilage extraction techniques while simple and robust, were recognised early in my candidature to be less than ideal for screening natural variants.. Previously published methods were often incomplete, time-consuming, and unnecessarily wasteful of precious seed stocks. Instead the new method described in Chapter 3 can be used to extract fractions of mucilage from small quantities of seed, which are still sufficient for chromatographic and other downstream analyses.

Chapter 4 is a published research article describing the unique aspects of seed mucilage polysaccharide accumulation, storage, and release in *Plantago ovata* (Phan *et al.* 2020, *Scientific Reports*). Literature describing the polysaccharide biology of most mucilage-producing species is lacking and as such has led to an overreliance on understanding from the well-characterised model species *Arabidopsis.* In this manuscript, work by Dr Jana Phan (submitted 2018) completed during her PhD candidature showing that in *P. ovata,* mucilage polysaccharides were deposited and stored in a different fashion to *Arabidopsis*, was complemented by collaborative work done during my candidature where we spatiotemporally defined *P. ovata* mucilage release characteristics. This resulted in the formulation of a new model to describe

mucilage-related processes in this species, and will be used to guide future work on Australian *Plantago* species that share some but not all features with *P. ovata.*

Chapter 5 is an unpublished research manuscript where variation in seed composition and structure was compared between twelve Australian *Plantago* species: commercial psyllium, three naturalised species and eight native species. In addition to an analysis of the functional mucilage polysaccharides, this research showed that *Plantago* seeds have a substantial endosperm that contains beneficial proteins and fats. Natural variation in these seed constituents is described and discussed in a biogeographic and evolutionary context.

Chapters 6 and 7 explore the influence that differences in *Plantago* seed composition and properties identified in Chapter 5 have on the in-food functionality of whole seed flour (WSF). Chapter 6 is an unpublished research manuscript where changes to the cooking/gelatinisation properties of rice flour and rice starch upon a small addition of *Plantago* WSF are described. Different WSFs have different influences on the gelatinisation properties with similarity observed between Australian species. Differences were attributed to mucilage content and structure and an explanatory model for a novel polysaccharide-polysaccharide interaction is proposed. In a more applied study presented in Chapter 7, *Plantago* WSF was added to gluten-free doughs which enhanced the rheology and proofing behaviour and led to improved loaf structure and texture. Differences in the degree of improvement were again attributed, in part, to the interaction described in Chapter 6 and an adapted model is presented.

Chapter 8 describes experiments where an aqueous extract was produced from seeds of four *Plantago* species (deemed to perform well in Chapters 6 and 7) and applied to two intestinal epithelial cell lines *in vitro*. *Plantago* seed extracts were found to enhance the viability of these cell lines which has gastrointestinal health and nutrition impacts.

It is likely that cell proliferation is enhanced by these extracts and based on characterisation of the extract, the constituents likely to be involved are discussed.

The final chapter, Chapter 9, presents a summary and general discussion of the findings of this work and suggests future research directions.

Music has played a significant role during my PhD candidature as both an escape and a tool to focus on writing. Each chapter was written to the sounds of an album, the details of which have been included on the cover page of each chapter. Included is a QR-style Spotify Code which can be imaged using the Spotify mobile app to listen to each album.

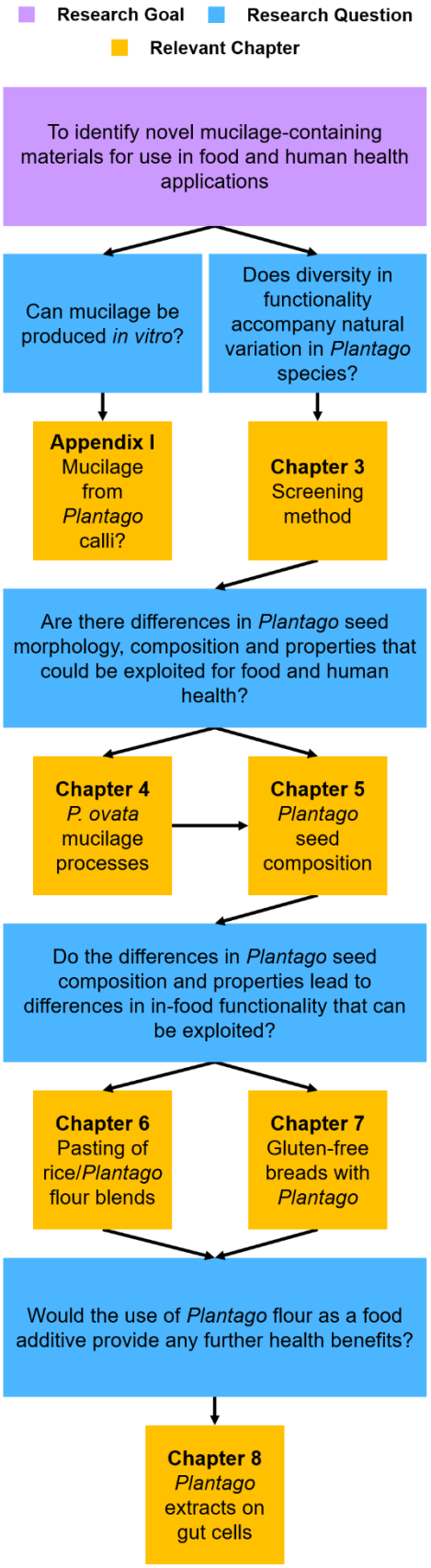

Figure 1.1. Schematic overview of the research questions that structured the thesis and its relevant research chapters

Figure 1.2. Schematic overview of the thesis structure

CHAPTER 2

Strategies for producing high quality natural hydrocolloids like psyllium gum for improved food and nutrition: a literature review

This chapter was written to the sounds of...

Album	IV
Artist	BADBADNOTGOOD
Favourite Song	In Your Eyes

HYDROCOLLOIDS AS FOOD ADDITIVES

Food product manufacturing is a massive global industry, with the total revenue of packaged foods expected to exceed USD 3 trillion by 2020 (Allied Analytics LLP, 2015). The industry is investing billions of dollars into innovative food production. Australia alone invested over AUD 900 million into research and development of agriculture and food manufacturing in 2015 (Chaustowski and Dolman, 2016). The success of many processed and manufactured foods lies in the manipulation of ingredients to meet customer expectations of sensory traits such as flavour and texture (Bourne, 2002).

Texture is often closely controlled by ingredients that alter the basic properties of the food system through their gelling, thickening, structuring or stabilisation properties. Such ingredients are usually members of a large group of compounds called hydrocolloids (Funami, 2017), a heterogeneous group of long-chain, often branched polymers (Saha and Bhattacharya, 2010). Many of these polymers do not easily form entire dissolution and can be physically separated from the solvent; however, they do form strong hydrophilic interactions with the solvent and so cannot be classified as a particulate suspension. These hydrocolloid mixtures are therefore more correctly classified as dispersions (Milani and Maleki, 2012). Usually hydrocolloids are added to modify sensory properties, particularly by enhancing viscosity and texture (Izydorczyk *et al.*, 2005; Saha and Bhattacharya, 2010; Funami, 2017), but hydrocolloids also have versatility in other roles such as structuring, stabilising, encapsulating and mimetic agents (Izydorczyk *et al.*, 2005).

Viscosifying and thickening agents

Viscosity refers to a material's flow and its resistance to being deformed under force. In liquid materials this is commonly referred to as 'thickness'. For example, water under the force of being poured deforms and spreads rapidly to fill its container, while honey takes far longer. This is because honey has a far greater viscosity than water (approximately 10 000 times more viscous) and resists deformation. Modifying a food's viscosity therefore alters its sensory properties, particularly in relation to texture and mouthfeel as it relates to perceived 'thickness' (Burey *et al.*, 2008). While viscosity can also be affected by interaction of concentrated solid particles in suspension (e.g. starch mixtures or concrete), the thickening effect of hydrocolloid-containing systems is caused when its free moving polymers must become sufficiently concentrated to form an interactive entangled network (Graessley, 1974; Heymans, 2000). In a dilute solution, hydrocolloids rarely form random interactions and thus viscosity remains unchanged but as the system becomes more concentrated, the polymers come into contact more frequently and the viscosity increases (Milani and Maleki, 2012). While the degree of viscosification or thickening effect is primarily determined by both the type and amount of hydrocolloid polymer present, the hydrocolloid's exact effect is also influenced by the native physical properties of the food system, like its pH and temperature (Burey *et al.*, 2008).

Non-Newtonian materials can exhibit Bingham plastic, shear thickening or shear thinning behaviour (Figure 2.1A) with the two latter states sometimes being time-dependent (rheopexy or thixotropy, respectively) (Figure 2.1B) (Milani and Maleki, 2012). Special behaviours in highly viscous systems are very often exploited in food, pharmaceutical and cosmetic technology for both practicality and consumer preference. A Bingham plastic material acts as solid until stress is applied which can be seen in many spreadable condiments like mayonnaise or peanut butter. Due to high

stress when being spread across a slice of bread, peanut butter transitions from a solid-like state to a viscous liquid, but once applied to the bread, the peanut butter returns to a solid state and no longer flows (Figure 2.1C). A material that is shear-thickening becomes more viscous under stress while a shear-thinning material becomes less viscous. Shear-thickening behaviour (and its time-dependent variant rheopexy) (Figure 2.1D) are uncommon and not often seen in food technology (Krokida *et al.*, 2007), but shear-thinning behaviour, and its time-dependent variant thixotropy, are very commonly exploited in food manufacturing. A classic example of shear-thinning behaviour is exhibited by the condiment ketchup. A highly viscous fluid at rest, ketchup is difficult to pour or squeeze from a bottle unless shaken. The stress applied from shaking causes the material to thin (become less viscous), becoming easier to dispense (Figure 2.1E). As the thinning effect increases with duration of shaking, ketchup more specifically exhibits time-dependent shear thinning or thixotropy.

Gelling agents

A gelling agent is used in food products to create a solid but soft texture (as for jelly), which is an attractive sensory property for consumers (Burey *et al.*, 2008). The traditional model of hydrocolloid gelation is sometimes considered a furthering of a viscosified or thickened dispersion because the dynamic viscosifying interactions become exponentially less transient until the polymer chains become entangled to form a stiff, three-dimensional network (Burey *et al.*, 2008) where solvent is contained within the interstices (Saha and Bhattacharya, 2010) (Figure 2.2). This is the typical ‘glass-like’ gel which is highly-disordered as network forms stochastically and thus would be unable to reorder with their neighbours and form homogenous assemblies. However this model prohibits dynamic reordering of biological gel structures like in cell walls and thus there is increasing evidence for dynamic ‘percolating’ gels where bond exchange

can occur among homotypic and heterotypic neighbours to assemble homogenous, potentially more effective networks (Li *et al.*, 2019).

Emulsifiers

Hydrocolloids are effective at emulsifying mixtures but do not employ combined hydrophilic and lipophilic properties (typical of commercial chemical emulsifiers) to combine immiscible components (Klose and Glicksman, 1972), instead generally relying on viscosification and/or surface activity. Some hydrocolloids are known to stabilise emulsions by adsorbing at interfaces, thereby isolating and electrostatically stabilising the interfaces between the two immiscible phases—known as a Pickering emulsion. Though not strictly emulsifiers (as they do not stabilise phase interfaces), other hydrocolloids may also stabilise immiscible mixtures simply by increasing the viscosity slowing droplet coalescence and subsequent phase separation (Wang *et al.*, 2011). The stabilisation of oil-in-water emulsions by hydrocolloid addition is particularly important to prevent the separation of condiments such as mayonnaise or salad dressing.

Stabilisers

In addition to emulsion stabilisation, hydrocolloids are also able to stabilise and prevent unwanted separation of foamed or frozen systems. The texture of frozen desserts like ice cream should be creamy and is often disrupted by the formation of ice crystals during freeze-thaw cycles. The separation of water within the system can be prevented by hydrophilic hydrocolloids which immobilise water molecules and prevent crystallisation (Regand and Goff, 2003). Ice crystal prevention is also important in a wide range of frozen goods as it can lead to syneresis, the separation and loss of water

from a frozen system, which can cause unwanted flavours and textures as well as freezer-burn (Ghosh and Coupland, 2008).

Encapsulating and film-forming agents

Hydrocolloids are used to create and/or reinforce edible films like those found on sausages (Klose and Glicksman, 1972; Milani and Maleki, 2012). These films are used to create a physical barrier that maintains the structure of foods while cooking and inhibits the bi-directional migration of moisture, aromas and oils (Izydorczyk *et al.*, 2005; Cazon *et al.*, 2016). Artificial sausage casings are arguably the best example, but novel hydrocolloid-based films are being used to prolong the shelf-life of a variety of perishable foods like cut meats or fruits (Ahmadi *et al.*, 2012; Jouki *et al.*, 2014; Mohammadi *et al.*, 2019).

Fat and gluten replacement

A facet of food technology that is becoming extremely important are the ‘free-from’ products. These are products that are consumed because they lack certain components that consumers opt out of eating for health reasons. Fat-reduced versions of high-fat products like mayonnaise or salad dressing rely on high viscosification by hydrocolloids to maintain the slippery texture that oils normally provide (Aghdaei *et al.*, 2014; Ladjevardi *et al.*, 2015; Fernandes and Salas-Mellado, 2017).

Formulations for fat-reduced products are much simpler to optimise as they often only require partial replacement which is much easier to achieve than making entirely fat-free products. Due to the severity of gluten intolerances, gluten reduction is not an option and thus total gluten replacement is essential. However, gluten has very unique properties that are not easily replicated but are essential in the production of high-quality baked goods. The hydration of a gluten-containing flour leads to the formation

of the three-dimensional gluten network (Shewry and Tatham, 1997). This imbues foods with positive chewy texture characteristics and helps to retain leavening gases produced during fermentation, assisting bread to rise (Figure 2.3A). A bread made from gluten-free flour will be unable to trap leavening gases and thus cannot effectively rise (Figure 2.3B). Hydrocolloids have some ability to replicate the function of gluten in bread by thickening gluten-free batters and preventing gas loss during bread rise. They can potentially create a three-dimensional network within the starch matrix, thus improving product structure and texture (Anton and Artfield, 2008).

Sources of hydrocolloids

Hydrocolloids are derived from several sources. While synthetic hydrocolloids do exist, biological hydrocolloids are far more common and are produced by a variety of land and marine plants, microbes, and animals (Table 2.1). With such a wide range of biological sources, hydrocolloid composition and structure is correspondingly diverse with many different glycan classes represented (Figure 2.4). Microbial hydrocolloids like xanthan gum are among the most commonly used (Garcia-Ochoa *et al.*, 2000), but plant-derived hydrocolloids are increasing in significance due to their ease of production and preference by consumers. Plant exudate gums are extruded from a point of stress (usually physical injury or fungal infection) and collected (e.g. gum arabic or gum ghatti), and seed gums are chemically extracted from endosperm tissue (e.g. guar gum or locust bean gum) (Izydorczyk *et al.*, 2005). These types of plant gums require extensive processing and refinement (adding to labour and production costs), while another class of plant hydrocolloid—seed mucilage—simply extrudes from the wetted seed coat of some species in a phenomenon called myxospermy (Phan and Burton, 2018). Currently, psyllium seed mucilage produced from milled husk is one of the most commercially significant seed hydrocolloids (Khaliq *et al.*, 2015), and is

beginning to permeate the food and pharmaceutical industries as a novel ingredient with excellent thickening and swelling properties.

PSYLLIUM

Historically, 'psyllium' referred to several species in the genus *Plantago*. Only *P. psyllium* (French Psyllium) and *P. ovata* (Blonde Psyllium) have been used for the commercial production of psyllium husk (Sharma and Koul, 1986). However, the unappealing dark brown husk colour of *P. psyllium* has led to it being displaced from the world market by the lighter *P. ovata* (Dhar *et al.*, 2005). *P. ovata* (Figure 2.5) is native to the Mediterranean and West Asia (Kumar, 2015), where it is called isabgol and ispaghula (Wiesner, 2013), though the commercial crop is usually referred to as psyllium. *P. ovata* is primarily produced for the seed husk that is milled from mature seeds (Figure 2.5D) (Bahrani, 1991; Van Craeyveld *et al.*, 2008) and used in various applications for its ability to produce mucilage upon contact with water. This mucilage is composed primarily of a hydrocolloid with excellent functional properties: a highly-branched heteroxylan (Sharma and Koul, 1986; Fischer *et al.*, 2004).

The majority of psyllium husk is sold as a dietary fibre supplement. Psyllium mucilage is poorly fermented by bacteria in the digestive system allowing it to pass through largely intact (Marlett *et al.*, 2000). The swelling of the psyllium mucilage increases faecal bulk and softness (Prajapati *et al.*, 2013), and acts as a lubricant, promoting laxation (Marlett *et al.*, 2000). There is increasing evidence that a diet supplemented with dietary fibre is an effective preventative treatment for irritable bowel syndrome, obesity, colon cancer, constipation, diabetes, high cholesterol, ulcerative colitis, atherosclerosis and inflammatory conditions like asthma (Ziai *et al.*, 2005; Van Craeyveld *et al.*, 2009; Mehmood *et al.*, 2011; Wiesner, 2013; Thorburn *et al.*, 2015; Gonçalves and Romano, 2016). Psyllium husk is also a livestock health supplement

where it is used to prevent glycaemic conditions (Moreaux *et al.*, 2011) and to flocculate ingested sand, preventing colic in horses (Landes *et al.*, 2008).

Psyllium mucilage is used in food technology for typical thickening and stabilisation properties (Milani and Maleki, 2012) but also as a fat substitute in the production of low-fat yoghurt and mayonnaise (Aghdaei *et al.*, 2014; Ladjevardi *et al.*, 2015). With gluten-free products now comprising a US$ 4.3 billion global industry (Research and Markets, 2017), great interest has now been placed in the utility of psyllium as a cost-effective textural corrector in gluten-free products (Zandonadi *et al.*, 2009; Cappa *et al.*, 2013). As gluten imbues dough with elasticity (Wieser, 2007), its exclusion in gluten-free products leads to unfavourable texture characteristics. Consumer satisfaction is significantly improved with the addition of texture modifiers like psyllium mucilage to gluten-free doughs (Mariotti *et al.*, 2009; Cappa *et al.*, 2013).

Industrially, psyllium husk has also been used as a disintegrant in pharmaceutical tablets (Pawar and Varkhade, 2014), a natural corrosion inhibitor (Mobin and Rizvi, 2016), an inexpensive alternative to agar in culture media (Jain *et al.*, 1997) and in the production of environmentally-responsible ‘green concretes’ (Minnesota Institute for Sustainable Transportation, 2017).

Agronomy of psyllium production

Plantago ovata is grown as a 120 – 130 day dry-season crop, suitable for cultivation in regions with well-drained, sandy soils (Dhar *et al.*, 2005). The small, light seeds are usually mixed with fine sand and broadcast sown to ensure dense planting (Najafi and Rezvani, 2002; Dhar *et al.*, 2005). Flood irrigation is performed as required, usually to a total of 4–5 irrigations over the growing season (Najafi and Rezvani, 2002; Dhar *et al.*, 2005; Bannayan *et al.*, 2008; Kumar, 2015). The understanding of *P. ovata*’s

nutrient requirements is poor, but may be fairly low. For example, a crop rotation including a leguminous crop is usually sufficient to meet nitrogen demand (Kumar, 2015), but a top dressing of nitrogen and phosphorus fertiliser can be used if continuous cropping is performed (Dhar *et al.*, 2005; Mandal *et al.*, 2008; Kumar, 2015). Flowering begins two months after sowing and is completed by five months, at which point whole plants are harvested by hand-sickling from just above ground level. The harvested plants are then heaped, sun-dried, threshed and winnowed (Dhar *et al.*, 2005). The seeds are collected and sold whole or milled to remove the husk (Kumar, 2015).

Constraints in psyllium production

There are several significant constraints in the production of *P. ovata* (psyllium), all of which can lead to significant losses in yield of seed or husk and reduction in the quality of mucilage produced.

P. ovata can be subject to massive yield losses in response to biotic stress. It can be infected by three major fungal wilt diseases such as downy mildew (*Peronospora plantaginis*) which tends to be the most damaging (resulting in greater than 50% yield losses) as it is difficult to detect, often striking at inflorescence emergence, reducing effective response time (Elwakil and Ghoneem, 1999; Dhar *et al.*, 2005; Mandal *et al.*, 2008). Cotton aphid (*Aphis gossypii)* is the major insect pest of *P. ovata*. Aphids appear at 50–60 days, where sap sucking during inflorescence emergence can lead to yield losses greater than 40% (Kumar, 2015). Competition from fast-germinating weeds is a significant contributing factor to poor crop establishment. If seeding is performed without light tillage, fast-germinating weeds will easily outcompete germinating *P. ovata* seeds.

Abiotic stresses and production constraints also limit supply and reduce quality. Climate is the most unpredictable and unavoidable constraint. Drought limits the availability of water from sources used for flood irrigation and unseasonable rainfall during vegetative growth increases transmission and severity of fungal infection (Kumar, 2015). Additionally, unseasonable rainfall at maturity leads to massive yield losses through seed shattering (Dhar *et al.*, 2005). A lack of modernised production techniques prevents any significant advances in the productivity of psyllium production. Mechanisation is nearly non-existent with sowing, weeding, harvesting, and post-harvest processing all traditionally done by hand (Dhar *et al.*, 2005). Introduction of agrochemicals has also been limited, particularly due to cultural practices and regulations associated with medicinal products (Kumar, 2015).

Commerce of psyllium production

Psyllium is an important crop for a number of South Asian nations, particularly India where North Gujarat, Western Rajasthan and Madhya Pradesh provinces export more than 80% of the world supply (Kumar, 2015) earning India approximately US$ 185 million in 2016 (Govt India Dept of Commerce, 2017a, 2017b). Export quantity relies on production in India, which in turn is affected by agronomic constraints. This leads to a clear supply and demand relationship (Figure 2.6). For example, between 2006/07 and 2007/08, export quantity from India increased and thus sufficient supply to consumers lead to steady prices. Conversely, after export quantities dropped in 2008/09, and again in 2009/10, the export price per tonne increased. These trends are likely to continue as demand for psyllium husk by the food, health and pharmaceutical sectors increases, highlighting the need for innovative production technologies and/or genetic improvement.

Genetic improvement of *Plantago ovata* (psyllium)

Selective breeding approaches to improving yield and quality traits in *P. ovata* are lengthy and difficult processes (Sarkar and Lal, 2015). Genetic variation in germplasm that have previously been used for breeding efforts is low. This was possibly due to *P. ovata*'s low chromosome number and exacerbated by small chromosome size, high abundance of heterochomatin and low chiasmata frequency which reduces the opportunity for spontaneous variation (Dhar *et al.*, 2005; Kotwal *et al.*, 2013),

Numerous approaches have been used to induce variability in *P. ovata* including mutagenesis and induced polyploidy. Two high-yielding commercial varieties—Niharika and Mayuri—were produced through mutagenesis (Lal *et al.*, 1998, 2007), but yield advantage over conventional varieties is minor (Kumar, 2015). Induced polyploidy showed promise in increasing seed weight, seed volume and tiller and inflorescence number, but any superiority diminished after several generations and was offset by reduced seed yield and germination success (Zadoo and Farooqi, 1977; Fougat, 2011). Finally, transgenic approaches have been shown to be a powerful tool to increase yield, improve drought tolerance and resist disease in other crops (Phillips, 2008) but the lack of a sequenced genome and a stable transformation technique in *P. ovata,* as well as heavy regulatory restraints have prevented a gene technology approach to improvement from being commercially viable.

While not ideal, conventional breeding for desired traits has been the only effective method of genetic improvement in psyllium, with a small number of commercial varieties released (Lal *et al.*, 1998, 2007; Kumar, 2015; Sarkar *et al.*, 2015). Current commercial varieties have been developed solely for increased yield, and efforts have not been made to address agronomic issues that may be the most significant cause of poor yield (Kumar, 2015). These agronomic issues underlie an inconsistent supply of

high-quality psyllium husk to industrial users globally, and pressure for genetic solutions or advancements in innovative production is higher than ever. This presents an opportunity to investigate more novel approaches to circumvent agronomic issues in the commercial *Plantago* variety such as scrutinising the suitability of close relatives that may be naturally-adapted to have desirable traits.

EXPLOITING NOVELTY IN THE *PLANTAGO* GENUS

The genus *Plantago*

The genus *Plantago* comprises more than 200 species with members found on all inhabited continents (Elliot and Jones, 1980). *Plantago* species are herbaceous, growing from a basal rosette at the root mass. Inflorescences are conspicuous, supported away from the vegetative mass by a peduncle and consist of many individual florets (Huisinga and Ayers, 1999; Tay, 2008) (Figure 2.5B)

For a cosmopolitan genus with several applications, *Plantago* species have not been extensively studied. *P. asiatica, P. lanceolata, P. major, P. maritima, P. media* and *P. ovata* are the most widely reported species in the literature, as rich sources of bioactive extracts of pharmaceutical significance (Grubešić *et al.*, 2005; Fons *et al.*, 2008; Yin *et al.*, 2010; Zhao *et al.*, 2014; Gonçalves and Romano, 2016; Navarrete *et al.*, 2016). *Plantago* species have also been used as models to study the genetics of male self-sterility (Wolff *et al.*, 1988; Rønsted *et al.*, 2002), the divergence of key growth characteristics in relation to climate (Atkin and Day, 1990; Covey-Crump *et al.*, 2002; Loveys *et al.*, 2003), bioaccumulation and phytoremediation of heavy metals (Baroni *et al.*, 2000), and the dynamics of arbuscular mycorrhizal interactions (Wang *et al.*, 2015; Zhang *et al.*, 2015).

As the source of commercially- and medicinally-important psyllium husk, *P. ovata* is the best-studied *Plantago* species. It has recently become an important model system in biomolecular studies as its heteroxylan-rich seed coat mucilage (Fischer *et al.*, 2004) is a highly amenable tissue for studying xylan synthesis. Jensen *et al.* (2011) were the first to use the integument layer of immature *P. ovata* seeds for transcriptional profiling of xylan synthesis genes, and further studies have revealed greater diversity in xylan biosynthesis genes than previously thought (Jensen *et al.*, 2013; Kotwal *et al.*, 2016). Recently, forward genetic analyses have been used to identify novel genes in a mutagenised *P. ovata* population (Cowley, 2016; Tucker *et al.*, 2017; Phan, 2018). Studying other members of the large *Plantago* genus could contribute to our understanding of mucilage production and its industrial applications and lead to optimal utilisation of products from *P. ovata* and other *Plantago* species.

Natural variation in *Plantago* spp.

Natural variation is arguably the most powerful resource for crop improvement. The success and productivity of commercial cereal crops is owed to the careful selection of naturally-occurring, advantageous traits in their ancient progenitors (William *et al.*, 2011). Today, natural variation is an extremely useful tool for novel gene identification (Mitchell-Olds and Schmitt, 2006), biomolecular characterisation and improving the understanding of plant development, physiology and adaptation (Alonso-Blanco *et al.*, 2009). Investigation of natural genetic variation has allowed greater understanding of the synthesis and properties of pectin-rich seed mucilage in *Arabidopsis* (North *et al.*, 2014; Saez-Aguayo *et al.*, 2014) and *Linum usitatissimum* (Aubert, 2014; Pavlov *et al.*, 2014). By contrast, few studies have been published studying natural variation in genera with xylan-rich seed mucilage like *Plantago*.

Natural variation in *Plantago* spp. has provided a unique resource for helping define the heteroxylan biosynthetic pathway. Recently, Phan et al. (2016) uncovered significant variation in seven members of the *Plantago* genus: *P. coronopus, P. cunninghamii, P. debilis, P. lanceolata, P. major, P. ovata* and *P. varia*. Monosaccharide and methylation linkage analysis was consistent with previous studies, showing that the major component of *Plantago* mucilage is heteroxylan (Samuelsen *et al.*, 1999; Chaplin, 2004; Fischer *et al.*, 2004; Guo *et al.*, 2008; Saghir *et al.*, 2008), however oligosaccharide mapping revealed that backbone substitution patterns vary substantially by species (Phan *et al.*, 2016). In particular, *P. cunninghamii* is hypothesised to have significantly lower levels of heteroxylan backbone substitution than *P. ovata*, which has a more complex backbone substitution pattern (Figure 2.8). Transcript analysis revealed that *P. ovata* had several abundant sequences encoding glycosyltransferase family (GT) 61 enzymes that have been previously implicated in β-1,2-xylosyltransferase and/or α-1,3-arabinosyltransferase activity—the attachment of xylose and arabinose moieties to the β-1,4-xylose backbone (Figure 2.7). Contrastingly, *P. cunninghamii* lacked an equivalent number of corresponding GT61 orthologues possibly leading to the lesser degree of backbone substitution found on the heteroxylan of its mucilage. Exploring xylan synthase genes in this way can identify genes responsible for novel linkages found in *Plantago* heteroxylan

In addition to revealing novel polysaccharide synthesis genes, natural variation in *Plantago* spp. mucilage heteroxylan structure can provide hydrocolloids with unique properties for use in food technology. It is known that polysaccharide structure dictates polymer conformation and interactivity with other polymers: factors that orchestrate the functional properties of the hydrocolloid. The functional properties of *Plantago* heteroxylan will therefore differ in response to the extent and chemical nature of its substitution. This was confirmed through rheological studies that found that differences

in the functional properties of separate layers of *P. ovata* seed mucilage arise from the degree of heteroxylan substitution (Yu *et al.*, 2017, 2018, 2019; Ren *et al.*, 2020; Zhou *et al.*, 2020). It would then follow that significant differences in functional properties are likely to accompany the natural variation in the heteroxylan structure within and between *Plantago* spp. (Figure 2.8) as revealed by Phan *et al.* (2016), which can be exploited as a versatile resource for studying the biosynthetic mechanisms and functional properties of xylan-rich mucilage, ultimately leading to novel industrial applications.

CONCLUSIONS

Plantago seed mucilage is a versatile food ingredient that is increasing in use due to its favourable functional properties. Currently only one species—*Plantago ovata*—is produced commercially but constraints in its production have impeded optimal industrial utilisation. It may be possible that another improved source of *Plantago* mucilage may lie within natural variants as it is unknown if other members of the *Plantago* genus produce mucilage with similar or better functional properties as the genus is yet to be thoroughly interrogated.

Table 2.1 Examples of common hydrocolloids used in food applications

Class	Derived From:	Name	Example of commercial source	Schematic glycan structure	Reference
Algal	Red seaweed	Agarose	*Gelidium amansii*	Figure 4L	(Araki, 1956)
		Carrageenan	*Kappaphycus alvarezii*	Figure 4M	(Ruiter and Rudolph, 1997)
	Brown seaweed	Alginate	*Macrocystis pyrifera*	Figure 4P	(Grasdalen *et al.*, 1981)
Animal		Gelatin	Animal bones and hide	-	-
		Chitosan	Exoskeletons of crustaceans	Figure 4O	(Islam *et al.*, 2017)
Microbial	Exopolysaccharide	Xanthan	*Xanthomonas campestris*	Figure 4F	(Paul *et al.*, 1986)
		Curdlan	*Agrobacterium* spp.	Figure 4D	(Shih *et al.*, 2009)
		Dextran	*Leuconostoc mesenteroides*	Figure 4E	(Paul *et al.*, 1986)
		Gellan	*Sphingomonas elodea*	Figure 4Q	(Jansson *et al.*, 1983)
Plant	Starchy plant tissues	Starch (amylose and amylopectin)	Cereals, tubers	Figure 4A,B	(Martin and Smith, 1995)
	Plant biomass	Cellulose derivatives	Agricultural biomass waste	Figure 4C	(Taylor, 2008)
		Pectin	Citrus peel and fruit pomace	Figure 4K	(Mohnen, 2008)
	Tree gums	Gum arabic	*Acacia* spp.	Figure 4R	(Williams and Phillips, 2003)
		Gum karaya	*Sterculia urens*	Figure 4U	(Williams and Phillips, 2003)
		Gum ghatti	*Anogeissus latifolia*	Figure 4T	(Williams and Phillips, 2003)
		Gum tragacanth	*Astragalus gummifer*	Figure 4V	(Williams and Phillips, 2003)
	Tubers	Konjac gel	*Amorphophallus konjac*	Figure 4G	(Williams *et al.*, 2000)
	Seed gums	Locust bean gum	*Ceratonia siliqua*	Figure 4H	(Dakia *et al.*, 2008)
		Senna gum	*Senna occidentalis*	Figure 4H	(Milani and Maleki, 2012)
		Guar gum	*Cyamopsis tetragonolobus*	Figure 4I	(Mudgil *et al.*, 2014)
		Tara gum	*Caesalpinia spinosa*	Figure 4I	(Wu *et al.*, 2015)
		Fenugreek gum	*Trigonella foenum-graecum*	Figure 4J	(Doyle *et al.*, 2009)
	Seed mucilage	Flaxseed mucilage	*Linum usitatissimum*	Figure 4N	(Naran *et al.*, 2008)
		Psyllium mucilage	*Plantago ovata*	Figure 4S	(Fischer *et al.*, 2004)

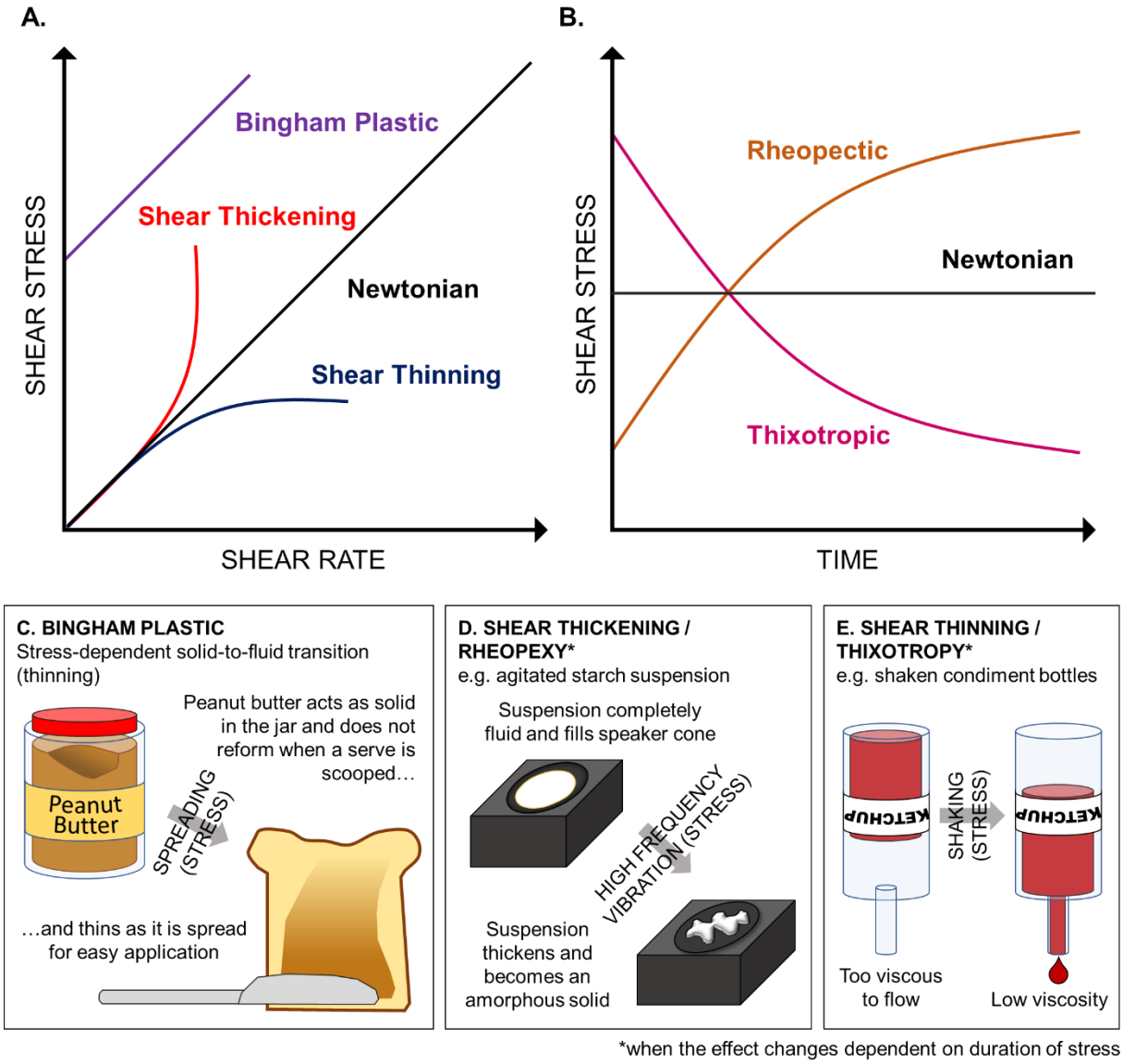

Figure 2.1. Description of types of viscoelastic behaviour. **A.** Shear rate dependence of Non-Newtonian materials compared to General Newtonian Behaviour **B.** Time-dependent shear thinning and shear thickening behaviour. **C.** Schematic examples of common materials exhibiting Non-Newtonian behaviour.

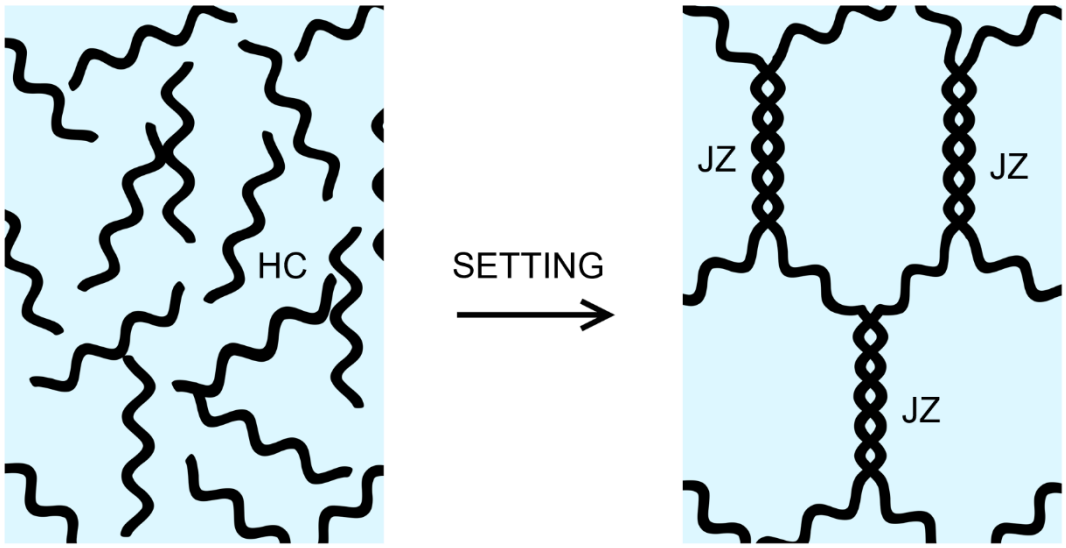

Figure 2.2. Simplified representation of traditional model of hydrocolloid gelation. Upon setting, the hydrocolloid molecules (HC) become entangled in junction zones (JZ) that form the basis of the three-dimensional structure of the gel matrix. (Adapted from de Vries 2004)

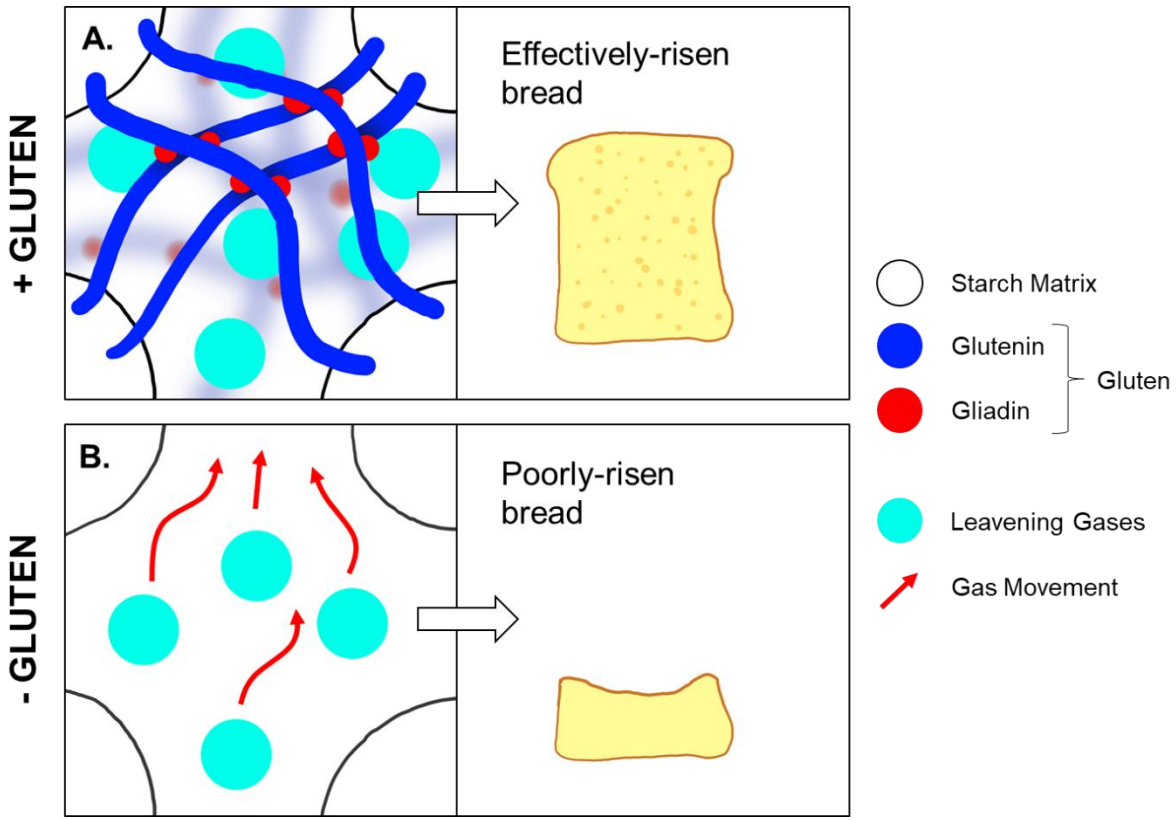

Figure 2.3. Function of gluten within leavened breads. **A.** Three-dimensional gluten network formation upon hydration traps gases produced during leavening and allows the bread to rise. **B.** A lack of gluten allows leavening gases to escape resulting in a poorly risen loaf.

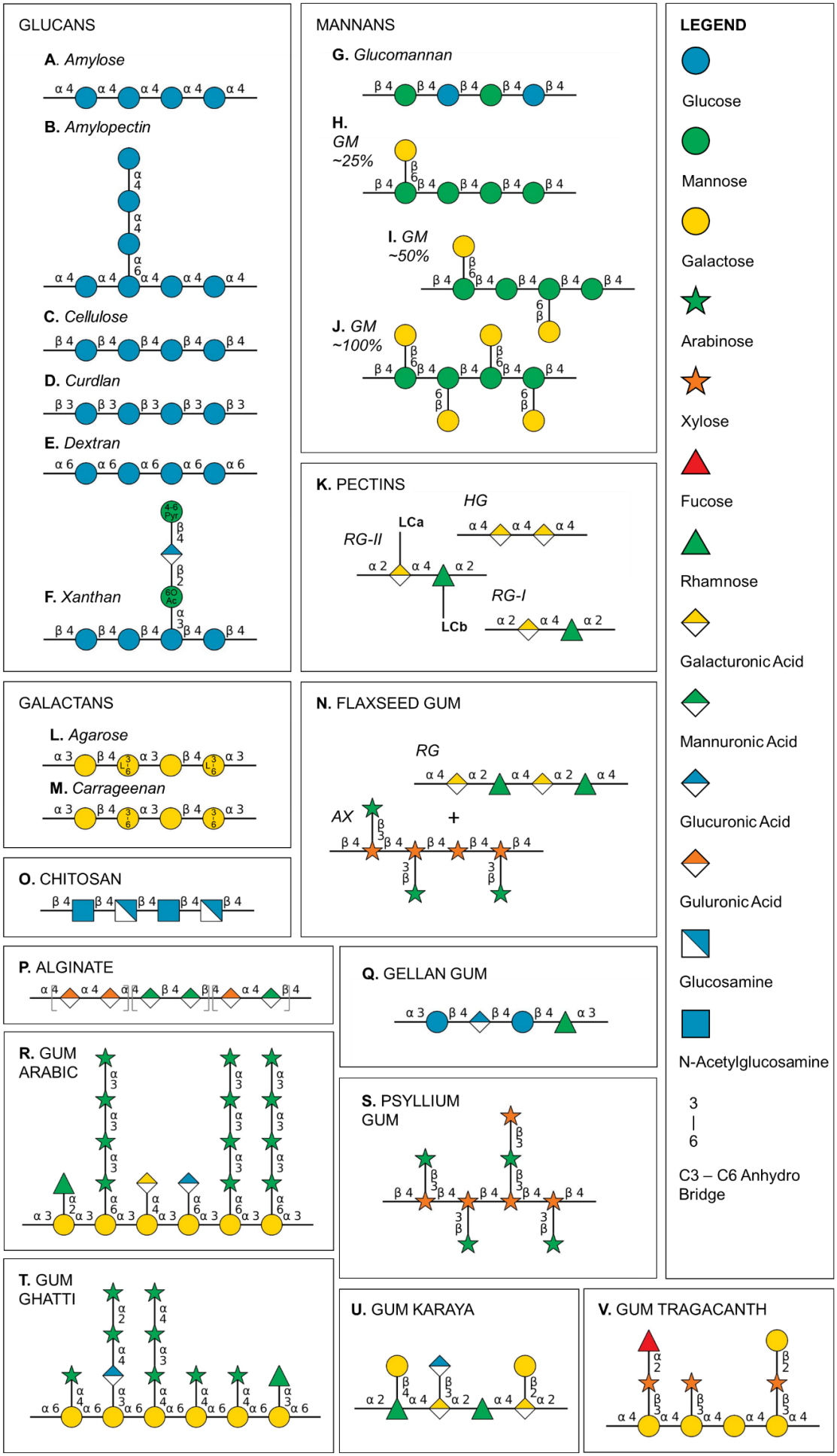
GLUCANS
A. Amylose
B. Amylopectin
C. Cellulose
D. Curdlan
E. Dextran
F. Xanthan
MANNANS
G. Glucomannan
H. GM ~25%
I. GM ~50%
J. GM ~100%
K. PECTINS
HG
RG-II
LCa
LCb
RG-I
GALACTANS
L. Agarose
M. Carrageenan
N. FLAXSEED GUM
RG
AX
O. CHITOSAN
P. ALGINATE
Q. GELLAN GUM
R. GUM ARABIC
S. PSYLLIUM GUM
T. GUM GHATTI
U. GUM KARAYA
V. GUM TRAGACANTH
LEGEND
Glucose
Mannose
Galactose
Arabinose
Xylose
Fucose
Rhamnose
Galacturonic Acid
Mannuronic Acid
Glucuronic Acid
Guluronic Acid
Glucosamine
N-Acetylglucosamine
C3 – C6 Anhydro Bridge

Figure 2.4. Schematic structures of common food hydrocolloids showing great complexity and diversity. Glucan-, mannan-, galactan-, and pectin-type glycans are grouped. Schematic structures were prepared based on references in Table 2.1 using the DrawGlycan-SNFG online tool (http://www.virtualglycome.org/DrawGlycan/) (Cheng *et al.*, 2017). Many specific structures (particularly those of tree gums and seed mucilages) have been generalised or are yet to be fully elucidated.

Abbreviations: GM = galactomannan (with approximate percentage of galactose substitution on the mannose backbone); HG = homogalacturonan; RG = rhamnogalacturonan; AX = arabinoxylan; LCa and LCb = lateral chain a and b, specific, highly-complex structures found in detail in Mohnen (2008).

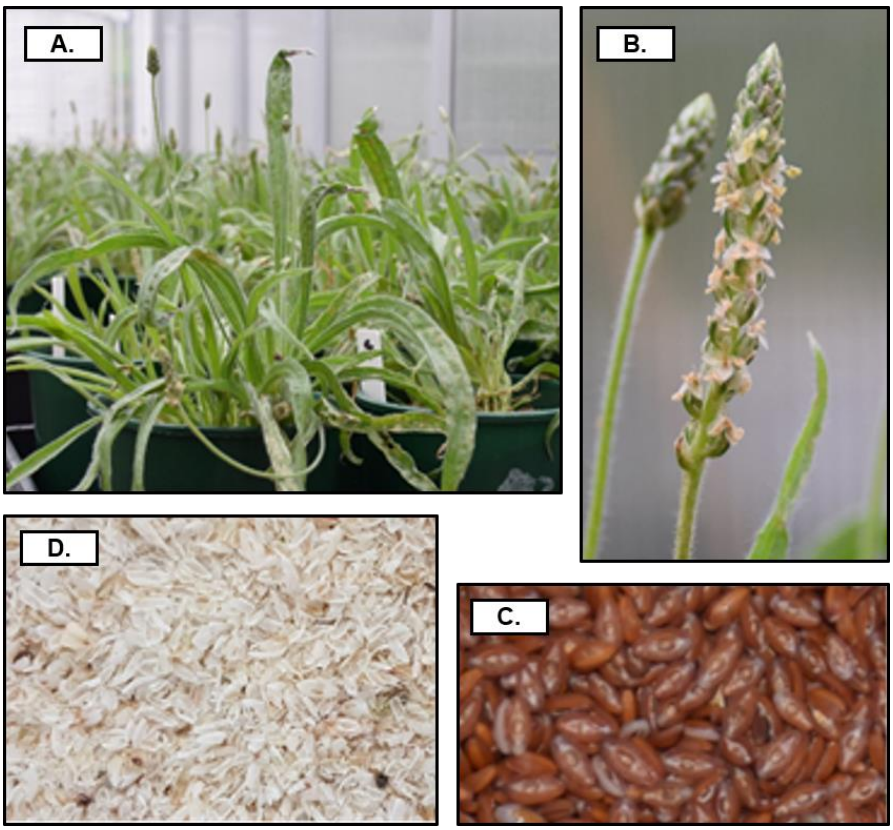

Figure 2.5. *Plantago ovata* (psyllium) is grown commercially to produce psyllium husk. **A.** Glasshouse-grown *P. ovata* in flower; **B.** *P. ovata* inflorescence undergoing anthesis; **C.** mature *P. ovata* seeds; **D.** milled commercial psyllium husk.

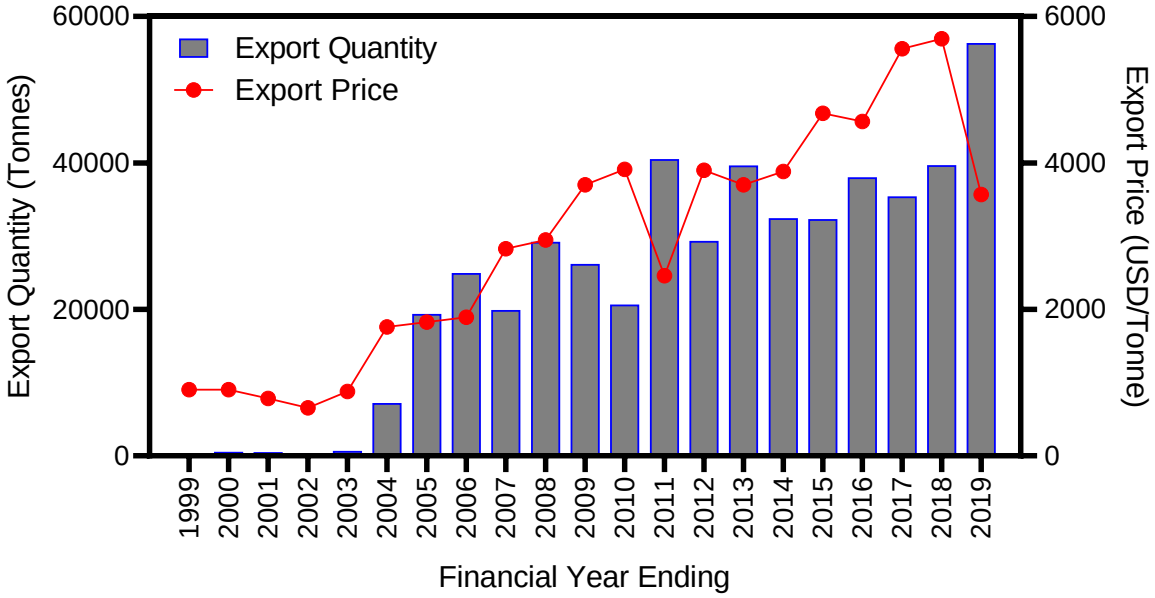

Figure 2.6. Trends of export quantity compared with export value of psyllium husk from 1999 to 2019 (adapted from Govt. India, Dept. of Commerce 2019a).

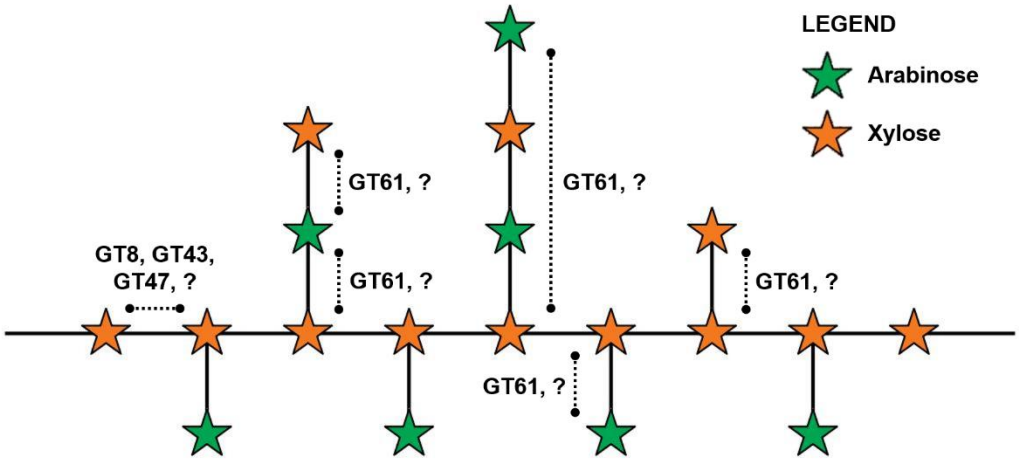

Figure 2.7. Schematic representation of the current understanding of heteroxylan synthesis. Enzymes of the glycosyltransferase families 8 (GT8), 43 (GT43) and 47 (GT47) have been implicated in the elongation of the xylan backbone (Rennie and Scheller, 2014) and glycosyltransferase 61 (GT61) enzymes have been implicated in the addition of various xylose, arabinose and oligosaccharide moieties onto the backbone (Anders *et al.*, 2012; Chiniquy *et al.*, 2012).

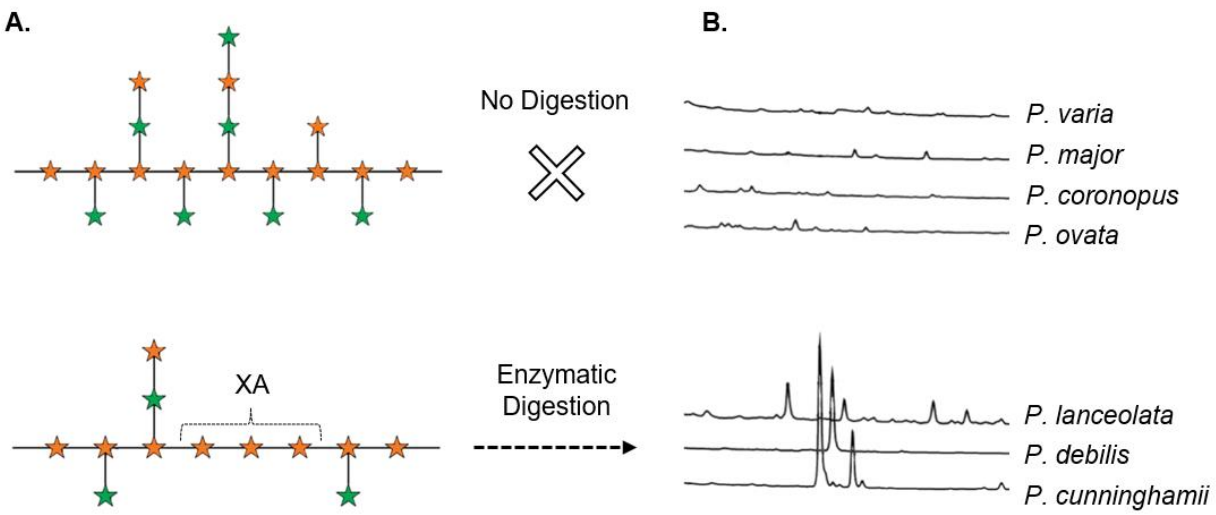

Figure 2.8. Oligosaccharide mapping reveals significant variation in heteroxylan structure in some *Plantago* species including reduced backbone substitution. **(B)** Chromatographic peaks represent oligosaccharides released by successful xylanase backbone digestion in *P. lanceolata, P. debilis* and *P. cunninghamii* possibly due to **(A)** reduced backbone substitution providing improved access to the xylan backbone (XA) by xylanase hydrolytic enzyme GH10 from *Cellvibrio mixtus.*

Adapted from Phan *et al.* (2016)

REFERENCES

Aghdaei, S. *et al.* (2014) 'Application of Isfarzeh seed (Plantago ovate L.) mucilage as a fat mimetic in mayonnaise.', *Journal of Food Science and Technology*, 51(10), pp. 2748–2754.

Ahmadi, R. *et al.* (2012) 'Development and characterization of a novel biodegradable edible film obtained from psyllium seed (Plantago ovata Forsk)', *Journal of Food Engineering*. Elsevier Ltd, 109(4), pp. 745–751.

Allied Analytics LLP (2015) *World Packaged Food - Market Opportunities and Forecasts, 2014-2020*.

Alonso-Blanco, C. *et al.* (2009) 'What has natural variation taught us about plant development, physiology, and adaptation?', *The Plant Cell*. Am Soc Plant Biol, 21(7), pp. 1877–1896.

Anders, N. *et al.* (2012) 'Glycosyl transferases in family 61 mediate arabinofuranosyl transfer onto xylan in grasses', *Proc Natl Acad Sci USA*, 109(3), pp. 989–993.

Anton, A. A. and Artfield, S. D. (2008) 'Hydrocolloids in gluten-free breads: A review', *International Journal of Food Sciences and Nutrition*, 59(1), pp. 11–23.

Araki, C. (1956) 'Structure of the agarose constituent of agar-agar', *Bulletin of the Chemical Society of Japan*, 29(4), pp. 543–544.

Atkin, O. and Day, D. (1990) 'A comparison of the respiratory processes and growth rate of selected Australian alpine and related lowland plant species', *Functional Plant Biology*, 17, pp. 517–526.

Aubert, M. (2014) *Seed mucilage formation and composition in Linum species*. University of Adelaide.

Bahrani, A. S. (1991) 'Processes for dehusking psyllium seeds', *US Patent Number 5020732*. Google Patents. Available at: http://www.google.com/patents/US5020732.

Bannayan, M. *et al.* (2008) 'Yield and seed quality of Plantago ovata and Nigella sativa under different irrigation treatments', *Industrial Crops and Products*, 27(1), pp. 11–16.

Baroni, F. *et al.* (2000) 'Antimony accumulation in Achillea ageratum, Plantago lanceolata and Silene vulgaris growing in an old Sb-mining area', *Environmental Pollution*, 109(2), pp. 347–352.

Bourne, M. (2002) *Food texture and viscosity: concept and measurement*. Academic press.

Burey, P. *et al.* (2008) 'Hydrocolloid gel particles: formation, characterization, and application.', *Critical reviews in food science and nutrition*, 48(5), pp. 361–77.

Cappa, C., Lucisano, M. and Mariotti, M. (2013) 'Influence of Psyllium, sugar beet fibre and water on gluten-free dough properties and bread quality', *Carbohydrate Polymers*. Elsevier Ltd., 98(2), pp. 1657–1666.

Cazon, P. *et al.* (2016) 'Polysaccharide-based films and coatings for food packaging: A review', *Food Hydrocolloids*, 68, pp. 136–148.

Chaplin, M. F. (2004) 'The structure of Plantago ovata arabinoxylan', in Williams, P. A. and Phillips, G. O. (eds) *Gums and Stabilisers for the Food Industry 12*. The Royal Society of Chemistry, pp. 509–516.

Chaustowski, R. and Dolman, S. (2016) *Australia's Food and Agribusiness sector - Data Profile*. Canberra.

Cheng, K., Zhou, Y. and Neelamegham, S. (2017) 'DrawGlycan-SNFG : a robust tool to render glycans and glycopeptides with fragmentation information', *Glycobiology*, 27(3), pp. 200–205.

Chiniquy, D. *et al.* (2012) 'XAX1 from glycosyltransferase family 61 mediates xylosyltransfer to rice xylan', *Proc Natl Acad Sci USA*, 109(42), pp. 17117–17122.

Covey-Crump, E. M., Attwood, R. G. and Atkin, O. K. (2002) 'Regulation of root respiration in two species of Plantago that differ in relative growth rate: the effect of short- and long-term changes in temperature', *Plant, Cell & Environment*, 25(11), pp. 1501–1513.

Cowley, J. M. (2016) *Analysis of Plantago mucilage mutants*. University of Adelaide.

Van Craeyveld, V., Delcour, J. A. and Courtin, C. M. (2008) 'Ball milling improves

extractability and affects molecular properties of psyllium (Plantago ovata Forsk) seed husk arabinoxylan', *Journal of Agricultural and Food Chemistry*, 56(23), pp. 11306–11311.

Van Craeyveld, V., Delcour, J. A. and Courtin, C. M. (2009) 'Extractability and chemical and enzymic degradation of psyllium (Plantago ovata Forsk) seed husk arabinoxylans', *Food Chemistry*, 112(4), pp. 812–819.

Dakia, P. *et al.* (2008) 'Composition and physicochemical properties of locust bean gum extracted from whole seeds by acid or water dehulling pre-treatment', *Food Hydrocolloids*, 22, pp. 807–818.

Dhar, M. *et al.* (2005) 'Plantago ovata: genetic diversity, cultivation, utilization and chemistry', *Plant Genetic Resources*, 3(2), pp. 252–263.

Doyle, J. P., Lyons, G. and Morris, E. R. (2009) 'New proposals on "hyperentanglement" of galactomannans: Solution viscosity of fenugreek gum under neutral and alkaline conditions', *Food Hydrocolloids*, 23(6), pp. 1501–1510.

Elliot, W. R. and Jones, D. L. (1980) 'Plantago L.', *Encyclopaedia of Australian plants suitable for cultivation*. Edited by W. R. Elliot and D. L. Jones. South Melbourne, AUS: Lothian Books.

Elwakil, M. A. and Ghoneem, K. M. (1999) 'Detection and location of seed-borne fungi of blonde psyllium and their transmission in seedlings', *Pakistan J. Biol. Sci*, 2(1), pp. 38–44.

Fernandes, S. and Salas-Mellado, M. (2017) 'Addition of chia seed mucilage for reduction of fat content in bread and cakes', *Food Chemistry*. Elsevier Ltd, 227, pp. 237–244.

Fischer, M. H. *et al.* (2004) 'The gel-forming polysaccharide of psyllium husk (Plantago ovata Forsk.)', *Carbohyd Res*, 339, pp. 2009–2017.

Fons, F., Gargadennec, A. and Rapior, S. (2008) 'Culture of Plantago species as bioactive components resources: a 20-year review and recent applications', *Acta Botanica Gallica*, 155(2), pp. 277–300.

Fougat, R. S. (2011) 'Effect of induced autotetraploidy in blond psyllium', *International Journal of Plant Sciences*, 6(1), pp. 2–5.

Funami, T. (2017) 'In vivo and rheological approaches for characterizing food oral processing and usefulness of polysaccharides as texture modifiers- A review', *Food Hydrocolloids*. Elsevier Ltd, 68, pp. 2–14.

Garcia-Ochoa, F. *et al.* (2000) 'Xanthan gum: Production, recovery, and properties', *Biotechnology Advances*, 18(7), pp. 549–579.

Ghosh, S. and Coupland, J. (2008) 'Factors affecting the freeze – thaw stability of emulsions', *Food Hydrocolloids*, 22, pp. 105–111.

Gonçalves, S. and Romano, A. (2016) 'The medicinal potential of plants from the genus Plantago (Plantaginaceae)', *Industrial Crops and Products*, 83, pp. 213–226.

Govt India Dept of Commerce (2017a) 'Psyllium husk (isobgul) 12119032 Export : Commodity-wise'.

Govt India Dept of Commerce (2017b) 'Psyllium seed (isobgul) 12119013 Export : Commodity-wise'.

Graessley, W. (1974) 'The Entanglement Concept in Polymer Rheology', *Advances in Polymer Science*, 16, pp. 1–179.

Grasdalen, H., Larsen, B. and Smisrod, O. (1981) '13C-NMR Studies of monomeric composition and sequence in alginate', *Carbohydrate Research1*, 89(2), pp. 179–191.

Grubešić, R. J. *et al.* (2005) 'Spectrophotometric method for polyphenols analysis: Prevalidation and application on Plantago L. species', *Journal of Pharmaceutical and Biomedical Analysis*, 39(3–4), pp. 837–842.

Guo, Q. *et al.* (2008) 'Fractionation and physicochemical characterization of psyllium gum', *Carbohydrate Polymers*, 73(1), pp. 35–43.

Heymans, N. (2000) 'Novel look at models for polymer entanglement', *Macromolecules*, 33(11), pp. 4226–4234.

Huisinga, K. D. and Ayers, T. J. (1999) 'Vascular Plants of Arizona: Plantaginaceae

Plantain Family', *J Ariz-Nev Acad Sci*, 32(1), pp. 62–76.

Islam, S., Bhuiyan, M. and Islam, M. (2017) 'Chitin and Chitosan: Structure, Properties and Applications in Biomedical Engineering', *Journal of Polymers and the Environment*. Springer US, 25(3), pp. 854–866.

Izydorczyk, M., Cui, S. W. and Wang, Q. (2005) 'Polysaccharide Gums: Structures, Functional Properties, and Applications', *Food Carbohydrates: Chemistry, Physical Properties, and Applications*, (March 2015), p. 43.

Jain, N., Gupta, S. and Babbar, S. B. (1997) 'Isubgol as an Alternative Gelling Agent for plant tissue culture media', 6(July), pp. 129–131.

Jansson, P.-E., Lingberg, B. and Sandford, P. (1983) 'Structural studies of gellan gum, an extracellular polysaccharide elaborate by Pseudomonas elodea', *Carbohydrate Polymers1*, 124(1), pp. 135–139.

Jensen, J. K. *et al.* (2011) 'The DUF579 domain containing proteins IRX15 and IRX15-L affect xylan synthesis in Arabidopsis', *Plant Journal*. Blackwell Publishing Ltd, 66(3), pp. 387–400.

Jensen, J. K., Johnson, N. and Wilkerson, C. G. (2013) 'Discovery of diversity in xylan biosynthetic genes by transcriptional profiling of a heteroxylan containing mucilaginous tissue', *Frontiers in Plant Science*, 4.

Jouki, M. *et al.* (2014) 'Effect of quince seed mucilage edible films incorporated with oregano or thyme essential oil on shelf life extension of refrigerated rainbow trout fillets', *International Journal of Food Microbiology*. Elsevier B.V., 174, pp. 88–97.

Khaliq, R. *et al.* (2015) 'Industrial Application Of Psyllium: An Overview', *ACTA Universitatis Cibiniensis*, 67(1).

Klose, R. and Glicksman, M. (1972) 'Gums', in Furia, T. E. (ed.) *CRC handbook of food additives*. 2d ed. Cleveland, Ohio: CRC Press, pp. 295–359.

Kotwal, S. *et al.* (2013) 'Molecular markers unravel intraspecific and interspecific genetic variability in Plantago ovata and some of its wild allies', *Journal of Genetics*, 92(2), pp. 293–298.

Kotwal, S. *et al.* (2016) 'De Novo Transcriptome Analysis of Medicinally Important Plantago ovata Using RNA-Seq', *PloS one*, 11(3), p. e0150273. Available at: http://www.ncbi.nlm.nih.gov/pmc/articles/PMC4778938/pdf/pone.0150273.pdf.

Krokida, M. K., Maroulis, Z. B. and Saravacos, G. D. (2007) 'Rheological properties of fluid fruit and vegetable puree products', *International Journal of Food Properties*, 4(2), pp. 179–200.

Kumar, J. (2015) *Good agricultural practices for isabgol*. Report for the Directorate of Medicinal and Aromatic Plants.

Ladjevardi, Z. S., Gharibzahedi, S. M. T. and Mousavi, M. (2015) 'Development of a stable low-fat yogurt gel using functionality of psyllium (Plantago ovata Forsk) husk gum', *Carbohydrate Polymers*. Elsevier Ltd., 125, pp. 272–280.

Lal, R. K. *et al.* (2007) 'Plantago ovata plant named "Mayuri"'. USA: Google Patents. Available at: https://www.google.com/patents/USPP17505.

Lal, R. K., Sharma, J. R. and Misra, H. O. (1998) 'Development of a new variety Niharika of Isabgol (Plantago ovata)', *Journal of Medicinal and Aromatic Plant Sciences*, 20, pp. 421–422.

Landes, A. D. *et al.* (2008) 'Fecal Sand Clearance Is Enhanced with a Product Combining Probiotics, Prebiotics, and Psyllium in??Clinically Normal Horses', *Journal of Equine Veterinary Science*, 28(2), pp. 79–84.

Li, X. *et al.* (2019) 'Polymer gel with a flexible and highly ordered three-dimensional network synthesized via bond percolation', *Science Advances*, 5(12), pp. 1–8.

Loveys, B. *et al.* (2003) 'Thermal acclimation of leaf and root respiration : an investigation comparing inherently fast- and slow- growing plant species', *Global Change Biology*, pp. 895–910.

Mandal, K., Saravanan, R. and Maiti, S. (2008) 'Effect of different levels of N, P and K on downy mildew (Peronospora plantaginis) and seed yield of isabgol (Plantago ovata)', *Crop Protection*, 27(6), pp. 988–995.

Mariotti, M. *et al.* (2009) 'The role of corn starch, amaranth flour, pea isolate, and

Psyllium flour on the rheological properties and the ultrastructure of gluten-free doughs', *Food Research International*. Elsevier Ltd, 42(8), pp. 963–975.

Marlett, J. A., Kajs, T. M. and Fischer, M. H. (2000) 'An unfermented gel component of psyllium seed husk promotes laxation as a lubricant in humans', *American Journal of Clinical Nutrition*, 72(3), pp. 784–789.

Martin, C. and Smith, M. (1995) 'Starch Biosynthesis', *The Plant Cell*, 7(July), pp. 971–985.

Mehmood, M. H. *et al.* (2011) 'Pharmacological basis for the medicinal use of psyllium husk (Ispaghula) in constipation and diarrhea', *Digestive Diseases and Sciences*, 56(5), pp. 1460–1471.

Milani, J. and Maleki, G. (2012) 'Hydrocolloids in Food Industry', *Food Industrial Processes*, p. 418.

Minnesota Institute for Sustainable Transportation (2017) *Sustainable Paving Project*. Available at: http://www.strans.org/trailpave.html (Accessed: 8 May 2017).

Mitchell-Olds, T. and Schmitt, J. (2006) 'Genetic mechanisms and evolutionary significance of natural variation in Arabidopsis', *Nature*. Nature Publishing Group, 441(7096), pp. 947–952.

Mobin, M. and Rizvi, M. (2016) 'Polysaccharide from Plantago as a Green Corrosion Inhibitor for Carbon Steel in 1M HCl Solution', *Carbohydrate Polymers*. Elsevier Ltd., 160, pp. 172–183.

Mohammadi, H. *et al.* (2019) 'Nanocomposite films with CMC, okra mucilage, and ZnO nanoparticles: Extending the shelf-life of chicken breast meat', *Food Packaging and Shelf Life*. Elsevier, 21(May), p. 100330.

Mohnen, D. (2008) 'Pectin structure and biosynthesis', *Current Opinion in Plant Biology*, 11, pp. 266–277.

Moreaux, S. J. J. *et al.* (2011) 'Psyllium Lowers Blood Glucose and Insulin Concentrations in Horses', *Journal of Equine Veterinary Science*, 31, pp. 160–165.

Mudgil, D., Barak, S. and Khatkar, B. S. (2014) 'Guar gum: processing, properties

and food applications—A Review', *Journal of Food Science and Technology*, 51(3), pp. 409–418.

Najafi, F. and Rezvani, M. (2002) 'Effects of irrigation regimes and plant densities on yield and argonomic characteristics of isabgol (Plantago ovata)', *Agricultural Sciences and Technology*, 12(2), pp. 56–65.

Naran, R., Chen, G. and Carpita, N. C. (2008) 'Novel rhamnogalacturonan I and arabinoxylan polysaccharides of flax seed mucilage.', *Plant physiology*, 148(1), pp. 132–41.

Navarrete, S. *et al.* (2016) 'Bioactive compounds, aucubin and acteoside, in plantain (Plantago lanceolata L.) and their effect on in vitro rumen fermentation', *Animal Feed Science and Technology*. Elsevier B.V., 222, pp. 158–167.

North, H. M. *et al.* (2014) 'Understanding polysaccharide production and properties using seed coat mutants: future perspectives for the exploitation of natural variants', *Ann Bot*, 114(6), pp. 1251–1263.

Paul, F., Morin, A. and Monsan, P. (1986) 'Microbial polysaccharides with actual potential industrial applications', *Biotechnology Advances*, 4(2), pp. 245–259.

Pavlov, A. *et al.* (2014) 'Variability of seed traits and properties of soluble mucilages in lines of the flax genetic collection of Vavilov Institute', *Plant Physiology and Biochemistry*. Elsevier Masson SAS, 80, pp. 348–361.

Pawar, H. and Varkhade, C. (2014) 'Isolation, characterization and investigation of Plantago ovata husk polysaccharide as superdisintegrant', *International Journal of Biological Macromolecules*. Elsevier B.V., 69, pp. 52–58.

Phan, J. *et al.* (2016) 'Differences in glycosyltransferase family 61 accompany variation in seed coat mucilage composition in Plantago spp.', *Journal of Experimental Botany*, 67(22), pp. 6481–6495.

Phan, J. (2018) *Using Plantago ovata as a proxy to study plant cell wall polysaccharide biosynthesis*. The University of Adelaide.

Phan, J. and Burton, R. A. (2018) 'New Insights into the Composition and Structure

of Seed Mucilage', *Annual Plant Reviews Online*, 1, pp. 1–41.

Phillips, T. (2008) 'Genetically modified organisms (GMOs): Transgenic crops and recombinant DNA technology', *Nature Education*, 1(1), p. 213.

Prajapati, V. D. *et al.* (2013) 'Pharmaceutical applications of various natural gums, mucilages and their modified forms', *Carbohydrate Polymers*. Elsevier Ltd., 92(2), pp. 1685–1699.

Regand, A. and Goff, H. D. (2003) 'Structure and ice recrystallization in frozen stabilized ice cream model systems', *Food Hydrocolloids*, 17, pp. 95–102.

Ren, Y. *et al.* (2020) 'Temperature fractionation, physicochemical and rheological analysis of psyllium seed husk heteroxylan', *Food Hydrocolloids*. Elsevier Ltd, 104(February), p. e105737.

Rennie, E. A. and Scheller, H. V. (2014) 'Xylan biosynthesis', *Curr Opin Biotech*, 26, pp. 100–107.

Research and Markets (2017) *Global Gluten-Free Food Market 2017-2021*. Available at: https://www.researchandmarkets.com/reports/4115447/global-gluten-free-food-market-2017-2021#pos-0.

Rønsted, N. *et al.* (2002) 'Phylogenetic relationships within Plantago (Plantaginaceae): Evidence from nuclear ribosomal ITS and plastid trnL-F sequence data', *Botanical Journal of the Linnean Society*, 139(4), pp. 323–338.

Ruiter, G. A. De and Rudolph, B. (1997) 'Carrageenan biotechnology', *Trends in Food Science and Technology*, 8(December), pp. 389–395.

Saez-Aguayo, S. *et al.* (2014) 'Local Evolution of Seed Flotation in Arabidopsis', *PLoS Genet*. Public Library of Science, 10(3), p. e1004221.

Saghir, S. *et al.* (2008) 'Structure characterization and carboxymethylation of arabinoxylan isolated from Ispaghula (Plantago ovata) seed husk', *Carbohydrate Polymers*. Elsevier Ltd, 74(2), pp. 309–317.

Saha, D. and Bhattacharya, S. (2010) 'Hydrocolloids as thickening and gelling agents in food: A critical review', *Journal of Food Science and Technology*, 47(6), pp. 587–

597.

Samuelsen, A. B. *et al.* (1999) ‘Structural studies of a heteroxylan from Plantago major L. seeds by partial hydrolysis, HPAEC-PAD, methylation and GC-MS, ESMS and ESMS/MS’, *Carbohydrate Research*, 315(3–4), pp. 312–318.

Sarkar, S. *et al.* (2015) ‘Inter and intra-specific genetic differentiation for agro-economical traits in Plantago germplasm’, *Industrial Crops and Products*. Elsevier B.V., 74, pp. 183–191.

Sarkar, S. and Lal, R. K. (2015) ‘Genetic variability of agronomical and economical traits in Psyllium germplasm’, *Industrial Crops and Products*. Elsevier B.V., 65, pp. 515–520.

Sharma, P. K. and Koul, A. K. (1986) ‘Mucilage in seeds of Plantago ovata and its wild allies’, *J Ethnopharmacol*, 17(3), pp. 289–295.

Shewry, P. R. and Tatham, A. S. (1997) ‘Disulphide bonds in wheat gluten proteins’, *Journal of Cereal Science*, 25(3), pp. 207–227.

Shih, I. *et al.* (2009) ‘Production and characterization of curdlan by Agrobacterium sp.’, *Biochemical Engineering Journal*, 43, pp. 33–40.

Tay, M. L. (2008) *Evolution of Australasian Plantago (Plantaginaceae)*. Victoria University of Wellington.

Taylor, N. G. (2008) ‘Cellulose biosynthesis and deposition in higher plants’, *New Phytologist*. Blackwell Publishing Ltd, 178(2), pp. 239–252.

Thorburn, A. N. *et al.* (2015) ‘Evidence that asthma is a developmental origin disease influenced by maternal diet and bacterial metabolites’, *Nature Communications*, 6.

Tucker, M. R. *et al.* (2017) ‘Dissecting the Genetic Basis for Seed Coat Mucilage Heteroxylan Biosynthesis in Plantago ovata Using Gamma Irradiation and Infrared Spectroscopy’, *Frontiers in Plant Science*, 8, p. 326.

Wang, B. *et al.* (2011) ‘Effect of gum Arabic on stability of oil-in-water emulsion stabilized by flaxseed and soybean protein’, *Carbohydrate Polymers*. Elsevier Ltd., 86(1), pp. 343–351.

Wang, M. *et al.* (2015) 'Effects of the Timing of Herbivory on Plant Defense Induction and Insect Performance in Ribwort Plantain (Plantago lanceolata L.) Depend on Plant Mycorrhizal Status', *Journal of Chemical Ecology*, 41(11), pp. 1006–1017.

Wieser, H. (2007) 'Chemistry of gluten proteins', *Food Microbiology*, 24(2), pp. 115–119.

Wiesner, J. (2013) *Assessment report on Plantago ovata Forssk., seminis tegumentum*, *Assessment Reports by the Committee on Herbal Medicinal Products (HMPC)*. Edited by B. Merz. London: European Medicines Agency.

William, A., Alain, B. and Maarten, V. (2011) *The world wheat book: a history of wheat breeding*. Lavoisier.

Williams, M. *et al.* (2000) 'A Molecular Description of the Gelation Mechanism of Konjac Mannan', *Biomacromolecules*, 1(1), pp. 440–450.

Williams, P. and Phillips, G. (2003) 'Gums: Properties of Individual Gums', in *Encyclopedia of Food Sciences and Nutrition*, pp. 2992–3001.

Wolff, K., Friso, B. and Van Damme, J. M. M. (1988) 'Outcrossing rates and male sterility in natural populations of *Plantago coronopus*', *Theoretical Applied Genetics*, 76, pp. 190–196.

Wu, Y. *et al.* (2015) 'The rheological properties of tara gum (Caesalpinia spinosa)', *Food Chemistry*. Elsevier Ltd, 168, pp. 366–371.

Yin, J. Y. *et al.* (2010) 'Chemical characteristics and antioxidant activities of polysaccharide purified from the seeds of Plantago asiatica L', *Journal of the Science of Food and Agriculture*, 90(2), pp. 210–217.

Yu, L. *et al.* (2017) 'Multi-layer mucilage of Plantago ovata seeds: Rheological differences arise from variations in arabinoxylan side chains', *Carbohydrate Polymers*. Elsevier Ltd., 165, pp. 132–141.

Yu, L. *et al.* (2018) 'Rheological and structural properties of complex arabinoxylans from Plantago ovata seed mucilage under non-gelled conditions', *Carbohydrate Polymers*. Elsevier, 193, pp. 179–188.

Yu, L. *et al.* (2019) ‘Multi-scale assembly of hydrogels formed by highly branched arabinoxylans from Plantago ovata seed mucilage studied by USANS/SANS and rheology’, *Carbohydrate Polymers*. Elsevier, 207, pp. 333–342.

Zadoo, S. N. and Farooqi, M. I. H. (1977) ‘Performance of autotetraploid blond psyllium’, *Indian Journal of Horticulture*. The Horticultural Society of India, 34(3), pp. 294–300.

Zandonadi, R. P., Botelho, R. B. A. and Araújo, W. M. C. (2009) ‘Psyllium as a Substitute for Gluten in Bread’, *Journal of the American Dietetic Association*. Elsevier Inc., 109(10), pp. 1781–1784.

Zhang, H. *et al.* (2015) ‘Plant carbon limitation does not reduce nitrogen transfer from arbuscular mycorrhizal fungi to Plantago lanceolata’, *Plant and Soil*, 396(1–2), pp. 369–380.

Zhao, H. *et al.* (2014) ‘Purification, characterization and immunomodulatory effects of Plantago depressa polysaccharides’, *Carbohydrate Polymers*. Elsevier Ltd., 112, pp. 63–72.

Zhou, P. *et al.* (2020) ‘Comparative study between cold and hot water extracted polysaccharides from Plantago ovata seed husk by using rheological methods’, *Food Hydrocolloids*, 101, p. 105465.

Ziai, S. A. *et al.* (2005) ‘Psyllium decreased serum glucose and glycosylated hemoglobin significantly in diabetic outpatients’, *Journal of Ethnopharmacology*, 102(2), pp. 202–207.

CHAPTER 3

A small-scale pipeline for rapid analysis of seed mucilage characteristics

Statement of Authorship

Title of Paper	A small-scale fractionation pipeline for rapid analysis of seed mucilage characteristics
Publication Status	☑ Published ☐ Accepted for Publication ☐ Submitted for Publication ☐ Unpublished and Unsubmitted work written in manuscript style
Publication Details	Cowley, J.M., Herliana, L., Neumann, K.A. *et al.* A small-scale fractionation pipeline for rapid analysis of seed mucilage characteristics. *Plant Methods* **16,** 20 (2020). https://doi.org/10.1186/s13007-020-00569-6

Principal Author

Name of Principal Author (Candidate)	James M. Cowley		
Contribution to the Paper	Conceived the study, designed and tested the method, analysed data, wrote the manuscript		
Overall percentage (%)	75%		
Certification:	This paper reports on original research I conducted during the period of my Higher Degree by Research candidature and is not subject to any obligations or contractual agreements with a third party that would constrain its inclusion in this thesis. I am the primary author of this paper.		
Signature		Date	19/5/2020

Co-Author Contributions

By signing the Statement of Authorship, each author certifies that:

i. the candidate's stated contribution to the publication is accurate (as detailed above);

ii. permission is granted for the candidate in include the publication in the thesis; and

iii. the sum of all co-author contributions is equal to 100% less the candidate's stated contribution.

Name of Co-Author	Lina Herliana		
Contribution to the Paper	Designed and conducted the mutant screen experiment. Assisted with data analysis and manuscript preparation.		
Signature		Date	9/6/2020

Name of Co-Author	Kylie A. Neumann		
Contribution to the Paper	Collected and assisted in data analysis for field trial quality testing		
Signature		Date	19/5/2020

Please cut and paste additional co-author panels here as required.

Name of Co-Author	Silvano Ciani		
Contribution to the Paper	Provided field trial materials for testing		
Signature		Date	19/5/2020

Name of Co-Author	Virna Cerne		
Contribution to the Paper	Provided field trial materials for testing		
Signature		Date	19/5/2020

Name of Co-Author	Rachel A. Burton		
Contribution to the Paper	Conceived the study and contributed to writing the manuscript		
Signature		Date	19/5/2020

Name of Co-Author			
Contribution to the Paper			
Signature		Date	

Name of Co-Author			
Contribution to the Paper			
Signature		Date	

Name of Co-Author			
Contribution to the Paper			
Signature		Date	

JOURNAL: Plant Methods

PUBLISHED: 2020, **16:20** https://doi.org/10.1186/s13007-020-00569-6

TITLE: A small-scale fractionation pipeline for rapid analysis of seed mucilage characteristics

AUTHORS: James M. Cowley[1,2], Lina Herliana[2], Kylie A. Neumann[1,2], Silvano Ciani[3], Virna Cerne[3], and Rachel A. Burton[1,2*]

*Corresponding author: rachel.burton@adelaide.edu.au

AFFILIATIONS: [1]Australian Research Council Centre of Excellence in Plant Cell Walls, School of Agriculture, Food and Wine, University of Adelaide, Waite Campus, Urrbrae, SA, Australia; [2]Australian Research Council Centre of Excellence in Plant Energy Biology, School of Agriculture, Food and Wine, University of Adelaide, Waite Campus, Urrbrae, SA, Australia; [3]Dr. Schär R&D Centre, AREA Science Park, Padriciano 99, 34149 Trieste, Italy

ABBREVIATIONS:

CWE = cold water extractable
HWE = hot water extractable
IAE = intense agitation extractable
DI water = deionized water
RG-I = rhamnogalacturonan I
QC = quality control
TOS = time of sowing
A:X Ratio = arabinose to xylose ratio
AX = arabinose + xylose (estimated heteroxylan content)
WT = wild type

Abstract

Background: Myxospermy is a process by which the external surfaces of seeds of many plant species produce mucilage – a polysaccharide-rich gel with numerous fundamental research and industrial applications. Due to its functional properties the mucilage can be difficult to remove from the seed and established methods for mucilage extraction are often incomplete, time-consuming, and unnecessarily wasteful of precious seed stocks.

Results: Here we tested the efficacy of several established protocols for seed mucilage extraction and then downsized and adapted the most effective elements into a rapid, small-scale extraction and analysis pipeline. Within four hours, three chemically- and functionally-distinct mucilage fractions were obtained from myxospermous seeds. These fractions were used to study natural variation and demonstrate structure-function links, to screen for known mucilage quality markers in a field trial, and to identify research and industry-relevant lines from a large mutant population.

Conclusion: The use of this pipeline allows rapid analysis of mucilage characteristics from diverse myxospermous germplasm which can contribute to fundamental research into mucilage production and properties, quality testing for industrial manufacturing, and progressing breeding efforts in myxospermous crops.

Keywords: Mucilage, myxospermy, extraction, polysaccharide, *Plantago ovata,* flax, chia, psyllium.

Background

In a process called myxospermy, seeds of many plants produce viscous polysaccharide gels called mucilage when imbibed in water. The mucilage of *Arabidopsis thaliana* has often been used as a proxy for studying cell wall biosynthesis (1–8). More recently other myxospermous species like *Linum usitatissimum* and *Plantago ovata* have also been adopted as genetic models (9–14) revealing the utility that novel systems can have in unravelling complex synthetic pathways. Furthermore, these novel model systems have the added benefit of being directly commercially-relevant. *P. ovata* (psyllium) and *L. usitatissimum* (flaxseed) mucilage are used as gums with varied applications in the food and health industries. Both are used as natural food structuring ingredients and gluten replacements (15–18) and are rich sources of dietary fibre shown to prevent various gastrointestinal diseases (19–21). A comprehensive myxospermous model system would allow gene-structure-function links to be made but there remains a technical disconnect between these facets. The functional study of myxospermous species preceded their use as genetic models and the scale and precision of the extraction techniques have generally not been updated since. A significant number of researchers use the methods of Sharma and Koul (22), Balke and Diosady (23), or similar. These methods are simple, effective and robust, using a magnetic stirrer to heat and agitate a seed/water mixture followed by straining to isolate released mucilage from seeds. However, there are several technical issues that limit the use of these techniques in screening applications. Firstly, the techniques are not high-throughput, generally requiring 3–4 hours to process a single sample (per magnetic stirrer). Secondly, the quantity of mucilage produced is excessive for downstream chromatographic and yield analyses which require milligram-scale quantities or less. Thirdly, the techniques often offer incomplete extraction, leaving a significant amount of mucilage adhered to the seed. It is also important to note that

seed mucilage is not homogenous. Its multi-layered nature is evident simply by visual inspection of stained expanded mucilage in nearly all species (24). The dual-layered nature of *Arabidopsis thaliana* mucilage has been the basis of many studies on cell wall polysaccharide biosynthesis (25) and Yu *et al.* (26–28) have recently highlighted the importance of fractionating mucilage to effectively unravel structural differences that underlie polysaccharide functionality.

Here we describe a pipeline suitable for the rapid extraction and fractionation of quantities of seed mucilage suitable for yield and chromatographic analyses. Within four hours, three chemically- and functionally-distinct fractions can be isolated from 24 samples per shaking incubator and the use of a shaking incubator allows adjustment in time, temperature and fractionation profile. The utility of this pipeline is demonstrated through its ability to: identify intergeneric and interspecific variation in seed mucilage extractability, yield and composition, screen for known quality parameters in field-grown myxospermous samples, and identify lines of interest from germplasm collections.

Methods

Materials

Arabidopsis thaliana seeds (ecotype *Columbia-0*) were grown as per Tucker *et al.,* (29). Flax (*Linum usitatissimum*) and chia (*Salvia hispanica*) seeds were purchased from Woolworths (Frewville, South Australia). *Plantago ovata* and *Plantago cunninghamii* seeds were obtained and bulked from sources listed in Phan *et al.,* (30). *P*. *ovata* varieties were grown in field trials conducted in 2017 and 2018 in Kununurra, Western Australia. Gamma-irradiated *P. ovata* mutants used for germplasm screening were obtained from a glasshouse-grown population described previously (10).

Once harvested or purchased, all seeds were dried at 37 °C for at least 72 hours and then stored in sealed containers at room temperature until analysis.

Reagents and Solutions

Ruthenium red hydrate (#C075) was purchased from ProSciTech, Australia and the staining solution was prepared at 0.01% w/v in water following Arsovski *et al.,* (5). To prevent bubble formation on the seed surfaces during imaging, the staining solution was sonicated for 5 min under vacuum to remove dissolved gases. KOH and HCl (Sigma-Aldrich) were made to a 0.2 M solution in water.

Mucilage staining

Expanded seed mucilage was observed *in situ* following Arsovski *et al.,* (5) to compare and validate extraction techniques. After positioning seeds on a microscope slide (Rowe GM2715, Australia) staining solution was added beneath a coverglass (ProSciTech No. 1, Australia) and images were captured on a dissecting microscope (Zeiss Stemi 2000-C, Germany) equipped with a colour digital camera (Zeiss AxioCam ERc 5s, Germany).

Conventional seed mucilage extraction techniques

The effectiveness of total mucilage extraction by the fractionation pipeline described here was validated against previously published methods by Balke and Diosady (23), Yu *et al.*, (26), Sharma and Koul, (22), and Voiniciuc *et al.* (4) . Balke and Diosady's method (also used previously by our group, Phan *et al.,* 2016) is simple, stirring seeds and water heated to 80 °C on a magnetic stirrer for 90 minutes after which the liberated mucilage is strained through nylon mesh to remove seeds. Yu *et al.*'s method uses an extended extraction (4 hr) with RT 0.2 M solution of KOH. Sharma and Koul's method combines seeds with dilute acid (0.2 M HCl) in a conical flask, which is stirred on a heated magnetic stirrer until the seeds have changed colour (20 minutes). Seeds are

strained through nylon mesh and washed twice with hot water. Finally, Voiniciuc's method uses the physical force (30 Hz for 30 min) of a tissue disruptor-type mixer mill.

Rapid small-scale mucilage fractionation pipeline

The rapid small scale fractionation of quantities of seed mucilage suitable for yield and chromatographic analyses was achieved using the following protocol incorporating elements of methods by Yu *et al.,* 2017 and Voiniciuc *et al.* 2015. For similarly sized seeds, seeds can be counted or for variably sized seeds 30 mg (+/- 0.5 mg) of seeds (exact mass recorded) can be weighed. Once the pre-extraction mass was recorded, seeds were added to a 2 mL microcentrifuge tube followed by 1.5 mL of RT DI H_2O (Figure 3.1A). Tubes were vortexed briefly to break surface tension and ensure all seeds are immersed. To obtain the first mucilage fraction (Figure 3.1B), tubes were incubated for 1.5 hr at 25 °C in a shaking incubator (Eppendorf ThermoMixer® Comfort, Germany) with agitation at 1300 rpm then centrifuged (Eppendorf 5424, Germany) for 2 min at 13,000 rpm. Ensuring that the pelleted adherent mucilage and seeds are not disturbed, the tubes were removed from the centrifuge and using a 1000 µL laboratory pipette, the supernatant—the cold water extractable (CWE) mucilage fraction—was transferred to a clean, pre-labelled microcentrifuge tube. This transfer may require multiple steps based on the volume of the supernatant. The volume of the tube contents comprising the pelleted mucilage and seeds was returned to approximately 1.5 mL with RT DI H_2O based on the tube markings (different samples may require slightly different volumes). To obtain the next mucilage fraction (Figure 3.1C), a similar process was employed but at a warmer temperature: tubes were incubated for 1.5 hr at 65 °C with agitation at 1300 rpm then centrifuged for 2 min at 13,000 rpm. Again the supernatant—the hot water extractable (HWE) mucilage fraction—was transferred to a clean, pre-labelled microcentrifuge tube using a 1000 µL laboratory pipette. After removal of the HWE fraction, the volume of the pellet is

significantly reduced as only the most extraction-resistant mucilage remains tightly adhered to the seed. After adjusting the volume of tube contents to approximately 1.5 mL with RT DI H_2O, the tubes were agitated intensely at 30 Hz for 10 min on a tissue disruptor-type mixer mill (Retsch MM400, Germany) using a microcentrifuge tube adapter (Figure 3.1D). Tubes were centrifuged for 2 min at 13,000 rpm and the supernatant—the intense agitation extractable (IAE) mucilage fraction—was transferred to a clean, pre-labelled microcentrifuge tube using a 1000 µL laboratory pipette.

From each sample, a cold water extractable (CWE), hot water extractable (HWE) and intense extraction resistant (IAE) fraction of seed mucilage has been obtained along with the corresponding demucilaged seeds (DMS) (Figure 3.1E). These four fractions were frozen at -80 °C for 24 hr and then freeze-dried (Labconco Freezone 6, US) to a constant weight. Freeze-dried mucilage and demucilaged seeds were transferred to a microbalance with 0.01 mg resolution (Shimadzu AUW220D, Japan) with fine-tip tweezers to calculate mucilage yield (Figure 3.1F).

Yield of mucilage fractions can be calculated using the following equation:

$$\text{Yield } (\%) = \left(\frac{\text{mass of freeze dried mucilage}}{\text{mass of seeds pre-extraction}}\right) \times 100$$

Optional - isolated fractions may be pipetted into a 2000 µL 96 well deep well plate (Eppendorf, Germany) in place of new microcentrifuge tubes which can become unwieldy when dealing with large sample numbers. The deep well plates can accommodate many samples and several plates will fit simultaneously into a freeze-drier unit for bulk processing.

Monosaccharide profiles of fractionated seed mucilage

Freeze-dried mucilage was dispersed in water at 2 mg/mL (w/v) and an 800 µL aliquot was added to 200 µL of 5M H_2SO_4 (final H_2SO_4 concentration of 1M) and hydrolysed at 100 °C for 3 hr as per Phan *et al.* (30). Monosaccharides released by acid hydrolysis were derivatised with 1-phenyl-3-methyl-5-pyrazoline (PMP) and then separated by reversed phase high performance liquid chromatography (RP-HPLC) following Comino *et al.* (31) with modifications to the column and eluents listed in Hassan *et al.* (32). Area under the peaks was compared to standard curves of mannose, ribose, rhamnose, glucuronic acid, galacturonic acid, glucose, galactose, xylose, arabinose and fucose (33).

Water absorption assay

After weighing 20 seeds into a 2 mL microcentrifuge tube, 1 g of water was added, and mucilage was allowed to expand undisturbed for 45 min at 25 °C. Using a 1 mL syringe without a needle, unabsorbed water was removed and weighed. Water absorption capacity can be calculated using the equation:

$$\text{Water absorption capacity (g/g)} = \frac{\text{Initial weight of water added - weight of unabsorbed water}}{\text{Initial weight of seeds added}}$$

Results and discussion

This protocol achieves total mucilage extraction

Figure 3.2 shows *P. ovata* seed with stained expanded seed mucilage before and after four methods of mucilage extraction. While hot water was effective at reducing the size of the mucilage envelope (Figure 3.2B), mucilage in the inner layer is more densely packed than the removed soluble fraction and thus a large amount of the mucilage remains (34). Yu *et al.* (26) reported that an extended (4 hr) extraction with 0.2 M KOH, a chaotropic agent, was sufficient to remove the adherent mucilage layer by disrupting hydrogen bonds in the mucilage. We confirm that this treatment is effective at removing

the majority of seed mucilage (Figure 3.2C) although the most strongly adherent portion remained on all treated seeds (n = 30). Mucilage removal in acid was similarly effective (Figure 3.2D), however the mode of action of the acid was to hydrolyse the mucilage *in situ* which is not useful if any downstream functional or linkage analyses are required. An appealing alternative was the non-chemical extraction method devised by Voiniciuc *et al.* (4) who were able to efficiently extract all adherent mucilage from *Arabidopsis* seeds using intense agitation on a tissue disruptor-type mixer mill. The physical force of the shaking was sufficient to disrupt the mucilage-seed attachment and disperse the polysaccharides. We corroborate the efficacy of this method on *P. ovata* where close to 100% of seed mucilage was removed (Figure 3.2E). We also observed that mucilage staining of seeds that sequentially underwent a hot water extraction before 0.2 M KOH, 0.2 M HCl or 30 Hz agitation were no different to those that were not extracted with hot water as a first step (data not shown).

The monosaccharide profiling of fractionated *P. ovata* mucilage shows that our small-scale fractionation technique is directly comparable to the larger scale technique published by Yu *et al.* (26), the original study by Guo *et al.* (35) on which their work is based and a similar work published earlier by Marlett & Fischer (36) (Supplementary Table S3.1).

The extraction pipeline effectively provides material for identifying variation in seed mucilage characteristics

Figure 3.3 shows the appearance of the expanded seed mucilage envelope of *A. thaliana* (a–d), *L. usitatissimum* (flaxseed) (e–h), *S. hispanica* (chia) (i–l), *P. ovata* (psyllium) (m–p) and an Australian native relative of psyllium, *P. cunninghamii* (q–t) before and after each mucilage fractionation step in the pipeline described here, which culminates in total extraction (Figure 3.4A). After CWE and HWE extraction, the mucilage envelope of *L. usitatissimum* and *A. thaliana* is significantly reduced in size

compared to *S. hispanica*, *P. ovata* and *P. cunninghamii*. These changes were reflected in the differences between the ratios of extracted fractions (Figure 3.4B), where *L. usitatissimum* and *A. thaliana* were most susceptible to extraction, yielding the largest proportion of water extractable (CWE + HWE) components. The easy removal of the delicate outer layer of mucilage in *A. thaliana* and *L. usitatissimum* is consistent with previous findings and established fractionation techniques (4,34,37–40). Contrastingly, *Plantago* and *S. hispanica* mucilage has been reported to require more effort to efficiently extract total mucilage. For *S. hispanica*, mucilage extraction in cold water is not efficient (41) while extended hot water extractions yield only slightly greater quantities (42–44). We corroborate these findings, reporting that only half of the mucilage is extractable by hot water (Figure 3.4B). Efficient mucilage extraction from *Plantago* species is also difficult, often requiring multiple physical and/or chemical extraction steps (26,35,36,45,46). While total yields of mucilage between *P. ovata* and *P. cunninghamii* were similar (Figure 3.4A), there are clear interspecific differences in the relative proportion of each fraction (Figure 3.4B). Changes in appearance of the mucilage envelope of *P. ovata* after CWE were more noticeable than for *P. cunninghamii,* which appears relatively unchanged and is reflected in CWE yield which was lower for *P. cunninghamii.* Yield of HWE mucilage was greater for *P. cunninghamii,* with less IAE mucilage than *P. ovata.*

Some, if not all, of the differences in the relative proportion of each mucilage fraction of the species studied can be ascribed to mucilage polysaccharide composition and the associated difference in properties. Monosaccharide analysis confirmed significant differences in mucilage composition between genera and species and their isolated mucilage fractions (Figure 3.4C). Monosaccharide analysis also confirmed previous findings that mucilage fractions from *A. thaliana* and *L. usitatissimum* are rich in rhamnose and galacturonic acid (4,47–50), components of pectin, a highly water-

soluble polysaccharide, the presence of which may contribute to overall ease of extraction in these species. It is the presence of minor mucilage components in the HWE and IAE fractions that are known to affect the mucilage properties including fractionality. In *A. thaliana*, monosaccharide profiling of the HWE and IAE fractions (containing the adherent mucilage) confirms previous findings of a molar reduction in rhamnose and galacturonic acid residues and an increase in non-cellulosic glucose, mannose, galactose and xylose (49,50), components of minor polysaccharides like xylan and glucomannan that are well-known to interact with and tether the adherent mucilage at the seed surface (4,7,51–53). Similarly, rhamnose and galacturonic acid residues were reduced in the HWE and IAE fractions of *L. usitatissimum*, along with increases in xylose and arabinose residues associated with heteroxylan, known to significantly alter the functional properties of RG-I (47). In *P. ovata and P. cunninghamii,* the three mucilage fractions contained high levels of xylose and arabinose (heteroxylan) with a smaller amount of rhamnose and galacturonic acid (pectin), congruent with previous findings by Phan *et al.* (30). Like both *A. thaliana* and *L. usitatissimum,* pectin-associated monosaccharides are enriched in the CWE fractionation and diminish with further fractions. While the presence of pectin has been proposed to modulate the extractability of the major heteroxylan component in *Plantago* mucilage, studies have shown that heteroxylan branching has the most significant influence on the mucilage properties including the extractability (26–28). In both *P. ovata* and *P. cunninghamii,* the ratio of arabinose to xylose residues (estimation of the degree of sidechain branching) increased with resistance to extraction, in line with those studies. However, more explicit structural characterisation will be needed to define the fine structure and its relationship to interspecific differences in extractability. The mucilage of *S. hispanica* is unique among the species studied in that its constituent polysaccharide(s) have not been found in any other genera (54). Its unique structure

containing xylose, glucose and glucuronic acid residues is consistent with the monosaccharide data (Figure 3.4C), although the molar ratios between the constituents varies by fraction suggesting that fine structure and/or interactions with minor components (from which the other monosaccharides detected are derived) influences the extractability.

The pipeline has utility in quality testing of mucilaginous species

The production of high-quality psyllium gum from *P. ovata* seeds is hampered by agronomic issues which cause poor quality, damaged seeds (55). Damaged seed coat allows leakage of endosperm components during extraction which alter the functional properties and cause significant discolouration due to phenolic browning which is undesirable in many applications (Cowley *et al.* unpublished data). As the functional component of psyllium gum, heteroxylan must be abundant and present at a consistent level to be considered good quality for industrial uses as the dilution of heteroxylan by the presence of contaminants will impact the functionality in optimised formulations. Four varieties of *P. ovata* were grown in three separate field trials with different times of sowing, a factor which, due to climatic conditions, was found to significantly affect seed quality (55,56). A suite of quality parameters is shown in Figure 3.5. Visual inspection was used to determine a baseline quality score for the four varieties at each trial (Figure 3.5A). Trial 2017a had the lowest damage score followed by 2017b and then 2017c. 2017c was deemed the poorest quality with consistently high seed damage. When mucilage was extracted using our pipeline, there were clear differences in yield, with the strongest effect related to time of sowing with only minor intervarietal influence (Figure 3.5B). Varieties grown at 2017b did not differ greatly in yield from the control, which was a high-quality field grown sample (QC). Conversely, varieties from 2017a and 2017c had higher mass yields after extraction. Monosaccharide profiling showed that mucilage synthesis was not disrupted as the arabinose to xylose (AX)

ratio was very similar between varieties and trials and not significantly different from the QC (Figure 3.5D). However, the quantity of heteroxylan in the mucilage (defined as total AX) differed between trials (Figure 3.5C). 2017b, confirmed as the most successful sample, had the highest proportion of AX and was closest to the QC. Correspondingly, 2017a and 2017c had lower proportions of AX indicating significant contamination from other components. Total AX is thereby inversely proportional to yield as a direct result of quality. No variety at any trial had AX as high as the QC, likely because seed of the QC sample was of exceptional quality.

Furthermore, known chemical markers have been defined indicating low quality or damaged seed. As one example, extreme damage of *P. ovata* seeds causes extensive leakage of endosperm components including mannose monosaccharides (Cowley *et al.* unpublished data). Trial 2017a was impacted by devastating unseasonable rainfall which physically damaged seed before harvesting (Figure 3.5E) and subsequently led to microbial growth, leading to detectable quantities of mannose in the extracted mucilage (Figure 3.5G). Mannose was found only in trace amounts in corresponding 2018 samples which were not weather damaged or microbially contaminated and more consistently high quality (Figure 3.5F).

The pipeline can be used for rapid screening of myxospermous germplasm

This pipeline has utility for rapid screening of mucilage yield traits in a germplasm set, demonstrated here using gamma-irradiated *P. ovata* mutants generated in a previous study (10). Total mucilage yield data (a pooling of CWE, HWE and IAE fractions) was obtained for a subset of 206 randomly-selected glasshouse-grown *P. ovata* mutants (Figure 3.6A). In 63% of mutants, mucilage yield was within a ±10% interval of WT yield (n = 131). Only 4% of mutants yielded 10% less mucilage than WT (n = 8), while 33% yielded over 10% more (n = 68). To validate this screen, a subset of the three lowest yielding (252-7, 768-9, and 1064-5) and three highest (743-4, 1072-12, and

776-5) mutants were selected for further analysis. Expanded mucilage architecture has been used previously to visually screen for altered mucilage phenotypes in mutants of *Arabidopsis* (4,57,58) and *Plantago* (10). Here we show variation in expanded mucilage architecture between the mutants (Figure 3.6B) where some are distinctly different to WT (252-7, 1064-5, 743-4, and 776-5) while others are WT-like (768-9 and 1072-12). The utility of the pipeline is proven two-fold in that it can identify highly-distinctive mutants which would be identified through typical visual screening techniques (like ruthenium red staining) but also mutants with more subtle changes to yield that may appear as WT. The validation set of mutant lines was subjected to further analysis which confirmed the differences observed in total mucilage yield were statistically significant compared to the WT. Differences observed in the size of the ruthenium red-stained mucilage envelopes and the amount of mucilage extracted may be linked to alterations in polysaccharide macromolecular properties. This was examined further by comparing the relative proportion of the three mucilage fractions (Figure 3.6D) with the water absorption capacity of the mucilage (Figure 3.6E).

While the total yield of mucilage was significantly decreased from WT in mutant 768-9, the ruthenium red phenotype, the ratio of mucilage fractions and the water absorption capacity were not significantly different from the WT. Contrastingly, the ratio of the three mucilage fractions was significantly altered in mutants 252-7, 1064-5, and 743-4 (*mucilage extractable with water* (*mew*) mutants) where the CWE and HWE fractions comprise most or all of the mucilage and the IAE fraction is significantly diminished or totally absent. In *mew* mutants, water absorption capacity is significantly reduced from the WT presumably due to a reduction in the stronger gelling, high water-holding capacity IAE mucilage fractions (26). The striking similarities in the phenotypes of the *mew* mutants suggests that they may contain mutant alleles. Importantly, *mew* mutant 252-7 has already been identified as a putative reduced mucilage xylan mutant

(10) and the characterisation of this class of mutant is ongoing (11). Mutant 776-5 represents a previously unseen class of *P. ovata* mucilage mutant (10,11,59). While this mutant has the highest total mucilage yield in the screened population, its water absorption capacity was unchanged from WT. Its unique compact ruthenium red phenotype and shift in the ratio of the three mucilage fractions suggests intrinsically different changes to the mucilage composition, with a novel causative mutation(s) compared to the *mew* mutants. The ease of distinguishing the *mew* mutants and mutant 776-5 within the mutant population shows that the pipeline can effectively identify putative mutants with perturbed seed development and/or mucilage synthesis, ideal for forward genetic studies.

In contrast to the *mew* mutants and mutant 776-5, it was found that while the ruthenium red and mucilage fractionation phenotype of mutant 1072-12 did not differ substantially from the WT, the total yield and related water absorption capacity was significantly increased. Mutant 1071-12 may therefore represent an important genotype for use in pre-breeding efforts due to its high mucilage yield without the aberrant changes to mucilage composition and properties which makes other mutants less suitable.

Conclusions

In this study we tested the efficacy of several established protocols for seed mucilage extraction and downsized and adapted the most effective elements into a small-scale, rapid extraction and analysis pipeline. We demonstrated the utility of this pipeline for investigating intergeneric and interspecific differences in seed mucilage characteristics, as well as for quality testing and germplasm screening of myxospermous plants. This pipeline is already regularly used in our research group increasing the analysis efficiency of a range of myxospermous species. It has also been adopted by a leading food manufacturer who relies on consistently high-quality

mucilage products. The use of this pipeline in fundamental research may improve our understanding of mucilage production and properties, ensure quality in food manufacturing, and aid in pre-breeding or breeding of myxospermous species—often classified as orphan crops—that could benefit from improved characterisation methods.

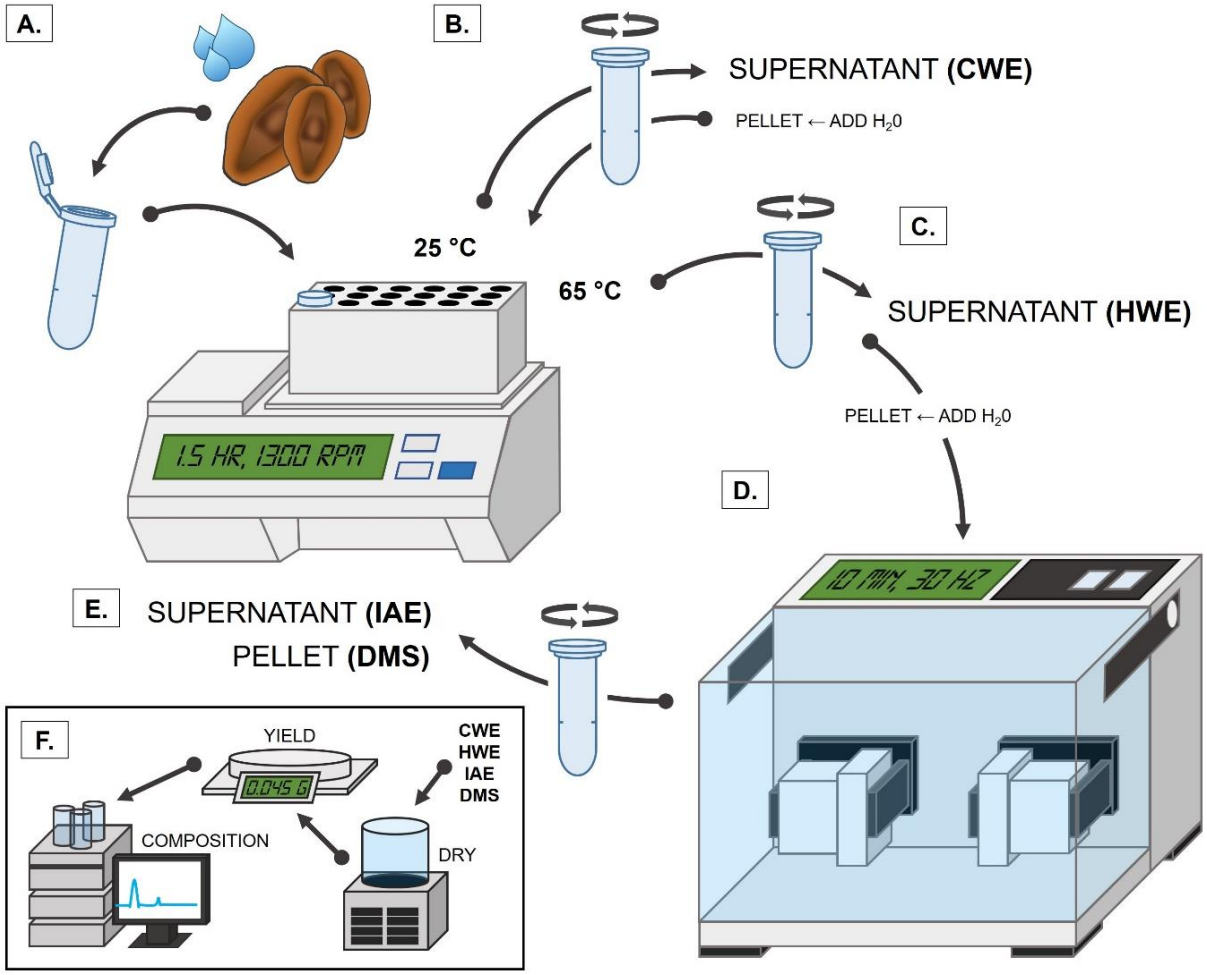

Figure 3.1. Schematic representation of pipeline used to extract small quantities of seed mucilage in discrete fractions for yield and chromatographic analysis. **(A)** Seeds and water are added to a microcentrifuge tube and incubated in a thermomixer-type shaking incubator at 25 °C for 1.5 hr with agitation. **(B)** After centrifugation, the cold water extractable (CWE) mucilage is removed and water is added to the pellet to restore the working volume. **(C)** The sample is incubated at 65 °C for 1.5 hr with agitation and after centrifugation the hot water extractable (HWE) mucilage is removed. Water is added to the pellet to restore the working volume. **(D)** Intense agitation by a mixer mill-type tissue disrupter is used to disrupt the seed-mucilage attachment. **(E)** After centrifugation, the intense agitation extractable (IAE) mucilage is removed. The pellet contains the demucilaged seeds (DMS). **F.** All fractions can be freeze-dried for yield and chromatographic analysis.

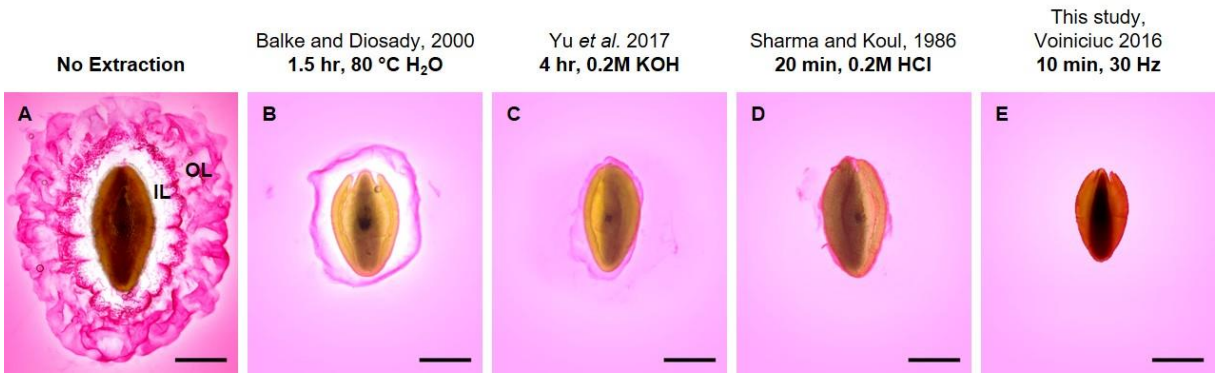

Figure 3.2. Seed mucilage that remains attached to *P. ovata* seeds after the application of various published extraction protocols and staining with 0.1% w/v ruthenium red. **(A)** The characteristic mucilage architecture of *P. ovata* seed mucilage. **(B)** After extended extraction in hot water the fine structure of the outer layer (OL) of mucilage has been lost leaving an inner adherent layer (IL). **(C)** The use of a chaotropic agent, KOH, significantly reduces the size of the mucilage envelope leaving only a film of mucilage that is resistant to chemical extraction. **(E)** Mucilage has been hydrolysed *in situ* and only a thin feathery layer remains. **(E)** Extraction by intense agitation leads to total mucilage removal.

Scale = 1 mm

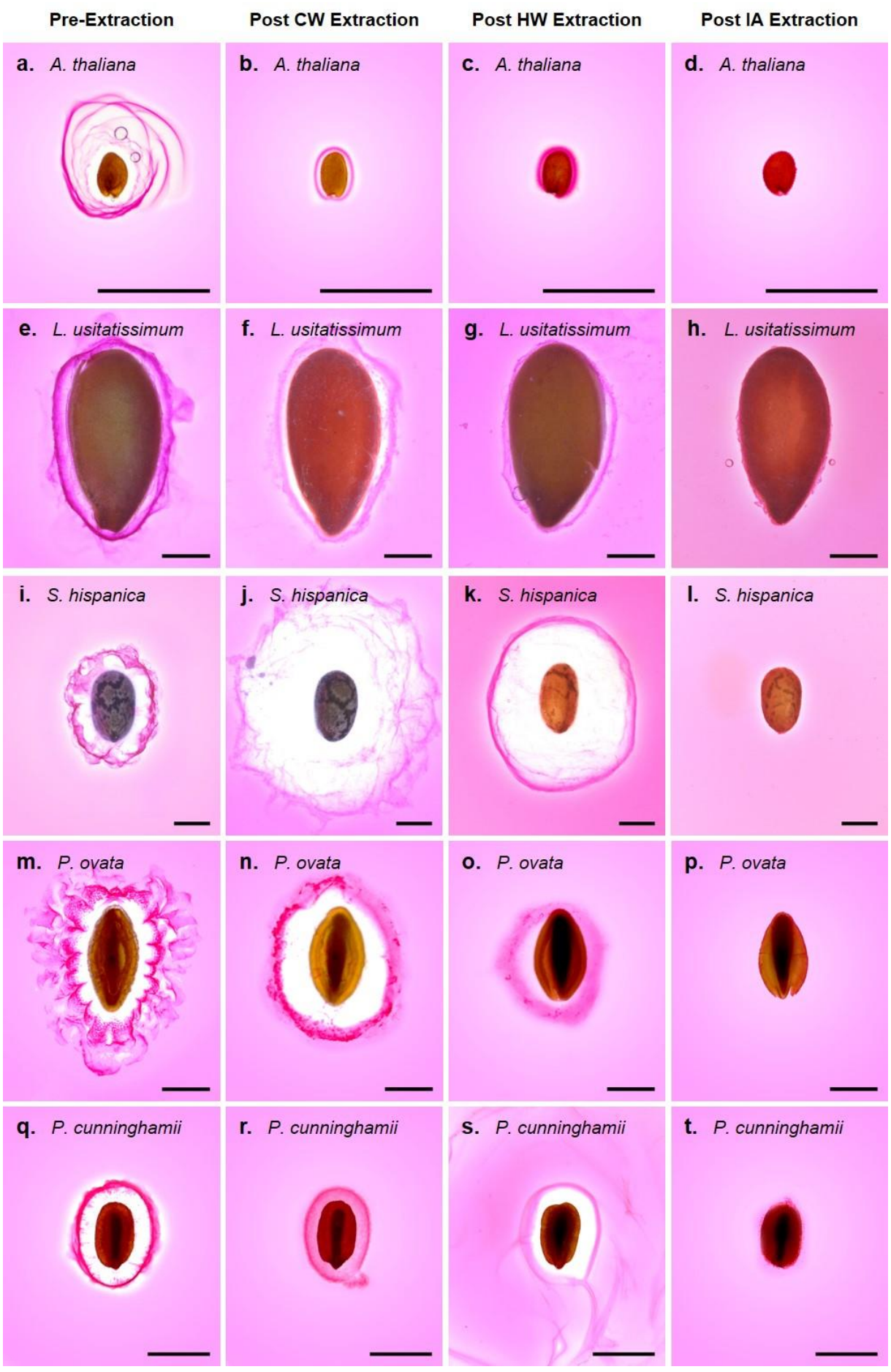
Pre-Extraction
Post CW Extraction
Post HW Extraction
Post IA Extraction
a. A. thaliana
b. A. thaliana
c. A. thaliana
d. A. thaliana
e. L. usitatissimum
f. L. usitatissimum
g. L. usitatissimum
h. L. usitatissimum
i. S. hispanica
j. S. hispanica
k. S. hispanica
l. S. hispanica
m. P. ovata
n. P. ovata
o. P. ovata
p. P. ovata
q. P. cunninghamii
r. P. cunninghamii
s. P. cunninghamii
t. P. cunninghamii

Figure 3.3. Visual inspection of the ruthenium red-stained seed mucilage of five myxospermous species (*Arabidopsis thaliana, Linum usitatissimum, Salvia hispanica, Plantago ovata* and *Plantago cunninghamii*) after sequential fractionation shows that the size of the mucilage envelope is sequentially changed corresponding to removal/dispersion of constituent polysaccharides. Note that images are not taken of the same seed as each seed was disposed of after imaging. Scale = 1 mm

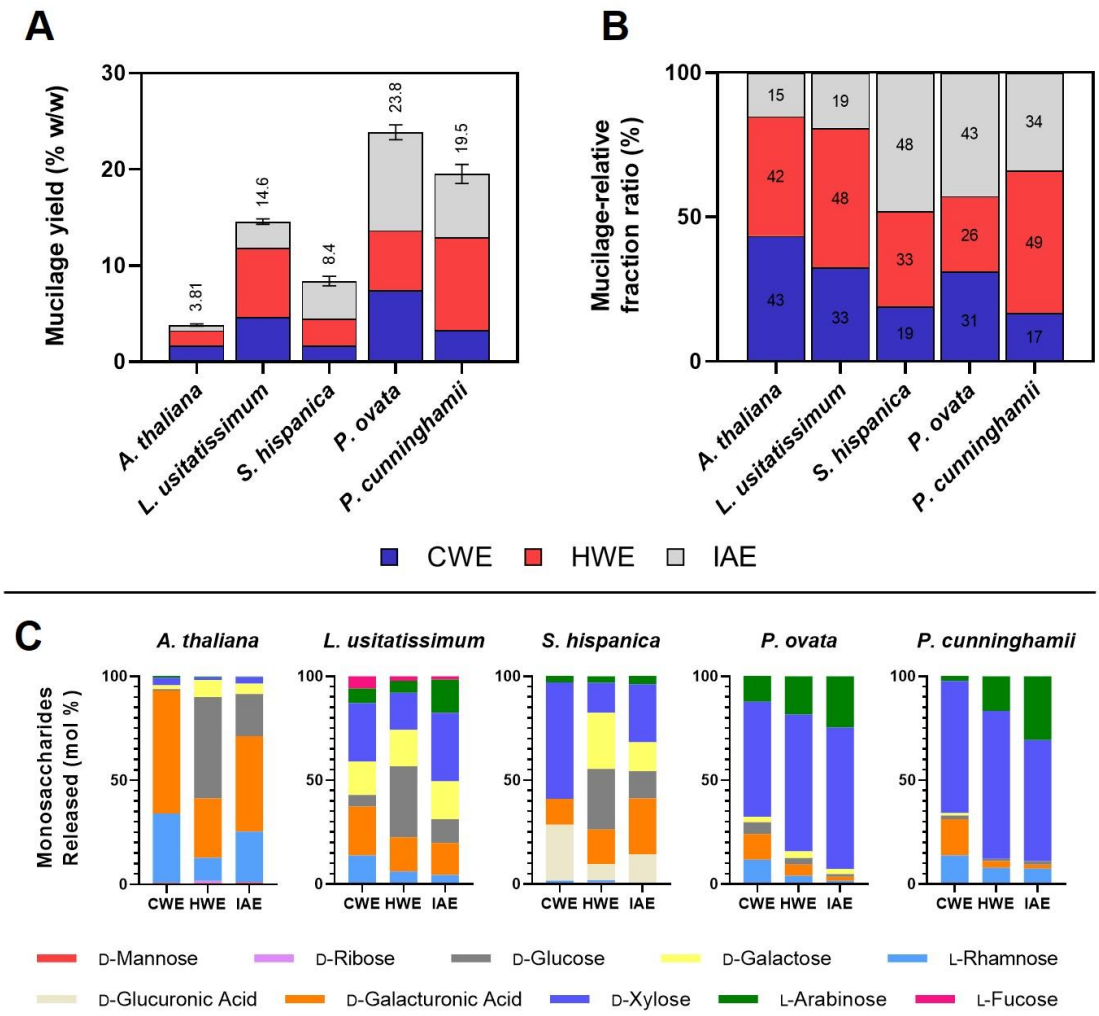

Figure 3.4. The extraction pipeline is effective at providing material suitable for identifying significant intergeneric and interspecific variation in seed mucilage yield, fractionation profile and composition. **(A)** Yield of total seed mucilage divided into constituent fractions. Error bars refer to standard deviation in total mucilage yield of five biological replicates. **(B)** Extractability of seed mucilage represented as the share of each fraction within total extracted mucilage. **(C)** Monosaccharide analysis of fractionated mucilage showing intergeneric, interspecific and intraspecific differences in mucilage chemical composition. Values presented are in molar ratio of quantified monosaccharides released by acid hydrolysis.

Abbreviations: CWE = cold water extractable; HWE = hot water extractable; IAE = intense agitation extractable.

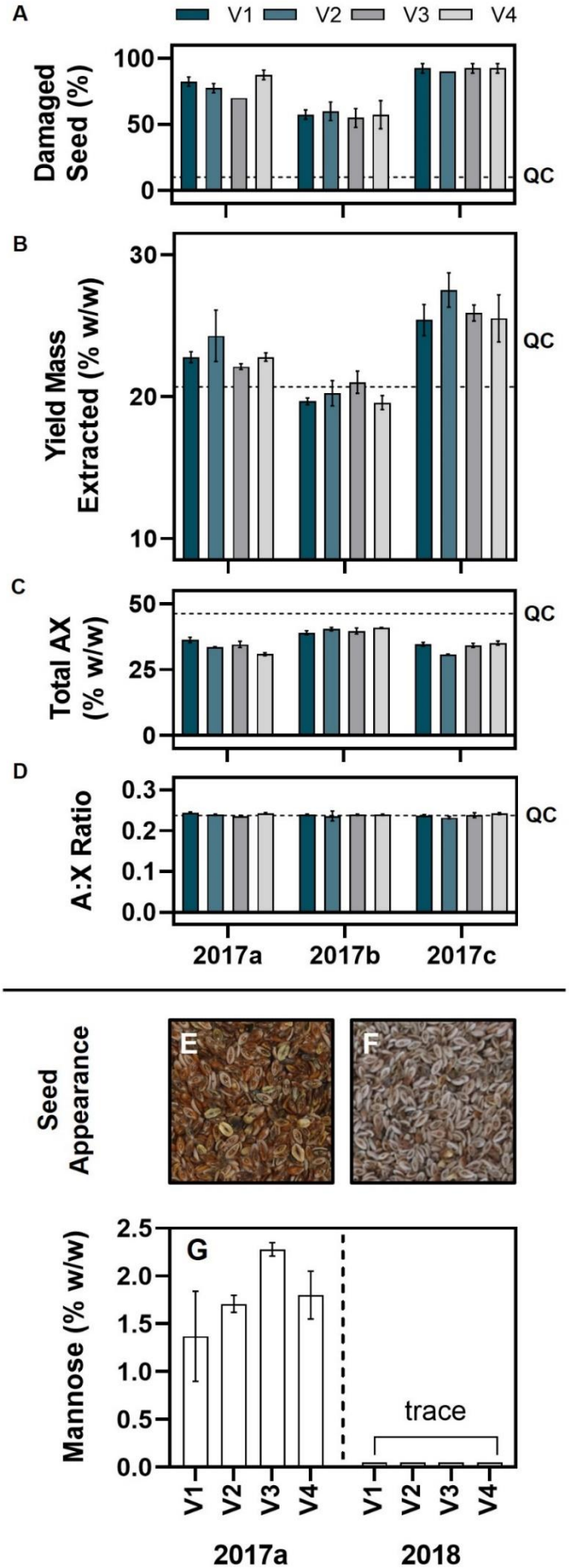
A
V1
V2
V3
V4
Damaged Seed (%)
100
50
0
QC
B
Yield Mass Extracted (% w/w)
30
20
10
QC
C
Total AX (% w/w)
50
25
0
QC
D
A:X Ratio
0.3
0.2
0.1
0.0
QC
2017a
2017b
2017c
Seed Appearance
E
F
Mannose (% w/w)
G
2.5
2.0
1.5
1.0
0.5
0.0
trace
V1
V2
V3
V4
V1
V2
V3
V4
2017a
2018

Figure 3.5. In field-grown samples of *Plantago ovata*, the extraction pipeline has utility in quality testing when coupled with yield and chromatographic analysis. **(A)** Visual inspection of damaged seed provides a baseline quality score. **(B)** Yield of total mucilage varied most significantly between times of sowing with a minor intervarietal effect. **(C)** Heteroxylan content (the proportion of arabinose and xylose residues in extracted mucilage) inversely related to mucilage yield and seed quality. **(D)** The ratio of arabinose to xylose residues in extracted mucilage (an approximation of heteroxylan branching) remains unchanged indicating that seed and mucilage development were unperturbed. **(E)** Seed grown at trial sites in 2017 is unevenly coloured, with many blackened seeds while **(F)** seeds grown at the same site in 2018 are more consistent, with the light-coloured husk material consistently visible on seeds. **(G)** In the 2017 field trials (analysed are samples from 2017a), significant quantities of mannose were identified by monosaccharide analysis in extracted mucilage of each variety grown indicative of seed damage-related endosperm leakage. Contrastingly, only trace amounts (well below the limit of quantitation) were found in the same varieties grown in the following year, 2018.

Dotted line in B, C, and D indicates the value of a quality control sample (QC). Error bars represent one standard deviation (some are small and not easily visible).

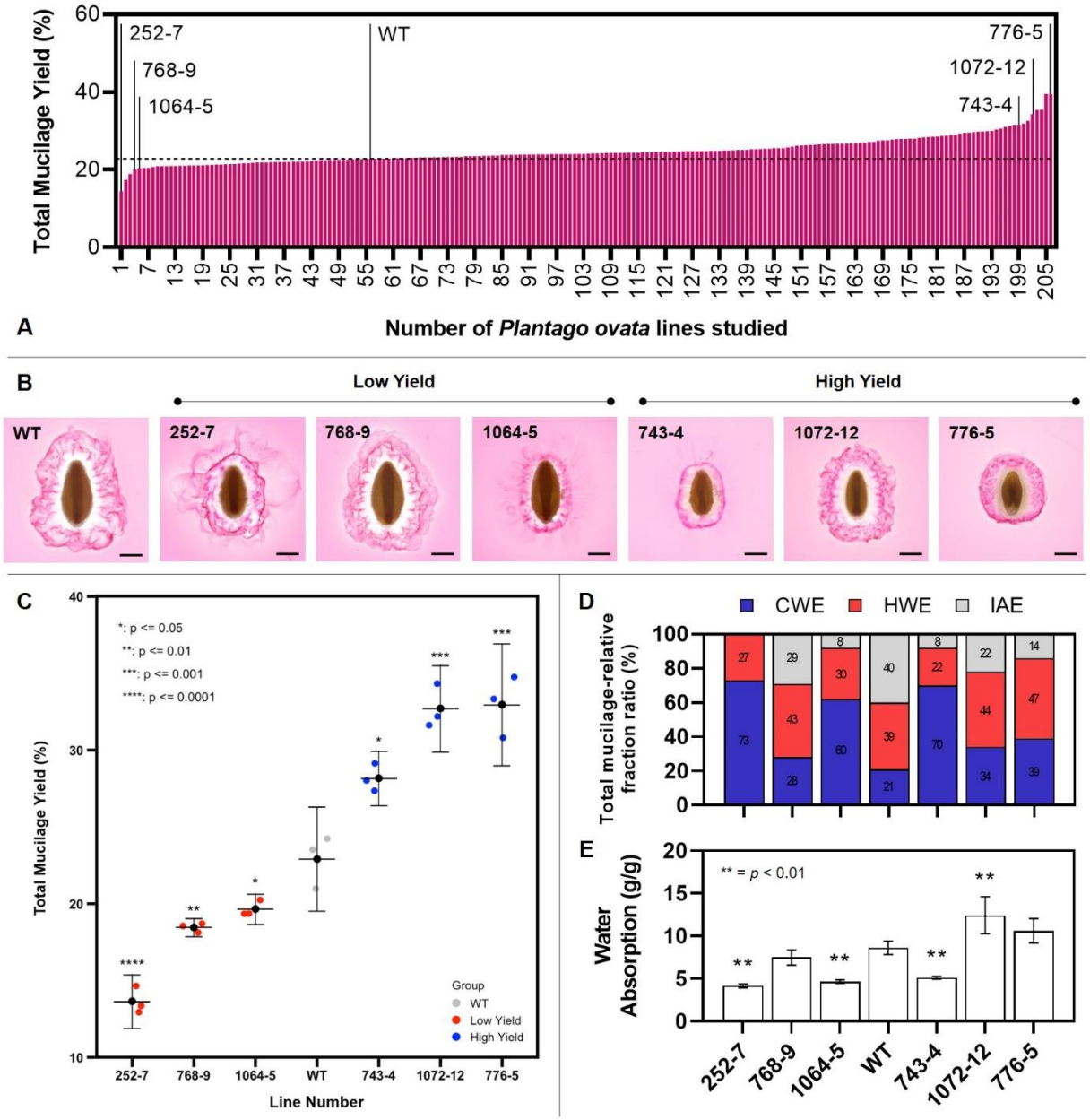

Figure 3.6. The extraction pipeline described here has utility in screening myxospermous germplasm. **(A)** Total seed mucilage yield of 206 *Plantago ovata* mutants screened using the extraction pipeline. **(B)** Mucilage architecture of a validation set including a wild type, three low yield and three high yield lines observed using ruthenium red staining (scale = 1 mm) **(C)** Verification of mucilage yield in the validation set. **(D)** Differences in the seed mucilage fractionation profile of the validation set **(E)** Water absorption by seed mucilage of the validation set.

Values in C and E are means while error bars represent one standard deviation from the mean. Asterisks denote statistical differences from WT (significance levels are included on the relevant figures) as determined by Student's t-test.

Supplementary Table 3.1. Monosaccharide summary of *Plantago ovata* mucilage fractionated by the small-scale extraction pipeline in comparison with previously published large scale techniques.

Fraction	Marlett & Fischer 2002[a]	Guo *et al.* 2008[b]	Yu *et al.* 2017[c]	This study
Heteroxylan-Relative Pectin Content (Rha+GalA:Xyl Ratio)				
CWE	0.679	0.286	0.426	0.438
HWE	trace R+G		trace R+G	trace R+G
IAE	-	trace R+G	trace R+G	trace R+G
Heteroxylan Branching (Ara:Xyl Ratio)				
CWE	0.200	0.232	0.211	0.222
HWE	0.285		0.301	0.281
IAE	-	0.345	0.341	0.364

a. From the work of Marlett and Fischer, psyllium husk fractions Fr C and Fr B are deemed comparable to CWE and HWE fractions, respectively. Their remaining fraction, Fr A, contained alkali insoluble husk material and thus is not directly comparable to the IAE fraction.
b. From Guo *et al.*'s work, psyllium husk fraction WE is deemed to be similar to a pooling of CWE and HWE while AEG 0.5 is deemed comparable to IAE
c. From Yu *et al.*'s work CW, HW and KOH fractions are deemed comparable to CWE, HWE and IAE fractions, respectively.

Declarations

Authors' Contributions:

JMC and RAB conceived the study. JMC designed and tested the method, analysed the data and wrote the manuscript. LH designed and conducted the mutant screen experiment, analysed the data and contributed to writing the manuscript. KAN collected and assisted in data analysis for field trial quality testing. SC and VC provided field trial material for testing the method. All authors read, edited and approved the final manuscript.

Funding:

This work was supported by the Australian Research Council Centres of Excellence in Plant Cell Walls (Grant No. 110001007) and Plant Energy Biology (Grant No. 140100008. JMC is supported by a PhD scholarship from the Australian Government's Research Training Program. LH is supported by the University of Adelaide's Adelaide Graduate Research Scholarship (AGRS).

Availability of data and materials:

The datasets used and analysed during this work are available from the corresponding author upon reasonable request.

Consent for publication:

All authors give consent for the data to be published.

Ethics:

Not applicable

Competing Interests:

The authors declare no competing interests.

Acknowledgements

The authors thank Dr Jana Phan and Dr Tina Bianco-Miotto for support and guidance and Shi Fang (Sandy) Khor for assistance with HPLC. We thank Siva Sivapalan, David McNeil and Mark Warmington from the Frank Wise Institute for Tropical Agriculture, Department of Primary Industries and Regional Development, Kununurra, WA for assistance in production of the field-grown seed samples. We thank Associate Professor Matthew Tucker for his assistance in developing the gamma-irradiated *Plantago ovata* mutant population and Dayton Bird from the Tucker Lab for the kind donation of *Arabidopsis* seeds used in this study. We thank members of the Burton Lab (RABLAB), the ARC Centre of Excellence in Plant Cell Walls and the ARC Centre of Excellence in Plant Energy Biology for useful discussions and support.

References

1. North HM, Berger A, Saez-Aguayo S, Ralet MC. Understanding polysaccharide production and properties using seed coat mutants: future perspectives for the exploitation of natural variants. Ann Bot. 2014/03/13. 2014;114(6):1251–63.

2. Western TL. The sticky tale of seed coat mucilages: production, genetics, and role in seed germination and dispersal. Seed Sci Res. 2012;22(01):1–25.

3. Arsovski AA, Haughn GW, Western TL. Seed coat mucilage cells of Arabidopsis thaliana as a model for plant cell wall research. Plant Signal Behav. 2010;5(7):796–801.

4. Voiniciuc C, Schmidt MH-W, Berger A, Yang B, Ebert B, Scheller HV, et al. MUCILAGE-RELATED10 Produces Galactoglucomannan That Maintains Pectin and Cellulose Architecture in Arabidopsis Seed Mucilage. Plant Physiol. 2015;

5. Arsovski AA, Popma TM, Haughn GW, Carpita NC, McCann MC, Western TL. AtBXL1 encodes a bifunctional β-d-xylosidase/α-l-arabinofuranosidase required for pectic arabinan modification in Arabidopsis mucilage secretory cells. Plant Physiol. 2009;150(3):1219–34.

6. Western TL. Isolation and Characterization of Mutants Defective in Seed Coat Mucilage Secretory Cell Development in Arabidopsis. Plant Physiol. 2001;127(3):998–1011.

7. Hu R, Li J, Yang X, Zhao X, Wang X, Tang Q, et al. Irregular xylem 7 (IRX7) is required for anchoring seed coat mucilage in Arabidopsis. Plant Mol Biol. 2016;92(1–2):25–38.

8. Ralet M-C, Crépeau M-J, Vigouroux J, Tran J, Berger A, Sallé C, et al. Xylans provide the structural driving force for mucilage adhesion to the Arabidopsis seed coat. Plant Physiol. 2016;171(1):165–78.

9. Jensen JK, Kim H, Cocuron J-C, Orler R, Ralph J, Wilkerson CG. The DUF579 domain containing proteins IRX15 and IRX15-L affect xylan synthesis in Arabidopsis. Plant J. 2011;66(3):387–400.

10. Tucker MR, Ma C, Phan J, Neumann K, Shirley NJ, Hahn MG, et al. Dissecting the Genetic Basis for Seed Coat Mucilage Heteroxylan Biosynthesis in Plantago ovata

Using Gamma Irradiation and Infrared Spectroscopy. Front Plant Sci. 2017;8(March):326.

11. Phan J. Using Plantago ovata as a proxy to study plant cell wall polysaccharide biosynthesis. The University of Adelaide; 2018.

12. Venglat P, Xiang D, Qiu S, Stone SL, Tibiche C, Cram D, et al. Gene expression analysis of flax seed development. BMC Plant Biol. 2011;11(April).

13. Renouard S, Cyrielle C, Lopez T, Lamblin F, Lainé E, Hano C. Isolation of nuclear proteins from flax (Linum usitatissimum L.) seed coats for gene expression regulation studies. BMC Res Notes. 2012;5:1–7.

14. Soto-Cerda BJ, Maureira-Butler I, Muñoz G, Rupayan A, Cloutier S. SSR-based population structure, molecular diversity and linkage disequilibrium analysis of a collection of flax (Linum usitatissimum L.) varying for mucilage seed-coat content. Mol Breed. 2012;30(2):875–88.

15. Kumar RK, Bejkar M, Du S, Serventi L. Flax and wattle seed powders enhance volume and softness of gluten-free bread. Food Sci Technol Int. 2018;0(0):108201321879580.

16. Haque A, Morris ER. Combined use of ispaghula and HPMC to replace or augment gluten in breadmaking. Food Res Int. 1994;27(4):379–93.

17. Mariotti M, Lucisano M, Ambrogina Pagani M, Ng PKWP, Pagani M, Ng PKWP. The role of corn starch, amaranth flour, pea isolate, and Psyllium flour on the rheological properties and the ultrastructure of gluten-free doughs. Food Res Int. 2009;42(8):963–75.

18. Cappa C, Lucisano M, Mariotti M. Influence of Psyllium, sugar beet fibre and water on gluten-free dough properties and bread quality. Carbohydr Polym. 2013;98(2):1657–66.

19. Anderson JW, Zettwoch N, Feldman T, Tietyen Clark J, Oeltgen P, Bishop CW. Cholesterol-Lowering Effects of Psyllium Hydrophilic Mucilloid for Hypercholesterolemic Men. Arch Intern Med. 1988;148(2):292–6.

20. Gunness P, Gidley MJ. Mechanisms underlying the cholesterol-lowering properties of soluble dietary fibre polysaccharides. Food Funct. 2010;1(2):149.

21. Prasad K. Dietary flax seed in prevention of hypercholesterolemic

atherosclerosis. Atherosclerosis. 1997;132(1):69–76.

22. Sharma PK, Koul AK. Mucilage in seeds of Plantago ovata and its wild allies. J Ethnopharmacol. 1986;17(3):289–95.

23. Balke DT, Diosady LL. Rapid aqueous extraction of mucilage from whole white mustard seed. Food Res Int. 2000;33(5):347–56.

24. Phan JL, Burton RA. New Insights into the Composition and Structure of Seed Mucilage [Internet]. Vol. 1, Annual Plant Reviews Online. 2018. 1–41 p.

25. Haughn GW, Western TL. Arabidopsis Seed Coat Mucilage is a Specialized Cell Wall that Can be Used as a Model for Genetic Analysis of Plant Cell Wall Structure and Function. Front Plant Sci. 2012;3:64.

26. Yu L, Yakubov GGE, Zeng W, Xing X, Stenson J, Bulone V, et al. Multi-layer mucilage of Plantago ovata seeds: Rheological differences arise from variations in arabinoxylan side chains. Carbohydr Polym. 2017;165:132–41.

27. Yu L, Yakubov GE, Gilbert EP, Sewell K, van de Meene AML, Stokes JR. Multi-scale assembly of hydrogels formed by highly branched arabinoxylans from Plantago ovata seed mucilage studied by USANS/SANS and rheology. Carbohydr Polym. 2019;207(December 2018):333–42.

28. Yu L, Yakubov GE, Martínez-Sanz M, Gilbert EP, Stokes JR. Rheological and structural properties of complex arabinoxylans from Plantago ovata seed mucilage under non-gelled conditions. Carbohydr Polym. 2018;193(March):179–88.

29. Tucker MR, Okada T, Hu Y, Scholefield A, Taylor JM, Koltunow AMG. Somatic small RNA pathways promote the mitotic events of megagametogenesis during female reproductive development in arabidopsis. Development. 2012;139(8):1399–404.

30. Phan JL, Tucker MR, Khor SF, Shirley NJ, Lahnstein J, Beahan C, et al. Differences in glycosyltransferase family 61 accompany variation in seed coat mucilage composition in Plantago spp. J Exp Bot. 2016;67(22):6481–95.

31. Comino P, Shelat K, Collins H, Lahnstein J, Gidley MJ. Separation and purification of soluble polymers and cell wall fractions from wheat, rye and hull less barley endosperm flours for structure-nutrition studies. J Agric Food Chem. 2013;61(49):12111–22.

32. Hassan AS, Houston K, Lahnstein J, Shirley N, Schwerdt JG, Gidley MJ, et al.

A Genome Wide Association Study of arabinoxylan content in 2-row spring barley grain. PLoS One. 2017;12(8):1–19.

33. Wood J, Tan H-T, Collins H, Yap K, Khor S, Lim W, et al. Genetic and environmental factors contribute to variation in cell wall composition in mature desi chickpea (Cicer arietinum L .) cotyledons. Plant Cell Environ. 2018;41(November 2017):2195–208.

34. Western TL, Skinner DJ, Haughn GW. Differentiation of Mucilage Secretory Cells of the Arabidopsis Seed Coat. Plant Physiol. 2000;122(2):345–56.

35. Guo Q, Cui SW, Wang Q, Christopher Young J. Fractionation and physicochemical characterization of psyllium gum. Carbohydr Polym. 2008;73(1):35–43.

36. Marlett JA, Fischer MH. Nutrient Metabolism A Poorly Fermented Gel from Psyllium Seed Husk Increases Excreta Moisture and Bile Acid Excretion in Rats. J Nutr. 2002;132(April 2002):2638–43.

37. Macquet A, Ralet MC, Kronenberger J, Marion-Poll A, North HM. In situ, chemical and macromolecular study of the composition of Arabidopsis thaliana seed coat mucilage. Plant Cell Physiol. 2007;48(7):984–99.

38. Voiniciuc C. Quantification of the Mucilage Detachment from Arabidopsis Seeds. Bio-protocol. 2016;6:1–9.

39. Mazza G, Biliaderis CG. Functional Properties of Flax Seed Mucilage. J Food Sci. 1989;54(5):1302–5.

40. Oomah BD, Kenaschuk EO, Cui W, Mazza G. Variation in the Composition of Water-Soluble Polysaccharides in Flaxseed. J Agric Food Chem. 1995;43(6):1484–8.

41. Capitani MI, Corzo-Rios LJ, Chel-Guerrero LA, Betancur-Ancona DA, Nolasco SM, Tomás MC. Rheological properties of aqueous dispersions of chia (Salvia hispanica L.) mucilage. J Food Eng. 2015;149:70–7.

42. Fernandes SS, Salas-Mellado M de las M. Addition of chia seed mucilage for reduction of fat content in bread and cakes. Food Chem. 2017;227:237–44.

43. Muñoz LA, Cobos A, Diaz O, Aguilera JM. Chia seeds: Microstructure, mucilage extraction and hydration. J Food Eng. 2012;108(1):216–24.

44. Segura-Campos M, Acosta-Chi Z, Rosado-Rubio G, Chel-Guerrero L, Betancur-Ancona D. Whole and crushed nutlets of chia (Salvia hispanica) from Mexico as a source of functional gums. Food Sci Technol. 2014;34(4):701–9.

45. Behbahani BA, Tabatabaei Yazdi F, Shahidi F, Hesarinejad MA, Mortazavi SA, Mohebbi M. Plantago major seed mucilage: Optimization of extraction and some physicochemical and rheological aspects. Carbohydr Polym. 2017;155:68–77.

46. Benaoun F, Delattre C, Boual Z, Ursu A V., Vial C, Gardarin C, et al. Structural characterization and rheological behavior of a heteroxylan extracted from *Plantago notata* Lagasca (Plantaginaceae) seeds. Carbohydr Polym. 2017;175:96–104.

47. Naran R, Chen G, Carpita NC. Novel rhamnogalacturonan I and arabinoxylan polysaccharides of flax seed mucilage. Plant Physiol. 2008;148(1):132–41.

48. Pavlov A, Paynel F, Rihouey C, Porokhovinova E, Brutch N, Morvan C. Variability of seed traits and properties of soluble mucilages in lines of the flax genetic collection of Vavilov Institute. Plant Physiol Biochem. 2014;80:348–61.

49. Voiniciuc C, Gunl M. Analysis of Monosaccharides in Total Mucilage Extractable from Arabidopsis Seeds. Bio-protocol. 2016;6:1–11.

50. Zhao X, Qiao L, Wu A-M. Effective extraction of Arabidopsis adherent seed mucilage by ultrasonic treatment. Sci Rep. 2017;7:40672.

51. Hu R, Li J, Wang X, Zhao X, Yang X, Tang Q, et al. Xylan synthesized by Irregular Xylem 14 (IRX14) maintains the structure of seed coat mucilage in Arabidopsis. J Exp Bot. 2016;67(5):1243–57.

52. Yu L, Shi D, Li J, Kong Y, Yu Y, Chai G, et al. CELLULOSE SYNTHASE-LIKE A2, a glucomannan synthase, is involved in maintaining adherent mucilage structure in *Arabidopsis* seed. Plant Physiol. 2014;164(4):1842–56.

53. Open PW, Grif JS, Tsai AY, Xue H, Seifert GJ, Mans SD, et al. SALT-OVERLY SENSITIVE5 Mediates Arabidopsis Seed Coat Mucilage Adherence and. 2014;165(July):991–1004.

54. Lin KY, Daniel JR, Whistler RL. Structure of chia seed polysaccharide exudate. Carbohydr Polym. 1994;23(1):13–8.

55. Kumar J. Good agricultural practices for isabgol. Report for the Directorate of Medicinal and Aromatic Plants; 2015.

56. McNeil DL. Growers' manual for production of Plantago ovata in the Ord irrigation area. ISBN Services; 2017. 75 p.

57. Macquet A, Ralet M-C, Loudet O, Kronenberger J, Mouille G, Marion-Poll A, et al. A Naturally Occurring Mutation in an Arabidopsis Accession Affects a -D-Galactosidase That Increases the Hydrophilic Potential of Rhamnogalacturonan I in Seed Mucilage. Plant Cell Online. 2007;19(12):3990–4006.

58. Sullivan S, Ralet M-C, Berger A, Diatloff E, Bischoff V, Gonneau M, et al. CESA5 is required for the synthesis of cellulose with a role in structuring the adherent mucilage of Arabidopsis seeds. Plant Physiol. 2011;156(4):1725–39.

59. Cowley J. Analysis of Plantago mucilage mutants. University of Adelaide; 2016.

Cowley *et al. Plant Methods* (2020) 16:20
https://doi.org/10.1186/s13007-020-00569-6

Plant Methods

RESEARCH Open Access

A small-scale fractionation pipeline for rapid analysis of seed mucilage characteristics

James M. Cowley[1,2], Lina Herliana[2], Kylie A. Neumann[1,2], Silvano Ciani[3], Virna Cerne[3] and Rachel A. Burton[1,2*]

Abstract

Background: Myxospermy is a process by which the external surfaces of seeds of many plant species produce mucilage—a polysaccharide-rich gel with numerous fundamental research and industrial applications. Due to its functional properties the mucilage can be difficult to remove from the seed and established methods for mucilage extraction are often incomplete, time-consuming and unnecessarily wasteful of precious seed stocks.

Results: Here we tested the efficacy of several established protocols for seed mucilage extraction and then downsized and adapted the most effective elements into a rapid, small-scale extraction and analysis pipeline. Within 4 h, three chemically- and functionally-distinct mucilage fractions were obtained from myxospermous seeds. These fractions were used to study natural variation and demonstrate structure–function links, to screen for known mucilage quality markers in a field trial, and to identify research and industry-relevant lines from a large mutant population.

Conclusion: The use of this pipeline allows rapid analysis of mucilage characteristics from diverse myxospermous germplasm which can contribute to fundamental research into mucilage production and properties, quality testing for industrial manufacturing, and progressing breeding efforts in myxospermous crops.

Keywords: Mucilage, Myxospermy, Extraction, Polysaccharide, *Plantago ovata*, Flax, Chia, Psyllium

Background

In a process called myxospermy, seeds of many plants produce viscous polysaccharide gels called mucilage when imbibed in water. The mucilage of *Arabidopsis thaliana* has often been used as a proxy for studying cell wall biosynthesis [1–8]. More recently other myxospermous species like *Linum usitatissimum* and *Plantago ovata* have also been adopted as genetic models [9–14] revealing the utility that novel systems can have in unravelling complex synthetic pathways. Furthermore, these novel model systems have the added benefit of being directly commercially-relevant. *P. ovata* (psyllium) and *L. usitatissimum* (flaxseed) mucilage are used as gums with varied applications in the food and health industries. Both are used as natural food structuring ingredients and gluten replacements [15–18] and are rich sources of dietary fibre shown to prevent various gastrointestinal diseases [19–21]. A comprehensive myxospermous model system would allow gene-structure–function links to be made but there remains a technical disconnect between these facets. The functional study of myxospermous species preceded their use as genetic models and the scale and precision of the extraction techniques have generally not been updated since. A significant number of researchers use the methods of Sharma and Koul [22], Balke and Diosady [23], or similar. These methods are simple, effective and robust, using a magnetic stirrer to heat and agitate a seed/water mixture followed by straining to isolate released mucilage from seeds. However, there are several technical issues that limit the use

*Correspondence: rachel.burton@adelaide.edu.au
[1] Australian Research Council Centre of Excellence in Plant Cell Walls, School of Agriculture, Food and Wine, University of Adelaide, Waite Campus, Urrbrae, SA, Australia
Full list of author information is available at the end of the article

of these techniques in screening applications. Firstly, the techniques are not high-throughput, generally requiring 3–4 h to process a single sample (per magnetic stirrer). Secondly, the quantity of mucilage produced is excessive for downstream chromatographic and yield analyses which require milligram-scale quantities or less. Thirdly, the techniques often offer incomplete extraction, leaving a significant amount of mucilage adhered to the seed. It is also important to note that seed mucilage is not homogenous. Its multi-layered nature is evident simply by visual inspection of stained expanded mucilage in nearly all species [24] The dual-layered nature of *Arabidopsis thaliana* mucilage has been the basis of many studies on cell wall polysaccharide biosynthesis [25] and Yu et al. [26–28] have recently highlighted the importance of fractionating mucilage to effectively unravel structural differences that underlie polysaccharide functionality.

Here we describe a pipeline suitable for the rapid extraction and fractionation of quantities of seed mucilage suitable for yield and chromatographic analyses. Within four hours, three chemically- and functionally-distinct fractions can be isolated from 24 samples per shaking incubator and the use of a shaking incubator allows adjustment in time, temperature and fractionation profile. The utility of this pipeline is demonstrated through its ability to: identify intergeneric and interspecific variation in seed mucilage extractability, yield and composition, screen for known quality parameters in field-grown myxospermous samples, and identify lines of interest from germplasm collections.

Methods

Materials

Arabidopsis thaliana seeds (ecotype *Columbia-0*) were grown as per Tucker et al. [29]. Flax (*Linum usitatissimum*) and chia (*Salvia hispanica*) seeds were purchased from Woolworths (Frewville, South Australia). *Plantago ovata* and *Plantago cunninghamii* seeds were obtained and bulked from sources listed in Phan et al. [30]. *P. ovata* varieties were grown in field trials conducted in 2017 and 2018 in Kununurra, Western Australia. Gamma-irradiated *P. ovata* mutants used for germplasm screening were obtained from a glasshouse-grown population described previously [10].

Once harvested or purchased, all seeds were dried at 37 °C for at least 72 h and then stored in sealed containers at room temperature until analysis.

Reagents and solutions

Ruthenium red hydrate (#C075) was purchased from ProSciTech, Australia and the staining solution was prepared at 0.01% w/v in water following Arsovski et al. [5]. To prevent bubble formation on the seed surfaces during imaging, the staining solution was sonicated for 5 min under vacuum to remove dissolved gases. KOH and HCl (Sigma-Aldrich) were made to a 0.2 M solution in water.

Mucilage staining

Expanded seed mucilage was observed in situ following Arsovski et al. [5] to compare and validate extraction techniques. After positioning seeds on a microscope slide (Rowe GM2715, Australia) staining solution was added beneath a coverglass (ProSciTech No. 1, Australia) and images were captured on a dissecting microscope (Zeiss Stemi 2000-C, Germany) equipped with a colour digital camera (Zeiss AxioCam ERc 5s, Germany).

Conventional seed mucilage extraction techniques

The effectiveness of total mucilage extraction by the fractionation pipeline described here was validated against previously published methods by Balke and Diosady [23], Yu et al. [26], Sharma and Koul [22], and Voiniciuc et al. [4]. Balke and Diosady's method (also used previously by our group, Phan et al. [30]) is simple, stirring seeds and water heated to 80 °C on a magnetic stirrer for 90 min after which the liberated mucilage is strained through nylon mesh to remove seeds. Yu et al.'s method uses an extended extraction (4 h) with RT 0.2 M solution of KOH. Sharma and Koul's method combines seeds with dilute acid (0.2 M HCl) in a conical flask, which is stirred on a heated magnetic stirrer until the seeds have changed colour (20 min). Seeds are strained through nylon mesh and washed twice with hot water. Finally, Voiniciuc's method uses the physical force (30 Hz for 30 min) of a tissue disruptor-type mixer mill.

Rapid small-scale mucilage fractionation pipeline

The rapid small scale fractionation of quantities of seed mucilage suitable for yield and chromatographic analyses was achieved using the following protocol incorporating elements of methods by Yu et al. [26] and Voiniciuc et al. [4]. For similarly sized seeds, seeds can be counted or for variably sized seeds 30 mg (±0.5 mg) of seeds (exact mass recorded) can be weighed. Once the pre-extraction mass was recorded, seeds were added to a 2 mL microcentrifuge tube followed by 1.5 mL of RT DI H_2O (Fig. 1a). Tubes were vortexed briefly to break surface tension and ensure all seeds are immersed. To obtain the first mucilage fraction (Fig. 1b), tubes were incubated for 1.5 h at 25 °C in a shaking incubator (Eppendorf ThermoMixer® Comfort, Germany) with agitation at 1300 rpm then centrifuged (Eppendorf 5424, Germany) for 2 min at 13,000 rpm. Ensuring that the pelleted adherent mucilage and seeds are not disturbed, the tubes were removed from the centrifuge and using a 1000 µL laboratory pipette, the supernatant—the cold water extractable (CWE) mucilage fraction—was

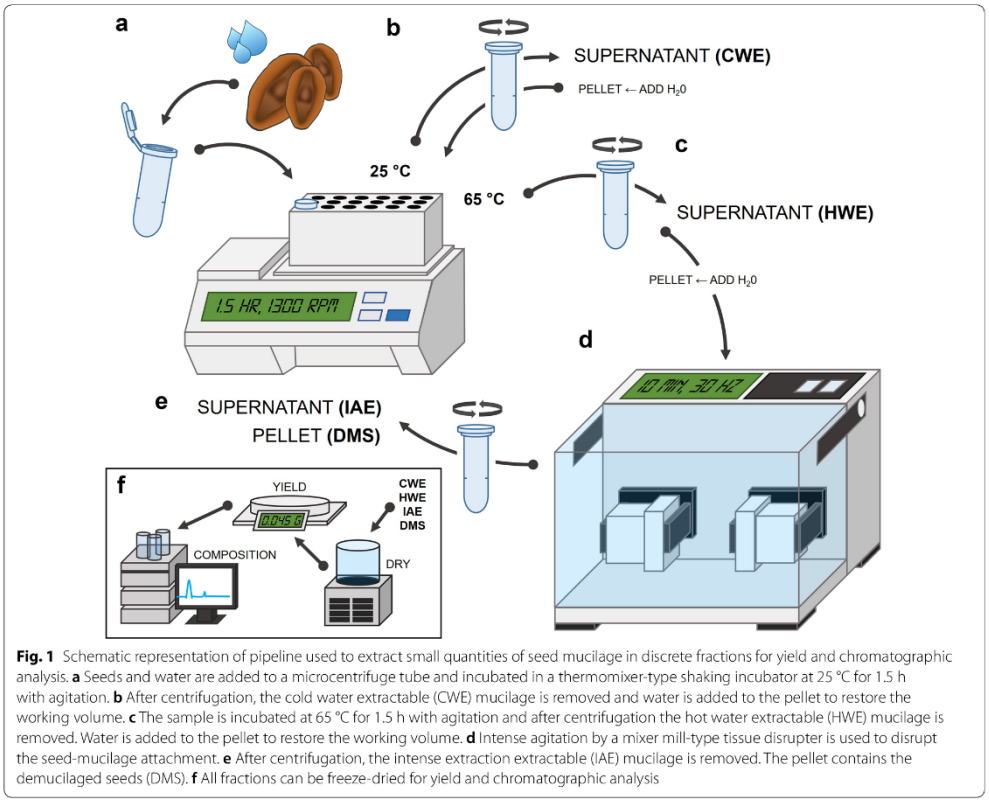

Fig. 1 Schematic representation of pipeline used to extract small quantities of seed mucilage in discrete fractions for yield and chromatographic analysis. **a** Seeds and water are added to a microcentrifuge tube and incubated in a thermomixer-type shaking incubator at 25 °C for 1.5 h with agitation. **b** After centrifugation, the cold water extractable (CWE) mucilage is removed and water is added to the pellet to restore the working volume. **c** The sample is incubated at 65 °C for 1.5 h with agitation and after centrifugation the hot water extractable (HWE) mucilage is removed. Water is added to the pellet to restore the working volume. **d** Intense agitation by a mixer mill-type tissue disrupter is used to disrupt the seed-mucilage attachment. **e** After centrifugation, the intense extraction extractable (IAE) mucilage is removed. The pellet contains the demucilaged seeds (DMS). **f** All fractions can be freeze-dried for yield and chromatographic analysis

transferred to a clean, pre-labelled microcentrifuge tube. This transfer may require multiple steps based on the volume of the supernatant. The volume of the tube contents comprising the pelleted mucilage and seeds was returned to approximately 1.5 mL with RT DI H_2O based on the tube markings (different samples may require slightly different volumes). To obtain the next mucilage fraction (Fig. 1c), a similar process was employed but at a warmer temperature: tubes were incubated for 1.5 h at 65 °C with agitation at 1300 rpm then centrifuged for 2 min at 13,000 rpm. Again the supernatant—the hot water extractable (HWE) mucilage fraction—was transferred to a clean, pre-labelled microcentrifuge tube using a 1000 µL laboratory pipette. After removal of the HWE fraction, the volume of the pellet is significantly reduced as only the most extraction-resistant mucilage remains tightly adhered to the seed. After adjusting the volume of tube contents to approximately 1.5 mL with RT DI H_2O, the tubes were agitated intensely at 30 Hz for 10 min on a tissue disruptor-type mixer mill (Retsch MM400, Germany) using a microcentrifuge tube adapter (Fig. 1d). Tubes were centrifuged for 2 min at 13,000 rpm and the supernatant—the intense agitation extractable (IAE) mucilage fraction—was transferred to a clean, pre-labelled microcentrifuge tube using a 1000 µL laboratory pipette.

From each sample, a cold water extractable (CWE), hot water extractable (HWE) and intense extraction resistant (IAE) fraction of seed mucilage has been obtained along with the corresponding demucilaged seeds (DMS) (Fig. 1e). These four fractions were frozen at − 80 °C for 24 h and then freeze-dried (Labconco Freezone 6, US) to a constant weight. Freeze-dried mucilage and demucilaged seeds were transferred to a microbalance with 0.01 mg resolution (Shimadzu AUW220D, Japan) with fine-tip tweezers to calculate mucilage yield (Fig. 1f).

Yield of mucilage fractions can be calculated using the following equation:

$$\text{Yield}(\%) = \left(\frac{\text{mass of freeze dried mucilage}}{\text{mass of seeds pre-extraction}}\right) \times 100.$$

Optional—isolated fractions may be pipetted into a 2000 µL 96 well deep well plate (Eppendorf, Germany) in place of new microcentrifuge tubes which can become unwieldy when dealing with large sample numbers. The deep well plates can accommodate many samples and several plates will fit simultaneously into a freeze-dried unit for bulk processing.

Monosaccharide profiles of fractionated seed mucilage

Freeze-dried mucilage was dispersed in water at 2 mg/mL (w/v) and an 800 µL aliquot was added to 200 µL of 5 M H_2SO_4 (final H_2SO_4 concentration of 1 M) and hydrolysed at 100 °C for 3 h as per Phan et al. [30]. Monosaccharides released by acid hydrolysis were derivatised with 1-phenyl-3-methyl-5-pyrazoline (PMP) and then separated by reversed phase high performance liquid chromatography (RP-HPLC) following Comino et al. [31] with modifications to the column and eluents listed in Hassan et al. [32]. Area under the peaks was compared to standard curves of mannose, ribose, rhamnose, glucuronic acid, galacturonic acid, glucose, galactose, xylose, arabinose and fucose [33].

Water absorption assay

After weighing 20 seeds into a 2 mL microcentrifuge tube, 1 g of water was added, and mucilage was allowed to expand undisturbed for 45 min at 25 °C. Using a 1 mL syringe without a needle, unabsorbed water was removed and weighed. Water absorption capacity can be calculated using the equation:

$$\text{Water absorption capacity}(\text{g/g}) = \frac{\text{Initial weight of water added} - \text{weight of unabsorbed water}}{\text{Initial weight of seeds added}}$$

Results and discussion

This protocol achieves total mucilage extraction

Figure 2 shows *P. ovata* seeds with stained expanded seed mucilage before and after four methods of mucilage extraction. While hot water was effective at reducing the size of the mucilage envelope (Fig. 2b), mucilage in the inner layer is more densely packed than the removed soluble fraction and thus a large amount of the mucilage remains [34]. Yu et al. [26] reported that an extended (4 h) extraction with 0.2 M KOH, a chaotropic agent, was sufficient to remove the adherent mucilage layer by disrupting hydrogen bonds in the mucilage. We confirm that this treatment is effective at removing the majority of seed mucilage (Fig. 2c) although the most strongly adherent portion remained on all treated seeds (n = 30). Mucilage removal in acid was similarly effective (Fig. 2d), however the mode of action of the acid was to hydrolyse the mucilage in situ which is not useful if any downstream functional or linkage analyses are required. An appealing alternative was the non-chemical extraction method devised by Voiniciuc et al. [4] who were able to efficiently extract all adherent mucilage from *Arabidopsis* seeds using intense agitation on a tissue disruptor-type mixer mill. The physical force of the shaking was sufficient to disrupt the mucilage-seed attachment and

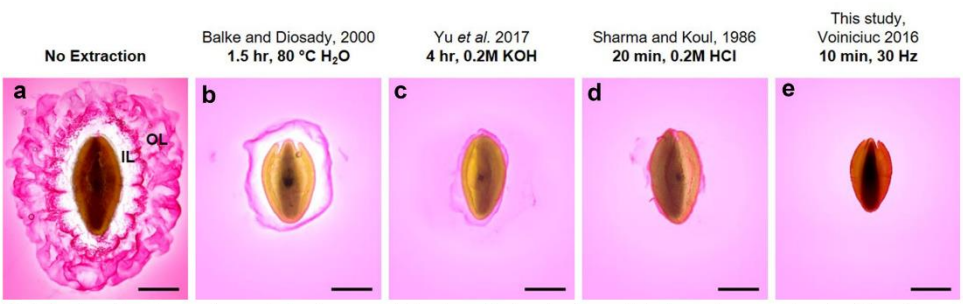

Fig. 2 Seed mucilage that remains attached to *P. ovata* seeds after the application of various published extraction protocols and staining with 0.1% w/v ruthenium red. **a** The characteristic mucilage architecture of *P. ovata* seed mucilage. **b** After extended extraction in hot water the fine structure of the outer layer (OL) of mucilage has been lost leaving an inner adherent layer (IL). **c** The use of a chaotropic agent, KOH, significantly reduces the size of the mucilage envelope leaving only a film of mucilage that is resistant to chemical extraction. **e** Mucilage has been hydrolysed in situ and only a thin feathery layer remains. **e** Extraction by intense agitation leads to total mucilage removal. Scale = 1 mm

disperse the polysaccharides. We corroborate the efficacy of this method on *P. ovata* where close to 100% of seed mucilage was removed (Fig. 2e). We also observed that mucilage staining of seeds that sequentially underwent a hot water extraction before 0.2 M KOH, 0.2 M HCl or 30 Hz agitation were no different to those that were not extracted with hot water as a first step (data not shown).

The monosaccharide profiling of fractionated *P. ovata* mucilage shows that our small-scale fractionation technique is directly comparable to the larger scale technique published by Yu et al. [26], the original study by Guo et al. [35] on which their work is based and a similar work published earlier by Marlett and Fischer [36] (Additional file 1: Table S1).

The extraction pipeline effectively provides material for identifying variation in seed mucilage characteristics

Figure 3 shows the appearance of the expanded seed mucilage envelope of *A. thaliana* (a–d), *L. usitatissimum* (flaxseed) (e–h), *S. hispanica* (chia) (i–l), *P. ovata* (psyllium) (m–p) and an Australian native relative of psyllium, *P. cunninghamii* (q–t) before and after each mucilage fractionation step in the pipeline described here, which culminates in total extraction (Fig. 4a). After CWE and HWE extraction, the mucilage envelope of *L. usitatissimum* and *A. thaliana* is significantly reduced in size compared to *S. hispanica*, *P. ovata* and *P. cunninghamii*. These changes were reflected in the differences between the ratios of extracted fractions (Fig. 4b), where *L. usitatissimum* and *A. thaliana* were most susceptible to extraction, yielding the largest proportion of water extractable (CWE + HWE) components. The easy removal of the delicate outer layer of mucilage in *A. thaliana* and *L. usitatissimum* is consistent with previous findings and established fractionation techniques [4, 34, 37–40]. Contrastingly, *Plantago* and *S. hispanica* mucilage has been reported to require more effort to efficiently extract total mucilage. For *S. hispanica*, mucilage extraction in cold water is not efficient [41] while extended hot water extractions yield only slightly greater quantities [42–44]. We corroborate these findings, reporting that only half of the mucilage is extractable by hot water (Fig. 4b). Efficient mucilage extraction from *Plantago* species is also difficult, often requiring multiple physical and/or chemical extraction steps [26, 35, 36, 45, 46]. While total yields of mucilage between *P. ovata* and *P. cunninghamii* were similar (Fig. 4a), there are clear interspecific differences in the relative proportion of each fraction (Fig. 4b). Changes in appearance of the mucilage envelope of *P. ovata* after CWE were more noticeable than for *P. cunninghamii*, which appears relatively unchanged and is reflected in CWE yield which was lower for *P. cunninghamii*. Yield of HWE mucilage was greater for *P. cunninghamii*, with less IAE mucilage than *P. ovata*.

Some, if not all, of the differences in the relative proportion of each mucilage fraction of the species studied can be ascribed to mucilage polysaccharide composition and the associated difference in properties. Monosaccharide analysis confirmed significant differences in mucilage composition between genera and species and their isolated mucilage fractions (Fig. 4c). Monosaccharide analysis also confirmed previous findings that mucilage fractions from *A. thaliana* and *L. usitatissimum* are rich in rhamnose and galacturonic acid [4, 47–50], components of pectin, a highly water-soluble polysaccharide, the presence of which may contribute to overall ease of extraction in these species. It is the presence of minor mucilage components in the HWE and IAE fractions that are known to affect the mucilage properties including fractionality. In *A. thaliana*, monosaccharide profiling of the HWE and IAE fractions (containing the adherent mucilage) confirms previous findings of a molar reduction in rhamnose and galacturonic acid residues and an increase in non-cellulosic glucose, mannose, galactose and xylose [49, 50], components of minor polysaccharides like xylan and glucomannan that are well-known to interact with and tether the adherent mucilage at the seed surface [4, 7, 51–53]. Similarly, rhamnose and galacturonic acid residues were reduced in the HWE and IAE fractions of *L. usitatissimum*, along with increases in xylose and arabinose residues associated with heteroxylan, known to significantly alter the functional properties of RG-I [47]. In *P. ovata and P. cunninghamii*, the three mucilage fractions contained high levels of xylose and arabinose (heteroxylan) with a smaller amount of rhamnose and galacturonic acid (pectin), congruent with previous findings by Phan et al. [30]. Like both *A. thaliana* and *L. usitatissimum*, pectin-associated monosaccharides are enriched in the CWE fractionation and diminish with further fractions. While the presence of pectin has been proposed to modulate the extractability of the major heteroxylan component in *Plantago* mucilage, studies have shown that heteroxylan branching has the most significant influence on the mucilage properties including the extractability [26–28]. In both *P. ovata* and *P. cunninghamii,* the ratio of arabinose to xylose residues (estimation of the degree of sidechain branching) increased with resistance to extraction, in line with those studies. However, more explicit structural characterisation will be needed to define the fine structure and its relationship to interspecific differences in extractability. The mucilage of *S. hispanica* is unique among the species studied in that its constituent polysaccharide(s) have not been found in any other genera [54]. Its unique structure containing xylose, glucose and glucuronic acid residues is consistent

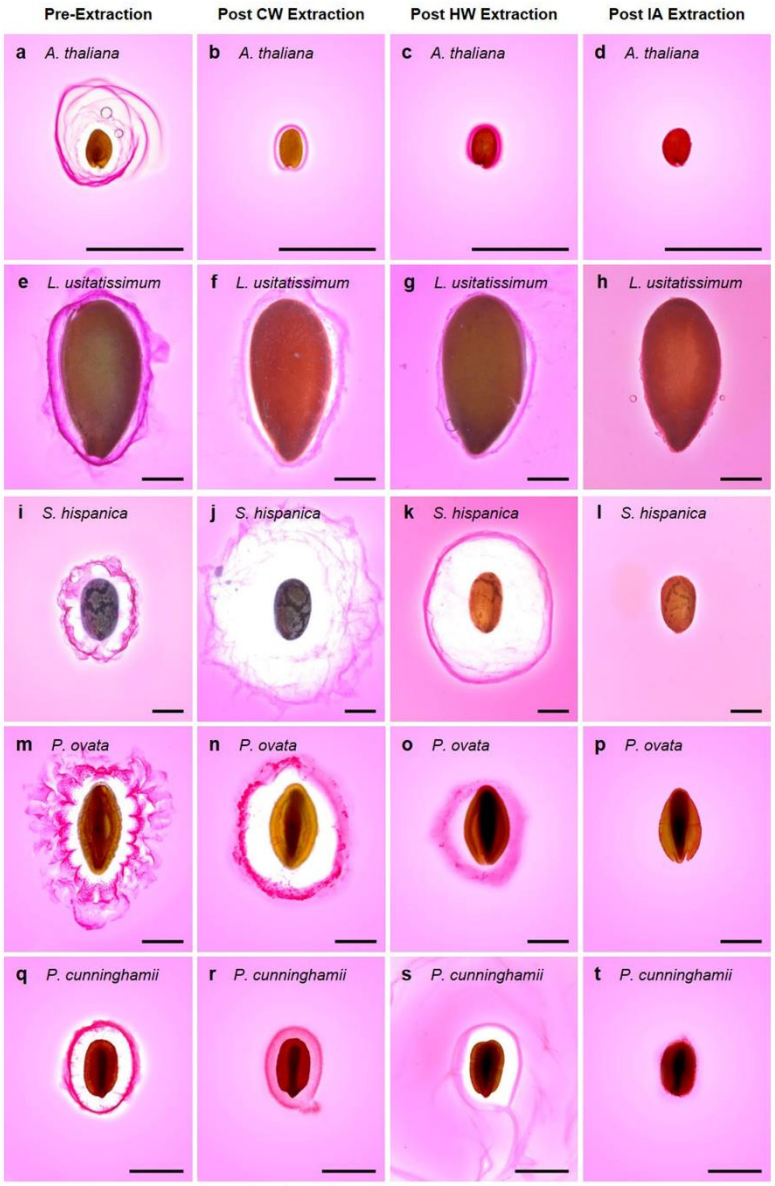

Fig. 3 Visual inspection of the ruthenium red-stained seed mucilage of five myxospermous species (*Arabidopsis thaliana*, *Linum usitatissimum*, *Salvia hispanica*, *Plantago ovata* and *Plantago cunninghamii*) after sequential fractionation shows that the size of the mucilage envelope is sequentially changed corresponding to removal/dispersion of constituent polysaccharides. Note that images are not taken of the same seed as each seed was disposed of after imaging. Scale = 1 mm

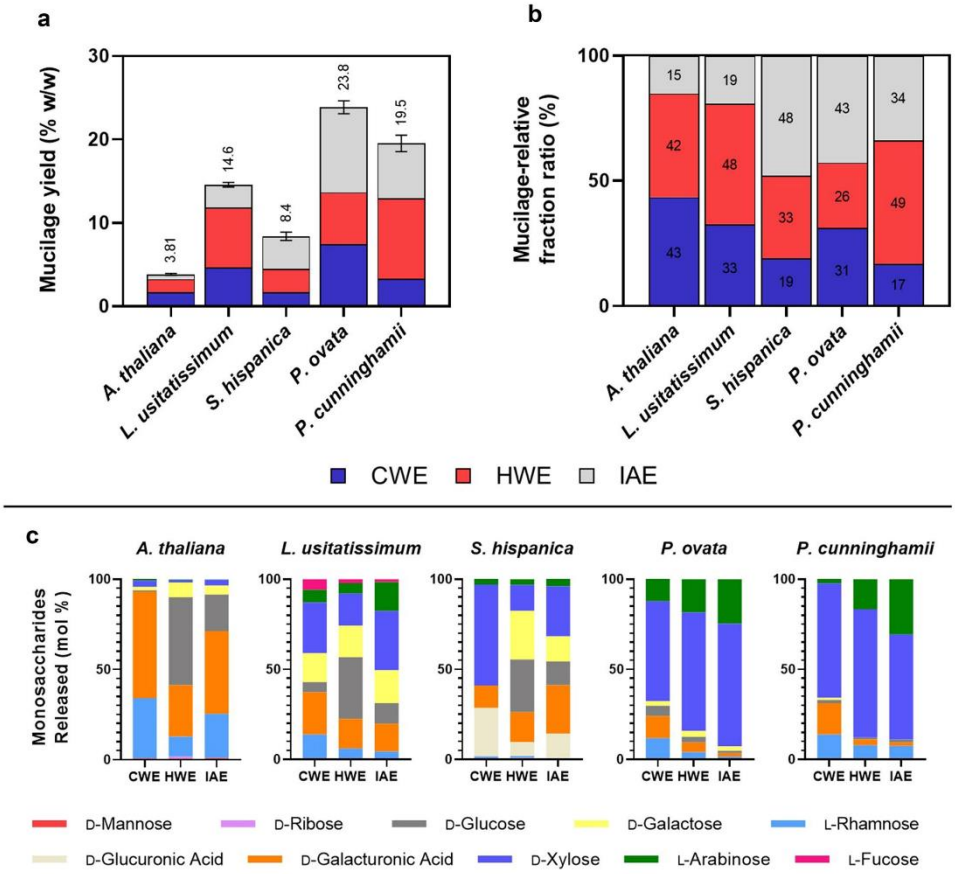

Fig. 4 The extraction pipeline is effective at providing material suitable for identifying significant intergeneric and interspecific variation in seed mucilage yield, fractionation profile and composition. **a** Yield of total seed mucilage divided into constituent fractions. Error bars refer to standard deviation in total mucilage yield of five biological replicates. **b** Extractability of seed mucilage represented as the share of each fraction within total extracted mucilage. **c** Monosaccharide analysis of fractionated mucilage showing intergeneric, interspecific and intraspecific differences in mucilage chemical composition. Values presented are in molar ratio of quantified monosaccharides released by acid hydrolysis. *CWE* cold water extractable, *HWE* hot water extractable, *IAE* intense agitation extractable

with the monosaccharide data (Fig. 4c), although the molar ratios between the constituents varies by fraction suggesting that fine structure and/or interactions with minor components (from which the other monosaccharides detected are derived) influences the extractability.

The pipeline has utility in quality testing of mucilaginous species

The production of high-quality psyllium gum from *P. ovata* seeds is hampered by agronomic issues which cause poor quality, damaged seeds [55]. Damaged seed coat allows leakage of endosperm components during extraction which alter the functional properties and cause significant discolouration due to phenolic browning which is undesirable in many applications (Cowley

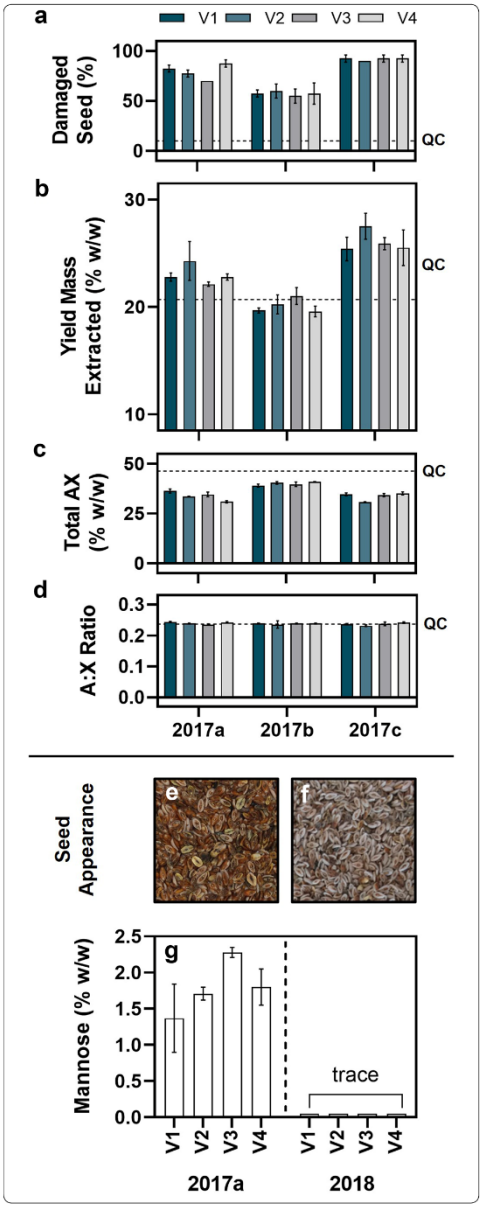

Fig. 5 In field-grown samples of *Plantago ovata*, the extraction pipeline has utility in quality testing when coupled with yield and chromatographic analysis. **a** Visual inspection of damaged seed provides a baseline quality score. **b** Yield of total mucilage varied most significantly between times of sowing with a minor intervarietal effect. **c** Heteroxylan content (the proportion of arabinose and xylose residues in extracted mucilage) inversely related to mucilage yield and seed quality. **d** The ratio of arabinose to xylose residues in extracted mucilage (an approximation of heteroxylan branching) remains unchanged indicating that seed and mucilage development were unperturbed. **e** Seed grown at trial sites in 2017 is unevenly coloured, with many blackened seeds while, **f** seeds grown at the same site in 2018 are more consistent, with the light-coloured husk material consistently visible on seeds. **g** In the 2017 field trials (analysed are samples from 2017a), significant quantities of mannose were identified by monosaccharide analysis in extracted mucilage of each variety grown indicative of seed damage-related endosperm leakage. Contrastingly, only trace amounts (well below the limit of quantitation) were found in the same varieties grown in the following year, 2018. Dotted line in **a**–**d** indicates the value of a quality control sample (QC). Error bars represent one standard deviation (some are small and not easily visible)

et al. unpublished data). As the functional component of psyllium gum, heteroxylan must be abundant and present at a consistent level to be considered good quality for industrial uses as the dilution of heteroxylan by the presence of contaminants will impact the functionality in optimised formulations. Four varieties of *P. ovata* were grown in three separate field trials with different times of sowing a factor which, due to climatic conditions, was found to significantly affect seed quality [55, 56]. A suite of quality parameters is shown in Fig. 5. Visual inspection was used to determine a baseline quality score for the four varieties at each trial (Fig. 5a). Trial 2017a had the lowest damage score followed by 2017b and then 2017c. 2017c was deemed the poorest quality with consistently high seed damage. When mucilage was extracted using our pipeline, there were clear differences in yield, with the strongest effect related to time of sowing with only minor intervarietal influence (Fig. 5b). Varieties grown at 2017b did not differ greatly in yield from the control, which was a high-quality field grown sample (QC). Conversely, varieties from 2017a and 2017c had higher mass yields after extraction. Monosaccharide profiling showed that mucilage synthesis was not disrupted as the arabinose to xylose (AX) ratio was very similar between varieties and trials and not significantly different from the QC (Fig. 5d). However, the quantity of heteroxylan in the mucilage (defined as total AX) differed between trials (Fig. 5c). 2017b, confirmed as the most successful sample, had the highest proportion of AX and was closest to the

QC. Correspondingly, 2017a and 2017c had lower proportions of AX indicating significant contamination from other components. Total AX is thereby inversely proportional to yield as a direct result of quality. No variety at any trial had AX as high as the QC, likely because seed of the QC sample was of exceptional quality.

Furthermore, known chemical markers have been defined indicating low quality or damaged seed. As one example, extreme damage of *P. ovata* seeds causes extensive leakage of endosperm components including mannose monosaccharides (Cowley et al. unpublished data). Trial 2017a was impacted by devastating unseasonable rainfall which physically damaged seed before harvesting (Fig. 5e) and subsequently led to microbial growth, leading to detectable quantities of mannose in the extracted mucilage (Fig. 5g). Mannose was found only in trace amounts in corresponding 2018 samples which were not weather damaged or microbially contaminated and more consistently high quality (Fig. 5f).

The pipeline can be used for rapid screening of myxospermous germplasm

This pipeline has utility for rapid screening of mucilage yield traits in a germplasm set, demonstrated here using gamma-irradiated *P. ovata* mutants generated in a previous study [10]. Total mucilage yield data (a pooling of CWE, HWE and IAE fractions) was obtained for a subset of 206 randomly-selected glasshouse-grown *P. ovata* mutants (Fig. 6a). In 63% of mutants, mucilage yield was within a ±10% interval of WT yield (n = 131). Only 4% of mutants yielded 10% less mucilage than WT (n = 8), while 33% yielded over 10% more (n = 68). To validate this screen, a subset of the three lowest yielding (252-7, 768-9, and 1064-5) and three highest (743-4, 1072-12, and 776-5) mutants were selected for further analysis. Expanded mucilage architecture has been used previously to visually screen for altered mucilage phenotypes in mutants of *Arabidopsis* [4, 57, 58] and *Plantago* [10]. Here we show variation in expanded mucilage architecture between the mutants (Fig. 6b) where some are distinctly different to WT (252-7, 1064-5, 743-4, and 776-5) while others are WT-like (768-9 and 1072-12). The utility of the pipeline is proven two-fold in that it can identify highly-distinctive mutants which would be identified through typical visual screening techniques (like ruthenium red staining) but also mutants with more subtle changes to yield that may appear as WT. The validation set of mutant lines was subjected to further analysis which confirmed the differences observed in total mucilage yield were statistically significant compared to the WT. Differences observed in the size of the ruthenium red-stained mucilage envelopes and the amount of mucilage extracted may be linked to alterations in polysaccharide macromolecular properties. This was examined further by comparing the relative proportion of the three mucilage fractions (Fig. 6d) with the water absorption capacity of the mucilage (Fig. 6e).

While the total yield of mucilage was significantly decreased from WT in mutant 768-9, the ruthenium red phenotype, the ratio of mucilage fractions and the water absorption capacity were not significantly different from the WT. Contrastingly, the ratio of the three mucilage fractions was significantly altered in mutants 252-7, 1064-5, and 743-4 (*mucilage extractable with water* (*mew*) mutants) where the CWE and HWE fractions comprise most or all of the mucilage and the IAE fraction is significantly diminished or totally absent. In *mew* mutants, water absorption capacity is significantly reduced from the WT presumably due to a reduction in the stronger gelling, high water-holding capacity IAE mucilage fractions [26]. The striking similarities in the phenotypes of the *mew* mutants suggests that they may contain mutant alleles. Importantly, *mew* mutant 252-7 has already been identified as a putative reduced mucilage xylan mutant [10] and the characterisation of this class of mutant is ongoing [11]. Mutant 776-5 represents a previously unseen class of *P. ovata* mucilage mutant [10, 11, 59]. While this mutant has the highest total mucilage yield in the screened population, its water absorption capacity was unchanged from WT. Its unique compact ruthenium red phenotype and shift in the ratio of the three mucilage fractions suggests intrinsically different changes to the mucilage composition, with a novel causative mutation(s) compared to the *mew* mutants. The ease of distinguishing the *mew* mutants and mutant 776-5 within the mutant population shows that the pipeline can effectively identify putative mutants with perturbed seed development and/or mucilage synthesis, ideal for forward genetic studies.

In contrast to the *mew* mutants and mutant 776-5, it was found that while the ruthenium red and mucilage fractionation phenotype of mutant 1072-12 did not differ substantially from the WT, the total yield and related water absorption capacity was significantly increased. Mutant 1071-12 may therefore represent an important genotype for use in pre-breeding efforts due to its high mucilage yield without the aberrant changes to mucilage composition and properties which makes other mutants less suitable.

Conclusions

In this study we tested the efficacy of several established protocols for seed mucilage extraction and downsized and adapted the most effective elements into a small-scale, rapid extraction and analysis pipeline. We demonstrated the utility of this pipeline for investigating intergeneric and interspecific differences in seed mucilage characteristics, as well as for quality testing and germplasm screening of myxospermous plants. This

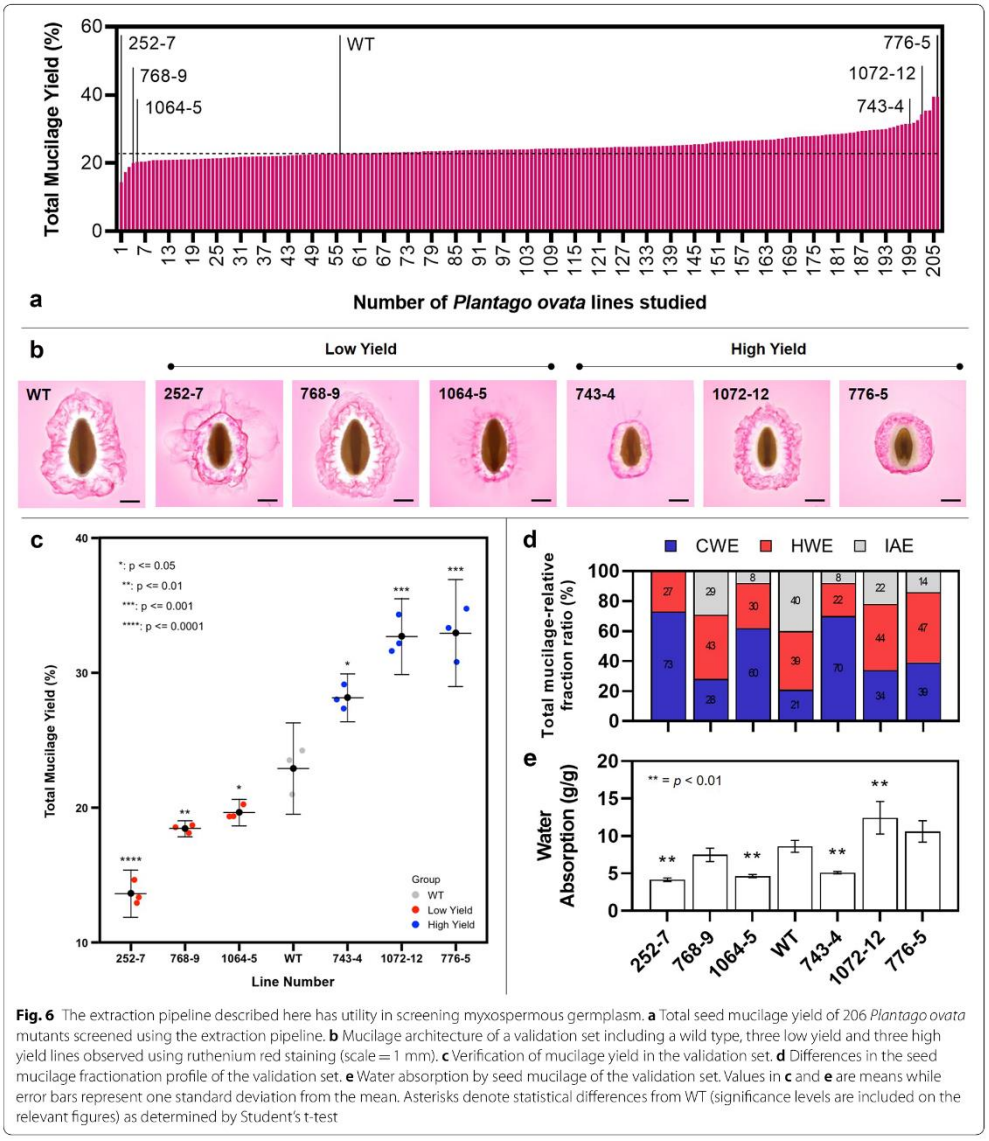

Fig. 6 The extraction pipeline described here has utility in screening myxospermous germplasm. **a** Total seed mucilage yield of 206 *Plantago ovata* mutants screened using the extraction pipeline. **b** Mucilage architecture of a validation set including a wild type, three low yield and three high yield lines observed using ruthenium red staining (scale = 1 mm). **c** Verification of mucilage yield in the validation set. **d** Differences in the seed mucilage fractionation profile of the validation set. **e** Water absorption by seed mucilage of the validation set. Values in **c** and **e** are means while error bars represent one standard deviation from the mean. Asterisks denote statistical differences from WT (significance levels are included on the relevant figures) as determined by Student's t-test

pipeline is already regularly used in our research group increasing the analysis efficiency of a range of myxospermous species. It has also been adopted by a leading food manufacturer who relies on consistently high-quality mucilage products. The use of this pipeline in fundamental research may improve our understanding of mucilage production and properties, ensure quality in food manufacturing, and aid in pre-breeding or breeding of myxospermous species—often classified as orphan crops—that could benefit from improved characterisation methods.

Supplementary information

Supplementary information accompanies this paper at https://doi.org/10.1186/s13007-020-00569-6.

Additional file 1: Table S1. Monosaccharide summary of *Plantago ovata* mucilage fractionated by the small-scale extraction pipeline in comparison with previously published large scale techniques.

Abbreviations

CWE: Cold water extractable; HWE: Hot water extractable; IAE: Intense agitation extractable; DI water: Deionized water; RG-I: Rhamnogalacturonan I; QC: Quality control; A:x Ratio: Arabinose to xylose ratio; AX: Arabinose + xylose (estimated heteroxylan content); WT: Wild type.

Acknowledgements

The authors thank Dr. Jana Phan and Dr. Tina Bianco-Miotto for support and guidance and Shi Fang (Sandy) Khor for assistance with HPLC. We thank Siva Sivapalan, David McNeil and Mark Warmington from the Frank Wise Institute for Tropical Agriculture, Department of Primary Industries and Regional Development, Kununurra, WA for assistance in production of the field-grown seed samples. We thank Associate Professor Matthew Tucker for his assistance in developing the gamma-irradiated *Plantago ovata* mutant population and Dayton Bird from the Tucker Lab for the kind donation of *Arabidopsis* seeds used in this study. We thank members of the Burton Lab (RABLAB), the ARC Centre of Excellence in Plant Cell Walls and the ARC Centre of Excellence in Plant Energy Biology for useful discussions and support.

Authors' contributions

JMC and RAB conceived the study. JMC designed and tested the method, analysed the data and wrote the manuscript. LH designed and conducted the mutant screen experiment, analysed the data and contributed to writing the manuscript. KAN collected and assisted in data analysis for field trial quality testing. SC and VC provided field trial material for testing the method. All authors edited the final manuscript. All authors read and approved the final manuscript.

Funding

This work was supported by the Australian Research Council Centres of Excellence in Plant Cell Walls (Grant No. 110001007) and Plant Energy Biology (Grant No. 140100008). JMC is supported by a PhD scholarship from the Australian Government's Research Training Program. LH is supported by the University of Adelaide's Adelaide Graduate Research Scholarship (AGRS).

Availability of data and materials

The datasets used and analysed during this work are available from the corresponding author upon reasonable request.

Ethics approval and consent to participate

Not applicable.

Consent for publication

All authors give consent for the data to be published.

Competing interests

The authors declare no competing interests.

Author details

[1] Australian Research Council Centre of Excellence in Plant Cell Walls, School of Agriculture, Food and Wine, University of Adelaide, Waite Campus, Urrbrae, SA, Australia. [2] Australian Research Council Centre of Excellence in Plant Energy Biology, School of Agriculture, Food and Wine, University of Adelaide, Waite Campus, Urrbrae, SA, Australia. [3] Dr. Schär R&D Centre, AREA Science Park, Padriciano 99, 34149 Trieste, Italy.

Received: 10 January 2020 Accepted: 14 February 2020
Published online: 24 February 2020

References

1. North HM, Berger A, Saez-Aguayo S, Ralet MC. Understanding polysaccharide production and properties using seed coat mutants: future perspectives for the exploitation of natural variants. Ann Bot. 2014;114(6):1251–63.
2. Western TL. The sticky tale of seed coat mucilages: production, genetics, and role in seed germination and dispersal. Seed Sci Res. 2012;22(01):1–25.
3. Arsovski AA, Haughn GW, Western TL. Seed coat mucilage cells of *Arabidopsis thaliana* as a model for plant cell wall research. Plant Signal Behav. 2010;5(7):796–801.
4. Voiniciuc C, Schmidt MHW, Berger A, Yang B, Ebert B, Scheller HV, et al. MUCILAGE-RELATED10 produces galactoglucomannan that maintains pectin and cellulose architecture in *Arabidopsis* seed mucilage. Plant Physiol. 2015;169(1):403–20.
5. Arsovski AA, Popma TM, Haughn GW, Carpita NC, McCann MC, Western TL. AtBXL1 encodes a bifunctional β-D-xylosidase/α-L-arabinofuranosidase required for pectic arabinan modification in *Arabidopsis* mucilage secretory cells. Plant Physiol. 2009;150(3):1219–34.
6. Western TL. Isolation and characterization of mutants defective in seed coat mucilage secretory cell development in *Arabidopsis*. Plant Physiol. 2001;127(3):998–1011.
7. Hu R, Li J, Yang X, Zhao X, Wang X, Tang Q, et al. Irregular xylem 7 (IRX7) is required for anchoring seed coat mucilage in *Arabidopsis*. Plant Mol Biol. 2016;92(1–2):25–38.
8. Ralet M-C, Crépeau M-J, Vigouroux J, Tran J, Berger A, Sallé C, et al. Xylans provide the structural driving force for mucilage adhesion to the *Arabidopsis* seed coat. Plant Physiol. 2016;171(1):165–78.
9. Jensen JK, Kim H, Cocuron J-C, Orler R, Ralph J, Wilkerson CG. The DUF579 domain containing proteins IRX15 and IRX15-L affect xylan synthesis in *Arabidopsis*. Plant J. 2011;66(3):387–400.
10. Tucker MR, Ma C, Phan J, Neumann K, Shirley NJ, Hahn MG, et al. Dissecting the genetic basis for seed coat mucilage heteroxylan biosynthesis in *Plantago ovata* using gamma irradiation and infrared spectroscopy. Front Plant Sci. 2017;8(March):326.
11. Phan J. Using Plantago ovata as a proxy to study plant cell wall polysaccharide biosynthesis. Adelaide: The University of Adelaide; 2018.
12. Venglat P, Xiang D, Qiu S, Stone SL, Tibiche C, Cram D, et al. Gene expression analysis of flax seed development. BMC Plant Biol. 2011;11(April):74.
13. Renouard S, Cyrielle C, Lopez T, Lamblin F, Lainé E, Hano C. Isolation of nuclear proteins from flax (*Linum usitatissimum* L.) seed coats for gene expression regulation studies. BMC Res Notes. 2012;5:1–7.
14. Soto-Cerda BJ, Maureira-Butler I, Muñoz G, Rupayan A, Cloutier S. SSR-based population structure, molecular diversity and linkage disequilibrium analysis of a collection of flax (*Linum usitatissimum* L.) varying for mucilage seed-coat content. Mol Breed. 2012;30(2):875–88.
15. Kumar RK, Bejkar M, Du S, Serventi L. Flax and wattle seed powders enhance volume and softness of gluten-free bread. Food Sci Technol Int. 2018. https://doi.org/10.1177/1082013218795808.
16. Haque A, Morris ER. Combined use of ispaghula and HPMC to replace or augment gluten in breadmaking. Food Res Int. 1994;27(4):379–93.
17. Mariotti M, Lucisano M, Ambrogina Pagani M, Ng PKWP, Pagani M, Ng PKWP. The role of corn starch, amaranth flour, pea isolate, and psyllium flour on the rheological properties and the ultrastructure of gluten-free doughs. Food Res Int. 2009;42(8):963–75.

18. Cappa C, Lucisano M, Mariotti M. Influence of psyllium, sugar beet fibre and water on gluten-free dough properties and bread quality. Carbohydr Polym. 2013;98(2):1657–66.
19. Anderson JW, Zettwoch N, Feldman T, Tietyen Clark J, Oeltgen P, Bishop CW. Cholesterol-lowering effects of psyllium hydrophilic mucilloid for hypercholesterolemic men. Arch Intern Med. 1988;148(2):292–6.
20. Gunness P, Gidley MJ. Mechanisms underlying the cholesterol-lowering properties of soluble dietary fibre polysaccharides. Food Funct. 2010;1(2):149.
21. Prasad K. Dietary flax seed in prevention of hypercholesterolemic atherosclerosis. Atherosclerosis. 1997;132(1):69–766.
22. Sharma PK, Koul AK. Mucilage in seeds of *Plantago ovata* and its wild allies. J Ethnopharmacol. 1986;17(3):289–95.
23. Balke DT, Diosady LL. Rapid aqueous extraction of mucilage from whole white mustard seed. Food Res Int. 2000;33(5):347–56.
24. Phan JL, Burton RA. New insights into the composition and structure of seed mucilage. Annu Plant Rev Online. 2018;1:1–41.
25. Haughn GW, Western TL. *Arabidopsis* seed coat mucilage is a specialized cell wall that can be used as a model for genetic analysis of plant cell wall structure and function. Front Plant Sci. 2012;3:64.
26. Yu L, Yakubov GGE, Zeng W, Xing X, Stenson J, Bulone V, et al. Multi-layer mucilage of Plantago ovata seeds: rheological differences arise from variations in arabinoxylan side chains. Carbohydr Polym. 2017;165:132–41.
27. Yu L, Yakubov GE, Gilbert EP, Sewell K, van de Meene AML, Stokes JR. Multi-scale assembly of hydrogels formed by highly branched arabinoxylans from *Plantago ovata* seed mucilage studied by USANS/SANS and rheology. Carbohydr Polym. 2019;207(December 2018):333–42.
28. Yu L, Yakubov GE, Martínez-Sanz M, Gilbert EP, Stokes JR. Rheological and structural properties of complex arabinoxylans from *Plantago ovata* seed mucilage under non-gelled conditions. Carbohydr Polym. 2018;193(March):179–88.
29. Tucker MR, Okada T, Hu Y, Scholefield A, Taylor JM, Koltunow AMG. Somatic small RNA pathways promote the mitotic events of megagametogenesis during female reproductive development in *Arabidopsis*. Development. 2012;139(8):1399–404.
30. Phan JL, Tucker MR, Khor SF, Shirley NJ, Lahnstein J, Beahan C, et al. Differences in glycosyltransferase family 61 accompany variation in seed coat mucilage composition in *Plantago* spp. J Exp Bot. 2016;67(22):6481–95.
31. Comino P, Shelat K, Collins H, Lahnstein J, Gidley MJ. Separation and purification of soluble polymers and cell wall fractions from wheat, rye and hull less barley endosperm flours for structure-nutrition studies. J Agric Food Chem. 2013;61(49):12111–22.
32. Hassan AS, Houston K, Lahnstein J, Shirley N, Schwerdt JG, Gidley MJ, et al. A genome wide association study of arabinoxylan content in 2-row spring barley grain. PLoS ONE. 2017;12(8):1–19.
33. Wood J, Tan H-T, Collins H, Yap K, Khor S, Lim W, et al. Genetic and environmental factors contribute to variation in cell wall composition in mature desi chickpea (*Cicer arietinum* L.) cotyledons. Plant Cell Environ. 2018;41(November 2017):2195–208.
34. Western TL, Skinner DJ, Haughn GW. Differentiation of mucilage secretory cells of the *Arabidopsis* seed coat. Plant Physiol. 2000;122(2):345–56.
35. Guo Q, Cui SW, Wang Q, Christopher YJ. Fractionation and physicochemical characterization of psyllium gum. Carbohydr Polym. 2008;73(1):35–433.
36. Marlett JA, Fischer MH. Nutrient metabolism a poorly fermented gel from psyllium seed husk increases excreta moisture and bile acid excretion in rats. J Nutr. 2002;132(April 2002):2638–43.
37. Macquet A, Ralet MC, Kronenberger J, Marion-Poll A, North HM. In situ, chemical and macromolecular study of the composition of *Arabidopsis thaliana* seed coat mucilage. Plant Cell Physiol. 2007;48(7):984–99.
38. Voiniciuc C. Quantification of the mucilage detachment from *Arabidopsis* seeds. Bio-protocol. 2016;6:1–9.
39. Mazza G, Biliaderis CG. Functional properties of flax seed mucilage. J Food Sci. 1989;54(5):1302–5.
40. Oomah BD, Kenaschuk EO, Cui W, Mazza G. Variation in the composition of water-soluble polysaccharides in flaxseed. J Agric Food Chem. 1995;43(6):1484–8.
41. Capitani MI, Corzo-Rios LJ, Chel-Guerrero LA, Betancur-Ancona DA, Nolasco SM, Tomás MC. Rheological properties of aqueous dispersions of chia (*Salvia hispanica* L.) mucilage. J Food Eng. 2015;149:70–7.
42. Fernandes SS, de las Mercedes Salas-Mellado M. Addition of chia seed mucilage for reduction of fat content in bread and cakes. Food Chem. 2017;227:237–44.
43. Muñoz LA, Cobos A, Diaz O, Aguilera JM. Chia seeds: microstructure, mucilage extraction and hydration. J Food Eng. 2012;108(1):216–24.
44. Segura-Campos M, Acosta-Chi Z, Rosado-Rubio G, Chel-Guerrero L, Betancur-Ancona D. Whole and crushed nutlets of chia (*Salvia hispanica*) from Mexico as a source of functional gums. Food Sci Technol. 2014;34(4):701–9.
45. Behbahani BA, Tabatabaei Yazdi F, Shahidi F, Hesarinejad MA, Mortazavi SA, Mohebbi M. Plantago major seed mucilage: optimization of extraction and some physicochemical and rheological aspects. Carbohydr Polym. 2017;155:68–77.
46. Benaoun F, Delattre C, Boual Z, Ursu AV, Vial C, Gardarin C, et al. Structural characterization and rheological behavior of a heteroxylan extracted from *Plantago notata* Lagasca (Plantaginaceae) seeds. Carbohydr Polym. 2017;175:96–104.
47. Naran R, Chen G, Carpita NC. Novel rhamnogalacturonan I and arabinoxylan polysaccharides of flax seed mucilage. Plant Physiol. 2008;148(1):132–41.
48. Pavlov A, Paynel F, Rihouey C, Porokhovinova E, Brutch N, Morvan C. Variability of seed traits and properties of soluble mucilages in lines of the flax genetic collection of Vavilov Institute. Plant Physiol Biochem. 2014;80:348–61.
49. Voiniciuc C, Gunl M. Analysis of monosaccharides in total mucilage extractable from *Arabidopsis* seeds. Bio-protocol. 2016;6:1–11.
50. Zhao X, Qiao L, Wu A-M. Effective extraction of *Arabidopsis* adherent seed mucilage by ultrasonic treatment. Sci Rep. 2017;7:40672.
51. Hu R, Li J, Wang X, Zhao X, Yang X, Tang Q, et al. Xylan synthesized by irregular xylem 14 (IRX14) maintains the structure of seed coat mucilage in *Arabidopsis*. J Exp Bot. 2016;67(5):1243–57.
52. Yu L, Shi D, Li J, Kong Y, Yu Y, Chai G, et al. CELLULOSE SYNTHASE-LIKE A2, a glucomannan synthase, is involved in maintaining adherent mucilage structure in *Arabidopsis* seed. Plant Physiol. 2014;164(4):1842–56.
53. Griffiths JS, Tsai AY, Xue H, Voiniciuc C, Sola K, Seifert GJ, et al. SALT-OVERLY SENSITIVE5 mediates *Arabidopsis* seed coat mucilage adherence and organization through pectins. Plant Physiol. 2014;165(July):991–1004.
54. Lin KY, Daniel JR, Whistler RL. Structure of chia seed polysaccharide exudate. Carbohydr Polym. 1994;23(1):13–8.
55. Kumar J. Good agricultural practices for isabgol. Report for the Directorate of Medicinal and Aromatic Plants; 2015.
56. McNeil DL. Growers' manual for production of *Plantago ovata* in the Ord irrigation area. ISBN Services; 2017. p. 75.
57. Macquet A, Ralet M-C, Loudet O, Kronenberger J, Mouille G, Marion-Poll A, et al. A naturally occurring mutation in an *Arabidopsis* accession affects a β-D-galactosidase that increases the hydrophilic potential of rhamnogalacturonan I in seed mucilage. Plant Cell Online. 2007;19(12):3990–4006.
58. Sullivan S, Ralet M-C, Berger A, Diatloff E, Bischoff V, Gonneau M, et al. CESA5 is required for the synthesis of cellulose with a role in structuring the adherent mucilage of *Arabidopsis* seeds. Plant Physiol. 2011;156(4):1725–39.
59. Cowley J. Analysis of Plantago mucilage mutants. Adelaide: University of Adelaide; 2016.

CHAPTER 4

The novel features of *Plantago ovata* seed mucilage accumulation, storage, and release

This chapter was written to the sounds of...	
Album	For Emma, Forever Ago
Artist	Bon Iver
Favourite Song	Re: Stacks

Statement of Authorship

Title of Paper	The novel features of *Plantago ovata* seed mucilage accumulation, storage and release
Publication Status	☑ Published ☐ Accepted for Publication ☐ Submitted for Publication ☐ Unpublished and Unsubmitted work written in manuscript style
Publication Details	Phan, J.L., Cowley, J.M, Neumann, K.A., *et al.* (2020) The novel features of *Plantago ovata* seed mucilage accumulation, storage and release. *Scientific Reports* https://doi.org/10.1038/s41598-020-68685-w

Candidate

Name of Candidate	James M. Cowley		
Contribution to the Paper	Performed compositional analyses, interpreted compositional and microscopy data, performed data analysis and formulated the model, contributed to writing the manuscript		
Overall percentage (%)	30%		
Certification:	This paper reports on original research I conducted during the period of my Higher Degree by Research candidature and is not subject to any obligations or contractual agreements with a third party that would constrain its inclusion in this thesis. I am a primary author of this paper.		
Signature		Date	19/5/2020

Co-Author Contributions

By signing the Statement of Authorship, each author certifies that:

i. the candidate's stated contribution to the publication is accurate (as detailed above);
ii. permission is granted for the candidate in include the publication in the thesis; and
iii. the sum of all co-author contributions is equal to 100% less the candidate's stated contribution.

Name of Principal Author	Jana Phan		
Contribution to the Paper	Conceived the study, performed experiments, wrote the manuscript.		
Signature		Date	9/6/2020

Name of Co-Author	Kylie A. Neumann		
Contribution to the Paper	Performed microscopy and assisted in compositional analyses		
Signature		Date	9/6/2020

Name of Co-Author	Lina Herliana		
Contribution to the Paper	Staged plants for developmental series		
Signature		Date	9/6/2020

Name of Co-Author	Lisa A. O'Donovan		
Contribution to the Paper	Performed sectioning and developmental microscopy		
Signature		Date	9/6/2020

Name of Co-Author	Rachel A. Burton		
Contribution to the Paper	Conceived the study and contributed to writing the manuscript		
Signature		Date	9/6/2020

Name of Co-Author			
Contribution to the Paper			
Signature		Date	

Name of Co-Author			
Contribution to the Paper			
Signature		Date	

Name of Co-Author			
Contribution to the Paper			
Signature		Date	

JOURNAL: Scientific Reports

PUBLISHED: 2020, **10, 11766** https://doi.org/10.1038/s41598-020-68685-w

TITLE: The novel features of *Plantago ovata* seed mucilage accumulation, storage and release

AUTHORS: Jana L. Phan[1#†], James M. Cowley[1,2#], Kylie A. Neumann[1,2‡], Lina Herliana[2], Lisa A. O'Donovan[2] and Rachel A. Burton[1,2*]

*Corresponding author, rachel.burton@adelaide.edu.au, +61 08 8313 6501

#These authors contributed equally

AFFILIATIONS: [1]Australian Research Council Centre of Excellence in Plant Cell Walls, School of Agriculture, Food and Wine, University of Adelaide, Waite Campus, Urrbrae, SA 5064, Australia

[2]Australian Research Council Centre of Excellence in Plant Energy Biology, School of Agriculture, Food and Wine, University of Adelaide, Waite Campus, Urrbrae, SA 5064, Australia

PRESENT ADDRESSES:

†Australian Academy of Science, Ian Potter House, 9 Gordon St, Canberra ACT 2601

‡IP Australia, PO Box 200, Woden ACT 2606

NUMBER OF TABLES: 0

NUMBER OF FIGURES: 7 (1,3,5,6,7 are colour)

WORD COUNT*:* 5114

NUMBER OF SUPPLEMENTARY TABLES AND FIGURES: 6

Running title:

Mucilage accumulation and release in *Plantago ovata* seeds.

Highlight*:*

Mucilage polysaccharide production and storage in *P. ovata* seeds is distinct from equivalent processes in *Arabidopsis* and mucilage is released directly by expansion upon seed imbibition*.*

Abstract:

Seed mucilage polysaccharide production, storage and release in *Plantago ovata* is strikingly different to that of the model plant *Arabidopsis*. We have used microscopy techniques to track the development of mucilage secretory cells and demonstrate that mature *P. ovata* seeds do not have an outer intact cell layer within which the polysaccharides surround internal columellae. Instead, dehydrated mucilage is spread in a thin homogenous layer over the entire seed surface and upon wetting expands directly outwards, away from the seed. Observing mucilage expansion in real time combined with compositional analysis allowed mucilage layer definition and the roles they play in mucilage release and architecture upon hydration to be explored. The first emergent layer of hydrated mucilage is rich in pectin, extremely hydrophilic, and forms an expansion front that functions to ’jumpstart’ hydration and swelling of the second layer. This next layer, comprising the bulk of the expanded seed mucilage, is predominantly composed of heteroxylan and appears to provide much of the structural integrity. Our results indicate that the synthesis, deposition, desiccation, and final storage position of mucilage polysaccharides must be carefully orchestrated, although many of these processes are not yet fully defined and vary widely between myxospermous plant species.

Keywords*:*

Plantago, seed mucilage, heteroxylan, pectin, myxospermy, psyllium

Abbreviations*:*

DPA	days post-anthesis
ESM	extruded seed mucilage
ML	mucilage layer
MSC	mucilage secretory cell
SEM	scanning electron microscopy

Introduction

Upon exposure to aqueous environments, seeds from myxospermous species extrude a polysaccharide-rich gel from their seed surface, often called mucilage. Numerous species display myxospermy and there are a range of possible evolutionary advantages of synthesising such a carbon-rich and energy-expensive substance[1]. Of all myxospermous species, the seed mucilage system of *Arabidopsis* is the best characterised. *Arabidopsis* seed mucilage has been used extensively as a proxy for the study of plant cell wall polysaccharide biosynthesis, enabling increased molecular characterisation of pectin biosynthesis, its main polysaccharide component[2], as well as the biosynthesis of cellulose[3,4] and several hemicelluloses[5–8], which are minor but integral components. Mucilage from other species can be highly diverse[1] and while *P. ovata* mucilage is also a complex mixture of polymers, it is predominantly heteroxylan with only a minor pectin component. While the pectin component is a near-linear rhamnogalacturonan[9–11], the *P. ovata* heteroxylan (accounting for around 90% of the mucilage polysaccharides) is highly complex with the current scientific consensus defining *P. ovata* heteroxylan comprising a β-(1,4)-linked-D-xylopyranose backbone, heavily substituted at O-2 and/or O-3 positions with various mono-, di- and oligosaccharide substitutions of α-L-arabinofuranose and β-D-xylopyranose[9,11,12]. It is likely that, as with other eudicots, the β-(1,4)-linked-D-xylopyranose backbone is synthesised by several members of glycosyltransferase (GT) families 43 and 47. There is strong evidence that GT47 protein IRX10-L, probably in concert with other GT43 and GT47 proteins, extends the backbone by adding UDP-xylose moieties[14,15]. GT61 family members have been implicated in both α-arabinosyltransferase and β-xylosyltransferase xylan backbone decoration activities in cereals[16,17], *Arabidopsis*[18,19] and *Plantago*[20], and copy number and type of GT61 was found to influence interspecific differences in *Plantago* heteroxylan fine structure[11]. The overall picture is

complicated even further in that different fractions (sometimes described as layers) of *P. ovata* mucilage contain heteroxylans of varying substitution patterns showing that, like *Arabidopsis* mucilage, it is a similarly complex but orchestrated network of polysaccharides[9,10,13]. To date, many xylan synthase genes, particularly those involved in backbone decoration, are still unknown.

P. ovata mucilage also has economic relevance, in that in its dry state it constitutes the basis of a dietary fibre supplement, called psyllium, that is widely consumed by humans to assist with laxation, relieving constipation[21,22], and to treat metabolic disorders like hypercholesterolaemia[23]. More recently, psyllium has become a key ingredient in gluten-free food, where it provides texture and structure in the absence of gluten[24–27]. Psyllium is produced by milling the dry polysaccharides off the seed surface[28] and is often referred to as the “husk” fraction. The ratio of husk to seed is approximately 1:3, with the discarded non-husk seed components often being used for animal or fish feed[29]. From an economic standpoint, the ability to understand mucilage polysaccharide production and therefore potentially increase the valuable husk fraction is a viable breeding target for this plant species.

As well as studying the biosynthesis of mucilaginous polymers, the mechanism of mucilage extrusion from the seed coat of *Arabidopsis* has also been thoroughly characterised. In *Arabidopsis*, seed mucilage polysaccharides accumulate in the apoplast of specialised seed coat cells called ‘mucilage secretory cells’ (MSCs). When the mucilage polysaccharides become hydrated, they swell and rupture the primary cell wall of the MSC, releasing the mucilage[30]. The MSCs in *Arabidopsis* differentiate from the outer-most integument cell layer of the ovule. *Arabidopsis* has an outer integument composed of two cell layers and an inner integument composed of three cell layers, both of maternal origin, which grow to surround the mature ovule[31]. After pollination, at approximately 7 days post-anthesis (DPA), starch granules begin to

accumulate in the MSCs and polysaccharide deposition starts in the peripheral "corners" of the cells. This pushes the protoplasm to form a central volcano-like structure in the cell. At 10 DPA this central column is reinforced by the deposition of secondary cell wall polysaccharides to form the columella. The columella is a prominent feature of the mature MSCs in *Arabidopsis* and the accumulated polysaccharides are deposited and stored around it, producing a doughnut-shaped ring. This structure results in the distinctive mature *Arabidopsis* seed coat patterning seen using SEM[32–34]. The details of MSC development, rupture and mucilage release are discussed in comprehensive reviews by Francoz *et al.*,[30] and Voiniciuc *et al.*,[35]. An important developmental stage during MSC development is the weakening of the radial primary cell walls of the MSCs at the end of columella formation, at approximately 13 DPA. This process enables the consequent fracturing and rupturing of the cell walls of the MSCs upon imbibition in an aqueous environment[32]. The rupturing allows the accumulated seed polysaccharides to be extruded almost instantaneously forming the distinctive mucilage envelope. Thus, MSCs of *Arabidopsis* are a highly-specialised seed coat cell with a clearly defined structure that is essential for correct seed mucilage extrusion. MSC development and mucilage release of *Linum usitatissimum* seeds, more commonly known as flax, has also recently been described, revealing an even more complex MSC structure[36]. The flax MSCs, embedded in the external surface of the seed coat were determined by Miart *et al.,*[36] to contain four discrete, laminated layers in the apoplast, each containing chemically- and functionally-distinct polysaccharides. Each of the layers and their polysaccharide contents act in concert to effectively hydrate the polysaccharides, mechanically forcing the radial cell wall to rupture in a peeling fashion and enabling mucilage to be released. In other species such as *Salvia hispanica* (chia) and *Coleus blumei*, the seed mucilage polysaccharides are stored in the outer epidermal cell layer(s) of a nutlet that encases the true seed

within[37,38], making these species myxocarpous rather than myxospermous. The events leading to the release of mucilage in these species have not been documented in detail but there appears to be great diversity in the mucilage extrusion structures between plant types[1].

The accumulation of seed mucilage polysaccharides in *P. ovata* has been investigated previously[39] and appears to be distinct from the process observed in the *Arabidopsis* MSCs. In the case of *P. ovata*, seed mucilage polysaccharides are deposited in the outer-most cell layer of a large integument. This single cell layer accumulates polysaccharides rapidly and the cells expand dramatically in size in a process that does not involve the formation of a central columella[39]. Beyond this, little is known about the precise development of these cells and so here we provide a detailed characterisation of the polysaccharide deposition and mucilage release processes of *P. ovata*, also enabling the formulation of a supporting model.

Results

Development of *P. ovata* mucilage secretory cells

P. ovata takes approximately 3.5 months to grow from germination through to maturity. The mature plants have long slender, straggly leaves and produce many spike-type infloresences (Supplementary Fig. 4.1). Development of *P. ovata* fruit on the spike and length of the inflorescence (and consequently yield per plant) are strongly dependent on the plant's health during growth and development. Each fruit or capsule contains two ovules, separated by a maternal disc and joined to the parent plant via a placenta (Fig. 4.1). *P. ovata* possesses a circumscissile capsule (also called a pyxis) that is firmly attached to the inflorescence at the proximal end of the fruit. When the fruit is mature, the seed dispersal mechanism involves dehiscence at the capsule equator causing the operculum to detach, enabling the seed to dislodge from the capsule. The

operculum, the point of attachment to the rachis, and the equator are indicated in Fig. 4.1A. After pollination, the fruits mature in approximately one month. At two weeks post-anthesis, the fruit has reached its full length and the seeds continue to develop inside, expanding widthways and filling the fruit.

Following successful fertilisation, the parenchyma cells of the integument layers differentiate rapidly (Fig. 4.2). The mucilage secretory cells (MSCs) of *P. ovata* seeds are easily observed at 1 DPA. They develop from the outermost single cell layer of the integument and lengthen as they accumulate starch granules (Fig. 4.2B and C). Substantial growth and elongation of the MSCs is observed from 3 to 5 DPA. Although it is difficult to discern discrete cellular compartments, it is likely that the empty space at the distal end of the cells where the polysaccharides accumulate, is the apoplast (Fig. 4.2D). By 9 DPA, the accumulated mucilage polysaccharides are hydrophilic enough to rupture the MSCs when they come into contact with aqueous solutions and it is technically challenging to obtain intact sections from this stage onwards. At 15 DPA all MSCs have ruptured and released their mucilage in fixed and sectioned developing seeds but it is possible to observe that the integument has been compressed to just a few cell layers between the MSCs and the seed endosperm. This compressed layer has disappeared almost completely by the time the seed is fully mature, leaving only a thin layer situated between the endosperm and the mucilage polysaccharide layer (Fig. 4.2H).

Composition of developing ovule cell walls

The cell walls of seed tissues at three key time points across early development were fluorescently immunolabelled with the primary antibodies LM11 (β-1,4-linked xylan backbone[40]) LM19 (un-esterified and partially esterified homogalacturonan[41]) and LM20 (methylesterified homogalacturonan[41]) and the carbohydrate-binding module CBM3a (crystalline cellulose[42]). At anthesis the ovule is minute but there was clear

binding by both LM20 (Fig. 4.3A1-3) and LM19 (Supplementary Fig. 4.2A), with the latter producing a strong signal in the integument tissue. There was a low level of CBM3a binding to the walls of both MSCs and integument cells (Fig. 4.3D1-3) and no binding by LM11 (Supplementary Fig. 4.2B). At 4 DPA, the MSCs are greatly elongated. The strongest signals are generated by LM20 in the MSC layer (Fig. 4.3B1-3) and CBM3a in both the MSC and integument cells (Fig. 4.3E1-3) but there was no labelling evident for LM19 (Supplementary Fig. 4.2C) or LM11 (Supplementary Fig. 4.2D). The final time point was at 6/7 DPA when the MSCs were becoming fragile due to the accumulation of mucilage polysaccharides. At this point the LM20 labelling was now restricted to the outside edge of the MSC layer and in cell corners bordering the integument tissue (Fig. 4.3C1-3). The CBM3a signal was still present in both the MSCs and integument though signals in the MSCs had become non-specific and amorphous compared to the integument where labelling of distinct walls was still present (Fig. 4.3F1-3). By 6/7 DPA there was no labelling by LM19 (Supplementary Fig. 4.2E) and minimal labelling by LM11 (Supplementary Fig. 4.2F).

Surface features of mature *P. ovata* seeds

The mature seeds of *P. ovata* have a deep scar on the ventral side resulting in a boat-shaped seed (Supplementary Fig. 4.3). The patterning of the dry seed surface on the dorsal side is polar. Where the inner surface of the fruit capsule has been pressed against the seed it is smoother (Fig. 4.4A). The seed surface is covered in hexagonal structures with a distinct wrinkled texture (Fig. 4.4B). The wrinkled patterning and hexagonal structures on the mature seed surface are lost once seeds have been imbibed in water (Fig. 4.4D). When the remaining seed mucilage is left to dry back onto the seed after hydration in cold water, the seed surface appears very smooth and high magnification SEM reveals little additional detail (Fig. 4.4E). The hexagonal structures are no longer visible, and the polarity observed prior to mucilage expansion (Fig. 4.4A)

has also been lost. This is in clear contrast to *Arabidopsis* where, after the same process, the seed surface morphology remains relatively unchanged and the columella is still clearly visible (Fig. 4F). Mature *P. ovata* seeds therefore do not have conventional seed coat cells and there is certainly no columella as found in *Arabidopsis* (Fig. 4.4C). Rather there is a dehydrated mucilage polysaccharide layer, underlain by a thin dark brown layer (which gives the seed its colour) both of which sit over the outer layer of the endosperm (Fig. 4.4G). The crushed integument layer is not at all visible in the mature seed.

Mucilage removal from mature *P. ovata* seeds

Different methods were used to remove the expanded mucilage from mature imbibed seeds of *P. ovata*. Although previous studies report no significant compositional differences between the different extraction methods[11], some physical differences were observed on the exposed seed surface (Supplementary Fig. 4.4). When mature seeds were placed into an aqueous fixative, the sequential washing steps removed most of the mucilage from the seed, leaving a thin resistant layer behind, as did extraction with hot water or 0.2M KOH (Supplementary Fig. 4.4). In contrast, when 0.1M HCl was used for extraction, the mild acid completely removed the mucilage layer from the entire seed (Supplementary Fig. 4.4D), probably hydrolysing it *in situ*[10], and in some patches it has also removed the underlying intensely-stained layer (Supplementary Fig. 4.4F).

Mucilage accumulation may be independent of embryo and endosperm development

From the mutant *P. ovata* population reported in Tucker *et al*.,[43], we selected a line, 69-1, that produces seeds with impaired development across a range of severity: seeds with a thickened translucent outer layer, incomplete endosperm filling, arrested embryo development, or a shrivelled appearance where it was difficult to determine if

an embryo was present (Fig. 4.5A1-5). Ruthenium red staining solution was applied to representative seeds and all types produced mucilage from the seed that was released into the aqueous environment. While different specific architectures were observed, two typical mucilage layers were recognisable in all but the shrivelled phenotype. These seeds may have been aborted early in development rather than representing a developmentally delayed phenotype (Fig. 4.5B5). While only 5% of seed are WT-like in the 69-1 bulk sample analysed, WT-level total mucilage yields, arabinose and xylan content and ratio were still obtained (Fig. 4.5C1-3).

Expansion of seed mucilage polysaccharides across time and space

Microscopy and monosaccharide analysis techniques were used to investigate changes in the composition and structure of the mucilage as it expanded from the seed surface. In order to define temporal mucilage expansion we tried to capture and describe the major stages using chemical profiling. By measuring the release of mucilage-related monosaccharides over 14.5 hrs we found that the major stages of mucilage expansion occurred within 60 min of imbibition (Supplementary Fig. 4.5). Monosaccharide analysis of serial fractions taken during the first 60 min of mucilage expansion clearly demonstrated a change in the composition of the expanded seed mucilage over time (Fig. 4.6A). Relative to total extracted sugars, there was a shift from pectin-dominant to heteroxylan-dominant monosaccharide composition during the initial stages. A sharp increase in the number of heteroxylan-associated monosaccharides (xylose and arabinose) was then observed, peaking at 20 min post imbibition (Fig. 4.6A) while pectin-derived monosaccharides (rhamnose and galacturonic acid) displayed the inverse, where they were most abundant at the start of seed imbibition and mucilage expansion, before tapering off considerably by 20 min (Fig. 4.6A).

Mature seeds were stained as described in Yu *et al.*,[9] and real-time mucilage expansion was observed dynamically using confocal microscopy (Fig. 4.6B). Two distinct layers of expanded mucilage were observed. A third mucilage layer adjacent to the seed coat reported by Yu *et al.*,[9] was not observed. The two mucilage layers, L1 and L2, have distinct structural features. L1 is the first to expand; it lacks clear structure and much of the Calcofluor White staining is associated with this layer. The expansion of L2 from the seed occurs soon after L1 but the sea anemone-like structures (Fig. 4.6B) are not observed until 2 min post imbibition. By 15 min, L1 has dispersed into the surrounding aqueous environment and by 20 min L2 has expanded in its entirety (Fig. 4.6B).

Discussion

Mucilage polysaccharide accumulation in the MSCs of *P. ovata* seeds follows a different developmental pattern to that occurring in the MSCs of *Arabidopsis*. The mechanism by which different cell layers are converted into seed tissues and the possible remodelling thereafter appears to be of central importance for MSC development in *P. ovata*. At some point during mid-development and perhaps after polysaccharide accumulation is complete, we propose that the MSC radial cell walls break down and collapse in a concertina-like fashion. The collapse is potentially to be driven by the outward pressure of the rapidly expanding embryo and endosperm tissues pushing the MSC outer walls against the inner capsule surface, releasing the accumulated mucilage polysaccharides into an amorphous layer that becomes sandwiched between the remnant distal and basal MSC walls (Fig. 4.2). The process of radial wall remodelling and/or disintegration may already be beginning by 6/7 DPA where discrete labelling present earlier in development is absent or has become non-specific and amorphous (Fig. 4.3C1-3 and 4.3F1-3). This is particularly evident for the

CBM3a labelling (Fig. 4.3F1-3). This is unlike the presence of the mucilage polysaccharides contained within intact discrete cells of the *Arabidopsis* (Fig. 4.4C and 4.4F) and flax[36] mature seed coats. From late development onwards it is clear that the MSCs of *P. ovata* do not contain a columella (Fig. 4.4B) and our hypothesis is that instead, laminated layers of dehydrated mucilage polysaccharides are present, following radial MSC wall disintegration, between the remnant distal MSC walls, inner capsule wall and the expanded endosperm tissue (Fig. 4.2 and 4.7B). At seed maturity when released from the dehiscent capsule, the dehydrated and highly compressed mucilage polysaccharides, originating from the obliterated MSC cells, (Fig. 4.2H, 4.4H and 4.7C) form a dense layer over the seed surface (Fig. 4.2C and 4.6C). Cross sections of the dry mature seed shows that the thickness of this mucilage layer ranges from 10–18 μm compared to the 80-90μm thickness of the MSCs at full elongation at 7 DPA (Fig. 4.2). This supports the compression of the MSCs as the seed matures, after which point the layer is so dense that the constituent polysaccharides do not label with monoclonal antibodies that bind well to the seed mucilage when expanded (Phan *et al.,*[11]; Fig. 2H).

In our SEM analysis of mature seeds, we observe a stark contrast in surface appearance before and after hydration (Fig. 4.4). After mucilage is hydrated and allowed to dry without fixation, we were no longer able to observe the wrinkled surface or characteristic hexagonal shapes of the underlying distal MSC wall remnants (Fig. 4.4D-E). We suggest that while the distal walls may have undergone a similar process of remodelling/weakening to the radial walls, they were protected from crushing as they lie perpendicular to the outward force of the expanding endosperm, pushed flat against the inner capsule surface, and thus remain present and visible in the mature seed. However these distal wall fragments are thin, not reinforced with cellulose (Fig. 4.3F1-3) and appear to be rich in pectin (Fig. 4.3C1-3) suggesting that they may be highly

soluble. We have previously observed 'hexagonal platelets' that stain strongly with Ruthenium Red to be released from *P. ovata* seeds very early in the hydration cascade and rapidly disintegrate or dissolve (Phan *et al.* [11], Fig. 1H). We suggest that these structures are the soluble remnants of the distal MSC walls. These are different to other cellulose-staining structures like the mucilage discs of the *Arabidopsis* mutant *fly1*[44] or plate cells of other *Plantago* species (Phan *et al.* [11], Fig. 1I-P; Cowley *et al.* unpublished data) which persist through mucilage hydration. When hydrated mucilage is left to dry back onto the seed (Fig. 4.4D and E), the distal MSC wall fragments may have already dissolved/disintegrated and are thus no longer discernible, so the hexagonal shapes are lost, unlike similarly treated *Arabidopsis* seeds which retain the lower portion of the ruptured MSCs (Fig. 4.4F). The still soft layer of mucilage polysaccharides released by the putative rupture of the *P. ovata* MSC radial walls in later development may also contribute to the polarity of striations on the dorsal side of the mature seed (Fig. 4.4A). This could occur as the proximal end of the seed is under more compression from the capsule wall, which imprints onto the surface of the polysaccharide layer as it dehydrates. Although the distal end of the seed also comes into contact with the capsule, at this end it does not adhere so tightly and is observed to readily detach when gently touched, thereby enabling seed dispersal. Interestingly, Boesewinkel[45] suggests that the seed coat of *Linum usitassimum* is also polar and that the 'slime-forming matter' is deposited on the outer surface of the epidermal seed coat cells. They also suggest that the cells underneath the outer epidermal seed coat cells, which are on the innermost layer of the inner integument, have thickened cell walls and are pigmented cells. These observations are strikingly similar to what we have observed in *P. ovata*; the mucilage is the outermost layer of the seed and is underlain by an intensely stained layer that may be pigment-rich (Fig. 4.2H). A similar structure was also described for *P. ovata* by Madgulkar *et al.*,[46]. These observations further

support our proposed mechanism of MSC development and disintegration, with the subsequent formation of a cell-free mucilage polysaccharide layer.

It is interesting to speculate about carbon flow through the *P. ovata* seed during development. There must be a balance between investment in maternal sporophytic tissue and the filial tissues i.e. the carbon supply must be split between mucilage polysaccharide biosynthesis and feeding the rapidly growing embryo and endosperm. It is possible that development of the MSCs from the outermost cell layer of the integument tissue, which is of maternal origin [31], could be favoured over zygotic development. This may explain our observation that MSC development and polysaccharide deposition for mucilage synthesis may occur independently of seed development since even developmentally-stalled and aborted seeds still make mucilage when imbibed (Fig. 4.5B1-5). While the specific architectures were different, two typical mucilage layers were recognisable and known *P. ovata* quality indicators[10], mucilage yield (Fig. 4.5C1) and heteroxylan content (Fig. 4.5C2) and composition (Fig. 4.5C3) were not significantly different to the wild-type ($p > 0.05$) showing that mucilage synthesis was uninterrupted. Garcia *et al*.,[47] demonstrated that development of the maternally-derived integument and the zygotic embryo and endosperm are coordinated to determine final Arabidopsis seed size. Of the various developmentally-impaired *P. ovata* seeds analysed here, none of them reached the same size as the wild-type, suggesting that although integument development and mucilage polysaccharide biosynthesis can occur independently of embryo and endosperm development, some coordination is needed in order to establish the correct size of the mature seed. It is possible that without outward pressure from the growing endosperm not only will the seed not reach mature size, but the MSC contents may not be correctly arranged and/or pressurised causing the diminished mucilage expansion shown here. Unlike *Arabidopsis*, several *Plantago* species are reported to contain specialised

nutrient transfer structures called haustoria that develop from the embryo sac. Haustoria have been characterised in the seeds of *P. lanceolata*[48], *P. major*[49], and *P. coronopus*, while those in *P. pumila* (also known as *P. exigua*) and *P. lagopus* are described briefly by Johri *et al*.,[50]. Cooper[48] observed haustoria "penetrating and digesting the outer portion of the ovule adjacent to the developing endosperm", in *P. lanceolata*, and this corresponds to the layer we have designated integument in *P. ovata*. Haustoria may function to directly connect the embryo and endosperm to surrounding integument cells, allowing a networked supply of carbon for growth and development. Eventually, the growing endosperm of *P. lanceolata* absorbs most of the surrounding integument and leaves only a few cell layers that lose most of their cytoplasmic contents and are squashed thin at maturity. Although Cooper[48] did not specifically state what this papery-thin layer could be, it is likely that they were describing the mucilage polysaccharide layer. Haustoria have not yet been reported in *P. ovata*, and we were unable to confirm their presence or absence in the developmental sections presented here. Thus, it remains unclear what mechanisms control the fate of the integument cells and this will be informative to investigate in the future.

The microscopy images of the developing MSCs (Fig. 4.2) raise questions regarding gene expression and regulation during the different developmental stages. During the early stages of MSC development at 3–5 DPA where rapid cell expansion is observed, the enzymes that are present may be synthesising the backbone of the immature pectin polymer i.e. one that still requires post-synthesis modification to become hydrophilic, as observed in *Arabidopsis*[51–53] and early stages of heteroxylan synthesis may also be occurring. The shift in the esterification status of the pectin in both the MSCs and the integument cell walls is clearly demonstrated in Figure 4.3 and Supplementary Figure 4.2, where tissues at anthesis label differently when compared

to four days later. However, at this magnification it is not possible to unequivocally define the location of the pectin – whether it is in the actual wall of the MSCs or in the apoplast and just pushed tightly against it will require detailed examination at the TEM level. There is a clear increase in the amount of crystalline cellulose in the walls of both the MSCs and the integument cells when tissues at anthesis and later at 4 and 7 DPA are compared. At these early stages there is minimal binding by the LM11 antibody which detects xylan suggesting there is no xylan present yet, even in the cell walls rather than the apoplast (Supplementary Fig. 4.2B, D and F). This lack of signal is consistent with our previous analyses, where later in development (13 DPA) many of the genes involved in xylan biosynthesis are transcriptionally active, such as the GT61, UXS, and UAM genes[11] which is only two days before the 15 DPA stage when the MSCs appear misshapen and possibly on the verge of extensive disintegration (Fig. 4.2G). It is possible that at 13 DPA these genes are more involved in polysaccharide post-synthesis modification, modifying the sidechain density and/or length in xylan and pectic polymers to enable correct mucilage expansion and final architecture upon imbibition in aqueous environments, but at this stage details are unknown. Future experiments are aimed at establishing the transcript abundance of gene sub-sets involved in synthesis of the pectic backbone including GT8, GAUT1 and GAUT7[54] members, the addition of minor substituents onto the pectin backbone and the biosynthesis of nascent and mature heteroxylan types. A precise temporal series employing laser capture microdissection of the developing MSCs, followed by RNAseq analysis will prove invaluable in this context.

Our microscopy analyses reveal that, in contrast to *Arabidopsis*, the seed mucilage release mechanism of *P. ovata* may be a physical process not dependent on cellular rupture followed by extrusion (Fig. 4.6B). Hence, for this species we suggest that it is more appropriate to describe the mechanism as an expansion rather than an

extrusion, similar to the extension of a concertina, where the mucilage starts to expand into the aqueous environment as it hydrates from the wrinkled appressed polysaccharide layer on the seed surface. Data demonstrating the change in mucilage composition and structure over time (Fig. 4.6) support this type of expansion process. The driving forces behind expansion of *P. ovata* seed mucilage could be derived from the differential hydrophilicity of the constituent mucilaginous polysaccharides. Pectin is most abundant in the first layer of mucilage to expand, L1 (Fig. 4.6B) and previous studies have described the outermost layer of the expanded seed mucilage to be a highly soluble, pectin-rich fraction[9,12,55]. In *P. ovata*, this seed mucilage fraction was easily extracted using cold water[9,10] and we propose that its function is to act as a primer, initiating mucilage expansion, and providing a hydration cascade triggering the swelling of the more gel-like and structurally-complex heteroxylan polymers located in subsequent fractions/layers (Supplementary Fig. 4.6). Compositional data supporting such patterns of polymer release have been reported previously[9,10,13], and now a model to illustrate this process, driven by polarised deposition and then expansion, is presented in Figure 7. To fulfil such a role the pectin-enriched fraction must be synthesised and/or deposited first into the distal end of the MSC, anchoring the mucilage to the seed to form L1, after which the structural polymers, including heteroxylan, are synthesised and/or deposited into the basal end of the cell to make L2 (Fig. 6A). A similar spatio-temporal pattern of polysaccharide synthesis and deposition was recently described by Miart *et al.*[36] who showed that RG-I (pectin) was synthesised in the two outermost layers of *L. usitatissimum* MSCs prior to synthesis of other polysaccharides in the layers beneath. The authors hypothesised that the arabinoxylan, xyloglucan and cellulose polysaccharides synthesised later in the inner layers provided a structural element that pressurised the outermost contents, enabling efficient mucilage release and anchoring the mucilage to the seed. Similarly, the

heterotypic interactions of various polymers including branched xylan, cellulose and arabinogalactan proteins are important for effective mucilage release and adherence in *Arabidopsis*[3,5,6,8,56,57]. In support of this temporal sequence of events, real-time qPCR analysis of cDNA from developing *L. usitatissimum* integument tissue shows that genes involved in pectin biosynthesis are transcriptionally active prior to those associated with xylan biosynthesis (M. Aubert, M. Tucker, R. Burton, University of Adelaide, unpublished data). The mucilage component of *P. ovata*, and likely many other species, is a complex network of heterogeneously distributed polysaccharides. Each polymer must be synthesised, deposited, and potentially modified, in a specific sequence and location during seed development to be able to fulfil the required mechanical functions enabling mucilage release, and supporting the structural functions of the material once it extends from the seed surface. The process of mucilage polysaccharide biosynthesis and deposition into the MSCs must therefore be a tightly regulated process, about which we have much to learn.

In future work, it would be valuable to characterise the MSCs of *Plantago* species such as *P. cunninghamii* that we have already confirmed to possess a similar seed surface arrangement to *P. ovata*, but that has a different expanded mucilage architecture[11]. Our preliminary characterisation of the MSCs of *P. ovata* has generated further questions regarding the biosynthesis and deposition of mucilaginous polysaccharides: how, where, and in what order are these polymers transported and deposited into the MSCs? What genes and regulatory elements are controlling this highly complex process? And what drives the fate of the integument cells? Should we be looking for signs of programmed cell death or a suite of cell wall degrading enzymes in this tissue? Combining further histological analysis of the developing seeds, with a focus on the MSCs and the integument tissue, with characterisation of the temporal regulation of mucilage biosynthetic transcripts may begin to answer some of these

questions. Our whole mount immunolabelling data suggests that hydrated heteroxylan is distributed in a specific digit-like pattern whilst immunolabelling of seed sections show that the heteroxylan and pectin are homogenously distributed throughout the expanded seed mucilage (Phan *et al.* 2016). It remains unclear how these polymers are deposited and distributed in both the developing MSCs, the mature mucilage polysaccharide layer, and the final expanded material. Thorough investigation of the developing MSCs in *P. ovata* may begin to shed some light upon these questions and allow us to fine tune our hypothetical model, whilst eventually providing tools to allow manipulation of the mucilage quantity and quality that could directly impact downstream applications and economics of psyllium use.

Materials and Methods

Plant materials and growth

Wild-type *Plantago ovata* and gamma-irradiated *P. ovata* mutant 69-1 were obtained from a population previously generated by Tucker *et al.,*[43]. Three 69-1 sister lines at M4 were tested to show that >95% of the seeds in each sister line displayed a developmentally delayed phenotype. The mutant line has not yet been backcrossed to wild type.

Plants were grown as per Phan *et al.,*[11]*.* To stage wild-type fruit development, fruits with freshly emerged anthers (erect and bright-yellow in colour) were marked and tagged with the date in order to harvest at the relevant day post-anthesis (DPA).

Observing *P. ovata* expanded seed mucilage

Ruthenium red: Mature *P. ovata* seeds were individually placed onto microscopy slides in a ruthenium red solution at a concentration of 0.01% (w/v) (ProSciTech, C075, Australia). Seeds were observed under a Zeiss Stemi 2000-C dissecting microscope

with an attached AxioCam ERc 5s camera. Seeds with impaired development were selected from the mutant line 69-1[43]

Time-lapse: Mature *P. ovata* seeds were prepared as per Yu *et al*.,[9]. In brief, dry mature *P. ovata* seeds were soaked overnight in stain solution comprised of 0.1% w/v Calcofluor White (Fluorescent Brightener 28, Sigma-Aldrich) and 0.4% w/v Direct Red 23 (Sigma-Aldrich) diluted in 80% ethanol. The seeds were removed from the staining solution and allowed to air dry before being adhered with a cyanoacrylate adhesive to the centre of a Petri dish. The Petri dish was mounted onto the stage of a Nikon A1R Laser Scanning Confocal with DS-Ri1 CCD camera and imaged prior to the addition of deionised water onto the seed at time = 0. Images were captured for 20 min in total at 1 min intervals.

Fixation, embedding, and sectioning of *P. ovata* developing fruit

Samples requiring fixation, embedding, and sectioning were processed as per Burton *et al*.,[58] and embedded tissue was sectioned at 1μm on an Ultramicrotome (Leica, EM UC6) using a diamond knife (DiATOME, Nidau, Switzerland). For non-aqueous fixation, PBS was replaced with an 80% ethanol solution. Sections were stained with Toluidine Blue (epoxy tissue stain, used undiluted, ProSciTech, C149, Australia). Sections were imaged under transmitted light differential interference contrast (DIC) using a Zeiss Axio Imager M2 (Carl Zeiss, Germany) fitted with a AxioCam MRm3 monochrome camera.

For fluorescence images, samples were fixed, embedded, and sectioned as above for non-aqueous fixation. Survey sections were stained with epoxy tissue stain (used undiluted, ProSciTech, Australia). For immunofluorescence, sections were incubated with monoclonal antibodies raised against pectin (LM19 and LM20) and arabinoxylan (LM11) (PlantProbes Leeds, UK) followed by an appropriate AlexaFluor 555 secondary

antibody (Invitrogen, USA). The His-tagged carbohydrate-binding module CBM3a (PlantProbes, Leeds, UK) was used with a triple indirect immunofluorescence labelling procedure as described previously[11,59]. Sections were counterstained using Calcofluor White (Fluorescent Brightener 28; Sigma-Aldrich) and mounted in glycerol. Images were obtained using an AxioCam 105 color camera fitted to a Zeiss fluorescence microscope (Axio Imager M2, Carl Zeiss, Germany) with 254/432 nm excitation/emission wavelength for Calcofluor White and 553/568 nm excitation/emission wavelength for LM11/LM19/LM20/CBM3a.

Scanning Electron Microscopy

Mature seeds of *P. ovata* and *Arabidopsis thaliana* ecotype *Columbia-0* were air-dried before and after mucilage hydration then sputter-coated with platinum at a thickness of 5 nm. Seeds were imaged at a working distance of 7.5 mm with an accelerating voltage of 3 kV using a Philips XL20 Scanning Electron Microscope (SEM) following Phan *et al.*,[11].

Mucilage extraction and compositional analysis

For temporal mucilage analysis, mucilage was collected by placing 1 g mature seeds into a wide-mouth sieve, placed in a water bath containing 40 mL of deionised water at room temperature with intermittent stirring. Fractions were collected at 5 min intervals by transferring the sieve and seeds into a fresh batch of deionised water. Mucilage extracted were freeze-dried to a constant weight and compositional analysis was conducted as per Hassan *et al.*[60]

For comparison of mutant 69-1 with the wild-type, mucilage was extracted from 40 seeds for 3 hr in 20 mL of deionised water heated to 80 °C and stirred vigorously on a heated magnetic stirrer. While still hot, the mucilage and seeds were transferred into a 50 mL tube and centrifuged for 10 min at 4000 rpm. The mucilage supernatant was

decanted into a new tube and freeze-dried to a constant weight. Yield per seed was calculated by dividing the freeze-dried mucilage mass by 40. Compositional analysis was conducted as per Hassan *et al.*[60]

Data availability

The datasets generated and/or analysed in this study are available from the corresponding author on reasonable request.

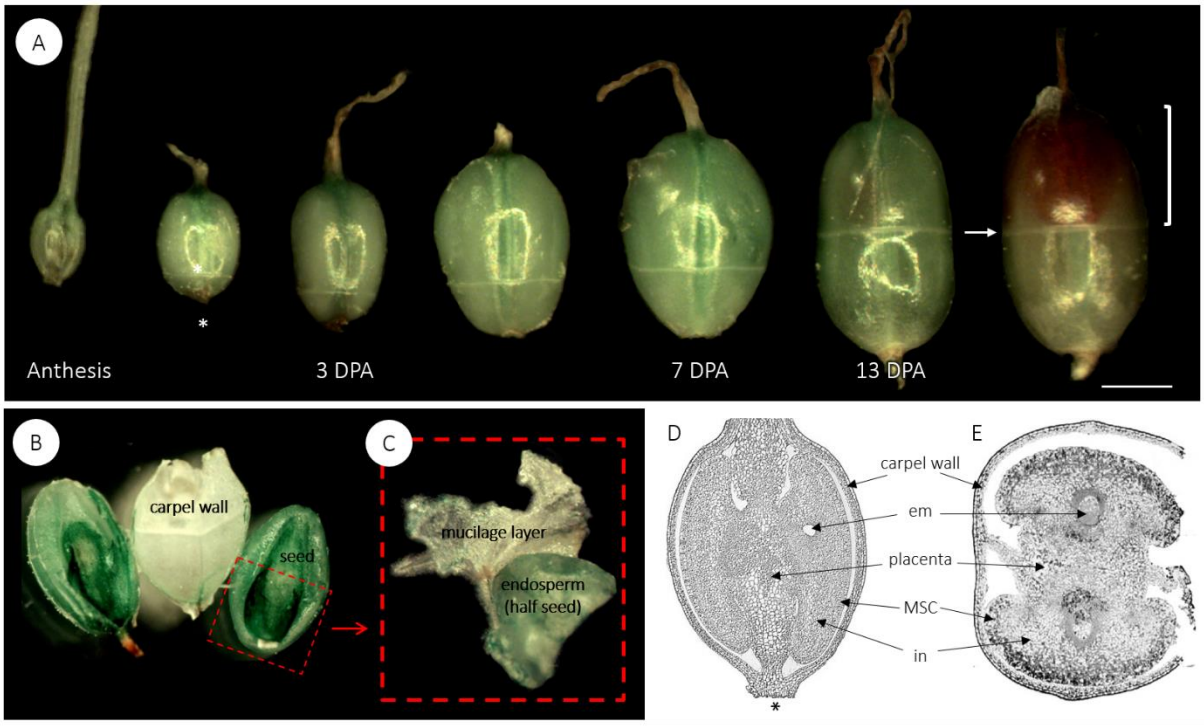

Figure 4.1. (A) The fruit development of *P. ovata*. Each fruit contains two ovules separated by placental tissue. *Plantago* species have a circumscissile capsule, also known as a pyxis. The arrow indicates the equator, where the zone of dehiscence is visible, the square bracket highlights the operculum, which detaches during dehiscence, and * indicates the end that joins the fruit to the rachis. Bar = 1 mm. **(B)** A dissected fruit at 13 DPA, showing two immature seeds and in **(C)** one of the seeds has been further dissected to show the mucilage polysaccharide layer, which has been peeled off the seed and is the remnant of the integument tissue. Longitudinal **(D)** and transverse **(E)** cross sections of a developing fruit at 7 DPA, stained with toluidine blue. em = embryo sac, MSC = mucilage secretory cells, in = integument.

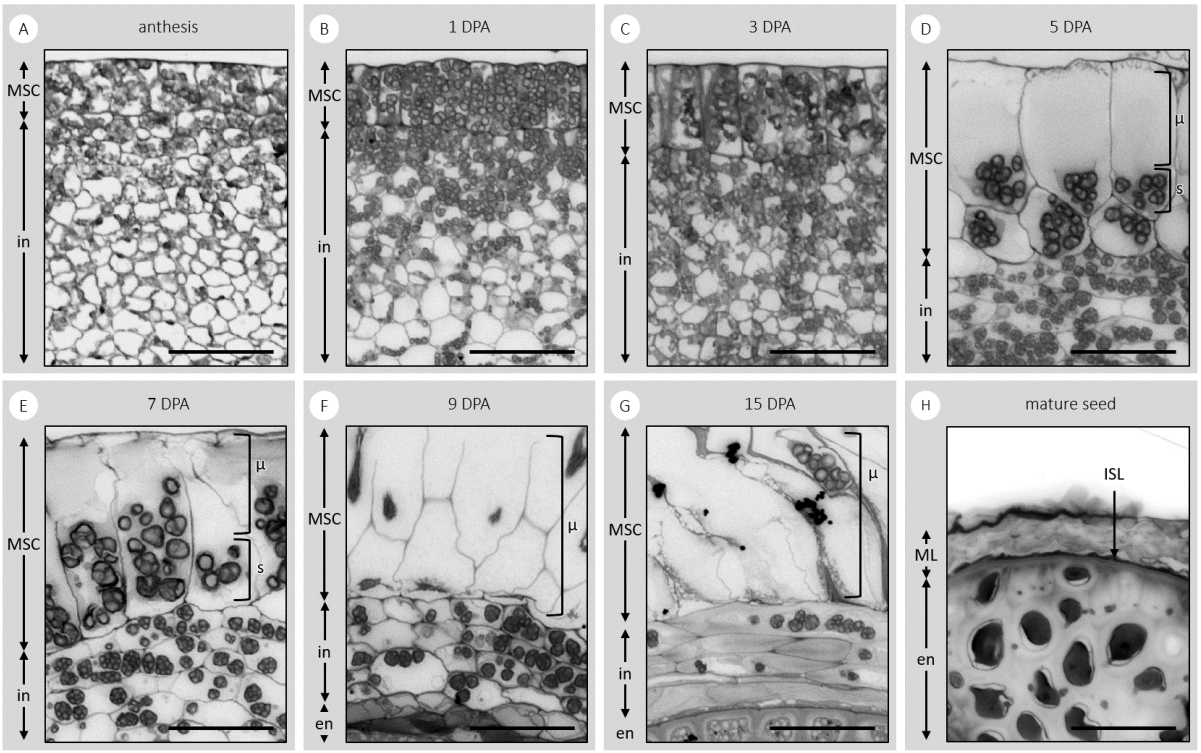

Figure 4.2. Toluidine blue-stained transverse sections of the developing integument of *P. ovata*. The sections show the tissues and components that are the: endosperm (en); integument (in); mucilage polysaccharides (μ); mucilage secretory cells (MSCs); mucilage polysaccharide layer (ML); intensely stained layer (ISL); and starch granules (s) at days post-anthesis (DPA). Scale bar = 50 μm.

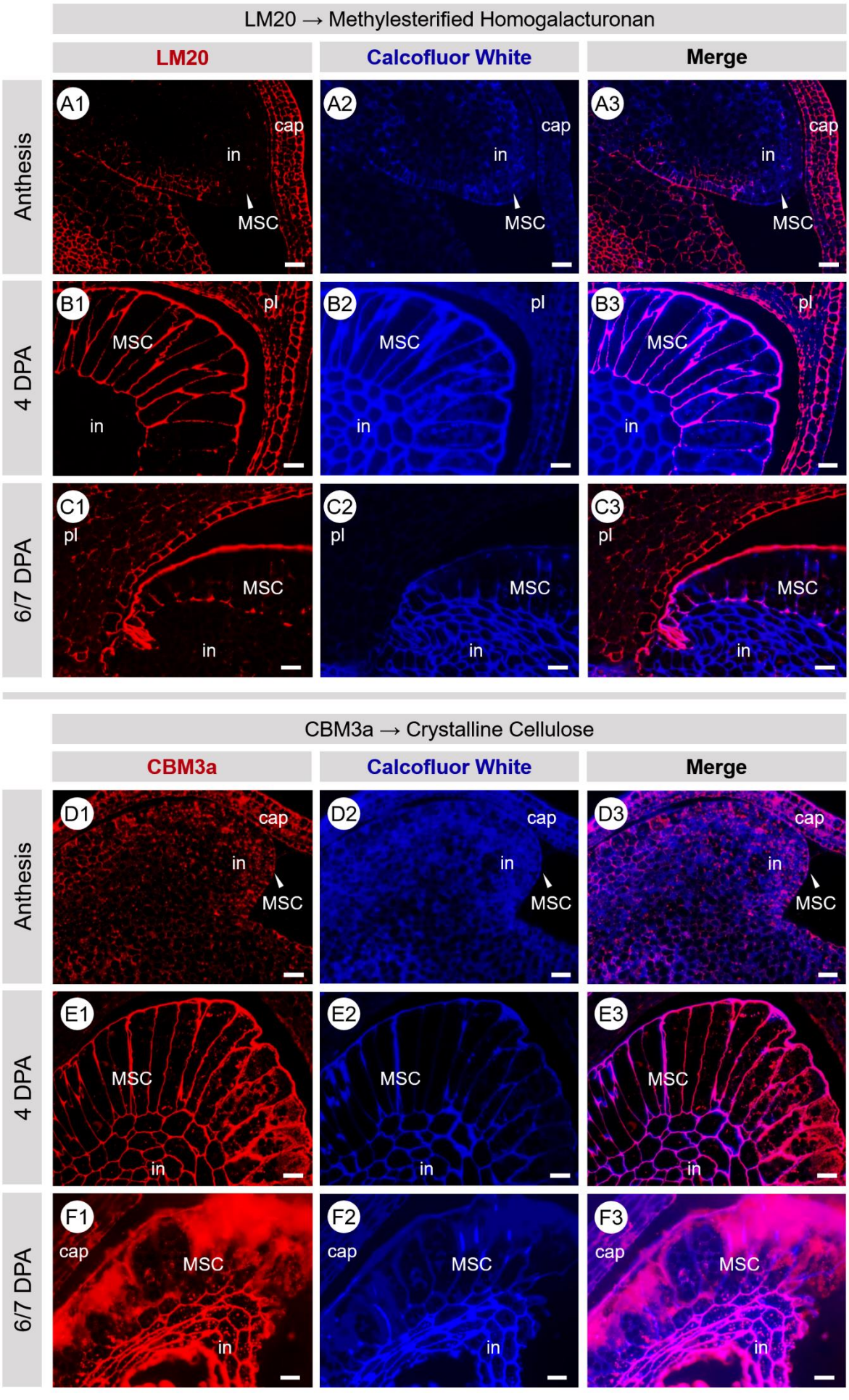
LM20 → Methylesterified Homogalacturonan
LM20
Calcofluor White
Merge
Anthesis
4 DPA
6/7 DPA
A1
A2
A3
B1
B2
B3
C1
C2
C3
cap
in
MSC
pl
CBM3a → Crystalline Cellulose
CBM3a
D1
D2
D3
E1
E2
E3
F1
F2
F3

Figure 4.3. Fluorescence micrographs of transverse sections of developing *P. ovata* seeds labelled with LM20 and CBM3a (red/pink) at anthesis **(A** and **D),** at 4 DPA **(B** and **E)** and at 6/7 DPA **(C** and **F)**. MSC cell walls show strong labelling of highly methylesterified HG (LM20) and crystalline cellulose (CBM3a) that diminishes in intensity and organisation as development/mucilage polysaccharide accumulation continues and/or as MSC cell walls disintegrate. Samples are counter-stained with calcofluor white (blue). Scale = 20 µm. DPA = days post anthesis

; HG = homogalacturonan; MSC = mucilage secretory cell; in = integument; pl = placenta; cap = capsule.

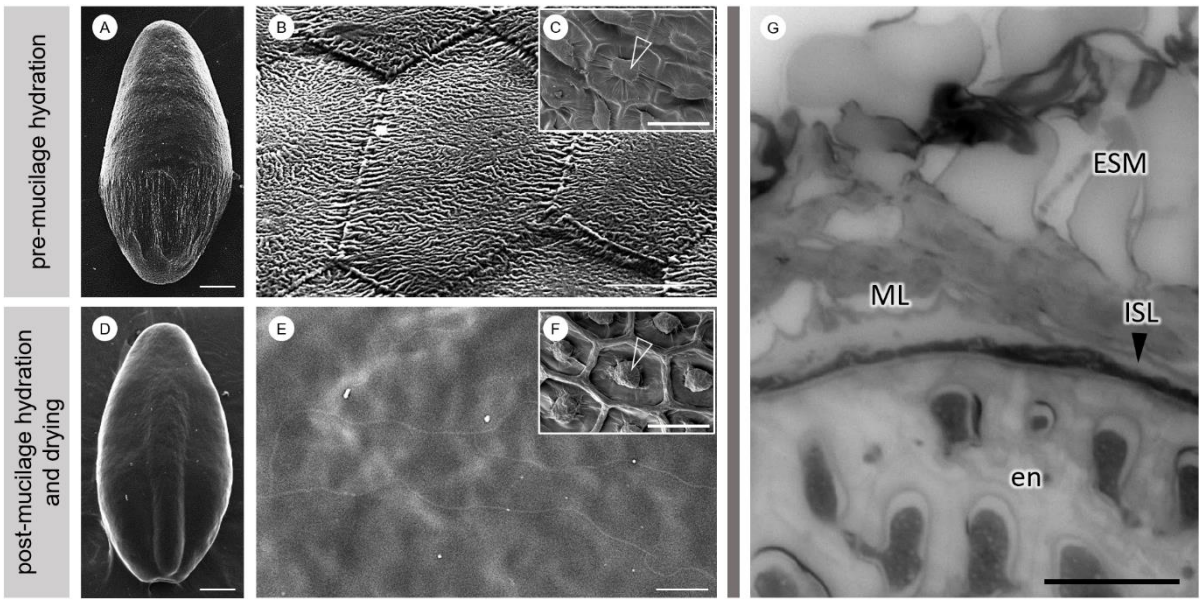

Figure 4.4. Scanning electron micrographs show that *P. ovata* does not contain a columella **(A** and **B)**. Inset **(C)** shows a scanning electron micrograph of the seed surface of *Arabidopsis* with the columella structure indicated with an arrowhead. In *P. ovata,* the wrinkled texture of the dry mucilage polysaccharide layer (ML) and hexagonal shapes of the distal MSC wall remnants disappear after mucilage is hydrated and allowed to dry back onto the seed surface, unfixed **(D** and **E),** leaving it extremely smooth. This contrasts with Arabidopsis where the distinct columella structure persists and remains clearly visible after the same process **(F)**. Toluidine blue-stained cross sections of the mature seeds fixed in aqueous fixative **(G)** reveal that the seed mucilage (ESM) expands from the ML, which sits on top of an intensely stained layer (ISL) that separates the mucilage polysaccharide layer from the endosperm. en = endosperm. Scales = A, D, G = 500 μm; B, E, H = 50 μm; C, F = 30 μm.

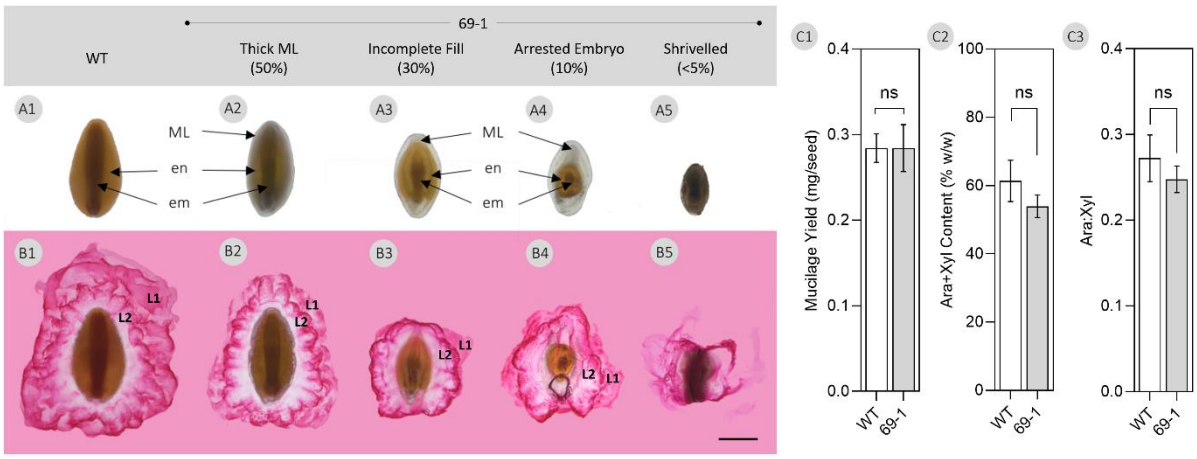

Figure 4.5. (A) Seeds were selected from developmentally-impaired gamma-irradiated *P. ovata* mutant 69-1 generated previously by Tucker *et al*. (2017). When these seeds were imbibed in a ruthenium red solution (0.01% w/v) for 10 min at room temperature **(B)** mucilage expanded from all seeds with different architectures but two typical mucilage layers (L1 and L2) were present. em = embryo; en = endosperm; ML = mucilage layer; WT = wild-type. Scale bar = 1 mm. (**C**) Analysis of mucilage yield and composition revealed no significant difference (ns) from the wild-type *(p* > 0.05, Student's t-test).

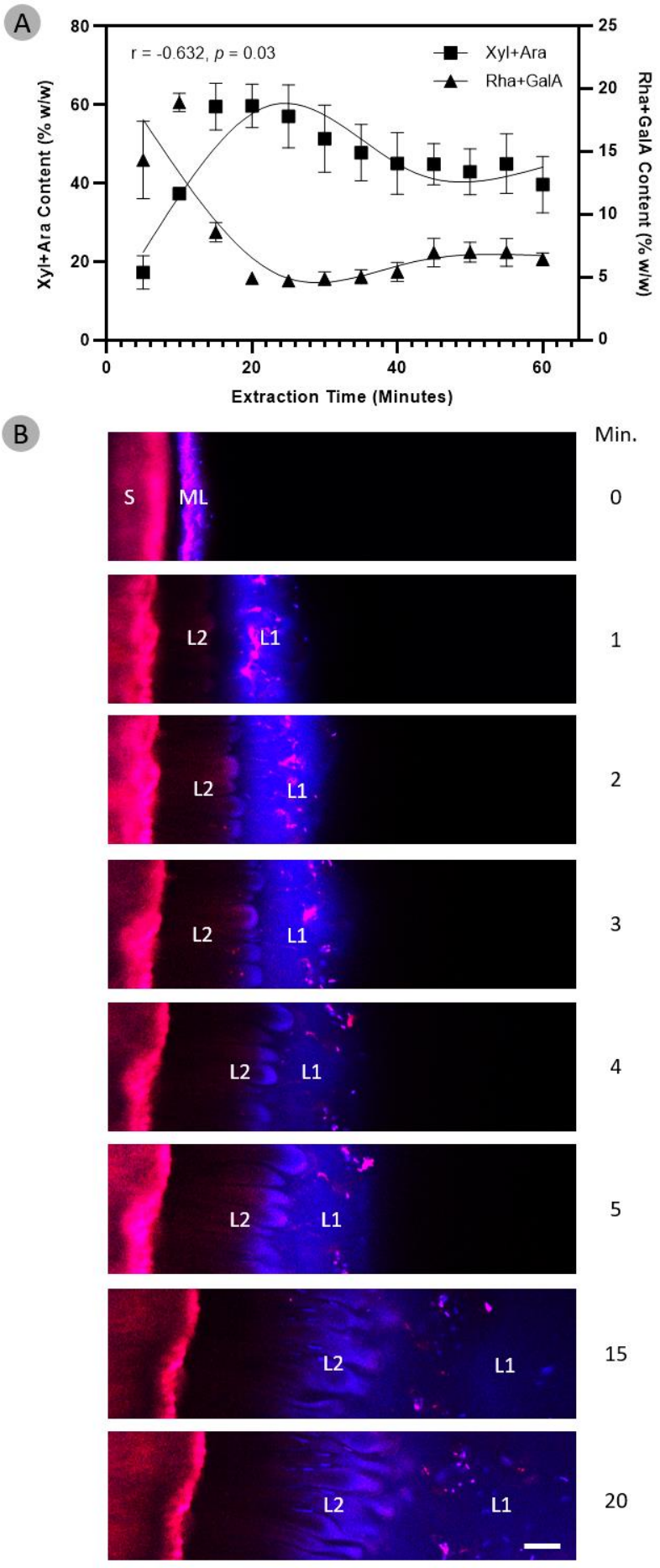
A
r = -0.632, p = 0.03
Xyl+Ara
Rha+GalA
Xyl+Ara Content (% w/w)
Rha+GalA Content (% w/w)
Extraction Time (Minutes)
B
Min.
S
ML
L2
L1
0
1
2
3
4
5
15
20

Figure 4.6. The composition and structure of seed mucilage changes over the course of its expansion. **(A)** Compositional analysis reveals pectin-associated monosaccharides (rhamnose and galacturonic acid) are most abundant during the initial expansion of mucilage and rapidly decrease in concentration thereafter. Heteroxylan-associated monosaccharides (xylose and arabinose) are also present in the initial expansion of mucilage, in almost similar amounts to pectin. Contrasting to pectin, the heteroxylan-associated monosaccharides rapidly increase in concentration and go on to make up the bulk of total expanded mucilage. Data have been fitted with cubic spline curves to highlight trends. **(B)** The dynamics of seed mucilage expansion in mature *P. ovata* seeds were observed in real-time over a period of 20 min using confocal microscopy. Seeds were pre-stained with 0.4% Direct Red 23 and 0.1% Calcofluor White. Upon imbibition in water, a sudden “explosion” of an extremely hydrophilic and non-structured mucilage layer emerges (L1). Following L1, a more structured and anemone-like layer of mucilage expands outwards (L2) and by 20min, L2 has reached its maximal expansion distance and L1 has mostly dissipated into the surrounding aqueous environment. Scale bar = 100 μm. S = mature seed, ML = mucilage polysaccharide layer on dry seed, L1 = layer 1, L2 = layer 2 N.B. time 0 min is a dry seed that has been pre-stained, water was added after this image was taken.

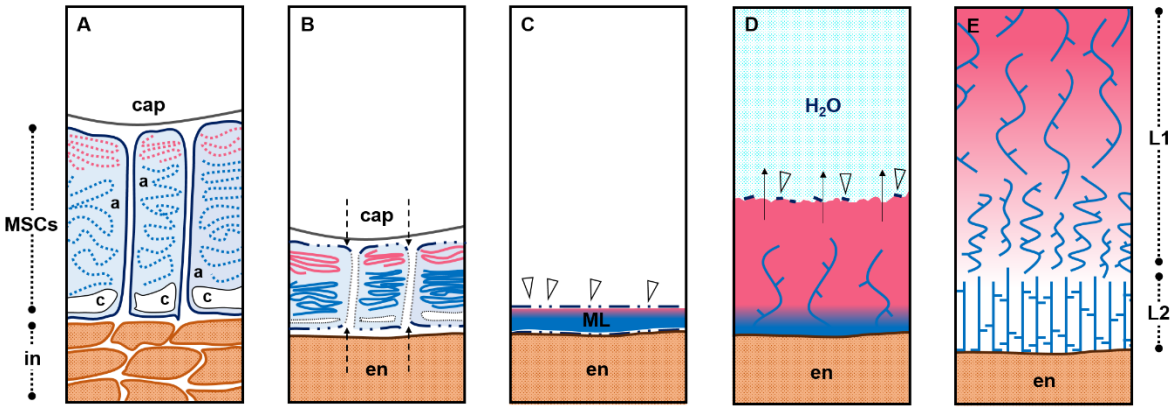

Figure 4.7. A proposed model of the polysaccharide deposition and mucilage expansion mechanism in *P. ovata*. **(A)** Mucilage polysaccharides pectin (pink) and heteroxylan (blue) are polarly synthesised and deposited into the outer apoplast (a) of mucilage secretory cells (MSCs), **(B)** which become compressed between the endosperm (en) and capsule wall (cap), obliterating the radial walls and releasing their contents into a **(C)** continuous laminated cell-free mucilage polysaccharide layer (ML) on the external seed surface when released from the capsule. **(D)** Upon exposure to an aqueous environment, the hydrophilic mucilage starts to expand outwards from the seed surface. The first layer to expand is rich in extremely hydrophilic and soluble pectin and is topped by fragile remnants of the distal MSC walls (arrowheads) that dissolve as hydration continues. This layer works to provide a hydration cascade to initiate and jumpstart hydration and swelling of the more gel-like, less hydrophilic polymers. **(E)** A hypothesised distribution of mucilaginous polysaccharides. The pink gradient is indicative of the distribution of pectin which is restricted to the periphery (or 'mucilage expansion front') of the expanded seed mucilage (as per Fig. 6) whilst the xylan polysaccharides (blue strands) are evenly distributed (Fischer *et al.*, 2004; Guo *et al.*, 2008; Yu *et al.*, 2017). In L1, the enrichment of pectin may proportionally modulate the solubility/extractability of xylan while in L2, pectin is not present and thus xylan polymers form a more robust, gel-like layer. in = integument; c = cytoplasm.

Supplementary Figure 4.1. *Plantago ovata* grown in a glass house. **(A)** shows a 2.5-month-old plant (ruler = 30 cm) and **(B)** shows 3.5-month-old plants with fully set inflorescences where the seed heads are almost completely dry and ready for harvesting. **(C)** shows a single inflorescence at ~3 months old, scale = 1 cm.

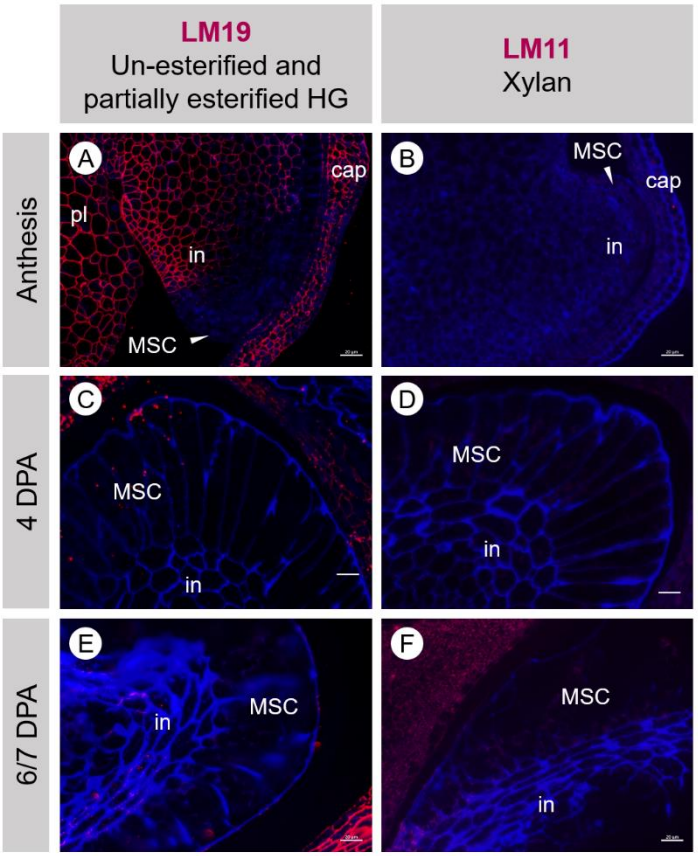

Supplementary Figure 4.2. From anthesis to the beginning of mucilage secretory cell (MSC) disintegration, minimal labelling of un-esterified/partially esterified homogalacturonan (HG) (LM19) and β-1,4-linked xylan backbone (LM11) is observed in developing seed tissues. Scale bar = 20 μm; MSC = mucilage secretory cell; in = integument.

Supplementary Figure 4.3. The mature seed of *P. ovata* has a deep scar on the proximal side**,** a remnant of where the seed was attached to the placental tissue and now forms the cymbiform shape of the seed.

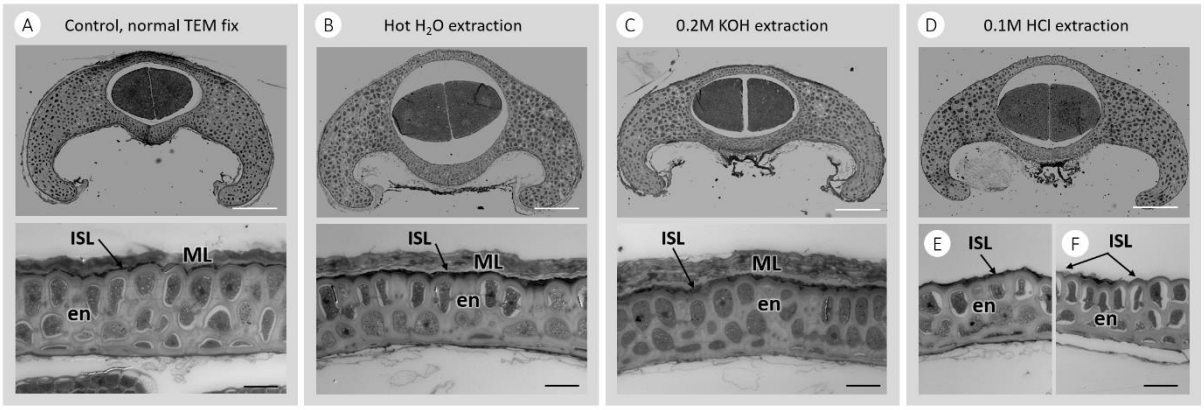

Supplementary Figure 4.4. Toluidine blue-stained transverse sections of mature *P. ovata* seeds after different methods of mucilage extraction. The expanded seed mucilage has been removed from the control **(A)** during the sequential washing steps required in tissue fixation, some mucilage remains tightly adhered to the seed after hot water extraction **(B)** or treatment with 0.2M KOH **(C).** Treatment with 0.1M HCl removed all the mucilage material **(D)** and **(E)** plus some sections of the intensely stained layer **(F).** All extractions were performed at 60°C for 3 hr on a magnetic stirrer. en = endosperm; ML = mucilage layer; ISL = intensely stained layer. Bars for whole seed = 200 μm, and the endosperm and mucilage layer = 20 μm.

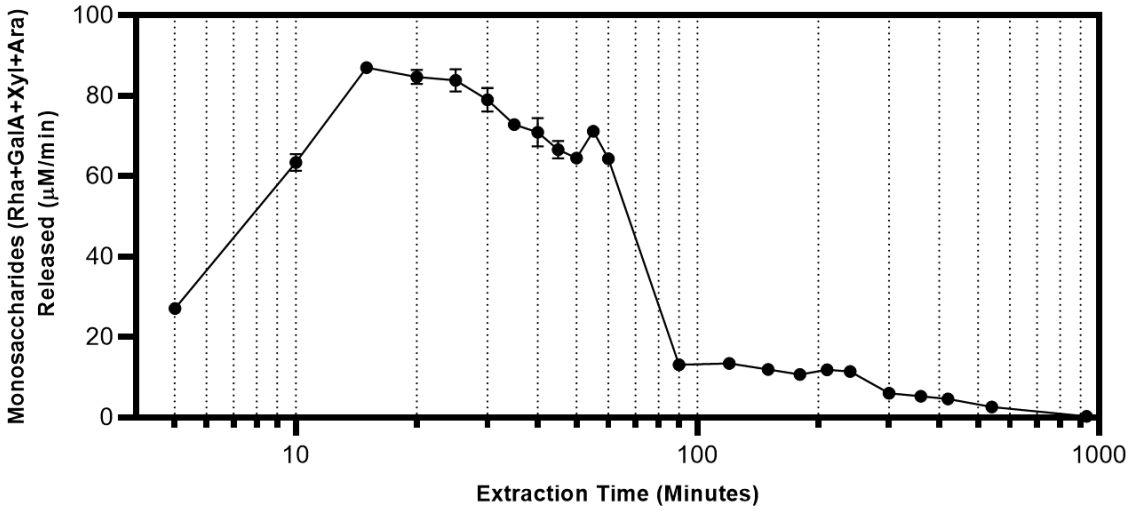

Supplementary Figure 4.5. Extraction of mucilage up to 60 mins from the start of imbibition effectively captures all major stages of *P. ovata* mucilage release. Semi-log plot shows that mucilage-related monosaccharide release tapers off sharply after 60 mins and only small quantities of monosaccharides are released in the subsequent 14.5 hours (870 mins).

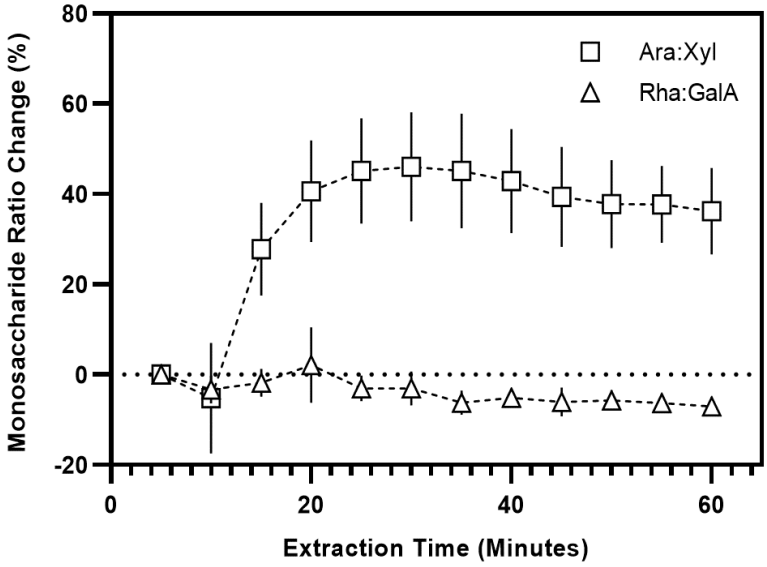

Supplementary Figure 4.6. While the pectin Rha:GalA ratio remains relatively unchanged between sequentially isolated fractions, the Ara:Xyl ratio gradually increases, suggesting increasing polysaccharide complexity through time. The monosaccharide ratio difference at an extraction time-point is calculated relative to the initial monosaccharide ratio at 5 min i.e. (initial ratio, 5 min / ratio at a timepoint, x min).

Declarations

Acknowledgements

The authors would like to thank Associate Professor Matthew R Tucker for ongoing scientific discussions. The authors acknowledge the facilities, and the scientific and technical assistance, of the Australian Microscopy & Microanalysis Research Facility at Adelaide Microscopy, The University of Adelaide, Waite Campus, for their assistance in using the SEM and confocal microscope and Dr Long Yu for assistance in developing a method to stain the mucilage of mature seeds. This work was supported by the Australian Research Council (ARC) Centre of Excellence in Plant Cell Walls (CE110001007) and Plant Energy Biology (CE140100008). JP was supported by a University of Adelaide's CJ Everard PhD Scholarship, a Grains Research and Development Corporation (GRDC) scholarship and a SARDI Bursary, JMC was supported by the Australian Government's Research Training Program and LH was supported by a University of Adelaide's Adelaide Graduate Research Scholarship.

Author contributions

JP and RAB conceived the study. JP, JMC, KAN, LH and LAO prepared materials and performed experiments. All authors contributed to the data analysis and interpretation. JP, JMC and RAB wrote the manuscript. All authors approved the final manuscript.

References

1. Phan, J. L. & Burton, R. A. New Insights into the Composition and Structure of Seed Mucilage. *Annu. Plant Rev. Online* **1**, 1–41 (2018).
2. Macquet, A., Ralet, M.-C., Kronenberger, J., Marion-Poll, A. & North, H. M. *In situ*, chemical and macromolecular study of the composition of *Arabidopsis thaliana* seed coat mucilage. *Plant Cell Physiol.* **48**, 984–99 (2007).
3. Harpaz-Saad, S. *et al.* Cellulose synthesis via the FEI2 RLK/SOS5 pathway and CELLULOSE SYNTHASE 5 is required for the structure of seed coat mucilage in *Arabidopsis*. *Plant J.* **68**, 941–953 (2011).
4. Yang, B. *et al.* TRM 4 is essential for cellulose deposition in Arabidopsis seed mucilage by maintaining cortical microtubule organization and interacting with CESA 3. *New Phytol.* **221**, 881–895 (2019).
5. Yu, L. *et al.* CELLULOSE SYNTHASE-LIKE A2, a glucomannan synthase, is involved in maintaining adherent mucilage structure in *Arabidopsis* seed. *Plant Physiol.* **164**, 1842–1856 (2014).
6. Voiniciuc, C., Günl, M., Schmidt, M. H.-W. & Usadel, B. MUCI10 produces galactoglucomannan that maintains pectin and cellulose architecture in *Arabidopsis* seed mucilage. *Plant Physiol.* **169**, 403–420 (2015).
7. Hu, R. *et al.* Xylan synthesized by Irregular Xylem 14 (IRX14) maintains the structure of seed coat mucilage in Arabidopsis. *J. Exp. Bot.* **67**, 1243–1257 (2016).
8. Hu, R. *et al.* Irregular xylem 7 (IRX7) is required for anchoring seed coat mucilage in Arabidopsis. *Plant Mol. Biol.* **92**, 25–38 (2016).
9. Yu, L. *et al.* Multi-layer mucilage of Plantago ovata seeds: Rheological differences arise from variations in arabinoxylan side chains. *Carbohydr. Polym.* **165**, 132–141 (2017).
10. Cowley, J. M. *et al.* A small-scale fractionation pipeline for rapid analysis of seed mucilage characteristics. *Plant Methods* **16**, 1–12 (2020).
11. Phan, J. L. *et al.* Differences in glycosyltransferase family 61 accompany variation in seed coat mucilage composition in Plantago spp. *J. Exp. Bot.* **67**, 6481–6495 (2016).

12. Fischer, M. H. *et al.* The gel-forming polysaccharide of psyllium husk (*Plantago ovata* Forsk). *Carbohydr. Res.* **339**, 2009–2017 (2004).

13. Ren, Y., Yakubov, G. E., Linter, B. R., Macnaughtan, W. & Foster, T. J. Temperature fractionation, physicochemical and rheological analysis of psyllium seed husk heteroxylan. *Food Hydrocoll.* (2020). doi:10.1016/j.foodhyd.2020.105737

14. Jensen, J. K., Johnson, N. R. & Wilkerson, C. G. Arabidopsis thaliana IRX10 and two related proteins from psyllium and Physcomitrella patens are xylan xylosyltransferases. *Plant J.* **80**, 207–215 (2014).

15. Urbanowicz, B. R., Peña, M. J., Moniz, H. A., Moremen, K. W. & York, W. S. Two Arabidopsis proteins synthesize acetylated xylan in vitro. *Plant J.* **80**, 197–206 (2014).

16. Chiniquy, D. *et al.* XAX1 from glycosyltransferase family 61 mediates xylosyltransfer to rice xylan. *Proc Natl Acad Sci USA* **109**, 17117–17122 (2012).

17. Anders, N. *et al.* Glycosyl transferases in family 61 mediate arabinofuranosyl transfer onto xylan in grasses. *Proc Natl Acad Sci USA* **109**, 989–993 (2012).

18. Voiniciuc, C., Gunl, M., Schmidt, M. H.-W. & Usadel, B. Highly Branched Xylan Made by IRREGULAR XYLEM14 and MUCILAGE-RELATED21 Links Mucilage to. *Plant Physiol.* **169**, 2481–2495 (2015).

19. Ralet, M.-C. *et al.* Xylans provide the structural driving force for mucilage adhesion to the Arabidopsis seed coat. *Plant Physiol* **171**, 165–178 (2016).

20. Jensen, J. K., Johnson, N. & Wilkerson, C. G. Discovery of diversity in xylan biosynthetic genes by transcriptional profiling of a heteroxylan containing mucilaginous tissue. *Front Plant Sci* **4**, (2013).

21. Marlett, J. A., Kajs, T. M. & Fischer, M. H. An unfermented gel component of psyllium seed husk promotes laxation as a lubricant in humans. *Am. J. Clin. Nutr.* **72**, 784–789 (2000).

22. McRorie, J. W. *et al.* Psyllium is superior to docusate sodium for treatment of chronic constipation. *Aliment. Pharmacol. Ther.* **12**, 491–497 (1998).

23. Anderson, J. W. *et al.* Cholesterol-lowering effects of psyllium intake adjunctive to diet therapy in men and women with hypercholesterolemia: Meta-analysis of

8 controlled trials. *Am. J. Clin. Nutr.* **71**, 472–479 (2000).

24. Cappa, C., Lucisano, M. & Mariotti, M. Influence of Psyllium, sugar beet fibre and water on gluten-free dough properties and bread quality. *Carbohydr. Polym.* **98**, 1657–1666 (2013).

25. Mancebo, C. M., San Miguel, M. Á., Martínez, M. M. & Gómez, M. Optimisation of rheological properties of gluten-free doughs with HPMC, psyllium and different levels of water. *J. Cereal Sci.* **61**, 8–15 (2015).

26. Fratelli, C., Muniz, D. G., Santos, F. G. & Capriles, V. D. Modelling the effects of psyllium and water in gluten-free bread: An approach to improve the bread quality and glycemic response. *J. Funct. Foods* **42**, 339–345 (2018).

27. Haque, A. & Morris, E. R. Combined use of ispaghula and HPMC to replace or augment gluten in breadmaking. *Food Res. Int.* **27**, 379–393 (1994).

28. Bahrani, A. S. Processes for dehusking psyllium seeds. *US Pat. Number 5020732* (1991).

29. Kumar, J. *Good agricultural practices for isabgol*. (2015).

30. Francoz, E., Ranocha, P., Burlat, V. & Dunand, C. *Arabidopsis* seed mucilage secretory cells: Regulation and dynamics. *Trends Plant Sci.* **20**, 515–524 (2015).

31. Schneitz, K., Huiskamp, M. & Pruitt, R. E. Wild-type ovule development in Arabidopsis thaliana: a light microscope study of cleared whole-mount tissue. *The Plant Journal* **7**, 731–749 (1995).

32. Windsor, J. B., Symonds, V. V., Mendenhall, J. & Lloyd, A. M. Arabidopsis seed coat development: Morphological differentiation of the outer integument. *Plant J.* **22**, 483–493 (2000).

33. Beeckman, T., Rycke, R. De, Viane, R. & Inzé, D. Histological study of seed coat development in *Arabidopsis thaliana*. *J. Plant Res.* **113**, 139–148 (2000).

34. Western, T. L., Skinner, D. J. & Haughn, G. W. Differentiation of mucilage secretory cells of the *Arabidopsis* seed coat. *Plant Physiol.* **122**, 345–56 (2000).

35. Voiniciuc, C., Yang, B., Schmidt, M. H.-W., Gunl, M. & Usadel, B. Starting to gel: How *Arabidopsis* seed coat epidermal cells produce specialized secondary cell walls. *Int. J. Mol. Sci.* **16**, 3452–3473 (2015).

36. Miart, F. *et al.* Cytological Approaches Combined With Chemical Analysis Reveals the Layered Nature of Flax Mucilage. *Front. Plant Sci.* **10**, 1–16 (2019).

37. Witzum, A. Mucilaginous plate pells in the nutlet epidermis of *Coleus blumei* Benth. (Labiatae). *Bot. Gaz.* **139**, 430–435 (1978).

38. Muñoz, L. A., Cobos, A., Diaz, O. & Aguilera, J. M. Chia seeds: Microstructure, mucilage extraction and hydration. *J. Food Eng.* **108**, 216–224 (2012).

39. Hyde, B. B. Mucilage-producing cells in the seed coat of *Plantago ovata*: Developmental fine structure. *Am. J. Bot.* **57**, 1197–1206 (1970).

40. Ruprecht, C. *et al.* A synthetic glycan microarray enables epitope mapping of plant cell wall glycan-directed antibodies. *Plant Physiol.* **175**, pp.00737.2017 (2017).

41. Verhertbruggen, Y., Marcus, S. E., Haeger, A., Ordaz-Ortiz, J. J. & Knox, J. P. An extended set of monoclonal antibodies to pectic homogalacturonan. *Carbohydr. Res.* **344**, 1858–1862 (2009).

42. Ruel, K., Nishiyama, Y. & Joseleau, J. P. Crystalline and amorphous cellulose in the secondary walls of Arabidopsis. *Plant Sci.* **193**–**194**, 48–61 (2012).

43. Tucker, M. R. *et al.* Dissecting the Genetic Basis for Seed Coat Mucilage Heteroxylan Biosynthesis in Plantago ovata Using Gamma Irradiation and Infrared Spectroscopy. *Front. Plant Sci.* **8**, 326 (2017).

44. Voiniciuc, C. *et al.* Flying saucer1 is a transmembrane RING E3 ubiquitin ligase that regulates the degree of pectin methylesterification in Arabidopsis seed mucilage. *Plant Cell* **25**, 944–959 (2013).

45. Boesewinkel, F. D. Development of ovule and testa of *Linum usitatssimum* L. *Acta Bot. Neerl.* **29**, 17–32 (1980).

46. Madgulkar, A., Rao, M. & Warrier, D. Characterization of Pysillium (*Plantago ovata*) polysaccharide and its uses. *Polysaccharides* 1–17 (2014). doi:10.1007/978-3-319-03751-6_49-1

47. Garcia, D., Fitz Gerald, J. N. & Berger, F. Maternal Control of Integument Cell Elongation and Zygotic Control of Endosperm Growth Are Coordinated to Determine Seed Size in Arabidopsis. *Plant Cell* **17**, 52–60 (2005).

48. Cooper, G. O. Development of the ovule and the formation of the seed in

Plantago lanceolata. *Am. J. Bot.* **29**, 577–581 (1942).

49. Mikesell, J. Anatomy of terminal haustoria in the ovule of Plantain (*Plantago major* L.) with taxonomic comparison to other angiosperm taxa. *Bot. Gaz.* **151**, 452–464 (1990).

50. Johri, B., Ambegaokar, K. & Srivastava, P. Plantaginales. in *Comparative Embryology of Angiosperms* 777–779 (Springer Berlin Heidelberg, 1992).

51. Saez-Aguayo, S. *et al.* PECTIN METHYLESTERASE INHIBITOR6 promotes *Arabidopsis* mucilage release by limiting methylesterification of homogalacturonan in seed coat epidermal cells. *Plant Cell* **25**, 308–23 (2013).

52. Macquet, A. *et al.* A naturally occurring mutation in an *Arabidopsis* accession affects a β-D-galactosidase that increases the hydrophilic potential of rhamnogalacturonan I in seed mucilage. *Plant Cell* **19**, 3990–4006 (2007).

53. Walker, M. *et al.* The transcriptional regulator LEUNIG_HOMOLOG regulates mucilage release from the *Arabidopsis* testa. *Plant Physiol.* **156**, 46–60 (2011).

54. Atmodjo, M. A., Hao, Z. & Mohnen, D. Evolving Views of Pectin Biosynthesis. *Annu. Rev. Plant Biol.* **64**, 747–779 (2013).

55. Guo, Q., Cui, S. W., Wang, Q. & Christopher Young, J. Fractionation and physicochemical characterization of psyllium gum. *Carbohydr. Polym.* **73**, 35–43 (2008).

56. Sullivan, S. *et al.* CESA5 is required for the synthesis of cellulose with a role in structuring the adherent mucilage of Arabidopsis seeds. *Plant Physiol* **156**, 1725–1739 (2011).

57. Ralet, M. *et al.* Xylans provide the structural driving force for mucilage adhesion to the *Arabidopsis* seed coat. *Plant Physiol.* **171**, 165–178 (2016).

58. Burton, R. A. *et al.* Over-expression of specific HvCslF cellulose synthase-like genes in transgenic barley increases the levels of cell wall (1,3;1,4)-β-D-glucans and alters their fine structure. *Plant Biotechnol. J.* **9**, 117–135 (2011).

59. Guillon, F. *et al.* Brachypodium distachyon grain: characterization of endosperm cell walls. *J. Exp. Bot.* **62**, 1001–1015 (2011).

60. Hassan, A. S. *et al.* A Genome Wide Association Study of arabinoxylan content in 2-row spring barley grain. *PLoS One* **12**, 1–19 (2017).

www.nature.com/scientificreports

SCIENTIFIC REPORTS
nature research

Check for updates

OPEN

The novel features of *Plantago ovata* seed mucilage accumulation, storage and release

Jana L. Phan[1,3,5], James M. Cowley[1,2,5], Kylie A. Neumann[1,2,4], Lina Herliana[2], Lisa A. O'Donovan[2] & Rachel A. Burton[1,2]✉

Seed mucilage polysaccharide production, storage and release in *Plantago ovata* is strikingly different to that of the model plant *Arabidopsis*. We have used microscopy techniques to track the development of mucilage secretory cells and demonstrate that mature *P. ovata* seeds do not have an outer intact cell layer within which the polysaccharides surround internal columellae. Instead, dehydrated mucilage is spread in a thin homogenous layer over the entire seed surface and upon wetting expands directly outwards, away from the seed. Observing mucilage expansion in real time combined with compositional analysis allowed mucilage layer definition and the roles they play in mucilage release and architecture upon hydration to be explored. The first emergent layer of hydrated mucilage is rich in pectin, extremely hydrophilic, and forms an expansion front that functions to 'jumpstart' hydration and swelling of the second layer. This next layer, comprising the bulk of the expanded seed mucilage, is predominantly composed of heteroxylan and appears to provide much of the structural integrity. Our results indicate that the synthesis, deposition, desiccation, and final storage position of mucilage polysaccharides must be carefully orchestrated, although many of these processes are not yet fully defined and vary widely between myxospermous plant species.

Abbreviations

DPA	Days post-anthesis
ML	Mucilage layer
MSC	Mucilage secretory cell
SEM	Scanning electron microscopy

Upon exposure to aqueous environments, seeds from myxospermous species extrude a polysaccharide-rich gel from their seed surface, often called mucilage. Numerous species display myxospermy and there are a range of possible evolutionary advantages of synthesising such a carbon-rich and energy-expensive substance[1]. Of all myxospermous species, the seed mucilage system of *Arabidopsis* is the best characterised. *Arabidopsis* seed mucilage has been used extensively as a proxy for the study of plant cell wall polysaccharide biosynthesis, enabling increased molecular characterisation of pectin biosynthesis, its main polysaccharide component[2], as well as the biosynthesis of cellulose[3,4] and several hemicelluloses[5–8], which are minor but integral components. Mucilage from other species can be highly diverse[1] and while *P. ovata* mucilage is also a complex mixture of polymers, it is predominantly heteroxylan with only a minor pectin component. While the pectin component is a near-linear rhamnogalacturonan[9–11], the *P. ovata* heteroxylan (accounting for around 90% of the mucilage polysaccharides) is highly complex with the current scientific consensus defining *P. ovata* heteroxylan comprising a β-(1,4)-linked-D-xylopyranose backbone, heavily substituted at O-2 and/or O-3 positions with various mono-, di- and oligosaccharide substitutions of α-L-arabinofuranose and β-D-xylopyranose[9,11,12]. It is likely that, as with other eudicots, the β-(1,4)-linked-D-xylopyranose backbone is synthesised by several members of

[1]Australian Research Council Centre of Excellence in Plant Cell Walls, School of Agriculture, Food and Wine, University of Adelaide, Waite Campus, Urrbrae, SA 5064, Australia. [2]Australian Research Council Centre of Excellence in Plant Energy Biology, School of Agriculture, Food and Wine, University of Adelaide, Waite Campus, Urrbrae, SA 5064, Australia. [3]Present address: Australian Academy of Science, Ian Potter House, 9 Gordon St, Canberra, ACT 2601, Australia. [4]Present address: IP Australia, PO Box 200, Woden, ACT 2606, Australia. [5]These authors contributed equally: Jana L. Phan and James M. Cowley. ✉email: rachel.burton@adelaide.edu.au

glycosyltransferase (GT) families 43 and 47. There is strong evidence that GT47 protein IRX10-L, probably in concert with other GT43 and GT47 proteins, extends the backbone by adding UDP-xylose moieties[14,15]. GT61 family members have been implicated in both α-arabinosyltransferase and β-xylosyltransferase xylan backbone decoration activities in cereals[16,17], *Arabidopsis*[18,19] and *Plantago*[20], and copy number and type of GT61 was found to influence interspecific differences in *Plantago* heteroxylan fine structure[11]. The overall picture is complicated even further in that different fractions (sometimes described as layers) of *P. ovata* mucilage contain heteroxylans of varying substitution patterns showing that, like *Arabidopsis* mucilage, it is a similarly complex but orchestrated network of polysaccharides[9,10,13]. To date, many xylan synthase genes, particularly those involved in backbone decoration, are still unknown.

Plantago ovata mucilage also has economic relevance, in that in its dry state it constitutes the basis of a dietary fibre supplement, called psyllium, that is widely consumed by humans to assist with laxation, relieving constipation[21,22], and to treat metabolic disorders like hypercholesterolaemia[23]. More recently, psyllium has become a key ingredient in gluten-free food, where it provides texture and structure in the absence of gluten[24–27]. Psyllium is produced by milling the dry polysaccharides off the seed surface[28] and is often referred to as the "husk" fraction. The ratio of husk to seed is approximately 1:3, with the discarded non-husk seed components often being used for animal or fish feed[29]. From an economic standpoint, the ability to understand mucilage polysaccharide production and therefore potentially increase the valuable husk fraction is a viable breeding target for this plant species.

As well as studying the biosynthesis of mucilaginous polymers, the mechanism of mucilage extrusion from the seed coat of *Arabidopsis* has also been thoroughly characterised. In *Arabidopsis*, seed mucilage polysaccharides accumulate in the apoplast of specialised seed coat cells called 'mucilage secretory cells' (MSCs). When the mucilage polysaccharides become hydrated, they swell and rupture the primary cell wall of the MSC, releasing the mucilage[30]. The MSCs in *Arabidopsis* differentiate from the outer-most integument cell layer of the ovule. *Arabidopsis* has an outer integument composed of two cell layers and an inner integument composed of three cell layers, both of maternal origin, which grow to surround the mature ovule[31]. After pollination, at approximately 7 days post-anthesis (DPA), starch granules begin to accumulate in the MSCs and polysaccharide deposition starts in the peripheral "corners" of the cells. This pushes the protoplasm to form a central volcano-like structure in the cell. At 10 DPA this central column is reinforced by the deposition of secondary cell wall polysaccharides to form the columella. The columella is a prominent feature of the mature MSCs in *Arabidopsis* and the accumulated polysaccharides are deposited and stored around it, producing a doughnut-shaped ring. This structure results in the distinctive mature *Arabidopsis* seed coat patterning seen using SEM[32–34]. The details of MSC development, rupture and mucilage release are discussed in comprehensive reviews by Francoz et al.[30], and Voiniciuc et al.[35]. An important developmental stage during MSC development is the weakening of the radial primary cell walls of the MSCs at the end of columella formation, at approximately 13 DPA. This process enables the consequent fracturing and rupturing of the cell walls of the MSCs upon imbibition in an aqueous environment[32]. The rupturing allows the accumulated seed polysaccharides to be extruded almost instantaneously forming the distinctive mucilage envelope. Thus, MSCs of *Arabidopsis* are a highly-specialised seed coat cell with a clearly defined structure that is essential for correct seed mucilage extrusion. MSC development and mucilage release of *Linum usitatissimum* seeds, more commonly known as flax, has also recently been described, revealing an even more complex MSC structure[36]. The flax MSCs, embedded in the external surface of the seed coat were determined by Miart et al.[36], to contain four discrete, laminated layers in the apoplast, each containing chemically- and functionally-distinct polysaccharides. Each of the layers and their polysaccharide contents act in concert to effectively hydrate the polysaccharides, mechanically forcing the radial cell wall to rupture in a peeling fashion and enabling mucilage to be released. In other species such as *Salvia hispanica* (chia) and *Coleus blumei*, the seed mucilage polysaccharides are stored in the outer epidermal cell layer(s) of a nutlet that encases the true seed within[37,38], making these species myxocarpous rather than myxospermous. The events leading to the release of mucilage in these species have not been documented in detail but there appears to be great diversity in the mucilage extrusion structures between plant types[1].

The accumulation of seed mucilage polysaccharides in *P. ovata* has been investigated previously[39] and appears to be distinct from the process observed in the *Arabidopsis* MSCs. In the case of *P. ovata*, seed mucilage polysaccharides are deposited in the outer-most cell layer of a large integument. This single cell layer accumulates polysaccharides rapidly and the cells expand dramatically in size in a process that does not involve the formation of a central columella[39]. Beyond this, little is known about the precise development of these cells and so here we provide a detailed characterisation of the polysaccharide deposition and mucilage release processes of *P. ovata*, also enabling the formulation of a supporting model.

Results

Development of *P. ovata* mucilage secretory cells. *P. ovata* takes approximately 3.5 months to grow from germination through to maturity. The mature plants have long slender, straggly leaves and produce many spike-type inflorescences (SI Fig. S1). Development of *P. ovata* fruit on the spike and length of the inflorescence (and consequently yield per plant) are strongly dependent on the plant's health during growth and development. Each fruit or capsule contains two ovules, separated by a maternal disc and joined to the parent plant via a placenta (Fig. 1). *P. ovata* possesses a circumscissile capsule (also called a pyxis) that is firmly attached to the inflorescence at the proximal end of the fruit. When the fruit is mature, the seed dispersal mechanism involves dehiscence at the capsule equator causing the operculum to detach, enabling the seed to dislodge from the capsule. The operculum, the point of attachment to the rachis, and the equator are indicated in Fig. 1A. After pollination, the fruits mature in approximately 1 month. At 2 weeks post-anthesis, the fruit has reached its full length and the seeds continue to develop inside, expanding widthways and filling the fruit.

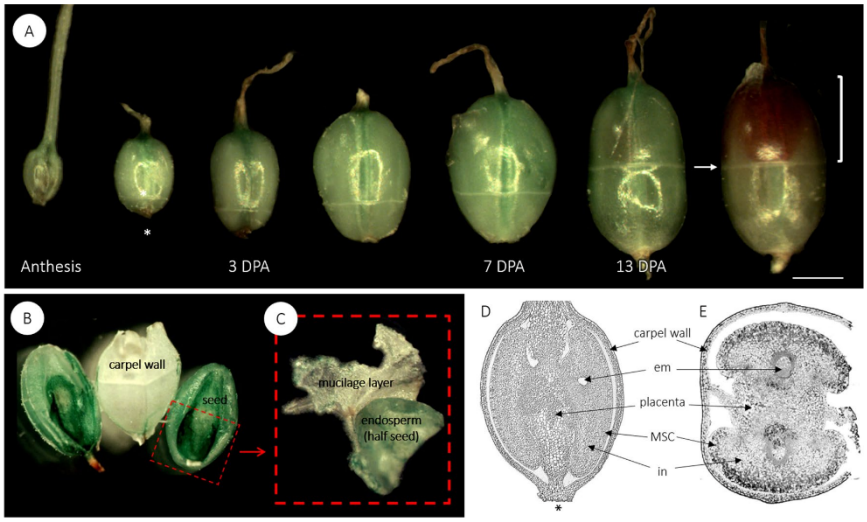

Figure 1. (**A**) The fruit development of *P. ovata*. Each fruit contains two ovules separated by placental tissue. *Plantago* species have a circumscissile capsule, also known as a pyxis. The arrow indicates the equator, where the zone of dehiscence is visible, the square bracket highlights the operculum, which detaches during dehiscence, and *indicates the end that joins the fruit to the rachis. Bar 1 mm. (**B**) A dissected fruit at 13 DPA, showing two immature seeds and in (**C**) one of the seeds has been further dissected to show the mucilage polysaccharide layer, which has been peeled off the seed and is the remnant of the integument tissue. Longitudinal (**D**) and transverse (**E**) cross sections of a developing fruit at 7 DPA, stained with toluidine blue. *Em* embryo sac, *MSC* mucilage secretory cells, *in* integument.

Following successful fertilisation, the parenchyma cells of the integument layers differentiate rapidly (Fig. 2). The MSCs of *P. ovata* seeds are easily observed at 1 DPA. They develop from the outermost single cell layer of the integument and lengthen as they accumulate starch granules (Fig. 2B,C). Substantial growth and elongation of the MSCs is observed from 3 to 5 DPA. Although it is difficult to discern discrete cellular compartments, it is likely that the empty space at the distal end of the cells where the polysaccharides accumulate, is the apoplast (Fig. 2D). By 9 DPA, the accumulated mucilage polysaccharides are hydrophilic enough to rupture the MSCs when they come into contact with aqueous solutions and it is technically challenging to obtain intact sections from this stage onwards. At 15 DPA all MSCs have ruptured and released their mucilage in fixed and sectioned developing seeds but it is possible to observe that the integument has been compressed to just a few cell layers between the MSCs and the seed endosperm. This compressed layer has disappeared almost completely by the time the seed is fully mature, leaving only a thin layer situated between the endosperm and the mucilage polysaccharide layer (Fig. 2H).

Composition of developing ovule cell walls. The cell walls of seed tissues at three key time points across early development were fluorescently immunolabelled with the primary antibodies LM11 (β-1,4-linked xylan backbone[40]) LM19 (un-esterified and partially esterified homogalacturonan[41]) and LM20 (methylesterified homogalacturonan[41]) and the carbohydrate-binding module CBM3a (crystalline cellulose[42]). At anthesis the ovule is minute but there was clear binding by both LM20 (Fig. 3A1–3) and LM19 (SI Fig. S2A), with the latter producing a strong signal in the integument tissue. There was a low level of CBM3a binding to the walls of both MSCs and integument cells (Fig. 3D1–3) and no binding by LM11 (SI Fig. S2B). At 4 DPA, the MSCs are greatly elongated. The strongest signals are generated by LM20 in the MSC layer (Fig. 3B1–3) and CBM3a in both the MSC and integument cells (Fig. 3E1–3) but there was no labelling evident for LM19 (SI Fig. S2C) or LM11 (SI Fig. S2D). The final time point was at 6/7 DPA when the MSCs were becoming fragile due to the accumulation of mucilage polysaccharides. At this point the LM20 labelling was now restricted to the outside edge of the MSC layer and in cell corners bordering the integument tissue (Fig. 3C1–3). The CBM3a signal was still present in both the MSCs and integument though signals in the MSCs had become non-specific and amorphous compared to the integument where labelling of distinct walls was still present (Fig. 3F1–3). By 6/7 DPA there was no labelling by LM19 (SI Fig. S2E) and minimal labelling by LM11 (SI Fig. S2F).

Surface features of mature *P. ovata* seeds. The mature seeds of *P. ovata* have a deep scar on the ventral side resulting in a boat-shaped seed (SI Fig. S3). The patterning of the dry seed surface on the dorsal side is polar. Where the inner surface of the fruit capsule has been pressed against the seed it is smoother (Fig. 4A). The seed

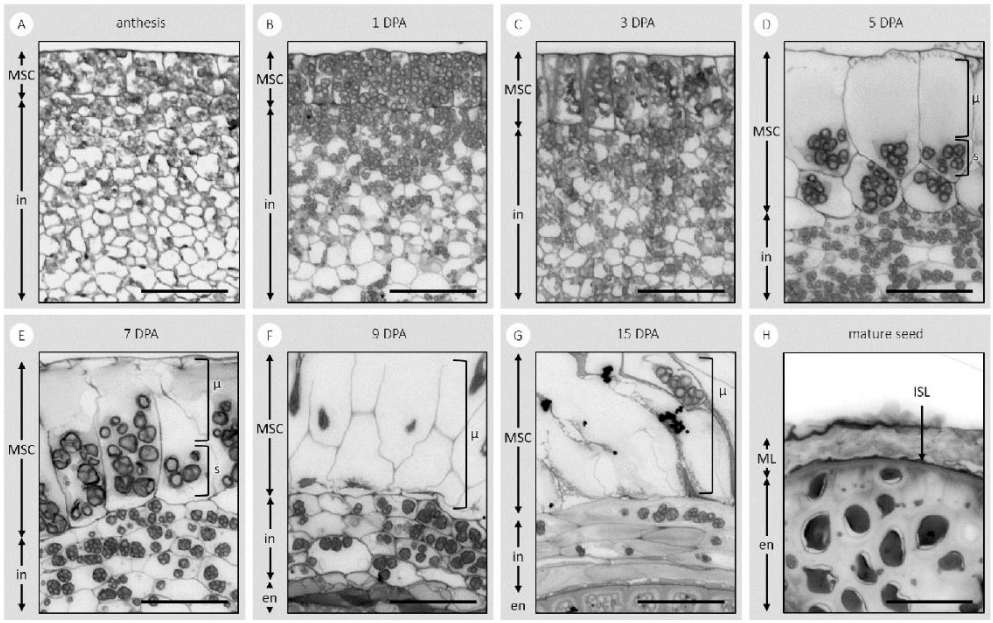

Figure 2. Toluidine blue-stained transverse sections of the developing integument of *P. ovata*. The sections show the tissues and components that are the: endosperm (en); integument (in); mucilage polysaccharides (μ); mucilage secretory cells (MSCs); mucilage polysaccharide layer (ML); intensely stained layer (ISL); and starch granules (s) at days post-anthesis (DPA). Scale bar 50 μm.

surface is covered in hexagonal structures with a distinct wrinkled texture (Fig. 4B). The wrinkled patterning and hexagonal structures on the mature seed surface are lost once seeds have been imbibed in water (Fig. 4D). When the remaining seed mucilage is left to dry back onto the seed after hydration in cold water, the seed surface appears very smooth and high magnification SEM reveals little additional detail (Fig. 4E). The hexagonal structures are no longer visible, and the polarity observed prior to mucilage expansion (Fig. 4A) has also been lost. This is in clear contrast to *Arabidopsis* where, after the same process, the seed surface morphology remains relatively unchanged and the columella is still clearly visible (Fig. 4F). Mature *P. ovata* seeds therefore do not have conventional seed coat cells and there is certainly no columella as found in *Arabidopsis* (Fig. 4C). Rather there is a dehydrated mucilage polysaccharide layer, underlain by a thin dark brown layer (which gives the seed its colour) both of which sit over the outer layer of the endosperm (Fig. 4G). The crushed integument layer is not at all visible in the mature seed.

Mucilage removal from mature *P. ovata* seeds. Different methods were used to remove the expanded mucilage from mature imbibed seeds of *P. ovata*. Although previous studies report no significant compositional differences between the different extraction methods[11], some physical differences were observed on the exposed seed surface (SI Fig. S4). When mature seeds were placed into an aqueous fixative, the sequential washing steps removed most of the mucilage from the seed, leaving a thin resistant layer behind, as did extraction with hot water or 0.2 M KOH (SI Fig. S4). In contrast, when 0.1 M HCl was used for extraction, the mild acid completely removed the mucilage layer from the entire seed (SI Fig. S4D), probably hydrolysing it in situ[10], and in some patches it has also removed the underlying intensely-stained layer (SI Fig. S4F).

Mucilage accumulation may be independent of embryo and endosperm development. From the mutant *P. ovata* population reported in Tucker et al.[43], we selected a line, 69-1, that produces seeds with impaired development across a range of severity: seeds with a thickened translucent outer layer, incomplete endosperm filling, arrested embryo development, or a shrivelled appearance where it was difficult to determine if an embryo was present (Fig. 5A1–5). Ruthenium red staining solution was applied to representative seeds and all types produced mucilage from the seed that was released into the aqueous environment. While different specific architectures were observed, two typical mucilage layers were recognisable in all but the shrivelled phenotype. These seeds may have been aborted early in development rather than representing a developmentally delayed phenotype (Fig. 5B5). While only 5% of seed are WT-like in the 69-1 bulk sample analysed, WT-level total mucilage yields, arabinose and xylan content and ratio were still obtained (Fig. 5C1–3).

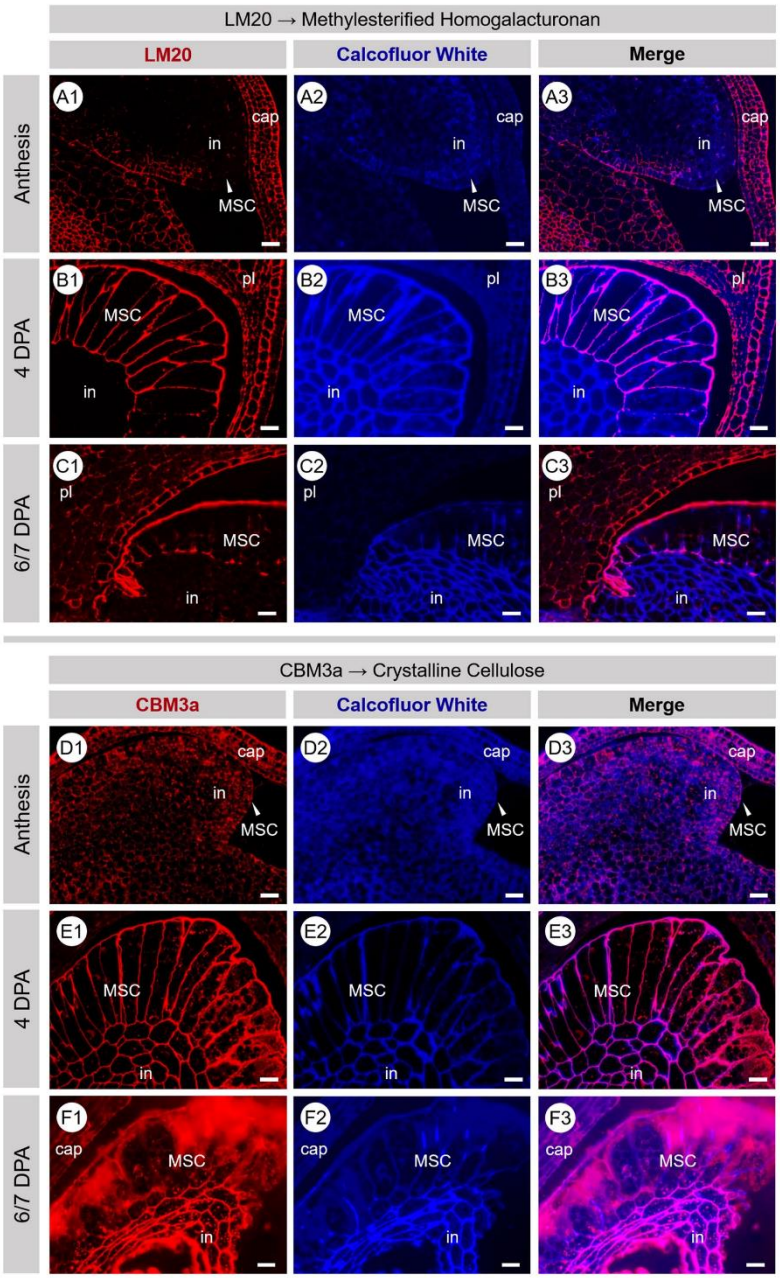

Figure 3. Fluorescence micrographs of transverse sections of developing *P. ovata* seeds labelled with LM20 and CBM3a (red/pink) at anthesis (**A**,**D**), at 4 DPA (**B**,**E**) and at 6/7 DPA (**C**,**F**). MSC cell walls show strong labelling of highly methylesterified HG (LM20) and crystalline cellulose (CBM3a) that diminishes in intensity and organisation as development/mucilage polysaccharide accumulation continues and/or as MSC cell walls disintegrate. Samples are counter-stained with calcofluor white (blue). Scale 20 µm. *DPA* days post-anthesis, *HG* homogalacturonan, *MSC* mucilage secretory cell, *in* integument, *pl* placenta, *cap* capsule.

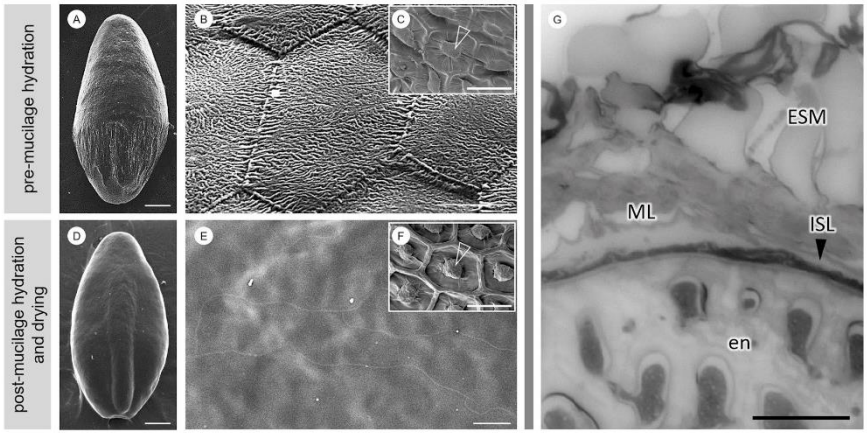

Figure 4. Scanning electron micrographs show that *P. ovata* does not contain a columella (**A**,**B**). Inset (**C**) shows a scanning electron micrograph of the seed surface of *Arabidopsis* with the columella structure indicated with an arrowhead. In *P. ovata,* the wrinkled texture of the dry mucilage polysaccharide layer (ML) and hexagonal shapes of the distal MSC wall remnants disappear after mucilage is hydrated and allowed to dry back onto the seed surface, unfixed (**D**,**E**), leaving it extremely smooth. This contrasts with *Arabidopsis* where the distinct columella structure persists and remains clearly visible after the same process (**F**). Toluidine blue-stained cross sections of the mature seeds fixed in aqueous fixative (**G**) reveal that the seed mucilage (ESM) expands from the ML, which sits on top of an intensely stained layer (ISL) that separates the mucilage polysaccharide layer from the endosperm. *En* endosperm. Scales **A**,**D**,**G** 500 µm; **B**,**E**,**H** 50 µm; **C**,**F** 30 µm.

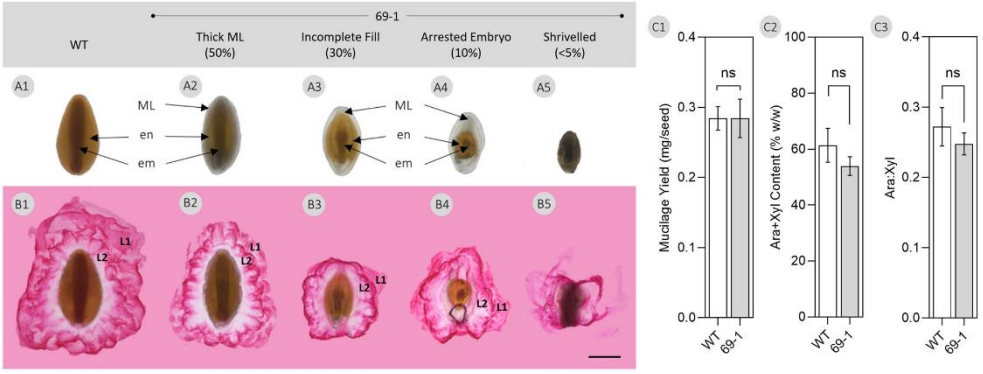

Figure 5. (**A**) Seeds were selected from developmentally-impaired gamma-irradiated *P. ovata* mutant 69-1 generated previously by Tucker et al.[43]. When these seeds were imbibed in a ruthenium red solution (0.01% w/v) for 10 min at room temperature (**B**) mucilage expanded from all seeds with different architectures but two typical mucilage layers (L1 and L2) were present. *em* embryo, *en* endosperm, *ML* mucilage layer, *WT* wild-type. Scale bar 1 mm. (**C**) Analysis of mucilage yield and composition revealed no significant difference (ns) from the wild-type ($p > 0.05$, Student's t test).

Expansion of seed mucilage polysaccharides across time and space. Microscopy and monosaccharide analysis techniques were used to investigate changes in the composition and structure of the mucilage as it expanded from the seed surface. In order to define temporal mucilage expansion we tried to capture and describe the major stages using chemical profiling. By measuring the release of mucilage-related monosaccharides over 14.5 h we found that the major stages of mucilage expansion occurred within 60 min of imbibition (SI Fig. S5). Monosaccharide analysis of serial fractions taken during the first 60 min of mucilage expansion clearly demonstrated a change in the composition of the expanded seed mucilage over time (Fig. 6A). Relative to total extracted sugars, there was a shift from pectin-dominant to heteroxylan-dominant monosaccharide composi-

tion during the initial stages. A sharp increase in the number of heteroxylan-associated monosaccharides (xylose and arabinose) was then observed, peaking at 20 min post imbibition (Fig. 6A) while pectin-derived monosaccharides (rhamnose and galacturonic acid) displayed the inverse, where they were most abundant at the start of seed imbibition and mucilage expansion, before tapering off considerably by 20 min (Fig. 6A).

Mature seeds were stained as described in Yu et al.[9], and real-time mucilage expansion was observed dynamically using confocal microscopy (Fig. 6B). Two distinct layers of expanded mucilage were observed. A third mucilage layer adjacent to the seed coat reported by Yu et al.[9], was not observed. The two mucilage layers, L1 and L2, have distinct structural features. L1 is the first to expand; it lacks clear structure and much of the Calcofluor White staining is associated with this layer. The expansion of L2 from the seed occurs soon after L1 but the sea anemone-like structures (Fig. 6B) are not observed until 2 min post imbibition. By 15 min, L1 has dispersed into the surrounding aqueous environment and by 20 min L2 has expanded in its entirety (Fig. 6B).

Discussion

Mucilage polysaccharide accumulation in the MSCs of *P. ovata* seeds follows a different developmental pattern to that occurring in the MSCs of *Arabidopsis*. The mechanism by which different cell layers are converted into seed tissues and the possible remodelling thereafter appears to be of central importance for MSC development in *P. ovata*. At some point during mid-development and perhaps after polysaccharide accumulation is complete, we propose that the MSC radial cell walls break down and collapse in a concertina-like fashion. The collapse is potentially driven by the outward pressure of the rapidly expanding embryo and endosperm tissues pushing the MSC outer walls against the inner capsule surface, releasing the accumulated mucilage polysaccharides into an amorphous layer that becomes sandwiched between the remnant distal and basal MSC walls (Fig. 2). The process of radial wall remodelling and/or disintegration may already be beginning by 6/7 DPA where discrete labelling present earlier in development is absent or has become non-specific and amorphous (Fig. 3C1–3,F1–3). This is particularly evident for the CBM3a labelling (Fig. 3F1–3). This is unlike the presence of the mucilage polysaccharides contained within intact discrete cells of the *Arabidopsis* (Fig. 4C,F) and flax[36] mature seed coats. From late development onwards it is clear that the MSCs of *P. ovata* do not contain a columella (Fig. 4B) and our hypothesis is that instead, laminated layers of dehydrated mucilage polysaccharides are present, following radial MSC wall disintegration, between the remnant distal MSC walls, inner capsule wall and the expanded endosperm tissue (Figs. 2, 7B). At seed maturity when released from the dehiscent capsule, the dehydrated and highly compressed mucilage polysaccharides, originating from the obliterated MSC cells, (Figs. 2H, 4H, 7C) form a dense layer over the seed surface (Figs. 2C, 6C). Cross sections of the dry mature seed shows that the thickness of this mucilage layer ranges from 10 to 18 µm compared to the 80 to 90 µm thickness of the MSCs at full elongation at 7 DPA (Fig. 2). This supports the compression of the MSCs as the seed matures, after which point the layer is so dense that the constituent polysaccharides do not label with monoclonal antibodies that bind well to the seed mucilage when expanded (Phan et al.[11]; Fig. 2H).

In our SEM analysis of mature seeds, we observe a stark contrast in surface appearance before and after hydration (Fig. 4). After mucilage is hydrated and allowed to dry without fixation, we were no longer able to observe the wrinkled surface or characteristic hexagonal shapes of the underlying distal MSC wall remnants (Fig. 4D–E). We suggest that while the distal walls may have undergone a similar process of remodelling/weakening to the radial walls, they were protected from crushing as they lie perpendicular to the outward force of the expanding endosperm, pushed flat against the inner capsule surface, and thus remain present and visible in the mature seed. However these distal wall fragments are thin, not reinforced with cellulose (Fig. 3F1–3) and appear to be rich in pectin (Fig. 3C1–3) suggesting that they may be highly soluble. We have previously observed 'hexagonal platelets' that stain strongly with Ruthenium Red to be released from *P. ovata* seeds very early in the hydration cascade and rapidly disintegrate or dissolve (Phan et al.[11], Fig. 1H). We suggest that these structures are the soluble remnants of the distal MSC walls. These are different to other cellulose-staining structures like the mucilage discs of the *Arabidopsis* mutant *fly1*[44] or plate cells of other *Plantago* species (Phan et al.[11], Fig. 1I–P; Cowley et al. unpublished data) which persist through mucilage hydration. When hydrated mucilage is left to dry back onto the seed (Fig. 4D,E), the distal MSC wall fragments may have already dissolved/disintegrated and are thus no longer discernible, so the hexagonal shapes are lost, unlike similarly treated *Arabidopsis* seeds which retain the lower portion of the ruptured MSCs (Fig. 4F). The still soft layer of mucilage polysaccharides released by the putative rupture of the *P. ovata* MSC radial walls in later development may also contribute to the polarity of striations on the dorsal side of the mature seed (Fig. 4A). This could occur as the proximal end of the seed is under more compression from the capsule wall, which imprints onto the surface of the polysaccharide layer as it dehydrates. Although the distal end of the seed also comes into contact with the capsule, at this end it does not adhere so tightly and is observed to readily detach when gently touched, thereby enabling seed dispersal. Interestingly, Boesewinkel[45] suggests that the seed coat of *Linum usitassimum* is also polar and that the 'slime-forming matter' is deposited on the outer surface of the epidermal seed coat cells. They also suggest that the cells underneath the outer epidermal seed coat cells, which are on the innermost layer of the inner integument, have thickened cell walls and are pigmented cells. These observations are strikingly similar to what we have observed in *P. ovata*; the mucilage is the outermost layer of the seed and is underlain by an intensely stained layer that may be pigment-rich (Fig. 2H). A similar structure was also described for *P. ovata* by Madgulkar et al.[46]. These observations further support our proposed mechanism of MSC development and disintegration, with the subsequent formation of a cell-free mucilage polysaccharide layer.

It is interesting to speculate about carbon flow through the *P. ovata* seed during development. There must be a balance between investment in maternal sporophytic tissue and the filial tissues i.e. the carbon supply must be split between mucilage polysaccharide biosynthesis and feeding the rapidly growing embryo and endosperm. It is possible that development of the MSCs from the outermost cell layer of the integument tissue, which is of

Figure 6. The composition and structure of seed mucilage changes over the course of its expansion. (**A**) Compositional analysis reveals pectin-associated monosaccharides (rhamnose and galacturonic acid) are most abundant during the initial expansion of mucilage and rapidly decrease in concentration thereafter. Heteroxylan-associated monosaccharides (xylose and arabinose) are also present in the initial expansion of mucilage, in almost similar amounts to pectin. Contrasting to pectin, the heteroxylan-associated monosaccharides rapidly increase in concentration and go on to make up the bulk of total expanded mucilage. Data have been fitted with cubic spline curves to highlight trends. (**B**) The dynamics of seed mucilage expansion in mature *P. ovata* seeds were observed in real-time over a period of 20 min using confocal microscopy. Seeds were pre-stained with 0.4% Direct Red 23 and 0.1% Calcofluor White. Upon imbibition in water, a sudden "explosion" of an extremely hydrophilic and non-structured mucilage layer emerges (L1). Following L1, a more structured and anemone-like layer of mucilage expands outwards (L2) and by 20 min, L2 has reached its maximal expansion distance and L1 has mostly dissipated into the surrounding aqueous environment. Scale bar 100 µm. *S* mature seed, *ML* mucilage polysaccharide layer on dry seed, *L1* layer 1, *L2* layer 2 N.B. time 0 min is a dry seed that has been pre-stained, water was added after this image was taken.

maternal origin[31], could be favoured over zygotic development. This may explain our observation that MSC development and polysaccharide deposition for mucilage synthesis may occur independently of seed development since even developmentally-stalled and aborted seeds still make mucilage when imbibed (Fig. 5B1–5). While the specific architectures were different, two typical mucilage layers were recognisable and known *P. ovata* quality indicators[10], mucilage yield (Fig. 5C1) and heteroxylan content (Fig. 5C2) and composition (Fig. 5C3) were not significantly different to the wild-type ($p > 0.05$) showing that mucilage synthesis was uninterrupted. Garcia et al.[47], demonstrated that development of the maternally-derived integument and the zygotic embryo and endosperm are coordinated to determine final *Arabidopsis* seed size. Of the various developmentally-impaired *P. ovata* seeds analysed here, none of them reached the same size as the wild-type, suggesting that although integument development and mucilage polysaccharide biosynthesis can occur independently of embryo and endosperm development, some coordination is needed in order to establish the correct size of the mature seed. It is possible that without outward pressure from the growing endosperm not only will the seed not reach mature size, but the MSC contents may not be correctly arranged and/or pressurised causing the diminished mucilage expansion shown here. Unlike *Arabidopsis*, several *Plantago* species are reported to contain specialised nutrient transfer structures called haustoria that develop from the embryo sac. Haustoria have been characterised in the seeds of *P. lanceolata*[48], *P. major*[49], and *P. coronopus*, while those in *P. pumila* (also known as *P. exigua*) and *P. lagopus* are described briefly by Johri et al.[50]. Cooper[48] observed haustoria "penetrating and digesting the outer portion of the ovule adjacent to the developing endosperm", in *P. lanceolata*, and this corresponds to the layer we have designated integument in *P. ovata*. Haustoria may function to directly connect the embryo and endosperm to surrounding integument cells, allowing a networked supply of carbon for growth and development. Eventually, the growing endosperm of *P. lanceolata* absorbs most of the surrounding integument and leaves only a few cell layers that lose most of their cytoplasmic contents and are squashed thin at maturity. Although Cooper[48] did not specifically state what this papery-thin layer could be, it is likely that they were describing the mucilage polysaccharide layer. Haustoria have not yet been reported in *P. ovata*, and we were unable to confirm their presence or absence in the developmental sections presented here. Thus, it remains unclear what mechanisms control the fate of the integument cells and this will be informative to investigate in the future.

The microscopy images of the developing MSCs (Fig. 2) raise questions regarding gene expression and regulation during the different developmental stages. During the early stages of MSC development at 3–5 DPA where rapid cell expansion is observed, the enzymes that are present may be synthesising the backbone of the immature pectin polymer i.e. one that still requires post-synthesis modification to become hydrophilic, as observed in *Arabidopsis*[51–53] and early stages of heteroxylan synthesis may also be occurring. The shift in the esterification status of the pectin in both the MSCs and the integument cell walls is clearly demonstrated in Fig. 3 and SI Fig. S2, where tissues at anthesis label differently when compared to four days later. However, at this magnification it is not possible to unequivocally define the location of the pectin—whether it is in the actual wall of the MSCs or in the apoplast and just pushed tightly against it will require detailed examination at the TEM level. There is a clear increase in the amount of crystalline cellulose in the walls of both the MSCs and the integument cells when tissues at anthesis and later at 4 and 7 DPA are compared. At these early stages there is minimal binding by the LM11 antibody which detects xylan suggesting there is no xylan present yet, even in the cell walls rather than the apoplast (SI Fig. S2B,D,F). This lack of signal is consistent with our previous analyses, where later in development (13 DPA) many of the genes involved in xylan biosynthesis are transcriptionally active, such as the GT61, UXS, and UAM genes[11] which is only two days before the 15 DPA stage when the MSCs appear misshapen and possibly on the verge of extensive disintegration (Fig. 2G). It is possible that at 13 DPA these genes are more involved in polysaccharide post-synthesis modification, modifying the sidechain density and/or length in xylan and pectic polymers to enable correct mucilage expansion and final architecture upon imbibition in aqueous environments, but at this stage details are unknown. Future experiments are aimed at establishing the transcript abundance of gene sub-sets involved in synthesis of the pectic backbone including GT8, GAUT1 and GAUT7[54] members, the addition of minor substituents onto the pectin backbone and the biosynthesis of nascent and mature heteroxylan types. A precise temporal series employing laser capture microdissection of the developing MSCs, followed by RNAseq analysis will prove invaluable in this context.

Our microscopy analyses reveal that, in contrast to *Arabidopsis*, the seed mucilage release mechanism of *P. ovata* may be a physical process not dependent on cellular rupture followed by extrusion (Fig. 6B). Hence, for this species we suggest that it is more appropriate to describe the mechanism as an expansion rather than an

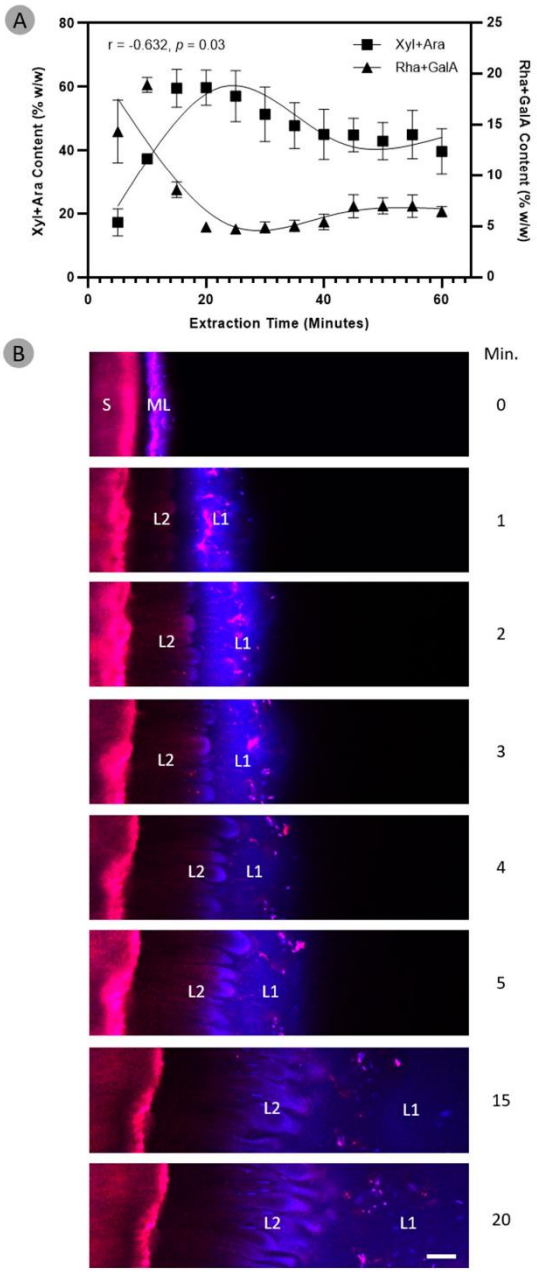
A
r = -0.632, p = 0.03
Xyl+Ara
Rha+GalA
Xyl+Ara Content (% w/w)
Rha+GalA Content (% w/w)
Extraction Time (Minutes)
B
Min.
S
ML
L2
L1
0
1
2
3
4
5
15
20

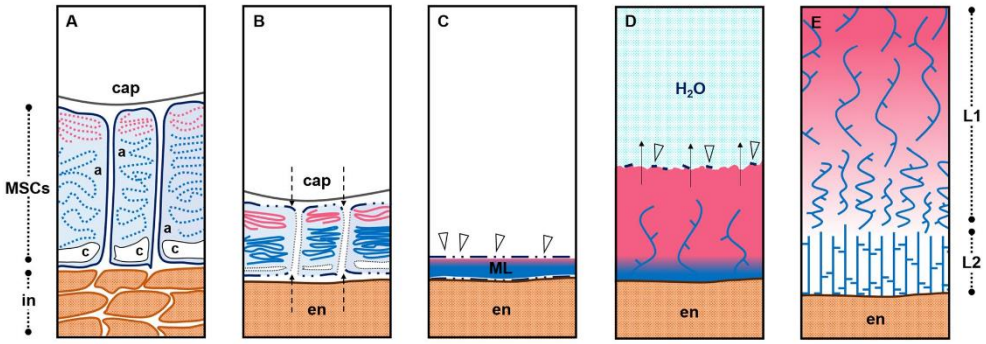

Figure 7. A proposed model of the polysaccharide deposition and mucilage expansion mechanism in *P. ovata*. (**A**) Mucilage polysaccharides pectin (pink) and heteroxylan (blue) are polarly synthesised and deposited into the outer apoplast (a) of mucilage secretory cells (MSCs), (**B**) which become compressed between the endosperm (en) and capsule wall (cap), obliterating the radial walls and releasing their contents into a (**C**) continuous laminated cell-free mucilage polysaccharide layer (ML) on the external seed surface when released from the capsule. (**D**) Upon exposure to an aqueous environment, the hydrophilic mucilage starts to expand outwards from the seed surface. The first layer to expand is rich in extremely hydrophilic and soluble pectin and is topped by fragile remnants of the distal MSC walls (arrowheads) that dissolve as hydration continues. This layer works to provide a hydration cascade to initiate and jumpstart hydration and swelling of the more gel-like, less hydrophilic polymers. (**E**) A hypothesised distribution of mucilaginous polysaccharides. The pink gradient is indicative of the distribution of pectin which is restricted to the periphery (or 'mucilage expansion front') of the expanded seed mucilage (as per Fig. 6) whilst the xylan polysaccharides (blue strands) are evenly distributed (Fischer et al.[12]; Guo et al.[55]; Yu et al.[9]). In L1, the enrichment of pectin may proportionally modulate the solubility/extractability of xylan while in L2, pectin is not present and thus xylan polymers form a more robust, gel-like layer. *In* integument, *c* cytoplasm.

extrusion, similar to the extension of a concertina, where the mucilage starts to expand into the aqueous environment as it hydrates from the wrinkled appressed polysaccharide layer on the seed surface. Data demonstrating the change in mucilage composition and structure over time (Fig. 6) support this type of expansion process. The driving forces behind expansion of *P. ovata* seed mucilage could be derived from the differential hydrophilicity of the constituent mucilaginous polysaccharides. Pectin is most abundant in the first layer of mucilage to expand, L1 (Fig. 6B) and previous studies have described the outermost layer of the expanded seed mucilage to be a highly soluble, pectin-rich fraction[9,12,55]. In *P. ovata*, this seed mucilage fraction was easily extracted using cold water[9,10] and we propose that its function is to act as a primer, initiating mucilage expansion, and providing a hydration cascade triggering the swelling of the more gel-like and structurally-complex heteroxylan polymers located in subsequent fractions/layers (SI Fig. S6). Compositional data supporting such patterns of polymer release have been reported previously[9,10,13], and now a model to illustrate this process, driven by polarised deposition and then expansion, is presented in Fig. 7. To fulfil such a role the pectin-enriched fraction must be synthesised and/or deposited first into the distal end of the MSC, anchoring the mucilage to the seed to form L1, after which the structural polymers, including heteroxylan, are synthesised and/or deposited into the basal end of the cell to make L2 (Fig. 6A). A similar spatio-temporal pattern of polysaccharide synthesis and deposition was recently described by Miart et al.[36] who showed that RG-I (pectin) was synthesised in the two outermost layers of *L. usitatissimum* MSCs prior to synthesis of other polysaccharides in the layers beneath. The authors hypothesised that the arabinoxylan, xyloglucan and cellulose polysaccharides synthesised later in the inner layers provided a structural element that pressurised the outermost contents, enabling efficient mucilage release and anchoring the mucilage to the seed. Similarly, the heterotypic interactions of various polymers including branched xylan, cellulose and arabinogalactan proteins are important for effective mucilage release and adherence in *Arabidopsis*[3,5,6,8,19,56]. In support of this temporal sequence of events, real-time qPCR analysis of cDNA from developing *L. usitatissimum* integument tissue shows that genes involved in pectin biosynthesis are transcriptionally active prior to those associated with xylan biosynthesis (Aubert et al., University of Adelaide, unpublished data). The mucilage component of *P. ovata*, and likely many other species, is a complex network of heterogeneously distributed polysaccharides. Each polymer must be synthesised, deposited, and potentially modified, in a specific sequence and location during seed development to be able to fulfil the required mechanical functions enabling mucilage release, and supporting the structural functions of the material once it extends from the seed surface. The process of mucilage polysaccharide biosynthesis and deposition into the MSCs must therefore be a tightly regulated process, about which we have much to learn.

In future work, it would be valuable to characterise the MSCs of *Plantago* species such as *P. cunninghamii* that we have already confirmed to possess a similar seed surface arrangement to *P. ovata*, but that has a different expanded mucilage architecture[11]. Our preliminary characterisation of the MSCs of *P. ovata* has generated further questions regarding the biosynthesis and deposition of mucilaginous polysaccharides: how, where, and

in what order are these polymers transported and deposited into the MSCs? What genes and regulatory elements are controlling this highly complex process? And what drives the fate of the integument cells? Should we be looking for signs of programmed cell death or a suite of cell wall degrading enzymes in this tissue? Combining further histological analysis of the developing seeds, with a focus on the MSCs and the integument tissue, with characterisation of the temporal regulation of mucilage biosynthetic transcripts may begin to answer some of these questions. Our whole mount immunolabelling data suggests that hydrated heteroxylan is distributed in a specific digit-like pattern whilst immunolabelling of seed sections show that the heteroxylan and pectin are homogenously distributed throughout the expanded seed mucilage (Phan et al.[11]). It remains unclear how these polymers are deposited and distributed in both the developing MSCs, the mature mucilage polysaccharide layer, and the final expanded material. Thorough investigation of the developing MSCs in *P. ovata* may begin to shed some light upon these questions and allow us to fine tune our hypothetical model, whilst eventually providing tools to allow manipulation of the mucilage quantity and quality that could directly impact downstream applications and economics of psyllium use.

Materials and methods

Plant materials and growth. Wild-type *P. ovata* and gamma-irradiated *P. ovata* mutant 69-1 were obtained from a population previously generated by Tucker et al.[43]. Three 69-1 sister lines at M4 were tested to show that > 95% of the seeds in each sister line displayed a developmentally delayed phenotype. The mutant line has not yet been backcrossed to wild type.

Plants were grown as per Phan et al.[11]. To stage wild-type fruit development, fruits with freshly emerged anthers (erect and bright-yellow in colour) were marked and tagged with the date in order to harvest at the relevant day post-anthesis (DPA).

Observing *P. ovata* expanded seed mucilage. *Ruthenium red.* Mature *P. ovata* seeds were individually placed onto microscopy slides in a ruthenium red solution at a concentration of 0.01% (w/v) (ProSciTech, C075, Australia). Seeds were observed under a Zeiss Stemi 2000-C dissecting microscope with an attached AxioCam ERc 5s camera. Seeds with impaired development were selected from the mutant line 69-1[43].

Time-lapse. Mature *P. ovata* seeds were prepared as per Yu et al.[9]. In brief, dry mature *P. ovata* seeds were soaked overnight in stain solution comprised of 0.1% w/v Calcofluor White (Fluorescent Brightener 28, Sigma-Aldrich) and 0.4% w/v Direct Red 23 (Sigma-Aldrich) diluted in 80% ethanol. The seeds were removed from the staining solution and allowed to air dry before being adhered with a cyanoacrylate adhesive to the centre of a Petri dish. The Petri dish was mounted onto the stage of a Nikon A1R Laser Scanning Confocal with DS-Ri1 CCD camera and imaged prior to the addition of deionised water onto the seed at time = 0. Images were captured for 20 min in total at 1 min intervals.

Fixation, embedding, and sectioning of *P. ovata* developing fruit. Samples requiring fixation, embedding, and sectioning were processed as per Burton et al.[57] and embedded tissue was sectioned at 1 µm on an Ultramicrotome (Leica, EM UC6) using a diamond knife (DiATOME, Nidau, Switzerland). For non-aqueous fixation, PBS was replaced with an 80% ethanol solution. Sections were stained with Toluidine Blue (epoxy tissue stain, used undiluted, ProSciTech, C149, Australia). Sections were imaged under transmitted light differential interference contrast (DIC) using a Zeiss Axio Imager M2 (Carl Zeiss, Germany) fitted with an AxioCam MRm3 monochrome camera.

For fluorescence images, samples were fixed, embedded, and sectioned as above for non-aqueous fixation. Survey sections were stained with epoxy tissue stain (used undiluted, ProSciTech, Australia). For immunofluorescence, sections were incubated with monoclonal antibodies raised against pectin (LM19 and LM20) and arabinoxylan (LM11) (PlantProbes Leeds, UK) followed by an appropriate AlexaFluor 555 secondary antibody (Invitrogen, USA). The His-tagged carbohydrate-binding module CBM3a (PlantProbes, Leeds, UK) was used with a triple indirect immunofluorescence labelling procedure as described previously[11,58]. Sections were counterstained using Calcofluor White (Fluorescent Brightener 28; Sigma-Aldrich) and mounted in glycerol. Images were obtained using an AxioCam 105 color camera fitted to a Zeiss fluorescence microscope (Axio Imager M2, Carl Zeiss, Germany) with 254/432 nm excitation/emission wavelength for Calcofluor White and 553/568 nm excitation/emission wavelength for LM11/LM19/LM20/CBM3a.

Scanning electron microscopy. Mature seeds of *P. ovata* and *Arabidopsis thaliana* ecotype *Columbia-0* were air-dried before and after mucilage hydration then sputter-coated with platinum at a thickness of 5 nm. Seeds were imaged at a working distance of 7.5 mm with an accelerating voltage of 3 kV using a Philips XL20 Scanning Electron Microscope (SEM) following Phan et al.[11].

Mucilage extraction and compositional analysis. For temporal mucilage analysis, mucilage was collected by placing 1 g mature seeds into a wide-mouth sieve, placed in a water bath containing 40 mL of deionised water at room temperature with intermittent stirring. Fractions were collected at 5 min intervals by transferring the sieve and seeds into a fresh batch of deionised water. Mucilage extracts were freeze–dried to a constant weight and compositional analysis was conducted as per Hassan et al.[59].

For comparison of mutant 69-1 with the wild-type, mucilage was extracted from 40 seeds for 3 h in 20 mL of deionised water heated to 80 °C and stirred vigorously on a heated magnetic stirrer. While still hot, the mucilage and seeds were transferred into a 50 mL tube and centrifuged for 10 min at 4,000 rpm. The mucilage supernatant

was decanted into a new tube and freeze–dried to a constant weight. Yield per seed was calculated by dividing the freeze–dried mucilage mass by 40. Compositional analysis was conducted as per Hassan et al.[59].

Data availability

The datasets generated and/or analysed in this study are available from the corresponding author on reasonable request.

Received: 12 March 2020; Accepted: 25 June 2020
Published online: 16 July 2020

References

1. Phan, J. L. & Burton, R. A. New insights into the composition and structure of seed mucilage. *Annu. Plant Rev. Online* **1**, 1–41 (2018).
2. Macquet, A., Ralet, M.-C., Kronenberger, J., Marion-Poll, A. & North, H. M. *In situ*, chemical and macromolecular study of the composition of *Arabidopsis thaliana* seed coat mucilage. *Plant Cell Physiol.* **48**, 984–999 (2007).
3. Harpaz-Saad, S. *et al.* Cellulose synthesis via the FEI2 RLK/SOS5 pathway and CELLULOSE SYNTHASE 5 is required for the structure of seed coat mucilage in *Arabidopsis*. *Plant J.* **68**, 941–953 (2011).
4. Yang, B. *et al.* TRM 4 is essential for cellulose deposition in Arabidopsis seed mucilage by maintaining cortical microtubule organization and interacting with CESA 3. *New Phytol.* **221**, 881–895 (2019).
5. Yu, L. *et al.* CELLULOSE SYNTHASE-LIKE A2, a glucomannan synthase, is involved in maintaining adherent mucilage structure in *Arabidopsis* seed. *Plant Physiol.* **164**, 1842–1856 (2014).
6. Voiniciuc, C., Günl, M., Schmidt, M.H.-W. & Usadel, B. MUCI10 produces galactoglucomannan that maintains pectin and cellulose architecture in *Arabidopsis* seed mucilage. *Plant Physiol.* **169**, 403–420 (2015).
7. Hu, R. *et al.* Xylan synthesized by Irregular Xylem 14 (IRX14) maintains the structure of seed coat mucilage in Arabidopsis. *J. Exp. Bot.* **67**, 1243–1257 (2016).
8. Hu, R. *et al.* Irregular xylem 7 (IRX7) is required for anchoring seed coat mucilage in Arabidopsis. *Plant Mol. Biol.* **92**, 25–38 (2016).
9. Yu, L. *et al.* Multi-layer mucilage of *Plantago ovata* seeds: Rheological differences arise from variations in arabinoxylan side chains. *Carbohydr. Polym.* **165**, 132–141 (2017).
10. Cowley, J. M. *et al.* A small-scale fractionation pipeline for rapid analysis of seed mucilage characteristics. *Plant Methods* **16**, 1–12 (2020).
11. Phan, J. L. *et al.* Differences in glycosyltransferase family 61 accompany variation in seed coat mucilage composition in *Plantago* spp.. *J. Exp. Bot.* **67**, 6481–6495 (2016).
12. Fischer, M. H. *et al.* The gel-forming polysaccharide of psyllium husk (*Plantago ovata* Forsk). *Carbohydr. Res.* **339**, 2009–2017 (2004).
13. Ren, Y., Yakubov, G. E., Linter, B. R., Macnaughtan, W. & Foster, T. J. Temperature fractionation, physicochemical and rheological analysis of psyllium seed husk heteroxylan. *Food Hydrocoll.* https://doi.org/10.1016/j.foodhyd.2020.105737 (2020).
14. Jensen, J. K., Johnson, N. R. & Wilkerson, C. G. *Arabidopsis thaliana* IRX10 and two related proteins from psyllium and *Physcomitrella patens* are xylan xylosyltransferases. *Plant J.* **80**, 207–215 (2014).
15. Urbanowicz, B. R., Peña, M. J., Moniz, H. A., Moremen, K. W. & York, W. S. Two Arabidopsis proteins synthesize acetylated xylan in vitro. *Plant J.* **80**, 197–206 (2014).
16. Chiniquy, D. *et al.* XAX1 from glycosyltransferase family 61 mediates xylosyltransfer to rice xylan. *Proc. Natl. Acad. Sci. USA* **109**, 17117–17122 (2012).
17. Anders, N. *et al.* Glycosyl transferases in family 61 mediate arabinofuranosyl transfer onto xylan in grasses. *Proc. Natl. Acad. Sci. USA* **109**, 989–993 (2012).
18. Voiniciuc, C., Gunl, M., Schmidt, M.H.-W. & Usadel, B. Highly branched Xylan made by IRREGULAR XYLEM14 and MUCILAGE-RELATED21 Links mucilage to. *Plant Physiol.* **169**, 2481–2495 (2015).
19. Ralet, M.-C. *et al.* Xylans provide the structural driving force for mucilage adhesion to the Arabidopsis seed coat. *Plant Physiol.* **171**, 165–178 (2016).
20. Jensen, J. K., Johnson, N. & Wilkerson, C. G. Discovery of diversity in xylan biosynthetic genes by transcriptional profiling of a heteroxylan containing mucilaginous tissue. *Front. Plant Sci.* **4**, 20 (2013).
21. Marlett, J. A., Kajs, T. M. & Fischer, M. H. An unfermented gel component of psyllium seed husk promotes laxation as a lubricant in humans. *Am. J. Clin. Nutr.* **72**, 784–789 (2000).
22. McRorie, J. W. *et al.* Psyllium is superior to docusate sodium for treatment of chronic constipation. *Aliment. Pharmacol. Ther.* **12**, 491–497 (1998).
23. Anderson, J. W. *et al.* Cholesterol-lowering effects of psyllium intake adjunctive to diet therapy in men and women with hypercholesterolemia: Meta-analysis of 8 controlled trials. *Am. J. Clin. Nutr.* **71**, 472–479 (2000).
24. Cappa, C., Lucisano, M. & Mariotti, M. Influence of Psyllium, sugar beet fibre and water on gluten-free dough properties and bread quality. *Carbohydr. Polym.* **98**, 1657–1666 (2013).
25. Mancebo, C. M., San Miguel, M. Á, Martínez, M. M. & Gómez, M. Optimisation of rheological properties of gluten-free doughs with HPMC, psyllium and different levels of water. *J. Cereal Sci.* **61**, 8–15 (2015).
26. Fratelli, C., Muniz, D. G., Santos, F. G. & Capriles, V. D. Modelling the effects of psyllium and water in gluten-free bread: An approach to improve the bread quality and glycemic response. *J. Funct. Foods* **42**, 339–345 (2018).
27. Haque, A. & Morris, E. R. Combined use of ispaghula and HPMC to replace or augment gluten in breadmaking. *Food Res. Int.* **27**, 379–393 (1994).
28. Bahrani, A. S. Processes for dehusking psyllium seeds. *US Pat. Number 5020732* (1991).
29. Kumar, J. *Good agricultural practices for isabgol.* (2015).
30. Francoz, E., Ranocha, P., Burlat, V. & Dunand, C. *Arabidopsis* seed mucilage secretory cells: Regulation and dynamics. *Trends Plant Sci.* **20**, 515–524 (2015).
31. Schneitz, K., Huiskamp, M. & Pruitt, R. E. Wild-type ovule development in *Arabidopsis thaliana*: A light microscope study of cleared whole-mount tissue. *Plant J.* **7**, 731–749 (1995).
32. Windsor, J. B., Symonds, V. V., Mendenhall, J. & Lloyd, A. M. Arabidopsis seed coat development: Morphological differentiation of the outer integument. *Plant J.* **22**, 483–493 (2000).
33. Beeckman, T., Rycke, R. D., Viane, R. & Inzé, D. Histological study of seed coat development in *Arabidopsis thaliana*. *J. Plant Res.* **113**, 139–148 (2000).
34. Western, T. L., Skinner, D. J. & Haughn, G. W. Differentiation of mucilage secretory cells of the *Arabidopsis* seed coat. *Plant Physiol.* **122**, 345–356 (2000).

35. Voiniciuc, C., Yang, B., Schmidt, M.H.-W., Gunl, M. & Usadel, B. Starting to gel: How *Arabidopsis* seed coat epidermal cells produce specialized secondary cell walls. *Int. J. Mol. Sci.* **16**, 3452–3473 (2015).
36. Miart, F. *et al.* Cytological approaches combined with chemical analysis reveals the layered nature of flax mucilage. *Front. Plant Sci.* **10**, 1–16 (2019).
37. Witzum, A. Mucilaginous plate pells in the nutlet epidermis of *Coleus blumei* Benth. (Labiatae). *Bot. Gaz.* **139**, 430–435 (1978).
38. Muñoz, L. A., Cobos, A., Diaz, O. & Aguilera, J. M. Chia seeds: Microstructure, mucilage extraction and hydration. *J. Food Eng.* **108**, 216–224 (2012).
39. Hyde, B. B. Mucilage-producing cells in the seed coat of *Plantago ovata*: Developmental fine structure. *Am. J. Bot.* **57**, 1197–1206 (1970).
40. Ruprecht, C. *et al.* A synthetic glycan microarray enables epitope mapping of plant cell wall glycan-directed antibodies. *Plant Physiol.* **175**, 00737 (2017).
41. Verhertbruggen, Y., Marcus, S. E., Haeger, A., Ordaz-Ortiz, J. J. & Knox, J. P. An extended set of monoclonal antibodies to pectic homogalacturonan. *Carbohydr. Res.* **344**, 1858–1862 (2009).
42. Ruel, K., Nishiyama, Y. & Joseleau, J. P. Crystalline and amorphous cellulose in the secondary walls of Arabidopsis. *Plant Sci.* **193–194**, 48–61 (2012).
43. Tucker, M. R. *et al.* Dissecting the genetic basis for seed coat mucilage heteroxylan biosynthesis in plantago ovata using gamma irradiation and infrared spectroscopy. *Front. Plant Sci.* **8**, 326 (2017).
44. Voiniciuc, C. *et al.* Flying saucer1 is a transmembrane RING E3 ubiquitin ligase that regulates the degree of pectin methylesterification in Arabidopsis seed mucilage. *Plant Cell* **25**, 944–959 (2013).
45. Boesewinkel, F. D. Development of ovule and testa of *Linum usitatssimum* L.. *Acta Bot. Neerl.* **29**, 17–32 (1980).
46. Madgulkar, A., Rao, M. & Warrier, D. Characterization of Pysillium (*Plantago ovata*) polysaccharide and its uses. *Polysaccharides* https://doi.org/10.1007/978-3-319-03751-6_49-1 (2014).
47. Garcia, D., FitzGerald, J. N. & Berger, F. Maternal control of integument cell elongation and zygotic control of endosperm growth are coordinated to determine seed size in Arabidopsis. *Plant Cell* **17**, 52–60 (2005).
48. Cooper, G. O. Development of the ovule and the formation of the seed in *Plantago lanceolata*. *Am. J. Bot.* **29**, 577–581 (1942).
49. Mikesell, J. Anatomy of terminal haustoria in the ovule of Plantain (*Plantago major* L.) with taxonomic comparison to other angiosperm taxa. *Bot. Gaz.* **151**, 452–464 (1990).
50. Johri, B., Ambegaokar, K. & Srivastava, P. *Plantaginales. Comparative Embryology of Angiosperms* 777–779 (Springer, Berlin, 1992).
51. Saez-Aguayo, S. *et al.* PECTIN METHYLESTERASE INHIBITOR6 promotes *Arabidopsis* mucilage release by limiting methylesterification of homogalacturonan in seed coat epidermal cells. *Plant Cell* **25**, 308–323 (2013).
52. Macquet, A. *et al.* A naturally occurring mutation in an *Arabidopsis* accession affects a β-D-galactosidase that increases the hydrophilic potential of rhamnogalacturonan I in seed mucilage. *Plant Cell* **19**, 3990–4006 (2007).
53. Walker, M. *et al.* The transcriptional regulator LEUNIG_HOMOLOG regulates mucilage release from the *Arabidopsis* testa. *Plant Physiol.* **156**, 46–60 (2011).
54. Atmodjo, M. A., Hao, Z. & Mohnen, D. Evolving views of pectin biosynthesis. *Annu. Rev. Plant Biol.* **64**, 747–779 (2013).
55. Guo, Q., Cui, S. W., Wang, Q. & Christopher Young, J. Fractionation and physicochemical characterization of psyllium gum. *Carbohydr. Polym.* **73**, 35–43 (2008).
56. Sullivan, S. *et al.* CESA5 is required for the synthesis of cellulose with a role in structuring the adherent mucilage of Arabidopsis seeds. *Plant Physiol.* **156**, 1725–1739 (2011).
57. Burton, R. A. *et al.* Over-expression of specific HvCslF cellulose synthase-like genes in transgenic barley increases the levels of cell wall (1,3;1,4)-β-D-glucans and alters their fine structure. *Plant Biotechnol. J.* **9**, 117–135 (2011).
58. Guillon, F. *et al.* Brachypodium distachyon grain: Characterization of endosperm cell walls. *J. Exp. Bot.* **62**, 1001–1015 (2011).
59. Hassan, A. S. *et al.* A Genome Wide Association Study of arabinoxylan content in 2-row spring barley grain. *PLoS One* **12**, 1–19 (2017).

Acknowledgements

The authors would like to thank Associate Professor Matthew R Tucker for ongoing scientific discussions. The authors acknowledge the facilities, and the scientific and technical assistance, of the Australian Microscopy and Microanalysis Research Facility at Adelaide Microscopy, The University of Adelaide, Waite Campus, for their assistance in using the SEM and confocal microscope and Dr Long Yu for assistance in developing a method to stain the mucilage of mature seeds. This work was supported by the Australian Research Council (ARC) Centre of Excellence in Plant Cell Walls (CE110001007) and Plant Energy Biology (CE140100008). JP was supported by a University of Adelaide's CJ Everard PhD Scholarship, a Grains Research and Development Corporation (GRDC) scholarship and a SARDI Bursary, JMC was supported by the Australian Government's Research Training Program and LH was supported by a University of Adelaide's Adelaide Graduate Research Scholarship.

Author contributions

J.P. and R.A.B. conceived the study. J.P., J.M.C., K.A.N., L.H. and L.A.O. prepared materials and performed experiments. All authors contributed to the data analysis and interpretation. J.P., J.M.C. and R.A.B. wrote the manuscript. All authors approved the final manuscript.

Additional information

Supplementary information is available for this paper at https://doi.org/10.1038/s41598-020-68685-w.

Correspondence and requests for materials should be addressed to R.A.B.

Reprints and permissions information is available at www.nature.com/reprints.

Publisher's note Springer Nature remains neutral with regard to jurisdictional claims in published maps and institutional affiliations.

CHAPTER 5

Seed characteristics and composition of Australian *Plantago* species: insights into drivers of natural variation and the nutritional value of whole seeds

This chapter was written to the sounds of...	
Album	Rainbow Valley
Artist	Matt Corby
Favourite Song	Light My Dart Up

Statement of Authorship

Title of Paper	Seed characteristics and composition of Australian *Plantago* species: insights into drivers of natural variation and the nutritional value of whole seeds
Publication Status	☐ Published ☐ Accepted for Publication ☐ Submitted for Publication ☑ Unpublished and Unsubmitted work written in manuscript style
Publication Details	

Principal Author

Name of Principal Author (Candidate)	James M. Cowley		
Contribution to the Paper	Conceived the study, performed experiments, analysed and interpreted data, wrote the manuscript		
Overall percentage (%)	80%		
Certification:	This paper reports on original research I conducted during the period of my Higher Degree by Research candidature and is not subject to any obligations or contractual agreements with a third party that would constrain its inclusion in this thesis. I am the primary author of this paper.		
Signature		Date	13/6/2020

Co-Author Contributions

By signing the Statement of Authorship, each author certifies that:

i. the candidate's stated contribution to the publication is accurate (as detailed above);
ii. permission is granted for the candidate in include the publication in the thesis; and
iii. the sum of all co-author contributions is equal to 100% less the candidate's stated contribution.

Name of Co-Author	Rachel A. Burton		
Contribution to the Paper	Conceived the study and contributed to writing the manuscript		
Signature		Date	13/6/20

TITLE: Seed characteristics and composition of Australian *Plantago* species: insights into drivers of natural variation and the nutritional value of whole seeds

AUTHORS: James M. Cowley[1,2] and Rachel A. Burton[1,2*]

AFFILIATIONS: [1]Australian Research Council Centre of Excellence in Plant Cell Walls, School of Agriculture, Food and Wine, University of Adelaide, Waite Campus, Urrbrae, SA, Australia; [2]Australian Research Council Centre of Excellence in Plant Energy Biology, School of Agriculture, Food and Wine, University of Adelaide, Waite Campus, Urrbrae, SA, Australia;

Abstract

Background and aims

Upon wetting, polysaccharides on the outer surface of *Plantago* seeds swell to form a gel-like coating called mucilage that has value as a food additive and bulking dietary fibre. However, the only commercially-relevant species, *P. ovata*, is plagued by many agronomy-related quality issues and could be more efficiently used as the non-mucilage-producing tissues, comprising the seed embryo and endosperm, are usually disposed of after milling. The aim of this study was to profile whole seeds of diverse *Plantago* species to identify potential new uses in food and industrial applications and reduce waste.

Methods

Histochemical, physicochemical and chromatographic analyses were used to profile seed composition and morphology of commercial psyllium, *P. ovata*, and 11 relatives, (three naturalised and eight native to Australia) and phylogenetic and distribution analyses were used to discuss evolutionary implications and possible trait adaptation.

Key results

There is substantial variation in *Plantago* mucilage yield and its properties, mainly as a consequence of differences in heteroxylan and pectin composition. We report for the first time that *Plantago* seeds have a substantial mannan-rich endosperm that contains health-promoting fermentable sugars, protein and fats. Composition profiles differ interspecifically but seeds of Australian native *Plantago* contain higher levels of health-promoting sugars, proteins and fats than the commercially-relevant species, *P. ovata*, plus abundant mucilage of differing compositions and properties.

Conclusion

Use of a whole seed *Plantago* flour retains the functionality of the seed mucilage, while also providing additional essential nutrients. Whole seed flour, particularly from species adapted to harsh Australian conditions, may therefore have many enhanced commercial and health benefits compared to purified *P. ovata* mucilage.

Keywords

Plantago; seed mucilage; myxospermy; natural variation; endosperm; nutrition; seed oil; heteroxylan; mannan; dietary fibre.

Introduction

Plants of the genus *Plantago* occur widely throughout the world. Traditionally, all parts of the plant are used (Samuelsen 2000; Heimler *et al.* 2007; Çoban *et al.* 2008; Moreno-Salazar *et al.* 2008; Zubair *et al.* 2016), but the seeds have particular importance as they produce a viscous gel upon wetting, called mucilage, that has many folk food and medicinal uses. For example, seeds of Australian *Plantago* species were pounded into a flour by Aboriginal and Torres Strait Islander peoples and combined with water to make a porridge thickened by the sticky mucilage (Low 1988; Gott 2006). Early British settlers also noted the palatability of Australian native *Plantago* seeds, exploiting the jelly-like mucilage to prepare sweetened desserts similar to sago pudding (Maiden 1898). More recently, *Plantago* seed mucilage has gained great industrial and medical significance. Commonly known as psyllium husk, the milled seed mucilage of *P. ovata* contains a highly-hydrophilic hemicellulose called heteroxylan (Phan *et al.* 2020), used to texturally mimic fat (Aghdaei *et al.* 2014) and gluten (Haque and Morris 1994; Cappa *et al.* 2013), and as a dietary fibre supplement to aid laxation (McRorie *et al.* 1998), treat hypercholesterolemia (Anderson *et al.* 2000), diabetes (Anderson *et al.* 1999), and irritable bowel syndrome (Bijkerk *et al.* 2009). While the clinical benefits of psyllium husk are generally attributed to the high viscosity of the heteroxylan, pre-clinical and *in vitro* studies showing free radical scavenging (Ye *et al.* 2011; Harput *et al.* 2012; Zhou *et al.* 2013; Gong *et al.* 2015; Han *et al.* 2016; Behbahani, Tabatabaei Yazdi, *et al.* 2017), immunomodulation (Huang *et al.* 2009, 2014; Jiang *et al.* 2014), and treatment of metabolic disorders (Romero *et al.* 2002; Galisteo *et al.* 2005; Samout *et al.* 2016; Yang *et al.* 2017) by extracts of whole *Plantago* seeds demonstrates that the non-husk/non-mucilage seed components (typically disposed of in commercial production) may have further beneficial effects. The concept of using whole seed *Plantago* flour as a less wasteful, more nutritious

alternative to psyllium husk is gaining interest and just recently unhusked *P. ovata* and *P. psyllium* flour were shown to be a useful hydrocolloid replacement in baking (Pejcz *et al.* 2018; Ziemichód *et al.* 2018). However, remarkably little is known about whole *Plantago* seed composition, particularly from a nutritional perspective, and how each component differs between species. The natural variation in such a diverse, cosmopolitan genus has already been a valuable resource to study polysaccharide biosynthesis (Jensen *et al.* 2013; Phan *et al.* 2016) and to obtain polymers with unique functional properties for industry (Saeedi *et al.* 2010, 2013; Yin *et al.* 2016; Behbahani, Shahidi, *et al.* 2017; Behbahani, Tabatabaei Yazdi, *et al.* 2017; Benaoun *et al.* 2017; Addoun *et al.* 2020). Since Australia is such a large, environmentally-diverse continent, it may boast species that are currently an untapped resource, perhaps even providing an alternative to *P. ovata*. Australian species would have the added advantage of being already adapted to demanding climatic conditions, and may be useful in overcoming production constraints of the current orphan crop (Kumar 2015).

Here we have compared the composition and morphology of seeds of commercial psyllium, *P. ovata*, to eleven related species naturalised or native to Australia. This has revealed great diversity in mucilage properties and composition and has provided the first comprehensive overview of *Plantago* seed composition, showing them to be rich in beneficial sugars, fats and protein, suggesting potentially valuable health effects from whole seed flour consumption. We also discuss the ecophysiological context of the natural variation described here.

Materials and methods

Diversity and distribution analysis

Distribution records of *Plantago* species were accessed in July 2020 from the Atlas of Living Australia (ALA) database at http://www.ala.org.au and spatial analysis and mapping were conducted using the ALA Spatial Portal. Distribution records were filtered for the following criteria: (1) Human observations, living and preserved specimens only; (2) Observations with both genus and species listed; (3) Observations with geographic coordinates; (4) New Zealand endemic species excluded; (5) Subspecies were combined with associated species records. Colour-coded 30 year (1960-1990) average annual rainfall data was obtained from the Bureau of Meteorology (Commonwealth of Australia) under use of the Creative Commons Attribution Australia Licence (CC BY 3.0 AU) (https://creativecommons.org/licenses/by/3.0/au/legalcode).

Plant growth

Seeds of twelve *Plantago* species were obtained from the sources listed in Supplementary Table 5.1. Seeds were vernalised dry for 48 hours at -20 °C prior to germination then imbibed in filtered (0.22 µm) sterilisation agent (50:50, 50% ethanol:4% bleach with 0.05% Triton X-100) for 1 min before replacing the sterilisation agent and incubating for another minute. This was repeated until the seeds had been imbibed in fresh sterilisation agent 5 times, after which the seeds were washed 5 times with filter-sterilised (0.22 µm) Milli-Q water. Seeds were spread onto pre-wetted autoclaved Whatman No. 1 paper in a sterile petri dish. Dishes were sealed, aluminium foil-wrapped and vernalised for another 48 hours at 4 °C. After vernalisation, plates were moved to a glasshouse with a day/night temperature of 23 °C/18 °C. Seeds were germinated for 10 days (3 days dark then 7 days exposed to the glasshouse day/night

light cycle) then transferred to coco-peat soil mixture in tall citrus pots. Plants were grown to maturity from June to December (Adelaide, Australia) with no supplemental light.

Phylogenetic analysis

Mature leaf tissue from *Plantago* plants was frozen at -80 °C and ground by stainless steel ball bearing for 30 sec at 30 Hz using a MM400 Mixer Mill (Retsch, Germany) fitted with 2 ml tube adapter. DNA was extracted from ground leaf tissue following Healey *et al.* (2014). Nuclear ribosomal internal transcribed spacer (ITS) regions were amplified by PCR using primers (Sun *et al.* 1994) and conditions listed in Supplementary Table 5.2. Amplified ITS regions were sequenced by AGRF (Adelaide, Australia). ITS sequences for other *Plantago* species were downloaded from Genbank using their accession numbers listed in Rønsted *et al.* (2002) and where possible, sequence identities were confirmed by MUSCLE nucleotide alignment with published sequences from Rønsted *et al.* (2002) and Tay *et al.* (2010). ITS sequences of *Veronica glandulosa*, AF313008.1 (Albach *et al.* 2001), and *V. salicornioides*, FJ024624.1 (Tay *et al.* 2010), were also downloaded from Genbank and used as outgroups as per Rønsted *et al.* (2002).

ITS sequences were trimmed using BMGE (Criscuolo and Gribaldo 2010) and the neighbour-joining comparison tree constructed in Geneious v8.1.3 (Biomatters Ltd, NZ) with the RAxML tree builder (Stamatakis 2006) using the GTR GAMMA nucleotide model with 500 rapid bootstrapping replicates.

Seed morphometric measurements

Seed length and width measurements were determined by image analysis. Images of seeds were taken at 1x magnification on an AxioImager M2 (Zeiss, Germany) fitted with an AxioCam 105 colour camera (Zeiss, Germany). Length and width of 20 seeds

per species were measured using ZEN 2012 software (Zeiss, Germany). To determine 1000 seed weight, seeds were manually counted and weighed.

Mucilage microscopy

Mucilage architecture was observed by whole mount immunolocalisation of heteroxylan using the LM11 antibody (McCartney *et al.* 2005) and ruthenium red staining following Phan *et al.* (2016). Ruthenium red used in this work (C075) was purchased from ProSciTech (Australia) and prepared as per Cowley *et al.* (2020).

Whole seed thin section microscopy and immunolabelling

Whole seeds were transversely halved with a razor blade and fixed and embedded as per Burton *et al.* (2011) modified to use the 80% ethanol fixative described in Phan *et al*. (2020). Fixed and embedded tissue was sectioned at 1 μm on an Ultramicrotome (Leica, EM UC6) using a diamond knife (DiATOME, Nidau, Switzerland). After staining thin sections with toluidine blue, internal seed structures were imaged with an AxioImager M2 (Zeiss, Germany) fitted with an AxioCam 105 colour camera (Zeiss, Germany). Endosperm mannan polysaccharides were immunolocalised using a 10-fold dilution of LM21 anti-(1,4)-β-mannan primary antibody (Kerafast, US). The secondary antibody, Alexa Fluor 555 goat anti-rat IgG, was applied at a 100-fold dilution. All fluorescent images were taken with a Zeiss M2 AxioImager with an AxioCam 506 mono black and white camera. Images were processed using ZEN 2012 software (Zeiss, Germany).

Seed mucilage fractionation and yield analysis

Mucilage was extracted and fractionated and yield traits were determined following Cowley *et al.* (2020) with no deviation from the described procedure. Briefly, 1 mL of water was added to 30 mg of seed and extracted at 25 °C for 1.5 hr with agitation. After brief centrifugation, the supernatant was transferred to a new tube (cold water

extractable (CWE) mucilage fraction) and the volume of the pellet-containing tube was returned to 1mL. The extraction was repeated again but at 65 °C to obtain the hot water extractable (HWE) mucilage fraction. Finally, the pellet (seeds with the most extraction resistant mucilage fraction) were agitated on a tissue disruptor-type mill at 30 Hz for 10 min to obtain the intense agitation extractable (IAE) fraction. Collected fractions were freeze-dried to a constant weight and compared to starting mass of seeds to determine the yield:

$$\text{Yield } (\%) = \left(\frac{\text{mass of freeze dried mucilage}}{\text{mass of seeds pre-extraction}} \right) \times 100$$

Mucilage water absorption capacity assay

The water absorption capacity was determined following Cowley *et al.* (2020) with modifications. As the seeds were of variable size, 30 mg were weighed into 2 mL microcentrifuge tubes and 1 g of deionized water was added to each tube. After briefly vortexing to break surface tension and submerge seeds, the seed mucilage was allowed to expand, undisturbed, for 45 min at room temperature (25 °C). After 45 min, a 1000 µL laboratory pipette was used to remove unabsorbed water, avoiding disturbing the seeds and their mucilage. Removed water was weighed and the water absorption capacity was determined using the following equation:

$$\text{Water absorption capacity } (g/g) = \frac{\text{Initial weight of water added - weight of unabsorbed water}}{\text{Initial weight of seeds added}}$$

Monosaccharide analysis

Monosaccharide profiles of fractionated mucilage (redispersed at 1 mg/mL in Milli-Q water) and milled whole seed flour were determined using reverse phase high performance liquid chromatography (RP-HPLC) of 1-phenyl-3-methyl-5-pyrazoline (PMP) derivatives following Cowley *et al.* (2020). Area under the peaks was compared

to standard curves of mannose, ribose, rhamnose, glucuronic acid, galacturonic acid, glucose, galactose, xylose, arabinose and fucose (Wood *et al.* 2018).

Soluble sugar extraction and profiling

Soluble sugars were extracted from whole seed flour following Vespreet *et al.* (2012) with modifications. Due to substantial mucilage gelling in water when attempting a sequential 80% ethanol and water extraction, soluble sugars were twice extracted from flour in 80% ethanol at 85 °C for 30 min on a mixer (700 rpm) at a final dilution of 1:40 (w/v, mg/µl). Supernatants were combined, diluted with water to 1:25000 (w/v, mg/µl) and 25 µl per sample were analysed by high pH anion exchange chromatography with pulsed amperometric detection (HPAEC–PAD) on a Dionex ICS-5000 system using a DionexCarboPAC™PA-20 column (3 x 150 mm) with a guard column (3 x 50 mm) kept at 30 °C and operated at a flow rate of 0.5 mL min-1. The eluents used were (A) 0.1 M sodium hydroxide and (B) 0.1 M sodium hydroxide with 1 M sodium acetate. The gradient used was: 0% (B) from 0-2 min, 20% (B) from 2-35 min, 100% (B) from 35-36.5 min, 0% (B) from 37.5-38.5 min. Detector temperature was maintained at 20 °C, data collection was at 2 Hz and the Gold Standard PAD waveform (std. quad. potential) was used.

Data acquisition, processing, and peak integration were performed using the Chromeleon™ version 7.1.3.2425 software (Thermo Scientific). Compounds were annotated and quantified based on peaks of available analytical standards. Glucose, fructose, sucrose, raffinose, 1-kestose, maltose, nystose and stachyose analytical standards were purchased from Sigma-Aldrich, while 1,1,1-kestopentaose was obtained from Bio-Strategy. A standard of planteose was purified and prepared from *Salvia hispanica* seed mucilage as per Xing *et al.* (2017). Schematic structures were

prepared using the DrawGlycan-SNFG online tool (http://www.virtualglycome.org/DrawGlycan/) (Cheng *et al.* 2017).

Protein analysis

Protein content of whole seed flour was determined by the Dumas method using a Rapid N Exceed bench top nitrogen analyser (Elementar, USA). Conversion factor was 6.25.

Lipid analysis

Total lipid in whole seed flour was determined by modified Folch method (1957) and fatty acid profiles were determined by gas chromatography of transesterified lipids following Liu *et al.* (2014). Multivariate principle component analysis for separation was performed in PAST software (version 3.25) (Hammer *et al.* 2001).

Energy Calculation

Energy content of whole seeds was estimated from the energy density of protein, carbohydrate, dietary fibre and fat components in whole *Plantago* seed (Food and Agriculture Organisation of the United Nations 1998). Average protein, carbohydrate, dietary fibre, and fat contents (% w/w) were obtained from whole seed protein, soluble sugar, monosaccharide, and lipid profiling analyses, respectively.

Results

Occurrence of mucilage among *Plantago* species

A neighbour-joining comparison of previously published *Plantago* nuclear ribosomal internally transcribed spacer (ITS) regions (Rønsted *et al.* 2002; Tay *et al.* 2010) and of the species studied here was used to produce a phylogenetic tree (Fig. 5.1). Using this tree, samples were ranked based on their relative genetic distance from the

outgroup and each other and this order is used in all subsequent figures to allow observation of trends between more distantly and more closely-related species.

The tree includes 63 of the roughly 200 species worldwide (Rahn 1996; Dhar *et al.* 2005) of which members from every continent are represented. From extensive review of the literature and experimental observations, 75% of species included in the tree have been confirmed to produce seed mucilage (n = 47), while the other 25% have not yet been reported in the literature but may also produce seed mucilage. It should also be noted that there are many other mucilage-producing *Plantago* species which have not had ITS regions sequenced (Grubert 1974).

Distribution of naturalised and Australian native *Plantago* species

In this work we have studied commercial psyllium (*P. ovata*) and 11 Australian relatives, three non-native but naturalised species (*P. coronopus, P. lanceolata*, and *P. major*), along with eight native species (*P. cunninghamii, P. paradoxa, P. turrifera, P. bellidioides, P. debilis, P. triantha, P. gaudichaudii, and P. varia*) which account for 87% of all recorded observations of *Plantago* species in Australia and New Zealand (Fig. 5.2A1 and 5.2A2). Distribution data obtained through observational and survey recordings in the Atlas of Living Australia shows that 37 species have been recorded in Australia, of which 26 are native (Fig. 5.2A-4) but non-native species are far more wide-spread and more extensively recorded (56% of observations) (Fig. 5.2A-3). Owing to their invasive nature *P. lanceolata*, *P. coronopus,* and *P. major* account for over half of all Australian observations (Fig. 5.2A-1) and represent the majority of observations of the 12 species studied here (61%) (Fig. 5.2B). Logically, the distribution of the naturalised species studied here is concentrated in areas of dense population, particularly on the Southern and Eastern Coasts (Fig. 5.2C) which are also areas of higher rainfall, like their European and Asian origins. Distribution of Australian native species is much more varied. Closely related *P. debilis, P. gaudichaudii* and *P.*

varia (Fig. 5.1) have a mostly coastal distribution, like the naturalised species, although they extend much farther into more arid, central regions. *P. cunninghamii* and *P. turrifera* are not found in coastal areas and are restricted to the arid central regions of the Eastern states and South Australia (Fig. 5.2C). Finally, Tasmanian-endemic species *P. triantha* and *P. paradoxa* are isolated to the high-elevation, high-rainfall regions of the island (and for *P. triantha* also New Zealand) and *P. bellidioides* is restricted to the Northern coast (Fig. 5.2C).

Seed mucilage characteristics

There is significant variation in expanded seed mucilage architecture of the *Plantago* species studied here (Fig. 5.3). We corroborate the same characteristics and differences in ruthenium red phenotype of *P. coronopus, P. lanceolata, P. ovata, P. major, P. cunninghamii*, *P. debilis* and *P. varia* described in detail by Phan *et al.* (2016). Here we studied five additional Australian native species and found, owing to their relatedness (Fig. 5.1), *P. turrifera* and *P. bellidioides* to be strikingly similar to *P. cunninghamii* and *P. debilis,* and *P. gaudichaudii* to be most similar to *P. varia*. These similarities were also found when immunolabelling the mucilage (Fig. 5.3a-l). Two further native species, *P. paradoxa* and *P. triantha,* despite their apparent genetic similarity to other native species (Fig. 5.1), produced a negligible mucilage envelope that was poorly distinguishable with ruthenium red staining (Fig. 5.3F and 5.4J) and only slightly more apparent with xylan-directed immunolabelling (Fig. 5.3f and 5.4j).

In this study we used our previously published mucilage fractionation method (Cowley *et al.* 2020) to investigate mucilage yield and fractionation traits (Fig. 5.4). There was significant interspecific variation in total yield (Fig. 5.4A) and fractionation profile (Fig. 5.4B) of seed mucilage. Total yield of mucilage was highest in *P. ovata* and comparatively lower in *P. lanceolata, P. paradoxa,* and *P. triantha.* Australian native species, *P. cunninghamii, P. turrifera, P. bellidioides, P. debilis, P. gaudichaudii* and *P.*

varia had quite similar total yield (Fig. 5.4A) and fractionation profiles (Fig. 5.4B) and their mucilage was poorly extractable using cold water (CWE). To complement mucilage extractability traits, the water absorption capacity by the mucilage of intact *Plantago* seeds was determined (Fig. 5.4C). Mucilage water absorption capacity (WAC) was found to vary substantially with *P. turrifera* and *P. bellidioides* having a significantly higher WAC than other species, while absorption by *P. lanceolata, P. paradoxa* and *P. triantha* was very low. A correlation study was performed to determine if there was a link between mucilage fractionation and yield traits and the observed differences in WAC (Fig. 5.4D). Logically, significant ($p < 0.05$) correlations between WAC and total mucilage content and WAC and the more gel-like extraction resistant mucilage fractions were found. The strongest correlation ($r = 0.73$, $p = 0.006$) with WAC was the proportion of hot water- and intense agitation extractable (HWE+IAE) mucilage.

The chemical composition of fractionated mucilage was determined by monosaccharide profiling which revealed both interspecific differences and trends (Fig. 5.5). Monosaccharide profiles were very similar between all fractions of all species, with xylose and arabinose comprising the majority of monosaccharides quantified along with rhamnose and galacturonic acid and minor quantities of glucose and galactose (Fig. 5.5A). Other monosaccharides for which standards were included, mannose, ribose, glucuronic acid, and fucose, were minute or not detected (data not shown). The relative abundance of each monosaccharide detected in the mucilage fractions, however, differed significantly. The arabinose to xylose ratio differed interspecifically and also between fractions. In almost all species, the arabinose to xylose ratio increases with extraction intensity (Fig. 5.5B). In *P. paradoxa*, the inverse was observed and in the CWE fraction of *P. triantha* the value was outside the expected range of less than 1 (1.28). These species produce minimal mucilage and

display poor monosaccharide recovery which explains some of the discrepancies. In *P. triantha* particularly, the CWE mucilage fraction is minute and the detected arabinose and xylose are likely not heteroxylan-derived. Values for HWE and IAE, more abundant fractions, are within the expected range (<1). The ratio of rhamnose to galacturonic acid was stable between fractions and differed minimally between species (Fig. 5.5A). Rhamnose and galacturonic acid, however, were found to be highly-enriched in the CWE fraction of all species (Fig. 5.5C) diminishing sometimes to the point of absence in subsequent fractions.

Plantago endosperm and embryo morphology and composition

Monosaccharide profiling revealed that mannose is the major non-cellulosic monosaccharide in whole seeds of all species, being the most abundant in 8 of 12 species studied here (Fig. 5.6A). Using a β-(1,4)-mannan-specific monoclonal antibody (Marcus *et al.* 2010) it was observed that *Plantago* species have a substantial endosperm with thick (grand median = 8.206 µm, Supplementary Fig. 5.1) mannan-rich walls (Fig. 5.6C–L). Minimal amounts of mannan were detected in the embryo but it was completely absent in the mucilage layer of all species except *P. cunninghamii* (Fig. 5.6G). However, mannose is completely absent in *P. cunninghamii* mucilage, even that tightly adhered to the seed (Cowley *et al.* 2020) suggesting that this is likely an artefact of non-specific binding in poorly-fixed mucilage. The endosperm cells also all contained tightly-packed spherical bodies (Supplementary Fig. 5.2) which are likely to be aleurone grains and/or oil bodies, similar to those seen in seed tissues of other species like *Cannabis sativa* (Schultz *et al.* 2020)

Soluble sugar profiling

Soluble sugar profiling was used to determine the content of rapidly-mobile non-starch reserve carbohydrates in the internal *Plantago* seed tissues (Fig. 5.7). Heat mapped

chromatographic data (Fig. 5.7A) show that the soluble sugar profiles are similar between all species with common major components, with most of the interspecific variation coming from differing abundances of the major sugars, sucrose (*β*-D-fructofuranosyl-(2→1)-*α*-D-glucopyranoside) and planteose (*α*-D-galactopyranosyl-(1→6)-*β*-D-fructofuranosyl-(2→1)-*α*-D-glucopyranoside) which account for up to 86% of the soluble sugar content (Supplementary Fig. 5.3). Some variation between profiles was evident between 2–5 min elution times but these components are (based on relative peak area; Supplementary Fig. 5.3) lowly abundant, minor sugars, possibly random mono- or di-saccharides. Quantification of extracted soluble sugars shows that the trisaccharide planteose is the major soluble sugar in seeds of the *Plantago* species studied here (up to 3.2% w/w), except in *P. lanceolata* where sucrose dominates, although followed by planteose (Fig. 5.7B). *P. lanceolata* also had the most unique soluble sugar profile in other ways: the trisaccharide raffinose (*β*-D-fructofuranosyl-(2→1)-*α*-D-glucopyranoside-(1→6)-*α*-D-galactopyranoside) and its higher homologue, the tetrasaccharide stachyose (*β*-D-fructofuranosyl-(2→1)-*α*-D-glucopyranoside-(1→6)-*α*-D-galactopyranosyl-(1→6)-*α*-D-galactopyranoside), which, present in minute quantities in other species, were additional major soluble sugars in *P. lanceolata*.

Currently unidentified, we also detected an additional sugar, Unknown 1 (Fig. 5.7A), eluting at approximately 14 mins in extracts of all species. Based on the relative chromatographic peak area, Unknown 1 appears to be a major soluble sugar in seven of the species tested, comparable to planteose amounts in *P. debilis* or *P. triantha* (Supplementary Fig. 5.3). Levels of other oligosaccharides included in the standard panel, 1-kestose, maltose, nystose, and 1,1,1-kestopentaose were tiny or not detected in the species studied here.

Morphometric and nutritional characteristics of *Plantago* seeds

Plantago seeds differ significantly in length, width and 1000 grain weight (Table 5.1) and can be categorised as small- or large-seeded (Supplementary Fig. 5.4). Seed size is not origin-specific as both native and non-native species are included in the small- and large-seeded categories (Supplementary Fig. 5.4).

To determine if there is any nutritional value in *Plantago* seeds that is normally overlooked, the seed nutrient (protein, carbohydrate, dietary fibre, and fat) composition was determined (Table 5.1). There is a significant amount of interspecific variation in the content of each nutrient. Compared to commercial psyllium (*P. ovata*) which lies at the extremes in three of four nutrients (Supplementary Fig. 5.5), the other species studied have less dietary fibre but more fat and more protein, with native species tending to have the highest protein content. In carbohydrate content, *P. ovata* is close to the median. *P. ovata* and *P. lanceolata* have a lower energy content than all other species due to their low protein and fat content (~900 kJ vs. ~1100 kJ).

After determining that *Plantago* seeds contain a modest fat content, we investigated the fatty acid composition of the seed oil (Table 5.1). The ratio of saturated (SFA) to unsaturated fatty acids (UFA) is relatively similar between species (Median = 1:5.2) but six of eight native species were slightly higher in UFA content, up to 33% more than *P. ovata* in *P. gaudichaudii* (1:6.4). The saturated fatty acid profiles are very similar between species with palmitic (16:0) and stearic acid (18:0) accounting for at least 94% of SFA species. The most variation in fatty acid profiles comes from differences in the UFA profile. Multivariate analysis shows that 89% of variance between the species is due to differences in the ratio of omega-3 to omega-6 UFAs (Supplementary Fig. 5.6). All native species except *P. triantha* separate from commercial psyllium and the naturalised species because they contain a much higher quantity of omega-3 UFA in the seed oil. Commercial psyllium seed contains the least omega-3 UFA (3.2% w/w) of the species studied followed by the naturalised species (at most 28% w/w in *P.*

coronopus). This is in clear contrast to the native species which contain an average of 39% omega-3 UFA (w/w), up to 54.5% in *P. turrifera*. When calculated as the omega-3 to omega-6 ratio, all native species have ratios greater than 1 (1.37–4.85) except *P. triantha* which has a very low ratio similar to non-native species which are all less than 1 (0.11–0.76). The yield of the major omega-3 UFA, alpha-linoleic acid (18:3) is particularly high in native species where, again, *P. turrifera* has the highest yield of 6.27% (w/w). There is also a small amount of variation (8%) from differences in the omega-6 to omega-9 UFA ratio. The omega-6 to omega-9 ratio was fairly similar between native species and much greater in naturalised species (up to 2.6 times greater than the native species average). Transaturated fatty acids were not present (data not shown).

Discussion

Seed mucilage is a ubiquitous, exploitable trait among *Plantago* species

Here the ubiquitous presence but variable nature of seed mucilage in *Plantago* is demonstrated. The *Plantago* species used in this study represent a good proportion of the genus instances recorded in the Atlas of Living Australia (87% of observations) (Fig. 5.2A). Only two native species not studied here had more than 250 observations and thus remaining species are considered very rare. Other non-native species (n = 8) have fewer than 150 recorded observations which could possibly be attributed to unsuccessful establishments, garden escapes, or misidentifications. The species studied in this work have different distributions and are found in a wide variety of environments and thus represent suitable genetic/interspecific variation in traits such as seed composition which have commercial value if properly scrutinised.

Substantial variation in *Plantago* seed mucilage characteristics may be an adaptive trait to cope with variable water availability in arid Australian environments

For such a high carbon-cost material, the evolutionary function of seed mucilage is largely unknown. Seed mucilage is a homoplastic trait with each occurrence having a unique and probably specific function that is often difficult to decipher. Numerous roles have been suggested including seed dispersal via animal hosts, seed retention via soil adherence, and protection against abiotic and biotic stresses (reviewed in Phan and Burton (2018)). The most commonly suggested role of seed mucilage, tolerating water deficit stress, was suggested by Grubert (1974) who noted that many mucilage-producing species were found in arid environments. However, in *Plantago*, mucilage-producing species are present in and adapted to a wide variety of habitats of varying water availability. In *Arabidopsis*, mucilage was not found to hasten the rate of water

uptake in the internal tissues of the seed, but rather acted as a reservoir for water at the seed surface while water uptake occurred (Saez-Aguayo *et al.* 2014). It is therefore likely that seed mucilage content and properties, rather than presence or absence, is key for tolerating a range of environments with variable water availability. This exact concept was recently studied using *Plantago* species as a model, where it was found that there is a significant relationship between seed mucilage content and seedling success under high levels of water deficit stress (Teixeira *et al.* 2019). It is likely that this relationship is found amongst the Australian *Plantago* species studied here and suggests that seed mucilage composition and properties also contribute to successful germination. Natural variation in *Plantago* mucilage properties is apparent even in the expanded mucilage architecture (Fig. 5.3). Species with the smallest mucilage envelope (relative to seed area) are those with low mucilage yield (Supplementary Fig. 5.7) and *P. lanceolata, P. paradoxa* and *P. triantha,* are species native to the wettest environments (Supplementary Fig. 5.8). *P. lanceolata* was introduced from the British Isles where average annual rainfall is over twice that of Australia (Smith 2004) and *P. paradoxa* and *P. triantha* are native to high-elevation regions of Tasmania (and *P. triantha* is also found in New Zealand) (Brown 1991) (Fig. 5.2C), some of the highest rainfall areas in the country. Six additional Australian *Plantago* species were used for ruthenium red mucilage staining to estimate mucilage quantity (Supplementary Fig. 5.9). Although seed availability was too low for mucilage extraction and subsequent analyses, this showed that these, like other Australian species from high-rainfall environments, also have minimal or very fragile mucilage envelopes.

Significant compositional variation may also explain differences in mucilage properties. The most easily-extracted *Plantago* seed fraction (CWE) contains abundant pectic monosaccharides, rhamnose and galacturonic acid, which are minimal in subsequent fractions (Fig. 5.5C). This is in line with our previous findings which suggest that the

pectin in highly hydrophilic first mucilage fractions acts to 'prime' and initiate mucilage expansion (Phan *et al.* 2020). Subsequent mucilage fractions which require more intense extraction conditions to obtain contain mostly xylose and arabinose, constituents of heteroxylan, in varying molar ratios. Yu *et al.* (2017) showed that the innermost layer(s) of mucilage in *P. ovata* was most gel-like as a result of high heteroxylan substitution complexity, corroborated in our previous publication (Phan *et al.* 2020) and by others (Ren *et al.* 2020; Zhou *et al.* 2020). Here, we show the same trends in other *Plantago* species where the second and third (HWE and IAE) mucilage fractions (akin to the inner layers described by Yu *et al.* (2017)) had the highest AX ratios, an indication of heteroxylan substitution complexity. Similarly, the HWE and IAE mucilage fractions of *P. cunninghamii*, *P. turrifera*, *P. bellidioides*, *P. debilis*, *P. gaudichaudii* and *P. varia* had particularly high AX ratios suggesting even more complex heteroxylan substitution (Fig. 5.5B), as indicated by minimal immunolabelling by LM11 because the unsubstituted/lowly-substituted backbone epitope is not present (Fig. 5.3c, g, h, k and l). The inner mucilage fractions in these species also represented a large proportion of the total mucilage (Fig. 5.4B) and analysis of the water absorption capacity (WAC) of mucilage on intact seeds (Fig. 5.4C) found WAC to be strongly correlated with both HWE ($r = 0.62$, $p = 0.032$) and IAE content ($r = 0.69$, $p = 0.013$) but the strongest correlation was a combination of the two ($r = 0.73$, $p = 0.006$) (Fig. 5.4D). Furthermore, the mucilage of these species is still apparent as retained, swollen envelopes even after extraction (compared to *P. lanceolata,* for example) (Supplementary Fig. 5.10) showing that the robustness of seed mucilage in Australian *Plantago* species is due, at least in part, to heteroxylan structure and resultant intermolecular bonds.

The data suggest that in Australian native *Plantago* species, the complexity of heteroxylan substitution leads to more complex intermolecular interactions. This

creates mucilage envelopes with differing properties, including resistance to removal and water absorption capacity that, in line with recent findings from Teixeira *et al.* (2019), is an adaptive trait to cope with variable water availability in arid Australian environments.

Plantago seeds contain abundant non-starch reserve carbohydrates

Agreeing with previous reports (Ahmed *et al.* 1965), soluble sugars are abundant in *Plantago* seeds (Fig. 5.7) with planteose and sucrose being the major sugars detected. Planteose (originally isolated from *Plantago* and named for the genus (Wattiez and Hans 1943)) is the major soluble sugar in seeds of all *Plantago* species studied here except *P. lanceolata* where only sucrose is higher. While minute quantities of the oligosaccharides raffinose and stachyose were detected in all species, these sugars are only abundant in *P. lanceolata* seeds, particularly stachyose where levels were similar to planteose. This agrees with previous findings where in a survey of a number of *Plantago* species, these sugars were only detected in seeds of *Plantago* Sect. *Arnoglossum* (now revised to Sect. *Lanceifolia*) of which *P. lanceolata* is the only member included here (Gorenflot and Bourdu 1962). An additional sugar, Unknown 1 (Fig. 5.7A), was also found in all species. Based on relative chromatographic peak area, Unknown 1 appears to be a major soluble sugar in seven of the species tested, with levels even comparable to planteose in *P. debilis* or *P. triantha* (Supplementary Fig. 5.3). As the chromatographic method used here elutes soluble sugars roughly by their degree-of-polymerisation (DP), it is likely that Unknown 1 is a tetra- or pentasaccharide (DP4–5) as it elutes after nystose (DP4) but before 1,1,1-kestopentaose (DP5). While the exact identity of this compound will be elucidated by mass spectrometry, we hypothesise that Unknown 1 is the tetrasaccharide sesamose (*α*-D-galactopyranosyl-(1→6)-*α*-D-galactopyranosyl-(1→6)-*β*-D-fructofuranosyl-(2→1)-*α*-D-glucopyranoside), a higher DP homologue of planteose, which while not reported

previously for *Plantago,* is found in tandem with planteose in other species (Hatanaka 1959).

In most seeds, starch exists as the main source of carbon during germination, and while initially starch is abundant in *Plantago* seeds (Cooper 1942; Hyde 1970; Phan *et al.* 2020) it is rapidly depleted to biochemically- and histochemically-undetectable levels during development (Phan 2012). In the absence of starch, it is likely that planteose, the principle reserve carbohydrate of a number of species (French *et al.* 1959; Jukes and Lewis 1974; Dey 1980; Wakabayashi *et al.* 2015), in concert with the other soluble sugars in *Plantago* seeds, including Unknown 1, is rapidly mobilised as a carbon source in the initial phases of germination. It is likely that at this point the endosperm is undergoing/beginning to undergo degradation to supply further carbon, but after a literature review, we found that while *Plantago* species are known to have a substantial endosperm (Youngken 1950; Bruneton 1995), its exact composition has not been defined. One report suggested that the hard endosperm cell walls of *P. ovata* must be comprised solely of reserve cellulose (Madgulker *et al.* 2014) but crystalline cellulose levels were found to be, at most, 4% (w/w) (Phan 2012). A clue is found in gene expression data where mannan synthesis genes have been found to be highly expressed in developing *P. ovata* seeds which also contain mannose monosaccharides (Jensen *et al.* 2011). Here we are the first to confirm that the endosperm of all *Plantago* species studied contains thickened cell walls that are rich in mannan (Fig. 5.6). The mannan-rich endosperm cell walls, like other species (Gong *et al.* 2005), gives *Plantago* seeds a ‘hard-seeded’ quality (Primack 1979; Miao *et al.* 1991) (for example, seeds of *P. ovata* require over four times the specific grinding energy compared to wheat (Dziki and Laskowski 2006; Ziemichód *et al.* 2018)) that must be altered for successful germination. Gong *et al.* (2005) reported that, in most species, endo-β-mannanase activity is only detectable after radicle emergence,

providing carbon for the post-germination seedling. We note that in *Plantago* seeds, minimal seed material remains after seedling emergence is complete (data not shown) showing that substantial bulk endosperm degradation also occurs at some point as a carbon supply for the seedling.

Based on findings in other species, we hypothesise that upon imbibition mobilisation of soluble sugars like planteose fuels rapid cell elongation that allows the radicle to puncture the micropylar endosperm, at which point hydrolases will begin/have begun to degrade the endosperm, further fuelling early seedling growth. The exact interplay and pattern of soluble sugar and endosperm polysaccharide mobilisation in *Plantago* seed germination is the subject of upcoming work.

Exploiting the array of beneficial constituents in whole *Plantago* seeds may provide additional benefits over mucilage products alone

India, the world's largest psyllium (*P. ovata*) exporter, produced 56,000 tonnes of psyllium husk in 2019/2020 which equates to over 160,000 tonnes of non-husk material (Govt India Dept of Commerce 2017a; b), comprising the inner tissues of the seeds that have been demonstrated here to be nutrient-rich. While the nutritional benefits of consuming viscous dietary fibres like psyllium husk are not in doubt, the underutilised inner seed tissues could also provide valuable human health benefits if consumed.

While the reserve carbohydrates that we report to be abundant in *Plantago* seeds are likely to be essential to germination, they also have medicinal and nutritional significance as fermentable dietary fibres. Fermentable dietary fibres are consumed by beneficial bacteria in our gut, producing short chain fatty acids like butyrate which is required to maintain colon health (Grady *et al.* 2019) and there is also mounting evidence that modulating the microbiome through dietary fibre supplementation has significant effects on a wide range of disease indications (for review see Lynch &

Pedersen (2016)). While *P. ovata* husk is not a fermentable dietary fibre and thus provides limited fermentation- and microbiome-related benefits (McRorie 2015), dehusked *P. ovata* seeds are reported to be fermentable, increasing faecal butyrate content in a clinical trial (Fernandez-Banares *et al.* 1999) and improving numerous digestibility markers compared to the husk in a pre-clinical study (Leng-Peschlow 1991). These findings demonstrate that at least one non-husk component in *Plantago* seeds is fermentable by gut microbiota. While its exact prebiotic properties are currently unknown (Xing *et al.* 2017), planteose, along with its homologues and other soluble sugars in *Plantago* seeds are likely fermentation candidates as many oligosaccharides are readily fermentable by beneficial bacteria in the gastrointestinal tract (Alander *et al.* 2001; Bruno-Barcena and Azcarate-Peril 2015). Endosperm polysaccharides are also likely to be fermentable compared to husk as diverse mannans and mannooligosaccharides released from mannan digestion have been shown to be well-fermented by a human faecal inoculum (Asano *et al.* 2003; Jonathan *et al.* 2012).

Within the endosperm cells are large aleurone grains and oil bodies which house the protein and fat content of the *Plantago* seeds. Protein levels are generally similar to previous reports of *Plantago* species (10–20% w/w) (Davison 1982; Romero-Baranzini *et al.* 2006; Mohamed *et al.* 2011; Ziemichód *et al.* 2018), but Australian *Plantago* species are generally higher compared to these reports and all are higher than commercial psyllium (*P. ovata*) (Table 1). *P. paradoxa* and *P. triantha* are very high in protein content, over 30% (w/w), which is higher than important grain legumes like chickpeas or lentil (24% and 26.1%, respectively) (Iqbal *et al.* 2006). *Plantago* protein has previously been reported to contain essential amino acids and is well digested (Romero-Baranzini *et al.* 2006) showing the potential of *Plantago* seeds as a protein source. Seeds of *Plantago* species are also rich in fats and all Australian species

contain more fat than commercial psyllium, *P. ovata* (Table 5.1). Of particular nutritional importance is the proportion of omega-3 and omega-6 UFAs which mammals are unable to synthesise and are thus essential. There is a growing body of evidence that omega-3 fatty acids, particularly long-chain fatty acids (LCFAs) EPA and DHA commonly obtained from consuming fish, are protective against cardiovascular diseases (Tocher *et al.* 2019). However many researchers conclude that the world's ecosystems could not sustainably supply the population with enough fish to provide the recommended EPA and DHA intake (Crawford *et al.* 2000) and thus sufficient intake of plant-derived UFAs to allow endogenous LCFA production from these precursors is recommended as an alternative. As plant-derived omega-3 (anti-inflammatory) and omega-6 (pro-inflammatory) (Harris and Harris 2006; Patterson *et al.* 2012) UFAs are competitively desaturated and elongated into LCFAs by the same pathways, it is important that the ratio of omega-3 to omega-6 is at the very least 1:1 (Simopoulos 2002) to reduce the risk of inflammation. However an omega-3 to omega-6 intake ratio of 4:1 is suggested to be ideal for promoting heart, liver and gut health (Calder 2006). Here we show that Australian native *Plantago* seeds have omega-3 to omega-6 ratios greater than the minimum adequate ratio of 1:1 (Table 5.1) and after extensive review of the literature we report that *P. turrifera* has the highest ratio of omega-3 to omega-6 fatty acids reported for any seed (4.85:1). This is higher than benchmark species *Linum usitatissimum* (flax) or *Salvia hispanica* (chia), with 3.44:1 and 3.08:1, respectively (Sargi *et al.* 2013), although total fat content was 50% and 30% lower in *P. turrifera* than these species, respectively. Consumption of *Plantago* seeds, particularly those of Australian natives like *P. turrifera*, may therefore contribute to improving the undesirable omega-3 to omega-6 ratio that is common in modern, western diets, and the associated health risks (Simopoulos 2002; Harris and Harris 2006).

Conclusions

In this study we have provided a more complete understanding of the composition and morphology of seeds of twelve *Plantago* species that grow in Australia, how they differ according to phylogenetic lineage, and what implications this may have for food and nutritional applications. We have shown that variation in mucilage content, structure and properties has probably developed as an adaptive trait to cope with water-deficit stress in arid Australian environments and provides wide differences in hydrocolloid functionality that can be exploited in industry. By profiling the nutrient content of the inner *Plantago* seed tissues, we show that current commercial production of psyllium in particular underutilises the nutritional value of whole *Plantago* seeds. The use of a whole seed *Plantago* product, particularly from those species native and adapted to harsh Australian conditions, may provide a more nutritious but still functional alternative to commercial psyllium husk. The consumption of a whole seed flour may also confer multiple nutritional benefits: minimally-fermented polysaccharides in the mucilage could benefit metabolic and gastrointestinal disorders that are improved when the viscosity and consistency of the gut digesta is increased, while fermentable fibres, lipids and micronutrients derived from the internal seed tissues could contribute to the improvement of a wide range of microbiome-, inflammatory- and oxidative stress-related disorders. Future work will investigate the functionality of whole seed *Plantago* flours in food technology and gut health.

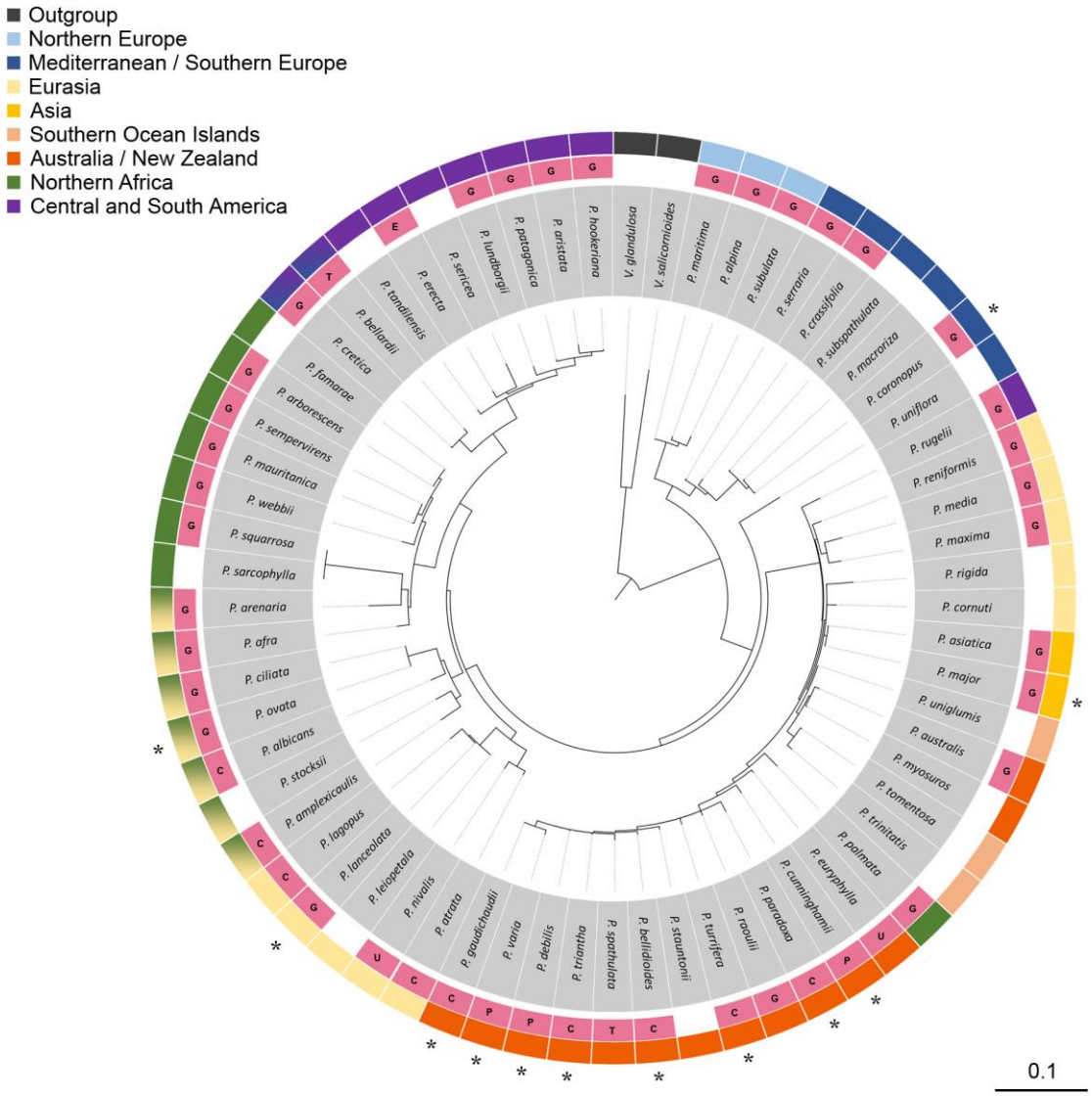

Figure 5.1. Neighbour-joining comparison of nuclear ribosomal DNA internally transcribed spacer (ITS) regions from 63 diverse *Plantago* species. Asterisks denote species sequenced and investigated in this study. Sequences of species without asterisks were obtained from Ronsted *et al.* (2002). Coloured segments in the outer ring denote outgroups and geographic origins with gradients denoting shared distribution. A pink segment in the inner circle indicates that the presence of seed mucilage has been confirmed in the literature (letters within the pink segment denote the specific reference). Species without a pink segment have not yet been examined rather than not producing mucilage. E = Evans *et al.* (1974); G = Grubert (1974); P = Phan *et al.* (2016); C = this study; U = unpublished observation by the authors.

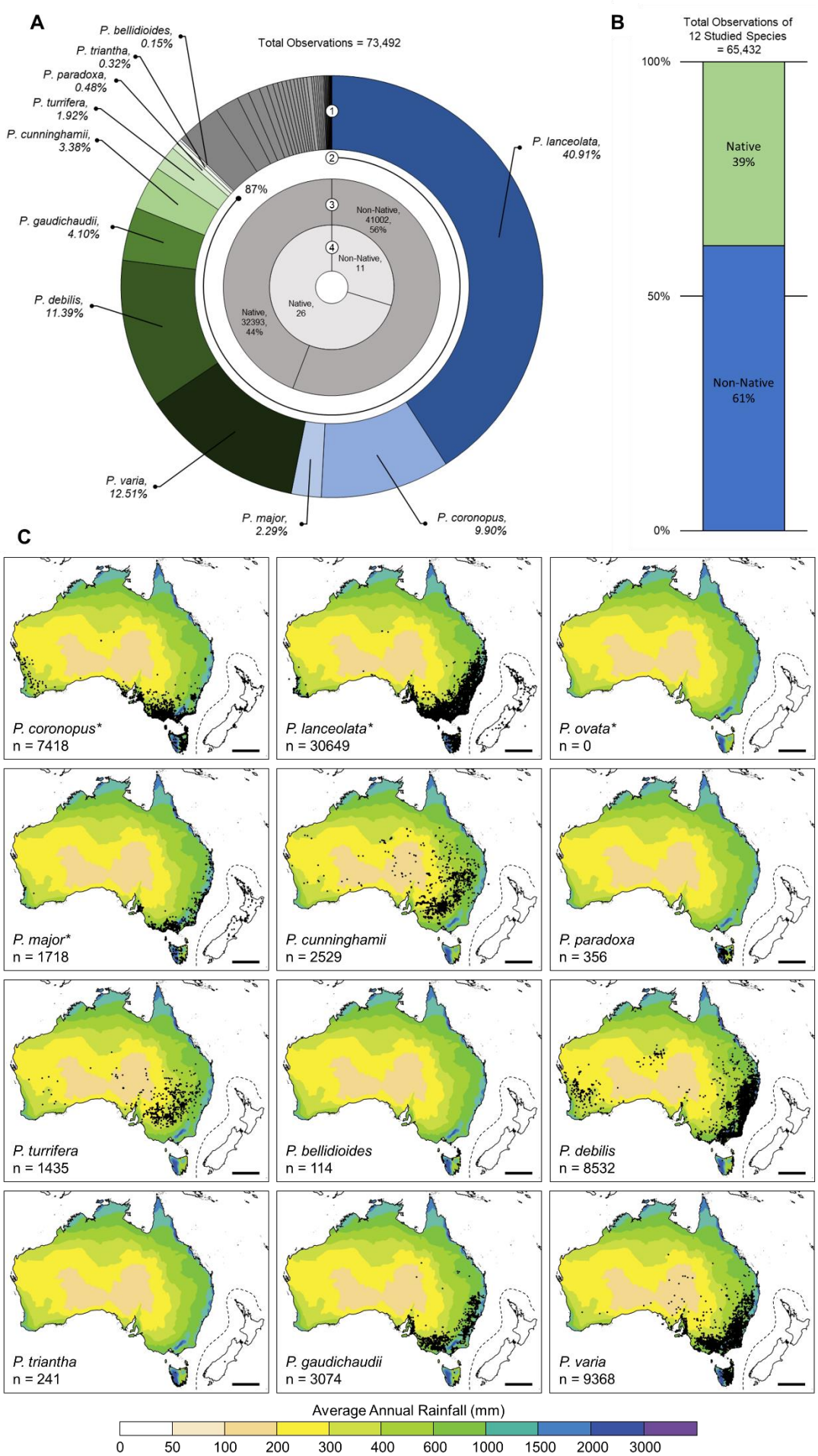
A
Total Observations = 73,492
P. bellidioides, 0.15%
P. triantha, 0.32%
P. paradoxa, 0.48%
P. turrifera, 1.92%
P. cunninghamii, 3.38%
P. gaudichaudii, 4.10%
P. debilis, 11.39%
P. varia, 12.51%
P. major, 2.29%
P. coronopus, 9.90%
P. lanceolata, 40.91%
87%
Non-Native, 41002, 56%
Non-Native, 11
Native, 26
Native, 32393, 44%
B
Total Observations of 12 Studied Species = 65,432
100%
50%
0%
Native 39%
Non-Native 61%
C
P. coronopus* n = 7418
P. lanceolata* n = 30649
P. ovata* n = 0
P. major* n = 1718
P. cunninghamii n = 2529
P. paradoxa n = 356
P. turrifera n = 1435
P. bellidioides n = 114
P. debilis n = 8532
P. triantha n = 241
P. gaudichaudii n = 3074
P. varia n = 9368
Average Annual Rainfall (mm)
0 50 100 200 300 400 600 1000 1500 2000 3000

Figure 5.2. **A1.** Proportions of recorded observations of *Plantago* species in Australia and New Zealand (excluding New Zealand endemic species) from the Atlas of Living Australia database (https://biocache.ala.org.au/occurrences/search?q=lsid%3Ahttps%3A%2F%2Fid.biodiversity.org.au%2Fnode%2Fapni%2F7745425 accessed on Thu Jul 02 11:33:30 AEST 2020.). The twelve species studied here are coloured while species not studied are grey. Non-native and/or naturalised and native species are coloured in shades of blue or green, respectively. **A2.** Species used in this study represent 87% of *Plantago* observations. **A3.** Proportion of native to non-native species in total *Plantago* observations. **A4.** Number of native species observed compared to non-native species. **B.** Proportion of non-native to native species in observations of the 12 species studied here. **C.** Distribution in Australia and New Zealand of 12 *Plantago* species studied here with colour-coded 30 year-average annual rainfall data. Species with asterisks are non-native and/or naturalised species. Dashed line indicates where the map was cropped to include New Zealand and maximise figure space. *P. ovata,* commercial psyllium, has not been reported in Australia or New Zealand and can be used as a blank map for reference.

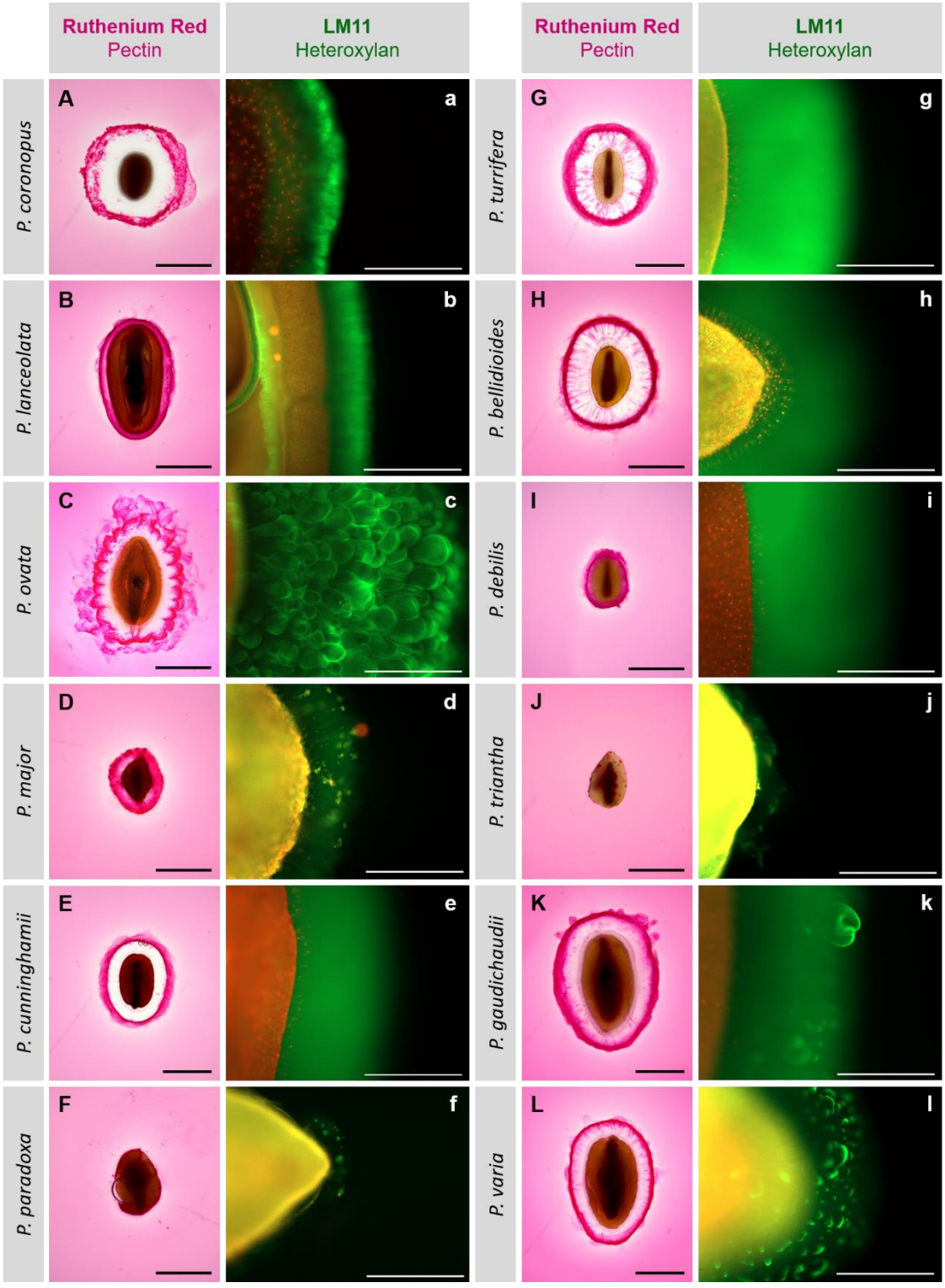

Figure 5.3. Expanded mucilage architecture of 12 *Plantago* species. Ruthenium red (dark pink) stains acidic polysaccharides at the mucilage periphery (A–L). Scale = 1 mm. Anti-xylan antibody LM11 (green) probes for xylan backbone epitopes in the inner mucilage layers (a-l) while the seed is counterstained with propidium iodide (red/yellow). Scale = 500 µm.

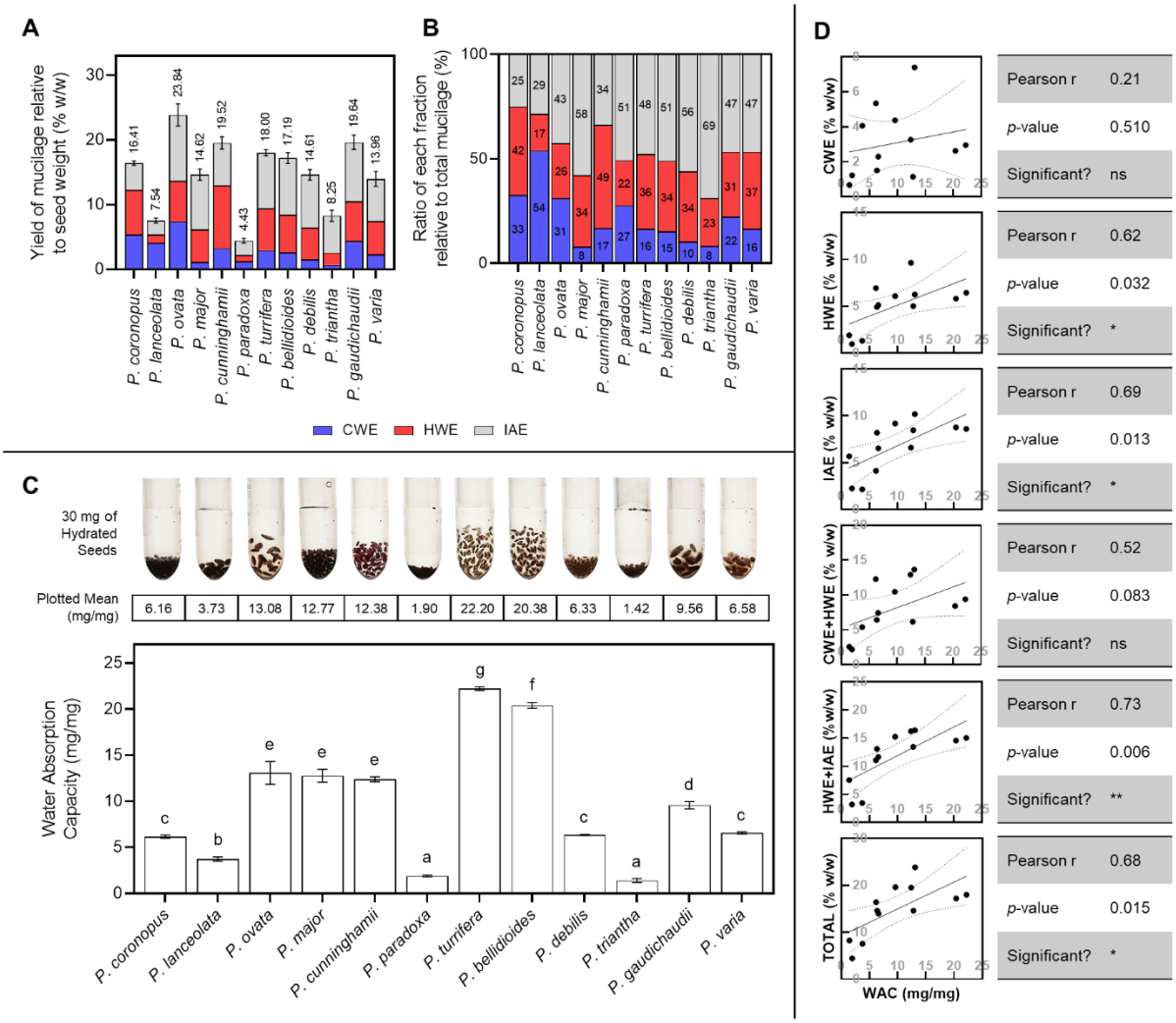

Figure 5.4. Seed mucilage yield, fractionation and water absorption traits of 12 *Plantago* species. **A.** Yield of mucilage as a share of whole seed. **B.** Quantity of each isolated mucilage fraction as share of total mucilage. Values within bars are plotted values rounded to the nearest integer. CWE = cold water extractable (blue); HWE = hot water extractable (red); IAE = intense agitation extractable (grey). **C.** Water absorption capacity of *Plantago* seeds. Above the plot are plotted mean values and a representative image of 30 mg of hydrated and swollen *Plantago* seeds. Samples sharing a letter are not significantly different to each other ($p > 0.05$). **D.** Study of correlations between water absorption capacity (WAC) and mucilage yield/fractionation traits (seed-relative traits from **A.**). Linear models plotted with 95% confidence bands. ns = not significant. Error bars in **A.** correspond to one standard deviation from the mean of total mucilage yield.

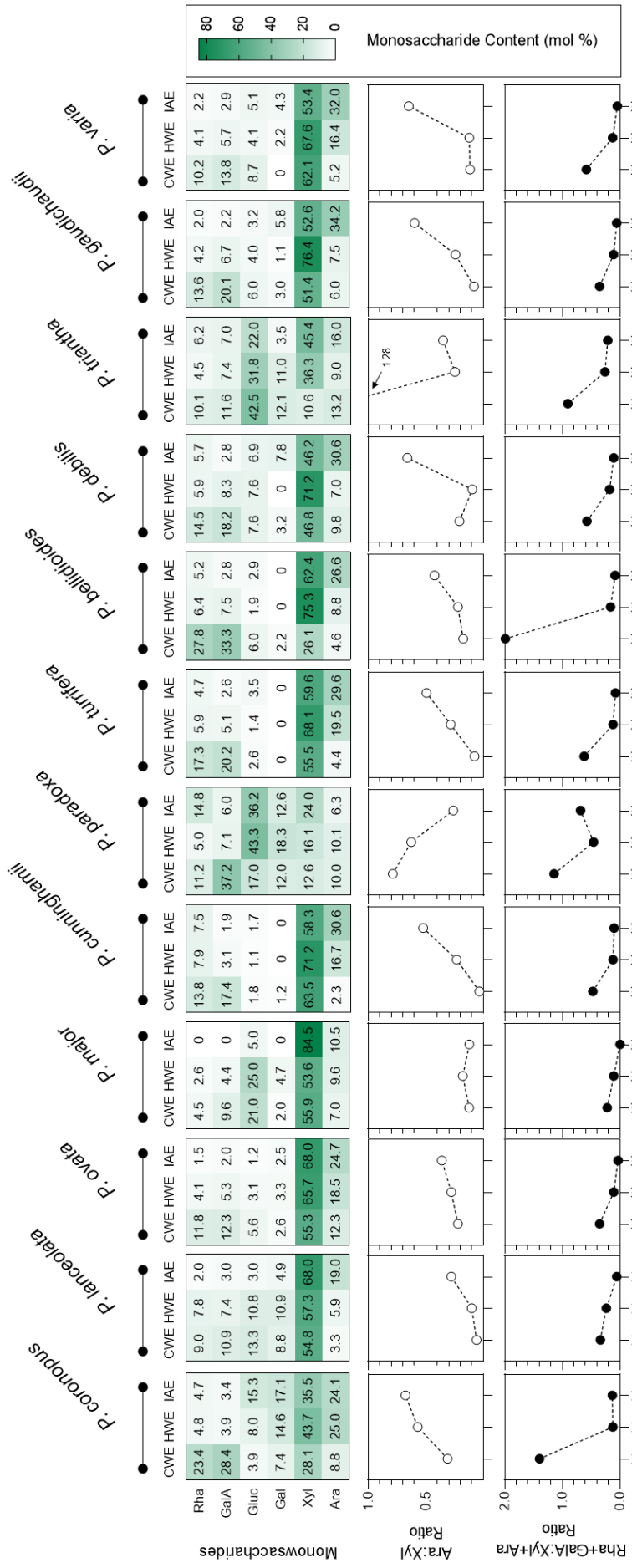

Figure 5.5. Chemical composition of fractionated mucilage from 12 *Plantago* species. **A.** Monosaccharide composition of each mucilage fraction. Heatmap of relative (molar) abundance of each monosaccharide in a fraction. **B.** Arabinose to xylose (Ara:Xyl) ratio in each fraction. **C.** Pectin (rhamnose and galacturonic acid) to heteroxylan (xylose and arabinose) (Rha+GalA:Xyl+Ara) ratio in each fraction. CWE = cold water extractable; HWE = hot water extractable; IAE = intense agitation extractable.

A

	Mannose	Rhamnose	Glucuronic Acid	Galacturonic Acid	Glucose	Galactose	Xylose	Arabinose
P. coronopus	11.43 ± 1.39	1.71 ± 0.25	nd	1.23 ± 0.18	3.05 ± 0.45	3.07 ± 0.32	5.52 ± 0.72	5.39 ± 0.68
P. lanceolata	19.39 ± 0.12	0.62 ± 0.01	nd	0.65 ± 0.00	5.23 ± 0.11	2.56 ± 0.04	3.80 ± 0.05	3.22 ± 0.04
P. ovata	12.67 ± 0.99	1.22 ± 0.02	nd	1.08 ± 0.02	2.35 ± 0.12	3.40 ± 0.10	18.83 ± 0.49	11.86 ± 0.08
P. major	11.84 ± 0.97	0.70 ± 0.04	0.65 ± 0.03	0.56 ± 0.01	5.98 ± 0.29	2.17 ± 0.05	8.85 ± 0.05	3.44 ± 0.08
P. cunninghamii	15.35 ± 0.58	3.19 ± 0.33	nd	1.15 ± 0.30	2.83 ± 0.20	1.50 ± 0.02	16.15 ± 1.36	8.32 ± 0.57
P. paradoxa	12.76 ± 0.13	1.58 ± 0.05	nd	0.50 ± 0.00	4.45 ± 0.14	2.53 ± 0.07	1.16 ± 0.01	2.20 ± 0.02
P. turrifera	18.67 ± 0.88	1.88 ± 0.08	nd	1.19 ± 0.08	3.01 ± 0.19	1.92 ± 0.11	14.05 ± 1.11	7.64 ± 0.66
P. bellidioides	12.02 ± 0.76	2.45 ± 0.05	nd	1.49 ± 0.03	2.74 ± 0.01	2.22 ± 0.02	13.02 ± 0.39	6.87 ± 0.14
P. debilis	18.18 ± 0.05	2.09 ± 0.03	nd	0.76 ± 0.00	3.97 ± 0.01	3.06 ± 0.02	8.23 ± 0.21	6.11 ± 0.17
P. triantha	20.25 ± 0.55	1.41 ± 0.03	nd	0.81 ± 0.02	4.77 ± 0.19	2.16 ± 0.06	3.14 ± 0.12	2.83 ± 0.14
P. gaudichaudii	11.91 ± 0.14	1.46 ± 0.01	nd	1.18 ± 0.02	3.98 ± 0.04	2.74 ± 0.01	13.59 ± 0.05	7.94 ± 0.05
P. varia	11.16 ± 0.20	1.55 ± 0.01	nd	0.99 ± 0.01	3.67 ± 0.00	3.12 ± 0.01	9.93 ± 0.14	6.93 ± 0.07

B

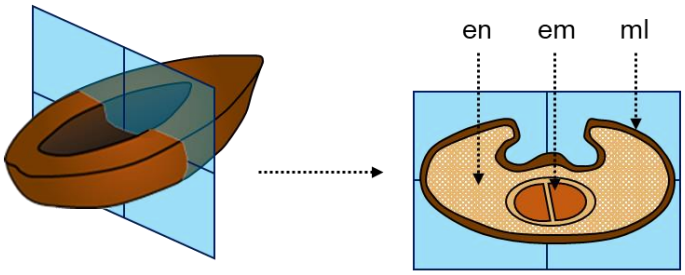

LM21 (anti-β-1,4-mannan) **Calcofluor White (glucan)**

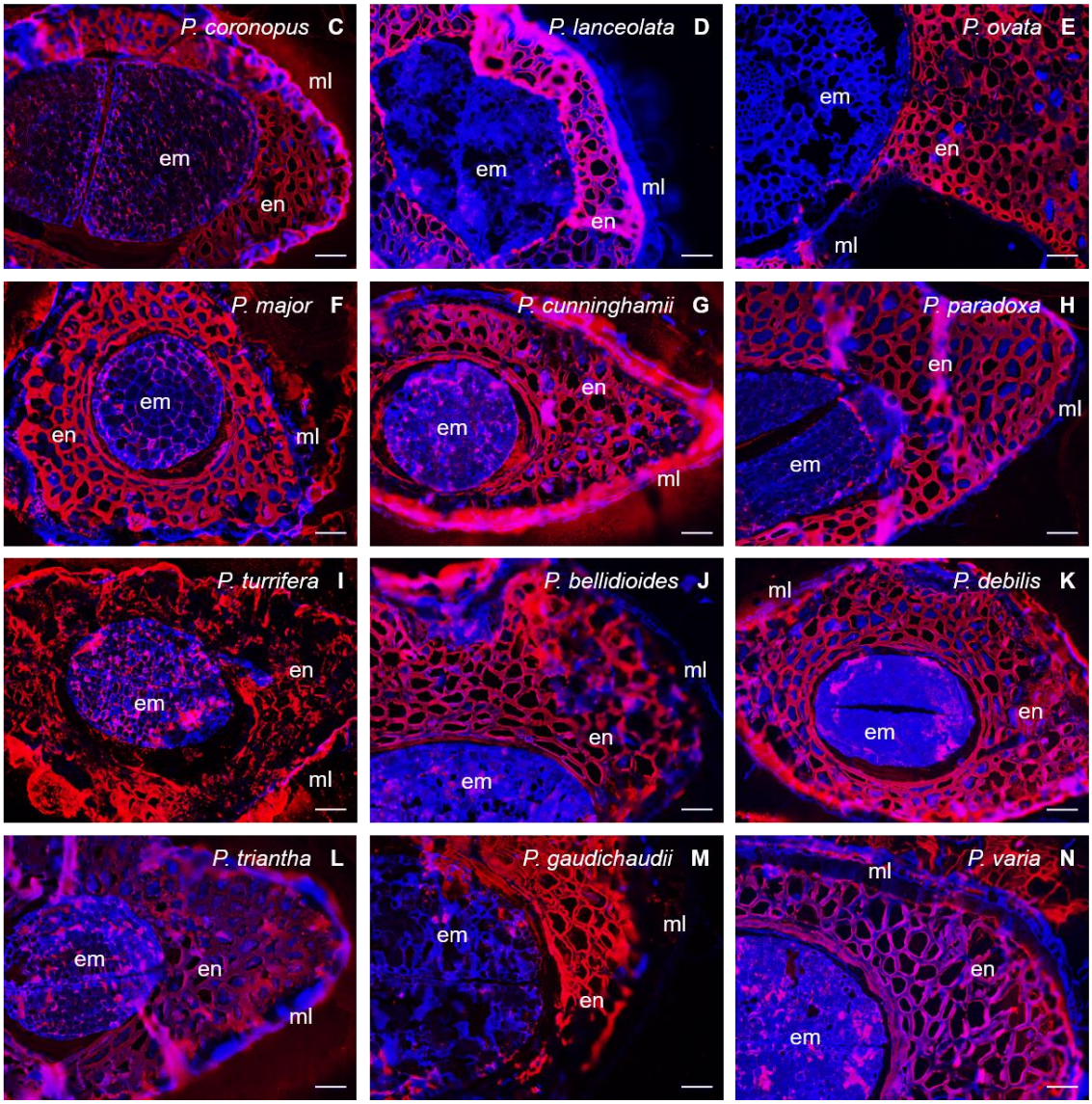

Figure 5.6. Profiling of the major polysaccharide in *Plantago* seed endosperm. **A.** Monosaccharide profiles of whole *Plantago* seeds (means, % w/w, with standard deviation). A grey scale (dark grey, highest value; white, lowest value) has been used to highlight the most abundant monosaccharides in a species. **B.** Schematic diagram of the orientation of thin sections taken from *Plantago* seeds. **C–N.** Immunodetection of mannan in *Plantago* endosperm cell walls by LM21 monoclonal antibody. Scale = 50 µm. Abbreviations: en = endosperm; em = embryo; ml = mucilage layer.

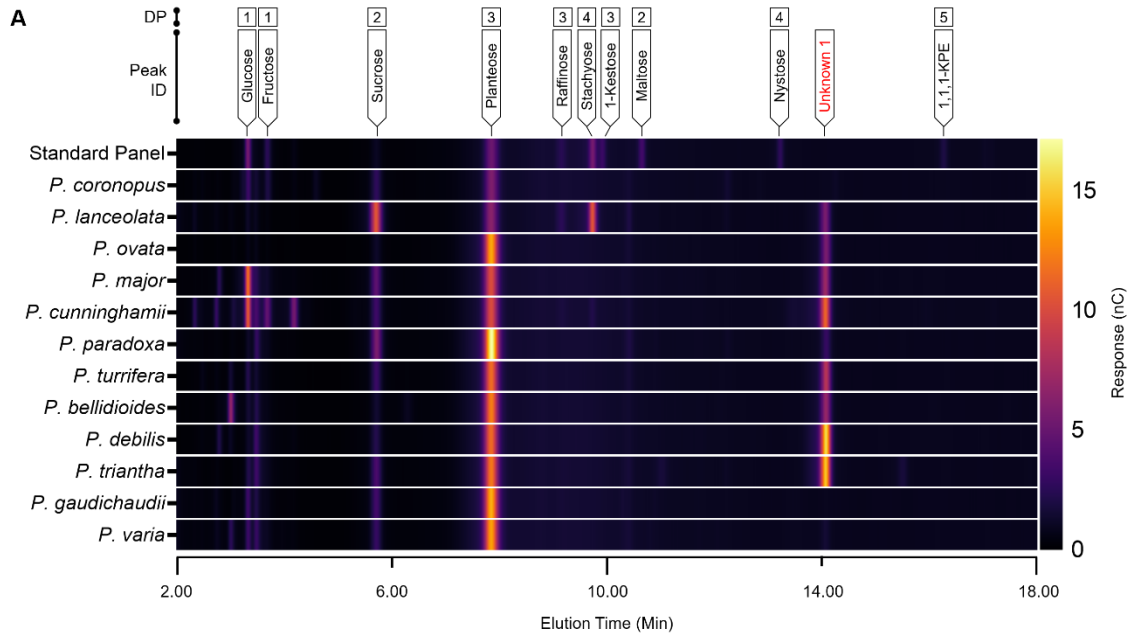

B

Legend Glucose, Galactose, Fructose

Simple Structure

	Glucose (µg/mg)	Fructose (µg/mg)	Sucrose (µg/mg)	Planteose (µg/mg)	Raffinose (µg/mg)	Stachyose (µg/mg)
P. coronopus	0.891 ± 0.003	1.400 ± 0.016	6.895 ± 0.000	9.823 ± 0.081	0.181 ± 0.020	0.001 ± 0.001
P. lanceolata	0.223 ± 0.012	0.150 ± 0.025	26.449 ± 0.114	10.233 ± 0.483	1.528 ± 0.039	8.170 ± 0.164
P. ovata	0.109 ± 0.004	0.090 ± 0.011	3.021 ± 0.080	25.645 ± 0.391	0.171 ± 0.086	0.016 ± 0.011
P. major	3.340 ± 0.007	0.265 ± 0.002	11.136 ± 0.003	17.953 ± 0.067	0.076 ± 0.004	0.004 ± 0.001
P. cunninghamii	0.400 ± 0.002	1.431 ± 1.009	6.144 ± 0.052	16.714 ± 0.575	0.378 ± 0.163	0.260 ± 0.180
P. paradoxa	0.131 ± 0.003	0.026 ± 0.004	14.565 ± 0.080	31.554 ± 0.102	0.071 ± 0.010	0.001 ± 0.001
P. turrifera	0.500 ± 0.012	0.011 ± 0.001	7.933 ± 0.193	21.224 ± 0.264	0.076 ± 0.008	0.011 ± 0.008
P. bellidioides	0.186 ± 0.003	0.044 ± 0.019	2.895 ± 0.002	22.081 ± 0.011	0.109 ± 0.010	0.001 ± 0.001
P. debilis	0.096 ± 0.008	0.001 ± 0.001	5.553 ± 0.044	20.968 ± 0.258	0.126 ± 0.068	0.003 ± 0.002
P. triantha	0.293 ± 0.002	0.008 ± 0.002	10.408 ± 0.829	22.201 ± 0.390	0.269 ± 0.068	0.001 ± 0.001
P. gaudichaudii	0.674 ± 0.006	0.080 ± 0.005	8.028 ± 0.292	24.239 ± 1.070	0.203 ± 0.011	0.018 ± 0.007
P. varia	0.489 ± 0.068	0.053 ± 0.028	7.235 ± 0.092	25.195 ± 0.200	0.116 ± 0.006	0.021 ± 0.003

Figure 5.7. Soluble sugar profiling of *Plantago* seeds. **A.** Chromatographic data presented in heatmap form to highlight differences in chromatographic profile between species. Chromatographic data has been cropped to an elution period that includes saccharides with a low degree-of-polymerisation (DP) (2–18 minutes). For simplicity, chromatographic data of standard runs (standard panel: a combined low DP saccharide suite, planteose and stachyose) were combined. **B.** Quantification of key low DP saccharides and their schematic structure. A grey scale (dark grey, highest value; white, lowest value) has been used to display differences in abundance of one type between species. Abbreviations: 1,1,1-KPE = 1,1,1-Kestopentaose

Table 1 Summary of morphometric and nutritional characteristics of seeds of 12 *Plantago* species.

	P. coronopus	*P. lanceolata*	*P. ovata*	*P. major*	*P. cunninghamii*	*P. paradoxa*	*P. turrifera*	*P. bellidioides*	*P. debilis*	*P. triantha*	*P. gaudichaudii*	*P. varia*
Seed Morphometric Characteristics												
Length (mm)	1.138 ± 0.132	2.679 ± 0.164	2.843 ± 0.224	1.144 ± 0.060	1.394 ± 0.111	1.556 ± 0.095	1.562 ± 0.044	1.563 ± 0.115	1.308 ± 0.071	1.236 ± 0.132	2.820 ± 0.292	2.495 ± 0.250
Width (mm)	0.740 ± 0.075	1.227 ± 0.143	1.448 ± 0.108	0.653 ± 0.081	0.822 ± 0.044	1.101 ± 0.087	0.840 ± 0.086	0.879 ± 0.079	0.717 ± 0.036	0.818 ± 0.07	1.490 ± 0.134	1.387 ± 0.142
1000 Grain Weight (mg)	205 ± 8	1508 ± 33	1618 ± 43	172 ± 5	364 ± 2	411 ± 17	355 ± 6	383 ± 8	288 ± 9	274 ± 4	1936 ± 102	1761 ± 24
Seed Nutrient Composition												
Energy (kJ/100g)	1176.15	844.89	898.30	1064.17	1260.15	1239.47	1174.72	1162.47	1109.70	1142.19	1209.43	1190.19
Protein (%)	19.91 ± 2.34	11.20 ± 0.08	11.42 ± 1.63	16.36 ± 0.35	19.53 ± 0.20	31.35 ± 2.16	18.03 ± 1.06	20.43 ± 0.22	13.80 ± 0.07	30.92 ± 0.35	24.05 ± 1.35	26.01 ± 0.80
Carbohydrate (%)	1.92 ± 0.02	4.68 ± 0.15	2.91 ± 0.11	3.28 ± 0.01	2.63 ± 0.58	4.63 ± 0.04	2.98 ± 0.10	2.53 ± 0.0	2.67 ± 0.08	3.32 ± 0.26	3.32 ± 0.28	3.31 ± 0.04
Dietary Fibre (%)	31.4 ± 2.99	35.47 ± 0.26	51.41 ± 0.63	34.19 ± 1.13	48.49 ± 2.52	25.19 ± 0.31	48.36 ± 2.33	40.80 ± 0.10	42.39 ± 0.35	35.38 ± 0.84	42.8 ± 0.05	37.34 ± 0.32
Fat (%)	14.45 ± 0.47	7.76 ± 0.54	7.08 ± 0.58	12.70 ± 0.44	13.14 ± 1.07	10.41 ± 1.28	11.51 ± 0.81	12.07 ± 0.04	12.90 ± 1.44	7.48 ± 1.78	8.80 ± 0.84	9.11 ± 0.47
Fatty Acid Composition of Seed Oil												
Saturated Fatty Acids Total (%)	16.85 ± 0.16	22.39 ± 0.37	17.20 ± 0.14	14.37 ± 1.33	15.01 ± 0.03	15.76 ± 0.02	14.37 ± 0.67	15.71 ± 0.11	18.73 ± 0.06	22.14 ± 0.21	13.44 ± 0.45	16.64 ± 0.17
Myristic Acid (14:0) (%)	0.04 ± 0.01	0.06 ± 0.01	0.06 ± 0.03	0.05 ± 0.02	0.09 ± 0.02	0.11 ± 0.00.	0.10 ± 0.02	0.09 ± 0.00	0.07 ± 0.00	0.09 ± 0.03	0.11 ± 0.03	0.14 ± 0.01
Pentadecylic Acid (15:0) (%)	0.08 ± 0.01	0.17 ± 0.01	0.12 ± 0.01	0.05 ± 0.02	0.05 ± 0.00	0.07 ± 0.02	0.05 ± 0.01	0.06 ± 0.01	0.04 ± 0.00	0.17 ± 0.00	0.05 ± 0.00	0.05 ± 0.00
Palmitic Acid (16:0) (%)	12.05 ± 0.15	17.52 ± 0.17	12.43 ± 0.13	10.23 ± 0.90	11.8 ± 0.11	11.84 ± 0.06	11.59 ± 0.45	12.64 ± 0.08	14.18 ± 0.12	17.59 ± 0.32	9.99 ± 0.32	12.84 ± 0.16
Margaric Acid (17:0) (%)	0.10 ± 0.01	0.13 ± 0.02	0.11 ± 0.01	0.15 ± 0.00	0.06 ± 0.01	0.09 ± 0.01	0.09 ± 0.02	0.08 ± 0.01	0.08 ± 0.00	0.13 ± 0.02	0.11 ± 0.01	0.12 ± 0.01
Stearic Acid (18:0) (%)	3.83 ± 0.03	3.70 ± 0.10	3.82 ± 0.06	2.82 ± 0.27	2.62 ± 0.17	3.11 ± 0.03	2.07 ± 0.18	2.18 ± 0.08	3.63 ± 0.02	3.46 ± 0.29	2.62 ± 0.13	2.85 ± 0.04
Arachidic Acid (20:0) (%)	0.50 ± 0.01	0.45 ± 0.05	0.42 ± 0.00	0.57 ± 0.06	0.26 ± 0.00	0.38 ± 0.01	0.24 ± 0.00	0.30 ± 0.02	0.41 ± 0.02	0.4 ± 0.00	0.35 ± 0.01	0.34 ± 0.01
Behenic Acid (22:0) (%)	0.17 ± 0.02	0.21 ± 0.01	0.19 ± 0.03	0.39 ± 0.04	0.12 ± 0.01	0.16 ± 0.01	0.12 ± 0.01	0.22 ± 0.03	0.19 ± 0.01	0.22 ± 0.06	0.13 ± 0.00.	0.18 ± 0.04
Lignoceric Acid (24:0) (%)	0.09 ± 0.01	0.15 ± 0.03	0.05 ± 0.06	0.11 ± 0.03	0.03 ± 0.04	0.00 ± 0.00	0.10 ± 0.00	0.15 ± 0.03	0.13 ± 0.03	0.09 ± 0.12	0.09 ± 0.02	0.11 ± 0.02
Unsaturated Fatty Acids Total (%)	82.99 ± 0.02	77.53 ± 0.48	82.76 ± 0.08	85.53 ± 1.41	84.92 ± 0.01	84.24 ± 0.02	85.58 ± 0.59	84.24 ± 0.04	81.19 ± 0.01	77.80 ± 0.30	86.43 ± 0.33	83.22 ± 0.03
ω-3 Total (%)	27.98 ± 0.02	6.74 ± 0.22	3.18 ± 0.12	12.31 ± 1.70	43.42 ± 0.03	32.09 ± 0.12	54.46 ± 0.71	41.35 ± 0.19	41.04 ± 0.06	7.69 ± 1.08	46.23 ± 0.29	42.69 ± 0.95
Alpha-Linoleic Acid (ALA) (18:3) (%)	27.98 ± 0.02	6.74 ± 0.22	3.18 ± 0.12	12.31 ± 1.70	43.42 ± 0.03	32.09 ± 0.12	54.46 ± 0.71	41.35 ± 0.19	41.04 ± 0.06	7.69 ± 1.08	46.23 ± 0.29	42.69 ± 0.95
ω-6 Total (%)	38.29 ± 0.09	43.99 ± 0.36	39.72 ± 0.29	52.30 ± 1.68	16.60 ± 0.20	23.38 ± 0.13	11.30 ± 0.16	18.67 ± 0.01	24.17 ± 0.10	45.70 ± 1.81	15.93 ± 0.14	19.48 ± 0.61
Linoleic Acid (18:2) (%)	38.22 ± 0.09	43.95 ± 0.42	39.65 ± 0.31	52.21 ± 1.69	16.57 ± 0.21	23.34 ± 0.19	11.26 ± 0.15	18.63 ± 0.01	24.15 ± 0.13	45.65 ± 1.74	15.91 ± 0.11	19.44 ± 0.60
Eicosadienoic Acid (20:2) (%)	0.06 ± 0.01	0.04 ± 0.06	0.07 ± 0.02	0.09 ± 0.01	0.03 ± 0.01	0.04 ± 0.06	0.04 ± 0.01	0.04 ± 0.00	0.02 ± 0.02	0.05 ± 0.07	0.02 ± 0.03	0.04 ± 0.01
ω-7 Total (%)	0.76 ± 0.01	1.73 ± 0.06	1.37 ± 0.03	1.10 ± 0.05	1.44 ± 0.04	1.16 ± 0.01	1.66 ± 0.02	1.31 ± 0.02	1.03 ± 0.00	1.73 ± 0.03	1.15 ± 0.04	1.14 ± 0.03
Palmitoleic Acid (16:1) (%)	0.08 ± 0.00	0.23 ± 0.02	0.16 ± 0.02	0.10 ± 0.01	0.21 ± 0.00	0.18 ± 0.02	0.26 ± 0.02	0.15 ± 0.01	0.16 ± 0.00	0.26 ± 0.02	0.15 ± 0.01	0.14 ± 0.02
cis-Vaccenic Acid (18:1) (%)	0.67 ± 0.01	1.49 ± 0.04	1.20 ± 0.05	0.99 ± 0.06	1.23 ± 0.04	0.99 ± 0.00	1.40 ± 0.01	1.17 ± 0.01	0.87 ± 0.00	1.47 ± 0.01	1.00 ± 0.02	1.00 ± 0.01
ω-9 Total (%)	15.96 ± 0.10	25.08 ± 0.15	38.49 ± 0.47	19.82 ± 1.91	23.46 ± 0.21	27.60 ± 0.29	18.15 ± 0.07	22.90 ± 0.26	14.96 ± 0.15	22.68 ± 3.17	23.13 ± 0.06	19.91 ± 0.34
Oleic Acid (18:1) (%)	15.83 ± 0.11	24.90 ± 0.13	38.12 ± 0.49	19.57 ± 1.88	23.35 ± 0.20	27.49 ± 0.34	18.07 ± 0.08	22.74 ± 0.25	14.87 ± 0.16	22.52 ± 3.13	23.00 ± 0.06	19.77 ± 0.33
Gondoic Acid (20:1) (%)	0.13 ± 0.01	0.18 ± 0.01	0.36 ± 0.02	0.26 ± 0.02	0.12 ± 0.02	0.12 ± 0.05	0.08 ± 0.01	0.16 ± 0.01	0.08 ± 0.01	0.16 ± 0.04	0.13 ± 0.01	0.14 ± 0.00
ω-3:ω-6	0.76 ± 0.04	0.16 ± 0.01	0.11 ± 0.04	0.28 ± 0.09	2.64 ± 0.06	1.37 ± 0.00	4.85 ± 0.09	2.24 ± 0.04	1.70 ± 0.01	0.17 ± 0.01	2.90 ± 0.01	2.22 ± 0.15
Yield of ALA (% w/w of whole seed)	4.04 ± 0.13	0.52 ± 0.02	0.23 ± 0.01	1.56 ± 0.16	5.71 ± 0.46	3.34 ± 0.40	6.27 ± 0.52	4.99 ± 0.00	5.29 ± 0.58	0.58 ± 0.22	4.07 ± 0.42	3.88 ± 0.12

Supplementary Table 5.1. Sources for all *Plantago* species used in this study. P, purchased; C, private land collected; R, collected and donated by researcher; S, seedbank withdrawal. ALA = Atlas of Living Australia. Seedbank accession records can be found at https://doi.org/10.26197/5dc21fa4f3b62

Species		Origin	Seedbank	ALA / Seedbank Accession Number
P. ovata	P	Austral Herbs, NSW, Australia	-	-
P. lanceolata	C	Panorama, SA, Australia	-	-
P. coronopus	C	Aldinga Beach, SA, Australia	-	-
P. major	P	Organics Australia, Australia	-	-
P. cunninghamii	R	St. George, Queensland, Australia	-	-
P. paradoxa	S	Central Plateau, Tasmania, Australia	Tasmanian Seed Conversation Centre	0008866-a
P. turrifera	C	Loxton, South Australia, Australia	-	-
P. bellidioides	S	Petal Point, Tasmania, Australia	Tasmanian Seed Conversation Centre	0008349-a
P. debilis	R	Charlwood, Queensland, Australia	-	-
P. triantha	S	Trial Harbour, Tasmania, Australia	Tasmanian Seed Conversation Centre	0009460-a
P. gaudichaudii	S	Mount Meredith, Victoria, Australia	Victorian Conservation Seedbank	MEL 2356648A
P. varia	R	Aranda Bushland, Australian Capital Territory, Australia	-	-
Species used in Supplementary Figure 5.9				
P. alpestris	S	Kosciuszko National Park, New South Wales, Australia	ANBG National Seedbank	748569.3
P. euryphylla	S	Kosciuszko National Park, New South Wales, Australia	ANBG National Seedbank	808038.3
P. glabrata	S	Wild Dog Creek, Tasmania, Australia	ANBG National Seedbank	609869.1
P. glacialis	S	Kosciuszko National Park, New South Wales, Australia	ANBG National Seedbank	797747.2
P. muelleri	S	Kosciuszko National Park, New South Wales, Australia	ANBG National Seedbank	808184.3
P. tasmanica	S	Central Plateau, Tasmania, Australia	Tasmanian Seed Conversation Centre	0004191-a

Supplementary Table 5.2. PCR parameters for amplification of nuclear ribosomal DNA internal transcribed spacer (ITS) regions used to produce *Plantago* phylogenetic tree.

Primers	
Forward ITS Primer (5'→ 3')	ACGAATTCATGGTCCGGTGAAGTGTTCG
Reverse ITS Primer (5'→ 3')	TAGAATTCCCCGGTTCGCTCGCCGTTAC

PCR Conditions	
Activation	95 °C for 2 min
Amplification Cycles	24 Cycles
Denaturation	95 °C for 30 sec
Annealing & Extension (Two-step PCR)	72 °C for 1 min
Final Extension	72 °C for 5 min

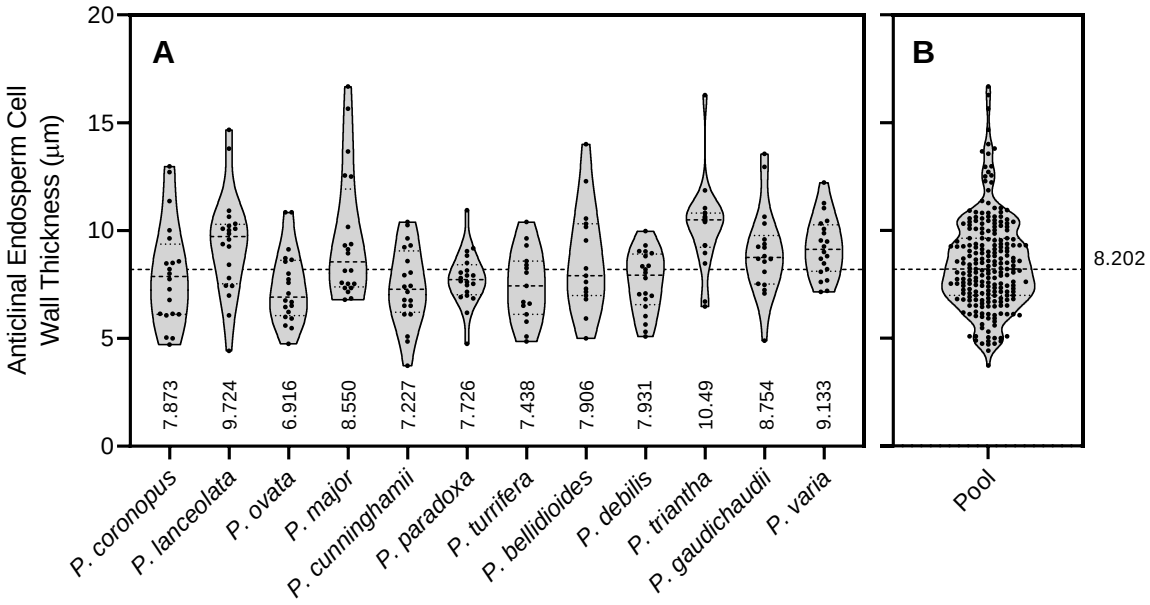

Supplementary Figure 5.1. Thickness of anticlinal *Plantago* endosperm cell walls. **A.** Values between x-axis tick marks and violin plots denote the median cell wall thickness measured in that sample. **B.** Dashed horizontal line denotes the grand median cell wall thickness from pooled measurements of each species. Cell wall thickness (n = 15–20) was measured using the measurement package of Adobe Photoshop CC 19.0

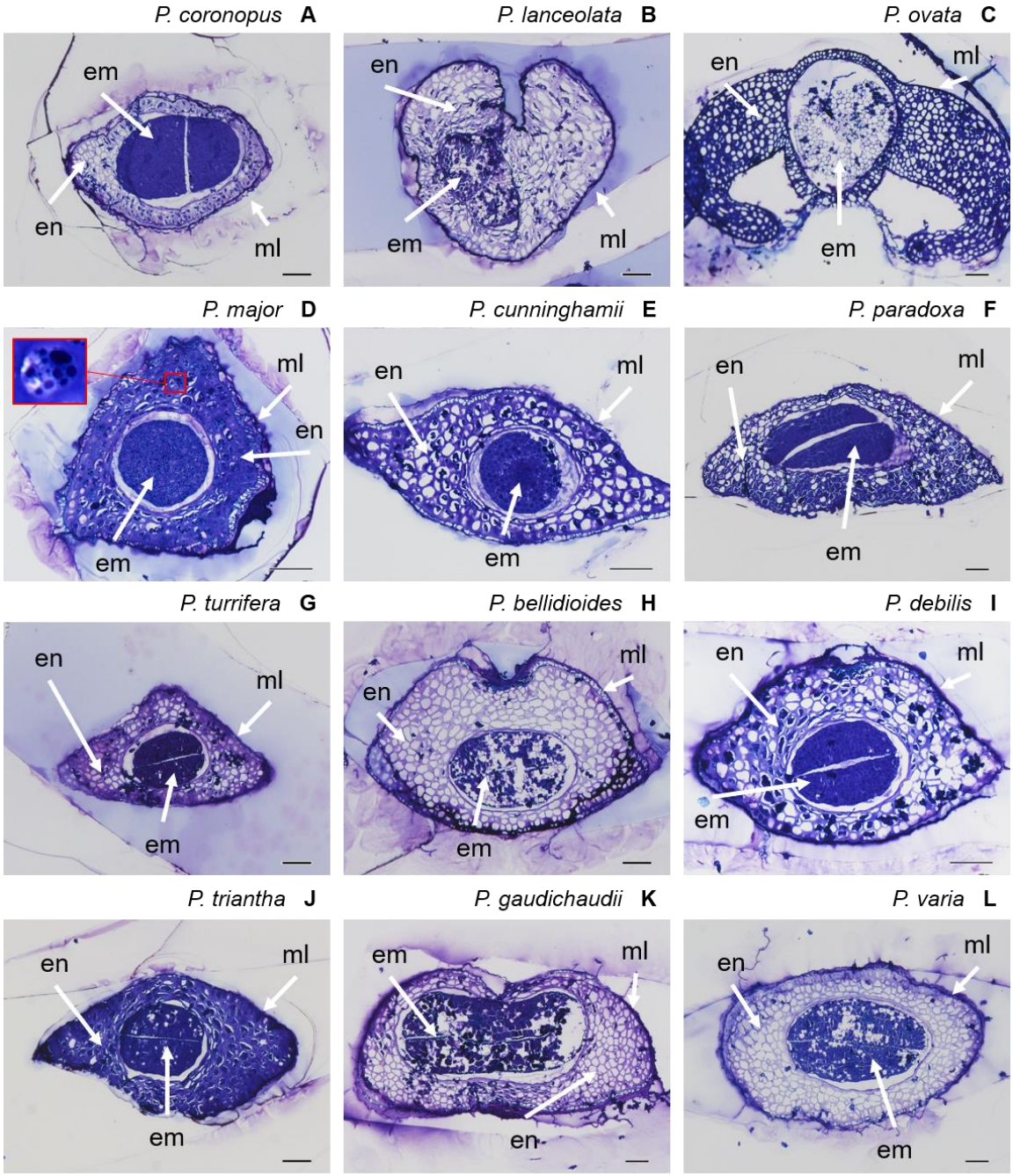

Supplementary Figure 5.2. Thin sections of mature *Plantago* seeds stained with Toluidine Blue O to show the major tissue types. Inset in D shows the spherical bodies typically contained within *Plantago* endosperm cells. These spherical bodies are present within endosperm cells of all species but are difficult to retain *in situ* when sectioning, positioning on slide and staining and are thus are sporadically present in images. Scale = 100 µm. Abbreviations: en = endosperm; em = embryo; ml = mucilage layer.

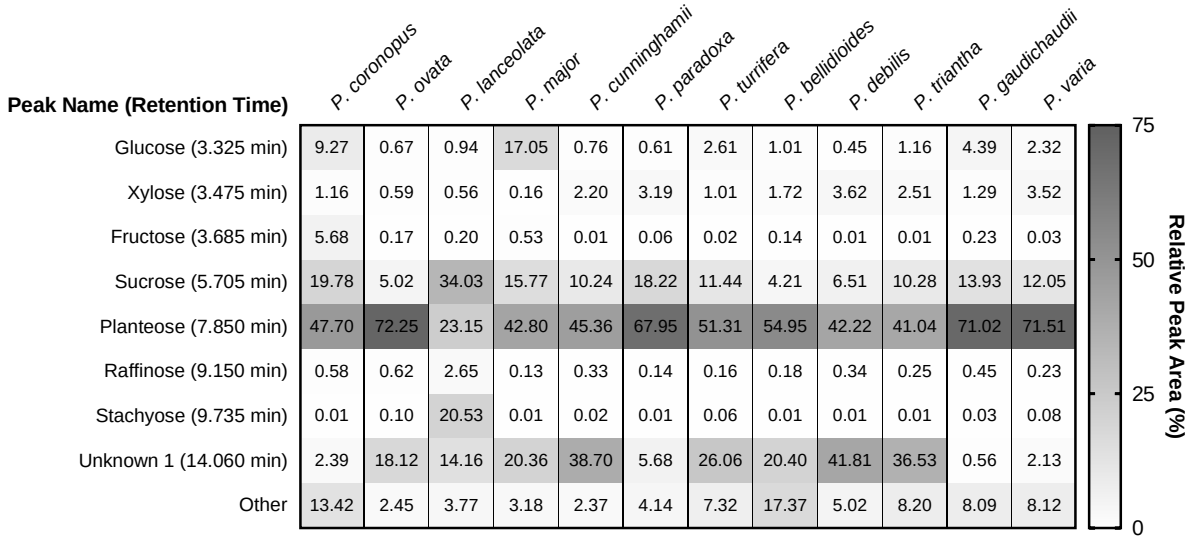

Supplementary Figure 5.3. Heatmap displaying the average relative peak area of soluble sugars extracted from *Plantago* seeds. Retention times of each peak are listed along with their assigned peak name. Values within each cell are the relative peak area of that component in that species.

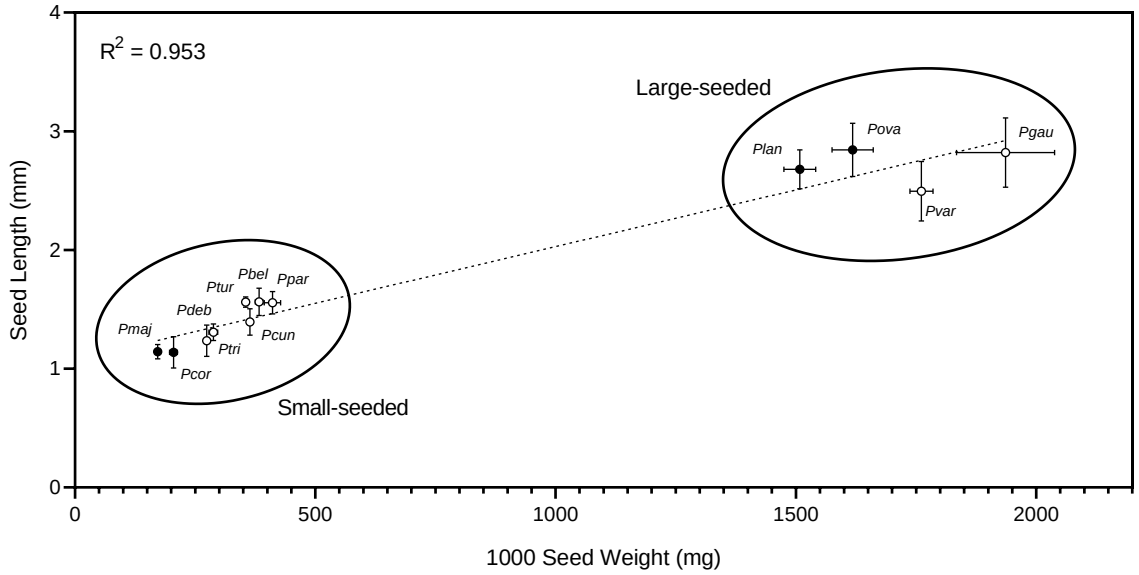

Supplementary Figure 5.4. Seeds of the *Plantago* species studied here can be grouped as small- or large-seeded, morphometrically and by mass. Seed size is not determined by geographic origin as both size groups contain both native (open circles) and naturalised species (filled circles). Error bars denote one standard deviation.

Abbreviations: Pbel = *P. bellidioides;* Pcor = *P. coronopus;* Pcun = *P. cunninghamii*; Pdeb = *P. debilis*; Pgau = *P. gaudichaudii;* Plan = *P. lanceolata;* Ppar = *P. paradoxa;* Ptri = *P. triantha;* Ptur = *P. turrifera;* Pvar = *P. varia.*

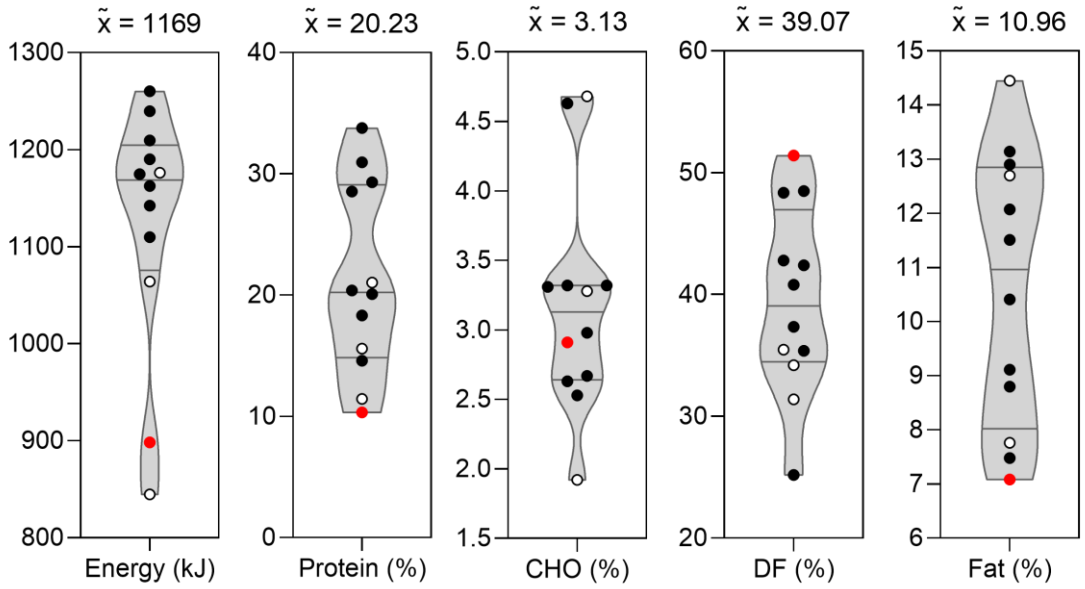

Supplementary Figure 5.5. Truncated violin plots displaying the data range of nutrient content in seeds of the 12 *Plantago* species studied here. Native species are denoted by black points, naturalised species are white points and the commercial species, *Plantago ovata,* is a red point. Median values (x̃) are included above each plot. Abbreviations: CHO = carbohydrates; DF = dietary fibre.

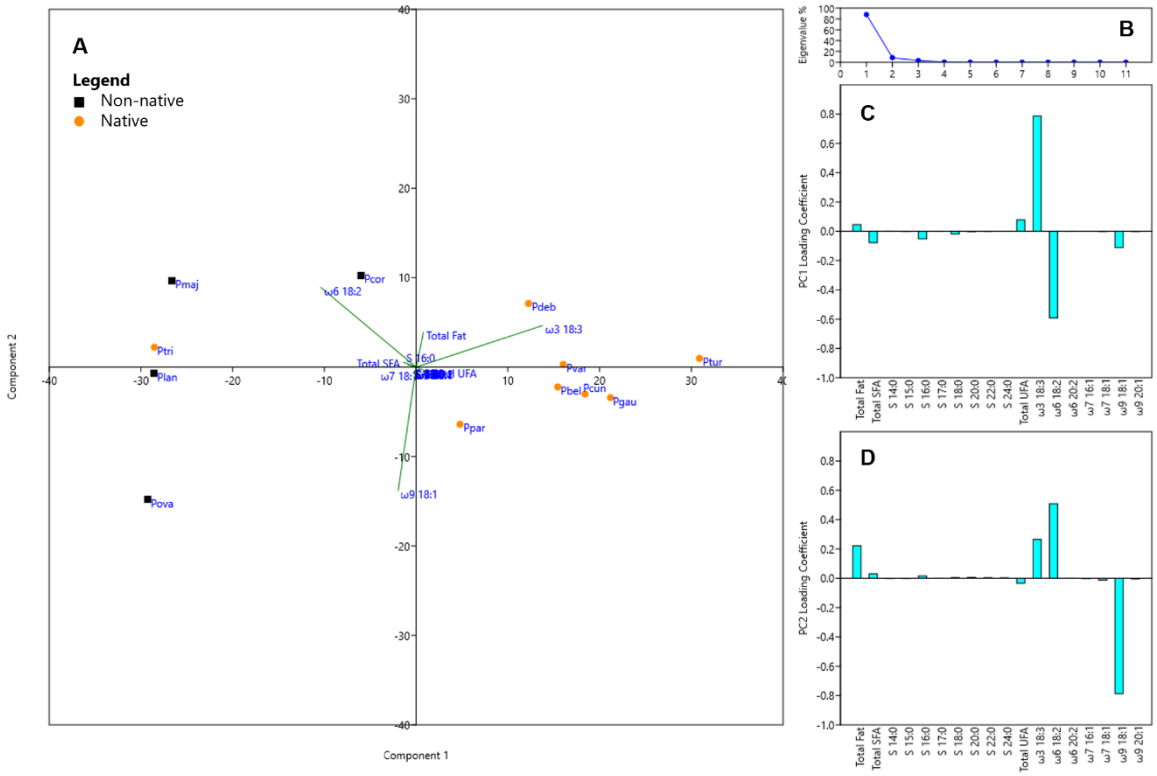

Supplementary Figure 5.6. Principle component analysis of fatty acid (FA) profiling. **A.** PCA biplot of PC1 and PC2 showing FA factors leading to species separation. **B.** Scree plot showing that PC1 and PC2 account for 98% of variance observed. **C.** Loading plot of PC1 and **D.** PC2. In PC1, most separation is due to a relationship between omega-3 (ω3 18:3) to omega-6 FAs (ω6 18:2) (89% of variance) while in PC2 the relationship is between omega-6 (ω6 18:2) and omega-9 FAs (ω9 18:1) (8% of variance).

Abbreviations: Pbel = *P. bellidioides;* Pcor = *P. coronopus;* Pcun = *P. cunninghamii*; Pdeb = *P. debilis*; Pgau = *P. gaudichaudii;* Plan = *P. lanceolata;* Ppar = *P. paradoxa;* Ptri = *P. triantha;* Ptur = *P. turrifera;* Pvar = *P. varia;* SFA = saturated fatty acids; UFA = unsaturated fatty acids.

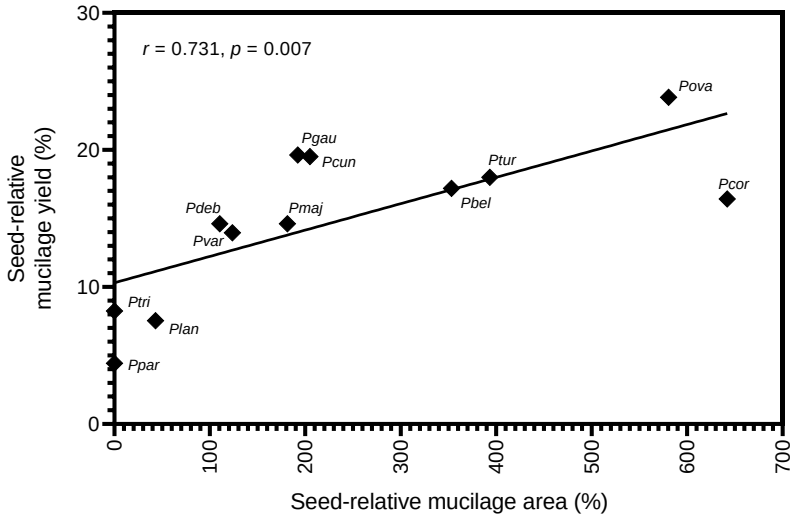

Supplementary Figure 5.7. There is a relationship between mucilage envelope size and mucilage yield in *Plantago* species. This is not always the case, as discussed previously with *Salvia hispanica* as an example where mucilage envelope is large with a proportionally low polysaccharide content (Cowley *et al.* 2020).

Abbreviations: Pbel = *P. bellidioides;* Pcor = *P. coronopus;* Pcun = *P. cunninghamii*; Pdeb = *P. debilis*; Pgau = *P. gaudichaudii;* Plan = *P. lanceolata;* Ppar = *P. paradoxa;* Ptri = *P. triantha;* Ptur = *P. turrifera;* Pvar = *P. varia*

Supplementary Figure 5.8. Locations of *Plantago* sample sources based on coordinates supplied with seedbank-withdrawn accessions or collection sites. Map sourced from Google Earth earth.google.com/web. *P. ovata* and *P. major* samples were purchased commercially, so origin information can only be assumed. White blips are naturalised species sourced locally. Green blips are Australian native species analysed in this study. Blue blips are other Australian native species used only in Supplementary Figure 12.

Abbreviations: Palp = *P. alpestris*; Pbel = *P. bellidioides;* Pcor = *P. coronopus;* Pcun = *P. cunninghamii*; Pdeb = *P. debilis*; Peur = *P. euryphylla;* Pgau = *P. gaudichaudii;* Pglb = *P. glabrata;* Pglc = *P. glacialis;* Plan = *P. lanceolata;* Pmue = *P. muelleri*; Ppar = *P. paradoxa;* Ptas = *P. tasmanica;* Ptri = *P. triantha;* Ptur = *P. turrifera;* Pvar = *P. varia.*

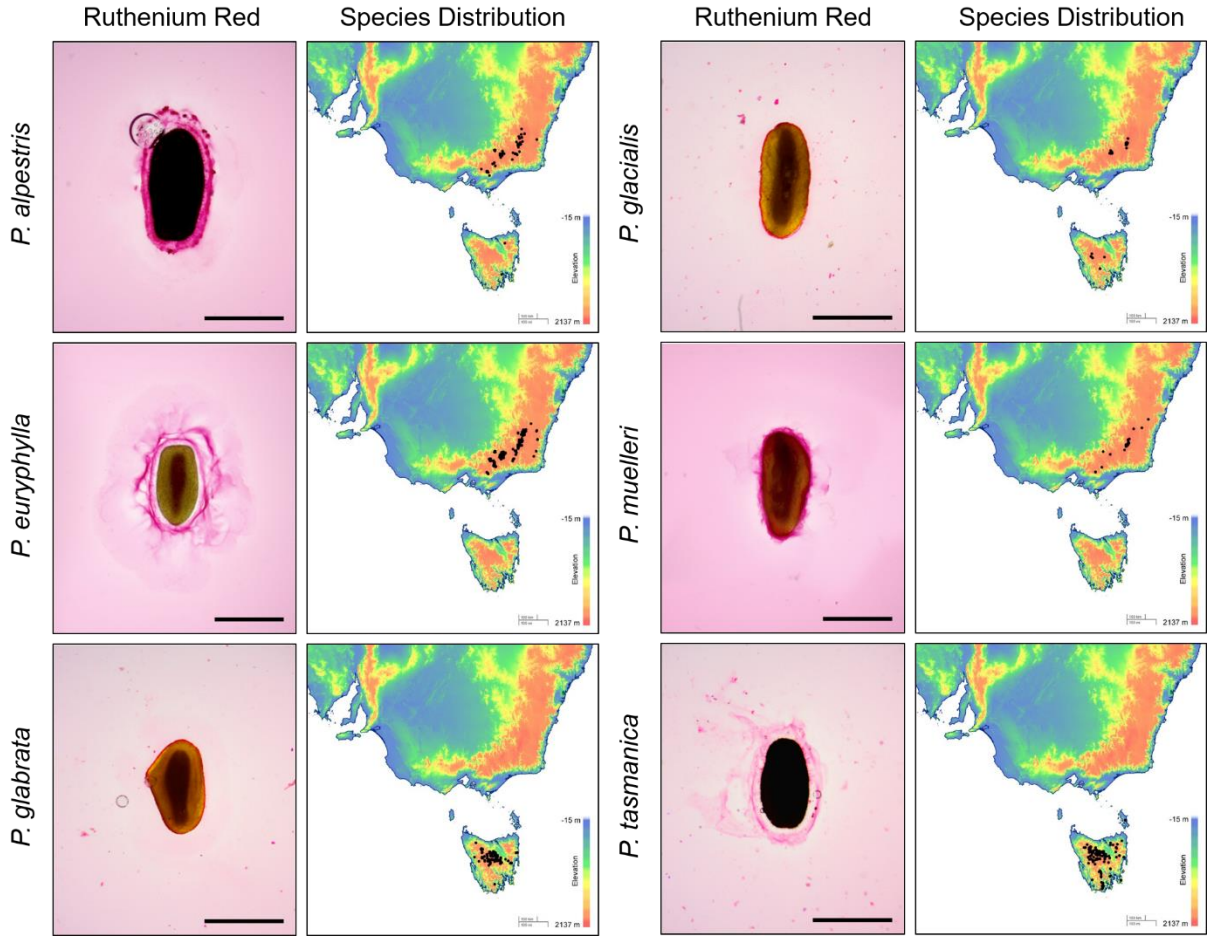

Supplementary Figure 5.9. A dense, high-energy cost mucilage envelope may not be advantageous in high elevation, high rainfall environments. Mucilage architecture of six additional native *Plantago* species (scale = 1mm) along with their distribution in South-Eastern Australia (recorded observations displayed as black dots). Heat map of geographic elevation is also displayed. Spatial distribution data extracted from the Atlas of Living Australia database in October 2019.

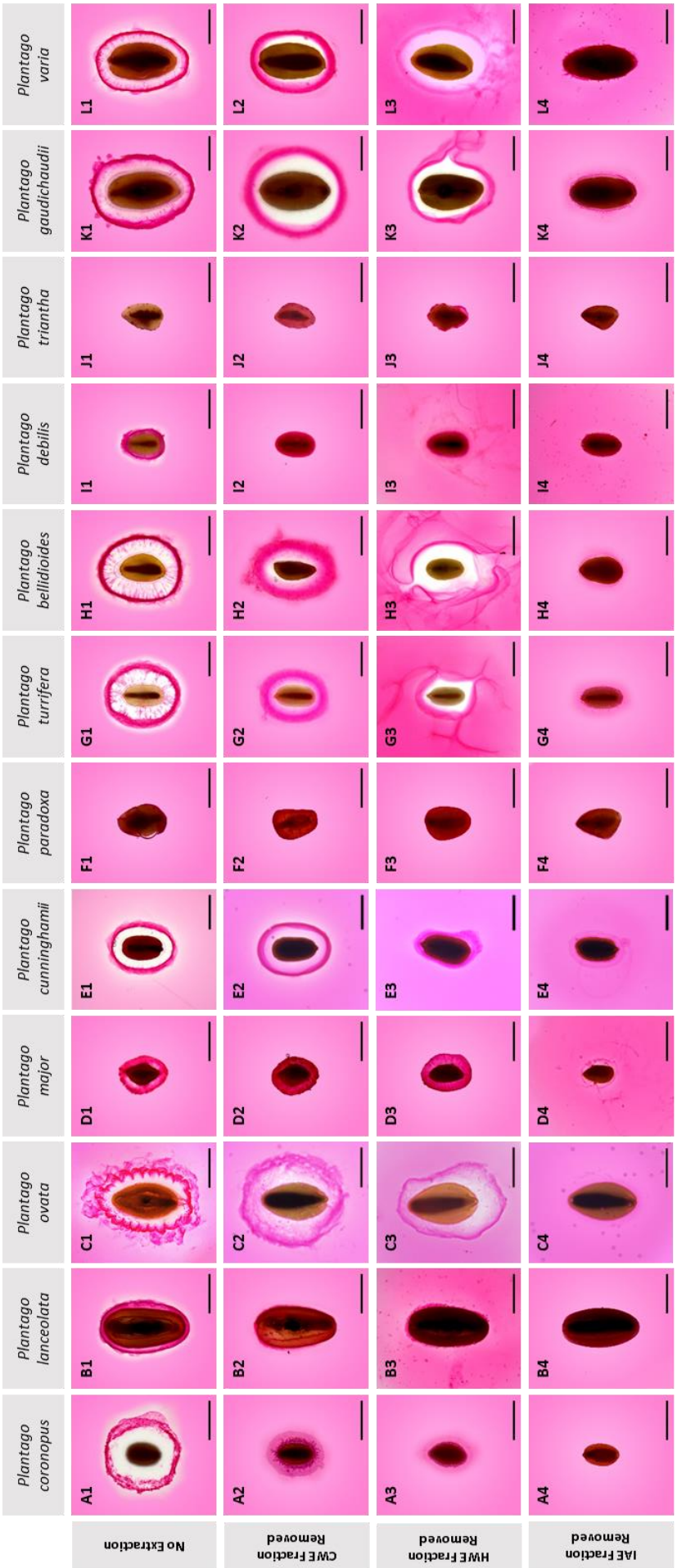

Supplementary Figure 5.10. Appearance of the mucilage envelope of each *Plantago* species after each step of fractionation protocol and staining with ruthenium red. Scale = 1 mm. CWE = cold water extractable; HWE = hot water extractable; IAE = intense agitation

Declarations

Acknowledgements

The authors acknowledge Dr Jana Phan for her hard work that paved the way for this study and Dr Tina Bianco-Miotto for continued support. The authors thank Kylie Neumann and Shi Fang (Sandy) Khor for excellent technical assistance, Dr Lisa O'Donovan for expert assistance in microtomy and microscopy, Dr Andrea Matros for valuable assistance with soluble sugar profiling, Dr Julian Schwerdt for advice on phylogenetic analysis, Sanjiv Satija and Mathieu Baes for assistance with protein analysis, and SAHMRI for lipid analysis.

The authors appreciate the valuable conservation work of the partners of the Australian Seedbank Partnership, particularly the ANBG National Seed Bank, Tasmanian Seed Conservation Centre and Victorian Conservation Seedbank, the collectors and the curators who generously provided some of the seed samples to allow this project to happen.

Authors' contributions:

JMC and RAB conceived the study. JMC conducted the experiments and wrote the manuscript. RAB contributed to data interpretation and writing the manuscript. Both authors read, edited and approved the final manuscript.

Funding:

This work was supported the Australian Research Council Centres of Excellence in Plant Cell Walls (Grant No. 110001007) and Plant Energy Biology (Grant No. 140100008). JMC is supported by a PhD scholarship from the Australian Government's Research Training Program.

Availability of data and materials:

The datasets used and analysed during this work are available from the corresponding author upon reasonable request.

Consent for publication:

All authors give consent for the data to be published.

Ethics:

Not applicable

Competing Interests:

The authors declare no competing interests.

References

Addoun N, Boual Z, Delattre C, *et al.* 2020. Structural features and rheological behavior of a water-soluble polysaccharide extracted from the seeds of Plantago ciliata Desf. *International Journal of Biological Macromolecules* **155**: 1333–1341.

Aghdaei S, Aalami M, Geefan S, Ranjbar A. **2014**. Application of Isfarzeh seed (Plantago ovate L.) mucilage as a fat mimetic in mayonnaise. *Journal of food science and technology* **51**: 2748–54.

Ahmed Z, Rizk A, Hammoud F. **1965**. Phytochemical Studies of Egyptian Plantago species. *Journal of Pharmaceutical Sciences* **156**: 1060–1062.

Alander M, Matto J, Kneifel W, *et al.* 2001. Effect of galacto-oligosaccharide supplementation on human faecal microflora and on survival and persistence of Bifidobacterium lactis Bb-12 in the gastrointestinal tract. *International Dairy Journal* **11**: 817–825.

Albach DC, Chase MW, Veroniceae V. **2001**. Paraphyly of Veronica (Veroniceae ; Scrophulariaceae): Evidence from the Internal Transcribed Spacer (ITS) Sequences of Nuclear Ribosomal DNA. *Journal of Plant Research* **114**: 9–18.

Anderson JW, Allgood LD, Lawrence A, *et al.* 2000. Cholesterol-lowering effects of psyllium intake adjunctive to diet therapy in men and women with hypercholesterolemia: meta-analysis of 8 controlled trials. *American Journal of Clinical Nutrition*: 472–479.

Anderson JW, Allgood LD, Turner J, Oeltgen PR, Daggy BP. **1999**. Effects of psyllium on glucose and serum lipid responses in men with type 2 diabetes and hypercholesterolemia. *American Journal of Clinical Nutrition* **70**: 466–473.

Asano I, Hamaguchi K, Fujii S, Iino H. **2003**. In Vitro Digestibility and Fermentation of Mannooligosaccharides from Coffee Mannan. *Food Science and Technology* **9**: 62–66.

Behbahani BA, Shahidi F, Yazdi FT, Mortazavi SA, Mohebbi M. **2017**. Use of Plantago major seed mucilage as a novel edible coating incorporated with Anethum

graveolens essential oil on shelf life extension of beef in refrigerated storage. *International Journal of Biological Macromolecules* **94**: 515–526.

Behbahani BA, Tabatabaei Yazdi F, Shahidi F, Hesarinejad MA, Mortazavi SA, Mohebbi M. **2017**. Plantago major seed mucilage: Optimization of extraction and some physicochemical and rheological aspects. *Carbohydrate Polymers* **155**: 68–77.

Benaoun F, Delattre C, Boual Z, *et al.* 2017. Structural characterization and rheological behavior of a heteroxylan extracted from *Plantago notata* Lagasca (Plantaginaceae) seeds. *Carbohydrate Polymers* **175**: 96–104.

Bijkerk CJ, De Wit NJ, Muris JWM, Whorwell PJ, Knottnerus JA, Hoes AW. **2009**. Soluble or insoluble fibre in irritable bowel syndrome in primary care? Randomised placebo controlled trial. *BMJ (Online)* **339**: 613–615.

Brown M. **1991**. A synopsis of the genus Plantago L. in Tasmania In: *Aspects of Tasmanian Botany*.65–74.

Bruneton J. **1995**. *Pharmacognosy, phytochemistry, medicinal plants*. Paris: Lavoisier.

Bruno-Barcena J, Azcarate-Peril M. **2015**. Galacto-oligosaccharides and colorectal cancer : Feeding our intestinal probiome. *Journal of Functional Foods* **12**: 92–108.

Burton RA, Collins HM, Kibble N, *et al.* 2011. Over-expression of specific HvCslF cellulose synthase-like genes in transgenic barley increases the levels of cell wall (1,3;1,4)-β-D-glucans and alters their fine structure. *Plant biotechnology journal* **9**: 117–135.

Calder PC. **2006**. n-3 Polyunsaturated fatty acids , inflammation, and inflammatory diseases. *American Journal of Clinical Nutrition* **83**.

Cappa C, Lucisano M, Mariotti M. **2013**. Influence of Psyllium, sugar beet fibre and water on gluten-free dough properties and bread quality. *Carbohydrate Polymers* **98**: 1657–1666.

Cheng K, Zhou Y, Neelamegham S. **2017**. DrawGlycan-SNFG : a robust tool to render glycans and glycopeptides with fragmentation information. *Glycobiology* **27**:

200–205.

Çoban T, Saltan G, Sever B, İşcan M. **2008**. Antioxidant Activities of Plants Used in Traditional Medicine in Turkey Antioxidant Activities of Plants Used in Traditional Medicine in Turkey. *Pharmaceutical Biology* **41**: 608–613.

Cooper GO. **1942**. Development of the ovule and the formation of the seed in *Plantago lanceolata*. *American Journal of Botany* **29**: 577–581.

Cowley JM, Herliana L, Neumann KA, Ciani S, Cerne V, Burton RA. **2020**. A small-scale fractionation pipeline for rapid analysis of seed mucilage characteristics. *Plant Methods* **16**: 1–12.

Crawford M, Galli C, Visioli F, Renaud S, Simopoulos AP, Spector AA. **2000**. Role of plant-derived omega-3 fatty acids in human nutrition. *Annals of Nutrition and Metabolism* **44**: 263–265.

Criscuolo A, Gribaldo S. **2010**. BMGE (Block Mapping and Gathering with Entropy): A new software for selection of phylogenetic informative regions from multiple sequence alignments. *BMC Evolutionary Biology* **10**.

Davison E. **1982**. Seed utilization by harvester ants In: *Ant-plant interactions*.1–6.

Dey PM. **1980**. Biosynthesis of planteose in Sesamum indicum. *FEBS Letters* **114**.

Dhar MK, Kaul S, Sareen S, Koul AK. **2005**. Plantago ovata: genetic diversity, cultivation, utilization and chemistry. *Plant Genet Resour* **3**: 252–263.

Dziki D, Laskowski J. **2006**. Influence of wheat grain mechanical properties on grinding energy requirements. *TEKA Kom. Mot. Energ. Roln.*: 45–52.

Fernandez-Banares F, Hinojosa J, Sanchez-Lombrana J, *et al.* 1999. Randomized Clinical Trial of Plantago ovata Seeds (Dietary Fiber) as Compared With Mesalamine in Maintaining Remission in Ulcerative Colitis. *The American Journal of Gastroenterology* **94**: 427–433.

Folch J, Lees M, Sloane Stanley G. 1957. A simple method for the isolation and purification of total lipid from animal tissues. *Journal of Biological Chemistry* **226**: 497–509.

Food and Agriculture Organisation of the United Nations. **1998**. *Calculation of the Energy Content of Foods - Energy Conversion Factors*. http://www.fao.org/3/Y5022E/y5022e04.htm.

French D, Youngquist RW, Lee A. **1959**. Isolation and Crystallization of Planteose from Mint. *Archives of Biochemistry and Biophysics* **85**: 471–473.

Galisteo M, Sánchez M, Vera R, *et al.* 2005. A diet supplemented with husks of Plantago ovata reduces the development of endothelial dysfunction, hypertension, and obesity by affecting adiponectin and TNF-alpha in obese Zucker rats. *The Journal of nutrition* **135**: 2399–2404.

Gong X, Bassel GW, Wang A, Greenwood JS. **2005**. The Emergence of Embryos from Hard Seeds is Related to the Structure of the Cell Walls of the Micropylar Endosperm , and not to Endo- b -mannanase Activity. *Annals of Botany*: 1165–1173.

Gong L, Zhang H, Niu Y, *et al.* 2015. A novel alkali extractable polysaccharide from plantago Asiatic L. seeds and its radical-scavenging and bile acid-binding activities. *Journal of Agricultural and Food Chemistry* **63**: 569–577.

Gorenflot R, Bourdu K. **1962**. Critères biochimiques et taxonomie expérimentale du genre Plantago. *Bulletin de la Société Botanique de France* **109**: 349–360.

Gott B. **2006**. Plant Species used by Aborigines of South-Eastern Australia.

Govt India Dept of Commerce. **2017a**. Psyllium seed (isobgul) 12119013 Export : Commodity-wise.

Govt India Dept of Commerce. **2017b**. Psyllium husk (isobgul) 12119032 Export : Commodity-wise.

Grady JO, Connor EMO, Shanahan F. **2019**. Review article : dietary fibre in the era of microbiome science. : 506–515.

Grubert M. **1974**. Studies on the distribution of myxospermy among seeds and fruits of Angiospermae and its ecological importance. *Acta Biologica Venezualica* **8**: 315–551.

Hammer Ø, Harper DAT, Ryan PD. **2001**. PAST: Paleotological statistics software

package for education and data analysis. *Palaeontologia electronica* **4**: 1–9.

Han N, Wang L, Song Z, *et al.* 2016. Optimization and antioxidant activity of polysaccharides from Plantago depressa. *International Journal of Biological Macromolecules* **93**, **Part A**: 644–654.

Haque A, Morris ER. **1994**. Combined use of ispaghula and HPMC to replace or augment gluten in breadmaking. *Food Research International* **27**: 379–393.

Harput US, Genc Y, Saracoglu I. **2012**. Cytotoxic and antioxidative activities of Plantago lagopus L. and characterization of its bioactive compounds. *Food and Chemical Toxicology* **50**: 1554–1559.

Harris WS, Harris WS. **2006**. The Omega-6 / Omega-3 Ratio and Cardiovascular Disease Risk : Uses and Abuses. *Current Atherosclerosis Reports* **8**: 453–459.

Hatanaka S. **1959**. Oligosaccharides in the Seeds of Sesamum indicum L. *Archives of Biochemistry and Biophysics* **82**: 188–194.

Healey A, Furtado A, Cooper T, Henry RJ. **2014**. Protocol: A simple method for extracting next-generation sequencing quality genomic DNA from recalcitrant plant species. *Plant Methods* **10**: 1–8.

Heimler D, Isolani L, Vignolini P, Tombelli S, Romani A. **2007**. Polyphenol Content and Antioxidative Activity in Some Species of Freshly Consumed Salads. *Journal of Agricultural and Food Chemistry* **55**: 1724–1729.

Huang D, Nie S, Jiang L, Xie M. **2014**. A novel polysaccharide from the seeds of Plantago asiatica L. Induces dendritic cells maturation through toll-like receptor 4. *International Immunopharmacology* **18**: 236–243.

Huang DF, Xie MY, Yin JY, *et al.* 2009. Immunomodulatory activity of the seeds of Plantago asiatica L. *Journal of Ethnopharmacology* **124**: 493–498.

Hyde BB. **1970**. Mucilage-producing cells in the seed coat of *Plantago ovata*: Developmental fine structure. *American Journal of Botany* **57**: 1197–1206.

Iqbal A, Khalil IA, Ateeq N, Khan MS. **2006**. Nutritional quality of important food legumes. *Food Chemistry* **97**: 331–335.

Jensen JK, Johnson N, Wilkerson CG. **2013**. Discovery of diversity in xylan biosynthetic genes by transcriptional profiling of a heteroxylan containing mucilaginous tissue. *Front Plant Sci* **4**.

Jensen JK, Kim H, Cocuron J-C, Orler R, Ralph J, Wilkerson CG. **2011**. The DUF579 domain containing proteins IRX15 and IRX15-L affect xylan synthesis in Arabidopsis. *Plant J* **66**: 387–400.

Jiang LM, Nie SP, Zhou HL, Huang DF, Xie MY. **2014**. Carboxymethylation enhances the maturation-inducing activity in dendritic cells of polysaccharide from the seeds of Plantago asiatica L. *International Immunopharmacology* **22**: 324–331.

Jonathan MC, Van Den Borne JJGC, Van Wiechen P, Souza Da Silva C, Schols HA, Gruppen H. **2012**. In vitro fermentation of 12 dietary fibres by faecal inoculum from pigs and humans. *Food Chemistry* **133**: 889–897.

Jukes C, Lewis D. **1974**. Planteose, the major soluble carbohydrate of seeds of Fraxinus excelsior. *Phytochemistry* **13**: 1519–1521.

Kumar J. **2015**. *Good agricultural practices for isabgol*. Report for the Directorate of Medicinal and Aromatic Plants.

Leng-Peschlow E. **1991**. Plantago ovata seeds as dietary fibre supplement : physiological and metabolic effects in rats. *British Journal of Nutrition* **66**: 331–349.

Liu G, Mühlhäusler BS, Gibson RA. **2014**. A method for long term stabilisation of long chain polyunsaturated fatty acids in dried blood spots and its clinical application. *Prostaglandins Leukotrienes and Essential Fatty Acids* **91**: 251–260.

Low T. **1988**. *Wild Food Plants of Australia*. North Ryde: Angus & Robertson Publishers.

Lynch S, Pedersen M. **2016**. The Human Intestinal Microbiome in Health and Disease. *The New England Journal of Medicine* **375**: 2369–2379.

Madgulker A, Rao M, Warrier D. **2014**. Characterization of Psyllium (Plantago ovata) Polysaccharide and Its Uses. *Polysaccharides*.

Maiden J. **1898**. A new indigenous food-plant. *Agricultural Gazette of NSW* **9**: 355.

Marcus SE, Blake AW, Benians TAS, *et al.* 2010. Restricted access of proteins to mannan polysaccharides in intact plant cell walls. *Plant Journal* **64**: 191–203.

McCartney L, Marcus SE, Knox JP. **2005**. Monoclonal Antibodies to Plant Cell Wall Xylans and Arabinoxylans. *Journal of Histochemistry & Cytochemistry* **53**: 543–546.

McRorie JW. **2015**. Psyllium is not fermented in the human gut. *Neurogastroenterology and Motility* **27**: 1681–1682.

McRorie JW, Daggy BP, Morel JG, Diersing PS, Miner PB, Robinson M. **1998**. Psyllium is superior to docusate sodium for treatment of chronic constipation. *Alimentary Pharmacology and Therapeutics* **12**: 491–497.

Miao S, Bazzaz F, Primack R. **1991**. Persistence of Maternal Nutrient Effects in Plantago Major: The Third Generation. *Ecology* **72**: 1634–1642.

Mohamed IK, Osama MA-F, El-Salam SMA, Mohamed ZE-O. **2011**. Biochemical studies on Plantago major L. and Cyamopsis tetragonoloba L. *International Journal of Biodiversity and Conservation* **3**: 83–91.

Moreno-Salazar S, Robles-Zepeda R, Johnson D. **2008**. Plant folk medicines for gastrointestinal disorders among the main tribes of Sonora , Mexico. *Fitoterapia* **79**: 132–141.

Patterson E, Wall R, Fitzgerald GF, Ross RP, Stanton C. **2012**. Health Implications of High Dietary Omega-6 Polyunsaturated Fatty Acids. *Journal of Nutrition and Metabolism* **2012**: 1–6.

Pejcz E, Spychaj R, Wojciechowicz-Budzisz A, Gil Z. **2018**. The effect of Plantago seeds and husk on wheat dough and bread functional properties. *LWT - Food Science and Technology* **96**: 371–377.

Phan J. **2012**. Xylans in Plantago species. *Honours Thesis*.

Phan J, Burton RA. **2018**. New Insights into the Composition and Structure of Seed Mucilage. *Annual Plant Reviews Online* **1**: 1–41.

Phan J, Cowley J, Neumann K, Burton R. **2020**. The novel features of Plantago ovata seed mucilage accumulation, storage and release. *Scientific Reports*.

Phan J, Tucker MR, Khor SF, *et al.* 2016. Differences in glycosyltransferase family 61 accompany variation in seed coat mucilage composition in Plantago spp. *Journal of Experimental Botany* **67**: 6481–6495.

Primack RB. **1979**. Reproductive Effort in Annual and Perennial Species of Plantago (Plantaginaceae). *The American Naturalist* **114**: 51–62.

Rahn K. **1996**. A phylogenetic study of the Plataginaceae. *Botanical Journal of the Linnean Society* **120**: 145–198.

Ren Y, Yakubov GE, Linter BR, MacNaughtan W, Foster TJ. **2020**. Temperature fractionation, physicochemical and rheological analysis of psyllium seed husk heteroxylan. *Food Hydrocolloids* **104**: 105737.

Romero-Baranzini AL, Rodriguez OG, Yanez-Farias GA, Barron-Hoyos JM, Rayas-Duarte P. **2006**. Chemical, physicochemical, and nutritional evaluation of Plantago (Plantago ovata Forsk). *Cereal Chemistry* **83**: 358–362.

Romero AL, West KL, Zern T, Fernandez ML. **2002**. The Seeds from Plantago ovata Lower Plasma Lipids by Altering Hepatic and Bile Acid Metabolism in Guinea Pigs 1. *American Society for Nutritional Sciences* **132**: 1194–1198.

Rønsted N, Chase MW, Albach DC, Bello MA. **2002**. Phylogenetic relationships within Plantago (Plantaginaceae): Evidence from nuclear ribosomal ITS and plastid trnL-F sequence data. *Botanical Journal of the Linnean Society* **139**: 323–338.

Saeedi M, Morteza-Semnani K, Ansoroudi F, Fallah S, Amin G. **2010**. Evaluation of binding properties of Plantago psyllium seed mucilage. *Acta pharmaceutica (Zagreb, Croatia)* **60**: 339–48.

Saeedi M, Morteza-Semnani K, Sagheb-Doust M. **2013**. Evaluation of Plantago major L. seed mucilage as a rate controlling matrix for sustained release of propranolol hydrochloride. *Acta pharmaceutica (Zagreb, Croatia)* **63**: 99–114.

Saez-Aguayo S, Rondeau-Mouro C, Macquet A, *et al.* 2014. Local Evolution of Seed Flotation in Arabidopsis. *PLoS Genet* **10**: e1004221.

Samout N, Ettaya A, Bouzenna H, Ncib S, Elfeki A, Hfaiedh N. **2016**. Beneficial

effects of Plantago albicans on high-fat diet-induced obesity in rats. *Biomedicine & Pharmacotherapy* **84**: 1768–1775.

Samuelsen AB. **2000**. The traditional uses, chemical constituents and biological activities of Plantago major L. A review. *Journal of Ethnopharmacology* **71**: 1–21.

Sargi SC, Silva BC, Munise H, *et al.* 2013. Antioxidant capacity and chemical composition in seeds rich in omega-3: chia , flax , and perilla. *Food Science and Technology* **33**: 541–548.

Schultz CJ, Lim WL, Khor SF, *et al.* 2020. Consumer and health-related traits of seed from selected commercial and breeding lines of industrial hemp, Cannabis sativa L. *Journal of Agriculture and Food Research* **2**: 100025.

Simopoulos AP. **2002**. The importance of the ratio of omega-6 / omega-3 essential fatty acids. *Biomedicine & Pharmacotherapy* **56**: 365–379.

Smith I. **2004**. An assessment of recent trends in Australian rainfall. *Australian Meteorological Magazine* **53**: 163–173.

Stamatakis A. **2006**. RAxML-VI-HPC: maximum likelihood-based phylogenetic analyses with thousands of taxa and mixed models Alexandros. *Phylogenetics* **22**: 2688–2690.

Sun Y, Skinner DZ, Liang GH, Hulbert SH. **1994**. Phylogenetic analysis of Sorghum and related taxa using internal transcribed spacers of nuclear ribosomal DNA. *Theoretical and Applied Genetics* **89**: 26–32.

Tay ML, Meudt HM, Garnock-Jones PJ, Ritchie PA. **2010**. DNA sequences from three genomes reveal multiple long-distance dispersals and non-monophyly of sections in Australasian Plantago (Plantaginaceae). *Australian Systematic Botany* **23**: 47–68.

Teixeira A, Iannetta P, Binnie K, Valentine TA, Toorop P. **2019**. Myxospermous seed-mucilage quantity correlates with environmental gradients indicative of water-deficit stress : Plantago species as a model. *Plant and Soil*: 1–14.

Tocher DR, Betancor MB, Sprague M, Olsen RE, Napier JA. **2019**. Omega-3 long-

chain polyunsaturated fatty acids, EPA and DHA: Bridging the gap between supply and demand. *Nutrients* **11**: 1–20.

Verspreet J, Pollet A, Cuyvers S, *et al.* 2012. A simple and accurate method for determining wheat grain fructan content and average degree of polymerization. *Journal of Agricultural and Food Chemistry* **60**: 2102–2107.

Wakabayashi T, Joseph B, Yasumoto S, Akashi T, Aoki T. **2015**. Planteose as a storage carbohydrate required for early stage of germination of Orobanche minor and its metabolism as a possible target for selective control. *Journal of Experimental Botany* **66**: 3085–3097.

Wattiez N, Hans M. **1943**. A holoside extracted from the seeds of Plantago major L. and Plantago ovata Forsk. *Bull Mem Acad R Med Belg* **8**: 386–396.

Wood J, Tan H-T, Collins H, *et al.* 2018. Genetic and environmental factors contribute to variation in cell wall composition in mature desi chickpea (Cicer arietinum L .) cotyledons. *Plant Cell and Environment* **41**: 2195–2208.

Xing X, Hsieh YSY, Yap K, *et al.* 2017. Isolation and structural elucidation by 2D NMR of planteose, a major oligosaccharide in the mucilage of chia (Salvia hispanica L.) seeds. *Carbohydrate Polymers* **175**: 231–240.

Yang Q, Qi M, Tong R, *et al.* 2017. Plantago asiatica L. Seed extract improves lipid accumulation and hyperglycemia in high-fat diet-induced obese mice. *International Journal of Molecular Sciences* **18**.

Ye CL, Hu WL, Dai DH. **2011**. Extraction of polysaccharides and the antioxidant activity from the seeds of Plantago asiatica L. *International Journal of Biological Macromolecules* **49**: 466–470.

Yin J-Y, Chen H-H, Lin H-X, Xie M-Y, Nie S-P. **2016**. Structural Features of Alkaline Extracted Polysaccharide from the Seeds of Plantago asiatica L. and Its Rheological Properties. *Molecules* **21**: 1181.

Youngken H. **1950**. *Textbook of pharmacognosy*. Philadelphia: Blakiston.

Yu L, Yakubov GGE, Zeng W, *et al.* 2017. Multi-layer mucilage of Plantago ovata

seeds: Rheological differences arise from variations in arabinoxylan side chains. *Carbohydrate Polymers* **165**: 132–141.

Zhou P, Eid M, Xiong W, *et al.* 2020. Comparative study between cold and hot water extracted polysaccharides from Plantago ovata seed husk by using rheological methods. *Food Hydrocolloids* **101**: 105465.

Zhou Q, Lu W, Niu Y, *et al.* 2013. Identification and quantification of phytochemical composition and anti-inflammatory, cellular antioxidant, and radical scavenging activities of 12 Plantago species. *Journal of Agricultural and Food Chemistry* **61**: 6693–6702.

Ziemichód A, Wójcik M, Różyło R. **2018**. Seeds of Plantago psyllium and Plantago ovata: Mineral composition, grinding, and use for gluten-free bread as substitutes for hydrocolloids. *Journal of Food Process Engineering*: 1–9.

Zubair M, Nybom H, Lindholm C, Brandner JM, Rumpunen K. **2016**. Promotion of wound healing by Plantago major L. leaf extracts – ex-vivo experiments confirm experiences from traditional medicine. *Natural Product Research* **30**: 622–624.

CHAPTER 6

Interaction of *Plantago* flour polysaccharides with amylose alters rice flour/starch pasting and retrogradation, suggesting a new model for synergistic interaction

This chapter was written to the sounds of...	
Album	Kingdoms in Colour
Artist	Maribou State
Favourite Song	Glasshouses

Statement of Authorship

Title of Paper	Interaction of *Plantago* flour polysaccharides with amylose alters rice flour/starch pasting and retrogradation, suggesting a new model for synergistic interaction
Publication Status	☐ Published ☐ Accepted for Publication ☐ Submitted for Publication ☑ Unpublished and Unsubmitted w ork w ritten in manuscript style
Publication Details	

Principal Author

Name of Principal Author (Candidate)	James M. Cowley		
Contribution to the Paper	Conceived the study, performed experiments, analysed and interpreted data, wrote the manuscript		
Overall percentage (%)	90%		
Certification:	This paper reports on original research I conducted during the period of my Higher Degree by Research candidature and is not subject to any obligations or contractual agreements with a third party that would constrain its inclusion in this thesis. I am the primary author of this paper.		
Signature		Date	19/5/2020

Co-Author Contributions

By signing the Statement of Authorship, each author certifies that:

i. the candidate's stated contribution to the publication is accurate (as detailed above);
ii. permission is granted for the candidate in include the publication in the thesis; and
iii. the sum of all co-author contributions is equal to 100% less the candidate's stated contribution.

Name of Co-Author	Tim J. Foster		
Contribution to the Paper	Provided materials and equipment for the study, assisted in data interpretation and contributed to writing the manuscript		
Signature		Date	19/5/2020

Name of Co-Author	Rachel A. Burton		
Contribution to the Paper	Contributed to writing the manuscript		
Signature		Date	19/5/2020

Please cut and paste additional co-author panels here as required.

Title: Interaction of *Plantago* flour polysaccharides with amylose alters rice flour/starch pasting and retrogradation, suggesting a new model for synergistic interaction

Authors: James M. Cowley[1], Tim J. Foster[2] & Rachel A. Burton[1]

Authors' Affiliations: [1]School of Agriculture, Food and Wine, University of Adelaide, Waite Campus, Urrbrae, SA, Australia and [2]School of Biosciences, University of Nottingham, Sutton Bonington Campus, Loughborough, Leicestershire, UK

Abstract

The seed composition of *Plantago* species varies substantially as a result of natural variation but little is known about how this influences their potential functionality as hydrocolloid replacements. To investigate this, changes to the pasting properties of rice flour (RF) and rice starch (RS) upon the addition of whole seed flour (WSF) prepared from eight diverse *Plantago* species were studied. Common structural characteristics of mucilage polysaccharides from four Australian native *Plantago* species promoted RF and RS granule swelling and altered pasting temperature to a far greater extent than those from the commercial species, *P. ovata.* Enhanced granule swelling caused more extensive leaching of amylose which appeared to interact with *Plantago* WSF polysaccharides. The hastening of gelation during retrogradation, reduction in syneresis and changes in heat stability-related pasting parameters upon a novel high heat pasting treatment suggested that polysaccharides from Australian native *Plantago* species can interact with starch exudates and form strong, viscoelastic gels. This could be due to the creation of a modified coupled network for which a model has been proposed. Clustering by genetic relatedness revealed that the influences of *Plantago* WSF on the properties of RF and RS were strongly linked by genetic similarity and thus putatively shared polysaccharide motifs. The data presented here clearly show that WSF of a number of *Plantago* species can be used as hydrocolloid replacements and that natural variation in seed composition across this genus is an untapped resource for selectively manipulating the quality and properties of starch-based food systems.

Introduction

Starch granules are composed of a heterogeneous mixture of linear amylose and highly-branched amylopectin polymers (Debet & Gidley, 2007). When heated, starch granules absorb water, swell and exude their contents into solution producing a continuous phase of water and leached polymers and a dispersed phase of swollen starch granules (Song *et al.*, 2006). The transformation of starch granules into a continuous matrix (pasting) is the basis of the production of cooked starch-based foods, and this process differs significantly in response to cooking conditions, starch origin, granule structure, morphology and composition as well as the presence of non-starch molecules (Buléon *et al.*, 1998). Hydrocolloids are well-known to alter the pasting of starches and flours due to their unique functional properties (Bemiller, 2011). Hydrocolloids are often used to improve the quality of starchy products by creating structure, improving moisture retention, controlling water mobility, and retarding aging from retrogradation (Liu *et al.*, 2019) all of which can improve shelf-life, product texture and consumer acceptability. Variation in pasting properties of starch-hydrocolloid blends have been ascribed to hydrogen bonding between hydroxyl groups of the starch and hydrocolloid components (Song *et al.*, 2006), synergistic phase separation in starch-hydrocolloid mixtures and physical reinforcement of the starch matrix (Bemiller, 2011; Yuris *et al.*, 2017). In addition to manipulating starch system quality, hydrocolloid-related changes to the pasting properties of starch/flour may be demonstrative of some functional properties of the hydrocolloid itself.

Hydrocolloids sourced from plants are becoming increasingly important food structuring ingredients particularly when consumers choose to avoid “non-natural” ingredients like derivatised celluloses (Horstmann *et al.*, 2018). Seeds of many plants become surrounded by a viscous polysaccharide layer called mucilage when they

come into contact with water, in a process called myxospermy (Phan & Burton, 2018). In food technology, the most common hydrocolloid derived from a myxospermous species is psyllium gum, a complex heteroxylan produced by milling husk from the seeds of *Plantago ovata* (Madgulkar *et al.*, 2014). Psyllium gum has been proven to have excellent utility as a versatile food ingredient due to its water-holding and viscoelastic properties (Haque *et al.*, 1993; Haque & Morris, 1994; Mariotti *et al.*, 2009; Ahmadi *et al.*, 2012; Cappa *et al.*, 2013; Mancebo *et al.*, 2015; Fratelli *et al.*, 2018). The use of whole seed flour (WSF) prepared from myxospermous seeds has gained interest as replacements for hydrocolloids due to their ease of processing and additional nutritional benefits normally lost during hydrocolloid isolation. While the use of WSF for manipulating starch-based food systems is increasingly prevalent (Pruska-Kędzior *et al.*, 2008; Steffolani *et al.*, 2014; Kumar *et al.*, 2018), the use of psyllium WSF is only rarely and recently reported in the literature (Pejcz *et al.*, 2018; Ziemichód *et al.*, 2018).

Structural complexity of *P. ovata* mucilage polysaccharides directly influences their functional properties (Yu *et al.*, 2017, 2018b, 2019; Ren *et al.*, 2020d; Zhou *et al.*, 2020). Recent research has found that there is significant variation in the structure, complexity and content of mucilage from near relatives of *P. ovata*, especially those native to Australia (Phan *et al.*, 2016) (Cowley, Chapter 5). A structure-function relationship has not yet been made in these novel species and genetic divergence may have led to the synthesis of polysaccharides with novel properties that remain unexploited.

The objective of this study was to assess how the diversity in seed composition of eight *Plantago* species influences their potential functionality as hydrocolloid replacements

by studying the influence of their addition on the pasting profiles and properties of rice flour (RF) and rice starch (RS) and the syneresis of RF pastes.

Methods and materials

Materials

Rice flour was purchased from Doves Farms (United Kingdom) and rice starch (S7260) was purchased from Sigma-Aldrich (Germany). Seeds of eight *Plantago* species were grown to maturity as per Cowley, Chapter 5, to produce bulk seed. Seed was ground to flour using a MM400 Mixer Mill (Retsch, Germany) and graded to 0.5 mm. Flours were stored dry at room temperature.

Phylogeny

Nuclear ribosomal DNA (nrDNA) internal transcribed spacer (ITS) region sequences for the accessions studied here were as described in Cowley, Chapter 5. ITS sequences were trimmed using BMGE (Criscuolo & Gribaldo, 2010) and the maximum-likelihood tree constructed in Geneious v8.1.3 (Biomatters Ltd, NZ) with the RAxML tree builder (Stamatakis, 2006) using the GTR GAMMA nucleotide model with 500 rapid bootstrapping replicates.

Mucilage microscopy

Seed mucilage architecture was observed by whole mount microscopy in ruthenium red as per Cowley *et al.* (2020). After positioning seeds on a microscope slide (Rowe GM2715, Australia) staining solution (0.01% ruthenium red hydrate, #C075, ProSciTech, Australia) was added beneath a coverglass (ProSciTech No. 1, Australia) and images were captured on a dissecting microscope (Zeiss Stemi 2000-C, Germany) equipped with a colour digital camera (Zeiss AxioCam ERc 5s, Germany).

Total seed mucilage extraction and fractionation

Total mucilage was extracted using a step-wise fractionation protocol following Cowley *et al.* (2020). Briefly, 30 mg of whole, unmilled seed was extracted for 1.5 h with 1.5 ml of deionised water at 25 °C and 1300 rpm agitation using a ThermoMixer® Comfort (Eppendorf, Germany). The samples were centrifuged for 2 min at 13000 rpm and the supernatant removed (cold water-extractable, CWE). Tube volume was made up to 1.5 ml with water and the extraction repeated at 65 °C. Supernatant from this step was the hot water-extractable (HWE) fraction. Tube volume was made up to 1.5 ml with DI water and the samples agitated at 30 Hz for 10 min on a MM400 Mixer Mill (Retsch, Germany) with a 2 mL tube adapter. Tubes were centrifuged at 13000 rpm for 2 min and the supernatant removed. This supernatant was the intense agitation extractable (IAE) fraction. In this study, three mucilage fractions (CWE, HWE and IAE) were homogenised at 80 °C for 3 hours with periodic vortexing to produce a total seed mucilage extract. Total seed mucilage extracts were freeze-dried to a constant weight for further analysis.

Monosaccharide analysis

Monosaccharide profiles of fractionated mucilage (redispersed at 1 mg/ml in Milli-Q water) and milled whole seed flour were determined using reverse phase high performance liquid chromatography (RP-HPLC) of 1-phenyl-3-methyl-5-pyrazoline (PMP) derivatives following Hassan *et al.* (2017). Area under the peaks was compared to standard curves of mannose, ribose, rhamnose, glucuronic acid, galacturonic acid, glucose, galactose, xylose, arabinose and fucose.

Preparation of rice flour/*Plantago* flour suspensions

Fifty milligrams (2% addition) or 100 mg (4% addition) of *Plantago* flour was blended with 2.5 g of rice flour or rice starch. Twenty-four grams of deionised water was added to the mixture and homogenised briefly by vigorous stirring. Control samples lacking *Plantago* flour were prepared following the same protocol.

Measurement of pasting properties

Pasting properties of rice flour-*Plantago* flour and rice starch-*Plantago* flour blends were determined by Rapid Visco-Analysis using an RVA Super 4 (Newport Scientific, Australia) for standard temperature pasting (<100 °C) or RVA 4800 (Perten Instruments, Sweden) for high temperature (>100 °C) based on Diaz-Calderon *et al.* (2018) with modifications. Suspensions were prepared as above in the RVA canister applicable to the device being used (standard or high temperature). Samples were held at 25 °C for 2 min before heating to 95 °C (standard temperature) or 140 °C (high temperature) at 12 °C/min, holding at 95/140 °C for 2.5 min before cooling to 25 °C at 12 °C/min where they were held for a final 2 min. For the first minute, the suspension was homogenised at 960 RPM. The remainder of the test was performed under constant stirring at 160 RPM.

The pasting parameters extracted were: pasting temperature (the temperature at which viscosity rapidly increases as a result of starch granule swelling upon the uptake of water), peak viscosity (the maximum viscosity obtained during heating), trough viscosity (the minimum viscosity obtained during hold at maximum temperature), breakdown viscosity (difference between peak and trough viscosities), final viscosity (viscosity at completion of the run), and setback viscosity (difference between final and trough viscosities).

Difference plot of pasting parameter (PP) values were calculated with the following equation:

$$\text{Difference plot values} = (\text{PP of WSF sample @ 140 °C-PP of control @ 140 °C})\text{-}(\text{PP of WSF sample @ 95 °C-PP of control @ 95 °C})$$

Pasting properties were measured in triplicate.

Measurement of syneresis

The extent of syneresis was measured on rice flour/*Plantago* flour blends at the 4% addition level. Pastes were prepared as per the measurement of standard temperature pasting properties. Triplicate samples of 5 g were stored at 4 °C for 14 days and water separated from the gels was removed every two days and weighed. Syneresis was calculated as the ratio of mass of water removed to the mass of the stored paste.

Statistical analysis

Data were analysed using GenStat 15th Edition (VSNi, UK). Statistical differences, where indicated, were analysed by ANOVA using Tukey's HSD post-hoc test ($p < 0.05$). The neighbour-joining comparison in Figure 6.8 and correlation matrix in Supplementary Figure 6.1 were prepared in Past 3.26 (Hammer *et al.*, 2001) using *Plantago* WSF-containing samples only (control omitted).

Results & discussion

Interspecific variation in *Plantago* seed composition

Variation in architecture of the expanded seed mucilage of the *Plantago* species studied here is shown in Figure 6.1. Ruthenium red is used to stain acidic polysaccharides at the periphery of expanded seed mucilage and is often used as a

diagnostic screening technique to estimate mucilage production capacity (Western *et al.*, 2000; Phan *et al.*, 2016; Tucker *et al.*, 2017; Cowley *et al.*, 2020). Here we show similarities in seed mucilage architecture of Australian native species that are likely due to their genetic relatedness (Figure 6.1A) (Phan *et al.,* 2016, Cowley, Chapter 5), despite their distant and varied environmental origins (Figure 6.1B).

We previously investigated the seed composition of twelve *Plantago* species in detail which included the eight species/accessions studied here. We showed that, in agreement with previous work (Davison, 1982; Romero-Baranzini *et al.*, 2006; Mohamed *et al.*, 2011; Ziemichód *et al.*, 2018), Australian *Plantago* species are rich in protein and fats and have a substantial mannan-rich endosperm, and that a great deal of natural variation occurs in the composition and properties of the seed mucilage (Cowley, Chapter 5). We described the monosaccharide composition of mucilage fractions obtained (Cowley, Chapter 5) using a published fractionation method (Cowley, Chapter 3) (Cowley *et al.*, 2020) and discussed the potential implications for functionality. A summary of the fractionation profiles and arabinose to xylose ratio (AX ratios) of the species studied here from Cowley, Chapter 5 are summarised in Table 6.1 along with that of the total seed mucilage extract from these species. The total yield of mucilage varied between species studied here, where *P. lanceolata* had a particularly low yield (7.55% w/w) and *P. ovata* had the highest yield (23.84% w/w) at over three times higher. The remaining species had a minimum of 14.62% w/w mucilage with a mean yield of 17.75% w/w. *Plantago* species also have differences in mucilage extractability, represented by the ratio between yields under extraction conditions of differing harshness (Cowley, Chapter 5). Guo *et al.* (2008) described that psyllium gum was comprised of differentially-extractable fractions and Yu *et al.* (2017) attributed this to increasing substitution complexity and subsequent stronger intermolecular interactions. The composition of extracted seed mucilage fractions of

the *Plantago* species studied was investigated by monosaccharide profiling where it was confirmed that heteroxylan comprises the major polysaccharide in mucilage of all species. However, the average level of backbone substitution, estimated from the AX ratio in total extracted mucilage, varies substantially (Table 6.1). *P. ovata* had an AX ratio of 0.27:1, close to that reported previously (Guo *et al.*, 2008; Phan *et al.*, 2016; Yu *et al.*, 2017). The average AX ratio was lower in *P. major* (0.14:1) and *P. lanceolata* (0.15:1) but higher in *P. bellidioides* (0.28:1), *P. cunninghamii* (0.31:1), *P. turrifera* (0.36:1) and *P. debilis* (0.43:1). These data suggest that heteroxylan from these species are structurally different from one another and that those from *P. bellidioides, P. cunninghamii, P. turrifera* and *P. debilis* are more heavily substituted than *P. ovata*. These differences were further highlighted when the mucilage was differentially extracted which shows even greater variation in the AX ratio. This variation corroborates previous studies that show that heteroxylan substitution (AX Ratio) increases with resistance to extraction and has a strong influence on the functional properties of the mucilage (Guo *et al.*, 2008; Yu *et al.*, 2017; Cowley *et al.*, 2020; Ren *et al.*, 2020d), and by extension in the whole seed flour of which it is a fraction..

Pasting properties of rice flour and rice starch blended with *Plantago* WSF

A pre-dispersed suspension of *Plantago* flour at the equivalent 4% addition level and in the absence of rice flour (RF) or starch (RS) showed negligible changes in viscosity using the starch RVA analysis settings (Figure 6.2). Demucilaged WSF flour addition also caused negligible changes to the pasting profile (Figure 6.2) of RF confirming that the mucilage is the most functional component in these experiments (Figure 6.2). The effect of a 2% and 4% addition of whole seed flour (WSF) of eight *Plantago* species had significant and varied effects on the pasting profile of RF (Figure 6.3 and Table 6.2) and RS (Figure 6.4 and Table 6.3).

Pasting Temperature

No viscosity was detected in RF suspensions until after sustained heating, typical of a dilute starchy suspension (Tester & Morrison, 1990). Once the starch granules begin to swell, their effective volume is increased, and the paste viscosity increases markedly (pasting temperature). In this study, a temperature of 88.95 ºC was required for pasting to begin in RF and 91.55 °C for RS, similar to some previous findings (Wang *et al.*, 2000), though pasting temperature varies substantially between flours and starches according to factors like suspension concentration, particle size and amylose content (Ahmed & Thomas, 2017). The onset of pasting can also be advanced or retarded in various ways by the presence of hydrocolloids (Shi & BeMiller, 2002).

The influence of *Plantago* mucilage polysaccharides on the pasting of RF has been seldom studied and where present has been limited to the commercially available species, *P. ovata* (psyllium gum). Cappa *et al.* (2013) studied the influence of blends of psyllium and sugar beet fibres on the pasting of a commercial gluten-free bread mixture and found that blends with a larger psyllium proportion reduced the pasting temperature but the effect was slight (~2 °C). Mancebo *et al.* (2015) reported a similarly small effect when studying the effect of psyllium and hydroxypropylmethylcellulose on RF-based gluten free bread and dough qualities. We corroborate these findings as at the 2% addition level, WSF of *P. ovata* along with *P. lanceolata* and *P. major* did not significantly change the pasting temperature of rice flour and at the 4% addition level that change was significant but only slight (<2.5 ºC) (Table 6.2). By contrast, blends containing both 2% and 4% additions of WSF of *P. cunninghamii*, *P. turrifera*, *P. bellidioides* and *P. debilis* substantially decreased the temperature at which the suspension viscosity markedly increased (>12 °C) (Table 6.2). The effect of these WSFs on the pasting onset can be described as two-stage swelling where a smaller

peak or shoulder precedes the primary pasting peak. Since early amylography studies it has been observed that hydrocolloids enhance the initial swelling of starch granules (Crossland & Favor, 1948; Goering & Schuh, 1967). It has been found that starches and flours heated in suspensions containing hydrocolloids like carboxymethylcellulose, xanthan gum, guar gum, or locust bean gum swell rapidly and earlier in the heating period due to direct hydrocolloid-starch interactions. Bean and Yamazaki (Bean & Yamazaki, 1978) found that carboxymethylcellulose caused an increase in first-stage granule swelling. Christianson *et al.* (1981) concluded that the initial stages of granule swelling were magnified in media containing xanthan gum, as viscosity was much higher and thus more work was required to move slightly swollen starch granules past one another, later corroborated by Sullo and Foster (2010). In our samples, this effect is likely as the magnitude of first stage swelling is mostly dependent on the addition level of *Plantago* WSF (ergo viscosity), but the time of peak initiation time remains constant. Studies have also since concluded that many hydrocolloids can interact directly with small quantities of amylose leached during the initial stages of starch granule swelling, further enhancing and hastening the onset of pasting (Liu *et al.*, 2003; Díaz-Calderón *et al.*, 2018). We corroborate this finding as the effect was also seen when blending *Plantago* WSF with purified RS (Figure 6.4), and the magnitude of the effect correlated with *Plantago* species, with reduced RF pasting temperature (Figure 6.3) showing that this phenomenon was also at play. In RS, a purer and more easily influenced system, *P. ovata* did significantly reduce pasting temperature (~14°C) but the effect was substantially greater for the species *P. cunninghamii*, *P. turrifera*, *P. bellidioides* and *P. debilis* (~20 °C) (Table 6.3) echoing the same trend and influence seen on RF. Interestingly, while *P. coronopus* only slightly reduced the pasting temperature of RF compared to the four aforementioned species, the effect was substantially greater in RS, comparable to *P. cunninghamii* or *P. bellidioides.* We

suggest the two-stage pasting seen in RF, along with the significantly decreased pasting temperature in both RF and RS blends, with *P. cunninghamii*, *P. turrifera*, *P. bellidioides* and *P. debilis* WSF is synergistic based on two effects. We conclude that structural characteristics shared by seed mucilage of these species allow it to interact directly with small amounts of amylose leached during the first stages of granule swelling, thus hastening pasting (peak time is also reduced). This effect is further magnified by the excellent water holding abilities of the mucilage, viscosifying the continuous phase to a greater extent than other species and allowing normally undetectable first stages of granule swelling to become exponentially magnified.

Peak Viscosity

Plantago WSF significantly increased the peak viscosity of RF (Table 6.2) and RS (Table 6.3) to varying degrees. In RF blends containing *P. ovata*, *P. lanceolata* and *P. major*, the magnitude of the increase of peak viscosity is roughly proportional to the addition level (Figure 6.3), while for *P. coronopus, P. cunninghamii*, *P. turrifera*, *P. bellidioides* and *P. debilis*, the increase from the control is significant but there is little difference between addition levels (Table 6.2). However, in purified RS blends containing *Plantago* WSF the magnitude of peak viscosity increase was roughly proportional to the addition level in all species (Figure 6.4) suggesting that the purified RS is more easily influenced. It is possible that non-starch polysaccharides are still present in RF leading to generally more substantial changes in purified RS. *P. lanceolata* had minimal effect on either material increasing peak viscosity by 7.4% at most (4% addition to RS).

For RF, the 4% addition of *P. major* WSF caused the greatest increase in peak viscosity (32% increase from control). For RS, *P. major* also caused a significant increase in peak viscosity (25% increase) but much greater effects were seen with

Australian native *Plantago* species on RS than RF. *P. debilis* caused the greatest increase in peak viscosity of RS at the 4% addition level (36% increase) with *P. cunninghamii, P. turrifera* and *P. bellidioides* causing ~30% increases. Increases in peak viscosity of starches in the presence of various hydrocolloids are consistently reported (Christianson *et al.*, 1981; Bahnassey & Breene, 1994; Liu *et al.*, 2003; Song *et al.*, 2006; Mudgil *et al.*, 2016; Díaz-Calderón *et al.*, 2018). The peak viscosity of starchy gluten-free bread mixtures blended with psyllium and sugar beet fibre were found to be higher in blends favouring psyllium (Cappa *et al.*, 2013). Similar but less significant effects were reported later when studying psyllium only (Mancebo *et al.*, 2015). Cappa *et al.* (2013) and Mancebo *et al.* (2015) attributed pasting viscosity changes of *P. ovata* mucilage (psyllium gum) to its strong water-binding capacity. Christianson *et al.* (1981) explained that hydrocolloids with strong water-binding (like psyllium) could thicken the suspension and enhance the forces exerted on the starch granules, increasing the paste viscosity. Sullo and Foster (2010) concluded that the behaviour of starch-hydrocolloid blends was not only dependent on the behaviour and viscosity of the starch and hydrocolloid separately, but also how they interact with one another. The water-holding capacity of the *Plantago* WSF polysaccharides will probably increase the effective concentration of starch granules and also promote starch-starch interactions (Sullo & Foster, 2010). However, this effect does not exclude others and it is likely that a composite effect is at play where both starch-starch and starch-hydrocolloid interactions contribute. It is known that interactions between hydrocolloids and granule-exuded amylose could hasten total amylose release and synergistically lead to a marked viscosity increase (Christianson *et al.*, 1981; Rojas *et al.*, 1999; Lai & Liao, 2002; Freitas *et al.*, 2003). Liu *et al.* (2003) corroborated similar effects but also reported that yellow mustard mucilage-amylose interactions simultaneously delayed peak viscosity by restricting granule swelling. It was also

reported that peak time can be delayed by the addition of xanthan gum (Weber *et al.*, 2009) and pullulan (Sheng *et al.*, 2018) as it physically restricted granule swelling. In our study we did not observe low pasting temperatures with delayed peak viscosity in RF or RS as was reported earlier. In fact, at the 4% addition level, peak time was advanced with most *Plantago* species (Figure 6.4) suggesting that the hastening of amylose leaching outweighed any granule swelling inhibition effect. We suggest that in addition to synergistic phase separation, the stimulation of granule swelling seen in the reduced pasting temperature and peak time of RF and RS is leading to more amylose being mobilised from the granule and increasing the peak viscosity.

Trough and Breakdown Viscosity

After peak viscosity is obtained, paste viscosity decreases due to the thixotropic behaviour of polymers aligning under shear stress (Fitzgerald *et al.*, 2003). The minimum viscosity reached and the difference between this value and the peak viscosity are important indicators of the resistance of starchy networks to disintegration (Sun *et al.*, 2014). In all RF and RS samples, trough viscosity was increased relatively linearly with addition level while a larger range of effects was seen in breakdown viscosities (Table 6.2 and Table 6.3). The breakdown viscosity was lowest in RF and RS samples containing *P. cunninghamii* (Table 6.2 and Table 6.3, respectively) indicating that these samples resisted disintegration and thixotropic viscosity loss (Heyman *et al.*, 2014). Interestingly, *Plantago* species closely related to *P. cunninghamii* did not have the same effect and generally breakdown viscosity was substantially higher in these samples. We suggest that this is related to the hastened granule breakdown reducing the presence of granule ghosts that remain ungelatinized and occupy volume in the suspension (Debet & Gidley, 2007; Yuris *et al.*, 2017). As

there is probably a proportional shift of granules to amylose released, samples with more amylose are more susceptible to thixotropic breakdown.

Final and Setback Viscosity

Final and setback viscosity describe retrogradation and associated gelation behaviour and are often used to describe the firmness and structure formation of cooked starches as they cool (Fitzgerald *et al.*, 2003). A large suite of changes to the retrogradation and gelation behaviour of RF and RS upon the addition of *Plantago* WSF can be seen in Figure 6.3 and Figure 6.4, respectively. *P. lanceolata* had no significant effect on the final or setback viscosities of either material. For RF samples containing *P. ovata* and *P. major* WSF, increases in the final and setback viscosities were roughly proportional to the addition level. For RS blends, this effect was only carried across in *P. major* samples as *P. ovata* WSF showed significantly less impact on the pasting of RS compared to RF. When blended with both RF and RS, the remaining *Plantago* species displayed significant but reproducible noise during the final stages of cooling (<40 °C) obscuring the true values of final and setback viscosities. However, noise at this time is explained by gelation occurring. Under the shear stress of the RVA paddle, the newly formed gel breaks and reforms continuously leading to the significant variation in paddle torque obscuring the true viscosity (Lai *et al.*, 2000). This effect has previously been seen when non-starch polysaccharides (mostly wheat arabinoxylan) were added to wheat starch (Sasaki *et al.*, 2000) and high concentrations of psyllium gum were added to maize starch (Belorio *et al.*, 2020). It was concluded that the highly swollen, extensively leached starch granules occupied a greater volume in these samples and concentrated the non-starch polysaccharides and leached exudates leading to greater intermolecular interactions which affected the viscoelasticity of the composite paste and led to gelation, also seen by Bahnassey and Breene (1994). Here, the extent and

intensity of noise during retrogradation of RF, and thus the extent of gelation, is both addition level and species dependent with similar trends seen for RS. There appears to be a connection between breakdown viscosity and the extent of gelation. *P. cunninghamii* samples showed breakdown resistance while other Australian natives were less resistant and likely enhanced the leaching of amylose into the continuous phase. It is likely that amylose leached from swollen granules by interaction with *Plantago* WSF polysaccharides (indicated by decreased pasting temperature, decreased peak time and increased peak viscosity) and changes to granule disintegration (shown by large breakdown values) lead to more molecules available to interact as the paste cooled (Weber *et al.*, 2009). Hastened gelation has been found to be a function of increased amylose in the continuous phase leading to more synergistic amylose-amylose and hydrocolloid-amylose interactions (Huang *et al.*, 2007). A similar compounding effect has been reported between extensively leached amylose and increasing concentrations of a complex polysaccharide from *Mesona chinensis* (Yuris *et al.*, 2017). The polysaccharide was reported to interact with exuded but granule-bound amylose molecules and form a dense three-dimensional interlinked network between the polysaccharide, amylose and granules. These concentration-dependent strong gels are consistent with those generated during the retrogradation phase in the presence of Australian native *Plantago* WSF. Compared with changes to the peak, trough and breakdown viscosities of RF and RS upon the addition of *P. cunninghamii, P. turrifera, P. bellidioides and P. debilis* WSF, changes to the retrograding paste properties were substantial. BeMiller (2011) explained that the stronger influence on final and setback viscosities is due to entropic changes in the polymers of the continuous phase which form exponentially more and more interactions until a threshold passes and gelation rapidly occurs (Yuris *et al.*, 2017).

Another possible mechanism for the significant change in viscoelastic properties in these samples is temperature-dependent phase separation. It has previously been reported that hydrocolloid-starch systems can phase separate in a temperature-dependent manner and lead to hastened gelation (Kim & Yoo, 2006; Ptaszek & Grzesik, 2007). We suggest that this effect is also a possibility and that strong gel network formation and separated phases may be operating synergistically.

Atypical peak in *P. ovata*

An atypical peak appears consistently in samples (~85 °C) containing *P. ovata* WSF during cooling within the trough viscosity region prior to retrogradation (Figure 6.3). In a review of the literature, analysis of pasting properties of starch-psyllium blends are rare (Habilla *et al.*, 2011; Cappa *et al.*, 2013; Mancebo *et al.*, 2015; Belorio *et al.*, 2020), with very few published RVA profiles, but Cappa *et al.* (2013) and Ren *et al.* (2020a,c) presented RVA profiles of psyllium husk-containing gluten-free formulations that exhibited the same atypical peak at roughly the same temperature (~85 °C). Additional peaks or ‘bumps’ have been reported previously where leached amylose aligns into lipid-associated crystalline helices that melted near 80 °C, exposing hydroxyl groups which immobilise free water, increase the effective concentration of the hydrocolloid and lead to a spike in viscosity. As the temperature dropped, the helices could not be maintained, the amylose reverted to random-coil formulation, and the viscosity spike diminished (Xu *et al.*, 1992). Some hydrocolloids influence or enhance this phenomenon (Rojas *et al.*, 1999). We found high concentration blends of purified RS and purified psyllium gum (both with minimal lipid content) could still produce the atypical peak (data not shown) so we suggest that in place of, or in addition to, an amylose-lipid complex, a transient amylose-psyllium gum complex is forming. It is possible that within this temperature range both amylose and psyllium polysaccharides

become only temporarily compatible. This phenomenon is not seen in WSF of any other *Plantago* species suggesting that psyllium is unique. It is also possible that the psyllium polysaccharide alone transiently adopts a different helical conformation with more exposed hydroxyl groups that only occurs at that temperature and so briefly changes the viscosity. As the temperature changes that conformation may return to the original form, returning the RVA profile to the expected shape.

Standard vs High Temperature Pasting Parameters.

Until recently, pasting studies have been temperature-limited to around 95 ºC to avoid artefacts as the temperature approaches boiling. There is an industrial need to assess the performance of starches at higher temperatures to determine their functionality under high temperature processing and how additives can influence this. Recently a new type of viscometer was released, RVA 4800, which is fitted with a sealed, self-pressurizing (~100 psi) module that allows pasting properties to be measured up to 140 ºC without boiling (Perten Instruments, 2018).

In the RF sample studied, pasting temperature and peak viscosity was similar between samples pasted to 95 °C or 140 °C as these parameters occur below 95°C and slight differences observed were attributed to sensitivity differences between devices used (Figure 6.5). The factors that differed significantly between heating ranges were the trough viscosity, breakdown viscosity and final viscosity which occur during continued heating. The trough viscosity was significantly reduced in RF heated to 140 °C (1252 cP), attributed to thixotropic breakdown of the starch network and possibly some thermal degradation (Liu *et al.*, 2019). Due to starch comprising most of the suspension, the trough viscosities were similarly reduced in samples containing *Plantago* WSF (Figure 6.5). The behaviours of *Plantago* WSF-containing suspensions

at high heat are therefore presented as differences (Figure 6.6) between the influence on RF pasted to 95 °C and RF pasted to 140 °C (for methods for calculation)

The difference in trough viscosity upon high heat was substantial in samples containing *P. coronopus*, *P. ovata* and *P. major* (Figure 6.6). In these samples, the trough viscosity was not significantly increased from the control at 140 °C upon the addition of either level of WSF indicating minimal improvements to granule or network heat stability. By contrast, the trough viscosity increases from the control in *P. cunninghamii, P. turrifera, P. bellidioides* and *P. debilis* formulations pasted to 140 °C was similar to when pasted to 95 °C (Figure 6.6). After standard temperature pasting (<95 °C), starch granules generally persist in dispersion as a swollen, hydrated shell called a granule 'ghost'. The viscosity of starch suspensions after exudation is due partly to the effective volume that these granule ghosts occupy within the dispersion (Hongsprabhas *et al.*, 2007). Debet and Gidley (Debet & Gidley, 2007) reported that the integrity of granule ghosts correlated with amylose content and thus the retention of amylose within or on the granule has often been associated with structural reinforcement, significantly reducing disintegration under shear stress (Biliaderis *et al.*, 1997; Aguirre-Cruz *et al.*, 2005). The same could be said of granule stability under high heat (> 130°C), which generally causes total granule disintegration from the melting of amylose double-helices (Debet & Gidley, 2007; Zhang *et al.*, 2020). We suggest that total granule disintegration has occurred in all samples (due to heat, shear and advanced swelling) but thermostable three-dimensional gel networks may be present in the Australian *Plantago* WSF-containing samples maintaining some structure and/or viscosity at such high heat. Further evidence for this is that after pasting to 140 °C, these samples maintained high final viscosity (Figure 6.5) and evidence of gelation (though much reduced from samples pasted to 95 °C) (Figure 6.5) while *P. major* addition appeared to not be thermoreversible as final viscosity in either addition level was not significantly

increased from the control (Figure 6.5). These data indicate that in samples containing *P. cunninghamii, P. turrifera, P. bellidioides* and *P. debilis,* the strong viscoelastic gel networks (seen as noise during retrogradation) are thermoreversible and the polysaccharides themselves are conformationally thermostable.

Syneresis of rice flour gels

The effects of a 4% addition of *Plantago* WSF on the structuring and storage stability of RF pastes was estimated through syneresis over a 14 day storage period (Figure 6.7). By storage day 4, measurable quantities of water had been ejected through syneresis in the control, *P. coronopus, P. lanceolata,* and *P. ovata* pastes while remaining samples did not begin syneresis until day 6. Rates and magnitude of syneresis diverged substantially during storage where by day 14 of storage, RF had lost substantially more mass through syneresis than samples containing *Plantago* WSF (Figure 6.7B). Samples containing *P. coronopus and P. lanceolata* reduced syneresis by ~25%, *P. ovata* by ~40% and the remaining samples an average of 50%. The samples with the lowest syneretic mass loss (~50%) were also those with a two-day onset delay. The presence of a network in these same samples means that the polysaccharides might have the ability to outcompete amylose resulting in fewer amylose-amylose interactions in favour of amylose-hydrocolloid interactions (Sudhakar *et al.*, 1996; Liu *et al.*, 2003). Fewer amylose-amylose interactions retards retrogradation improving product stability (Charoenrein *et al.*, 2011). It is likely that the interactions between amylose and *Plantago* WSF polysaccharides seen in changes in the pasting profile of RF (Figure 6.3) are delaying the onset and reducing the magnitude of syneresis by creating phase continuity through a continuous network that resists the settling of particles and thus the migration of water to the surface of the gel. Higher viscosity and higher water-holding capacity will also further reduce mass lost

through syneresis (Lee *et al.*, 2002). This effect is also likely in samples containing *Plantago* WSF which have strong water-holding and viscosifying abilities.

Proposal for a new synergistic interaction model

Mucilage polysaccharides and differences in their composition and content contribute to most, if not all, of the changes to the behaviour of RF and RS reported here. As demucilaged WSF and low mucilage-content *P. lanceolata* WSF led to minimal changes to all parameters tested, we confirm that mucilage polysaccharides in *Plantago* WSF are the functional component that alters the pasting properties of RF and RS. The remaining species had comparable yields of mucilage that were differentially extractable, likely as a result of structure-related intermolecular interactivities. Comparing the properties of *P. ovata* and *P. turrifera* or *P. major* and *P. debilis* (pairs with comparable mucilage content but different AX ratios) we suggest that substitution differences allow polysaccharides from Australian *Plantago* to form different synergistic interactions with starch exudates and/or other *Plantago* polysaccharides. When changes to the pasting properties seen in this study are presented in heat map form and clustered by genetic relatedness, we can hypothesise that the differences are a result of variation in polysaccharide structure (Figure 6.8). It is therefore likely that structural features shared between polysaccharides of Australian native *Plantago* species allow similar interactions with starch exudates during cooking. However, in this study we could not statistically correlate AX ratio with the properties described herein (Supplementary Figure 6.1) suggesting that structural influences are more complicated than can be represented simply by AX ratio and/or substitution complexity alone.

Yu *et al.* (2017; 2018; 2019) defined *Plantago ovata* heteroxylan interactions as ‘mucin-like’ where comb-like sidechain substitutions could interconnect to form gel-like

networks where the traditional backbone-backbone junction zone model of gelation (Burey *et al.*, 2008) was not possible due to extensive substitution. We now build on this hypothesis and suggest that heteroxylans from varied *Plantago* sources are indeed highly substituted but have 'blocky' backbone substitution patterns with regions of high complexity unpatterned substitutions and regions of regularly patterned backbone. Blocky polymer structure has been identified in a number of polymer types and evidence shows that this has a strong influence on intermolecular associations and related functional properties (Abbaszadeh *et al.*, 2014; Kool *et al.*, 2014). In galactomannans with blocky structures, regions of bare backbone were concluded to interact directly with the helix of algal polymers in binary mixtures (Cairns *et al.*, 1987) and form synergistic coupled networks. Similarly, differentially-extractable fractions of locust bean gum (a galactomannan) were found to have a variably blocky structure that allows them to form correspondingly variable backbone-backbone interactions with helical xanthan (Lundin & Hermansson, 1995). These models have generally defined 'blocks' of unsubstituted backbone as, logically, being essential to forming these heterotypic backbone-backbone interactions. However, recent evidence has now shown that plant polysaccharides like galactoglucomannan and glucuronoxylan are able to interact with helical cellulose polymers despite the interactive region of backbone not necessarily being unsubstituted (Busse-Wicher *et al.*, 2016; Grantham *et al.*, 2017; Yu *et al.*, 2018a). Instead, dedicated regions of backbone with regular substitution patterns are able to adopt a two-fold screw conformation, where all backbone substitutions were located in the same plane exposing the backbone to form backbone-backbone interactions. The same hypothesis regarding backbone-backbone interactions in the presence of high substitution had also been arrived at independently (Morris *et al.*, 1981). Morris *et al.*'s 'hyperentanglement' model describes the same polymer interaction and was also supported when evidence of

these associations were found in highly substituted galactomannans including fenugreek gum which is almost entirely substituted (Goycoolea *et al.*, 1995; Doyle *et al.*, 2009). Importantly, recent microscopic and rheological evidence has now been reported that supports the homotypic interactions between highly-substituted *P. ovata* heteroxylan fractions (Ren *et al.*, 2020d) and also heterotypic interactions between *P. ovata* heteroxylan and fibrillated cellulose (Ren *et al.*, 2020b), presenting an opportunity to speculate on the existence of, as discussed by the authors, similar fold-dependent backbone-backbone associations in highly-substituted heteroxylan-type polymers.

Combining our data, recent findings from Ren *et al.* (2020b,d), and these models we now hypothesise that *Plantago* mucilage heteroxylans contain backbone regions that are helix-compatible and helix-incompatible. Compatible regions could form heterotypic coupled network interactions with amylose polymers while incompatible regions with high substitution are free to form the mucin-like homotypic interactions with helix-incompatible regions of other *Plantago* mucilage heteroxylans and/or possibly heterotypic interactions with similarly complex polymers like amylopectin. This interaction is proposed to be a modified version of the coupled network model defined by Cairns *et al.* (1987) (Figure 6.9D) and this new model is presented in Figure 6.9E. The complex substitutions within the helix-incompatible regions is still hypothesised to form the mucin-like interactions described by Yu *et al.* (2017; 2018; 2019) and the changes to the pasting onset and viscoelastic properties of the gels formed during retrogradation are a direct result of these complex synergistic interactions. We suggest that these interactions would neatly explain all the changes to the pasting properties observed. Interaction with amylose during initial granule swelling acts to advance granule leaching reducing the pasting temperature and altering the peak, trough and breakdown viscosities. After total granule leaching is achieved more amylose is

available to interact with *Plantago* mucilage heteroxylan which is then able to form further interactions (the nature of which are dependent on the complexity and/or regularity of substitutions) leading to the modified coupled networks which have different viscoelastic properties during retrogradation. The modified coupled networks have some heat resistance, resulting in minimal changes to trough, breakdown and final viscosities upon a novel high heat treatment (highlighting their potential in high-temperature processing like retorting, jet cooking or extrusion). Finally, the substantial reduction in syneresis of RF gels suggests phase continuity in the modified coupled network, resisting separation and water loss during storage.

Conclusions and Future Directions

We conclude that natural variation in the composition of mucilage-containing seeds of *Plantago* species was sufficient to cause a suite of changes to the pasting of RF and RS. We present a hypothesis that the properties described here are a result of *Plantago* mucilage polysaccharides forming heterotypic interactions with amylose helices in ways similar to other polymers (Cairns *et al.*, 1987; Lundin & Hermansson, 1995; Grantham *et al.*, 2017; Yu *et al.*, 2018a; Ren *et al.*, 2020b), in tandem with homotypic interactions with other *Plantago* mucilage polysaccharides. The recent evidence of polysaccharide-helical polymer associations makes this hypothesis highly compelling and such combinations of heterotypic and homotypic associations may have important practical implications for effective network formation in binary systems (Foster, 1992; Díaz-Calderón *et al.*, 2018). The hypothesis will be probed further in future publications by employing microscopy of pasted mixtures to assess starch granule morphology changes and the contribution of phase separation, as well as more explicit structural and functional characterisation of WSF polysaccharides, perhaps through discrete fractionation techniques which have yielded great insight for *P. ovata*

(Yu *et al.*, 2017; Ren *et al.*, 2020d). Additionally, we highlight the utility of whole seed flour of myxospermous species as hydrocolloid replacements and show that they may be an untapped resource for selectively manipulating and altering the properties of starch-based food systems. We prove that by scrutinising relatives of a commercially-relevant species like *P. ovata,* an orphan crop plagued by agronomic constraints, we can identify species adapted to grow in harsh Australian conditions that also have significant functional food crop potential.

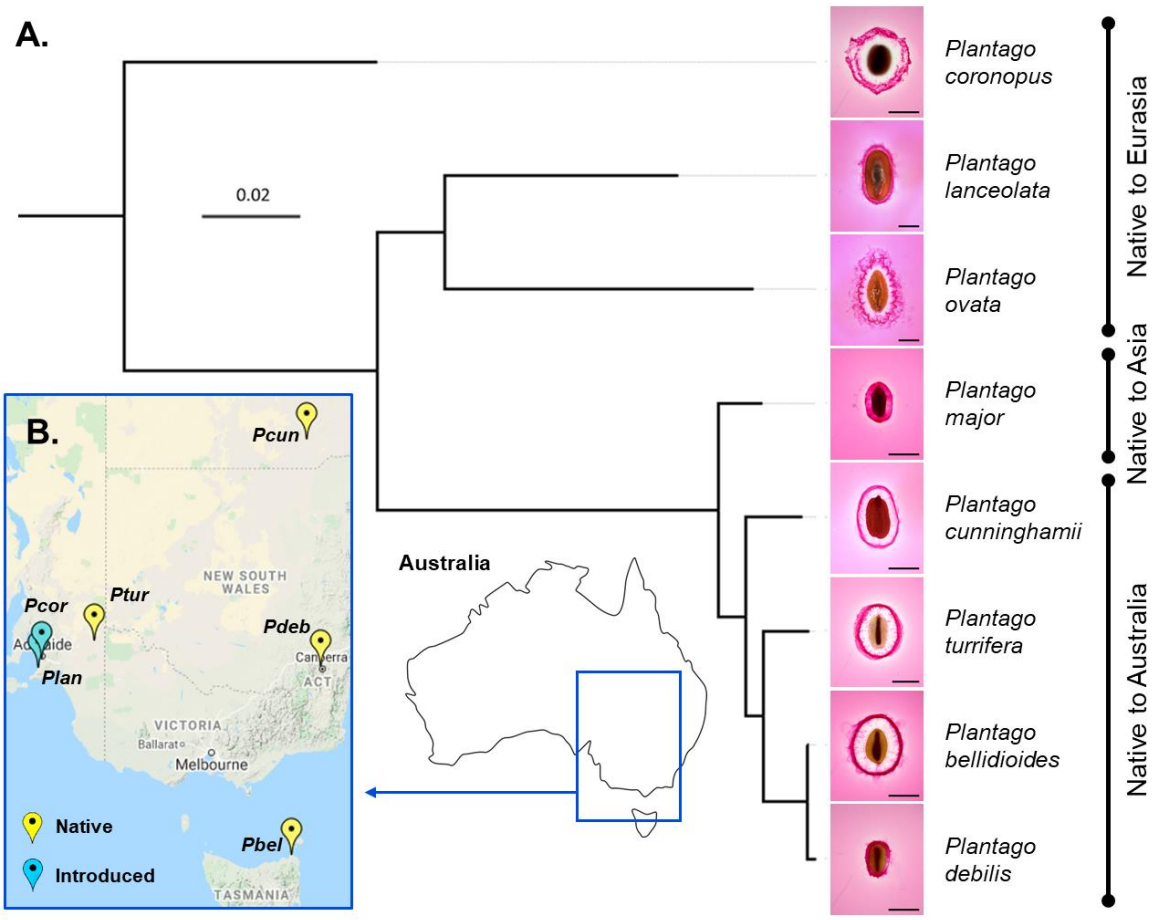

Figure 6.1. A. Maximum-likelihood tree of internal transcribed spacer regions estimating genetic relatedness of *Plantago* species studied. Trends in expanded mucilage architecture as seen with ruthenium red staining correspond to genetic relatedness. Ruthenium red scale = 1 mm. **B.** Geographic origin of Australian *Plantago* species studied here. *P. ovata* is not known to occur in Australia. While naturalised in many places in Eastern Australia, the *P. major* sample studied here was commercially sourced. Map sourced from Google Earth earth.google.com/web

Abbreviations: *Pcor = P. coronopus, Plan = P. lanceolata, Pcun = P. cunninghamii, Ptur = P. turrifera, Pbel = P. bellidioides, Pdeb = P. debilis.*

Table 6.1. Yield and arabinose to xylose (AX) ratio of fractionated and total mucilage extracts from eight *Plantago* species.

CWE = cold water extractable; HWE = hot water extractable; IAE = intense agitation extractable

	CWE Fraction[a]		HWE Fraction[a]		IAE Fraction[a]		Total	
Species	**Yield (%)**	**AX Ratio**	**Yield (%)**	**AX Ratio**	**Yield (%)**	**AX Ratio**	**Yield (%)[a]**	**AX Ratio**
P. coronopus	5.34	0.31	6.94	0.57	4.13	0.68	16.41	0.53
P. lanceolata	4.07	0.06	1.32	0.10	2.16	0.28	7.55	0.15
P. ovata	7.40	0.22	6.26	0.28	10.18	0.36	23.84	0.27
P. major	1.14	0.12	5.02	0.18	8.46	0.12	14.62	0.14
P. cunninghamii	3.27	0.04	9.64	0.23	6.61	0.52	19.52	0.31
P. turrifera	2.96	0.08	6.46	0.29	8.60	0.50	18.02	0.36
P. bellidioides	2.62	0.18	5.80	0.22	8.77	0.43	17.19	0.28
P. debilis	1.51	0.21	4.92	0.10	8.19	0.66	14.62	0.43

[a]Yield and monosaccharide data for fractionated mucilage (CWE, HWE, and IAE) and yield data for total mucilage was obtained previously in Cowley, Chapter 5

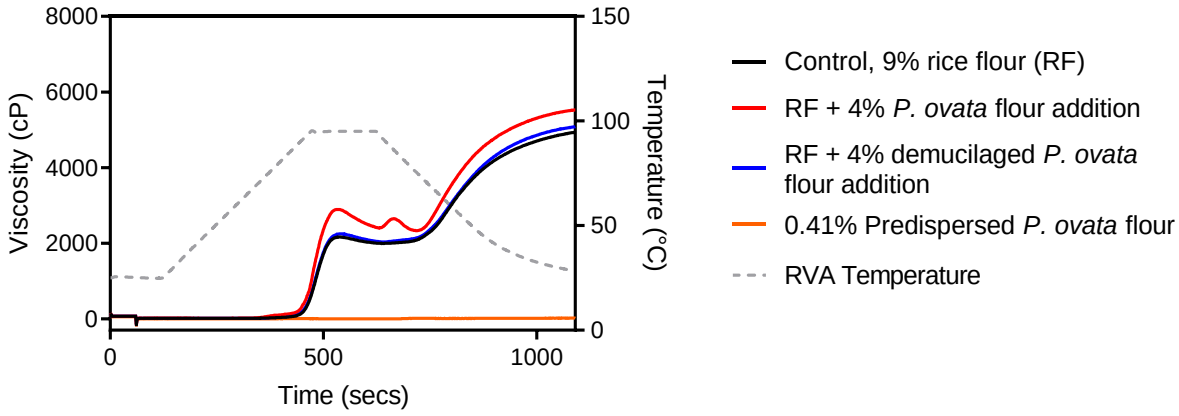

Figure 6.2. RVA (Rapid Visco Analyser) profiles of 9% rice flour (RF) suspension (black line), 9% rice flour + 4% *P. ovata* flour addition suspension (red line), 9% rice flour + 4% demucilaged *P. ovata* flour addition suspension (blue line) and 0.41% (equivalent to a 4% addition) *P. ovata* suspension (orange line).

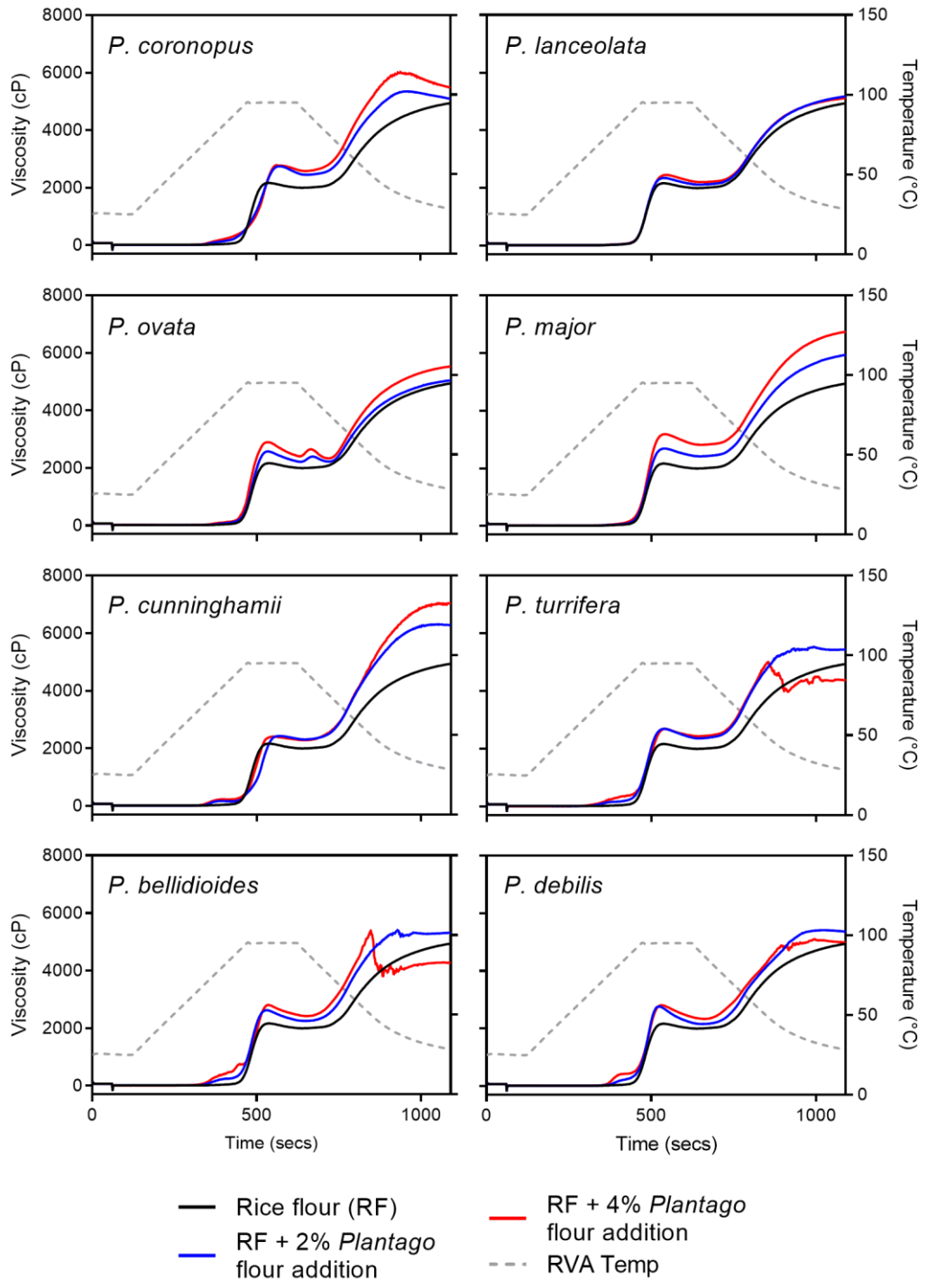

Figure 6.3. Changes in the RVA (Rapid Visco Analyser) profile of rice flour upon the addition of WSF from eight *Plantago* species at 2% or 4% addition levels.

Table 6.2 Pasting properties of rice flour upon a 2% or 4% addition of flour from eight *Plantago* species. Values are means ± SD

2% Sample Addition

Pasting Parameter	Control (Rice Flour)	*P. coronopus*	*P. lanceolata*	*P. ovata*	*P. major*	*P. cunninghamii*	*P. turrifera*	*P. bellidioides*	*P. debilis*
Pasting Temperature (°C)	88.95 ± 0.31^{d}	86.07 ± 0.83^{c}	88.5 ± 0.28^{d}	88.0 ± 0.69^{d}	87.68 ± 0.16^{d}	70.50 ± 0.48^{a}	70.25 ± 0.87^{a}	70.68 ± 1.01^{a}	76.87 ± 0.30^{b}
Peak Viscosity (cP)	2166 ± 6^{a}	2747 ± 53^{f}	2257 ± 54^{b}	2576 ± 40^{d}	2687 ± 10^{ef}	2433 ± 18^{c}	2692 ± 16^{ef}	2625 ± 15de	2761 ± 2^{f}
Trough Viscosity (cP)	1969 ± 12^{a}	2446 ± 46^{e}	2030 ± 45^{a}	2211 ± 42^{bc}	2382 ± 23de	2306 ± 31^{cd}	2356 ± 57de	2252 ± 11^{bc}	2153 ± 10^{b}
Breakdown Viscosity (cP)	196 ± 17^{ab}	301 ± 95^{bcd}	246 ± 20^{bc}	367 ± 32^{d}	306 ± 15^{bcd}	127 ± 14^{a}	335 ± 62^{cd}	374 ± 5^{d}	608 ± 9^{e}
Final Viscosity (cP)	4937 ± 99^{a}	5091 ± 147^{abc}	5178 ± 111^{abcd}	5044 ± 26^{ab}	5933 ± 108^{e}	6272 ± 78^{f}	5437 ± 123^{d}	5289 ± 93^{bcd}	5359 ± 100^{cd}
Setback Viscosity (cP)	2967 ± 91^{bc}	2644 ± 153^{a}	3076 ± 96^{bc}	2835 ± 62^{ab}	3551 ± 112^{d}	3966 ± 108^{e}	3080 ± 72^{bc}	3037 ± 104^{bc}	3206 ± 90^{c}

4% Sample Addition

Pasting Parameter	Control (Rice Flour)	*P. coronopus*	*P. lanceolata*	*P. ovata*	*P. major*	*P. cunninghamii*	*P. turrifera*	*P. bellidioides*	*P. debilis*
Pasting Temperature (°C)	88.95 ± 0.31^{e}	84.97 ± 0.36^{c}	88.53 ± 0.08^{e}	87.15 ± 0.53^{d}	86.47 ± 0.32^{d}	69.07 ± 0.45^{a}	69.95 ± 0.33^{a}	69.20 ± 0.13^{a}	73.57 ± 0.19^{b}
Peak Viscosity (cP)	2166 ± 6^{a}	2792 ± 25^{cd}	2303 ± 13^{b}	2898 ± 44^{d}	3186 ± 78^{e}	2412 ± 50^{b}	2688 ± 38^{c}	2809 ± 24^{cd}	2807 ± 80^{cd}
Trough Viscosity (cP)	1969 ± 12^{a}	2574 ± 16^{e}	2044 ± 11^{a}	2404 ± 30^{cd}	2782 ± 44^{f}	2281 ± 32^{b}	2432 ± 45^{d}	2420 ± 31^{cd}	2333 ± 49^{bc}
Breakdown Viscosity (cP)	196 ± 17^{ab}	231 ± 14^{b}	348 ± 39^{c}	565 ± 26^{e}	404 ± 35^{c}	131 ± 25^{a}	266 ± 12^{b}	389 ± 8^{c}	476 ± 30^{d}
Final Viscosity (cP)	4937 ± 99^{b}	5480 ± 25^{c}	5112 ± 55^{b}	5525 ± 59^{c}	6736 ± 86^{d}	7025 ± 147^{e}	4356 ± 66^{a†}	4273 ± 66^{a†}	4986 ± 70^{b†}
Setback Viscosity (cP)	2967 ± 91^{c}	2906 ± 40^{c}	3005 ± 49^{c}	3192 ± 44^{d}	3953 ± 43^{e}	4744 ± 115^{f}	1947 ± 15^{a†}	1853 ± 52^{a†}	2654 ± 21^{b†}

Different letters indicate a significant difference ($p < 0.05$) between parameters in a row. † refers to values that are inaccurate to the true value due to gelation-related noise during retrogradation.

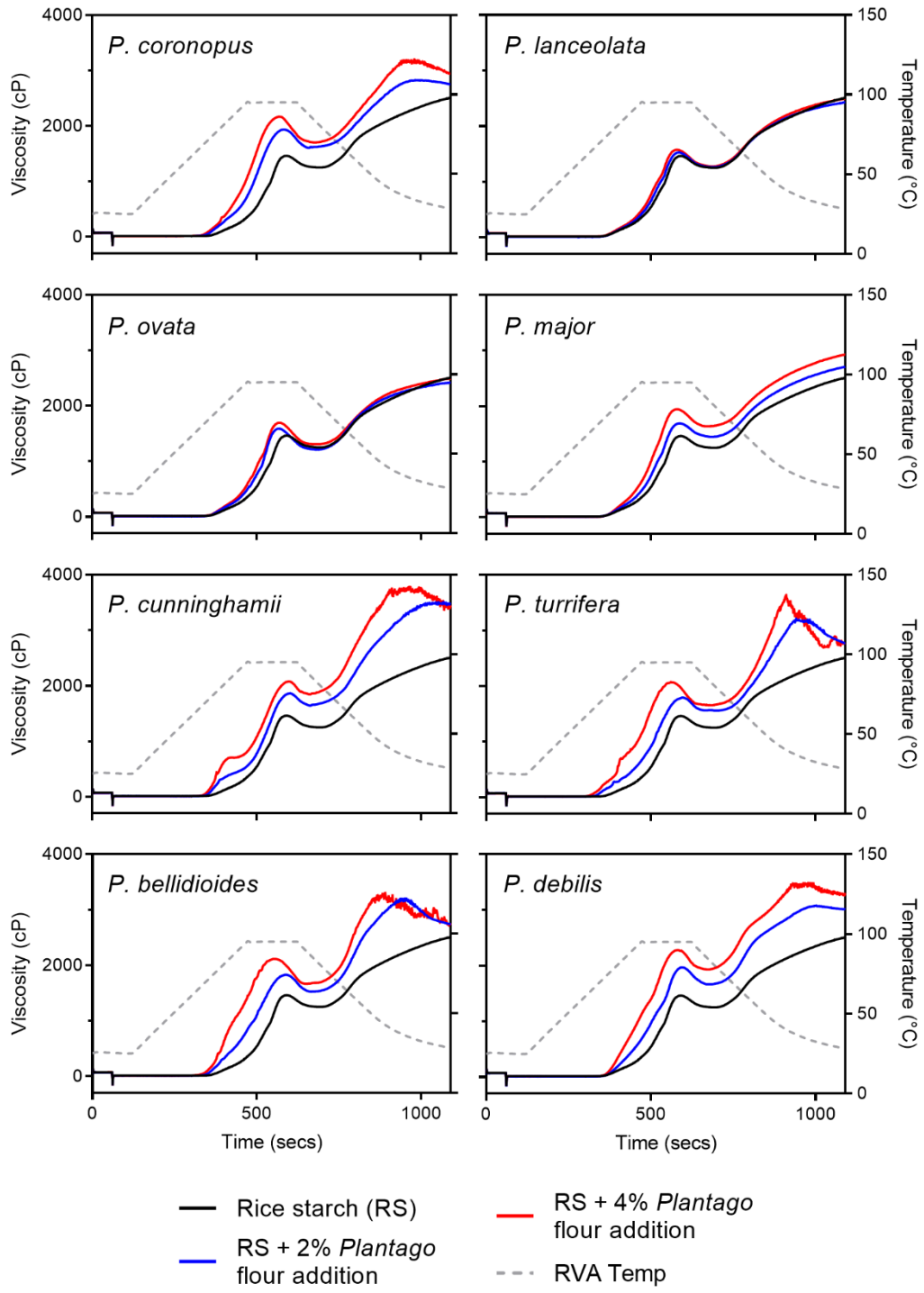

Figure 6.4. Changes in the RVA (Rapid Visco Analyser) profile of rice starch upon the addition of WSF from eight *Plantago* species at 2% and 4% addition levels

Table 6.3. Pasting properties of rice starch upon a 2% or 4% addition of flour from eight *Plantago* species. Values are means ± SD

2% Sample Addition

Pasting Parameter	Control (Rice Starch)	*P. coronopus*	*P. lanceolata*	*P. ovata*	*P. major*	*P. cunninghamii*	*P. turrifera*	*P. bellidioides*	*P. debilis*
Pasting Temperature (°C)	91.55 ± 0.05^{f}	71.87 ± 0.25^{b}	88.93 ± 0.26^{e}	77.28 ± 1.38^{c}	86.95 ± 0.83^{d}	71.23 ± 0.03^{b}	68.57 ± 0.4^{a}	71.3 ± 0.31^{b}	76.00 ± 0.4^{c}
Peak Viscosity (cP)	1460 ± 13^{a}	1937 ± 23^{ef}	1524 ± 6^{ab}	1561 ± 62^{b}	1685 ± 23^{c}	1862 ± 22de	1794 ± 15^{d}	1829 ± 12^{d}	1975 ± 20^{f}
Trough Viscosity (cP)	1247 ± 22^{a}	1601 ± 44^{cde}	1257 ± 4^{a}	1158 ± 42^{a}	1445 ± 1^{b}	1637 ± 17de	1557 ± 11^{cd}	1520 ± 36^{bc}	1660 ± 76^{e}
Breakdown Viscosity (cP)	213 ± 9^{a}	336 ± 45^{cd}	265 ± 10^{abc}	403 ± 20^{d}	248 ± 24^{ab}	225 ± 17^{a}	235 ± 4^{ab}	309 ± 25^{bc}	315 ± 57^{bc}
Final Viscosity (cP)	2503 ± 33^{b}	2751 ± 16^{c}	2423 ± 3^{ab}	2383 ± 23^{a}	2707 ± 16^{c}	3463 ± 78^{e}	2766 ± 2^{c}	2740 ± 43^{c}	3009 ± 14^{d}
Setback Viscosity (cP)	1256 ± 11^{bc}	1688 ± 8^{e}	1167 ± 1^{a}	1333 ± 20^{cd}	1256 ± 19^{bc}	2406 ± 56^{f}	1211 ± 9^{ab}	1220 ± 7^{ab}	1349 ± 62^{d}

4% Sample Addition

Pasting Parameter	Control (Rice Starch)	*P. coronopus*	*P. lanceolata*	*P. ovata*	*P. major*	*P. cunninghamii*	*P. turrifera*	*P. bellidioides*	*P. debilis*
Pasting Temperature (°C)	91.55 ± 0.05^{f}	70.4 ± 0.52^{b}	86.7 ± 0.83^{e}	75.48 ± 0.79^{d}	76.5 ± 0.33^{d}	69.05 ± 0.17^{b}	66.83 ± 0.69^{a}	69.4 ± 0.26^{b}	73.65 ± 0.54^{c}
Peak Viscosity (cP)	1460 ± 13^{a}	2173 ± 47^{f}	1576 ± 12^{b}	1700 ± 15.39^{c}	1946 ± 18^{d}	2080 ± 18^{e}	2075 ± 17^{e}	2116 ± 23^{ef}	2283 ± 40^{g}
Trough Viscosity (cP)	1247 ± 22^{a}	1700 ± 69^{bc}	1273 ± 23^{a}	1304 ± 43.27^{a}	1632 ± 37^{b}	1840 ± 29^{cd}	1653 ± 37^{b}	1665 ± 40^{b}	1929 ± 110^{d}
Breakdown Viscosity (cP)	213 ± 9^{a}	473 ± 42^{e}	303 ± 34^{ab}	396 ± 38^{bcde}	314 ± 23^{abc}	241 ± 38^{a}	421 ± 22^{cde}	451 ± 32de	354 ± 72^{bcd}
Final Viscosity (cP)	2503 ± 33^{a}	2942 ± 42^{b}	2494 ± 4^{a}	2492 ± 78^{a}	2925 ± 82^{b}	3449 ± 78^{c}	2775 ± 156^{b}	2725 ± 32^{ab}	3268 ± 156^{c}
Setback Viscosity (cP)	1256 ± 11^{abcd}	1882 ± 58^{e}	1221 ± 20^{abc}	1436 ± 83^{d}	1293 ± 52^{bcd}	2399 ± 81^{f}	1121 ± 158^{ab}	1060 ± 23^{a}	1339 ± 71^{cd}

Different letters indicate a significant difference ($p < 0.05$) between parameters in a row

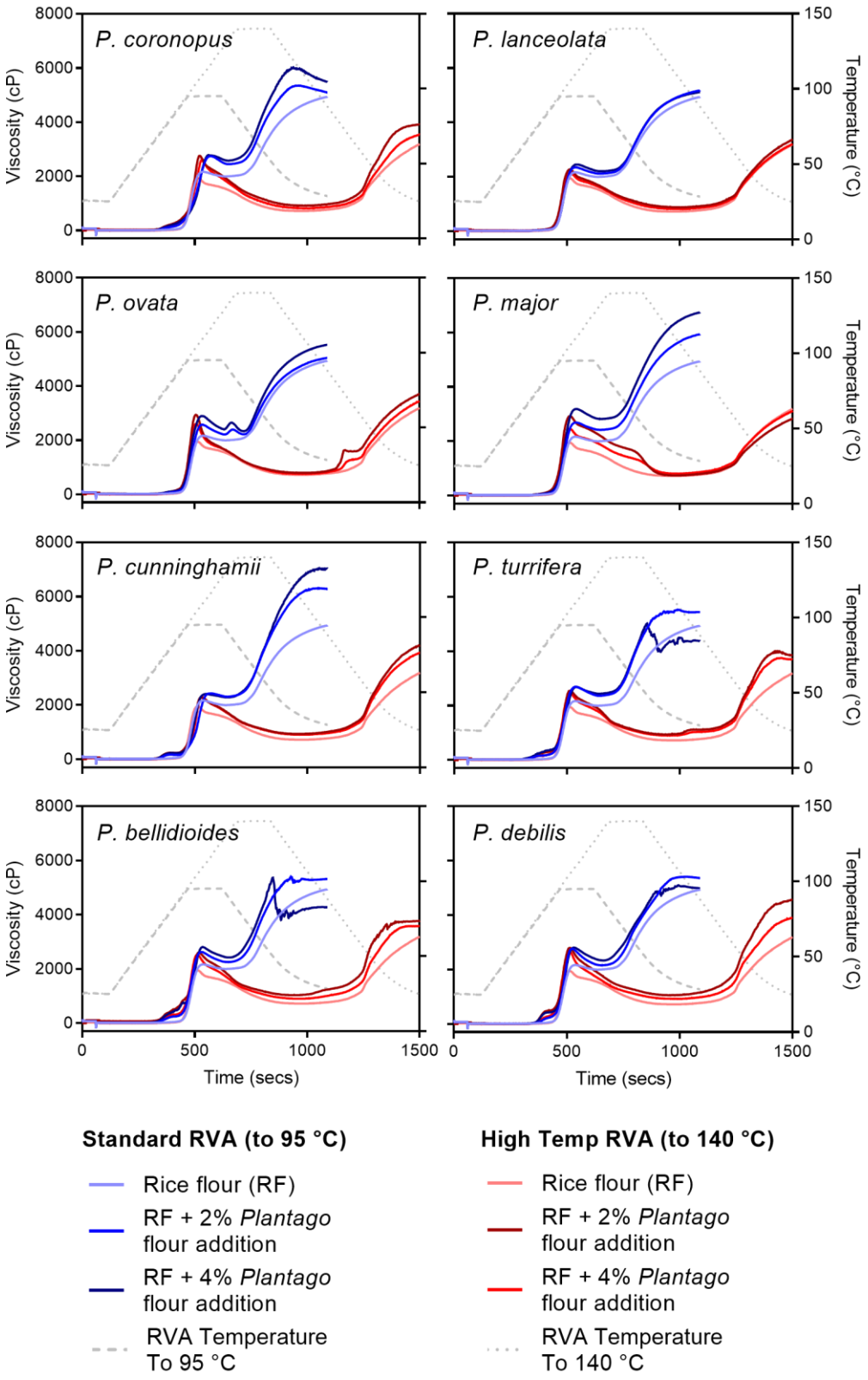

Figure 6.5. Comparison of RVA (Rapid Visco Analyser) profiles of rice flour supplemented with WSF from eight *Plantago* species at two addition levels (2% or 4%) heated to two temperatures (95 °C or 140 °C).

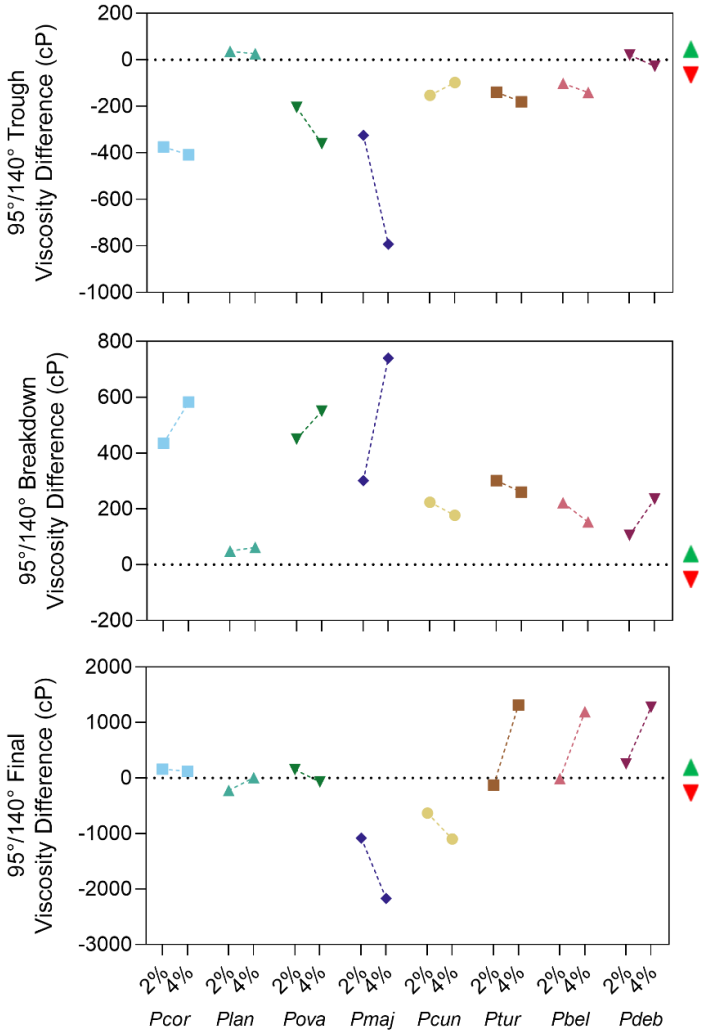

Figure 6.6. Difference plots of heat stability-related pasting parameters of rice flour upon a 2% or 4% addition of WSF from eight *Plantago* species. Difference parameters for each pasting parameter were calculated between the control (0%) and each addition level (2% or 4%) of each species at both RVA (Rapid Visco Analyser) temperatures. The values plotted are the difference between the calculated difference parameter of each addition level at 95 °C and 140 °C. Green upward triangle = increase in parameter after heating to 140 °C. Red downward triangle = decrease in parameter after heating to 140 °C. Values plotted are averages. Lines correspond to guide-to-eye only. Abbreviations: *Pcor = P. coronopus, Plan = P. lanceolata, Pova = P. ovata, Pmaj = P. major, Pcun = P. cunninghamii, Ptur = P. turrifera, Pbel = P. bellidioides, Pdeb = P. debilis.*

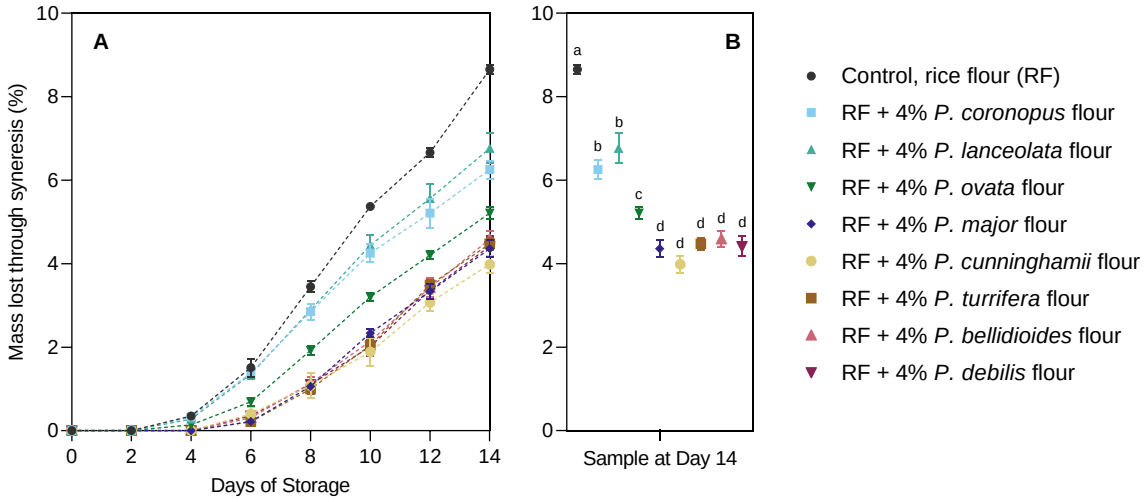

Figure 6.7. A. The effect of a 4% addition of WSF from eight *Plantago* species on the syneresis of 9% rice flour pastes over a 14 day period when stored at 4 °C. Lines displayed correspond to guide-to eye only. **B**. Statistical differences in the final mass of water lost through syneresis after 14 days of storage.

Samples sharing the same letter are not significantly different ($p > 0.05$); values shown are means ± SD.

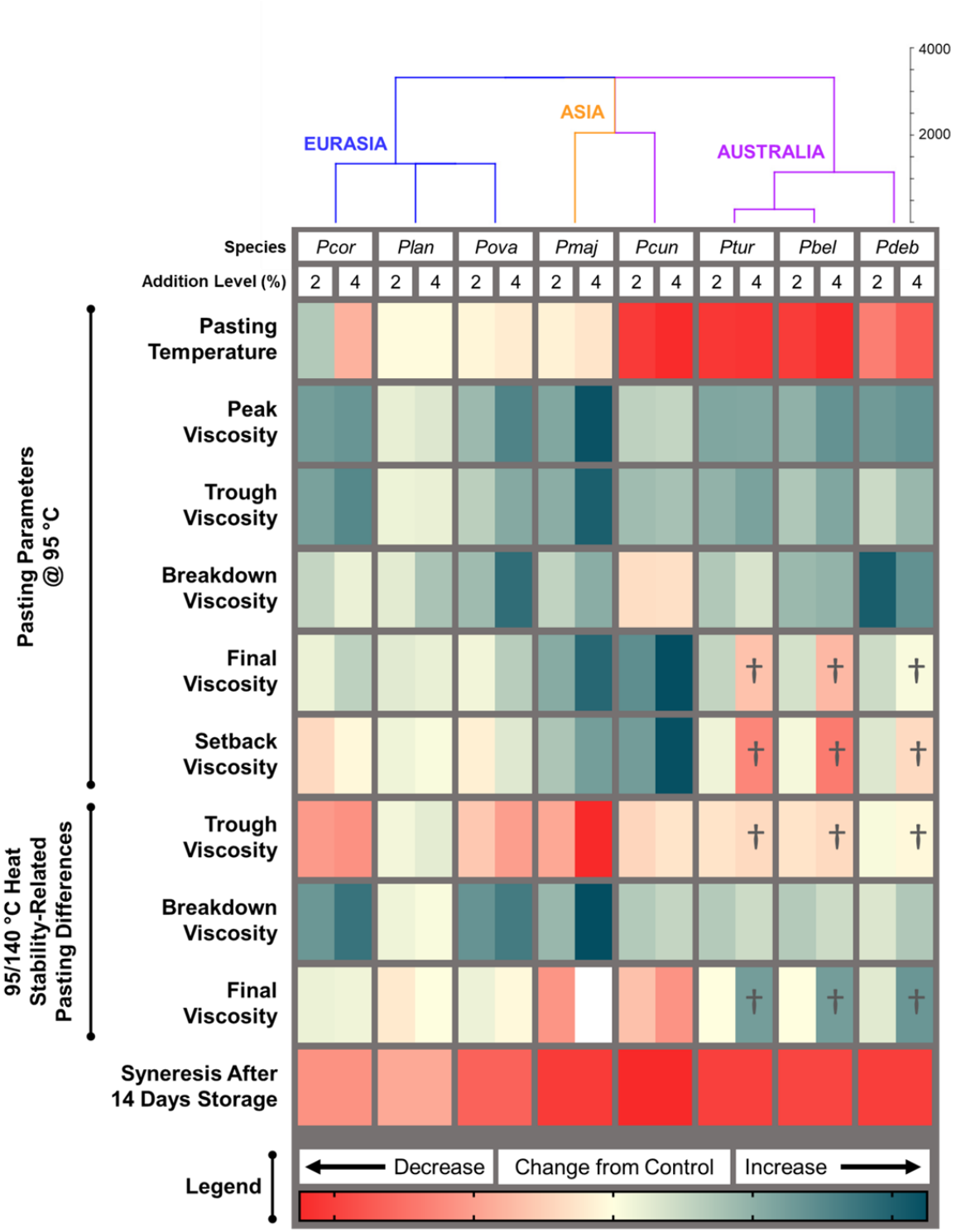
4000
2000
EURASIA
ASIA
AUSTRALIA
Species
Pcor
Plan
Pova
Pmaj
Pcun
Ptur
Pbel
Pdeb
Addition Level (%)
2 4 2 4 2 4 2 4 2 4 2 4 2 4 2 4
Pasting Parameters @ 95 °C
Pasting Temperature
Peak Viscosity
Trough Viscosity
Breakdown Viscosity
Final Viscosity
Setback Viscosity
95/140 °C Heat Stability-Related Pasting Differences
Trough Viscosity
Breakdown Viscosity
Final Viscosity
Syneresis After 14 Days Storage
Legend
Decrease
Change from Control
Increase

Figure 6.8. Clustered heat map allowing a generalised visualisation of the relationship between genetic relatedness and the changes to pasting-related qualities of rice flour upon the 2% or 4% addition of WSF from eight *Plantago* species. Each sample's pasting parameter has been normalised to the control value (rice flour with no *Plantago* addition, a value of zero). The largest (positive or negative) change observed in a sample parameter was converted to its additive inverse and these positive and negative values were used as that parameter's equidistant maximum and minimum respectively. † refers to values that were very inaccurate to the true value due to gelation-related noise. Dendrogram displayed is a neighbour-joining comparison of values in the heatmap and stratigraphically-constrained by order of genetic relatedness estimated from ITS sequences (Figure 6.1). Colour coding of the dendrogram corresponds to the geographic origin of each species.

Abbreviations: *Pcor = P. coronopus, Plan = P. lanceolata, Pova = P. ovata, Pmaj = P. major, Pcun = P. cunninghamii, Ptur = P. turrifera, Pbel = P. bellidioides, Pdeb = P. debilis.*

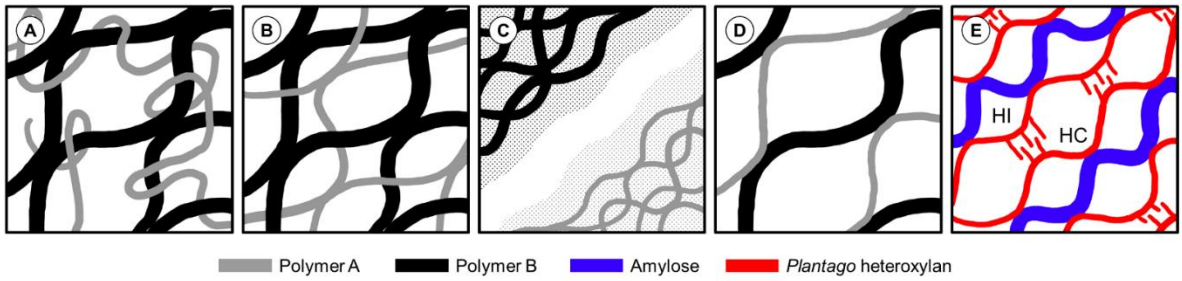

Figure 6.9. Models describing five binary gel network structures that may describe the complex interactions between *Plantago* WSF polysaccharides and starch granule exudates that lead to changes in rice flour and rice starch pasting properties. **A** Secondary polymer-containing network **B** Interpenetrating networks **C** Phase-separated networks **D** Coupled networks adapted from Cairns *et al.* (1987). **E** modified coupled network model proposed here.

Abbreviations: HI = helix-incompatible region of *Plantago* heteroxylan. HC = helix-compatible region of *Plantago* heteroxylan.

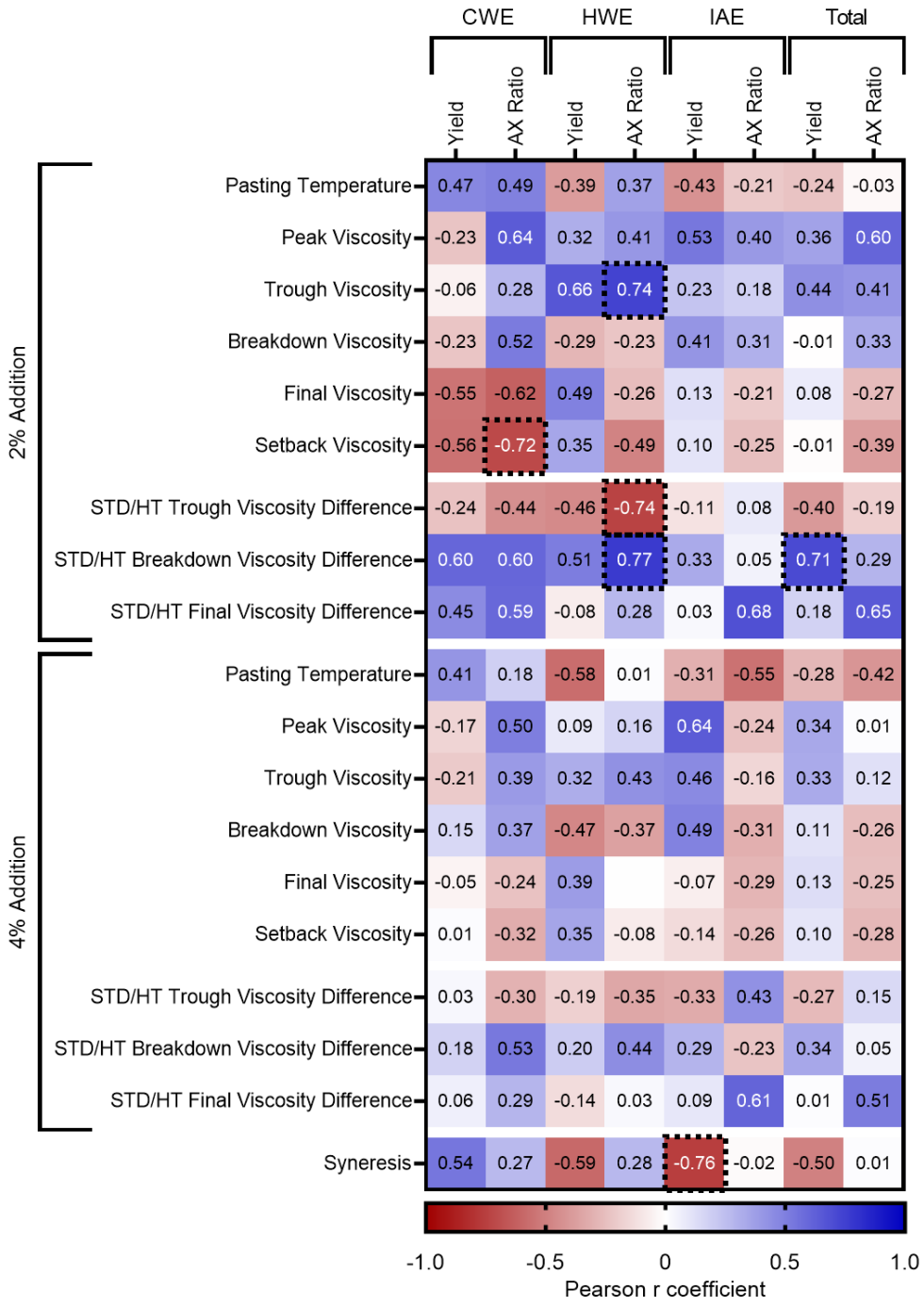

Supplementary Figure 6.1. Correlation study of *Plantago* mucilage traits (x-axis) with pasting qualities (y-axis). Significant correlations ($p > 0.05$) are denoted by dashed black boxes

Abbreviations: CWE = cold water extractable mucilage; HWE = hot water extractable mucilage; IAE = intense agitation extractable mucilage; AX = arabinose to xylose; HT = high temperature RVA setting.

Supplementary Table 6.1. Monosaccharide analysis of total extracted seed mucilage from eight *Plantago* species. Values are means ± standard deviation in %mol/mol. nd = not detected.

	D-Man	D-Rha	D-GlcA	D- GalA	D-Glc	D-Gal	D-Xyl	L-Ara
P. coronopus	nd	8.2 ± 0.5	nd	8.7 ± 0.3	7.5 ± 0.0	13.0 ± 0.1	40.8 ± 0.6	21.7 ± 0.2
P. lanceolata	1.9 ± 0.0	5.8 ± 0.5	3.5 ± 0.0	6.6 ± 0.1	14.6 ± 0.6	10.9 ± 0.3	49.2 ± 0.2	7.4 ± 0.1
P. ovata	nd	2.9 ± 0.0	nd	3.3 ± 0.0	1.3 ± 0.3	2.9 ± 0.0	70.4 ± 0.6	19.0 ± 0.2
P. major	0.8 ± 0.0	1.0 ± 0.0	5.3 ± 0.2	1.7 ± 0.4	10.2 ± 0.3	2.4 ± 0.0	69.3 ± 0.2	9.3 ± 0.1
P. cunninghamii	nd	8.7 ± 0.3	nd	3.7 ± 0.1	0.9 ± 0.4	0.7 ± 0.0	65.7 ± 0.6	20.3 ± 0.1
P. turrifera	nd	5.7 ± 0.0	nd	4.0 ± 0.2	1.5 ± 0.5	0.6 ± 0.1	64.9 ± 0.6	23.4 ± 0.1
P. bellidioides	nd	6.7 ± 0.4	nd	5.6 ± 0.2	0.9 ± 0.1	1.2 ± 0.5	67.1 ± 0.5	18.5 ± 0.2
P. debilis	nd	6.6 ± 0.0	nd	3.6 ± 0.1	7.0 ± 0.5	6.4 ± 0.0	53.4 ± 0.3	23.2 ± 0.1

Acknowledgements

The authors would like to thank Yi Ren for supplying rice flour, rice starch and technical and formulation advice. The authors would like to thank Tina Bianco-Miotto for manuscript input, and Khatija Nawaz, Kylie Neumann and Shi Fang Khor for technical support and plant management. JMC acknowledges the financial support of the Australian Government's Research Training Program and the Farrer Memorial Trust and the Barr-Smith Travelling Scholarship for funding the PhD travel that made this research possible.

References

Abbaszadeh A, Lad M, Janin M, Morris GA, MacNaughtan W, Sworn G, Foster TJ. **2014**. A novel approach to the determination of the pyruvate and acetate distribution in xanthan. *Food Hydrocolloids* **44**: 162–171.

Aguirre-Cruz A, Méndez-Montealvo G, Solorza-Feria J, Bello-Pérez LA. **2005**. Effect of carboxymethylcellulose and xanthan gum on the thermal, functional and rheological properties of dried nixtamalised maize masa. *Carbohydrate Polymers* **62**: 222–231.

Ahmadi R, Kalbasi-Ashtari A, Oromiehie A, Yarmand MS, Jahandideh F. **2012**. Development and characterization of a novel biodegradable edible film obtained from psyllium seed (Plantago ovata Forsk). *Journal of Food Engineering* **109**: 745–751.

Ahmed J, Thomas L. **2017**. Pasting Properties of Starch: Effect of Particle Size, Hydrocolloids and High Pressure. *Glass Transition and Phase Transitions in Food and Biological Materials*: 427–451.

Bahnassey YA, Breene WM. **1994**. Rapid Visco-Analyzer (RVA) Pasting Profiles of Wheat, Corn, Waxy Corn, Tapioca and Amaranth Starches (A. hypochondriacus and A cruentus) in the Presence of Konjac Flour, Gellan, Guar, Xanthan and Locust Bean Gums. *Starch - Stärke* **46**: 134–141.

Bean MM, Yamazaki WT. **1978**. Wheat Starch Gelatinization in Sugar Solutions. *Cereal Chem* **55**: 936–944.

Belorio M, Marcondes G, Gómez M. **2020**. Influence of psyllium versus xanthan gum in starch properties. *Food Hydrocolloids*: 105843.

Bemiller JN. **2011**. Pasting, paste, and gel properties of starch-hydrocolloid combinations. *Carbohydrate Polymers* **86**: 386–423.

Biliaderis CG, Arvanitoyannis I, Izydorczyk MS, Prokopowich DJ. **1997**. Effect of hydrocolloids on gelatinization and structure formation in concentrated waxy maize and wheat starch gels. *Starch/Staerke* **49**: 278–283.

Buléon A, Colonna P, Planchot V, Ball S. **1998**. Starch granules: structure and

biosynthesis. *International journal of biological macromolecules* **23**: 85–112.

Burey P, Bhandari BR, Howes T, Gidley MJ. **2008**. Hydrocolloid gel particles: formation, characterization, and application. *Critical reviews in food science and nutrition* **48**: 361–77.

Busse-Wicher M, Li A, Silveira RL, Pereira CS, Tryfona T, Gomes TCF, Skaf MS, Dupree P. **2016**. Evolution of Xylan Substitution Patterns in Gymnosperms and Angiosperms: Implications for Xylan Interaction with Cellulose. *Plant Physiol* **171**: 2418–2431.

Cairns P, Miles MJ, Morris VJ, Brownsey GJ. **1987**. X-Ray fibre-diffraction studies of synergistic, binary polysaccharide gels. *Carbohydrate Research* **160**: 411–423.

Cappa C, Lucisano M, Mariotti M. **2013**. Influence of Psyllium, sugar beet fibre and water on gluten-free dough properties and bread quality. *Carbohydrate Polymers* **98**: 1657–1666.

Charoenrein S, Tatirat O, Rengsutthi K, Thongngam M. **2011**. Effect of konjac glucomannan on syneresis, textural properties and the microstructure of frozen rice starch gels. *Carbohydrate Polymers* **83**: 291–296.

Christianson D, Hodge J, Osborne D, Detroy R. **1981**. Gelatinization of wheat starch as modified by xanthan gum, guar gum, and cellulose gum. *Cereal chemistry* **58**: 513–517.

Cowley JM, Herliana L, Neumann KA, Ciani S, Cerne V, Burton RA. **2020**. A small-scale fractionation pipeline for rapid analysis of seed mucilage characteristics. *Plant Methods* **16**: 1–12.

Criscuolo A, Gribaldo S. **2010**. BMGE (Block Mapping and Gathering with Entropy): A new software for selection of phylogenetic informative regions from multiple sequence alignments. *BMC Evolutionary Biology* **10**: 1–21.

Crossland L, Favor H. **1948**. Starch gelatinization studies. II. A method for showing the stages in swelling of starch during heating in the amylograph. *Cereal Chemistry* **25**: 213–220.

Davison E. **1982**. Seed utilization by harvester ants. In: Ant-plant interactions. 1–6.

Debet MR, Gidley MJ. **2007**. Why do gelatinized starch granules not dissolve completely? Roles for amylose, protein, and lipid in granule 'ghost' integrity. *Journal of Agricultural and Food Chemistry* **55**: 4752–4760.

Díaz-Calderón P, MacNaughtan B, Hill S, Foster T, Enrione J, Mitchell J. **2018**. Changes in gelatinisation and pasting properties of various starches (wheat, maize and waxy maize) by the addition of bacterial cellulose fibrils. *Food Hydrocolloids* **80**: 274–280.

Doyle JP, Lyons G, Morris ER. **2009**. New proposals on 'hyperentanglement' of galactomannans: Solution viscosity of fenugreek gum under neutral and alkaline conditions. *Food Hydrocolloids* **23**: 1501–1510.

Fitzgerald MA, Martin M, Ward RM, Park WD, Shead HJ. **2003**. Viscosity of rice flour: A rheological and biological study. *Journal of Agricultural and Food Chemistry* **51**: 2295–2299.

Foster T. **1992**. Conformation and Properties of Xanthan Variants.

Fratelli C, Muniz DG, Santos FG, Capriles VD. **2018**. Modelling the effects of psyllium and water in gluten-free bread: An approach to improve the bread quality and glycemic response. *Journal of Functional Foods* **42**: 339–345.

Freitas RA, Gorin PAJ, Neves J, Sierakowski MR. **2003**. A rheological description of mixtures of a galactoxyloglucan with high amylose and waxy corn starches. *Carbohydrate Polymers* **51**: 25–32.

Goering K, Schuh M. **1967**. The properties of the starch from Phalaris canariensis. *Cereal Chemistry* **44**: 532–538.

Goycoolea FM, Morris ER, Gidley MJ. **1995**. Viscosity of galactomannans at alkaline and neutral pH: evidence of 'hyperentanglement' in solution. *Carbohydrate Polymers* **27**: 69–71.

Grantham NJ, Wurman-Rodrich J, Terrett OM, Lyczakowski JJ, Stott K, Iuga D, Simmons TJ, Durand-Tardif M, Brown SP, Dupree R, *et al.* 2017. An even pattern

of xylan substitution is critical for interaction with cellulose in plant cell walls. *Nature Plants* **3**: 859–865.

Guo Q, Cui SW, Wang Q, Christopher Young J. **2008**. Fractionation and physicochemical characterization of psyllium gum. *Carbohydrate Polymers* **73**: 35–43.

Habilla C, Sim SY, Aziah N, Cheng LH. **2011**. The properties of jelly candy made of acid-thinned starch supplemented with konjac glucomannan or psyllium husk powder. *International Food Research Journal* **18**: 213–220.

Hammer Ø, Harper DAT, Ryan PD. **2001**. PAST: Paleotological statistics software package for education and data analysis. *Palaeontologia Electronica* **4**: 1–9.

Haque A, Morris ER. **1994**. Combined use of ispaghula and HPMC to replace or augment gluten in breadmaking. *Food Research International* **27**: 379–393.

Haque A, Richardson RK, Morris ER. **1993**. Xanthan-like ' weak gel ' rheology from dispersions of ispaghula seed husk. *Carbohydrate Polymers* **22**: 223–232.

Hassan AS, Houston K, Lahnstein J, Shirley N, Schwerdt JG, Gidley MJ, Waugh R, Little A, Burton RA. **2017**. A Genome Wide Association Study of arabinoxylan content in 2-row spring barley grain. *PLoS ONE* **12**: 1–19.

Heyman B, De Vos WH, Depypere F, Van der Meeren P, Dewettinck K. **2014**. Guar and xanthan gum differentially affect shear induced breakdown of native waxy maize starch. *Food Hydrocolloids* **35**: 546–556.

Hongsprabhas P, Israkarn K, Rattanawattanaprakit C. **2007**. Architectural changes of heated mungbean, rice and cassava starch granules: Effects of hydrocolloids and protein-containing envelope. *Carbohydrate Polymers* **67**: 614–622.

Horstmann SW, Axel C, Arendt EK. **2018**. Water absorption as a prediction tool for the application of hydrocolloids in potato starch-based bread. *Food Hydrocolloids* **81**: 129–138.

Huang M, Kennedy JF, Li B, Xu X, Xie BJ. **2007**. Characters of rice starch gel modified by gellan, carrageenan, and glucomannan: A texture profile analysis study. *Carbohydrate Polymers* **69**: 411–418.

Kim C, Yoo B. **2006**. Rheological properties of rice starch-xanthan gum mixtures. *Journal of Food Engineering* **75**: 120–128.

Kool MM, Gruppen H, Sworn G, Schols HA. **2014**. The influence of the six constituent xanthan repeating units on the order-disorder transition of xanthan. *Carbohydrate Polymers* **104**: 94–100.

Kumar RK, Bejkar M, Du S, Serventi L. **2018**. Flax and wattle seed powders enhance volume and softness of gluten-free bread. *Food Science and Technology International* **0**: 1–10.

Lai LS, Liao CL. **2002**. Steady and dynamic shear rheological properties of starch and decolorized Hsian-tsao leaf gum composite systems. *Cereal Chemistry* **79**: 58–63.

Lai KP, Steffe JF, Ng PKW. **2000**. Average shear rates in the Rapid Visco Analyser (RVA) mixing system. *Cereal Chemistry* **77**: 714–716.

Lee MH, Baek MH, Cha DS, Park HJ, Lim ST. **2002**. Freeze-thaw stabilization of sweet potato starch gel by polysaccharide gums. *Food Hydrocolloids* **16**: 345–352.

Liu H, Eskin NAM, Cui SW. **2003**. Interaction of wheat and rice starches with yellow mustard mucilage. *Food Hydrocolloids* **17**: 863–869.

Liu S, Yuan TZ, Wang X, Reimer M, Isaak C, Ai Y. **2019**. Behaviors of starches evaluated at high heating temperatures using a new model of Rapid Visco Analyzer – RVA 4800. *Food Hydrocolloids* **94**: 217–228.

Lundin L, Hermansson AM. **1995**. Supermolecular aspects of xanthan-locust bean gum gels based on rheology and electron microscopy. *Carbohydrate Polymers* **26**: 129–140.

Madgulkar A, Rao M, Warrier D. **2014**. Characterization of Psyllium (Plantago ovata) Polysaccharide and Its Uses. *Polysaccharides* **1**: 1–17.

Mancebo CM, San Miguel MÁ, Martínez MM, Gómez M. **2015**. Optimisation of rheological properties of gluten-free doughs with HPMC, psyllium and different levels of water. *Journal of Cereal Science* **61**: 8–15.

Mariotti M, Lucisano M, Ambrogina Pagani M, Ng PKWP, Pagani M, Ng PKWP.

2009. The role of corn starch, amaranth flour, pea isolate, and Psyllium flour on the rheological properties and the ultrastructure of gluten-free doughs. *Food Research International* **42**: 963–975.

Mohamed IK, Osama MA-F, El-Salam SMA, Mohamed ZE-O. **2011**. Biochemical studies on Plantago major L. and Cyamopsis tetragonoloba L. *International Journal of Biodiversity and Conservation* **3**: 83–91.

Morris ER, Cutler AN, Ross-Murphy SB, Rees DA, Price J. **1981**. Concentration and shear rate dependence of viscosity in random coil polysaccharide solutions. *Carbohydrate Polymers* **1**: 5–21.

Mudgil D, Barak S, Khatkar BS. **2016**. Effect of partially hydrolyzed guar gum on pasting, thermo-mechanical and rheological properties of wheat dough. *International Journal of Biological Macromolecules* **93**: 131–135.

Pejcz E, Spychaj R, Wojciechowicz-Budzisz A, Gil Z. **2018**. The effect of Plantago seeds and husk on wheat dough and bread functional properties. *LWT - Food Science and Technology* **96**: 371–377.

Perten Instruments. **2018**. Assessing ingredient performance using the RVA 4800.

Phan J, Burton RA. **2018**. New Insights into the Composition and Structure of Seed Mucilage. *Annual Plant Reviews Online* **1**: 1–41.

Phan J, Tucker MR, Khor SF, Shirley NJ, Lahnstein J, Beahan C, Bacic A, Burton RA. **2016**. Differences in glycosyltransferase family 61 accompany variation in seed coat mucilage composition in Plantago spp. *Journal of Experimental Botany* **67**: 6481–6495.

Pruska-Kędzior A, Kędzior Z, Gorący M, Pietrowska K, Przybylska A, Spychalska K. **2008**. Comparison of rheological, fermentative and baking properties of gluten-free dough formulations. *European Food Research and Technology* **227**: 1523–1536.

Ptaszek P, Grzesik M. **2007**. Viscoelastic properties of maize starch and guar gum gels. *Journal of Food Engineering* **82**: 227–237.

Ren Y, Linter BR, Foster TJ. **2020a**. Starch replacement in gluten free bread by

cellulose and fibrillated cellulose. *Food Hydrocolloids* **107**: 105957.

Ren Y, Linter BR, Foster TJ. **2020b**. Cellulose fibrillation and interaction with psyllium seed husk heteroxylan. *Food Hydrocolloids* **104**: 105725.

Ren Y, Linter BR, Linforth R, Foster TJ. **2020c**. A comprehensive investigation of gluten free bread dough rheology, proving and baking performance and bread qualities by response surface design and principal component analysis. *Food & Function*.

Ren Y, Yakubov GE, Linter BR, MacNaughtan W, Foster TJ. **2020d**. Temperature fractionation, physicochemical and rheological analysis of psyllium seed husk heteroxylan. *Food Hydrocolloids* **104**: e105737.

Rojas JA, Rosell CM, Barber CB De. **1999**. Pasting properties of different wheat flour-hydrocolloid systems. *Food Hydrocolloids* **13**: 27–33.

Romero-Baranzini AL, Rodriguez OG, Yanez-Farias GA, Barron-Hoyos JM, Rayas-Duarte P. **2006**. Chemical, physicochemical, and nutritional evaluation of Plantago (Plantago ovata Forsk). *Cereal Chemistry* **83**: 358–362.

Sasaki T, Yasui T, Matsuki J. **2000**. Influence of non-starch polysaccharides isolated from wheat flour on the gelatinization and gelation of wheat starches. *Food Hydrocolloids* **14**: 295–303.

Sheng L, Li P, Wu H, Liu Y, Han K, Gouda M, Tong Q, Ma M, Jin Y. **2018**. Tapioca starch-pullulan interaction during gelation and retrogradation. *LWT - Food Science and Technology* **96**: 432–438.

Shi X, BeMiller JN. **2002**. Effects of food gums on viscosities of starch suspensions during pasting. *Carbohydrate Polymers* **50**: 7–18.

Song JY, Kwon JY, Choi J, Kim YC, Shin M. **2006**. Pasting properties of non-waxy rice starch-hydrocolloid mixtures. *Starch/Staerke* **58**: 223–230.

Stamatakis A. **2006**. RAxML-VI-HPC: maximum likelihood-based phylogenetic analyses with thousands of taxa and mixed models Alexandros. *Phylogenetics* **22**: 2688–2690.

Steffolani E, de la Hera E, Pérez G, Gómez M. **2014**. Effect of Chia (Salvia hispanica

L.) Addition on the Quality of Gluten-Free Bread. *Journal of Food Quality* **37**: 309–317.

Sudhakar V, Singhal RS, Kulkarni PR. **1996**. Starch-galactomannan interactions: Functionality and rheological aspects. *Food Chemistry* **55**: 259–264.

Sullo A, Foster TJ. **2010**. Characterisation of Starch / Cellulose blends. *Annual Transactions of the Nordic Rheology* **18**: 1–7.

Sun Q, Xing Y, Qiu C, Xiong L. **2014**. The pasting and gel textural properties of corn starch in glucose, fructose and maltose syrup. *PLoS ONE* **9**.

Tester RF, Morrison WR. **1990**. Swelling and gelatinization of cereal starches. I. Effects of amylopectin, amylose and lipids. *Cereal Chemistry* **67**: 551–557.

Tucker MR, Ma C, Cozzlino D, Phan JL, Neumann K, Shirley NJ, Burton RA. **2017**. *Dissecting the genetic basis for seed coat mucilage biosynthesis in Plantago ovata using gamma irradiation and infrared spectroscopy*.

Wang HH, Sun DW, Zeng Q, Lu Y. **2000**. Effect of pH, corn starch and phosphates on the pasting properties of rice flour. *Journal of Food Engineering* **46**: 133–138.

Weber FH, Clerici MTPS, Collares-Queiroz FP, Chang YK. **2009**. Interaction of guar and xanthan gums with Starch in the Gels Obtained from Normal, Waxy and High-amylose Corn starches. *Starch/Staerke* **61**: 28–34.

Western TL, Skinner DJ, Haughn GW. **2000**. Differentiation of Mucilage Secretory Cells of the Arabidopsis Seed Coat. *Plant Physiol* **122**: 345–356.

Xu A, Ponte J, Chung O. **1992**. Bread crumb amylograph studies. II. Cause of unique properties. *Cereal chemistry* **69**: 502–507.

Yu L, Lyczakowski JJ, Pereira CS, Kotake T, Yu X, Li A, Mogelsvang S, Skaf MS, Dupree P. **2018a**. The patterned structure of galactoglucomannan suggests it may bind to cellulose in seed mucilage. *Plant Physiology* **178**: 1011–1026.

Yu L, Yakubov GE, Gilbert EP, Sewell K, van de Meene AML, Stokes JR. **2019**. Multi-scale assembly of hydrogels formed by highly branched arabinoxylans from Plantago ovata seed mucilage studied by USANS/SANS and rheology. *Carbohydrate Polymers* **207**: 333–342.

Yu L, Yakubov GE, Martínez-Sanz M, Gilbert EP, Stokes JR. **2018b**. Rheological and structural properties of complex arabinoxylans from Plantago ovata seed mucilage under non-gelled conditions. *Carbohydrate Polymers* **193**: 179–188.

Yu L, Yakubov GE, Zeng W, Xing X, Stenson J, Bulone V, Stokes JJR. **2017**. Multi-layer mucilage of Plantago ovata seeds: Rheological differences arise from variations in arabinoxylan side chains. *Carbohydrate Polymers* **165**: 132–141.

Yuris A, Goh KKT, Hardacre AK, Matia-Merino L. **2017**. Understanding the interaction between wheat starch and Mesona chinensis polysaccharide. *LWT - Food Science and Technology* **84**: 212–221.

Zhang Y, Li M, You X, Fang F, Li B. **2020**. Impacts of guar and xanthan gums on pasting and gel properties of high-amylose corn starches. *International Journal of Biological Macromolecules* **146**: 1060–1068.

Zhou P, Eid M, Xiong W, Ren C, Ai T, Deng Z, Li J, Li B. **2020**. Comparative study between cold and hot water extracted polysaccharides from Plantago ovata seed husk by using rheological methods. *Food Hydrocolloids* **101**: 105465.

Ziemichód A, Wójcik M, Różyło R. **2018**. Seeds of Plantago psyllium and Plantago ovata: Mineral composition, grinding, and use for gluten-free bread as substitutes for hydrocolloids. *Journal of Food Process Engineering* **12931**: 1–9.

CHAPTER 7

Augmenting rice flour-based gluten-free breads with naturalised and Australian native *Plantago* seeds

This chapter was written to the sounds of...

Album	What Comes Next
Artist	Cosmo's Midnight
Favourite Song	Polarised

Statement of Authorship

Title of Paper	Augmenting rice flour-based gluten-free breads with naturalised and Australian native *Plantago* seeds
Publication Status	☐ Published ☐ Accepted for Publication ☐ Submitted for Publication ☑ Unpublished and Unsubmitted w ork w ritten in manuscript style
Publication Details	

Principal Author

Name of Principal Author (Candidate)	James M. Cowley		
Contribution to the Paper	Conceived the study, performed experiments, analysed and interpreted data, wrote the manuscript		
Overall percentage (%)	85%		
Certification:	This paper reports on original research I conducted during the period of my Higher Degree by Research candidature and is not subject to any obligations or contractual agreements with a third party that would constrain its inclusion in this thesis. I am the primary author of this paper.		
Signature		Date	19/5/2020

Co-Author Contributions

By signing the Statement of Authorship, each author certifies that:

i. the candidate's stated contribution to the publication is accurate (as detailed above);
ii. permission is granted for the candidate in include the publication in the thesis; and
iii. the sum of all co-author contributions is equal to 100% less the candidate's stated contribution.

Name of Co-Author	Yi Ren		
Contribution to the Paper	Assisted in method development and data interpretation		
Signature		Date	19/5/2020

Name of Co-Author	Tim J. Foster		
Contribution to the Paper	Provided materials and equipment for the study, assisted in data interpretation and contributed to writing the manuscript		
Signature		Date	19/5/2020

Name of Co-Author	Rachel A. Burton		
Contribution to the Paper	Contributed to writing the manuscript		
Signature		Date	19/5/2020

Name of Co-Author			
Contribution to the Paper			
Signature		Date	

Name of Co-Author			
Contribution to the Paper			
Signature		Date	

Name of Co-Author			
Contribution to the Paper			
Signature		Date	

Name of Co-Author			
Contribution to the Paper			
Signature		Date	

Name of Co-Author			
Contribution to the Paper			
Signature		Date	

Abstract

The aim of this research was to assess the influence of natural variation in composition of mucilage-producing seeds of psyllium (*Plantago ovata)* and six of its relatives—three Australian naturalised (*P. coronopus, P. lanceolata* and *P. major*) and three Australian native (*P. cunninghamii, P. turrifera* and *P. debilis*) species—on the rheological, textural and physical properties of gluten-free (GF) dough and bread made from rice flour. With the exception of one species, doughs with a 4% addition of *Plantago* whole seed flour (WSF) had significantly increased elasticity (G'). Variation in dough physical properties were possibly due to differences in the loss tangent, relating to the dough's extensibility/ability to flow, which was significantly improved in psyllium-containing loaves and even more so when WSF from two Australian species, *P. cunninghamii* and *P. turrifera* was added. Improvements to rheological properties of *Plantago* WSF-containing doughs modulated the kinetics of dough growth during proofing and led to collapse resistance. Doughs which successfully proofed, produced GF breads with increased specific volume, improved crumb structure, and improved textural characteristics like springiness and cohesiveness which are generally lacking in GF formulations. Psyllium produced high quality doughs and breads but two Australian species, *P. turrifera* and *P. cunninghamii,* produced doughs with improved rheological properties and GF breads with greater volume, improved crumb structure and improved textural properties. Here we show the significant potential of *Plantago* species adapted to grow in the harsh Australian climate as new functional food crops.

Introduction

Coeliac disease is a chronic autoimmune enteropathy triggered by ingestion of gluten proteins from wheat, barley and rye. Gluten-related immune responses in the digestive system trigger gastrointestinal irritation and inflammatory lesions, eventually leading to villi atrophy and associated malabsorption conditions (Green & Jabri, 2003). Currently the only effective treatment for the 1% to 2% of the population that suffer from coeliac disease and other gluten-related disorders is adherence to a strict, lifelong gluten-free (GF) diet (Anton and Artfield, 2008). From those following a GF diet, there is often a demand for GF versions of typically gluten-containing products, like baked goods, which must be enhanced with a suitable texture modifier to have consumer acceptance. As such, the market for GF products, and the texture modifiers required for their production, is ever-growing.

Leavened breads are arguably the most difficult baked goods to create without gluten. In breadmaking, the entanglement of gluten proteins creates a mechanically-robust three-dimensional network (Shewry & Tatham, 1997; Tilley *et al.*, 2001; Wieser, 2007) capable of trapping CO_2 during leavening allowing a dough to rise effectively, giving it an airy yet robust texture essential to consumers (Haque *et al.*, 1994). GF breads are unable to rise effectively and so have low volume, a powdery or crumbly texture and high crumb hardness (Hager & Arendt, 2013). GF bread must therefore be augmented with ingredients and additives that can replicate the viscoelastic properties of gluten in order to produce products with satisfactory consumer appeal (Lazaridou *et al.*, 2007). Non-gluten flours and purified starches are the most common base ingredients which are often combined with one or more hydrocolloids to strengthen and viscosify the dough (Anton & Artfield, 2008). The most commonly-used polymer for gluten replacement is hydroxypropylmethylcellulose (HPMC), a semi-synthetic derivative of

cellulose with excellent viscoelastic properties (Foschia *et al.*, 2016). While HPMC is found in 40%–50% of GF breads, consumers tend to respond negatively to such synthetic hydrocolloids in the ingredient list (Horstmann *et al.*, 2018), making natural polysaccharides, like those from plants, a more appealing alternative.

Plant exudate gums like gum arabic are extruded from a point of stress (usually physical injury or fungal infection) and collected, and seed gums like guar or locust bean gum are chemically extracted from endosperm tissue (Izydorczyk *et al.*, 2005; Pollard *et al.*, 2008). These types of plant gums require processing and refinement, while another class of plant hydrocolloid—seed mucilage—simply extrudes from the wetted seed coat of some species in a process called myxospermy (Western, 2012). The most commercially significant seed mucilage is psyllium gum, which is milled from the seeds of *Plantago ovata* and used extensively as a dietary fibre supplement and more recently as a functional food ingredient (Madgulkar *et al.*, 2014). Psyllium gum is predominantly a complex heteroxylan with a structure that has proven difficult to define, but the current data consensually define the polysaccharide as having a β-(1,4)-linked-D-xylopyranose backbone, variably substituted at O-2 and/or O-3 positions with mono-, di- and oligosaccharide substitutions of α-L-arabinofuranose and β-D-xylopyranose in various combinations and linkages (Fischer *et al.*, 2004; Phan *et al.*, 2016; Yu *et al.*, 2017).

Psyllium gum is often used to replace gluten in GF baking. Haque *et al.* were the first to report that the fibrillar ‘weak gel’ network of psyllium gum (1993) was sufficient to support gas cell formation and facilitate proofing of GF bread (1994; 1994). This was later supported in work by others (Cappa *et al.*, 2013; Mancebo *et al.*, 2015; Fratelli *et al.*, 2018). Fundamentally, the addition of psyllium improves workability of GF dough (Mariotti *et al.*, 2009), likely as a result of improved rheological properties of the dough

that have also been reported (Collar *et al.*, 2015; Mancebo *et al.*, 2015). Zandonadi *et al.* (2009) showed that improved dough and bread qualities led to good acceptability of psyllium-containing GF breads in both coeliac and non-coeliac individuals. The overwhelming majority of these studies have focussed on purified psyllium gum, the production of which is less than optimal, as 75% of the seed is discarded after removal of the husk (containing the psyllium gum). Whole psyllium seeds contain 7.5 times more protein, less sodium, more minerals including zinc and magnesium, and beneficial compounds like acteoside and antioxidants - these are not present in the husk (Patel *et al.*, 2016, 2019; Ziemichód *et al.*, 2018). *Plantago* seeds also contain low molecular weight saccharides and mannan (Cowley, Chapter 5) which may have prebiotic and/or nutritional properties (Jonathan *et al.*, 2012; Xing *et al.*, 2017), and while nutritional studies using whole psyllium seeds are rare, one study found that psyllium seeds reduced serum cholesterol while the same effect not was seen with psyllium husk (Gelissen *et al.*, 1994). The use of a whole seed *Plantago* flour, which contains the functional mucilage polysaccharides along with the beneficial phytonutrients, is a way to reduce waste, bolster a product's nutritional profile, while improving its functional properties.

Whole seed powders of myxospermous seeds are rarely seen in the literature as ingredients in GF bread. Flaxseed (*Linum usitatissimum*) and chia (*Salvia hispanica*) flour are the most reported. The incorporation of flaxseed meal has repeatedly been reported to increase specific volume and reduce hardness of GF baked goods (Pruska-Kędzior *et al.*, 2008; Ozkoc & Seyhun, 2015; Sung & Chai, 2017; Kumar *et al.*, 2018; Ziemichód *et al.*, 2020), while chia flour improves the mixing and thermal properties of GF flour (Moreira *et al.*, 2013) subsequently improving quality and acceptability of GF breads (Steffolani *et al.*, 2014; Sandri *et al.*, 2017). To the best of our knowledge, the use of whole seed *Plantago* flour in bread has only been reported twice in the literature.

Pejcz *et al.* (2018) found that adding *Plantago ovata* (blond psyllium) and *P. psyllium* (dark psyllium) flour to wheat bread improved dough hydration and the antioxidant content but competition with gluten for water was observed. Ziemichód *et al.* (2018) reported that the addition of whole and ground *P. psyllium* seeds increased the specific volume of GF bread while *P. ovata* whole and ground seeds had no significant effect. These and all known studies using *Plantago* seed components—including purified gums—as ingredients in baking have been confined to *P. ovata* and occasionally, *P. psyllium,* providing an opportunity to study the suitability of the 200+ other members of the *Plantago* genus (Elliot & Jones, 1980).

Phan *et al.* (2016) have reported significant diversity in the composition of seed mucilage of Australian native *Plantago* species. More recently, Yu *et al.* (2017, 2018) reported that for *P. ovata*, rheological differences in fractionated seed mucilage were a result of varied heteroxylan substitution patterns. Recently, we have studied seed composition in Australian *Plantago* species in more detail (Cowley, Chapter 5) and shown that differences in mucilage heteroxylan structure led to changes in the pasting properties of rice flour (RF) (Cowley, Chapter 6). Heteroxylan substitution-related rheological and starch pasting variation plausibly suggest differences in food functionality and thus the natural variation in heteroxylan reported by Phan *et al.* (Phan *et al.*, 2016) and Cowley (Chapter 5) may be exploited in food technology.

Here, we studied the impact on RF-based GF breads of the addition of whole seed flour (WSF) from commercial psyllium, *P. ovata*, and six of its relatives found in Australia: three naturalised, *P. coronopus, P. lanceolata* and *P. major,* and three Australian native species *P. cunninghamii, P. turrifera* and *P. debilis.*

Methods and materials

Materials

Rice flour (RF) was purchased from Doves Farms (United Kingdom). Caster sugar, table salt and sunflower oil were purchased from Sainsbury's (UK) and yeast (*Saccharomyces cerevisiae*) was purchased from Allinson (UK). Seeds of seven *Plantago* species were grown to maturity as per Cowley (Chapter 5) to produce bulk seed. Seed was ground to flour using a MM400 Mixer Mill (Retsch, Germany) and graded to 0.5 mm. Dry ingredients and oil were stored dry at room temperature. Yeast was stored dry at +4 °C.

Dough rheological properties

Doughs used for rheological tests were prepared in triplicate at breadmaking formulation levels but excluding dried yeast. Viscoelastic properties of baking dough formulations were determined by dynamic oscillatory tests on a Physica MCR 301 Rheometer (Anton Paar, Germany) using 25 mm serrated parallel plate geometry (PP25/P2) with a gap of 2 mm. Excess dough was trimmed and the newly exposed surface was coated in a thin layer of mineral oil to prevent moisture loss. Samples were rested for 500 sec. Oscillatory measurement of the storage (*G'*) and loss (*G"*) dynamic moduli was performed at 30°C (proofing temperature) within a frequency range of 0.6 to 600 rad/s. The frequency sweep was performed at a constant strain of 0.02%, within the linear viscoelastic region which was determined previously by amplitude sweep (0.01–10 000% strain) (data not shown). The dynamic moduli, *G'* and *G"*, were extracted at 1 Hz and the loss tangent (Tan δ) was calculated as the ratio between *G"* and *G'*.

Dough proofing dynamics

Proofing kinetics were studied following Vidaurre-Ruiz *et al.* (2019) with modifications. Dough was moulded into a cylinder (Ø 22 mm) in the centre of a Petri dish. Cylinders were removed and the doughs were proofed in an incubator at 30°C for 85 min. Dishes were scanned (C7270i, Canon, Japan) prior to and after rest and every 10 min during proofing. Images were analysed using the measurement function of Photoshop CC 2018 (Adobe, USA). Rest spread (RS) was calculated as the difference in dough circumference at 0 min and 10 min. Proofing changes are presented as the difference between the dough circumference at the time of measurement and after 10 min rest.

Breadmaking

The impact of additions of *Plantago* flour to baking quality of a RF-based GF bread was assessed with baking tests. The effect of *Plantago* flour alone was studied by a 4% addition to a RF-based formulation based on work by Ren *et al.* (2020a) without other hydrocolloids or purified starches. The basic formulation consisted of 4 g of *Plantago* flour per 100g rice flour, 5 g caster sugar, 2 g table salt, 1.5 g dried yeast, 120 g of water and 5 g of sunflower oil. Control breads were produced without the addition of *Plantago* flour.

Doughs and breads were prepared at between two and four replicates (based on material limitations) and baking and subsequent analyses were performed within one day.

Baking procedure

Water and oil were added to the combined dry ingredients and mixed in a multi-speed tilt-head stand mixer (Chef Premier, Kenwood Ltd, UK) with a silicone-edged creaming beater (AT501, Kenwood Ltd) for 7 min at a constant speed. A 200 g amount of dough was transferred to a baking paper-lined multi-size (7.5 cm×7.5 cm×10 cm) anodised

cake pan (10034, Silverwood, UK). The pan was sealed with cling film to maintain humidity and doughs proofed at 30°C for 85 min in an incubator (KB115, Binder, Germany). Proofing of each dough formulation was monitored at the time of baking tests by placing a 10 g sample of dough into a measuring cylinder and proofed at 30 °C for 85 minutes, recording the volume every 10 minutes. The change in dough volume is presented as the difference between the volume at the measurement time and the initial volume.

Loaves were baked at 230°C for 40 min in a deck oven (Compacta, Tom Chandley, UK), then cooled to room temperature for 1 hr before measurements were taken.

Bread qualities

Bake loss

Bake loss (water and CO_2 released during baking) was recorded as the difference between dough weight and loaf weight.

$$Bake\ Loss\ (\%) = \frac{Weight\ of\ dough - weight\ of\ cooled\ loaf}{Weight\ of cooled\ loaf}$$

Loaf volume and specific volume

Loaf volume was measured as the displacement of a mass of rapeseeds of known density (Ren *et al.*, 2020c). Specific volume was calculated as the ratio of the loaf volume to the loaf weight.

Loaf imagery and crumb structure

Loaves were sliced into 1.25 cm slices (four full slices, two crusts). The central slice surfaces were used for C-Cell imagery. Loaf crumb structure including cell diameter

and wall thickness was evaluated using the C-Cell Bread Imaging System (Calibre Control International Ltd., UK) as per the manufacturer's standardised procedure.

Crumb colour

Crumb colour of the central slice surfaces were measured by colourimeter (ColorQuest XE, HunterLab, USA) as per the manufacturer's standard procedure. To account for variation in darkness caused by bread porosity, five measurements were taken at random across the subsample and averaged for a single replicate. Values *L** (lightness/darkness), *a** (greenness/redness), and *b** (yellowness/blueness) were obtained and the difference values between control and sample loaves (Δ*L**, Δ*a**, and Δ*b**) and the total colour difference ΔE* (CIE 2000) were calculated using the ColorTools add-in for MS Excel (http://rgbcmyk.com.ar/en/xla-2/). Hue angle was calculated using the equation below (Fernandes & Salas-Mellado, 2017):

$$\text{Hue Angle } (°) = \tan^{-1}\left(\frac{b^*}{a^*}\right)$$

The hue family was categorised based on the hue angle: 15 ± 7.5° = warm red; 30 ± 7.5° = orange; 45 ± 7.5° = warm yellow; 60 ± 7.5° = mid yellow; 75 ± 7.5° = cool yellow.

Textural properties of bread crumb

A 30 mm cylindrical punch was used to remove a central representative subsample from each of the four slices for texture analysis. Crumb texture was assessed by texture profile analysis (TPA) using a texture analyser (TA.HD*plus*, Stable Micro Systems, UK) fitted with a 30 kg load cell and 100mm aluminium compression platen (P/100, Stable Micro Systems). Pre-test, test, and post-test speeds were 1 mm/s with a target of 65% strain. Hardness, springiness, chewiness and cohesiveness values were calculated by the standard TPA analytical macro.

The TPA ratio was calculated as the ratio between all four TPA parameters.

$$TPA\ Ratio = (((Hardness/Cohesiveness)/Springiness)/Chewiness)$$

Moisture Analysis

Moisture analysis was performed by weighing the two central crumb subsamples in an aluminium pan before drying at 105°C for 24 hours and weighing again. Moisture content was calculated as the difference between fresh weight and dry weight.

Statistical analysis

Data were analysed using GenStat 15th Edition (VSNi, UK). Statistical differences, where indicated, were analysed by ANOVA using Tukey's HSD post-hoc test ($p < 0.05$).

Results & discussion

Rheological properties of gluten-free doughs augmented with *Plantago* whole seed flour

The variation in rheological dynamic moduli of GF doughs under frequency sweep are shown in Figure 7.1, while rheological parameters extracted at 1 Hz are shown in Table 7.1. In all formulations, the storage modulus (*G'*) was greater than the loss modulus (*G''*) regardless of frequency indicating solid-elastic behaviour (Figure 7.1). Similar behaviour was reported in GF formulations by others, especially those containing psyllium (Mariotti *et al.*, 2009; Cappa *et al.*, 2013; Collar *et al.*, 2015; Mancebo *et al.*, 2015). At 1 Hz (Table 7.1), all species except *P. lanceolata* significantly increased dough elasticity (*G'*) with *P. turrifera* dough having the greatest increase from the control dough. These data correlate closely with visual appearance (data not shown)

where control and *P. lanceolata* doughs were runny with a batter-like consistency while the remaining formulations were elastic and dough-like. Psyllium gum may form synergistic interactions with starch forming a co-polymer network reinforcing the flour matrix (Mariotti *et al.*, 2009; Collar *et al.*, 2015) and significantly increasing *G' and G''*. We have previously reported new evidence of complex synergistic interactions between the mucilage of *Plantago* whole seed flour and RF amylose (Cowley, Chapter 6). Species showing evidence of extensive synergistic interaction (atypical amylographic peaks (*P. ovata*) or viscoelastic gel formation during retrogradation (*P. coronopus, P. cunninghamii, P. debilis* and *P. turrifera*) were generally those with high *G' and G''* further supporting the presence and effect of a co-polymer network on GF dough rheological properties. Differences in *G'* between *Plantago* WSF-containing formulations were significant but moderate while differences in the loss tangent—Tan δ—representing the ratio between viscous (*G''*) and elastic (*G'*) behaviour were larger. The loss tangent, Tan *δ*, was less than 1 in all formulations indicating gel-like behaviour. Control, *P. coronopus, P. lanceolata* and *P. major* doughs had similarly low values for Tan *δ* (<0.156), while *P. cunninghamii* and *P. turrifera* doughs had the highest value of Tan *δ* (>0.204). A loss tangent of 1 indicates a balance between solid and elastic behaviour. Doughs with high *G'* and low *G''* (low Tan *δ*) are sensorially described as 'stiff and snappy' and are resistant to extension (Collar *et al.*, 2015), often leading to mechanical failure under force (Weipert, 1990; Edwards *et al.*, 1999). Dough extensibility is important in GF doughs as they often have low *G'* giving a batter-like consistency, and the combination of low *G'* and low Tan *δ* mean that dough will rise rapidly under the force of gas development but will succumb to shortness, lack of extensibility and will collapse (Weipert, 1990; Ronda *et al.*, 2013). Therefore, a balance between *G'* and Tan *δ* is likely required to ensure mechanical durability during proofing and baking.

Proofing behaviour of *Plantago* flour-augmented gluten-free doughs

The behaviour of *Plantago* WSF-augmented doughs during proofing is shown in Figure 7.2. Kinetic parameters of proofing were calculated by the change in dough area over time and the growth modelled using the Gompertz model (Tjørve & Tjørve, 2017; Vidaurre-Ruiz *et al.*, 2019). The Gompertz model had good agreement with the experimental data (R^2 = 0.983–0.999) showing it to be suitable to estimate kinetic parameters.

When the mould was removed, doughs containing *Plantago* WSF changed in rest spread volume and proofed volume to different degrees (Table 2) dependent on the dough elasticity. Control and *P. lanceolata* doughs had low elasticity (low *G'*) and thus spread significantly, while in other *Plantago* WSF-containing doughs spread was up to 75% less than the control. The amount of rest spread was negatively correlated with storage modulus (*G'*) (Supplementary Figure 1, r = -0.88, *p* = 0.003) showing that elasticity was impacting mechanical robustness. The maximum rate of growth (V_{max}) estimated by the Gompertz model differs significantly between formulations. We found that V_{max} was greatest in *P. cunninghamii, P. turrifera* and *P. debilis* and lowest in control and *P. lanceolata* doughs. These data show a strong negative correlation with rest spread (Supplementary Figure 1, r = -0.79, *p* = 0.021). This contradicts the findings of Viduarre-Ruiz *et al*. (2019) who found that their most fluid formulation (greatest rest spread) had the greatest V_{max}. We suggest that in our doughs with high elasticity, the internal pressure from CO_2 produced during proofing is higher in doughs that are not spreading so when internal pressure becomes sufficiently high, volume change is rapid. This also corresponded with the time to the inflection point of the growth curve (X) where the inflection occurred sooner as the growth rate was not dampened by the spread of the dough caused by the lack of elasticity. These similar effects are seen in

dough proofed vertically in a measuring cylinder (Supplementary Figure 7.2) where the volume of control and *P. lanceolata* doughs began to increase sooner and had a more gradual rate of increase compared to other formulations.

The data obtained from the kinetic parameters agrees with data from vertically proofed doughs (Supplementary Figure 7.2). Many authors have concluded that if volume expansion was not controlled, either by controlling fermentation time or altering the rheological properties, the doughs will proof too rapidly and succumb to collapse under gravity (Lazaridou *et al.*, 2007; Cappa *et al.*, 2016; Mir *et al.*, 2016; Kumar *et al.*, 2018). The development of *P. ovata*, *P. major*, *P. cunninghamii*, *P. turrifera* and *P. debilis* doughs were successful with no substantial collapse during proofing, while control and *P. lanceolata* doughs had significant rapid collapse and *P. coronopus* had slight collapse.

***Plantago* flour-augmented gluten-free bread quality evaluation**

The structure of GF loaves and their cellularity is shown in Figure 7.3. The control and *P. coronopus* loaves have a low, flat-topped profile indicating collapse during proofing, while the *P. lanceolata* and *P. major* loaves have a ‘horned’ appearance more characteristic of collapse during baking. *P. ovata, P. cunninghamii, P. turrifera* and *P. debilis* loaves all maintained high profiles with domed tops, however *P. debilis* loaves did show slight evidence of collapse-related bowing not present in *P. ovata, P. cunninghamii* or *P. turrifera* loaves. The high-profile loaves also had few holes and small alveoli, while the low profile and ‘horned’ loaves had substantial holes and large alveoli, particularly for *P. major*. Collapsed loaves also show evidence of alveolar coalescence having extensive alveolar border irregularity, again, particularly noticeable in *P. major* loaves.

The quality characteristics of *Plantago* WSF-augmented GF breads are presented in Table 7.3. Baking loss describes the dough mass lost as CO_2 and water lost during proofing and baking and is a strong indicator of gas retention (Gan *et al.*, 1990; Alvarez-Jubete *et al.*, 2009). In doughs with significant collapse, baking loss is high due to mass ejection of gases during the collapse event. The greatest baking loss was therefore seen in control, *P. coronopus* and *P. lanceolata* loaves which have evidence of significant collapse and low specific volume. The loaves that had no significant collapse, *P. ovata, P. cunninghamii* and *P. turrifera,* correspondingly had the lowest bake loss. Loaves containing *Plantago* WSF had significantly higher moisture content than the control, but moisture content was similar between formulations indicating that most of the baking loss was through ejection of CO_2.

Loaves containing *Plantago* WSF significantly increased the specific volume from the control. The increase in *P. coronopus* and *P. lanceolata* loaves was slight, while in *P. ovata*, *P. debilis*, *P. cunninghamii*, *P. turrifera*, and *P. major* loaves the increase was greater (Table 7.3). *P. turrifera, P. cunninghamii* and *P. major* loaves had the greatest specific volume, with these findings also being reflected in the actual volume of the loaves. It was previously reported that a 5% replacement of *P. ovata* did not significantly increase the specific volume of RF-based GF bread while *P. psyllium* WSF only slightly increased specific volume (Ziemichód *et al.*, 2018). The differences reported here are attributed to formulation differences. Ziemichód *et al.* (2018) opted for replacement (5 g in 95 g of RF) compared to the addition (4 g in 100 g of RF) used in this study. *Plantago* seeds contain minimal starch (Phan, 2012) so the effect of reduction of starch is likely responsible. Differences in ingredients used are also possible. While both studies have used RF as a base ingredient, it is known that RF particle size differences can strongly influence the quality of GF bread (de la Hera *et al.*, 2013). The differences in specific volume between *Plantago* species studied here

are likely due to structure-related differences in functional properties of the seed hydrocolloids. *Plantago* hydrocolloids are predominantly complex heteroxylan (Cowley, Chapter 5) (Phan *et al.*, 2016) and functional differences in these types of heteroxylans are a result of physical entanglement and hydrogen bonding between side chains (Yu *et al.*, 2017, 2018, 2019). We have previously reported significant differences in mucilage composition and content of the *Plantago* species studied here (Cowley, Chapter 5) and suggest that differences in specific volume correspond to dough reinforcement and network formation as a result of complex side chain interactions like that reported by Cowley (Chapter 6), Yu *et al.* (2017; 2018; 2019) and Ren *et al.* (2020d)

Weak doughs are not only prone to gas movement out of the loaf but also within the loaf. Gas expansion in doughs with poor structuring can lead to coalescence of alveoli as the cells expand and intercalate combining their contents and wall content. This is a function of collapse during proofing, baking, or both and thus stronger doughs will resist this. Alveolar formation and coalescence can be observed through the average alveolar diameter of the crumb and thickness of intraalveolar walls (Table 7.3). *P. cunninghamii* and *P. turrifera* loaves had alveoli 29% smaller than the control while loaves containing *P. major* WSF had alveoli that were 36% larger. Coalescence leads to thickened walls between the already enlarged alveoli. The thickness of the intraalveolar walls is therefore correlated with their average diameter (Supplementary Figure 1, r = 0.77). The loaf with largest alveoli, *P. major* had the thickest walls while *P. cunninghamii* and *P. turrifera* with the smallest alveoli had the thinnest walls.

Bread crumb texture

Inconsistent or poor crumb structure leads to poor textural characteristics. The results of texture profile analysis (TPA) of the GF bread crumb are presented in Table 7.4.

Hard crumb is typical of poorly leavened GF breads and is perceived as staleness and thus unappealing, so low hardness is ideal. Crumb hardness was significantly increased from the control in all *Plantago*-containing loaves except *P. turrifera* and *P. debilis*. The moderate crumb hardness observed even in leavened loaves is likely an effect of the highly-hydrophilic *Plantago* mucilage (Cowley, Chapter 5) binding water and reducing the effective dough water content. It has often been reported that GF formulations containing the highly-hydrophilic psyllium mucilage are particularly susceptible to this (Cappa *et al.*, 2013; Mancebo *et al.*, 2015; Fratelli *et al.*, 2018). A more effective bread rise leading to dilution of crumb within the loaf area would ameliorate this effect creating a softer crumb even under insufficient hydration. This explains the non-significant change in hardness in *P. turrifera* bread, the loaf with the greatest volume (Table 7.3) and most effectively proofed structure (Figure 7.3). Furthermore, *P. coronopus* and *P. major* loaves exhibited the greatest hardness as a result of the most extensive collapse. Control and *P. lanceolata* loaves also had significant collapse but *P. lanceolata* WSF contains less mucilaginous polysaccharides than *P. coronopus* and *P. major* (Cowley, Chapter 5). *P. coronopus* and *P. major* loaves would therefore have a greater hydration deficit, in addition to extensive collapse, compounding the high hardness in comparison to *P. lanceolata* or control loaves. Furthermore, Demirkesen *et al.* (2014) reported a significant positive correlation between hardness and pore size ($r = 0.87$). In this study, we were unable to find a significant correlation between these factors (Supplementary Figure 1, $r = 0.43$) but we suggest that the effects of porosity variation in collapsed loaves may have skewed the correlation as *P. ovata* and *P. turrifera* loaves were effectively proofed with small alveoli and also relatively soft texture compared to collapsed and large-pored loaves like *P. major*.

Gluten's ability to form structure imbues a bread with mechanical robustness and subsequent positive textural traits like cohesiveness, springiness, and chewiness (Moore *et al.*, 2004). As GF breads lack gluten's internal cohesion they are prone to fracture and crumbliness and thus increased cohesiveness is desirable (Demirkesen *et al.*, 2014). The addition of hydrocolloid(s) has the ability, to some extent, to replicate gluten-like structure within a GF bread (Lazaridou *et al.*, 2007; Anton & Artfield, 2008). Psyllium is particularly effective as Ziemichód *et al.* (2018) reported that *P. ovata* WSF- and *P. psyllium* WSF-augmented GF breads had high cohesiveness. This agrees with this study where cohesiveness was significantly increased in all *Plantago* WSF-containing formulations except *P. coronopus,* while springiness and chewiness were significantly increased in all *Plantago* WSF-containing formulations (Table 7.4). The greatest increases are seen in loaves containing *P. major, P. cunninghamii* and *P. turrifera.* The high level of cohesiveness, chewiness and springiness in *P. cunninghamii* and *P. turrifera* bread crumb is attributed to system structuring (Haque & Morris, 1994). We have previously reported that polysaccharides in *P. cunninghamii* and *P. turrifera* WSF have a strong gelling influence on starches during pasting due to their water affinity and probable synergism with granule exudates (Cowley, Chapter 6). In this study, we report corresponding data that *P. cunninghamii* and *P. turrifera* form GF doughs with high storage modulus (*G'*). The presence of gel-forming polysaccharides that reinforce the RF matrix would explain the high *G'* along with the high cohesiveness, springiness, and chewiness in these samples. These factors follow effective proofing and resultant crumb structure. Demirkesen *et al.* (2014) reported significant negative correlation between pore size and cohesiveness and pore size and springiness in GF loaves. As a result of alveolar coalescence during rapid collapse, *P. major* loaves had large pores while effectively proofed *P. cunninghamii* and *P. turrifera* loaves had small pores (Figure 7.3 and Table 7.3). While we initially could not confirm

the strong negative correlation reported by Demirkesen *et al.* (2014), we suggest that porosity variation in *P. major* (large variation in pore size, Figure 7.3; large standard deviation, Table 7.3) was strongly influencing the correlation. Alveoli size at the top of the loaf is very large, while alveoli in the bottom section (where the subsamples for TPA were taken) are smaller and more regular. If *P. major* is excluded from the correlation study (or alveolar size from the bottom loaf half is used), we can corroborate Demirkesen *et al.* (2014)'s negative correlation between porosity and cohesiveness (r = -0.76) and porosity and springiness (r = -0.78). We do note that Demirkesen *et al.* (2014) used a lower strain (25% vs 65%) and thus likely had less deformation in their samples, however we suggest that the same principles apply and thus we agree that system structuring that allows gas retention during proofing and baking also imbues positive textural qualities to GF breads.

We propose that the trade-off between loaf hardness, a negative attribute for bread, and positive texture attributes can be generalised in the ratio between TPA parameters, dubbed the TPA ratio, and can be used as a prediction of acceptability. While *P. major* loaves did have good cohesiveness, springiness and chewiness values (comparable to that of *P. cunninghamii* and *P. turrifera*), the proportion of loaf hardness raised its TPA ratio. Owing to modest hardness values, the TPA ratio was ultimately lowest in loaves containing *P. cunninghamii* and *P. turrifera*. These GF breads may have greater consumer acceptability due to a balance between textural characteristics.

Bread crumb colour

Table 7.5 shows the effect that adding *Plantago* WSF had on the perceptible colour of GF bread crumb. The polished white rice flour used is bright white in colour while the whole grain *Plantago* WSFs are various shades of brown (Supplementary Figure 7.3). Correspondingly, the addition of *Plantago* WSF darkened all formulations after baking

($\Delta L^* \neq 0$), though only significantly in *P. coronopus, P. major, P. cunninghamii* and *P. debilis* loaves. Addition of *Plantago* WSF significantly reddened the crumb colour ($\Delta a^* > 0$) with the greatest change being seen in *P. debilis, P. cunninghamii* and *P. ovata*. The effect of *Plantago* WSF addition on Δb^* had a wider range of effects than Δa^* with formulations showing both yellow and blue tones ($\Delta b^* > 0$ and $\Delta b^* < 0$). Pejcz *et al.* (2018) reported similar changes in crumb colour when comparing psyllium husk and psyllium WSF as ingredients in wheat bread. They suggested that WSF significantly darkened and reddened the crumb due to higher levels of phenolic compounds that underwent enzymatic browning during baking. This was corroborated later by Ziemichód *et al.* (2018). We propose non-enzymatic browning like the Maillard reaction as an alternative or additional explanation since in other unrelated experiments (data not presented) we observed the most significant progressive darkening at temperatures >70 °C, well beyond the optimal temperature of polyphenol or catechol oxidase (Queiroz *et al.*, 2008). Such Maillard reactions were proposed to darken mixtures of psyllium husk polysaccharides and protein in a previous study (Niu *et al.*, 2019).

The value of ΔE* displays the total perceptible colour difference between the samples and the control while the hue angle is used to interpret the hue family to broadly class the crumb colour (Table 7.4). The crumb colour of *P. turrifera* was most similar to the control, also a cool yellow hue, while *P. debilis* was starkly different, a purplish warm red. This is interesting given that raw *P. turrifera* and *P. debilis* WSFs are similarly light in colour (Supplementary Figure 7.3). The stark difference between the two may reflect differences in phenolic or other oxidative pigment composition or Maillard reaction capacity. Depending on the product, the impact of colour change is not always negative. GF breads made from purified starches are lighter in colour than white wheat bread and thus natural ‘earthy’ colours from additives can be desirable (Gallagher *et*

al., 2003). It is also known that colours, particularly those perceived as natural, influence expectation of sensory experience and perceived and actual nutritional value and this may influence consumer acceptability (Stintzing & Carle, 2004; Wei *et al.*, 2012).

Conclusions & future directions

This study shows that whole seed flour from psyllium (*Plantago ovata*) and its near relatives, particularly those adapted to Australian conditions, have untapped potential as replacements for hydrocolloids in GF baking.

The results presented here show that natural variation in mucilage content and structure are influencing the functionality of *Plantago* WSF in GF breadmaking. Our recent publication (Cowley, Chapter 6) has discussed an interaction between *Plantago* heteroxylan and starch granule exudates that create a synergistic coupled network altering the pasting profiles of rice flour and rice starch, and the viscoelastic properties of these pastes during cooking (Cowley, Chapter 6). These effects will be present during breadmaking when exudates are released from the granules but does not explain the viscoelastic changes in doughs before cooking when granules are still intact. Importantly, our model for the synergistic interactions between amylose and *Plantago* heteroxylan also includes heteroxylan-heteroxylan interactions which still occur in uncooked doughs (Figure 7.5). We hypothesise that within the dough, particles of *Plantago* WSF become hydrated and the mucilage becomes swollen, occupying intergranular spaces. The mucilage heteroxylan, remaining anchored to the WSF particles by the mucilage envelope, may begin to interact with heteroxylan from other WSF particles forming the mucin-like interactions described by Yu *et al.* (2017) (Figure 7.5A). These interactions, along with occupation of intergranular space by the WSF particles, may act to reinforce the flour matrix leading to improved rheological

properties and proofing dynamics. A similar hypothesis, where psyllium's competition for water prior to system heating synergistically increased rheological behaviour, has been reported (Ren *et al.*, 2020b,c). Discrete differences in these properties are a result of interspecific differences in heteroxylan substitution and content and their associated interactivity (Cowley, Chapter 5 and Cowley, Chapter 6). The effect of mucilage content is at play, as we suggest that the minimal quality improvement in *P. lanceolata*-containing loaves is due, at least in part, to *P. lanceolata* WSF's low mucilage content, a result corroborated in our previous publication (Cowley, Chapter 6). However, this cannot be the case when comparing *P. turrifera*, *P. cunninghamii* or *P. debilis* loaves to the commercial species *P. ovata,* as these species have significantly less mucilage but comparable or greater viscoelasticity. This is most evident when comparing *P. turrifera* and *P. ovata,* where the former has ~25% less mucilage yet produces more rheologically-robust doughs with greater flow/extensibility. The improved rheological properties of these doughs leads to higher quality GF breads. We suggest that more intermolecular interactions through greater heteroxylan complexity (Average AX Ratio = *P. turrifera,* 0.36:1 vs *P. ovata,* 0.27:1; Cowley (Chapter 6)) akin to that described by Yu *et al.* (2017; 2018; 2019) and Ren *et al.* (2020d) is likely involved. This hypothesis is further supported by the comparison of bread and dough quality between *P. major* and *P. debilis,* where the two species have the same yield of mucilage but markedly different AX ratios (Cowley, Chapter 5 and Cowley, Chapter 6). We hypothesise that a higher heteroxylan substitution rate in Australian *Plantago* species would explain greater improvements to bread and dough qualities as a result of more complex heteroxylan-heteroxylan interactions. The heteroxylan-heteroxylan interaction hypothesis also complements our model (Cowley, Chapter 6) where we hypothesise that regions of *Plantago* heteroxylan are selectively compatible with helical polymers like amylose. When cooking begins and the starch

granules in the dough begin to gelatinise, the helix-compatible regions of heteroxylan are still free to form coupled networks with extruded amylose, further reinforcing the bread matrix during and after cooking (Figure 7.5B). Similar to this, it was previously observed that *P. ovata* heteroxylan and fibrillated cellulose became thermodynamically-compatible after heating, forming a different type of synergistic interaction to that prior to heat treatment (Ren *et al.*, 2020b). *Plantago* species that showed the strongest evidence of coupled networks (atypical amylographic peaks and gelation during retrogradation) (Cowley, Chapter 6) also generally have high dough and bread quality showing that heteroxylan from *Plantago* WSF may be influencing breadmaking in different ways both before and during cooking.

While we are currently unable to precisely link particular structural motifs to favourable mucilage properties, future efforts will focus on more explicit structural characterisation and in-depth rheological analysis to decipher this further. Future work could also aim to optimise bread quality to commercial formulations by manipulating water content and proofing times.

We conclude from this research that native *Plantago* species adapted to grow in the harsh Australian climate, particularly *P. turrifera,* have significant potential as new functional food crops. Furthermore, we demonstrate the untapped potential of natural variation in myxospermous plants for selectively manipulating food quality.

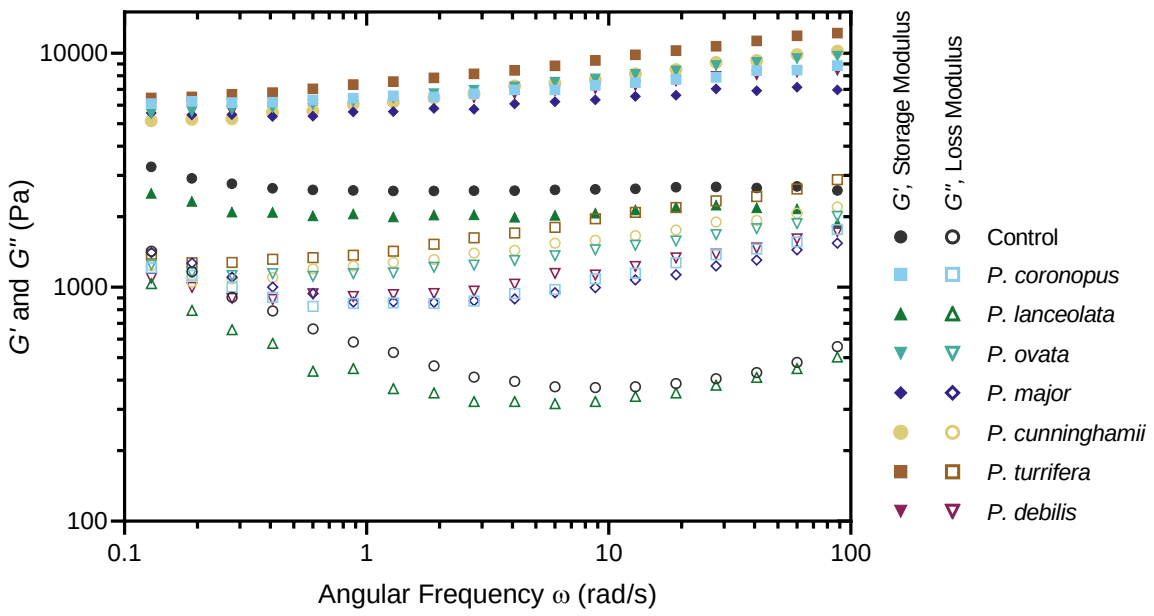

Figure 7.1. Variation in storage (*G',* closed symbols) and loss (*G"*, open symbols) moduli with frequency of *Plantago* flour-augmented rice flour-based gluten free doughs. The control dough is rice flour without the addition of *Plantago* flour. Plots are averages of three replicates.

Table 7.1. Rheological properties of rice-flour based gluten-free bread doughs augmented with the addition of whole seed *Plantago* flour

Rheological Properties	Control	*P. coronopus*	*P. lanceolata*	*P. ovata*	*P. major*	*P. cunninghamii*	*P. turrifera*	*P. debilis*
Storage Modulus *G'* (Pa) – 1 Hz	2609.5 ± 25.3^{a}	6978.5 ± 555.1^{bc}	2028.2 ± 201.9^{a}	7520.4 ± 153.7^{c}	6216.4 ± 374.6^{b}	7441.2 ± 429.1^{c}	8832.0 ± 408.6^{d}	6926.0 ± 249.3^{bc}
Loss Modulus *G''* (Pa) – 1 Hz	375.6 ± 6.4^{a}	977.6 ± 83.2^{bc}	317.6 ± 34.8^{a}	1362.9 ± 47.7^{d}	947.6 ± 49.4^{b}	1543.0 ± 91.7^{d}	1801.9 ± 106.8^{e}	1146.1 ± 19.1^{c}
Loss Tangent Tan δ – 1 Hz	0.144 ± 0.004^{a}	0.140 ± 0.000^{a}	0.156 ± 0.002^{b}	0.181 ± 0.003^{d}	0.152 ± 0.002^{b}	0.207 ± 0.003^{e}	0.204 ± 0.003^{e}	0.165 ± 0.004^{c}

Different letters indicate a significant difference ($p < 0.05$) between parameters in a row

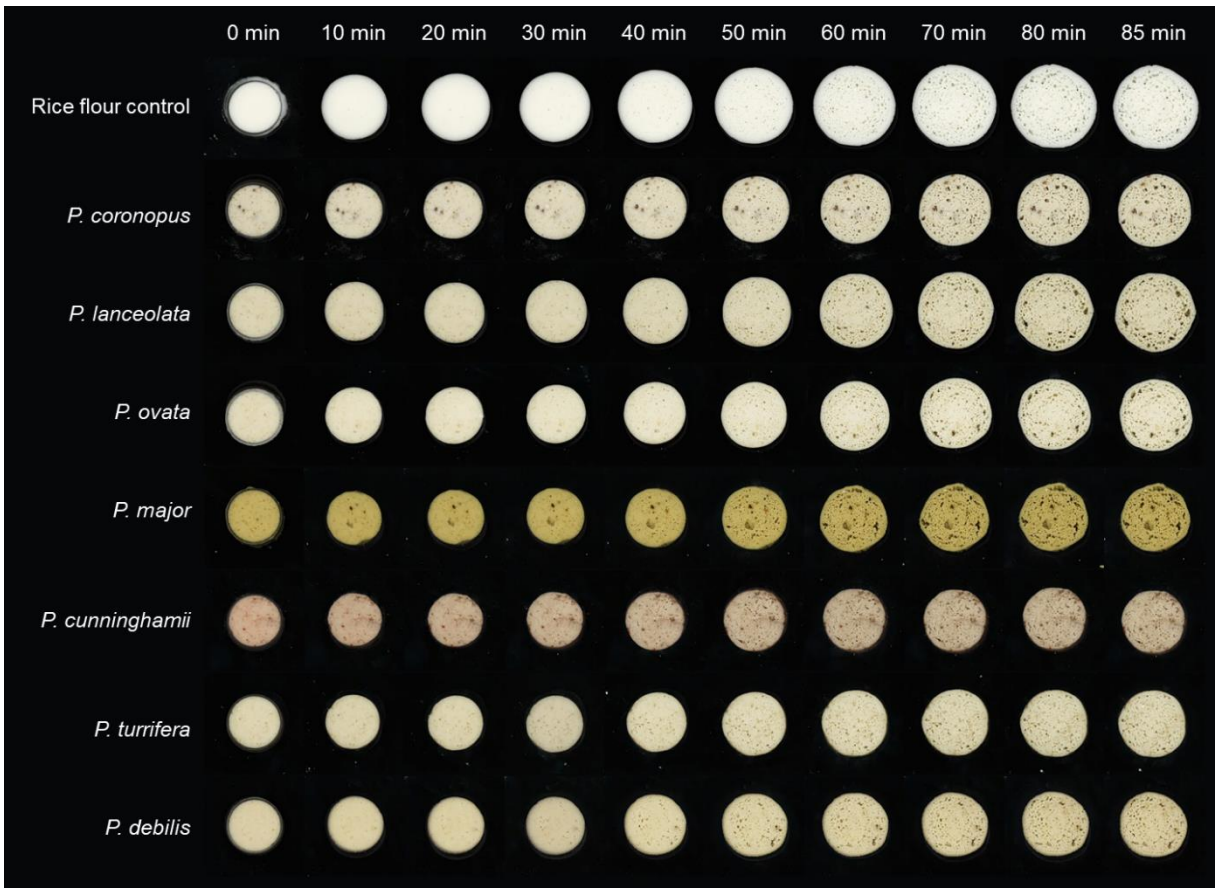

Figure 7.2. Representative images of changes in dough volume during proofing of gluten-free bread doughs augmented with the addition of whole seed *Plantago* flour.

Table 7.2. Proofing kinetic parameters of gluten-free bread doughs augmented with the addition of whole seed *Plantago* flour.

Kinetic Parameter	Control	*P. coronopus*	*P. lanceolata*	*P. ovata*	*P. major*	*P. cunninghamii*	*P. turrifera*	*P. debilis*
Rest Spread (%)	38.04 ± 1.82^{f}	17.65 ± 0.76^{d}	25.56 ± 1.00^{e}	17.54 ± 0.61^{d}	16.80 ± 1.12^{cd}	11.12 ± 1.68^{ab}	9.60 ± 0.26^{a}	13.82 ± 0.11^{bc}
Proofing Growth (%)	43.14 ± 1.52^{d}	38.50 ± 1.25^{cd}	43.61 ± 0.44^{d}	38.02 ± 2.14^{bc}	33.30 ± 1.05^{ab}	30.61 ± 3.91^{a}	33.99 ± 1.51^{ab}	30.89 ± 1.78^{a}
V_{max} (min^{-1})	0.046 ± 0.001^{a}	0.058 ± 0.003^{ab}	0.036 ± 0.004^{a}	0.061 ± 0.002^{abc}	0.085 ± 0.001^{bcd}	0.079 ± 0.010^{cd}	0.103 ± 0.020^{d}	0.088 ± 0.013^{cd}
X (min)	38.12 ± 0.52^{b}	40.22 ± 1.02^{bc}	42.16 ± 1.81^{c}	42.94 ± 0.98^{c}	38.56 ± 0.57^{b}	33.22 ± 0.89^{a}	34.63 ± 0.94^{a}	33.16 ± 1.92^{a}
Gompertz Model Fit (R^2)	0.994	0.991	0.997	0.999	0.983	0.991	0.991	0.990

Different letters indicate a significant difference ($p < 0.05$) between parameters in a row

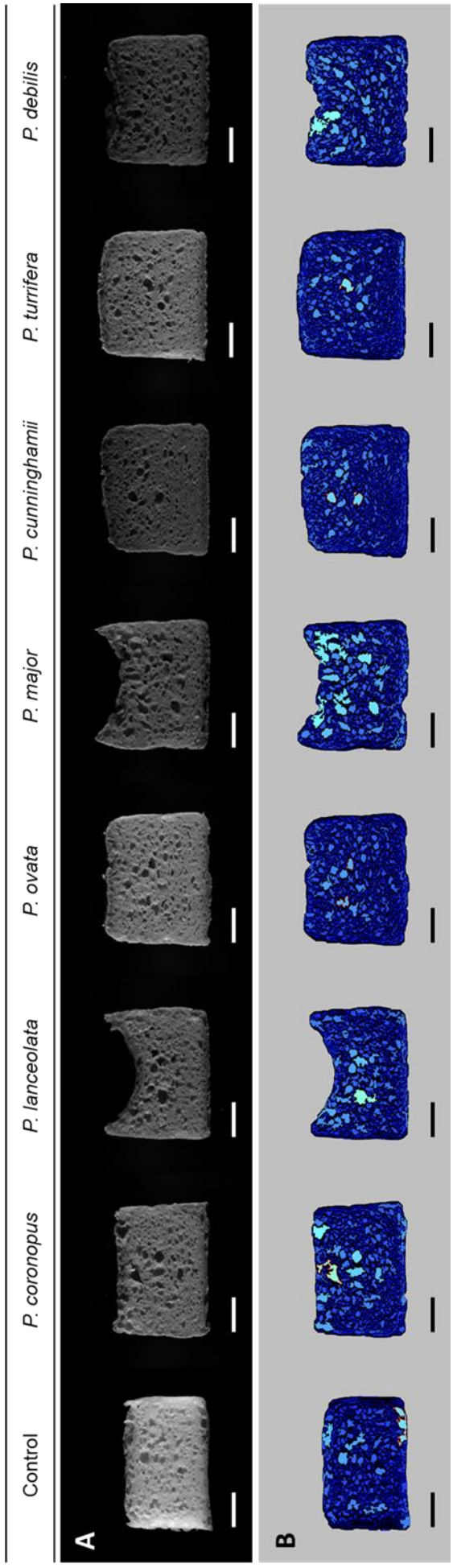

Figure 7.3. Representative images of rice flour-based gluten-free breads augmented by the addition of whole seed *Plantago* flour. **A.** Raw images of mid-loaf slices. **B.** C-Cell cellularity of the same slice. Scale = 2 cm

Table 7.3. Quality characteristics of rice flour-based gluten-free breads augmented with whole seed *Plantago* flour. Values are means ± standard deviation.

Quality parameters	Control	*P. coronopus*	*P. lanceolata*	*P. ovata*	*P. major*	*P. cunninghamii*	*P. turrifera*	*P. debilis*
Baking loss (%)	21.58 ± 0.8^{d}	21.59 ± 0.06^{d}	22.88 ± 0.42^{d}	18.64 ± 0.58^{bc}	19.39 ± 0.04^{c}	16.35 ± 0.02^{a}	17.24 ± 0.12^{ab}	19.75 ± 0.05^{c}
Specific volume (mL/g)	1.479 ± 0.023^{a}	1.666 ± 0.005^{b}	1.665 ± 0.001^{b}	1.805 ± 0.004^{c}	1.976 ± 0.006^{d}	1.877 ± 0.047^{cd}	1.946 ± 0.006^{d}	1.851 ± 0.037^{cd}
Actual volume (mL)	236.03 ± 5.19^{a}	263.79 ± 0.56^{b}	257.41 ± 0.20^{b}	294.07 ± 0.83^{c}	317.16 ± 0.43^{d}	314.68 ± 7.11^{d}	324.68 ± 0.69^{d}	295.47 ± 7.04^{c}
Crumb moisture content (%)	53.77 ± 0.05^{a}	55.57 ± 0.01^{c}	55.05 ± 0.02^{b}	55.88 ± 0.07^{c}	55.92 ± 0.18^{c}	55.82 ± 0.04^{c}	55.86 ± 0.07^{c}	55.70 ± 0.11^{c}
Average alveoli diameter (mm)	2.280 ± 0.006^{bc}	2.369 ± 0.108^{bc}	2.690 ± 0.145^{cd}	1.847 ± 0.029^{ab}	3.108 ± 0.238^{d}	1.623 ± 0.081^{a}	1.709 ± 0.019^{a}	2.552 ± 0.150^{cd}
Average intraalveolar wall thickness (mm)	0.457 ± 0.003^{ab}	0.479 ± 0.003^{c}	0.524 ± 0.010^{de}	0.505 ± 0.005^{cd}	0.540 ± 0.014^{e}	0.448 ± 0.004^{a}	0.469 ± 0.001^{ab}	0.513 ± 0.000^{de}

Different letters indicate a significant difference ($p < 0.05$) between parameters in a row

Table 7.4. Texture profile analysis (TPA) of rice flour-based gluten-free breads augmented with *Plantago* flour. Values are means ± standard deviation.

TPA Parameter	Control	*P. coronopus*	*P. lanceolata*	*P. ovata*	*P. major*	*P. cunninghamii*	*P. turrifera*	*P. debilis*
Hardness (g)	2579 ± 121^{a}	3344 ± 191^{bc}	3154 ± 73^{b}	3157 ± 62^{b}	3824 ± 8^{c}	3335 ± 222^{b}	2924 ± 135^{a}	3074 ± 57^{ab}
Cohesiveness	0.875 ± 0.009^{a}	0.880 ± 0.012^{a}	0.923 ± 0.014^{b}	0.915 ± 0.005^{b}	0.939 ± 0.000^{b}	0.944 ± 0.002^{c}	0.945 ± 0.004^{c}	0.920 ± 0.006^{b}
Springiness	0.329 ± 0.006^{a}	0.454 ± 0.008^{b}	0.526 ± 0.010^{cd}	0.525 ± 0.004^{cd}	0.585 ± 0.011^{de}	0.602 ± 0.019^{e}	0.614 ± 0.002^{e}	0.484 ± 0.036^{bc}
Chewiness (g)	1193 ± 19^{a}	1859 ± 75^{b}	1971 ± 4^{b}	1984 ± 35^{b}	2605 ± 25^{d}	2365 ± 202^{cd}	2138 ± 12^{c}	1845 ± 34^{b}
TPA Ratio	7.51	4.50	3.30	3.31	2.67	2.48	2.36	3.74

Different letters indicate a significant difference ($p < 0.05$) between parameters in a row

Table 7.5. Crumb colour parameters of rice flour-based gluten-free breads augmented with whole seed *Plantago* flour.

Colour Parameters	Control	*P. coronopus*	*P. lanceolata*	*P. ovata*	*P. major*	*P. cunninghamii*	*P. turrifera*	*P. debilis*
*L**	51.79 ± 0.69^{d}	46.39 ± 1.94^{c}	49.88 ± 0.08^{cd}	49.98 ± 1.03^{cd}	40.13 ± 1.60^{b}	38.02 ± 0.29^{b}	47.32 ± 1.43^{cd}	32.34 ± 0.57^{a}
Δ*L**	-	-5.41	-1.91	-1.81	-11.66	-13.77	-4.48	-19.45
*a**	-1.21 ± 0.10^{a}	1.43 ± 0.05^{b}	2.82 ± 0.07^{d}	6.66 ± 0.15^{f}	2.13 ± 0.04^{c}	5.85 ± 0.03^{e}	1.43 ± 0.05^{b}	6.88 ± 0.08^{f}
Δ*a**	-	2.64	4.03	7.87	3.34	7.06	2.64	8.09
*b**	4.13 ± 0.19^{b}	6.99 ± 0.29^{d}	5.56 ± 0.34^{c}	7.42 ± 0.08^{d}	11.01 ± 0.50^{e}	3.98 ± 0.04^{b}	5.02 ± 0.26^{bc}	0.93 ± 0.10^{a}
Δ*b**	-	2.87	1.44	3.29	6.89	-0.15	0.89	-3.20
ΔE*	-	9.67	6.57	10.55	13.12	16.14	5.20	20.92
Hue Angle (°)	73.67	78.44	63.11	48.09	79.05	34.23	74.10	7.70
Hue Family	Cool Yellow	Cool Yellow	Mid Yellow	Warm Yellow	Cool Yellow	Orange	Cool Yellow	Warm Red

Where applicable, different superscript letters indicate a significant difference ($p < 0.05$) between parameters in a row

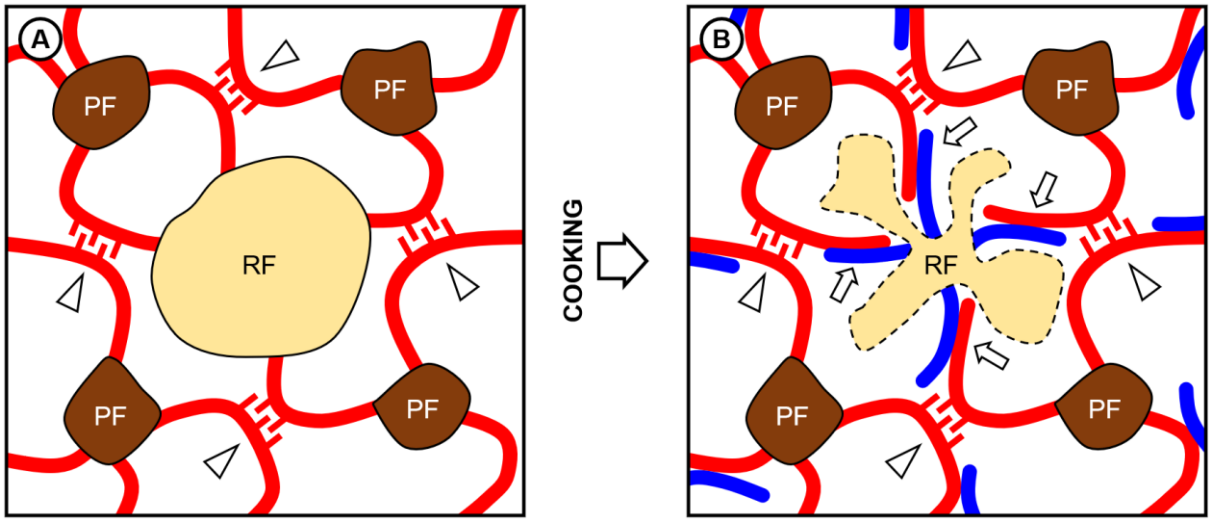

Figure 7.4. Model showing the hypothesised interaction between rice flour and *Plantago* WSF particle exudates that augments gluten-free breadmaking. **A** Before baking *Plantago* WSF particles (PF) absorb water and exude mucilage polysaccharides (red) which form homotypic interactions (arrowheads). Mucilage interactions between *Plantago* WSF particles and subsequent swelling reinforces the dough before cooking. **B** During cooking, starch breakdown in the rice flour particles (RF) causes amylose (blue) to be released which is free to form heterotypic interactions with helix-compatible regions of the *Plantago* WSF polysaccharides (arrows), forming a more complete GF loaf matrix.

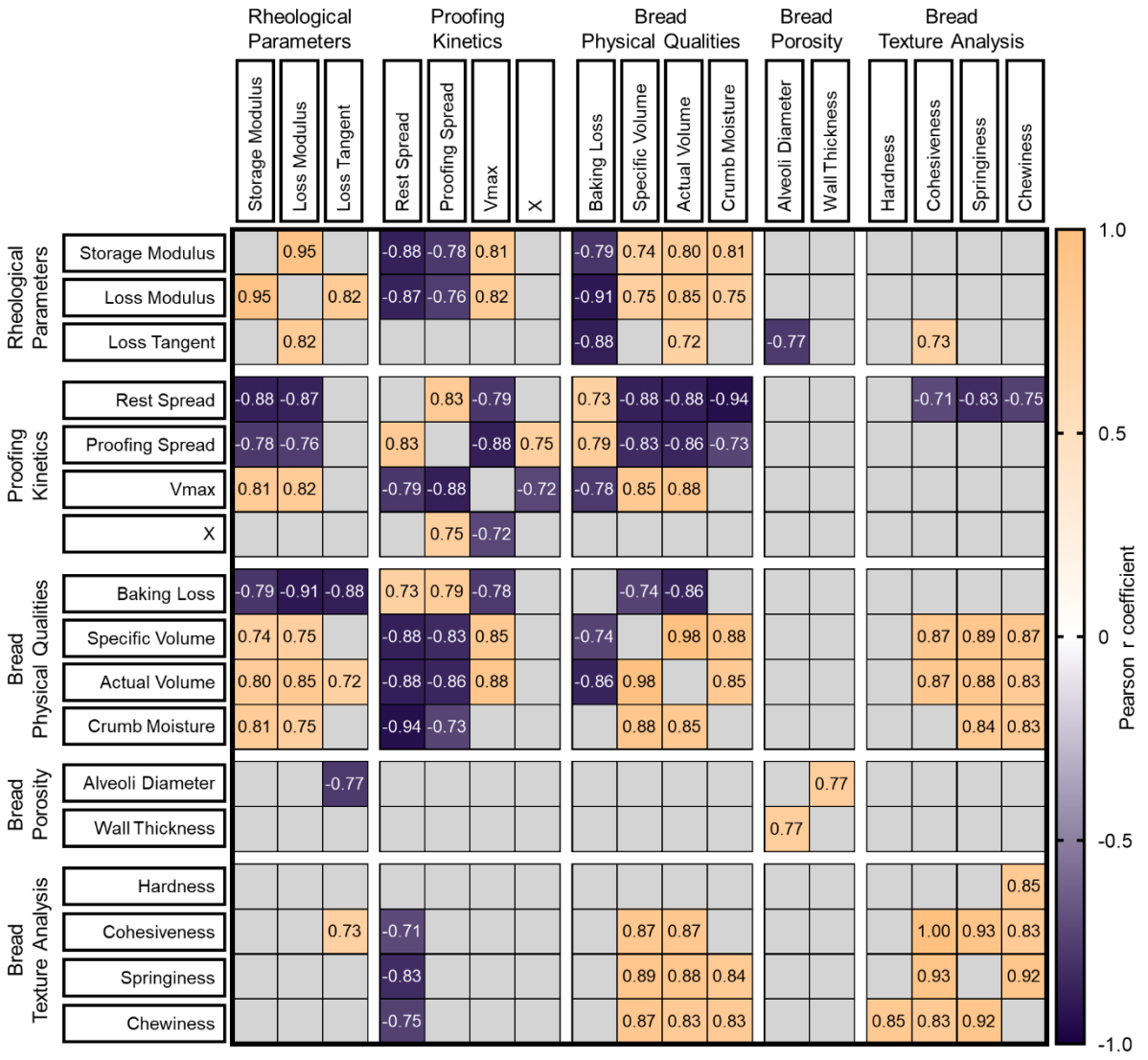

Supplementary Figure 7.1. Correlation matrix of dough rheological and bread quality parameters. Parameters are grouped by analysis type. Pearson r coefficients are only shown for statistically significant correlations ($p < 0.05$). Grey cells are insignificant correlations

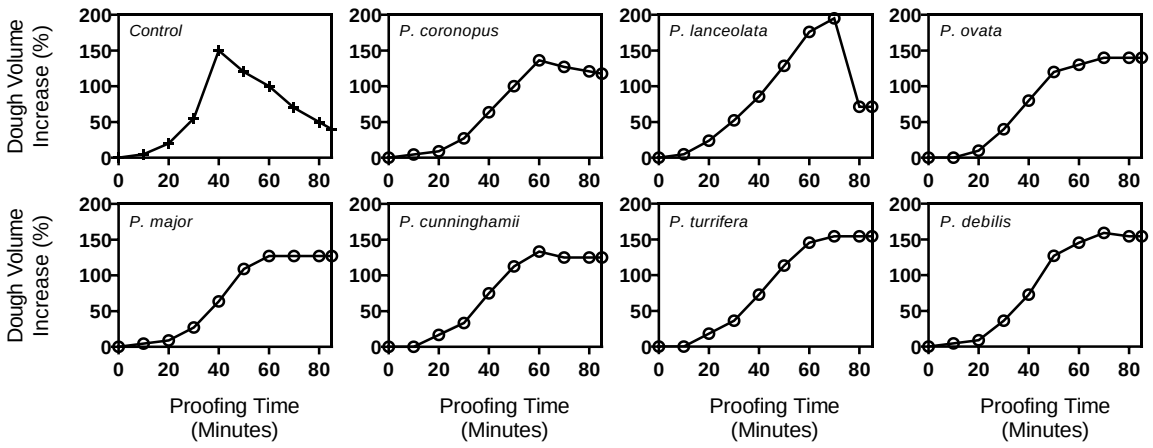

Supplementary Figure 7.2. Changes in vertical dough volume during proofing of rice flour-based gluten-free bread doughs augmented with *Plantago* flour.

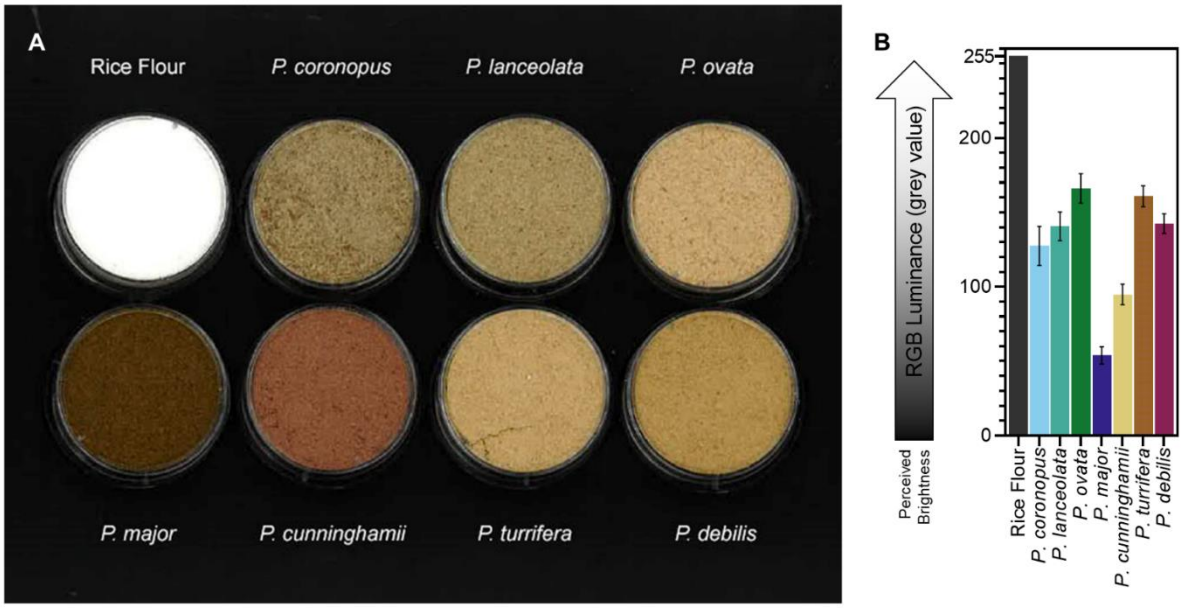

Supplementary Figure 7.3. A. Visual appearance of the samples of rice and *Plantago* flour studied**. B.** Perceived pixel luminance of the flour samples measured using Fiji ImageJ 1.51.

Acknowledgements

The authors would like to acknowledge Kylie Neumann, Shi Fang (Sandy) Khor, Khatija Nawaz for technical assistance and Dr Tina Bianco-Miotto and Dr Gleb Yakubov for continued support. JMC is supported by the Australian Government's Research Training Program and acknowledges the generous financial support of the Farrer Memorial Trust Travelling Scholarship and the Barr Smith Travelling Scholarship in Agriculture for funding the travel that made this study possible.

References

Alvarez-Jubete L, Auty M, Arendt EK, Gallagher E. **2009**. Baking properties and microstructure of pseudocereal flours in gluten-free bread formulations. *European Food Research and Technology* **230**: 437–445.

Anton AA, Artfield SD. **2008**. Hydrocolloids in gluten-free breads: A review. *International Journal of Food Sciences and Nutrition* **59**: 11–23.

Cappa C, Barbosa-Cánovas G V., Lucisano M, Mariotti M. **2016**. Effect of high pressure processing on the baking aptitude of corn starch and rice flour. *LWT - Food Science and Technology* **73**: 20–27.

Cappa C, Lucisano M, Mariotti M. **2013**. Influence of Psyllium, sugar beet fibre and water on gluten-free dough properties and bread quality. *Carbohydrate Polymers* **98**: 1657–1666.

Collar C, Conte P, Fadda C, Piga A. **2015**. Gluten-free dough-making of specialty breads: Significance of blended starches, flours and additives on dough behaviour. *Food Science and Technology International* **21**: 523–536.

Demirkesen I, Kelkar S, Campanella OH, Sumnu G, Sahin S, Okos M. **2014**. Characterization of structure of gluten-free breads by using X-ray microtomography. *Food Hydrocolloids* **36**: 37–44.

Edwards NM, Dexter JE, Scanlon MG, Cenkowski S. **1999**. Relationship of creep-recovery and dynamic oscillatory measurements to durum wheat physical dough properties. *Cereal Chemistry* **76**: 638–645.

Elliot WR, Jones DL. **1980**. Plantago L. (WR Elliot and DL Jones, Eds.). *Encyclopaedia of Australian plants suitable for cultivation*.

Fernandes S, Salas-Mellado M. **2017**. Addition of chia seed mucilage for reduction of fat content in bread and cakes. *Food Chemistry* **227**: 237–244.

Fischer MH, Yu N, Gray GR, Ralph J, Anderson L, Marlett JA. **2004**. The gel-forming polysaccharide of psyllium husk (Plantago ovata Forsk.). *Carbohyd Res* **339**: 2009–2017.

Foschia M, Horstmann S, Arendt EK, Zannini E. **2016**. Nutritional therapy – Facing the gap between coeliac disease and gluten-free food. *International Journal of Food Microbiology* **239**: 113–124.

Fratelli C, Muniz DG, Santos FG, Capriles VD. **2018**. Modelling the effects of psyllium and water in gluten-free bread: An approach to improve the bread quality and glycemic response. *Journal of Functional Foods* **42**: 339–345.

Gallagher E, Gormley T, Arendt E. **2003**. Crust and crumb characteristics of gluten free breads. *Journal of Food Engineering* **56**: 153–161.

Gan Z, Angold RE, Williams MR, Ellis PR, Vaughan JG, Galliard T. **1990**. The microstructure and gas retention of bread dough. *Journal of Cereal Science* **12**: 15–24.

Gelissen I, Brodie B, Eastwood M. **1994**. Effect of Plantago ovata (psyllium) husk and seeds on sterol metabolism: studies in normal and ileostomy subjects. *American Journal of Clinical Nutrition* **59**: 395–400.

Green P, Jabri B. **2003**. Coeliac Disease. *The Lancet* **362**: 383–391.

Hager AS, Arendt EK. **2013**. Influence of hydroxypropylmethylcellulose (HPMC), xanthan gum and their combination on loaf specific volume, crumb hardness and crumb grain characteristics of gluten-free breads based on rice, maize, teff and buckwheat. *Food Hydrocolloids* **32**: 195–203.

Haque A, Morris ER. **1994**. Combined use of ispaghula and HPMC to replace or augment gluten in breadmaking. *Food Research International* **27**: 379–393.

Haque A, Morris ER, Richardson RK. **1994**. Polysaccharide substitutes for gluten in non-wheat bread. *Carbohydrate Polymers* **25**: 337–344.

Haque A, Richardson RK, Morris ER. **1993**. Xanthan-like ’ weak gel ’ rheology from dispersions of ispaghula seed husk. *Carbohydrate Polymers* **22**: 223–232.

Horstmann SW, Axel C, Arendt EK. **2018**. Water absorption as a prediction tool for the application of hydrocolloids in potato starch-based bread. *Food Hydrocolloids* **81**: 129–138.

Izydorczyk M, Cui SW, Wang Q. **2005**. Polysaccharide Gums: Structures, Functional Properties, and Applications. *Food Carbohydrates: Chemistry, Physical Properties, and Applications*: 43.

Jonathan MC, Van Den Borne JJGC, Van Wiechen P, Souza Da Silva C, Schols HA, Gruppen H. **2012**. In vitro fermentation of 12 dietary fibres by faecal inoculum from pigs and humans. *Food Chemistry* **133**: 889–897.

Kumar RK, Bejkar M, Du S, Serventi L. **2018**. Flax and wattle seed powders enhance volume and softness of gluten-free bread. *Food Science and Technology International* **0**: 1–10.

de la Hera E, Martinez M, Oliete B, Gómez M. **2013**. Influence of Flour Particle Size on Quality of Gluten-Free Rice Cakes. *Food and Bioprocess Technology* **6**: 2280–2288.

Lazaridou A, Duta D, Papageorgiou M, Belc N, Biliaderis CG. **2007**. Effects of hydrocolloids on dough rheology and bread quality parameters in gluten-free formulations. *Journal of Food Engineering* **79**: 1033–1047.

Madgulkar A, Rao M, Warrier D. **2014**. Characterization of Psyllium (Plantago ovata) Polysaccharide and Its Uses. *Polysaccharides* **1**: 1–17.

Mancebo CM, San Miguel MÁ, Martínez MM, Gómez M. **2015**. Optimisation of rheological properties of gluten-free doughs with HPMC, psyllium and different levels of water. *Journal of Cereal Science* **61**: 8–15.

Mariotti M, Lucisano M, Ambrogina Pagani M, Ng PKWP, Pagani M, Ng PKWP. **2009**. The role of corn starch, amaranth flour, pea isolate, and Psyllium flour on the rheological properties and the ultrastructure of gluten-free doughs. *Food Research International* **42**: 963–975.

Mir SA, Shah MA, Naik HR, Zargar IA. **2016**. Influence of hydrocolloids on dough handling and technological properties of gluten-free breads. *Trends in Food Science and Technology* **51**: 49–57.

Moore MM, Schober TJ, Dockery P, Arendt EK. **2004**. Textural comparisons of gluten-free and wheat-based doughs, batters, and breads. *Cereal Chemistry* **81**: 567–

575.

Moreira R, Chenlo F, Torres MD. **2013**. Effect of chia (Sativa hispanica L.) and hydrocolloids on the rheology of gluten-free doughs based on chestnut flour. *LWT - Food Science and Technology* **50**: 160–166.

Niu Y, Xia Q, Jung W, Yu L. **2019**. Polysaccharides-protein interaction of psyllium and whey protein with their texture and bile acid binding activity. *International Journal of Biological Macromolecules* **126**: 215–220.

Ozkoc SO, Seyhun N. **2015**. Effect of Gum Type and Flaxseed Concentration on Quality of Gluten-Free Breads Made from Frozen Dough Baked in Infrared-Microwave Combination Oven. *Food and Bioprocess Technology* **8**: 2500–2506.

Patel MKM, Mishra A, Jha B. **2016**. Non-targeted Metabolite Profiling and Scavenging Activity Unveil the Nutraceutical Potential of Psyllium (Plantago ovata Forsk). *Frontiers in plant science* **7**: 431.

Patel MK, Tanna B, Gupta H, Mishra A, Jha B. **2019**. Physicochemical, scavenging and anti-proliferative analyses of polysaccharides extracted from psyllium (Plantago ovata Forssk) husk and seeds. *International Journal of Biological Macromolecules* **133**: 190–201.

Pejcz E, Spychaj R, Wojciechowicz-Budzisz A, Gil Z. **2018**. The effect of Plantago seeds and husk on wheat dough and bread functional properties. *LWT - Food Science and Technology* **96**: 371–377.

Phan J. **2012**. Xylans in Plantago species. *University of Adelaide, Honours Thesis*.

Phan J, Tucker MR, Khor SF, Shirley NJ, Lahnstein J, Beahan C, Bacic A, Burton RA. **2016**. Differences in glycosyltransferase family 61 accompany variation in seed coat mucilage composition in Plantago spp. *Journal of Experimental Botany* **67**: 6481–6495.

Pollard MA, Kelly R, Fischer PA, Windhab EJ, Eder B, Amadò R. **2008**. Investigation of molecular weight distribution of LBG galactomannan for flours prepared from individual seeds, mixtures, and commercial samples. *Food Hydrocolloids* **22**: 1596–1606.

Pruska-Kędzior A, Kędzior Z, Gorący M, Pietrowska K, Przybylska A, Spychalska K. **2008**. Comparison of rheological, fermentative and baking properties of gluten-free dough formulations. *European Food Research and Technology* **227**: 1523–1536.

Queiroz C, Mendes Lopes ML, Fialho E, Valente-Mesquita VL. **2008**. Polyphenol oxidase: Characteristics and mechanisms of browning control. *Food Reviews International* **24**: 361–375.

Ren Y, Linter BR, Foster TJ. **2020a**. Starch replacement in gluten free bread by cellulose and fibrillated cellulose. *Food Hydrocolloids* **107**: 105957.

Ren Y, Linter BR, Foster TJ. **2020b**. Cellulose fibrillation and interaction with psyllium seed husk heteroxylan. *Food Hydrocolloids* **104**: 105725.

Ren Y, Linter BR, Linforth R, Foster TJ. **2020c**. A comprehensive investigation of gluten free bread dough rheology, proving and baking performance and bread qualities by response surface design and principal component analysis. *Food & Function*.

Ren Y, Yakubov GE, Linter BR, MacNaughtan W, Foster TJ. **2020d**. Temperature fractionation, physicochemical and rheological analysis of psyllium seed husk heteroxylan. *Food Hydrocolloids* **104**: e105737.

Ronda F, Pérez-Quirce S, Angioloni A, Collar C. **2013**. Impact of viscous dietary fibres on the viscoelastic behaviour of gluten-free formulated rice doughs: A fundamental and empirical rheological approach. *Food Hydrocolloids* **32**: 252–262.

Sandri LTB, Santos FG, Fratelli C, Capriles VD. **2017**. Development of gluten-free bread formulations containing whole chia flour with acceptable sensory properties. *Food Science and Nutrition* **5**: 1021–1028.

Shewry PR, Tatham AS. **1997**. Disulphide bonds in wheat gluten proteins. *Journal of Cereal Science* **25**: 207–227.

Steffolani E, de la Hera E, Pérez G, Gómez M. **2014**. Effect of Chia (Salvia hispanica L.) Addition on the Quality of Gluten-Free Bread. *Journal of Food Quality* **37**: 309–317.

Stintzing FC, Carle R. **2004**. Functional properties of anthocyanins and betalains in plants, food, and in human nutrition. *Trends in Food Science and Technology* **15**: 19–

38.

Sung WC, Chai P-S. **2017**. Effect of Flaxseed Flour and Xanthan Gum on Gluten-Free Cake Properties. *Journal of Food and Nutrition Research* **5**: 717–728.

Tilley KA, Benjamin RE, Bagorogoza KE, Okot-Kotber BM, Prakash O, Kwena H. **2001**. Tyrosine cross-links: Molecular basis of gluten structure and function. *Journal of Agricultural and Food Chemistry* **49**: 2627–2632.

Tjørve KMC, Tjørve E. **2017**. The use of Gompertz models in growth analyses, and new Gompertz-model approach: An addition to the Unified-Richards family. *PLoS ONE* **12**: 1–17.

Vidaurre-Ruiz J, Matheus-Diaz S, Salas-Valerio F, Barraza-Jauregui G, Schoenlechner R, Repo-Carrasco-Valencia R. **2019**. Influence of tara gum and xanthan gum on rheological and textural properties of starch-based gluten-free dough and bread. *European Food Research and Technology* **0**: 0.

Wei ST, Ou LC, Luo MR, Hutchings JB. **2012**. Optimisation of food expectations using product colour and appearance. *Food Quality and Preference* **23**: 49–62.

Weipert D. **1990**. The Benefits of Basic Rheometry in Studying Dough Rheology. *Cereal Chemistry* **67**.

Wieser H. **2007**. Chemistry of gluten proteins. *Food Microbiology* **24**: 115–119.

Xing X, Hsieh YSY, Yap K, Ang ME, Lahnstein J, Tucker MR, Burton RA, Bulone V. **2017**. Isolation and structural elucidation by 2D NMR of planteose, a major oligosaccharide in the mucilage of chia (Salvia hispanica L.) seeds. *Carbohydrate Polymers* **175**: 231–240.

Yu L, Yakubov GE, Gilbert EP, Sewell K, van de Meene AML, Stokes JR. **2019**. Multi-scale assembly of hydrogels formed by highly branched arabinoxylans from Plantago ovata seed mucilage studied by USANS/SANS and rheology. *Carbohydrate Polymers* **207**: 333–342.

Yu L, Yakubov GE, Martínez-Sanz M, Gilbert EP, Stokes JR. **2018**. Rheological and structural properties of complex arabinoxylans from Plantago ovata seed mucilage

under non-gelled conditions. *Carbohydrate Polymers* **193**: 179–188.

Yu L, Yakubov GE, Zeng W, Xing X, Stenson J, Bulone V, Stokes JJR. **2017**. Multi-layer mucilage of Plantago ovata seeds: Rheological differences arise from variations in arabinoxylan side chains. *Carbohydrate Polymers* **165**: 132–141.

Zandonadi RP, Botelho RBA, Araújo WMC. **2009**. Psyllium as a Substitute for Gluten in Bread. *Journal of the American Dietetic Association* **109**: 1781–1784.

Ziemichód A, Różyło R, Dziki D. **2020**. Impact of Whole and Ground-by-Knife and Ball Mill Flax Seeds on the Physical and Sensorial Properties of Gluten-Free Bread. *Processes* **8**: 1–15.

Ziemichód A, Wójcik M, Różyło R. **2018**. Seeds of Plantago psyllium and Plantago ovata: Mineral composition, grinding, and use for gluten-free bread as substitutes for hydrocolloids. *Journal of Food Process Engineering* **12931**: 1–9.

CHAPTER 8

Crude aqueous extracts from novel Australian *Plantago* flours increase viability of rat IEC-6 and human Caco-2 intestinal epithelial cells

This chapter was written to the sounds of...

Album	Ribbons
Artist	Bibio
Favourite Song	Curls

Statement of Authorship

Title of Paper	Crude aqueous extracts from novel Australian *Plantago* flours increase viability of rat IEC-6 and human Caco-2 intestinal epithelial cells
Publication Status	☐ Published ☐ Accepted for Publication ☐ Submitted for Publication ☑ Unpublished and Unsubmitted work written in manuscript style
Publication Details	

Principal Author

Name of Principal Author (Candidate)	James M. Cowley		
Contribution to the Paper	Conceived the study, performed extract preparation, extract characterisation, cell culture experiments, data analysis, prepared figures and wrote the manuscript		
Overall percentage (%)	70%		
Certification:	This paper reports on original research I conducted during the period of my Higher Degree by Research candidature and is not subject to any obligations or contractual agreements with a third party that would constrain its inclusion in this thesis. I am the primary author of this paper.		
Signature		Date	16/6/2020

Co-Author Contributions

By signing the Statement of Authorship, each author certifies that:

i. the candidate's stated contribution to the publication is accurate (as detailed above);
ii. permission is granted for the candidate in include the publication in the thesis; and
iii. the sum of all co-author contributions is equal to 100% less the candidate's stated contribution.

Name of Co-Author	Jacqueline P. Barsby		
Contribution to the Paper	Performed cell culture and cell viability assays		
Signature		Date	16/6/2020

Name of Co-Author	Shalem Y. Leemaqz		
Contribution to the Paper	Performed statistical analysis of cell viability experiments		
Signature		Date	16/6/2020

Please cut and paste additional co-author panels here as required.

Name of Co-Author	Susan E. P. Bastian		
Contribution to the Paper	Provided access to the cell culture facility, cells and reagents		
Signature		Date	23/6/2020

Name of Co-Author	Tina Bianco-Miotto		
Contribution to the Paper	Conceived the study, provided reagents, supervision and intellectual input		
Signature		Date	16/6/2020

Name of Co-Author	Rachel A. Burton		
Contribution to the Paper	Conceived the study, provided reagents, supervision and intellectual input		
Signature		Date	16/6/2020

Name of Co-Author			
Contribution to the Paper			
Signature		Date	

Name of Co-Author			
Contribution to the Paper			
Signature		Date	

Name of Co-Author			
Contribution to the Paper			
Signature		Date	

TITLE: Crude aqueous extracts from novel Australian *Plantago* flours increase viability of rat IEC-6 and human Caco-2 intestinal epithelial cells

AUTHORS: James M. Cowley[1], Jacqueline P. Barsby[1], Shalem Y. Leemaqz[2], Susan E. P. Bastian[1], Tina Bianco-Miotto[1,2] and Rachel A. Burton[1]

AFFILIATIONS:

[1]School of Agriculture, Food and Wine, & Waite Research Institute, University of Adelaide, Waite Campus, Urrbrae, SA, Australia

[2]Robinson Research Institute, University of Adelaide, Adelaide, SA, Australia

Abstract

Plants of the *Plantago* genus occur worldwide and their seeds are frequently used as food and folk medicines. We recently showed that a number of Australian native *Plantago* species produce seeds that are highly nutritious, versatile food ingredients though little is known about their potential health benefits and safety. Using a mild aqueous extraction at human body temperature (37 °C), we have produced an extract from seed flour to determine the safety of these novel food ingredients in addition to some health-promoting properties. We used fluorometry, chromatography and antioxidant assays to characterise extracts from commercial psyllium, *P. ovata,* and three Australian relatives *P. cunninghamii*, *P. turrifera* and *P. debilis*. The extracts had antioxidant properties, were rich in minerals and protein and particularly high in soluble polysaccharides and oligosaccharides extracted from the seed endosperm and mucilage. To determine any potential cytotoxicity associated with the *Plantago* seed flours, we performed dose-response MTT cell viability assays on rat IEC-6 and human Caco-2 intestinal epithelial cells after treatment with the aqueous extracts. Using this technique, we found no evidence of cytotoxicity, even at high doses, and instead found that all extracts enhanced cell viability, with the extract from *P. turrifera* being the most effective ($p < 0.05$). We hypothesise that cell viability is enhanced through changes in cell death and/or proliferation, possibly due to the bioactive polysaccharides that are abundant in the extract. Further work will aim to identify what extract components promote cell viability in the way observed here and to characterise the underlying mechanisms.

Background

Plantago is a diverse, cosmopolitan genus of plants from the order Lamiales. Due to their abundance, *Plantago* landraces are used widely in food and folk remedies (Samuelsen, 2000) but compared to the only commercially-grown species, *P. ovata,* generally little is known about their potential hazards nor are there clinical data supporting their health benefits. In experimental terms, this is often investigated by treating mammalian cells *in vitro* with extracts from medicinal plants and measuring the cytotoxic effects. Many cell lines are used for this purpose, but in testing novel food products, the 'gold standard' cell lines, IEC-6 derived from rat small intestine epithelium and Caco-2 derived from human large intestine epithelium, are used due to their enterocytic characteristics particularly at high confluence (Sambruy *et al.*, 2001). Many studies find cytotoxicity when applying highly purified and concentrated extracts and previous studies on *Plantago* have relied on relatively harsh physical or chemical extraction techniques which may produce such toxin-enriched extracts. For example, solvent-based extraction techniques seem to enrich potentially cytotoxic compounds like polyphenolic compounds, flavonoids, terpenes and phenylethanoid glycosides from *Plantago* leaves and seeds (Gálvez *et al.*, 2003; Velasco-Lezama *et al.*, 2006; Beara, Lesjak, Cetijevic-Simin, *et al.*, 2012; Beara, Lesjak, Or, *et al.*, 2012; Harput *et al.*, 2012; Kartini *et al.*, 2014) in great excess of human digestive system-accessible levels. More recently, Huh7 human hepatocarcinoma and HeLa human cervical adenocarcinoma cell lines exhibited only mild cytotoxicity (compared to methanolic extracts) when treated with crude aqueous extracts from *P. ovata* seeds (Patel *et al.*, 2019). However, this aqueous extraction was performed in very hot water (90 °C), well beyond human body temperature (37 °C) again possibly producing a non-biologically relevant extract.

Here we developed a technique to produce an aqueous extract under more mild conditions than most previously reported methods, by using water at human body temperature (37 °C). While the traditional use of *Plantago* seeds by Australian Aboriginal and Torres Strait Islander peoples is documented (Low, 1988; Gott, 2006), their potential health benefits and safety are unknown. Therefore, the aim of this study was to identify health-promoting properties and determine any potential cytotoxicity by treating rat IEC-6 and human Caco-2 intestinal epithelial cells with aqueous extracts from seeds of four *Plantago* species (commercial psyllium, *P. ovata,* and three Australian native relatives, *P. cunninghamii, P. turrifera* and *P. debilis*) that we have previously shown to be nutritious and versatile food ingredients (Cowley, Chapter 5; Cowley, Chapter 6; Cowley, Chapter 7).

Materials and methods

Preparation of Crude Aqueous Extracts

Mature *Plantago* seeds were grown and bulked from sources listed in Cowley (Chapter 5) and milled to flour following Cowley (Chapter 6). Four grams of *Plantago* flour was extracted in 200 mL of deionized water at 37 °C on a heated magnetic stirrer for 3 hours with moderate agitation. While still warm, the extracted mixture was added to a 500 mL centrifugation bottle and debris was pelleted by centrifugation at 10000 rpm for 5 min (Beckman J2-21, US). The supernatant was carefully decanted from the pellet, homogenised in a water bath at 37 °C for 30 min, then poured into trays and frozen at -80 °C. Crude aqueous extracts were freeze-dried to a constant weight (Labconco Freezone 6, US). From duplicate extractions, yield was determined as the percentage of freeze-dried extract mass to initial mass of flour. For further analysis, extracts were pooled and dispersed at a concentration of 5 mg/mL (w/v) in deionized water for chemical analyses or sterile PBS (Life Technologies) for cell culture assays.

Monosaccharide Profiling

Freeze-dried mucilage was dispersed in water at 2 mg/mL (w/v) and an 800 µL aliquot was added to 200 µL of 5M H_2SO_4 (final H_2SO_4 concentration of 1M) and hydrolysed at 100 °C for 3 h as per Phan *et al.* (2016). Monosaccharides released by acid hydrolysis were derivatised with 1-phenyl-3-methyl-5-pyrazoline (PMP) following Comino *et al.* (2013) and then separated by reversed phase high performance liquid chromatography (RP-HPLC) with modifications to the column and eluents listed in Hassan *et al.* (2017). Area under the peaks was compared to standard curves of mannose, ribose, rhamnose, glucuronic acid, galacturonic acid, glucose, galactose, xylose, arabinose and fucose (Wood *et al.*, 2018). Monosaccharide profiles were determined from duplicate analyses.

Protein Content

Extract protein contents were determined fluorometrically by Qubit Protein Assay Kit (Invitrogen, US) in triplicate as per the manufacturer's instructions.

Mineral Analysis

Ultra-trace element analysis by inductively coupled plasma-mass spectrometry (ICP-MS) was performed on freeze-dried extracts and their source flour following Hofstee *et al.* (2019). A routine calibration standard set was run prior to samples with a spiked quality control run after every 6 samples followed by a wash step. All runs were spiked with ^{45}Sc, ^{89}Y, ^{115}In, ^{159}Tb internal standards to ensure recovery. Analysis was performed fee-for-service by the Perkins Pregnancy Research Laboratory (Griffith University, Australia) and data presented are the average of two technical repeats with minimal error.

Mineral extractability was determined with the following equation:

$$\text{Extractability } (\%) = \frac{(C^F \times M^F)}{(C^E \times M^E)} \times 100$$

Where C^F and C^E refer to the mineral concentration in mg/kg in source flour and extract, respectively, and M^F and M^E refer to the mass in grams of flour used for extraction and recovered extract respectively.

Antioxidant Assays

Antioxidant properties of extracts were determined in triplicate by Ferric Reducing Antioxidant Power (FRAP) (Benzie and Strain, 1996) and DPPH Scavenging (Shi *et al.*, 2012) assays, and related to the phenolic content as determined by Folin-Ciocalteu Assay (Ainsworth and Gillespie, 2007).

Cell Culture

IEC-6 (ATCC CRL-1592) and Caco-2 (ATCC HTB-37) cells were cultured in Gibco Dulbecco's Modified Eagle Medium (DMEM; Life Technologies, US) with 10% Fetal Bovine Serum (FBS; Sigma, US) and antibiotics and antimycotics (Sigma, US). The cells were maintained in a 37 °C incubator with 5% CO_2 in 75 cm^2 flasks (Greiner Bio-One, Austria) and the cells were washed and media changed every 72 hours. Cells were passaged to 7080% confluence and split at a 1:3 ratio by using Trypsin (Gibco, US) to dissociate the cells from the bottom of the flask. Viable cell counts were performed by trypan blue exclusion (Gibco, US) and counted by standard procedure with a haemocytometer on an inverted microscope (Olympus, Japan).

Cell Viability Assay

A dose-response cell viability assay was performed by a method adapted from Kumar *et al.* (2019). IEC-6 or Caco-2 cells were plated in flat-bottom 96 well plates (Corning, US) at a concentration of 1×10^5 cells/well in 50µL, then left for 24 hours to adhere to the plasticware. Extracts (5 mg/mL) were diluted to 500 µg/mL DMEM+FBS and then

two-fold serial dilutions were prepared (500, 250, 125 and 62.5 µg/mL). The extract treatments (50 µL) were applied to triplicate wells, and the plate was left to incubate for another 24 hours. A solution of 3-(4,5-dimethylthiazol-2-yl)-2,5-diphenyltetrazolium bromide (MTT; Invitrogen, US) was prepared in PBS to 1 mg/mL, filter-sterilized (0.22 µm), and 50 µL was added to each well and the plate was incubated for a further 4 hours. A 100 µL volume of dimethyl sulfoxide (DMSO; Sigma-Aldrich, US) was added to each well, the plate was covered in aluminium foil and agitated slightly on an orbital shaker for 15 min to extract the formazan product. Absorbance was read using a Multiskan Spectrum (Thermo Scientific, US) microplate spectrophotometer at 570 nm. The cell viability was calculated as a percentage of the vehicle control value:

$$\text{Cell Viability (\%)} = \frac{abs^{570}\ \text{(sample)}}{abs^{570}\ \text{(control)}} \times 100$$

Independent cell viability assays were performed on four separate passages.

Statistical Analysis

Statistical differences in antioxidant capacities were determined using GraphPad Prism 8.4.0. Statistical differences were determined by ANOVA with Tukey's Honestly Significant Difference post-hoc test ($p > 0.05$) and EC_{50} of DPPH radical scavenging was determined using the inhibitor vs normalised response model (variable slope) (Chen *et al.*, 2013) with good agreeance to the experimental data ($R^2 = 0.89–0.99$).

Cell viability assay data were analysed using R version 3.6.1 (R Core Team, 2012). Marginal models were fitted using Generalized Estimating Equations, accounting for repeated experiments assuming an independence working correlation structure. Cubic splines were used to explore the non-linear dose-response relationship of concentration on cell viability. Separate marginal models were fitted with categorical concentrations to allow for comparisons to the vehicle control.

Results and discussion

Preparation and compositional analysis of crude aqueous extracts from whole seed *Plantago* flours

To reduce the chance of enriching cytotoxic compounds as is common with typical hydroalcoholic or high temperature extraction techniques, we recently developed a mild aqueous extraction method performed at human body temperature (37 °C) to isolate water-extractable constituents from seed flour (Barsby *et al.* unpublished). This extraction process is presented schematically in Figure 8.1 and its use generated a crude aqueous body temperature extract from *P. ovata*, *P. cunninghamii, P. turrifera* and *P. debilis* flour, hereafter referred to as POE, PCE, PTE and PDE, respectively. The efficiency of the extraction process varied between samples but PCE had the highest yield (26.4%) (Figure 8.1E). Yields were significantly lower than the most efficient extraction reported previously for this method (~40%, Barsby *et al.* unpublished) though this high yield from flaxseed (*Linum usitatissimum*) was possibly due in part to its mucilage being readily-extractable, which we determined previously (Cowley *et al.*, 2020). By contrast, yields from the *Plantago* flours studied here were more similar to that of chia (*Salvia hispanica*) in the same study, a species also found to have difficult-to-extract mucilage (Muñoz *et al.*, 2012; Segura-Campos *et al.*, 2014; Capitani *et al.*, 2015; Fernandes and Salas-Mellado, 2017; Cowley *et al.*, 2020).

To characterise constituents of the extracts, we have used protein, monosaccharide, and mineral profiling techniques (Figure 8.2). While crude plant storage proteins are not known to have bioactive properties, it was important to account for as much of the extract as possible and solubilised proteins were detected in all extracts (Figure 8.2A). Due to its water solubility (Shewry *et al.*, 1995), the vast majority of the extracted

protein in *Plantago* extracts is likely to be albumin with a small globulin component possible in line with previous reports (Romero-Baranzini *et al.*, 2006).

As sugars, both low and high molecular weight, are generally highly soluble/dispersable in water it was hypothesised that they would comprise a large proportion of the extract mass. Monosaccharide analysis was performed to determine the sugar content and to make assumptions on their saccharide sources based on previous findings. Monosaccharides were the largest quantified constituent in the extracts, accounting for around half of the mass (Figure 8.2B). Monosaccharides detected in the extracts are highly consistent with known saccharides found in seeds of the species studied here (Cowley, Chapter 5) (Phan *et al.*, 2016). The major polysaccharides in *Plantago* seeds are found in seed mucilage and endosperm cell walls. Monosaccharides associated with seed mucilage (rhamnose and galacturonic acid from pectin and xylose and arabinose from heteroxylan) accounted for between 50% and 78% of quantified monosaccharides while those from endosperm wall mannan (mannose) accounted for at most 8.5% of quantified monosaccharides. This is consistent with the physicochemical properties of these two polysaccharide types where the endosperm mannan is structural and possibly crystalline giving it low solubility while the seed mucilage is highly hydrophilic. The remaining quantified monosaccharides, glucose and galactose, are consistent with highly-soluble low molecular weight reserve sugars found in these species (Cowley, Chapter 5) (Ahmed *et al.*, 1965).

Minerals are stored in seeds often as inclusions in bodies in the endosperm and embryo, positioned to rapidly mobilise during germination. Minerals primed for rapid mobilisation should be easily extracted by the technique used here and we report minerals to be present in the extracts (Figure 8.2A) at similar total levels (~3.5% w/w). Comparing mineral content of the extracts with their source flour allows some

estimation of their enrichment or extraction efficiency. In terms of absolute mineral concentration, 8 of 14 minerals measured were more concentrated in the extracts than the source flour (Figure 8.3A). Na, Mg, K and Ca are highly abundant cationic minerals and were well extracted by the technique used here, though we do note that greater than 100% recovery of Na was seen in some samples. This is typical of some contamination in the extraction water (Na is difficult to completely remove by filtering) and was exacerbated by the sensitivity of the quantification technique. This was particularly evident in *P. turrifera* where Na was not present in the flour but present in the extract, though at lower levels than other samples (Figure 8.3A). Essential minerals Fe, Co, Ni and Cu were generally higher in absolute concentration in the extracts which may boost the benefits of these nutrients. Recovery of Fe, Co, Ni and Cu was also generally good, varying somewhat between samples, but was consistently more efficient than Cr, Mn, Zn, and Mo which were lower in absolute concentration in the extracts than their source flour with very poor extraction efficiency (<15% recovery) (Figure 8.3B). Reasons underpinning the differences in mineral extraction efficiency are complicated but may be due to sequestration in phytin crystals locked in intact vacuoles (Otegui *et al.*, 2002) and/or poor removal of mineral inclusions from protein/lipid bodies in the seeds (Prego *et al.*, 1998).

After these analyses we found that between 27% and 48% of the extract remained uncharacterised (Figure 8.2B). A similar gap in extract constituent identity was observed in our previous study (Barsby *et al.*, unpublished), but identification/quantification was more complete here. As with previous work, we suggest that the unaccounted mass is likely to be comprised of water-soluble phytochemicals like C- and B-group vitamins and polyphenolic secondary metabolites, intact membrane-encapsulated protein bodies that are inaccessible to the fluorometric quantification used here, with a portion of unpelleted insoluble particulate matter likely.

Future work should aim to improve this extraction technique with greater biological relevance by employing a simulated peptic digestion at low pH and in the presence of enzymes, shown to be effective as an *in vitro* digestion model (Glahn *et al.*, 1998).

Antioxidant properties of *Plantago* flour extracts

To determine any potential antioxidant properties, we employed three benchmark antioxidant assays (Figure 8.4). Polyphenolic compounds are major water-soluble plant antioxidants and their relative content in the extracts was determined by Folin-Ciocalteu assay (Figure 8.4A). Phenolic content was highest in extracts from Australian native species. Phenolic content of all extracts was relatively low (less than 100 mg GAE/g) compared to extracts from vegetative and structural tissues of many species, but is within a typical range for seeds (Soong and Barlow, 2004) which are richer in other water-extractable components that may dilute the phenolic content in the extract. To determine the antioxidant action of the extracts, two different radical scavenging assays were employed. The ferric reducing antioxidant potential (FRAP) assay showed low antioxidant activity compared to ascorbic acid, the positive control (<0.2 vs ~20 mmol Fe^{2+}/g) (Figure 8.4B), however a study of 30 aqueous plant extracts found that FRAP capacity was always far lower than the positive control with a median value of 1.54 mmol Fe^{2+}/g (Dudonné *et al.*, 2009), much closer to the values seen in this study. To complement the FRAP assay we tested the capacity of the extracts to scavenge 2,2-diphenyl-1-picrylhydrazyl (DPPH) radicals (Figure 8.4C). In this dose-response assay, we found the extracts to be effective antioxidants with even low doses exhibiting scavenging activity (~20%). By estimating the EC_{50} values using a mathematical model we showed that extracts from Australian native species (PCE, PTE and PDE) are between 35% and 48% more effective antioxidants than POE.

To determine why the extracts appear to scavenge ferric and DPPH radicals differently, we analysed data from an extensive comparative study of plant-derived antioxidants

and related assays and found that while phenolic content, FRAP capacity and DPPH scavenging activity are strongly correlated, the correlation between FRAP and DPPH more frequently decoupled (Dudonné *et al.*, 2009). This would indicate that the assays are differentially responsive to individual antioxidants. We corroborated these conclusions, finding that while FRAP was strongly correlated with phenolic content (r = 0.77), DPPH had no correlation (r = 0.12). It is possible that the FRAP assay is preferentially detecting the action of phenolic compounds in the extracts while DPPH scavenging is a broader antioxidant measure, and thus may account for antioxidant activity of polysaccharides that are enriched in the extracts. This would corroborate previous studies that found polysaccharides isolated from *Plantago* seeds have antioxidant capacity due to the high number of hydroxyl groups on the highly substituted backbone (Yin *et al.*, 2010; Han *et al.*, 2016; Niu *et al.*, 2017).

Effect of *Plantago* flour extracts on IEC-6 and Caco-2 Cell Viability

Widely useful in cell biology, cell viability assays are often used to determine the cytotoxicity of a chemical or a mixture and are required as the first toxicological indication when introducing novel food ingredients or drugs (Stoddart, 2011). To provide an indication of any potential toxicity, we treated IEC-6 and Caco-2 cell lines with increasing concentrations of *Plantago* extracts and measured their viability by MTT assay (Figure 8.5 and Figure 8.6, respectively). Data presented here show that even the highest doses of *Plantago* extracts do not exhibit cytotoxic effects on IEC-6 or Caco-2 cells. Cubic spline models were used to study the non-linear relationship between dose and cell viability and indicated that only one treatment significantly reduced cell viability from the vehicle control: the lowest dose tested, 62.5 µg/mL, of PDE on Caco-2 cells (Figure 8.6B). However, since for higher doses the statistically significant effect was lost, it is likely to be an artefact of the cubic (third-order polynomial) modelling on what may be a linear relationship i.e. no impact of PDE (or

POE) on viability of Caco-2 compared to the vehicle control. The treatment of IEC-6 cells led to a significant increase in cell viability in the highest two doses of all four *Plantago* extracts tested here. At the highest dose, 500 µg/mL, PCE and PTE increased cell viability by around 30% from the vehicle control, while increases from POE and PDE were statistically significant but more modest at around 8%. Changes in the viability of Caco-2 cells were smaller and only the highest tested dose, 500 µg/mL, of PTE led to a statistically significant increase in cell viability (17% increase from the vehicle control). Patterns of the effect on cells were similar between both IEC-6 and Caco-2 where PCE and PTE both exhibited a pronounced upward curve while POE and PDE models were flatter. It was found that there was a strong positive correlation (r = 0.81) between viability effects of each extract on both cell types. The comparable effect on both cell lines is not unexpected due to the biomolecular similarity of the two cell lines (both intestine epithelium-derived and exhibiting enterocytic characteristics) and a similar result was also observed in our previous study (Barsby *et al.*, unpublished).

After review of the literature, we hypothesise that several factors are contributing to the enhancement of cell viability, which are summarised in Figure 8.7. Two main factors can lead to increased cell viability: a decrease in cell death or an increase in cell proliferation.

Cell death/apoptosis is often reduced when cells are protected against oxidative stress. Protection against induced oxidative stress by *Plantago* seed extracts has not been reported for any cell line *in vitro* but seed extracts from several species have been shown to have strong antioxidant properties linked to several constituents including phenolic secondary metabolites, minerals and polysaccharides (Yin *et al.*, 2010; Ye *et al.*, 2011; Zhou *et al.*, 2013; Han *et al.*, 2016; Niu *et al.*, 2017; Patel *et al.*, 2019). We identified that antioxidant minerals are present in the extracts in varying abundance

with iron and copper micronutrients particularly enriched in the extracts and possibly providing some oxidative protection (Hercberg *et al.*, 2006; Kilari *et al.*, 2010). Many polysaccharides are also well documented to protect against induced oxidative stress *in vitro*, however those from *Plantago* are seldom studied. Polysaccharides purified from *Ganoderma* and *Hizikia* mushrooms have been shown to reduce cell death by protecting against induced oxidative stress in IEC-6 cells (Choi *et al.*, 2010; G. Jiang *et al.*, 2018), an effect suggested to be linked to high polysaccharide substitution like that in *Plantago* (Yu *et al.*, 2017). Given their abundance in the extracts (Figure 8.2A), it is also compelling that particular motifs like rhamnose and arabinose side-chains in polysaccharides from *Aloe* and arabinose side chains in heteroxylan from rice bran were found to be key to the protective effect against induced oxidative stress (Kang *et al.*, 2014; Mendez-Encinas *et al.*, 2019). Given the antioxidant capacity of the extracts (Figure 8.4), it is possible that a reduction in oxidative stress is involved in the increase in cell viability observed in this study. However, as oxidative stress was not specifically induced, we suggest that the enhancement of cell proliferation is the more likely candidate.

A higher rate of cell proliferation means that more viable cells are produced and thus would lead to a higher cell viability measure. Several components that we have identified in the extracts could enhance cell proliferation. While a compound effect of multiple extract components is likely to be responsible, we hypothesise that extracted polysaccharides, particularly those derived from mucilage, play a key role as they comprise the largest part of the extract, they chemically vary substantially between species, and there are numerous indications in the literature of several bioactive properties. However, despite *Plantago* polysaccharides being relatively common dietary fibre supplements, we found no previous reports in the literature of the cytotoxic/proliferative effects of *Plantago* polysaccharides on any enterocyte cell lines

in vitro. In lieu of this, we have based our hypothesis on indications from studies of a) the effects of other polysaccharides on IEC-6/Caco-2 cells or b) the effects of *Plantago* polysaccharides on other cell types. Oral ingestion of polysaccharides extracted from *Acmella oleracea* was found to induce proliferation of rat enterocytes *in vivo* (Maria-Ferreira *et al.*, 2014), complemented by a follow-up study showing that purified, undigested *A. oleracea* polysaccharides still exhibited proliferative effects in Caco-2 cells *in vitro* (Maria-Ferreira *et al.*, 2018) potentially due to the activation of Toll-like receptors. A role for receptor activation was found in another study where proliferation was enhanced in *Capsosiphon fulvescens* polysaccharide-treated IEC-6 cells though the activation of the MAPK signalling pathway, a key pathway involved in cell proliferation. Polysaccharides from *P. ovata* seeds were not found to have significant cytotoxic effects on Vero green monkey kidney, HEp-2 human laryngeal, HeLa human cervical or HaCaT human skin cells (Deters *et al.*, 2005; Kulkarni *et al.*, 2005), all epithelial cell lines like IEC-6 and Caco-2, indicating no toxicity even at very high doses, in line with our findings. In fact, polysaccharides purified from *Plantago* seeds have been found to have proliferative effects on cells *in vitro.* From RNA analysis of activated signal pathways, it was found that aqueous extracts of *P. ovata* seeds (almost entirely composed of mucilage polysaccharides) could initiate the signal transduction cascade of keratinocyte growth factor (KGF) receptors in outer membranes and significantly increase the proliferation of HaCaT cells (Deters *et al.*, 2005). Additionally, polysaccharides isolated from *P. depressa* and *P. asiatica* seeds increase proliferation and maturation of dendritic cells (Huang *et al.*, 2014; Zhao *et al.*, 2014; Hu *et al.*, 2016) with this effect enhanced when the polysaccharides were modified by carboxymethylation (Jiang *et al.*, 2014) or acetylation (L. Jiang *et al.*, 2018) indicating that sidechains may be specifically interacting. Another study supported this by showing that the proliferation-enhancing effects of heteroxylan on a human enterocyte

line were masked when the polysaccharides were cross-linked, rendering the sidechains inaccessible (Mendez-Encinas *et al.*, 2019). A specific role for polysaccharide sidechains may explain the differential effects on cell viability between the different extracts as the polysaccharides extracted vary most based on sidechain substitution patterns (Cowley, Chapter 5) (Phan *et al.*, 2016; Cowley *et al.*, 2020). This could indicate that motifs influencing cell viability are more abundant or more effectual in PCE and PTE polysaccharides (which enhance cell viability to a greater degree than POE or PDE) and future diagnostic purification and hydrolysis could aid in the investigation of this hypothesis.

Conclusions and future directions

By treating two intestinal epithelial cell lines *in vitro* with mild aqueous extracts from seeds of four *Plantago* species we show that the seeds are unlikely to be toxic and may in fact provide gastrointestinal health-promoting benefits. Extracts from *P. cunninghamii* and *P. turrifera* flour were found to significantly increase cell viability of IEC-6 cells by around 30% and Caco-2 cells by around 15%. We hypothesise that several components in the extracts may have combined or even synergistic effects with highly-substituted polysaccharides from the seed mucilage possibly playing a key role in enhancing cell proliferation or protecting against oxidative stress. These activities could be confirmed through cell proliferation assays and imaging/marker analysis of cells with chemically-induced oxidative stress, respectively. Future work will aim to chromatographically purify these polysaccharides and subsequently treat cells to confirm their hypothesised role in enhancing cell viability while selective enzymatic hydrolysis of side chains may reveal which motifs have bioactivity. Similarly, diagnostic separation of other extract constituents is also possible and may unravel their roles in what are likely to be a complicated mix of bioactivities.

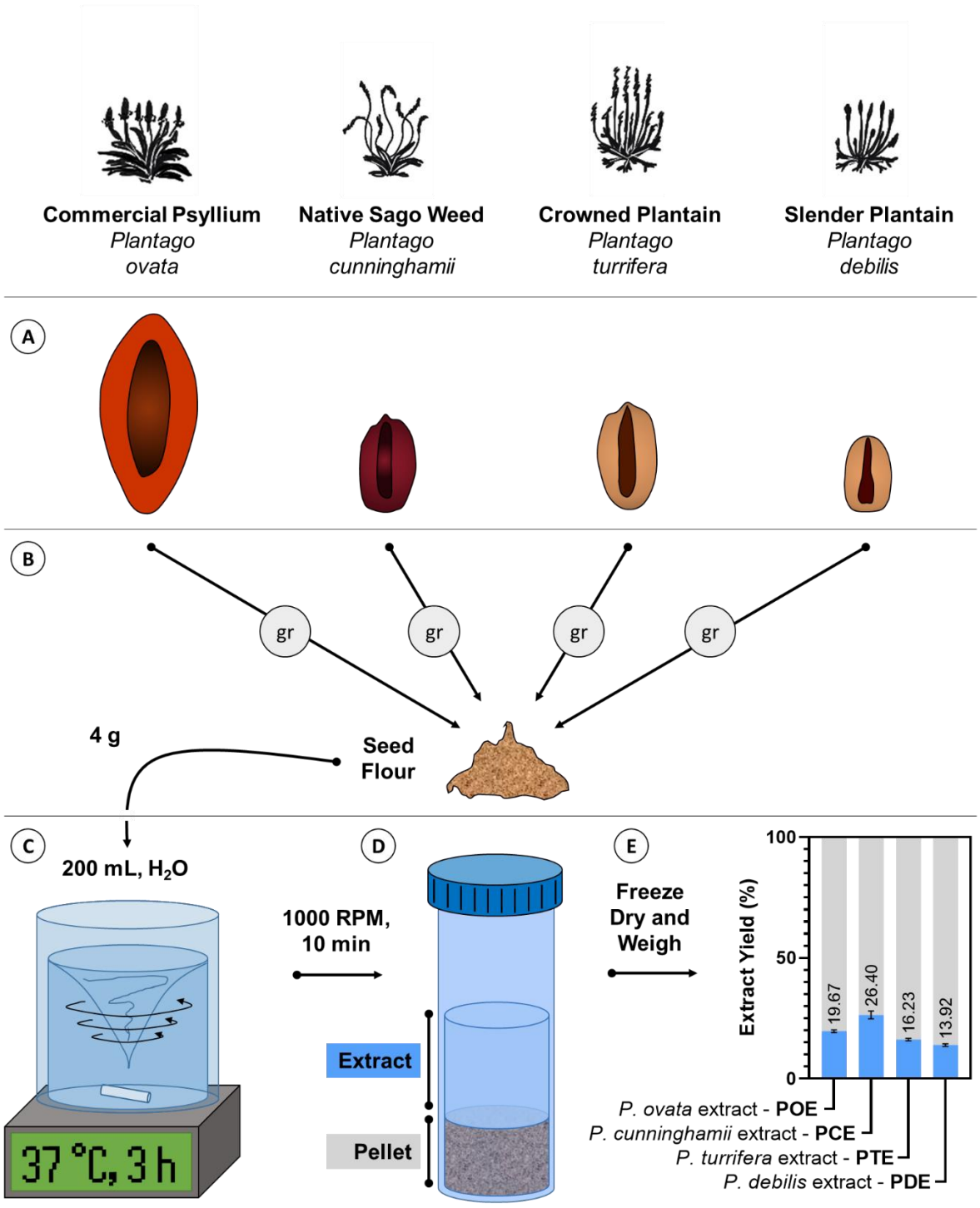

Figure 8.1. Schematic diagram of crude body temperature aqueous extract preparation. **A.** Whole, unextracted seeds are **B.** ground (gr) to flour. **C.** 5 g of seed flour was extracted in body temperature (37 °C) water for 3 h with intense mixing. **D.** Debris was pelleted by centrifugation and the aqueous extracts were decanted and dried. **E.** Dried extracts were weighed and compared against the starting material to determine the extract yield (mean ± SEM).

A

	POE	PCE	PTE	PDE
Protein Content				
Protein (% w/w)	10.52 ± 0.36	3.68 ± 0.04	6.16 ± 0.18	4.06 ± 0.10
Monosaccharide Content				
D-Mannose (% w/w)	1.53 ± 0.01	2.69 ± 0.03	2.36 ± 0.00	3.64 ± 0.05
D-Ribose (% w/w)	nd	nd	nd	nd
D-Rhamnose (% w/w)	2.24 ± 0.05	4.02 ± 0.02	2.96 ± 0.01	3.23 ± 0.06
D-Glucuronic Acid (% w/w)	nd	nd	nd	nd
D-Galacturonic Acid (% w/w)	3.37 ± 0.30	3.44 ± 0.21	3.78 ± 0.36	4.01 ± 0.62
D-Glucose (% w/w)	8.47 ± 0.08	8.32 ± 0.06	11.25 ± 0.79	11.50 ± 0.00
D-Galactose (% w/w)	5.93 ± 0.05	3.34 ± 0.05	4.48 ± 0.01	5.69 ± 0.08
D-Xylose (% w/w)	22.57 ± 0.22	33.89 ± 0.57	12.57 ± 0.11	9.36 ± 0.17
L-Arabinose (% w/w)	6.60 ± 0.00	9.96 ± 0.19	5.99 ± 0.04	5.79 ± 0.07
L-Fucose (% w/w)	nd	nd	nd	nd
Total (% w/w)	50.72 ± 0.55	65.66 ± 0.71	43.39 ± 1.02	43.23 ± 1.06
Mineral Content				
Na (mg/kg)	1229.22	1618.68	244.93	1036.22
Mg (mg/kg)	2357.01	3629.49	3493.11	4630.37
K (mg/kg)	28897.76	20253.84	23548.93	22922.30
Ca (mg/kg)	3443.80	4279.98	6674.34	6586.46
Cr (mg/kg)	3.30	2.05	1.96	1.87
Mn (mg/kg)	16.72	25.87	40.22	29.31
Fe (mg/kg)	67.70	54.44	78.37	84.53
Co (mg/kg)	0.53	0.04	0.20	0.03
Ni (mg/kg)	0.93	0.67	0.71	0.76
Cu (mg/kg)	18.78	24.36	44.40	24.16
Zn (mg/kg)	10.33	7.82	27.77	5.02
Se (mg/kg)	0.52	0.22	0.29	1.36
Mo (mg/kg)	0.47	0.10	0.15	0.32
I (mg/kg)	925.23	896.66	724.65	710.93
Total (% w/w)	3.697	3.079	3.488	3.603

B

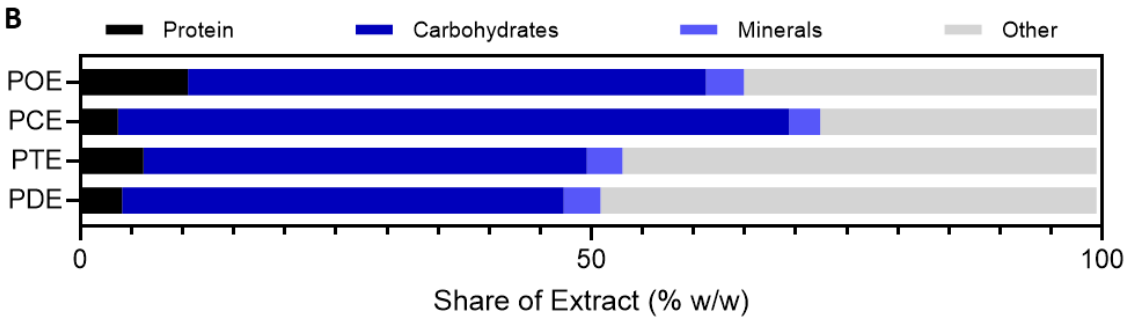

Figure 8.2. Summary of extract composition. **A.** Extract protein, monosaccharide, and mineral profiles. Values presented for protein and monosaccharide content are averages ± SEM while minerals are averages only (small error between technical repeats not shown). ND = not detected. **B.** Stacked graph summarising the quantified components in the extracts.

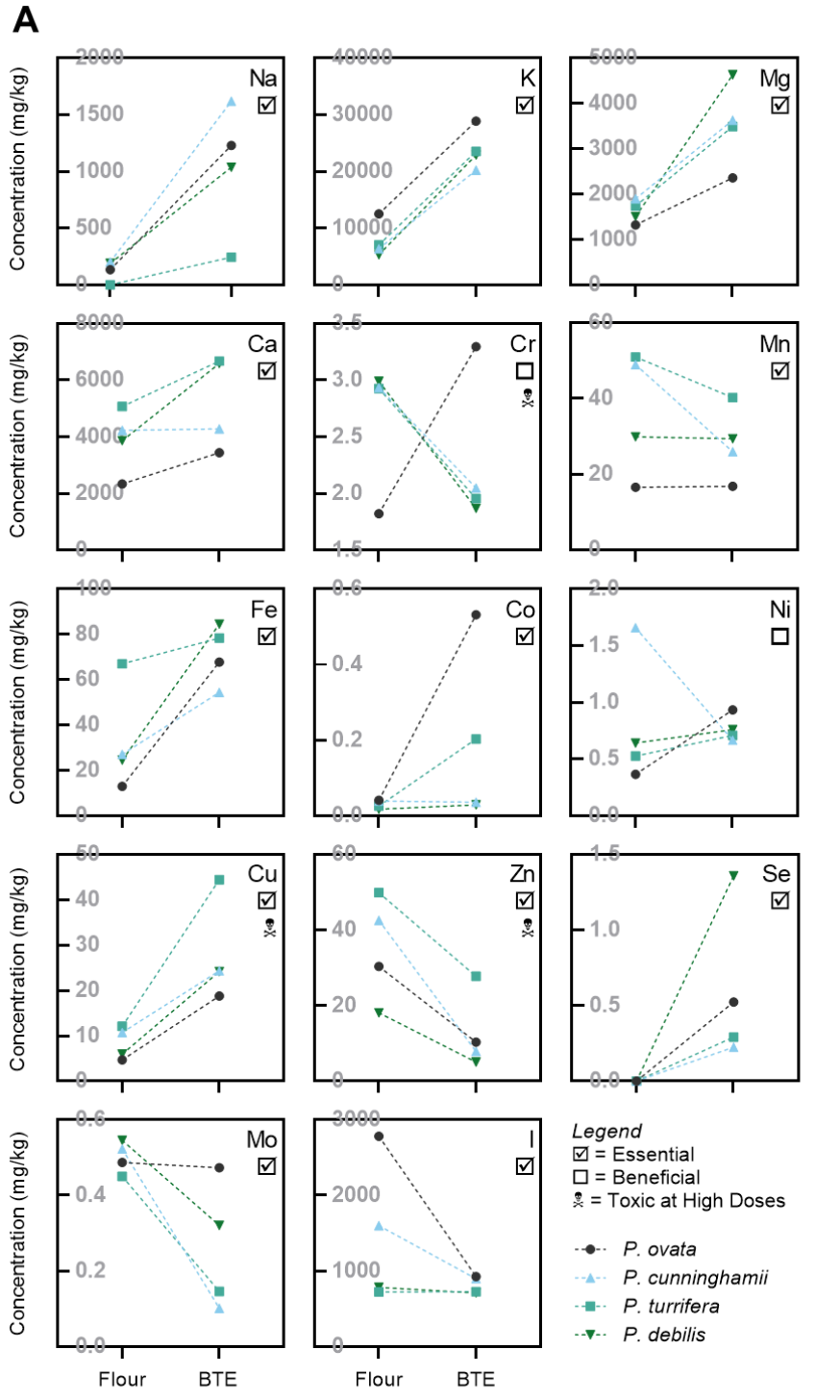
A
Concentration (mg/kg)
Na
K
Mg
Ca
Cr
Mn
Fe
Co
Ni
Cu
Zn
Se
Mo
I
Flour
BTE
Legend
☑ = Essential
☐ = Beneficial
☠ = Toxic at High Doses
P. ovata
P. cunninghamii
P. turrifera
P. debilis

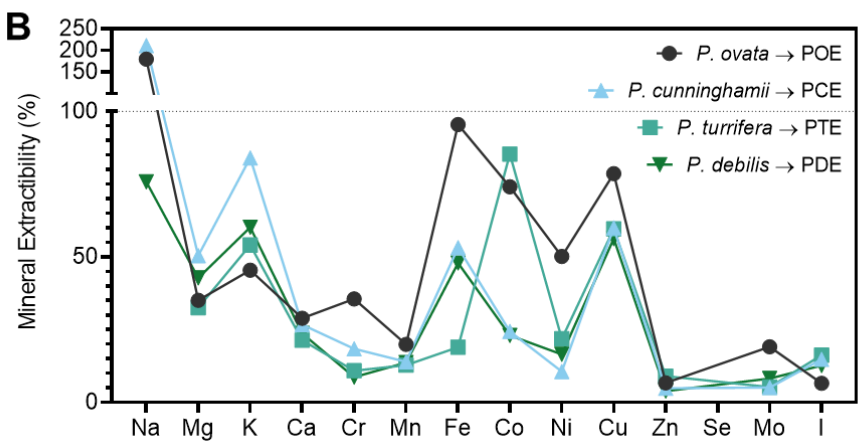
B
Mineral Extractibility (%)
P. ovata → POE
P. cunninghamii → PCE
P. turrifera → PTE
P. debilis → PDE
Na Mg K Ca Cr Mn Fe Co Ni Cu Zn Se Mo I

Figure 8.3. Mineral profiling comparing extracts to their source flour. **A.** Change in absolute mineral concentration from source flour to extract. **B.** Extractability of minerals from *Plantago* seed flour represented as the percentage of the whole seed sample found in the extract. Missing points denote those unable to be calculated due to values below the quantitation limit.

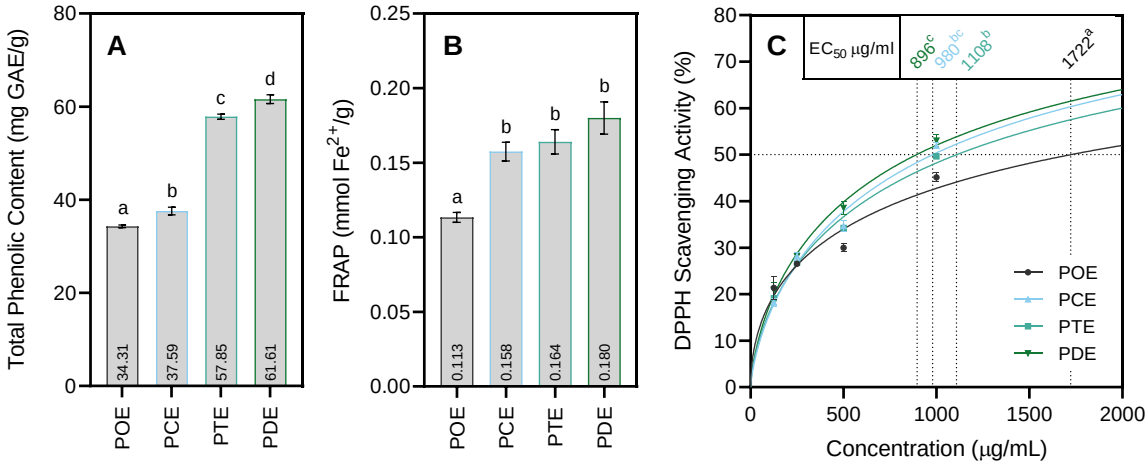

Figure 8.4. Antioxidant properties of *Plantago* flour extracts **A.** Total phenolic content **B.** Ferric reducing antioxidant potential (FRAP) **C.** 2,2-diphenyl-1-picrylhydrazyl (DPPH) radical scavenging activity.

Values are means ± SEM. Values within the bars are the plotted mean. Different letters at error bars and superscripts with the EC_{50} values in **C** indicate significant differences ($p < 0.05$) between extracts.

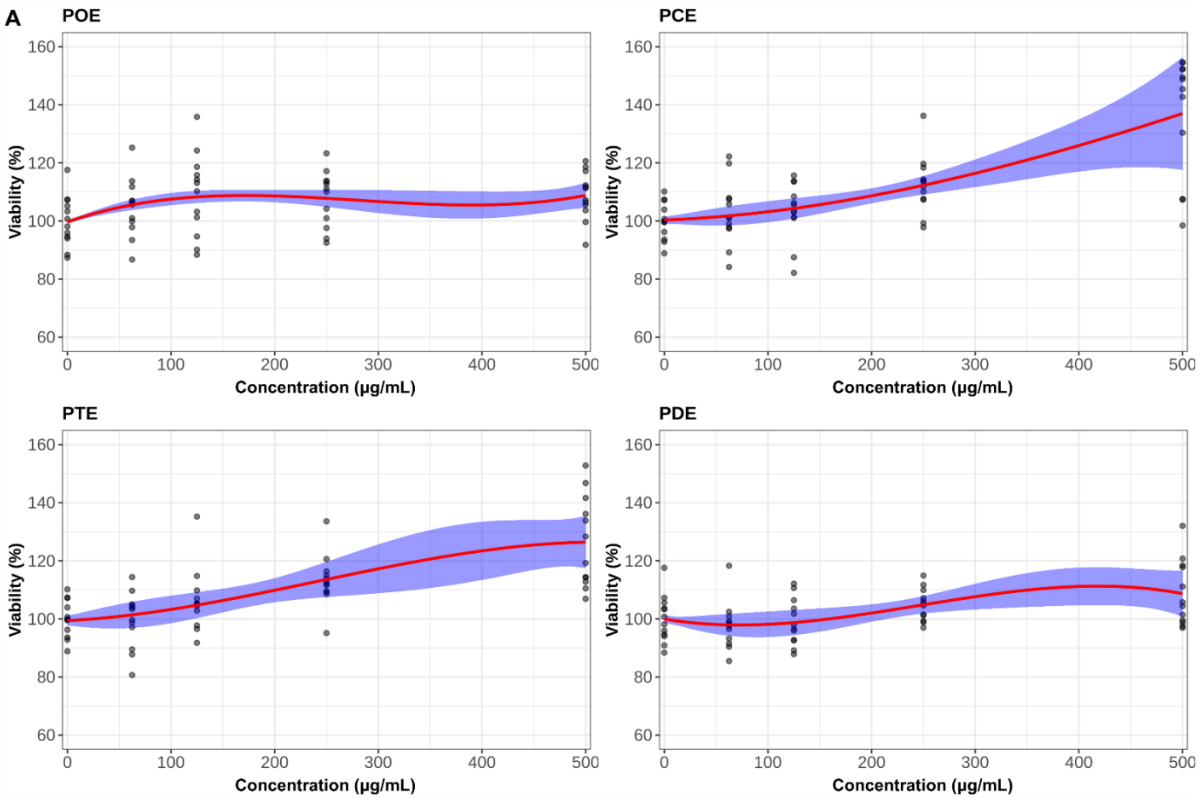

B

		POE	PCE	PTE	PDE
Control, 0 µg/mL	Estimated Mean ± SEM	100.00 ± 0.00	100.00 ± 0.00	100.00 ± 0.00	100.00 ± 0.00
	p-value	-	-	-	-
62.5 µg/mL	Estimated Mean ± SEM	**104.61 ± 1.10**	102.75 ± 2.85	99.55 ± 4.29	97.68 ± 2.74
	p-value	**<0.0001**	0.3343	0.9156	0.3978
125 µg/mL	Estimated Mean ± SEM	**109.15 ± 1.40**	103.47 ± 1.81	**106.33 ± 1.34**	98.95 ± 2.94
	p-value	**<0.0001**	0.0544	**<0.0001**	0.7212
250 µg/mL	Estimated Mean ± SEM	**107.60 ± 1.50**	**112.51 ± 1.58**	**113.18 ± 3.05**	**104.80 ± 1.48**
	p-value	**<0.0001**	**<0.0001**	**<0.0001**	**0.0012**
500 µg/mL	Estimated Mean ± SEM	**108.83 ± 2.14**	**136.99 ± 9.68**	**126.47 ± 4.46**	**108.70 ± 3.94**
	p-value	**<0.0001**	**0.0001**	**<0.0001**	**0.0272**

Figure 8.5. Dose-response of IEC-6 cell viability after treatment with *Plantago* flour extracts. **A.** Plotted dose-response models. **B.** Table of estimated mean viability plus the *p*-value of model contrasts comparing cell viability in a treatment to the vehicle control. Bolded values are statistically significant when compared to the vehicle control ($p > 0.05$).

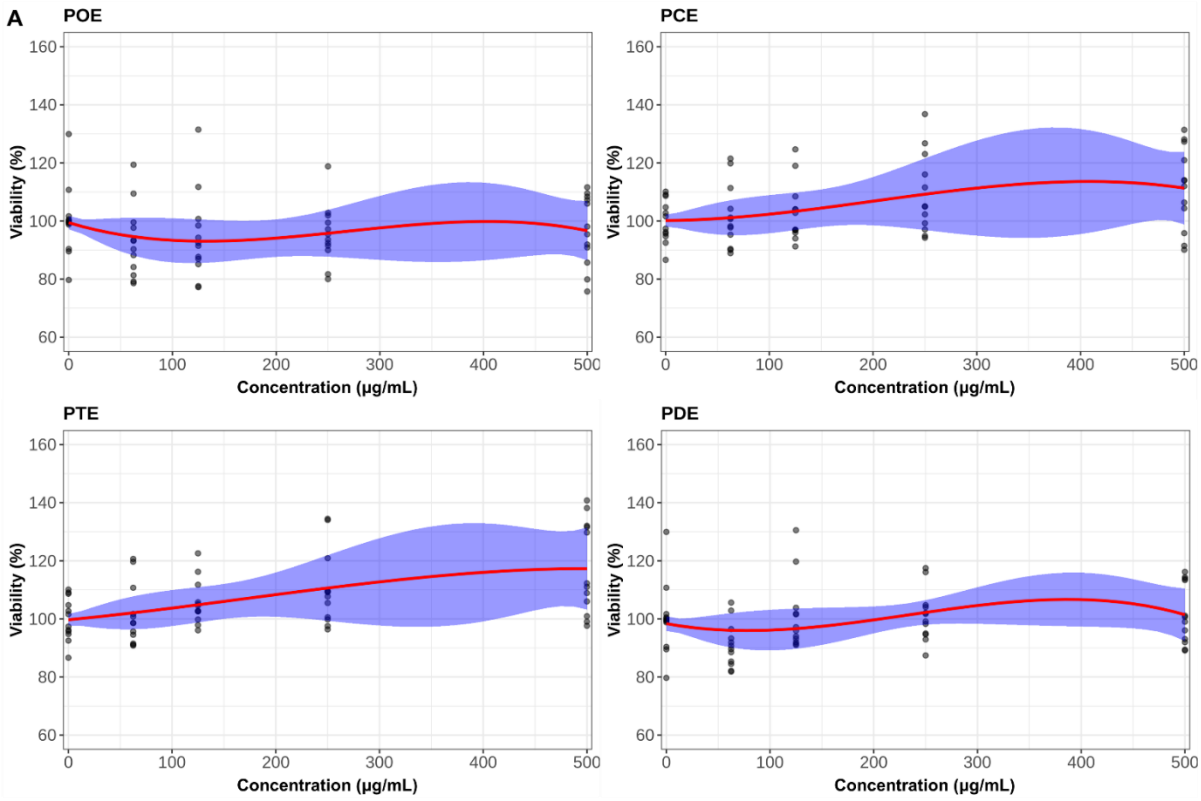

B

		POE	PCE	PTE	PDE
Control, 0 µg/mL	Estimated Mean ± SEM	100.00 ± 0.00	100.00 ± 0.00	100.00 ± 0.00	100.00 ± 0.00
	p-value	-	-	-	-
62.5 µg/mL	Estimated Mean ± SEM	92.86 ± 4.52	101.61 ± 4.98	101.19 ± 4.72	**91.07 ± 3.15**
	p-value	0.1137	0.7461	0.8003	**0.0046**
125 µg/mL	Estimated Mean ± SEM	94.59 ± 5.07	102.92 ± 3.63	105.64 ± 3.37	101.01 ± 4.35
	p-value	0.286	0.4224	0.0941	0.8171
250 µg/mL	Estimated Mean ± SEM	95.39 ± 4.06	109.33 ± 6.27	110.43 ± 5.74	101.13 ± 1.97
	p-value	0.2558	0.1372	0.0690	0.5662
500 µg/mL	Estimated Mean ± SEM	96.69 ± 5.10	111.32 ± 6.25	**117.35 ± 7.03**	101.52 ± 4.51
	p-value	0.5160	0.0702	**0.0136**	0.7365

Figure 8.6. Dose-response of Caco-2 cell viability after treatment with *Plantago* flour extracts. **A.** Plotted dose-response models. **B.** Table of mean viability plus the *p*-value of model contrasts comparing cell viability in a treatment to the vehicle control. Bolded values are statistically significant when compared to the vehicle control ($p > 0.05$).

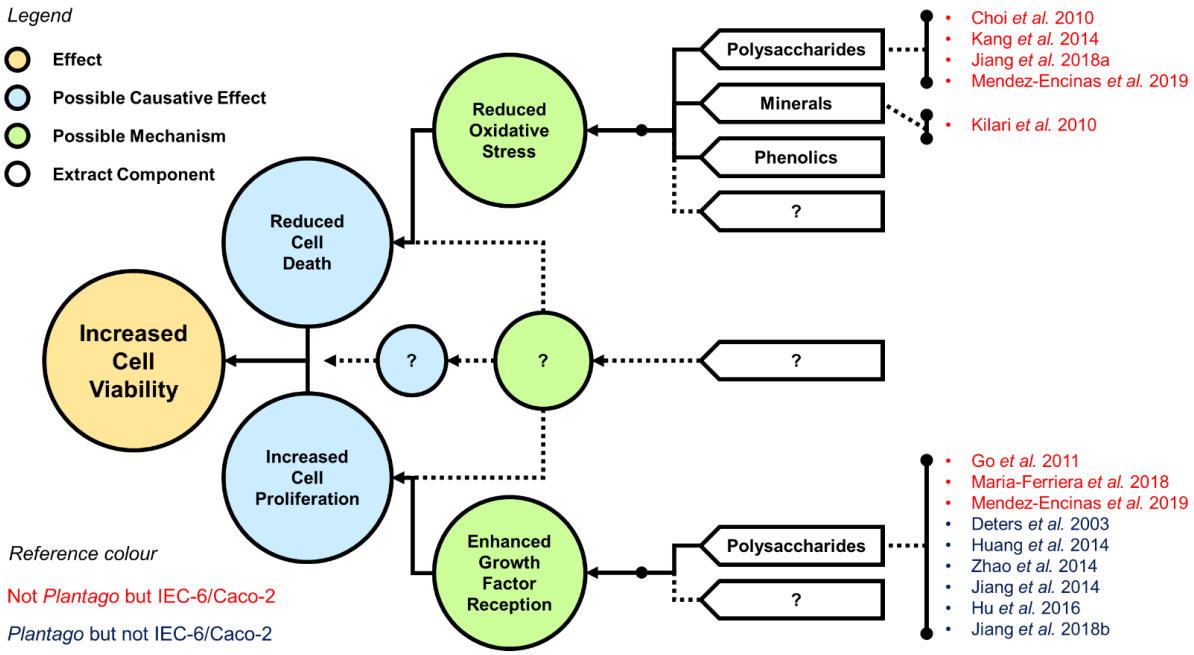

Figure 8.7. Flowchart summarising possible therapeutic effects of *Plantago* flour extract components that may lead to increased IEC-6 and Caco-2 cell viability, as inferred from available published results.

Declarations

Authors' Contributions

JMC, RAB and TBM conceived the experiments. JMC performed the extract preparation, extract characterisation, data analysis, prepared figures and wrote the manuscript. JPB and JMC performed the cell culture experiments. SYL performed statistical analysis of the cell culture experiments. SEPB provided access to the cell culture facility, cells and reagents. RAB and TBM also provided reagents, supervision and intellectual input.

Acknowledgments

The authors would like to thank Anh Nguyen for assistance and training in mammalian cell culture techniques and Shi Fang (Sandy) Khor for technical assistance.

References

Ahmed, Z., Rizk, A. and Hammoud, F. (1965) 'Phytochemical Studies of Egyptian Plantago species', *Journal of Pharmaceutical Sciences*, 156(1954), pp. 1060–1062.

Ainsworth, E. A. and Gillespie, K. M. (2007) 'Estimation of total phenolic content and other oxidation substrates in plant tissues using Folin-Ciocalteu reagent', *Nature Protocols*, 2(4), pp. 875–877.

Beara, I., Lesjak, M., Or, D., *et al.* (2012) 'Comparative analysis of phenolic profile, antioxidant, anti-inflammatory and cytotoxic activity of two closely-related Plantain species: Plantago altissima L. and Plantago lanceolata L.', *LWT - Food Science and Technology*, 47, pp. 64–70.

Beara, I., Lesjak, M., Cetijevic-Simin, D., *et al.* (2012) 'Phenolic profile, antioxidant, anti-inflammatory and cytotoxic activities of endemic Plantago reniformis G. Beck', *Food Research International*, 49, pp. 501–507.

Benzie, I. F. F. and Strain, J. J. (1996) 'The Ferric Reducing Ability of Plasma (FRAP) as a Measure of "' Antioxidant Power '": The FRAP Assay', 76, pp. 70–76.

Capitani, M. I. *et al.* (2015) 'Rheological properties of aqueous dispersions of chia (Salvia hispanica L.) mucilage', *Journal of Food Engineering*. Elsevier Ltd, 149, pp. 70–77.

Chen, Z., Bertin, R. and Froldi, G. (2013) 'EC50 estimation of antioxidant activity in DPPH* assay using several statistical programs', *Food Chemistry*. Elsevier Ltd, 138(1), pp. 414–420.

Choi, E. Y., Hwang, H. J. and Nam, T. J. (2010) 'Protective effect of a polysaccharide from Hizikia fusiformis against ethanol-induced cytotoxicity in IEC-6 cells', *Toxicology in Vitro*. Elsevier Ltd, 24(1), pp. 79–84.

Comino, P. *et al.* (2013) 'Separation and purification of soluble polymers and cell wall fractions from wheat, rye and hull less barley endosperm flours for structure-nutrition studies', *J Agric Food Chem*, 61(49), pp. 12111–12122. Available at: http://pubs.acs.org/doi/pdfplus/10.1021/jf403558u.

Cowley, J. M. *et al.* (2020) 'A small- scale fractionation pipeline for rapid analysis of seed mucilage characteristics', *Plant Methods*. BioMed Central, 16(20), pp. 1–12.

Deters, A. M., Smiatek, T. and Hensel, A. (2005) 'Ispaghula (Plantago ovata) Seed Husk Polysaccharides Promote Proliferation of Human Epithelial Cells (Skin Keratinocytes and Fibroblasts) via Enhanced Growth Factor Receptors and Energy Production'.

Dudonné, S. *et al.* (2009) 'Comparative study of antioxidant properties and total phenolic content of 30 plant extracts of industrial interest using DPPH, ABTS, FRAP, SOD, and ORAC assays', *Journal of Agricultural and Food Chemistry*, 57(5), pp. 1768–1774.

Fernandes, S. and Salas-Mellado, M. (2017) 'Addition of chia seed mucilage for reduction of fat content in bread and cakes', *Food Chemistry*. Elsevier Ltd, 227, pp. 237–244.

Gálvez, M. *et al.* (2003) 'Cytotoxic effect of Plantago spp. on cancer cell lines', *Journal of Ethnopharmacology*, 88, pp. 125–130.

Glahn, R. P. *et al.* (1998) 'Caco-2 Cell Ferritin Formation Predicts Nonradiolabeled Food Iron Availability in an In Vitro Digestion/Caco-2 Cell Culture Model', *The Journal of Nutrition*, 128(9), pp. 1555–1561.

Gott, B. (2006) 'Plant Species used by Aborigines of South-Eastern Australia'. Clayton, Vic: Monash University.

Han, N. *et al.* (2016) 'Optimization and antioxidant activity of polysaccharides from Plantago depressa', *International Journal of Biological Macromolecules*. Elsevier B.V., 93, Part A, pp. 644–654.

Harput, U. S., Genc, Y. and Saracoglu, I. (2012) 'Cytotoxic and antioxidative activities of Plantago lagopus L. and characterization of its bioactive compounds', *Food and Chemical Toxicology*. Elsevier Ltd, 50(5), pp. 1554–1559.

Hassan, A. S. *et al.* (2017) 'A Genome Wide Association Study of arabinoxylan content in 2-row spring barley grain', *PLoS ONE*, 12(8), pp. 1–19.

Hercberg, S., Czernichow, S. and Galan, P. (2006) 'Antioxidant vitamins and minerals in prevention of cancers: lessons from the SU.VI.MAX study', *British Journal of Nutrition*, 96(S1), pp. S28–S30.

Hofstee, P. *et al.* (2019) 'Maternal selenium deficiency during pregnancy in mice increases thyroid hormone concentrations, alters placental function and reduces fetal growth', *The Journal of Physiology*, 0, pp. 1–21.

Hu, Z. *et al.* (2016) 'Immunomodulation activity of alkali extract polysaccharide from Plantago asiatic L . seeds', *RSC Advances*, 6, pp. 76312–76317.

Huang, D. *et al.* (2014) 'A novel polysaccharide from the seeds of Plantago asiatica L. Induces dendritic cells maturation through toll-like receptor 4', *International Immunopharmacology*. Elsevier B.V., 18(2), pp. 236–243.

Jiang, G. *et al.* (2018) 'Protective effects of a: Ganoderma atrum polysaccharide against acrylamide induced oxidative damage via a mitochondria mediated intrinsic apoptotic pathway in IEC-6 cells', *Food and Function*, 9(2), pp. 1133–1143.

Jiang, L. *et al.* (2018) 'Acetylation Modification Improves Immunoregulatory Effect of Polysaccharide from Seeds of Plantago asiatica L .', *Journal of Chemistry*, 2018, pp. 1–10.

Jiang, L. M. *et al.* (2014) 'Carboxymethylation enhances the maturation-inducing activity in dendritic cells of polysaccharide from the seeds of Plantago asiatica L.', *International Immunopharmacology*. Elsevier B.V., 22(2), pp. 324–331.

Kang, M. C. *et al.* (2014) 'In vitro and in vivo antioxidant activities of polysaccharide purified from aloe vera (Aloe barbadensis) gel', *Carbohydrate Polymers*. Elsevier Ltd., 99, pp. 365–371.

Kartini *et al.* (2014) 'HPTLC simultaneous quantification of triterpene acids for quality control of Plantago major L. and evaluation of their cytotoxic and antioxidant activities', *Industrial Crops & Products*. Elsevier B.V., 60, pp. 239–246.

Kilari, S., Pullakhandam, R. and Nair, K. M. (2010) 'Zinc inhibits oxidative stress-induced iron signaling and apoptosis in Caco-2 cells', *Free Radical Biology and Medicine*. Elsevier Inc., 48(7), pp. 961–968.

Kulkarni, G. *et al.* (2005) 'In vitro cytotoxicity and in vivio acute toxicity of selected polysaccharide hydrogels as pharmaceutical excipients', *Oriental Pharmacy and Experimental Medicine*, 5(1), pp. 29–36.

Kumar, P., Nagarajan, A. and Uchil, P. D. (2019) 'Analysis of Cell Viability by the MTT Assay', pp. 469–472.

Low, T. (1988) *Wild Food Plants of Australia*. North Ryde: Angus & Robertson Publishers.

Maria-Ferreira, D. *et al.* (2014) 'Rhamnogalacturonan from Acmella oleracea (L.) R.K. Jansen: Gastroprotective and ulcer healing properties in rats', *PLoS ONE*, 9(1).

Maria-Ferreira, D. *et al.* (2018) 'Rhamnogalacturonan, a chemically-defined polysaccharide, improves intestinal barrier function in DSS-induced colitis in mice and human Caco-2 cells', *Scientific Reports*, 8(1), pp. 1–14.

Mendez-Encinas, M. A. *et al.* (2019) 'Arabinoxylan-Based Particles: In Vitro Antioxidant Capacity and Cytotoxicity on a Human Colon Cell Line', *Medicina*, 55(349), pp. 1–19.

Muñoz, L. A. *et al.* (2012) 'Chia seeds: Microstructure, mucilage extraction and hydration', *Journal of Food Engineering*, 108(1), pp. 216–224.

Niu, Y. *et al.* (2017) 'A new heteropolysaccharide from the seed husks of Plantago asiatica L. with its thermal and antioxidant properties', *Food Funct.*

Otegui, M. S., Capp, R. and Staehelin, L. A. (2002) 'Developing seeds of Arabidopsis store different minerals in two types of vacuoles and in the endoplasmic reticulum', *Plant Cell*, 14(6), pp. 1311–1327.

Patel, M. K. *et al.* (2019) 'Physicochemical, scavenging and anti-proliferative analyses of polysaccharides extracted from psyllium (Plantago ovata Forssk) husk and seeds', *International Journal of Biological Macromolecules*. Elsevier B.V., 133, pp. 190–201.

Phan, J. *et al.* (2016) 'Differences in glycosyltransferase family 61 accompany variation in seed coat mucilage composition in Plantago spp.', *Journal of Experimental Botany*, 67(22), pp. 6481–6495.

Prego, I., Maldonado, S. and Otegui, M. (1998) 'Seed structure and localization of reserves in Chenopodium quinoa', *Annals of Botany*, 82(4), pp. 481–488.

R Core Team (2012) 'R: A language and environment for statistical computing'. Available at: http://www.r-project.org/.

Romero-Baranzini, A. L. *et al.* (2006) 'Chemical, physicochemical, and nutritional evaluation of Plantago (Plantago ovata Forsk)', *Cereal Chemistry*, 83(4), pp. 358–362.

Sambruy, Y. *et al.* (2001) 'Intestinal Cell Culture Models: Applications in Toxicology and Pharmacology', *Cell Biology and Toxicology*, 17, pp. 301–317.

Samuelsen, A. B. (2000) 'The traditional uses, chemical constituents and biological activities of Plantago major L. A review', *Journal of Ethnopharmacology*, 71(1), pp. 1–21.

Segura-Campos, M. *et al.* (2014) 'Whole and crushed nutlets of chia (Salvia hispanica) from Mexico as a source of functional gums', *Food Science and Technology (Campinas)*, 34(4), pp. 701–709.

Shewry, P. R., Napier, J. A. and Tatham, A. S. (1995) 'Seed Storage Proteins: Structures and Biosynthesis', *The Plant Cell*, 7(July), pp. 945–956.

Shi, M. *et al.* (2012) 'Bioactivity of the crude polysaccharides from fermented soybean curd residue by Flammulina velutipes', *Carbohydrate Polymers*. Elsevier Ltd., 89(4), pp. 1268–1276.

Soong, Y. Y. and Barlow, P. J. (2004) 'Antioxidant activity and phenolic content of selected fruit seeds', *Food Chemistry*, 88(3), pp. 411–417.

Stoddart, M. (2011) 'Cell Viability Assays: Introduction', in *Mammalian Cell Viability: Methods and Protocols*, pp. 1–7.

Velasco-Lezama, R. *et al.* (2006) 'Effect of Plantago major on cell proliferation in vitro', *Journal of Ethnopharmacology*, 103, pp. 36–42.

Wood, J. *et al.* (2018) 'Genetic and environmental factors contribute to variation in cell wall composition in mature desi chickpea (Cicer arietinum L .) cotyledons', *Plant Cell and Environment*, 41(November 2017), pp. 2195–2208.

Ye, C. L., Hu, W. L. and Dai, D. H. (2011) 'Extraction of polysaccharides and the antioxidant activity from the seeds of Plantago asiatica L.', *International Journal of Biological Macromolecules*. Elsevier B.V., 49(4), pp. 466–470.

Yin, J. Y. *et al.* (2010) 'Chemical characteristics and antioxidant activities of polysaccharide purified from the seeds of Plantago asiatica L', *Journal of the Science of Food and Agriculture*, 90(2), pp. 210–217.

Yu, L. *et al.* (2017) 'Multi-layer mucilage of Plantago ovata seeds: Rheological differences arise from variations in arabinoxylan side chains', *Carbohydrate Polymers*. Elsevier Ltd., 165, pp. 132–141.

Zhao, H. *et al.* (2014) 'Purification, characterization and immunomodulatory effects of Plantago depressa polysaccharides', *Carbohydrate Polymers*. Elsevier Ltd., 112, pp. 63–72.

Zhou, Q. *et al.* (2013) 'Identification and quantification of phytochemical composition and anti-inflammatory, cellular antioxidant, and radical scavenging activities of 12 Plantago species', *Journal of Agricultural and Food Chemistry*, 61(27), pp. 6693–6702.

CHAPTER 9

Summary and future directions

This chapter was written to the sounds of...

Album	Parcels
Artist	Parcels
Favourite Song	Tieduprightnow

Thesis Summary

Work presented in this thesis has demonstrated the feasibility of using mucilage-containing flour from seeds of diverse *Plantago* species in food and human health applications.

Typical seed mucilage extraction techniques are often incomplete, time-consuming and are not adapted for use with precious seed stocks. In Chapter 3, we developed a small-scale method for fractionating seed mucilage from just a few milligrams of seed that can be performed on multiple samples in parallel. The fractionation technique provides information about the macromolecular properties of the mucilage polysaccharides including extractability, yield and composition. The utility of the method was proven in its ability to (1) discern intergeneric, interspecific and intraspecific variation in mucilage properties, (2) screen for known mucilage quality traits in field grown samples and (3) identify lines of interest from a mucilage-producing germplasm set.

Data presented in Chapter 3 reiterated the differences in mucilage properties between the model species *Arabidopsis* and *Plantago* species and further highlighted the need to better understand mucilage-related processes in *Plantago*. In Chapter 4, the mucilage accumulation, storage and release mechanism of *P. ovata* is described, and demonstrated to be different to *Arabidopsis* in a number of aspects. Understanding the way *P. ovata* mucilage polysaccharides form a laminated cell-free layer on the mature seed surface has significant implications for the mucilage release process. Mucilage release was determined to be a passive process of hydration and expansion away from the seed, mediated by specific types of polysaccharides. Understanding the mucilage release dynamics in *P. ovata* has direct implications for interpreting mucilage functionality in other *Plantago* species.

In Chapter 5, we described the natural variation in seed composition and morphology of twelve Australian *Plantago* species. Using microscopic and chromatographic techniques we showed that *Plantago* species have a substantial mannan-rich endosperm with abundant low molecular weight reserve sugars which may represent untapped fermentable dietary fibres. Australian *Plantago* species were also found to be potentially more nutritious than commercial psyllium as they contain more protein and beneficial fats. Using the published method described in Chapter 3 we also expanded on previous knowledge of *Plantago* mucilage properties by showing that the composition of differentially-extracted fractions of mucilage differs within a species while trends were clear between same fractions of different species. These findings complemented the sequential layer-mediated mucilage release/hydration model described in Chapter 4 by showing that the composition of the fractions could be related directly to other *in situ* functional properties like the water absorption capacity which differed between species. These differences in functionality, in addition to findings of beneficial nutrients in non-mucilage producing seed tissues, highlighted the possibility of using flours prepared from different *Plantago* species as hydrocolloids in food production.

In Chapters 6 and 7, we described the use of *Plantago* flour as hydrocolloid replacements in starchy food systems. In Chapter 6, different flours were found to exert variable influences on the gelatinisation and storage properties of rice flour and rice starch, but distinct similarities were observed between Australian species. Changes were attributed to mucilage content and structure and an explanatory model for a novel polysaccharide-polysaccharide interaction was developed. This model was expanded further in Chapter 7, where *Plantago* flour was found to strengthen gluten-free doughs, directly leading to improved bread structure and texture. Variation in the degree of

improvement was attributed, in part, to the polysaccharide-polysaccharide interaction described in Chapter 6 and an adapted, complementary model was developed.

In Chapter 5, we showed that *Plantago* flour was a nutritious ingredient that in Chapter 7 was shown to significantly improve the quality of gluten-free products through an interaction studied and described in Chapter 6. In Chapter 8 we were interested in any further health benefits that could occur through the consumption of *Plantago* flour-containing food and health products. In this study, we treated *in vitro*-grown small and large intestinal epithelial cells with aqueous extracts prepared from four *Plantago* flours deemed to perform well in Chapters 6 and 7. It was found that no flour was cytotoxic and high doses of flour extract from Australian native *Plantago* species were found to enhance viability of these cell lines. A possible link was made between mucilage heteroxylans that were in the extract and the enhancement of cell viability, and possible mechanisms for inducing cell proliferation were discussed.

In summary, we have (1) developed a robust method for screening mucilage properties in precious seed stocks (Chapter 3) which aided in (2) demonstrating that mucilage-related processes in *P. ovata* are not necessarily comparable to those in model species *Arabidopsis* (Chapter 4). (3) Whole *Plantago* seeds contain beneficial nutrients that are typically wasted during manufacturing and natural variation in seed composition may lead to variations in functional properties (Chapter 5) which (4) we demonstrated through their use as hydrocolloid replacements in starchy food systems (Chapters 6 and 7). (5) The use of *Plantago* flour as food additives may have added benefits as antioxidant sources and promote gut cell health (Chapter 8).

Limitations and Future Directions

1 – Explicit polysaccharide structural characterisation

We recognise that a significant limitation of this work is the non-structural nature of chemical analyses used to characterise the functional polysaccharides. As mentioned throughout the thesis, monosaccharide profiling provides the ability to only estimate the degree of substitution based on molar ratios of each monosaccharide with insight from previous structural analyses in these systems. It will be extremely insightful to continue to structurally characterise key polysaccharide types identified in this study in order to better understand their functionality. A continued collaboration with the University of Nottingham's School of Biosciences and a new collaboration with the University of Cambridge will combine Nuclear Magnetic Resonance (NMR) techniques with Polysaccharide Analysis using Carbohydrate Electrophoresis (PACE) to define the fine structural differences in mucilage heteroxylan structure.

Furthermore, details about the composition and fine structure of mannan polysaccharides found to be abundant in the *Plantago* endosperm cell walls are unknown. Again, a collaboration with the University of Cambridge will employ PACE to elucidate and compare mannan structures.

2 – Define heteroxylan 'blockiness' and its effect on polysaccharide interactivity

Preliminary work is beginning to show that variation in heteroxylan 'blockiness' may change with fractionation. Combining structural characterisation techniques mentioned above with more fundamental and in-food functionality analyses may further unpick the mode of heterotypic polysaccharide interactions described in Chapters 6 and 7 and the implications it may have for industrial use.

3 – Agronomic traits of Australian *Plantago* species

From this work, we have anecdotal evidence of Australian *Plantago* species displaying several agronomic advantages over commercial psyllium including drought, salt, and disease tolerance and resistance to shattering. It would be extremely useful to experimentally confirm these advantages which would have a huge impact on their potential commercial expansion and use. Such experiments, along with field trials to determine production feasibility, are planned.

4 – Diversity in mucilage accumulation, storage and release mechanisms in *Plantago*

Preliminary findings during this work (not presented) suggest that some but not all features of mucilage accumulation, storage and release described for *P. ovata* in Chapter 4 are shared in Australian *Plantago* species. It would be interesting to mirror the work in Chapter 4 in a study focussed on a key Australian species like *P. cunninghamii*, which is known to have a similar surface morphology but different expanded mucilage architecture. Notably, *P. cunninghamii* (along with many other species studied in this thesis) release specialised seed coat cells that reside within the expanded mucilage envelope and it is interesting to speculate on the 'scaffolding' role these may have on the robustness of the expanded mucilage envelope. Developmental characterisation including transcriptomic analysis, perhaps through laser capture microdissection, may give further insight into the function of these cells and the synthesis and deposition of the mucilage polysaccharides they associate with.

5 – Gastrointestinal benefits of *Plantago* seed consumption

We have shown that diversity in heteroxylan content and structure play a significant role in the in-food functionality of *Plantago* whole seed flour. These structural

differences may have added health benefits in a number of ways, one of which we studied in Chapter 8. Commercial psyllium heteroxylan is a useful dietary fibre that promotes laxation due to the water holding ability of its complex sidechains, but this property appears to directly prevent its fermentation in the human gut. It is possible that structural differences found in other *Plantago* species studied here may allow them to be fermentable or partially-fermentable in the gut. A partially-fermentable heteroxylan would be of great interest as it may provide the laxative benefits of commercial psyllium while still providing a fermentable material for the microbiome to produce beneficial short chain fatty acids (SCFA). *In vitro* fermentation work to determine fermentability and SCFA production could be complemented with pre-clinical and clinical nutritional studies to assess differential effects on animal and human health and even shifts in the microbiome.

APPENDICES

This chapter was written to the sounds of...

Album	Flying
Artist	Garth Stevenson
Favourite Song	The Southern Sea

Appendix I

Cellular debris, not mucilage polysaccharides, dominate extracts of *Plantago ovata* and *Plantago lanceolata* calli grown *in vitro*

James M. Cowley, Lina Herliana, Natalie S. Betts and Rachel A. Burton

https://doi.org/10.1101/2020.06.15.153395

This contradictory result pre-print posted to bioRxiv reports on research performed in the first few months of my PhD candidature when the project was still under development. One research area of interest was the efficient *in vitro* production of mucilage polysaccharides reported in many publications. Replicating the techniques, we found the methods to be flawed and the pre-print reports on data demonstrating this, which we thought important to provide to the research community interested in mucilage polysaccharides.

Cellular debris, not mucilage polysaccharides, dominate extracts of *Plantago ovata* and *Plantago lanceolata* calli grown *in vitro*

James M. Cowley*, Lina Herliana, Natalie S. Betts, and Rachel A. Burton

Australian Research Council Centre of Excellence in Plant Cell Walls, School of Agriculture, Food and Wine, University of Adelaide, Waite Campus, Urrbrae, SA, Australia. *Corresponding author: james.cowley@adelaide.edu.au

Abstract

Mucilage is a hydrophilic mixture of polysaccharides produced by seeds of many species, and used in research, industrial processes and as human health supplements. As such, demand often outweighs supply. In recent years, several researchers have reported that mucilage can be produced efficiently from *in vitro*-cultured calli as a direct 'plant-less' alternative to seed mucilage; however, this mucilage has not been rigorously characterised. Here we replicate previously published culturing and extraction procedures and couple them with compositional analysis to determine whether the mucilage produced from *Plantago ovata* and *P. lanceolata* calli are similar to seed mucilage. Our monosaccharide profiling and microscopy show that, while calli derived from either seedling hypocotyls or roots yield more material than seeds using the same extraction techniques, the majority of extract mass is cellular debris. Debris polysaccharide composition was significantly different to seed mucilage from both species. Plant tissue culture as an alternative source of high yields of useful mucilage polysaccharides, at least by these and similar methods, is likely to not be possible.

Keywords

Mucilage; *in vitro*; *Plantago;* callus; mucilaginous callus; polysaccharide; plant tissue culture

Introduction

Upon wetting, seeds of many plant species produce a sticky gel coating called mucilage. Mucilage consists primarily of highly hydrophilic polysaccharides, whose composition differs greatly between species[1]. Seed mucilage has research significance as a tool to study polysaccharide biosynthesis[2], industrial significance as food hydrocolloids[3], and health applications as viscous dietary fibres[4]. Demand for mucilage-producing seeds like psyllium (*Plantago ovata*) often exceeds supply due to agronomic constraints and large requirements in industrial and pharmaceutical applications, and so alternate sources of mucilage polysaccharides, such as *in vitro* production, is desirable.

Since early tissue culture experiments, increases in exogenous auxins were found to stimulate polysaccharide production[5–8]. Notably, calli of *Arabidopsis thaliana* stimulated with an exogenous auxin (2,4-

dichlorophenoxyacetic acid; 2,4-D) would produce polysaccharides with a cell wall-like composition[8]. Undifferentiating calli producing polysaccharides with no assigned function or localisation—mucilage—are therefore referred to as mucilaginous calli (Figure 1). More recently, significant interest has been placed on mucilaginous calli as *ex planta* sources of commercial mucilage. It has been reported that mucilage produced from mucilaginous calli can be easily extracted to yield quantities significantly higher than seed-derived mucilage. Recent work reported that calli derived from *Plantago lanceolata*[9], *P. ovata*[10,11], *P. major*[12], *Lepidium sativum*[13,14], *Linum usitatissimum*[15] and several *Alyssum* species[16] could produce significantly (up to 10×) more mucilage than their respective seeds. As seed-derived mucilage from all of these species are important folk remedies, and that from *L. usitatissimum* and *Plantago* species have established industrial applications, this sort of efficient alternative production system would be of significant commercial interest. However, no studies have rigorously compared the composition and/or functional properties of callus- versus seed-derived mucilage to assess the feasibility of *in vitro* mucilage production. Due to our research group's interest in seed mucilage, we were curious about the efficiency and possible applications of such methods so the aim of this work was to compare the composition of mucilage produced by calli to seed mucilage from two *Plantago* species.

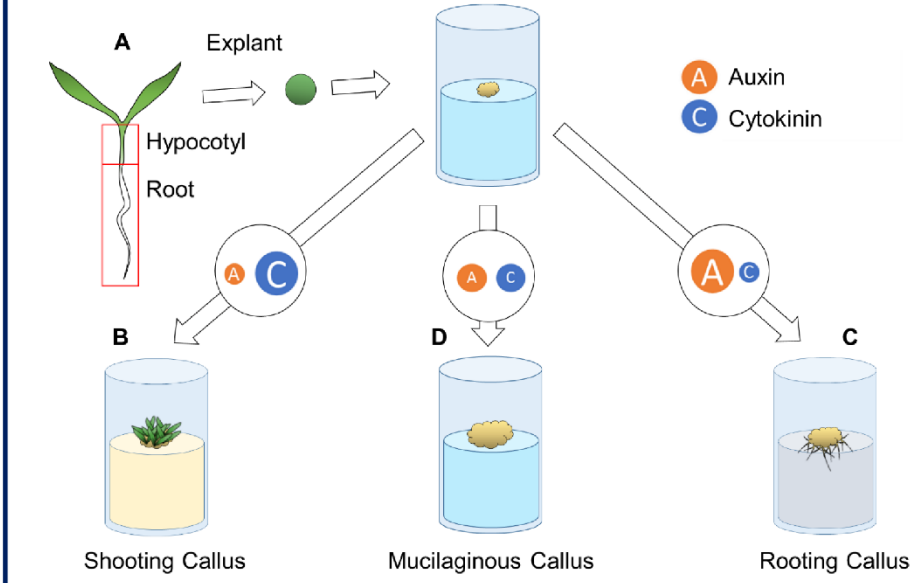

Figure 1. Varying levels of exogenous plant growth regulators can induce morphologically different calli *in vitro*. **A.** Pluripotent plant tissue explants (often hypocotyl or root) are used to induce callus. **B.** Low auxin:cytokinin favours shoot regeneration. **C.** High auxin:cytokinin favours root regeneration. **D.** When auxin and cytokinin are balanced, cells do not differentiate into distinct tissues and are referred to as mucilaginous calli.

Results and Discussion

As a preliminary study, we performed tissue culture experiments on two seed mucilage-producing species established in our lab, *P. ovata* and *P. lanceolata.* These species were selected as they have similar germination times and conditions, and both produce heteroxylan-rich seed mucilage but with easily-distinguishable differences in polysaccharide fine structure[17].

For optimisation of callogenesis, we opted for a 3×3 factorial arrangement of treatments

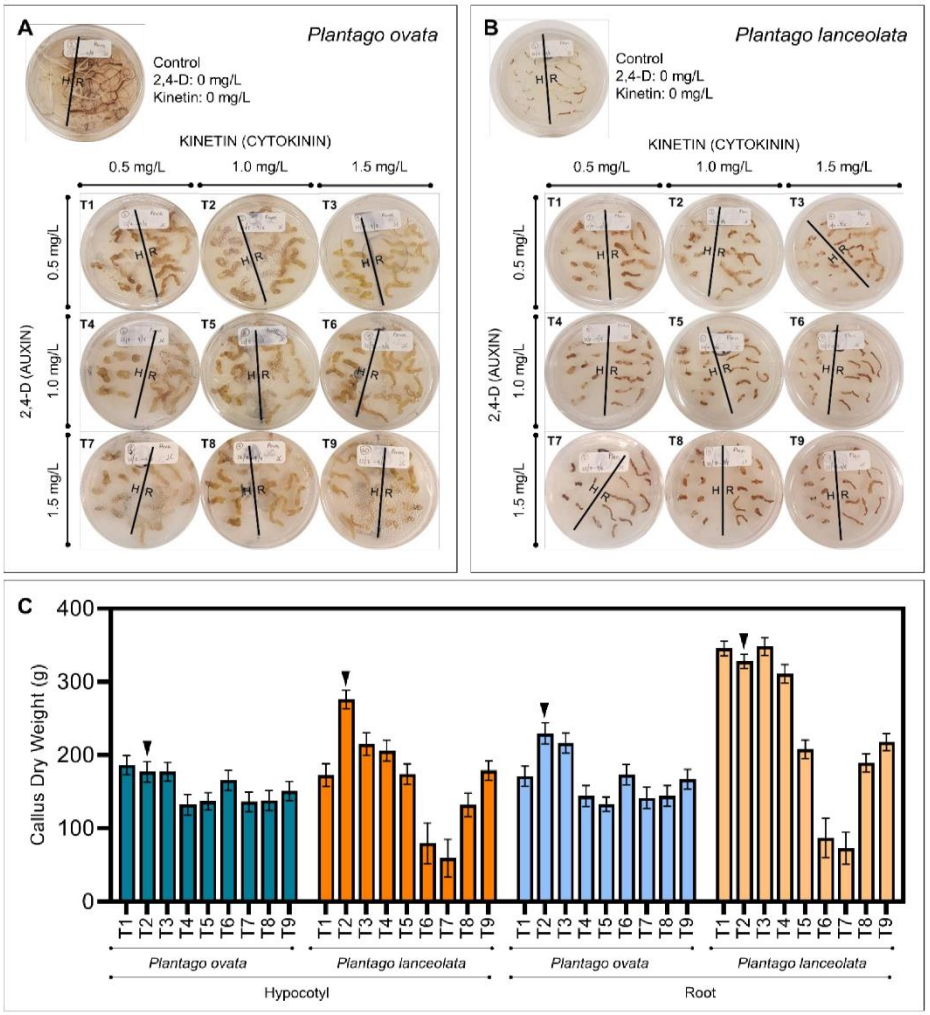

Figure 2. Effect of varying auxin and cytokinin ratios on *Plantago* callus morphology and yield. **A, B** Callus induction and morphology of (**A**) *P. ovata* and (**B**) *P. lanceolata* calli at 4 weeks. H, hypocotyl explant; R, root explant. **C.** Dry weight of calli after 8 weeks reveals that the effect of auxin and cytokinin are similar between species and explant type. Arrowhead denotes treatment 2 (T2), the highest yielding treatment that was used for composition analysis.

(Table 1) using 2,4-D and kinetin (KIN) as the auxin and cytokinin, respectively, and using 10 day old hypocotyl and root tissues as explants. While the explant tissues of both species wilted rapidly in the absence of any hormones (T0 treatment), addition of any combination of hormones induced callogenesis (Figure 2A and 2B). Morphology of calli ranged from dark and compact to cream-coloured, soft and friable, and calli from *P. ovata* tended to be softer and wetter than that of *P. lanceolata*. Treatments T2 and T3 (lower 2,4-D to KIN) produced larger, softer, wetter-looking calli than other treatments; the dry weights of T2 and T3 calli were consistently highest across all treatments (Figure 2C), with T2 yielding the highest sum and grand mean for all replicates. The same treatment (0.5 mg/L 2,4-D with 1.0

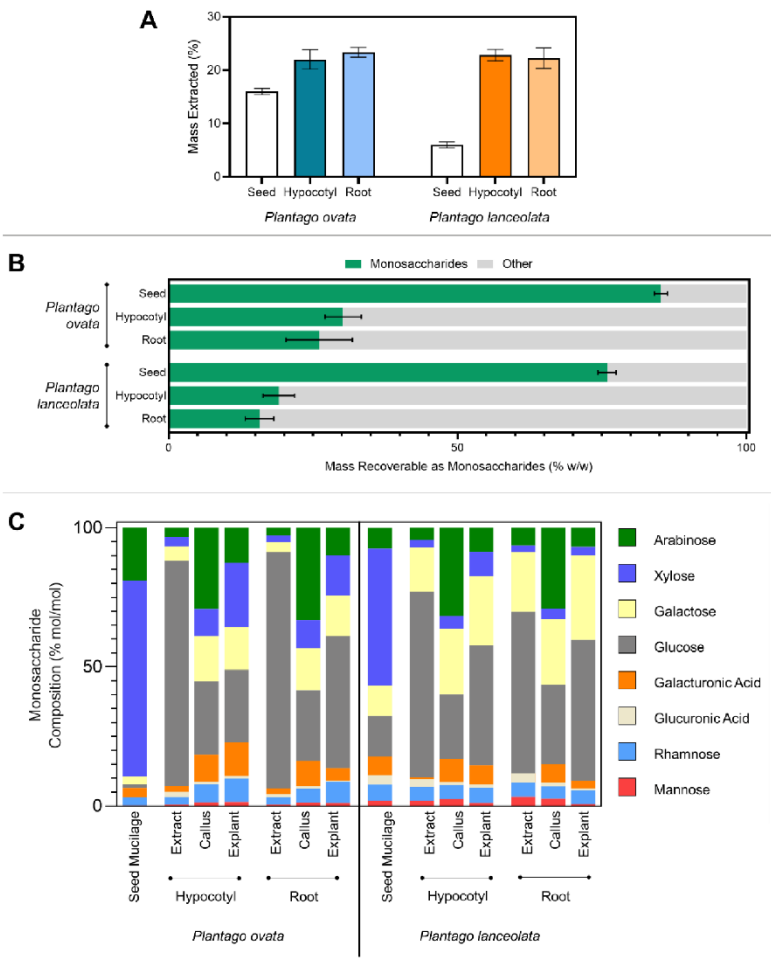

Figure 3. Yield and compositional analysis of *Plantago* callus extracts. **A.** Yield of extract from callus exceeds that of seed. **B.** Quantification of the proportion of extracts that could be recovered as monosaccharides. **C.** Molar monosaccharide profiles of extracts derived from various sources.

mg/L KIN) had also been reported to produce very high callus induction rate, growth rate and mucilage yield from *P. ovata* hypocotyls[11] and leaves[10]. Previous studies of mucilage production from *Plantago*-derived calli reported that the largest calli yielded the most mucilage[9,11], so T2 calli from both species and explant types were used for mucilage compositional analysis.

Mucilage was extracted from freeze-dried T2 calli alongside mature seeds. In line with previous findings[9,10,16], the mass yield of material extracted from calli exceeded that extracted from seed in both species, but yield from both types of callus was comparable (Figure 3A). As mucilage is predominantly polysaccharide[1], monosaccharide profiling was used to assess the composition of callus-derived extracted material (Figure 3B and 3C). While seed-derived mucilage from both *P. ovata* and *P. lanceolata* is clearly predominantly mono- or polysaccharide, material extracted from calli of both species had far more mass than could be accounted for as hydrolysed monosaccharides. While seed-derived mucilage is typically 70–90% polysaccharides[18,19], only 15–30% of material extracted from calli could be recovered as monosaccharides after acid hydrolysis (Figure 3B). Comparing the molar monosaccharide composition of each sample, neither hypocotyl nor root callus-derived extracted material had a composition comparable to seed mucilage (Figure 3C). Monosaccharides present in callus-derived extracted material from both species were overwhelmingly glucose,

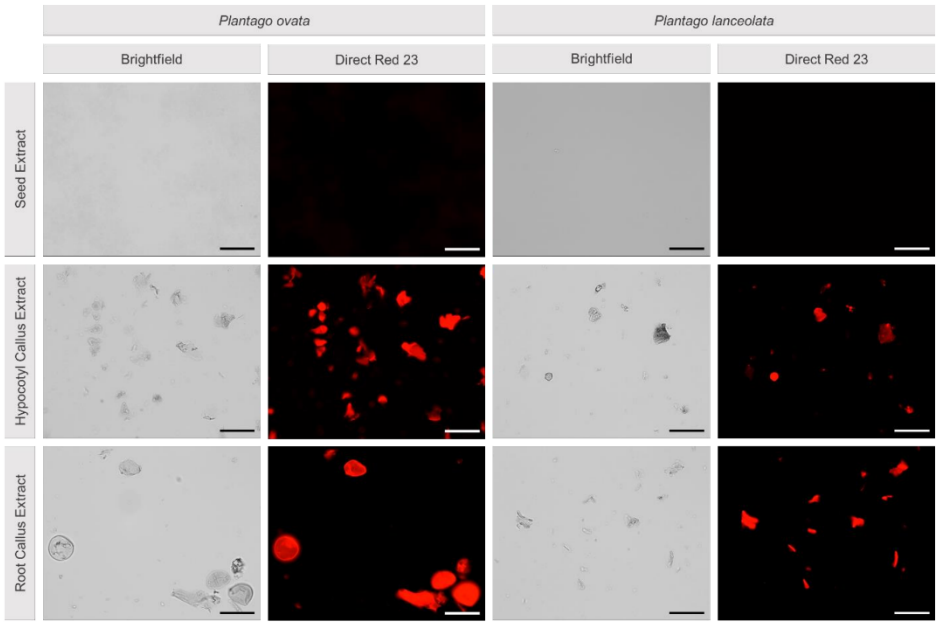

Figure 4. Microscopic analysis of *Plantago* seed and callus extracts. Cellular debris visible under brightfield stain positively with Direct Red 23. Scale bar = 100 µm.

compared with xylose-rich seed-derived mucilage (Figure 3C). As cellulose is resistant to the hydrolysis used here, the excess glucose is likely to be free cellular glucose or derived from starch. Though occurring in slightly different ratios, the remaining monosaccharides in the callus-derived extract corresponded to those in the post-extraction callus, which in turn corresponded to the composition of the fresh explant material (Figure 3C). The presence of arabinose, galactose and glucose were also reported for *L. sativum* callus mucilage[13] but, similar to our results, these monosaccharides could only account for at most 20% of the mucilage mass. Furthermore, the molar ratios of these monosaccharides do not correspond to previous reports of the composition of *L. sativum* seed mucilage[20]. A similar compositional disconnect between hairy root culture-derived mucilage and gum of *Astragalus gummifer* has also been reported[21]. These findings indicate that callus-extracted monosaccharides are derived from non-cellulosic polysaccharides in the source cell walls, in line with some previous work[22], rather than an extracellular mucilage.

The callus extract mass that was not recoverable by monosaccharide analysis was substantial, and characterising the remaining material may shed light on why extract yields are, in agreement with findings here, reported to be so high. Based on the crude extraction techniques we hypothesised that the remaining mass may simply be insoluble debris. Using microscopic analysis we show that extracts from calli contain abundant particulate matter which is not present in corresponding extracts from seeds (Figure 4). Using the cellulose specific stain Direct Red 23[23], it is clear that the debris is predominantly cellulosic wall material produced by the harsh extraction techniques and not effectively removed by filtering prior to further analysis. Even semi-intact, but somewhat damaged entire cells can be seen in *P. ovata* root callus extracts (Figure 4). Cellulosic materials are recalcitrant to hydrolysis by the technique used here, explaining the loss of mass recovery.

Conclusion

While previous reports of highly efficient *in vitro* mucilage production was an exciting premise, here we have shown that *Plantago* callus-derived extracted material, referred to by others as “mucilage”, is predominantly cellular debris, with a very different compositional profile to seed-derived mucilage from the same species. Previous reports of high yields are likely to be the result of ineffective filtering of cellular debris produced from harsh extraction techniques. Our monosaccharide analysis shows callus “mucilage” to have a low non-cellulosic polysaccharide content (only 21–35% of the content of seed mucilage), with an overall monosaccharide profile analogous to cell wall material from both callus and the source explant. We conclude that plant tissue culture as an alternative source of mucilage polysaccharides, at least by the methods followed here, is not likely to be possible.

Methods

Explant preparation and callus induction

P. ovata and *P. lanceolata* seeds were obtained from a previous study by Phan *et al.*[17]. Seeds were placed in an autoclaved stainless steel tea strainer and surface sterilised by sequential immersion for 1 min in filter-sterilised: 50% ethanol (once), 1:1 ethanol (50%) and bleach (4% hypochlorite) with 0.05% Triton X-100) (five times), and water (five times). Sterilised seeds were spread on sterile Whatman No. 1 filter paper in a Petri dish, wetted with 3 ml sterile water. Petri dishes were sealed with Parafilm, and seeds vernalised for 48 h at 4 °C before germination on a south-facing windowsill (Adelaide, Australia) for 10 days. Ten hypocotyl and ten root segments were aseptically excised from 10 day-old seedlings using a sterile scalpel and placed onto culture media (30 mg/L sucrose, 4.43 mg/L MS basal medium (PhytoTech, M519), 9% agarose) with different concentrations of 2,4-dichlorophenoxyacetic acid (2,4-D) (Astral Scientific, KB0745) and kinetin (KIN) (Astral Scientific, DB0166) (Table 1). Calli were incubated in the dark at 25 °C for 8 weeks, with subculturing every 2 weeks. Four replicates were prepared for each treatment and divided between two independent incubators.

At 8 weeks old, calli were harvested into 10 mL tubes, frozen at -80 °C and freeze-dried to a constant weight (approximately 72 hr)..

Table 1. *Hormone treatments*

Treatment	2,4-D (mg/L)	KIN (mg/L)
T0	0.0	0.0
T1	0.5	0.5
T2	0.5	1.0
T3	0.5	1.5
T4	1.0	0.5
T5	1.0	1.0
T6	1.0	1.5
T7	1.5	0.5
T8	1.5	1.0
T9	1.5	1.5

Mucilage extraction

Freeze-dried 8 week old calli were lightly ground using a mortar and pestle prior to mucilage extraction. In line with previous publications[10,11,16], mucilage was extracted from calli and seeds following the method of Sharma and Koul[24] with some modifications described by Cowley *et al.,* [25]. Briefly, 1.5 mL of milli-Q water was added to 50 mg of ground callus or seeds. Mixtures were extracted at 95°C for 30 minutes on a shaking incubator (Thermomixer Comfort, Eppendorf, Germany). Extracts were filtered through layered fine tulle (Spotlight, Australia) and freeze-dried for yield and monosaccharide analysis. This extraction was also tested with 0.1 M HCl (in place of water) as per Sharma and Koul[24]. No difference in yield or composition was observed, in line with our previous study[25]. As such, the hot water method was chosen for ease of handling and safety reasons.

Monosaccharide analysis

Composition of mucilage extracted from seeds and callus, post-extraction callus material, and corresponding fresh explant material was determined by monosaccharide profiling following Cowley *et al.,*[25].

Microscopy

Freeze-dried extracts were dispersed at 2 mg/mL in 0.22 µm filtered milli-Q water. An aliquot of 967 µL was added to 33 µL of 5% w/v Direct Red 23 (Sigma-Aldrich) (1 in 30 dilution; final stain concentration of 0.165% w/v) and incubated in the dark at room temperature for 20 mins. One hundred microlitres of stain/extract was placed on a microscope slide and a cover slip placed on top.

Samples were imaged with a Zeiss M2 AxioImager with an AxioCam 506 mono black and white camera. Images were processed using ZEN 2012 software (Zeiss, Germany)

Data analysis

Data analysis was performed in GraphPad Prism 8.4.0.

Acknowledgements

This work was funded by the ARC Centre of Excellence in Plant Cell Walls (Grant No. 110001007). JMC is supported by a PhD scholarship from the Australian Government's Research Training Program. The authors thank Rohan Singh for technical advice in plant tissue culture.

References

1. Phan, J. L. & Burton, R. A. New Insights into the Composition and Structure of Seed Mucilage. *Annu. Plant Rev. Online* **1**, 1–41 (2018).
2. Haughn, G. W. & Western, T. L. Arabidopsis Seed Coat Mucilage is a Specialized Cell Wall that Can be Used as a Model for Genetic Analysis of Plant Cell Wall Structure and Function. *Front Plant Sci* **3**, 64 (2012).
3. Soukoulis, C., Gaiani, C. & Hoffmann, L. Plant seed mucilage as emerging biopolymer in food industry applications. *Curr. Opin. Food Sci.* (2018). doi:10.1016/j.cofs.2018.01.004
4. Khaliq, R., Tita, O., Antofie, M. M. & Sava, C. Industrial Application Of Psyllium: An Overview. *ACTA Univ. Cibiniensis* **67**, (2015).
5. VanDerWoude, W. J. J. *et al.* Auxin (2,4-D) stimulation (in vivo and in vitro) of polysaccharide synthesis in plasma membrane fragments isolated from onion stems. *Biochem. Biophys. Res. Commun.* **46**, 245–253 (1972).
6. Bolwell, G. P. & Northcote, D. H. Induction by growth factors of polysaccharide synthases in bean cell suspension cultures. *Biochem. J.* **210**, 509–515 (1983).
7. Asamizu, T., Nakano, N. & Nishi, A. Changes in non-cellulosic cell-wall polysaccharides during the growth of carrot cells in suspension cultures. *Planta* **158**, 166–174 (1983).
8. Goto, N. Stimulation of polysaccharide formation by 2,4-dichlorophenoxyacetic acid in callus tissues of Arabidopsis thaliana. *Physiol. Plant.* (1986).
9. Mirmasumi, M., Ebrahimzadeh, H. & Tabatabaei, S. M. F. Mucilage Production In Tissue Culture of Plantago lanceolata. *J. Agric. Sci. Technol.* **3**, 155–160 (2001).
10. Gupta, M., Kour, B., Kaul, S. & Dhar, M. Mucilage Synthesis in Callus Cultures of Plantago ovata Forsk. *Natl. Acad. Sci. Lett.* **38**, 103–106 (2015).
11. Golkar, P., Amooshahi, F. & Arzani, A. In vitro synthesis of mucilage in Plantago ovata Forsk affected by genotypes and culture media. *Herba Pol.* **63**, 53–66 (2017).
12. Farzan, F., Shooshtari, L. & Ghorbanpour, M. Callus induction in plantain (Plantago major L .) for in vitro production of mucilage. *Int. J. Biosci.* **6655**, 55–60 (2014).
13. Golkar, P., Hadian, F. & Koohi Dehkordi, M. Production of a new mucilage compound in Lepidium sativum callus by optimizing in vitro growth conditions. *Nat. Prod. Res.* **33**, 130–135 (2019).
14. Hadian, F., Koohi-Dehkordi, M. & Golkar, P. Evaluation of in vitro mucilage and lepidine biosynthesis in different genotypes of Lepidium sativum Linn originated from Iran. *South African J. Bot.* **127**, 91–95 (2019).
15. Kavianifar, S., Ghodrati, K., Badi, N. H. & Etminan, A. Effects of Nano Elicitors on Callus Induction and Mucilage Production in Tissue Culture of Linum usitatissimum L. *J. Med. Plants* **17**, 45–54 (2018).
16. Afshar, B. & Golkar, P. Mucilage synthesis by in vitro cell culture in different species of Alyssum. *BioTechnologia* **2**, 79–86 (2016).
17. Phan, J. L. *et al.* Differences in glycosyltransferase family 61 accompany variation in seed coat mucilage composition in Plantago spp. *J. Exp. Bot.* **67**, 6481–6495 (2016).
18. Varkhade, C. B. & Pawar, H. A. Spectrophotometric Estimation of Total Polysaccharides in Plantago ovata Husk Mucilage. *Int. J. Chem. Pharm. Anal.* **1**, 2–4 (2013).
19. Hesarinejad, M. A. *et al.* The effects of concentration and heating-cooling rate on rheological properties of Plantago lanceolata seed mucilage. *Int. J. Biol. Macromol.* **115**, 1260–1266 (2018).
20. Behrouzian, F., Razavi, S. M. A. & Phillips, G. O. Cress seed (Lepidium sativum) mucilage, an overview. *Bioact. Carbohydrates Diet. Fibre* **3**, 17–28 (2014).

21. Isa, T., Ogasawara, T. & Kaneko, H. Induction of Hairy-Root from Astragalus Plant, and Mucilage Production by the Hairy-Root. *Plant Tissue Cult. Lett.* **6**, 134–137 (1989).

22. Bacic, A., Moody, S., Mccomb, J., Hinch, J. & Clarke, A. Extracellular Polysaccharides From Shaken Liquid Cultures of Zea mays. *Funct. Plant Biol.* **14**, 633 (1987).

23. Liesche, J., Ziomkiewicz, I. & Schulz, A. Super-resolution imaging with Pontamine Fast Scarlet 4BS enables direct visualization of cellulose orientation and cell connection architecture in onion epidermis cells. *BMC Plant Biol.* **13**, (2013).

24. Sharma, P. K. & Koul, A. K. Mucilage in seeds of Plantago ovata and its wild allies. *J Ethnopharmacol* **17**, 289–295 (1986).

25. Cowley, J. M. *et al.* A small- scale fractionation pipeline for rapid analysis of seed mucilage characteristics. *Plant Methods* **16**, 1–12 (2020).

Appendix II - Career and Research Skills Training (CaRST)

What is Career and Research Skills Training (CaRST)?

Career and Research Skills Training (CaRST) is a specialised training and development program for Higher Degree by Research (HDR) students at the University of Adelaide.

CaRST comprises the ‘Development Component of the Structured Program’ and student participation extends from enrolment to thesis submission. HDRs are required to complete a minimum number of CaRST hours by thesis submission: 120 hours for PhDs and 60 hours for MPhils. Activities must also be distributed across all four domains identified in the Researcher Development Framework from Vitae.

CaRST Record

Below is a record of the activities that I completed during my PhD Candidature as per the requirements of the Career and Research Skills Training (CaRST) program

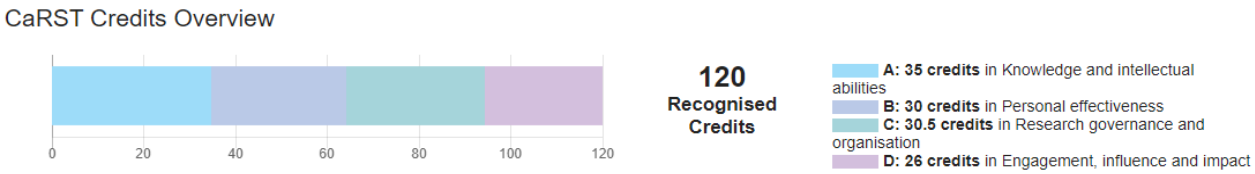

Date Completed	Type	Activity Description	Domain	Hours
29/03/2017	Experiential	Grant Application - 2017 MDPI Agriculture Travel Award	C	3
30/03/2017	Experiential	ARC CoE Plant Cell Walls - Journal Club: organisation, presentation and attendance	A	8
5/04/2017	Core	CaRST Information Session	C	2
6/04/2017	Core	Postgraduate Research Induction	B	2
31/05/2017	Experiential	Grant Application - 2017 Farrer Memorial Trust Travelling Scholarship in Agriculture	C	3
4/06/2017	Experiential	Community Outreach - Children's University Demonstrator Profile Video	D	4
4/06/2017	Experiential	Community Outreach - Children's University Regional Lecture Series	D	10
4/06/2017	Experiential	Online Researcher Profile	B	1
1/09/2017	Experiential	Core Component of the Structure Program	B	15
1/09/2017	Experiential	Core Component of the Structure Program	C	4
3/10/2017	Experiential	Conference Attendance - ComBio 2017, Adelaide	B	9
4/10/2017	Experiential	Research Communication - Poster: Combio 2017, Adelaide	D	3
28/11/2017	Training	FreezerPro Biobank Management for Researchers	C	1.5
4/01/2018	Training	Workshop - Animate Your Science	D	2
4/01/2018	Training	Workshop - Customized Onsite LCMS QTOF Techniques and Operation	A	25
4/01/2018	Training	Workshop - Engaging Allies for Change: LGBTI Inclusion	D	2
20/04/2018	Training	Lecture - Demystifying Research Metrics	A	1
20/04/2018	Training	Lecture - The Imposter Syndrome	B	3
20/04/2018	Training	Lecture - You & Your Supervisor: Communication and win-win skills as an HDR	D	2
1/05/2018	Experiential	Grant Application - 2018 Barr Smith Travelling Scholarship in Agriculture	C	3
18/08/2018	Experiential	Conference Attendance - Plant Biology Europe 2018	C	12
18/08/2018	Experiential	Research Communication - Poster: Plant Biology Europe, 2018	D	3
20/08/2018	Experiential	Research Communication - Seminar: Lunch and Learn at PepsiCo, Leicester, UK	A	1
27/09/2018	Training	Working with GMOs - Gene Technology Training	C	1

CaRST Completion Certificate

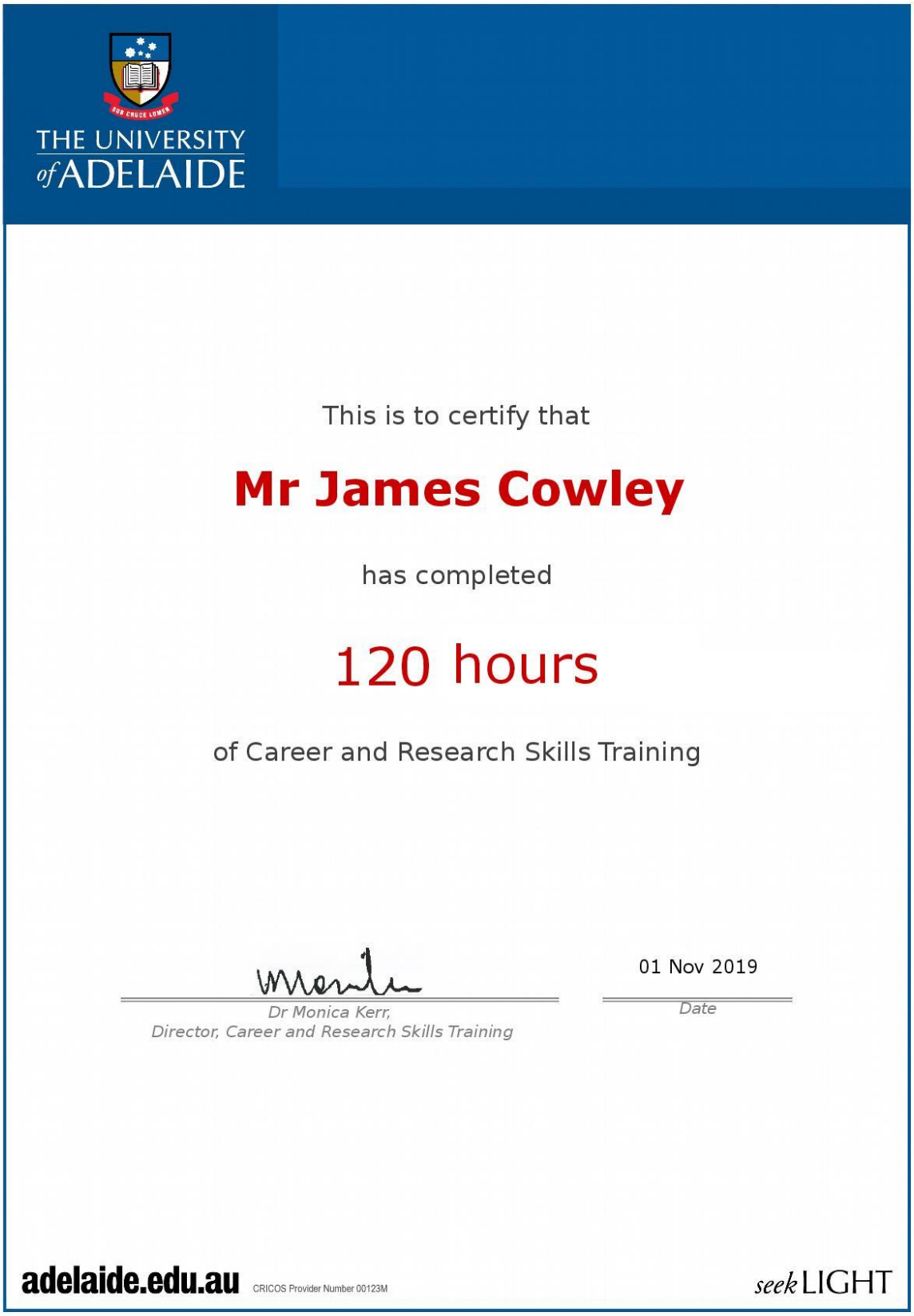

Appendix III – Conference Posters

ComBio 2017, Adelaide, Australia

Below is the poster that I presented at ComBio 2017 based on work completed during my honours year and continued during my PhD Candidature.

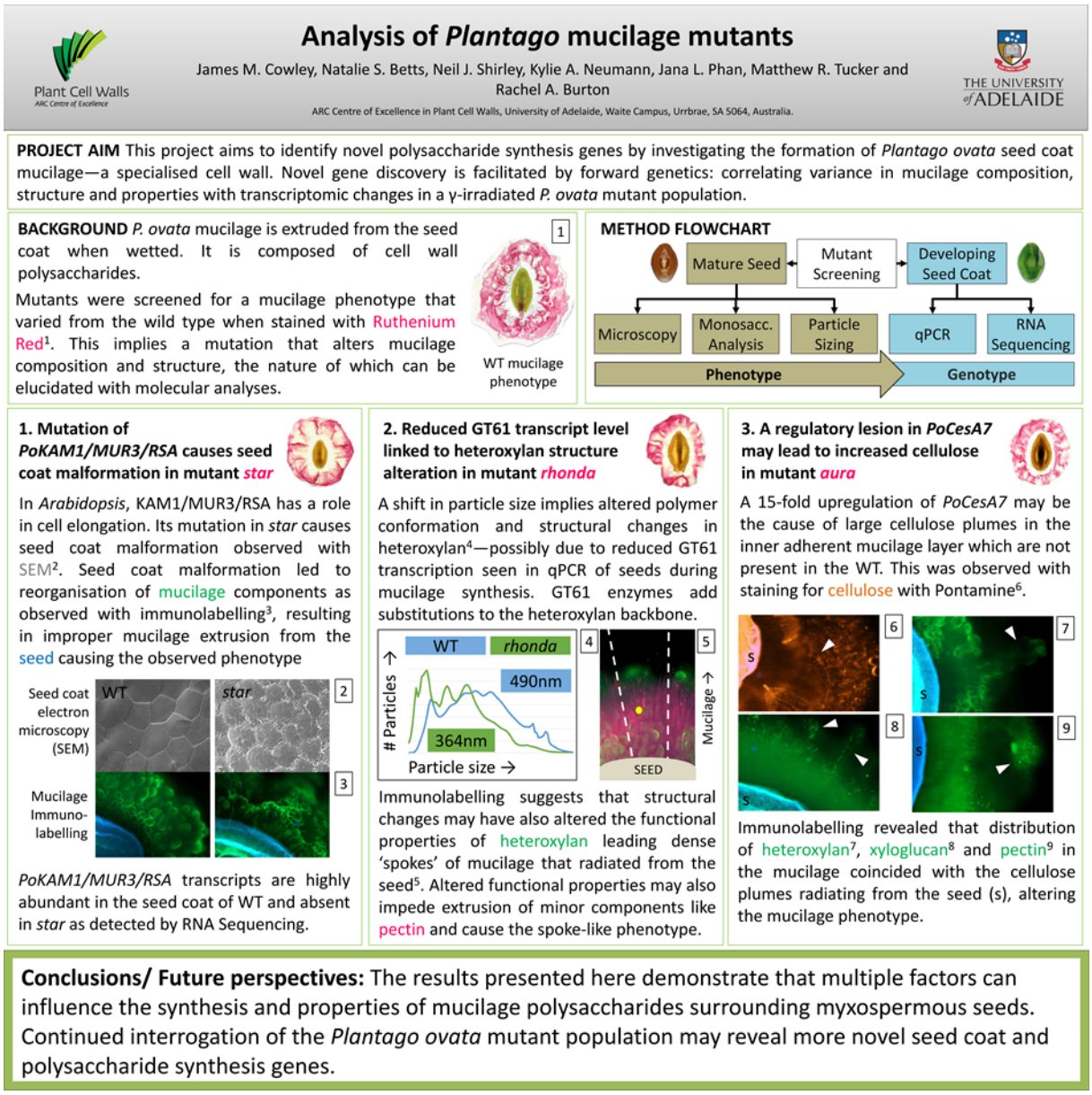

Plant Biology Europe,

June 2018, Copenhagen, Denmark

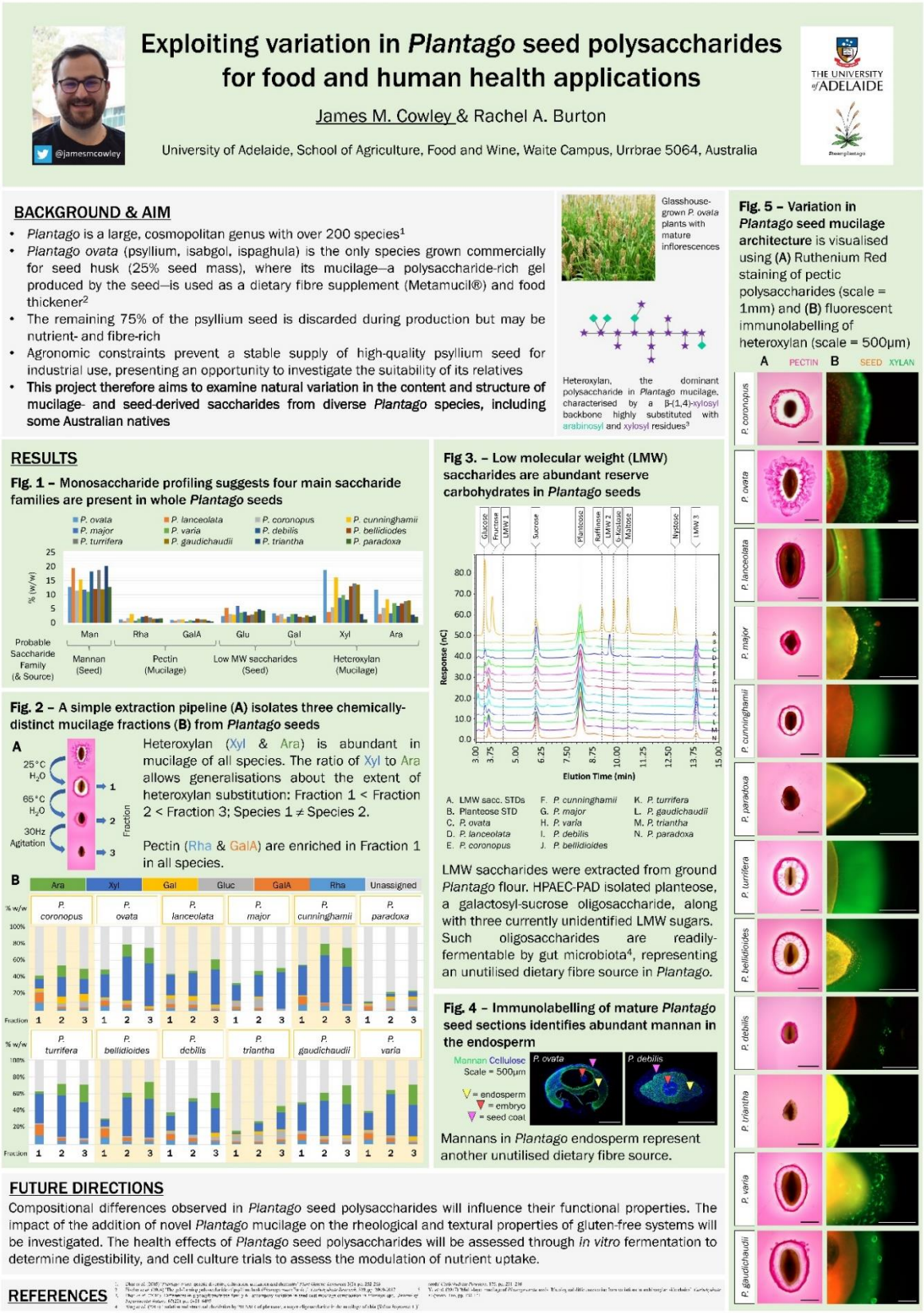

Australian Institute of Food Science and Technology Meeting,

January 2019, Adelaide, Australia

Augmenting gluten-free breads with naturalised and Australian native *Plantago* seeds

James M. Cowley[1], Yi Ren[2], Timothy J. Foster[2] & Rachel A. Burton[2]

✉ james.cowley@adelaide.edu.au

University of Adelaide, School of Agriculture, Food and Wine, Waite Campus, Urrbrae 5064, Australia[1]
University of Nottingham, School of Biosciences, Sutton Bonington Campus, Leicestershire LE12 5RD, UK[2]

THE UNIVERSITY of ADELAIDE

The University of Nottingham

BACKGROUND & AIM

- *Plantago* seeds extrude diverse, complex polysaccharides that form networks capable of simulating some functions of gluten in gluten-free (GF) foods
- Psyllium (*P. ovata*) is the only commercially-grown species
- Whole psyllium seeds and seeds of its near relatives are yet to be used as functional food ingredients.
- **The aim of this project is to assess the functionality of diverse *Plantago* flours as ingredients in GF breads.**

1. Differences in extrusion architecture are related to different polysaccharide structures resulting from natural variation between *Plantago* species. When stained with ruthenium red, hydrophilic polysaccharides extruded from *Plantago* seeds can be observed. The geographic origin of each species is indicated and are ordered (L to R) by increasing genetic distance from the most recent common ancestor. **Scale=1mm**

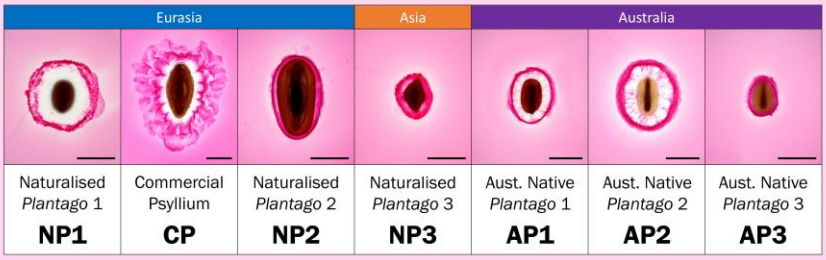

2a. Small additions of *Plantago* flour can enhance the pasting process of rice flour (RF), the process by which the continuous starch matrix of bread is formed. In the example below, a Rapid Visco Analyser (RVA) was used to determine that a 4% addition of AP1 flour drastically reduced the temperature at which pasting (PT) of RF began. This indicates that AP1 has a high water-holding capacity. Additionally, AP1 greatly increased peak (PV) and final (FV) viscosities indicating AP1 has strong gelling properties. Polysaccharide gel networks can reinforce gluten-less starch matrices.

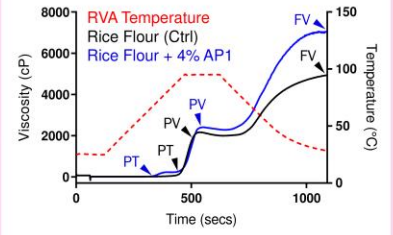

2b. A wide range of enhancements to RF pasting was observed. Differences appear to accompany natural diversity in polysaccharide structure. Furthermore, effects cluster by genetic relatedness. This is most apparent in AP1, -2 and -3.

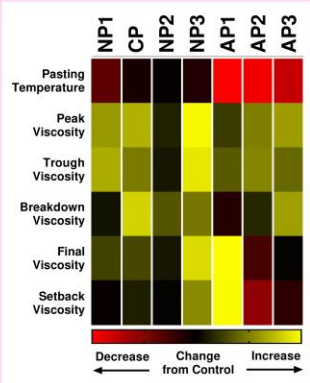

3. In breadmaking, a 4% addition of *Plantago* flour to rice flour-based GF doughs increases fundamental strength and extensibility. Dynamic oscillatory tests on breadmaking dough formulations revealed that the *Plantago* flour-derived polysaccharide gel network led to an increase in the amount of energy stored under deformation (storage modulus G'), characteristic of increased elasticity. This indicates a transition from a liquid batter to a strong dough. While G' was similar between most *Plantago* species, the loss factor Tan δ—representing extensibility—was highest in AP1 and AP2 doughs.

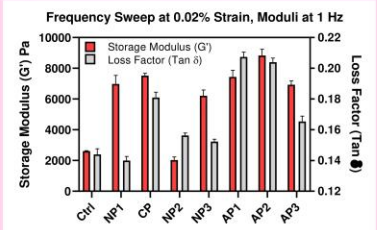

4. Improvements to RF pasting and dough rheological properties manifests as effectively leavened GF loaves. While NP1, NP3 and AP3 doughs had storage moduli (G') similar to that of AP1 and AP2, their lower loss factors indicate reduced extensibility, required to resist structural failure under proofing tension. This manifests as collapsed loaves (▻), while the higher loss factor (extensible) doughs did not collapse. Uncollapsed loaves had greater specific volume. Using texture profile analysis (TPA), it was found that while volume increased, loaf hardness was not reduced. This is likely due to the robust gel network. However, the gel network's presence increased the cohesiveness and springiness of the loaves, particularly in AP1 and AP2 loaves. These are essential mouthfeel characteristics that GF loaves typically lack.

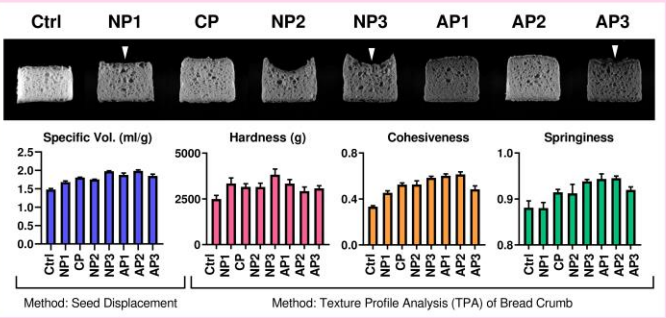

CONCLUSIONS AND FUTURE DIRECTIONS

The results of this study show that whole seed *Plantago* flour from diverse sources can be used to augment the quality of GF baking formulations. Future work will be aimed at developing commercial formulations implementing additional hydrocolloids that can further improve loaf specific volume and reduce loaf hardness. Additionally, the dietary implications of using a whole seed additive which contains bioactive compounds will be studied. This may bolster the profile of GF formulations which are typically nutritionally-poor.

TEAM PLANTAGO